



Fisheries and Oceans
Canada

Pêches et Océans
Canada

Ecosystems and
Oceans Science

Sciences des écosystèmes
et des océans

Canadian Science Advisory Secretariat (CSAS)

Research Document 2017/077

Newfoundland and Labrador Region

Coast of Bays seawater vertical and horizontal structure (2009-13): Hydrographic structure, spatial variability and seasonality based on the Program for Aquaculture Regulatory Research (PARR) 2009-13 oceanographic surveys

S. Donnet, S. Cross, P. Goulet and A.W. Ratsimandresy

Science Branch
Fisheries and Oceans Canada
Po Box 5667
St. John's, NL A1C 5X1

Foreword

This series documents the scientific basis for the evaluation of aquatic resources and ecosystems in Canada. As such, it addresses the issues of the day in the time frames required and the documents it contains are not intended as definitive statements on the subjects addressed but rather as progress reports on ongoing investigations.

Research documents are produced in the official language in which they are provided to the Secretariat.

Published by:

Fisheries and Oceans Canada
Canadian Science Advisory Secretariat
200 Kent Street
Ottawa ON K1A 0E6

[http://www.dfo-mpo.gc.ca/csas-sccs/
csas-sccs@dfo-mpo.gc.ca](http://www.dfo-mpo.gc.ca/csas-sccs/csas-sccs@dfo-mpo.gc.ca)



© Her Majesty the Queen in Right of Canada, 2018
ISSN 1919-5044

Correct citation for this publication:

Donnet, S., Cross, S., Goulet, P., and Ratsimandresy, A.W. 2018. Coast of Bays seawater vertical and horizontal structure (2009-13): Hydrographic structure, spatial variability and seasonality based on the Program for Aquaculture Regulatory Research (PARR) 2009-13 oceanographic surveys. DFO Can. Sci. Advis. Sec. Res. Doc. 2017/077. viii + 255 p.

TABLE OF CONTENTS

ABSTRACT.....	VII
RÉSUMÉ	VIII
INTRODUCTION	1
PREVIOUS STUDIES.....	3
MATERIAL AND METHODS.....	5
EQUIPMENT.....	5
FIELD WORK.....	6
DATA PROCESSING AND QUALITY ASSURANCE / QUALITY CONTROL (QA/QC)	12
DATA VISUALISATION AND ANALYSES.....	12
RESULTS	15
HERMITAGE BAY – BAY D’ESPOIR(HB-BDE)	15
FORTUNE BAY – BELLE BAY (FB – BB)	23
CONNAIGRE PENINSULA (CP)	27
DISCUSSION.....	31
HYDROGRAPHIC CHARACTERISTICS.....	31
SHORT TERM VARIATIONS	41
STUDY LIMITATIONS.....	41
CONCLUSION AND RECOMMENDATIONS	42
ACKNOWLEDGEMENTS	43
REFERENCES	43
APPENDIX A(I): HERMITAGE BAY – BAY D’ESPOIR (HB-BDE) VERTICAL SECTIONS.....	46
APPENDIX A(II): HERMITAGE BAY – BAY D’ESPOIR(HB-BDE) VERTICAL SECTIONS SUMMARY TABLES.....	99
APPENDIX A(III): HERMITAGE BAY – BAY D’ESPOIR(HB-BDE) SURFACE MAPS.....	108
APPENDIX B(I): FORTUNE BAY – BELLE BAY (FB-BB) VERTICAL SECTIONS	142
APPENDIX B(II): FORTUNE BAY – BELLE BAY (FB-BB) VERTICAL SECTIONS SUMMARY TABLES.....	159
APPENDIX B(III): FORTUNE BAY – BELLE BAY (FB-BB) SURFACE MAPS.....	163
APPENDIX C(I): CONNAIGRE PENINSULA (CP) VERTICAL SECTIONS.....	176
APPENDIX C(II): CONNAIGRE PENINSULA (CP) VERTICAL SECTIONS SUMMARY TABLES	219
APPENDIX C(III): CONNAIGRE PENINSULA (CP) SURFACE MAPS	226
APPENDIX D: CTD DATA PROCESSING STEPS	251
APPENDIX E: SAGONA ISLAND WIND RECORDS.....	254

LIST OF FIGURES

Figure 1: Study Area with the locations of the aquaculture licences (as of November 2015; source: Department of Fisheries and Aquaculture 2015.....	2
Figure 2: Instrumentation.	7
Figure 3: CTD data collection temporal resolution.....	9
Figure 4: CTD data collection program, casts (black dots) spatial coverage from June 2009 to July 2011.	10
Figure 5: CTD data collection program, casts (black dots) spatial coverage from May 2012 to September 2013.	11
Figure 6: Key along channel transects.	13
Figure 7: Basins and sills of the Hermitage Bay – Bay d’Espoir (HB-BDE) region.	17
Figure 8: Basins and sills of the Belle Bay (BB) region.....	24
Figure 9: Basins and sills of the CP region.....	28
Figure 10: BDE (April-May 2010), BB (May 2011) and CP (May 2011) hydrographic sections.	33
Figure 11: BDE hydrographic zones.....	38
Figure 12: BB hydrographic zones.	39
Figure 13: CP hydrographic zones.....	40

LIST OF TABLES

Table 1: Instrument specifications.....	6
Table 2: Data collection summary.	8

LIST OF ACRONYMS

Acronym	Name	Description
ADCP	Acoustic Doppler Current Profiler	Oceanographic instrument measuring current using acoustic method (i.e., current meter)
BBE	Belle Bay East	Hydrographic transect and zone
BBN	Belle Bay North	Hydrographic zone
BBW	Belle Bay West	Hydrographic transect and zone
BB-MB	Belle Bay – Mal Bay	Hydrographic transect
BDE	Bay d'Espoir	Major bay of interest
BDE-DA	BDE Development Association	Local society promoting economic development
BIS	Bois Island South	Hydrographic zone
CCB	Central Connaigre Bay	Hydrographic zone
CCGS	Canadian Coast Guard Research Vessel (Ship)	Scientific vessel used for the hydrographic surveys
CB	Connaigre Bay	Major bay of interest
CP	Connaigre Peninsula	Broad region encompassing Connaigre Bay, Harbour Breton - Northern Arm and Great Bay de L'eau
CTD	Conductivity, Temperature and Depth	Oceanographic instrument measuring temperature, conductivity and pressure. The latter two measurements are usually converted to salinity and depth
DIVA	Data Interpolating Variational Analysis	Sophisticated spatial interpolation method based on a cost function (Variational Inverse Method) and finite element solver
EB	East Bay	Hydrographic transect and zone and sub-region of Bay d'Espoir
FB	Fortune Bay	Major bay of interest
FB-BB	Fortune Bay - Belle Bay	Major bay of interest
FB-LH	Fortune Bay – Long Harbour	Hydrographic transect
GBDE	Great Bay de l'Eau	Major bay of interest
GHB	Great Harbour Bight	Hydrographic zone of Connaigre Bay
GPS	Global Positioning System	Satellite navigation system
HB	Hermitage Bay	Major bay of interest
HB-BDE	Hermitage Bay - Bay d'Espoir	Major bay of interest
HB-NA	Harbour Breton - Northeast Arm	Major bay of interest
HC	Hermitage Channel	Major underwater channel ending in Hermitage Bay
IHB	Inner Hermitage Bay	Hydrographic zone
LaP	Lampidoes Passage	Hydrographic zone and sub-region of Bay d'Espoir
LaP-	Lampidoes Passage –	Hydrographic transect
UBDE	Upper BDE section	-
LBDE	Lower Bay d'Espoir	Hydrographic zone and sub-region of Bay d'Espoir
LBDE-NB	Lower Bay d'Espoir– North Bay	Hydrographic transect
LCW	Labrador Current Water	Water mass carried over by the Labrador Current
LGBDE	Lower Great Bay De l'Eau	Hydrographic zone
LiP	Little Passage	Hydrographic transect and zone of Bay d'Espoir

LIST OF ACRONYMS

Acronym	Name	Description
LH	Long Harbour	Major estuary of interest located in Fortune Bay
LHB-NA	Lower Harbour Breton – Northeast Arm	Hydrographic zone
MSRL	Marine Science Research Laboratory	Academic research facility (presently Ocean Science Centre)
MSW	Modified Slope Water	Deep water mass present below about 200 m in the Laurentian channel, Hermitage Channel and flowing into some of our bays of interest
NACS	Natural Areas of Canadian Significance	Parks Canada designation of areas of ecological interest
NAFO	Northwest Atlantic Fisheries Organization	Fisheries organisation based in Canada to manage Northwest Atlantic fisheries stocks
NB	North Bay	Hydrographic zone and sub-region of Bay d'Espoir
OCB	Outer Connaigre Bay	Hydrographic zone
OHB	Outer Hermitage Bay	Hydrographic zone
PARR	Program for Aquaculture Regulatory Research (PARR)	DFO Program
ODV	Ocean Data View	Oceanographic software used to graphically represent and analyze the in-situ observations
QA/QC	Quality Assessment/Quality Control	Methods used to assess the quality of the in-situ observations (i.e., data)
SBE	Seabird	Oceanographic instrumentation company manufacturing the Conductivity, Temperature and Depth (CTD) instruments used for this study
UBDE	Upper Bay d'Espoir	Hydrographic zone and sub-region of Bay d'Espoir
UCB	Upper Connaigre Bay	Hydrographic transect and zone
UGBDE	Upper Great Bay De l'Eau	Hydrographic zone
UHB-NA	Upper Harbour Breton Northeast Arm	Hydrographic zone
UTC	Coordinated Universal Time	Time zone/time standard
WGS84	World Geodetic System 1984	Horizontal coordinate system

ABSTRACT

Upon a recent rapid increase of the finfish aquaculture industry in the Coast of Bays, an area of the South Coast of Newfoundland (9 fold production growth from 2003 to 2013), Fisheries and Oceans Canada (DFO) carried out a research project to better understand the physical oceanography of the area. This report is the second of a series aiming to provide an oceanographic knowledge baseline of the Coast of Bays (i.e., data and analyses) to help manage and ensure the sustainable growth of the aquaculture industry. This report presents the analysis of 790 water profiles of temperature, salinity and dissolved oxygen concentration sampled at 276 stations over the course of a 5-year oceanographic program (2009-13). The profiles were analyzed using along-channel vertical sections plots (i.e., transects), surface property maps and water masses statistics.

The results of this study highlight the hydrographic structure of three distinct geographical regions: a very stratified fjord subject to large freshwater runoff (Bay d'Espoir), a large stratified bay subject to important freshwater runoff (Belle Bay) and a peninsula producing limited amount of freshwater discharge and consisting of two open bays and one narrow inlet (Connaigre Peninsula). As a result of the geographical variation of freshwater inputs, the surface layer characteristics (temperature, salinity, dissolved oxygen and pycnocline depth) vary significantly among the bays studied. Below the seasonal surface layer, two main water masses were identified and are unevenly distributed across the area; due mainly to topographic features which impede or limit water exchanges (i.e., sills). Short-term (i.e., order of hours to days), seasonal and inter-annual variations are also discussed but their assessment, and understanding, is limited by the spatial and temporal resolution. Similarly, the physical processes responsible for those variations are poorly understood. Further research would be needed to address those important knowledge gaps.

Based on these geographical differences across regions and within each of the bay studied, hydrographic zones are defined and may be used, in conjunction with other relevant factors, for aquaculture management purposes.

Data used and presented in this report are available at the [Government of Canada's Open Data website](#).

**Structure verticale et horizontale de l'eau de mer de la Coast of Bays (2009-13):
Structure hydrographique, variabilité spatiale et saisonnalité basée sur les levés
océanographiques du Programme de recherche sur la réglementation de
l'aquaculture (PRRA) 2009-13**

RÉSUMÉ

À la suite d'une récente augmentation rapide de l'industrie de l'aquaculture de poissons dans la côte des baies, une région de la côte sud de Terre-Neuve (production multiplié par 9 de 2003 à 2013), Pêches et Océans Canada a mené un projet de recherche pour mieux comprendre l'océanographie physique de la région. Ce rapport est le deuxième d'une série visant à fournir une base de connaissances océanographiques sur le littoral des baies (données et analyses) afin d'aider à gérer et assurer la croissance durable de l'industrie aquacole. Ce rapport présente l'analyse de 790 profils de température, salinité et concentration en oxygène dissous échantillonnés à 276 stations au cours d'un programme océanographique de cinq ans (2009-2013). Les profils ont été analysés à l'aide de tracés de sections verticales (transects), de cartes de propriétés de surface et de statistiques des masses d'eau.

Les résultats de cette étude mettent en évidence la structure hydrographique de trois régions géographiques distinctes: un fjord très stratifié soumis à un important ruissellement d'eau douce (Bay D'Espoir), une grande baie stratifiée soumise à un ruissellement d'eau douce notable (Belle Bay) et une péninsule produisant une quantité limitée d'eau douce et se composant de deux baies ouvertes sur l'océan et d'un bras de mer étroit (péninsule de Connaigre). En raison de la variation géographique des apports en eau douce, les caractéristiques de la couche superficielle (température, salinité, oxygène dissous et profondeur de la pycnocline) varient de façon significative entre les baies étudiées. Au-dessous de la couche superficielle saisonnière, deux masses d'eau principales ont été identifiées et sont réparties de façon inégale dans la zone; principalement en raison de caractéristiques topographiques qui entravent ou limitent les échanges d'eau (seuils). Les variations saisonnières et interannuelles à court terme (c'est-à-dire de l'ordre des heures à jours) sont aussi examinées mais aussi leur évaluation, et leur compréhension, est limitée par la résolution spatiale et temporelle des données. De même, les processus physiques responsables de ces variations sont mal compris. Des recherches plus approfondies seraient nécessaires pour combler ces lacunes importantes.

Sur la base de ces différences géographiques entre les régions et dans chacune des baies étudiées, des zones hydrographiques sont définies et peuvent être utilisées, en parallèle avec d'autres facteurs pertinents, à des fins de gestion de l'industrie aquacole.

Les données utilisées et présentées dans ce rapport sont disponibles au [le site Web des données ouvertes du gouvernement du Canada](#).

INTRODUCTION

This report is the second of a series that aims to describe the physical oceanography of the Coast of Bays, an area of the Newfoundland South Coast (Figure 1). The Coast of Bays area is currently experiencing a rapid growth of its aquaculture industry (from 2,600 t in 2003 to 22,196 t in 2013, or about 9 fold in 10 years, of salmonid production [Department of Fisheries and Aquaculture 2014a]), leading to the necessity of developing new regulations in environmental management such as the implementation of Bay Management Areas (BMAs, Chang et al. 2014). One of the main purposes of this document is to provide baseline physical oceanographic information to serve as a scientific basis to those regulations.

In Newfoundland and Labrador (NL), the provincial the provincial Department of Fisheries, Forestry and Agrifoods (formerly the Department of Fisheries and Aquaculture), together with the finfish industry recently implemented a BMAs policy, similar to that of New Brunswick, to better manage the growth and ensure sustainability of aquaculture activity in the Coast of Bays (Department of Fisheries and Aquaculture 2014b). The BMAs policy established in New Brunswick consists in implementing single-year-class farming and in partitioning salmon farm areas into Management Areas based on a combination of oceanographic, fish health and business considerations (Chang et al. 2014). The oceanographic considerations rely largely on potential for water exchanges between farm sites based on tidal excursions; with the underlying objective of minimizing the connections among farms to reduce risks of cross-contaminations (Chang et al. 2007). However, scientific basis for defining those BMAs in Newfoundland is limited as there is little understanding of the oceanography.

The previous report of the series (Donnet et al. 2017) focused on describing the area's geography, hydrology and oceanography. In particular, it provided a description of the tides and coastal freshwater input as well as a detailed description of the bathymetry. Another key element to the understanding of the physical oceanography of a given region is its water structure characteristics and seasonality (or variability, more generally) which both influence and represent the dynamics that occur. A good understanding of the hydrographic characteristics and dynamics is essential to the sustainable development and management of aquaculture sites, as they have a key influence on: carrying capacity, fish growth optimization and health, pathogen dispersion and management, seafloor enrichment and other environmental interactions.

Funded by Fisheries and Oceans Canada's (DFO) Program for Aquaculture Regulatory Research (PARR) initiative, an oceanographic monitoring program took place between the years of 2009 and 2013. The program included the collection of Conductivity, Temperature and Depth (CTD), Acoustic Doppler Current Profiler (ADCP) and Drifter data. The results of the CTD measurement program are presented and analysed here.

The specific objectives of this work were to:

- Provide an updated and more comprehensive description of the vertical and horizontal hydrographic structure, highlighting its spatial and temporal variability;
- To identify and enhance the understanding of the areas of water exchange and mixing;
- Provide data and information to initialize and verify a coastal water circulation numerical model currently being implemented by Fisheries and Oceans Canada.

The first two objectives allowed us to delineate 'hydrographic zones' (i.e., zone of common or similar hydrographic characteristics) which may be used to assist with the delineation of BMAs as well as to provide useful information regarding pathogen (e.g., sea lice) development and

mortality. The third objective will allow the model to provide with more robust delineations that will be presented in other publication(s). The report is structured as follow: first, a review of the literature and current knowledge of the area is provided, a description of the instrumentation and methods used for this study is then presented followed by a description of the results and a discussion. A short conclusion with key recommendations is provided at the end of the manuscript.

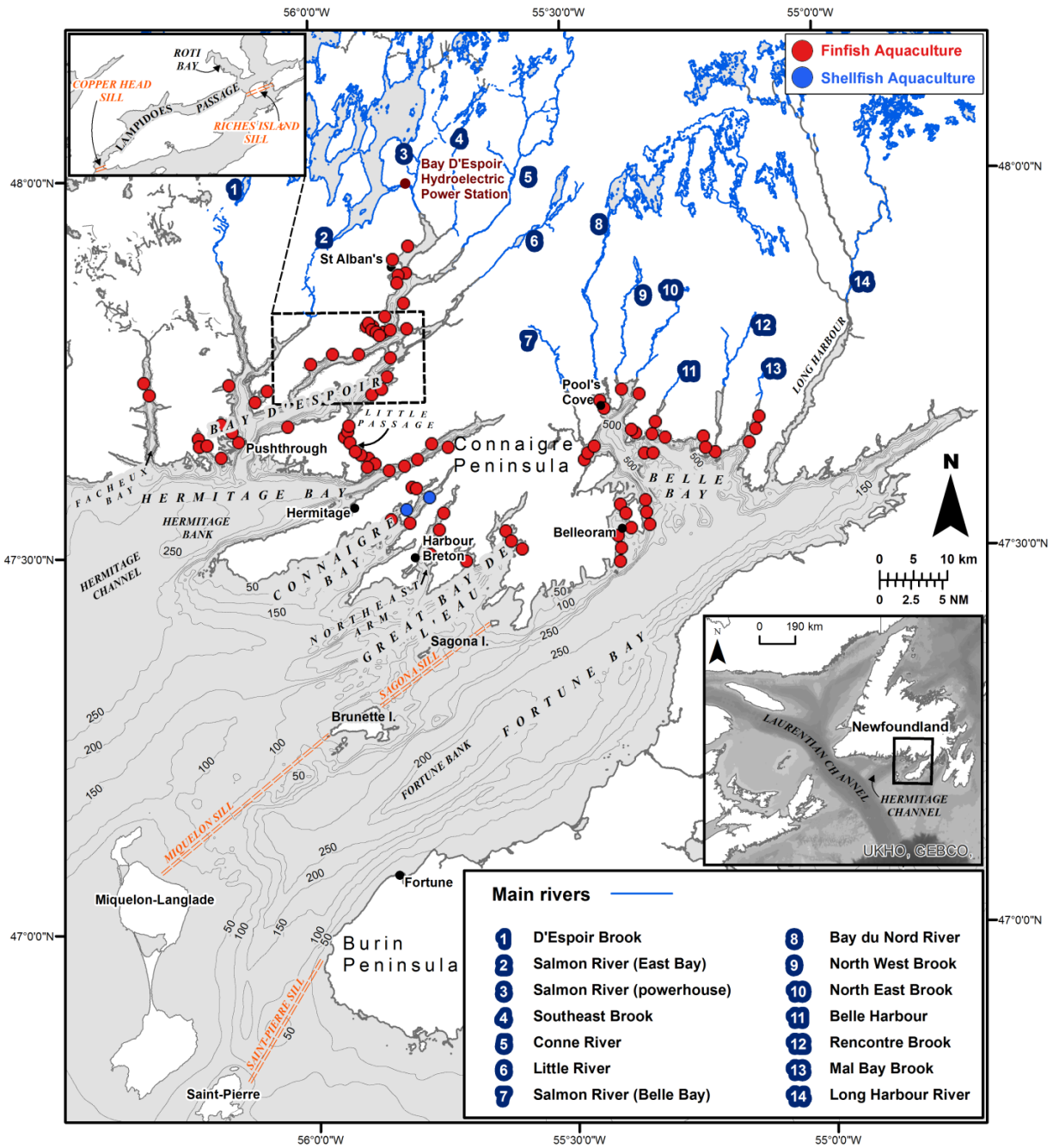


Figure 1: Study Area with the locations of the aquaculture licences (as of November 2015; source: [Department of Fisheries and Aquaculture 2015](#)).

PREVIOUS STUDIES

The horizontal and vertical hydrographic structure have been previously investigated and described by de Young (1983) and Richard and Hay (1984). The de Young (1983) study focused on the Hermitage Channel (HC) up to Hermitage Bay (HB) and Fortune Bay (FB) area, whereas the program of Richard and Hay (1984) dealt with both HB and Bay d'Espoir (BDE) (Figure 1). The oceanographic section described by Richard and Hay (1984) covered part of the Lower BDE section (LBDE) and Lampidoes Passage – Upper BDE section (LaP-UBDE) presented in this report (Figure 6). Publications based on and further work expanding the de Young (1983) thesis study about FB deep water dynamics continued until the mid-1990s (de Young and Hay 1987, Hay and de Young 1989, and White and Hay 1994). Measurements reported by de Young (1983), de Young and Hay (1987) and Hay and de Young (1989) included CTD data collected in June 1981, December 1981, February-March 1982, May 1982, June 1982, July 1982 and November 1982, while White and Hay (1994) reported results from data collected in June 1984 and September 1984. Spring and fall conditions were reported by Richard and Hay (1984) with measurements done in May 1982, November 1982, June 1983, November 1983 and April 1984. Most of those earlier works focused on deep-water renewal processes and provided limited information on the near-surface conditions.

In addition to these regional studies, a comprehensive survey of the Newfoundland South Coast, including the northern arm of BDE and few stations in HB was conducted in August 1982 and reported by Yurick and Vanstone (1983) as part of Parks Canada studies of marine Natural Areas of Canadian Significance (NACS). Temperature and salinity data at few sites in the study area and as far as Placentia and St. Mary's Bay were also reported with an emphasis on winter and summer near-surface conditions in the Marine Science Research Laboratory (MSRL) aquaculture feasibility study of 1980 and in the BDE Development Association (BDE-DA) study of 1984 (also related to aquaculture). Additional surface sampling (bottles, CTD casts and moored instruments) were carried out in BDE by Fisheries and Oceans Canada in the late 90s and early-2000s around aquaculture sites as part of assimilative capacity (Tlusty et al. 1999) and species performance studies (Pepper et al. 2003 and 2004). In addition, stations within the HC and the general winter-spring oceanographic conditions of the Northwest Atlantic Fisheries Organization (NAFO) Subdivision 3Ps area (including the Coast of Bays and Placentia Bay areas and adjacent continental shelf) used to be regularly reported by Fisheries and Oceans Canada in support of the annual Atlantic Cod assessments, the latest one being that of Colbourne and Murphy (2008).

De Young (1983) and Richard and Hay (1984) described the presence of two main water masses in the area: the Labrador Current Water (LCW) mixed with winter cooled water and the Modified Slope Water (MSW; first described by McLellan 1957). The LCW is advected into the region from the Avalon Channel (to the east of St Pierre sill) as part of the inshore branch of the LC; the MSW is typically found over the continental slope and reaches the South Coast through the Laurentian and Hermitage channels. The cold and relatively fresh LCW mixed with winter cooled water ($T < 2^{\circ}\text{C}$; $S = 32-33$) was found from 25 to 175 m while the relatively warm and salty MSW ($T = 4-6^{\circ}\text{C}$; $S = 34.5$) was generally found below 200 m depth. Both water masses (LCW-winter cooled water mix and MSW) were found in HC and in BDE up to Copper Head sill (Figure 1). In the inner basin of BDE (LaP-UBDE), only the LCW-winter cooled water mix was found due to blockage of the deep MSW by the Copper Head and Riches island sills (Figure 1).

Richard and Hay (1984) showed that a decrease of the cold and relatively fresh intermediate water volume (mix LCW-winter cooled water) occurs from spring to fall. They also found that the intermediate layer was colder and fresher in spring and warmer and more saline water in fall. The upper boundary of the warm and saline deep water (MSW) was observed to vary seasonally (by about 50 m), consistent with the seasonal upwelling mechanism described by de

Young (1983) and described further below. Examining the small seasonal changes in temperature (by about 0.5°C) and salinity (by about 0.5 or less) of the deep water, Richard and Hay (1984) also found that annual, and at least partial, renewal of the deep BDE 'outer basin' water (B3 in Figure 7) and bi-annual renewal of the inner basin (B5 and B6 in Figure 7) deep water occur. The renewal of BDE outer basin deep water was further corroborated by the examination of the dissolved oxygen (DO) concentration which showed little differences between the HC and BDE outer basin at depth.

In FB, deep-water renewal of the main basin was shown to occur through two seasonal mechanisms (de Young 1983; de Young and Hay 1987, Hay and de Young 1989). In winter, dense, warm and saline MSW is advected above the Miquelon sill due to upwelling-favorable northwest or northeast winds. During the summer, slightly less dense, cold and relatively fresh LCW flows over the St Pierre sill due to prevailing southwest winds and gradually replace through horizontal advection and associated mixing the dense, warm and saline bottom water. White and Hay (1994) further showed that this summertime renewal involving LCW origin is strongly modulated by the tides as well as other possible mechanisms such as bottom-trapped waves and/or internal seiches. All those processes take place below sill depth (i.e., below about 100 m) and significant mixing involved with those deep water renewals was suggested as evidenced by the very weak stratification observed in FB basin below that depth. Due to this seasonal renewal involving water masses of distinct temperatures, a seasonal horizontal gradient develops within FB below sill depth: colder water at the head and warmer water at the mouth is found in fall-winter while warmer water at the head and colder water at the mouth is found in spring-summer. Although separated from FB basin by a sill of about 209 m maximum depth (S1, Figure 8), the few measurements done in the western deep basin of Belle Bay (BB) indicated that deep-water renewal eventually occurs there also as a result of the water exchanges happening in FB basin (de Young 1983).

At the surface, a clear seasonal cycle was reported in HB and BDE by Richard and Hay (1984): cold and more saline water was found in spring; warmer and fresher water found in fall. Maximum thickness of the surface layer was observed in fall and minimum thickness in spring. Near-surface temperatures as low as about 1.5°C were observed in spring (May 1982) and slightly more than 8°C were observed in fall (November 1983) with some inter-annual variation. Near-surface salinities of about 31 were observed in spring (May 1982) and less than 21 in fall (November 1982). This seasonal cycle seemed counter-intuitive to Richard and Hay (1984) since the freshwater discharge of the BDE generating station, the largest contributor of the region, peaks in winter. Seasonal prevailing wind from the southwest, containing the freshwater surface lens within BDE and freshwater runoff influence in HC from the Gulf of St. Lawrence peaking in late summer were proposed as hypotheses to the fall salinity minimum found in most of the HB-BDE region. Focussing on the near-surface and aquaculture related issues, Tlusty et al. (1999) and Pepper et al. (2003, 2004) reported a surface layer thickness of about 5 m maximum, varying both temporally and spatially along the fjord. A close look at their figures reveal a surface layer of 2-4 m, both in winter (cold, near 0°C , and 0-10 in salinity) and in late spring (about 12°C and 8-30 in salinity) at stations located in LaP-UBDE, Roti Bay, south of Bois Island and in Little Passage. The salinity gradient of their measurements appeared to be as high as about 20/m in winter and about 10/m in summer in UBDE. All along the South Coast in general, and in BDE in particular, Yurick and Vanstone (1983) indicated coherence between the near-surface temperatures and salinities, where lower salinities were found along with warm temperatures. Maximum near-surface temperature along the coast (and outside the fjords) was observed in HB with a value of 16.2°C and was generally higher than 17°C within most fjords, including BDE. The lowest near-surface salinity measured was in HB (less than 29) separated by about 15 km from the highest salinity measured (about 32.5), off Facheux Bay's entrance,

highlighting the existence of a relatively strong front in HB. Within most fjords including BDE, a shallow, low-salinity layer was typically found within the first 5-10 m.

In FB, important seasonality was noted by de Young (1983), who reported near-surface temperature rising from about 5°C in spring (May 1982) to about 11-12°C in summer (July 1982). An indication of winter conditions is also given in his results, with sub-zero temperatures (about -0.5°C) within the upper 100-150 m in February 1982, a severe winter with respect to cooling and wind mixing conditions (de Young 1983). The surface 'mixed-layer' was found warmer and thicker at the head of the bay and colder and thinner towards St. Pierre, an effect attributed to the freshwater input from Belle Bay by de Young (1983).

Examination of the DO concentration generally showed elevated values (about 11 mg/L) within the near-surface and low concentrations (less than 7 mg/L) at depth in the deep outer basin and in HC in early summer (June 1982). Low concentrations (7 mg/L) were also found in the upper part of the bay (LaP-UBDE and Roti Bay) below ice cover in February 1981 and March 1982 in the upper 25 m. Tlustý et al. (1999), however, did not find critically low DO concentration levels during their winter surveys of 1997, reporting values of about 8 mg/L or greater, on average at six aquaculture sites in the upper bay (LaP-UBDE and Roti Bay); within the upper 5 m and at 1 m above the bottom. DO measurements from late spring (June 1982) are also reported by de Young (1983); they indicate that, while near-surface water oxygen concentrations were not fully saturated at the time of sampling (highest measured was about 70%), no areas of anoxia were found in FB. The lowest DO concentration values measured were associated with the influx of MSW whereas LCW was found to carry high levels of DO (greater than 11 mg/L) into the bay. de Young (1983) furthermore found that by the time the deep water reached the head of FB (i.e., the mouth of BB), DO concentration had decrease by about 1.4 mg/L.

MATERIAL AND METHODS

EQUIPMENT

The water temperature, conductivity, oxygen and pressure were measured using Seabird (SBE) CTD (conductivity, temperature, and depth) instruments from which salinity and density were derived. Two main models were used: 25 and 19 plus V2 (Figure 2 and Table 1). Both instruments are medium frequency sampling devices (4 Hz and 8 Hz for the SBE19 and SBE25, respectively) designed to profile at rates of the order of 0.5-1 meter per second. The May 2013 survey used a higher frequency SBE25 (model 25plus, 16 Hz sampling rate). Along with the CTD, the SBE instruments were equipped with a dissolved oxygen (DO) sensor (SBE43 model). A summary of the technical specifications of the instruments and sensors used is presented in Table 1.

Table 1: Instrument specifications.

-	SBE 25 and SBE 25plus	SBE 19plus V2
Conductivity (S/m)	0 – 7 range +/- 0.0003 accuracy ⁽¹⁾ 0.00004 resolution	0 – 9 range +/- 0.0005 accuracy ⁽¹⁾ 0.00005 resolution
Temperature (°C)	-5 to +35 range +/- 0.002 accuracy 0.0003 resolution	-5 to +35 range +/- 0.005 accuracy 0.0001 resolution
Pressure (dbar)	0 – 600/1000 range ⁽²⁾ +/- 0.1% ⁽³⁾ accuracy 0.002% ⁽³⁾ resolution	0 – 600 range +/- 0.1% ⁽³⁾ accuracy 0.002% ⁽³⁾ resolution
Disolved Oxygen	0-120% ⁽⁴⁾ range 2% ⁽⁵⁾ accuracy	0-120% ⁽⁴⁾ range 2% ⁽⁵⁾ accuracy

1. Over calibration range (about 0 to 6 S/m); goes down to about 0.001 S/m outside calibration range
2. varying between instruments used
3. full scale range; most of the instruments used were rated to 870 psi range (~600 dbar)
4. % of surface saturation
5. % of saturation

FIELD WORK

Typical CTD field work consists of lowering the instrumentation package (usually mounted in a cage or rosette) from the side of the vessel (port or starboard) using a winch and a block (Figure 2). Data recording can either be done internally and/or on board when using a deck unit (i.e., computer allowing real time communication with the instrument and data visualisation). All data presented here were collected in 'self-contain mode' (i.e., autonomous) with no deck unit and extracted directly from the instrument internal memory. In addition to the CTD casts, other tasks such as bottle sampling, drop video camera, ADCP mooring deployments, drifter deployments, plankton net sampling, etc. also took place. The results of the data collected from those other tasks will be presented in subsequent reports.

760 CTD profiles were collected from June 2009 to November 2013 in 11 surveys, accounting for a total of 52 days at sea (Table 2 and

Figure 3). Some duplicate profiles were collected for quality control (QC) purposes and 276 sites were sampled overall, resulting in a given station surveyed an average of just less than 3 times during the 5 years measurement period. However, some stations were sampled as many as 6 times and other stations were sampled only once. Major surveys in June 2009, April 2010, May 2011, May 2012 and May 2013 were performed using Canadian Coast Guard Research Vessels (CCGS Shamook from 2009 to 2011, CCGS Vladykov in 2013); smaller scale surveys such as September 2012 or more inshore surveys such as September 2009 were carried out using a 25' Rosborough type boat. Sampling times were recorded in standard Universal Time Coordinated (UTC). Instruments were synchronized using the field computer's clock and adjusted to UTC using a Global Positioning System device (GPS). Position of the casts were recorded using on-board GPS as World Geodetic System 1984 (WGS84) coordinates.



Figure 2: Instrumentation.

The area of study is roughly delimited from 47 to 48°N and 54.5 to 56.5°W (Figure 1). Spatial coverage varied from survey to survey and year to year (Figure 4 and Figure 5). While most of the stations were about 3 km apart, spatial resolution was generally higher along the cross-channel sections. Typically, the area of interest (i.e., Coast of Bays) could not be sampled as a whole for a given survey and the Hermitage Bay (HB) - Bay d'Espoir(BDE) and Fortune Bay (FB) - Belle Bay (BB) regions were never sampled together. The HB-BDE region was the focus of the sampling during the first two years of the program (2009 and 2010) whereas the Connaigre Peninsula (CP) region, which include Connaigre Bay (CB), Harbour Breton - Northeast Arm (HB-NA) and Great Bay de l'Eau (GBDE), was sampled more frequently the later years of the program (from 2012). FB-BB region was the least visited region of all with sampling only in May and July 2011 (

Figure 3).

Overall, the measurements were mainly carried out in spring (April-May) and early to late summer (June-September). The last survey of the program was executed in fall (November 2013). A common classification for Atlantic Canada has: January-March as winter months, April-June as spring months, July-September as summer months and October-December as fall months such as defined in Petrie et al.' climatology studies (1996a and 1996b). In the context of this report, June 2009 is considered as a summer month since the survey occurred late in the month (18-23). Similarly, data collected in April 2010, May 2011, May 2012 and May 2013 shall be considered comparable in terms of seasonal timing since the 2010 data was collected at the end of April – early May and the 2011, 2012 and 2013 data was collected in the first days of the month of May.

Table 2: Data collection summary.

Field work date and vessel	Instrument	Total # of casts	# stations HB - BDE	# stations FB - BB	# stations CP	# days survey
18-23 June 2009 CCGS Shamook	SBE25	128	106	0	0	6
21-26 September 2009 Rosborough	SBE25	47	46	0	0	4
28 April – 03 May 2010 CCGS Shamook	SBE25 SBE19plusV2	103	98	0	0	6
15-16 July 2010 Rosborough	SBE19plusV2	16	0	0	15	2
04-09 May 2011 CCGS Shamook	SBE19plusV2	70	0	39	14	6
03-05 July 2011 Rosborough	SBE19plusV2	13	0	13	0	3
04-07 May 2012 CCGS Shamook	SBE19plusV2	89	22	0	51	5
14-17 July 2012 Rosborough	SBE19plusV2	5	0	0	5	3
22-24 September 2012 Rosborough	SBE19plusV2	8	7	0	0	3
03-09 May 2013 CCGS Vladykov	SBE25 SBE25plus	103	20	0	61	7
03-09 November 2013 CCGS Vladykov	SBE25 SBE25plus SBE19plusV2	178	58	0	36	7

CTD Gantt Chart - All Seabird Data 2009-2013

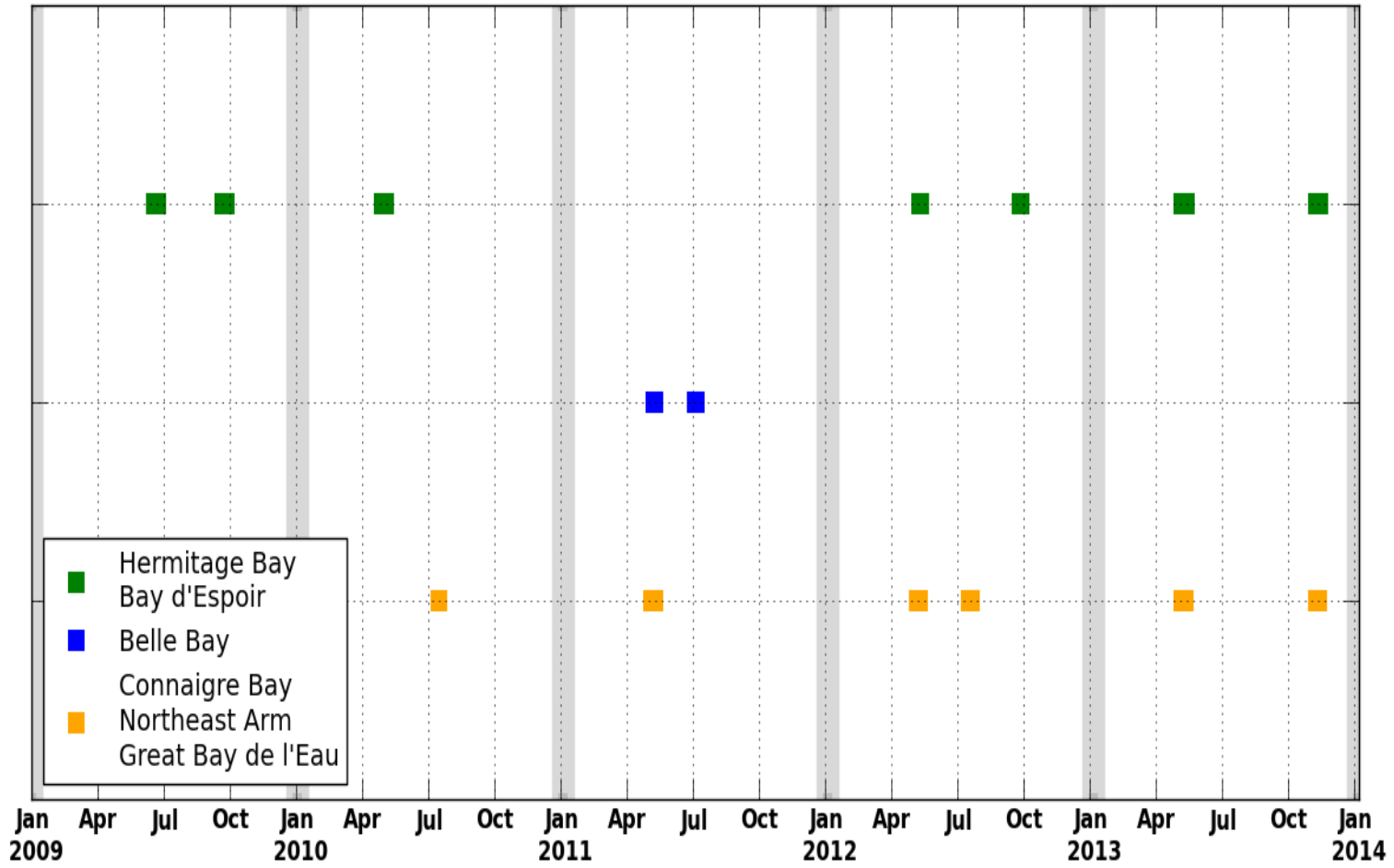


Figure 3: CTD data collection temporal resolution.

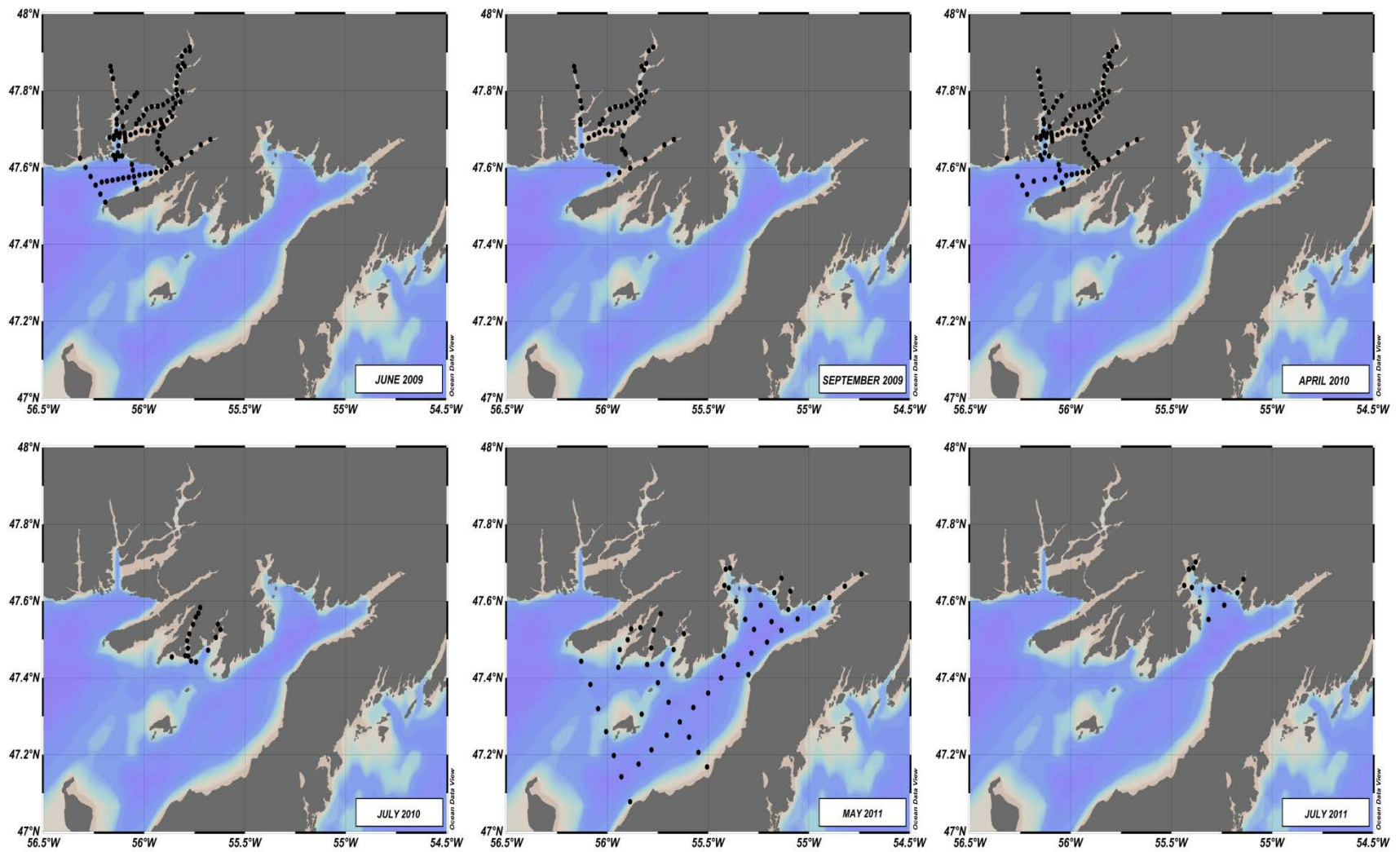


Figure 4: CTD data collection program, casts (black dots) spatial coverage from June 2009 to July 2011.

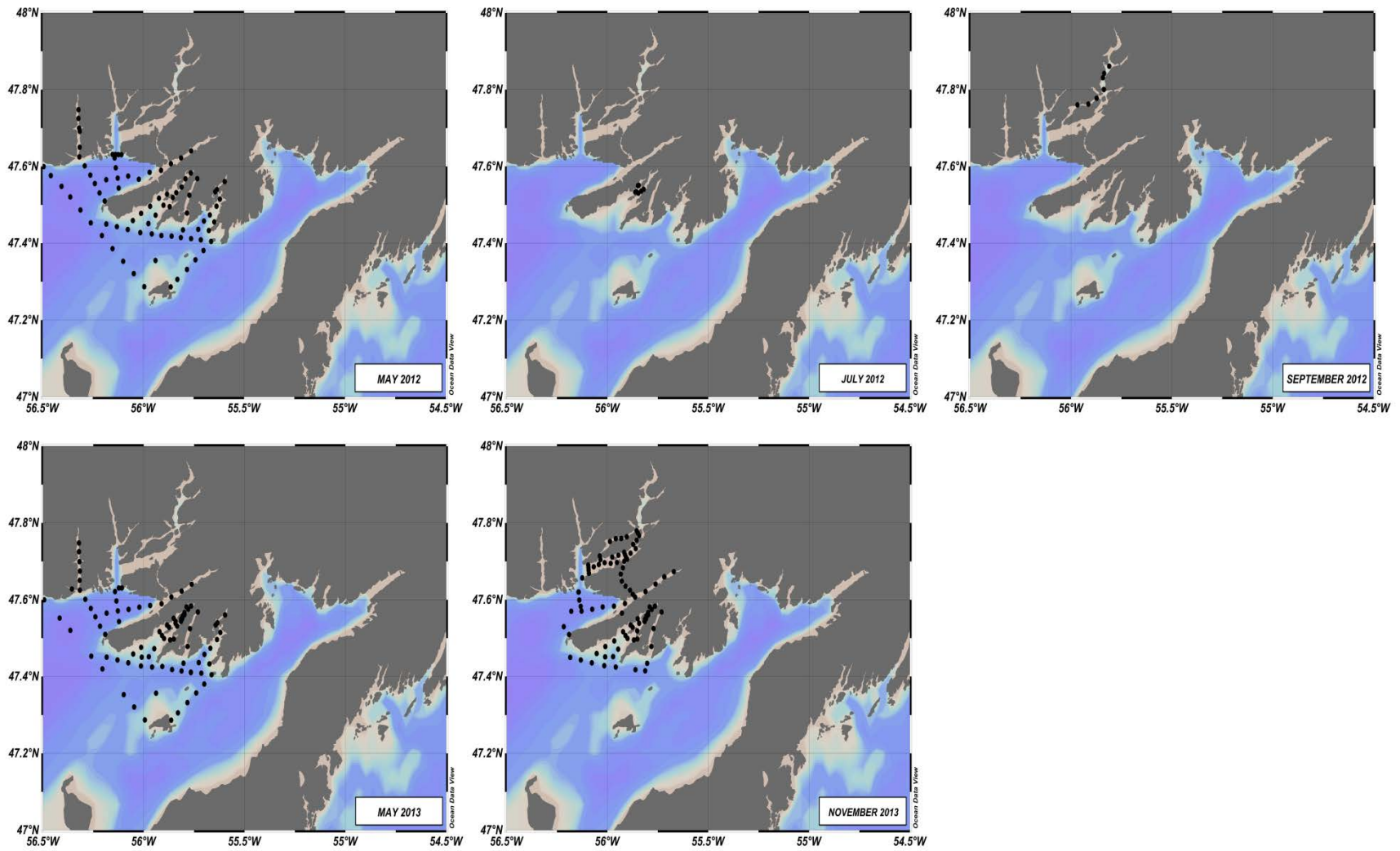


Figure 5: CTD data collection program, casts (black dots) spatial coverage from May 2012 to September 2013.

DATA PROCESSING AND QUALITY ASSURANCE / QUALITY CONTROL (QA/QC)

Data processing and QA/QC followed SBE recommended procedures and consisted of seven steps (Appendix D).

Data were first converted from raw binary form (typically voltages and frequencies) to ASCII data as engineering units and then went through a series of filters to account for sensors response times, thermal lag and spikes. To correct the surface data noise due to the sensors acclimation (i.e., soak time), which are common to CTD measurements, a special filter was developed 'in-house' in order to extract good data as close as possible to the surface. An illustration of the results of this filter is presented in Appendix D (Figure D1). Overall, the filter worked very well and allowed the extraction of data as close as 1 or 2 m to the surface, corresponding to the average 'soak depth'. Due to the physical size of the instrumentation, which is about 1 m in height, boat size and CTD winch setup and to frequent unfavourable sea-state, the closest measurement from the surface was 2 m for the most part.

Filtered data were then vertically averaged into regularly spaced bins (1 m) which allows easier data handling and profile comparisons (Thomson and Emery 2014).

Numerous duplicates were taken during the surveys and cross-comparisons between the instruments were conducted at the NAFC facilities (i.e., tank tests). The CTD used for this study were also all sent back to the manufacturer for calibration in March 2012. Results of the cross-comparisons done in the lab over the course of a year between November 2013 and 2014 indicated uncertainty between the instruments of about 0.005°C, 0.004 for salinity, 0.1 dbar and 0.12 mg/L for DO (about 1% saturation). Based on factory calibrations, drifts of about 0.0003°C, 0.003 in Salinity, 0.03 dbar and 0.18 mg/L in DO (less than 1.5% saturation) per year were found. Both results indicate that the instruments performed well and within specifications and qualitative check on surveys' duplicates did not indicate differently.

DATA VISUALISATION AND ANALYSES

Processed data were graphically represented using the Ocean Data View (ODV) software (Schlitzer 2015). Prior to being imported into and displayed by ODV, all the files from a given instrument of a given survey were merged into one file. Bathymetry data of the study area (Donnet et al. 2017) were also imported to ODV as a gridded file and as section-specific files. Sections of interest were first digitalised to follow the main channels as closely as possible using ArcGIS prior to be imported (as points of latitude, longitude and depth). The results of this digitalisation are also presented in Donnet et al. (2017).

As interpolating data is never without trade-off (e.g., balance between loss of small scale features and need for filling gaps), an effort was made on adjusting the interpolation scheme to yield to the best results. The Data Interpolating Variational Analysis (DIVA) gridding method (Troupin et al. 2012) was chosen. The complex bathymetry and coastline of the area were considered for the interpolation (i.e., used as boundaries) and the interpolation aimed to respect the following key criteria: vertical resolution of 1 m was to be kept and horizontal interpolation was not to span over distances much larger than the average distance between stations (about 3 km).

Based on their geographical characteristics (Donnet et al. 2017), the study area was divided in three regions: HB-BDE, FB-BB and CP (CB, HB-NA and GBDE). For each region, two types of plots were produced: vertical sections and property maps. For each section, statistics of water masses were also produced. Results (plots and tables) of the HB - BDE region, FB - BB region and CP region are presented in separate Appendices (A, B and C, respectively) corresponding to the three regions; these are described below in separate sections. For each region, the water

horizontal and vertical structure as well as seasonality and inter-annual variability are described with an emphasis on the near-surface region (0-20 m depth).

Vertical sections are presented along selected key transect. Transect generally run along the main channels as described in Donnet et al. (2017) and as shown in Figure 6. Two main set of plots are provided for each transect: one presenting the full depth and a second one for 0-20 m. The latter allows a more detailed presentation of the near-surface layer structure and is directly relevant to fish farming activities which typically use 15-20 m height fish cages in our study area. Property maps at fixed depths were created to illustrate the spatial hydrographic variability and near-bottom conditions within the domain studied. Based on previously collected information of the study area summarized above and relevance to fish farming activities (cage heights and near-bottom information for benthic habitat studies), five depths were selected for property maps display: surface (2 m), 20 m, 75 m, 250 m and near-bottom. Due to the geographical variation of the deep water layer, the 250 m depth maps were not created for the FB-BB and CP region. The near-bottom maps were created using the deepest data from each cast, which generally was a few meters above the bottom except in areas deeper than 600 m which was the operational limit of most of the instruments used.

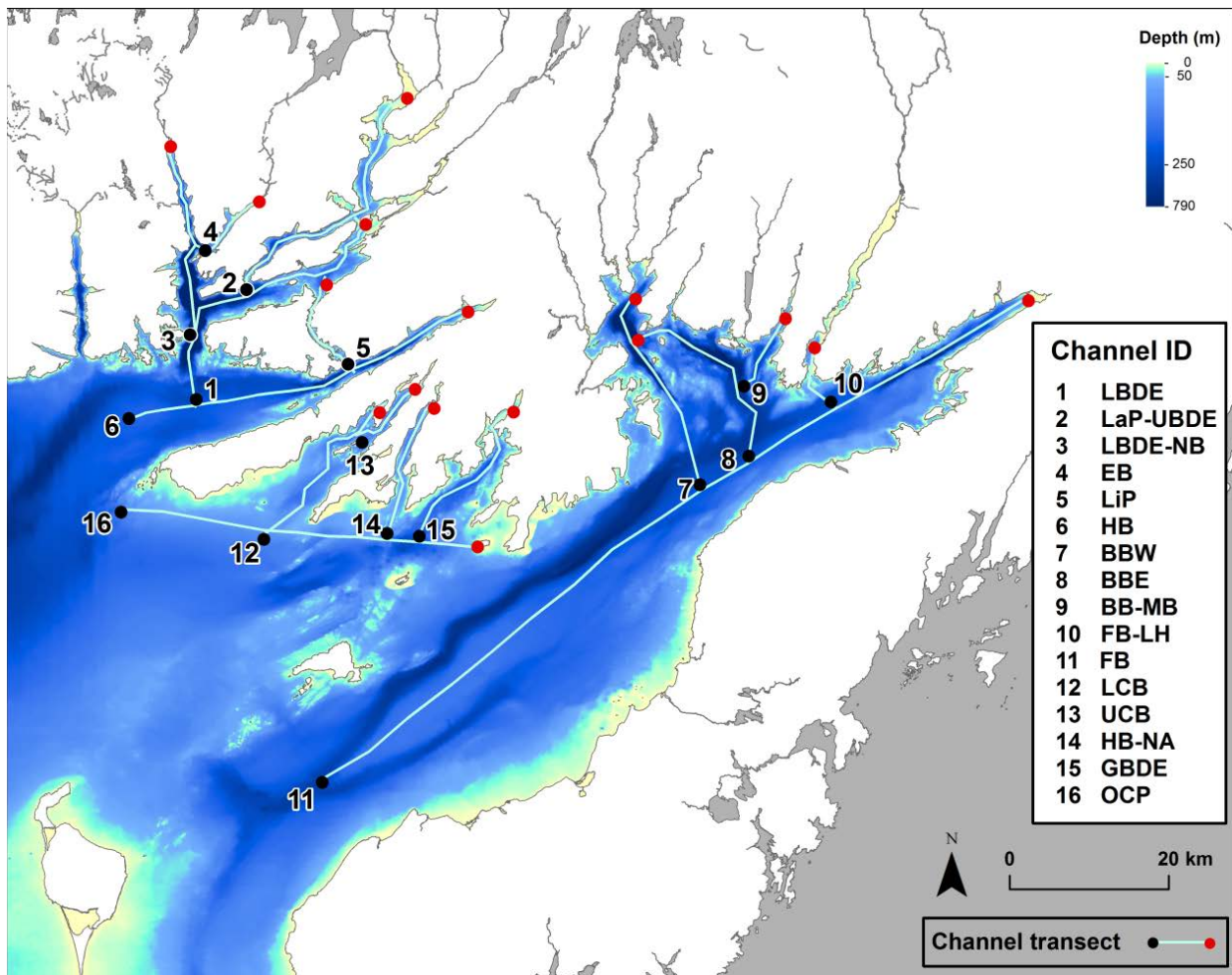


Figure 6: Key along channel transects.

Vertical sections and property maps consist of five subplots representing temperature ($^{\circ}\text{C}$), salinity, potential density anomaly (kg/m^3), oxygen concentration (mg/L) and oxygen saturation

(%) at atmospheric pressure. A sixth subplot shows the stations used for the interpolation on a map. Color scales and isoline scales were kept the same for all plots to allow easier comparisons among seasons, transects and regions except for the salinity plots due to very different freshwater conditions existing from one region to another (Donnet et al. 2007). The temperature scale ranges from 0°C to 15°C with isolines every 1°C; the salinity scale ranges from 0 to 35 for HB-BDE, 25 to 35 for FB-BB and from 30 to 35 for CP with isolines every 0.5 (vertical sections) or 1 (property maps and 0-20 m BDE sections); the potential density anomaly scale ranges from 15 kg/m³ to 30 kg/m³ with isolines every 0.5 kg/m³ (vertical sections) or 1 kg/m³ (property maps and 0-20 m BDE sections); dissolved oxygen concentration scale ranges from 6 mg/L (hypoxic conditions upper limit for salmon) to 12 mg/L with isolines every 0.5 mg/L; oxygen saturation scale ranges from 50% to 100% with isolines every 5%.

On the vertical sections plots, CTD stations are represented by small black dotted lines and main section distances are annotated on the companion map. On the property maps, CTD stations are represented by small black dots. Each individual plot was checked visually to ensure realistic interpolation results. When data were too scarce and interpolation resulted in an under or over estimation (i.e., interpolated values significantly different from adjacent measurements), a polygon was created and used as a mask.

Salinity was derived using the UNESCO algorithms (Fofonoff and Millard 1983) and is thus expressed without units. The potential density anomaly was calculated using ODV built-in algorithms and represents pure freshwater (1,000 kg/m³) density subtracted from the potential density calculated using the TEOS-10 functions (IOC 2010) and at atmospheric pressure. It represents the density that the water would be if brought at the surface adiabatically and it allows a more direct understanding of the water masses dynamics. The DO concentration and saturation were calculated based on Owens and Millard (1985) and Garcia and Gordon (1992) algorithms and using the SBE data processing software (Appendix D). DO concentration is presented here in units of mg/L, a unit commonly used in aquaculture science. DO percent saturation is calculated based on saturation at atmospheric pressure; that is the theoretical value the water parcel of a given temperature and salinity would have at the sea-surface.

As companion to the vertical sections plots, summary tables providing statistics of the water masses of each section were produced. In those tables, the following parameters were calculated for up to three layers (surface, intermediate and deep):

- T_min: minimum Temperature (°C), minimum Temperature gradient (°C/m) or minimum Thermocline depth (m)
- T_max: maximum Temperature (°C), maximum Temperature gradient (°C/m) or maximum Thermocline depth (m)
- T_mean: mean Temperature (°C), mean Temperature gradient (°C m) or mean Thermocline depth (m)
- S_min: minimum Salinity, minimum Salinity gradient (/m) or minimum Halocline depth (m)
- S_max: maximum Salinity, maximum Salinity gradient (/m) or maximum Halocline depth (m)
- S_mean: mean Salinity, mean Salinity gradient (/m) or mean Halocline depth (m)
- DO_min: minimum DO concentration (mg/L), minimum DO gradient (mg/l) or minimum oxycline depth (m)
- DO_max: maximum DO concentration (mg/L), maximum DO gradient (mg/l) or maximum oxycline depth (m)

-
- DO_mean: mean DO concentration (mg/L), mean DO gradient (mg/l) or mean oxycline depth (m)
 - ST_min: minimum potential density anomaly (kg/m^3), minimum potential density anomaly gradient ($\text{kg/m}^3/\text{m}$) or minimum pycnocline depth (m)
 - ST_max: maximum potential density anomaly (kg/m^3), maximum potential density anomaly gradient ($\text{kg/m}^3/\text{m}$) or maximum pycnocline depth (m)
 - ST_mean: mean potential density anomaly (kg/m^3), mean potential density anomaly gradient ($\text{kg/m}^3/\text{m}$) or mean pycnocline depth (m)
 - 2°C_D: mean depths of the 2°C isotherm (upper and lower boundary), (m)
 - Dz: thickness of the intermediate layer based on the 2°C isotherm mean depths (m)
 - 5°C_D: depth of the 5°C isotherm below 100 m depth (m)

Thermocline, halocline, oxycline and pycnocline depths were calculated as the depth of maximum temperature, salinity, DO and potential density anomaly gradient within the upper 0-100 m depth, respectively. The surface layer is defined as the upper 0-20 m, the intermediate layer as bounded by the 2°C isotherm and the deep layer as bounded by the 5°C, below 100 m depth. The definitions of the intermediate (commonly referred to as the Cold Intermediate Layer (CIL) in the literature; e.g., Colbourne et al. 2015) and deep layer were based on the results of the previous studies done in the study area and summarised above.

RESULTS

HERMITAGE BAY – BAY D’ESPOIR(HB-BDE)

Geography

The HB-BDE region is divided in sections as follows (Figure 6 and Figure 7): Hermitage Bay (HB, 6 in Figure 6), Lower Bay d’Espoir(LBDE, 1 in Figure 6), Lampidoes Passage – Upper Bay d’Espoir (LaP-UBDE, 2 in Figure 6), Lower Bay d’Espoir–North Bay (LBDE-NB, 3 in Figure 6), East Bay (EB, 4 in Figure 6) and Little Passage (LiP, 5 in Figure 6), with total lengths of about 46 km, 39 km, 38 km, 25 km, 11 km and 16 km respectively. The bathymetry of the region with its main basins and sills described in Donnet et al. (2017) is reproduced as Figure 7. Interpolated profiles of the full water column and surface layer (0-20 m depth) are presented in Appendix A(i), sorted in the order listed above (HB, LBDE, LaP-UBDE, LBDE-NB, EB and LiP) and chronologically for each section. Corresponding summary tables are presented in Appendix A(ii). Interpolated property maps are presented in Appendix A(iii), sorted in chronological order and from shallow (surface, 2 m depth) to deep (near-bottom).

For this region, the term “outer basin” will be used to refer to the basin B3 (Figure 7), while the term “inner basin” will be used to refer to the basins B4, B5-B7, B10 and B11, depending of the context. In HB, the term “outer” and “inner” refers to the part of the bay located to the west (B1) and to the east (B2) of sill S1, respectively.

HB, itself the inner end of the larger feature HC (Figure 1), is a fairly large bay, about 17 km across from the tip of the CP to Facheux Bay, greatly narrowing eastward to an inner part less than 2 km wide, about 25 km long and about 464 m maximum depth. The inner part of HB is separated from the outer part by a sill (S1 in Figure 7) of about 303 m maximum depth. The bay also consists of a deep channel to the north, the inner end of the HC, and a shallower area to south, referred in this report as Hermitage Bank (Figure 1). BDE is a fairly long and narrow fjord

consisting of two main arms and numerous smaller features. Its maximum length is about 30 km northward and 50 km eastward and it is about 2 km wide on average (Donnet et al. 2017). BDE is separated from HB by a sill of about 291 m maximum depth at its largest entrance (S2 in Figure 7) and by a sill of about 109 m maximum depth at its narrowest entrance, Little Passage, (S10 in Figure 7). 10 main basins and 11 main sills were identified in the HB-BDE region by Donnet et al. (2017) (Figure 7). The maximum depth of 792 m is found in the BDE outer basin (B3 in Figure 7) while the shallowest basin, with a maximum depth of 59 m, is found in the upper, northeast, part of the bay (B7 in Figure 7). Three basins are within a depth range of 150-200 m (B6, B9 and B10 in Figure 7), two basins within 250-300 m depth range (B4 and B5 in Figure 7), two basins within 350-400 m depth range (B1 and B8 in Figure 7) and two basins are more than 400 m deep (B2 and B3 in Figure 7).

The HB-BDE region is subject to significant freshwater runoff, particularly in BDE where a major power generation plant (604 MW, [NL Hydro 2017](#)) is operating. The annual average freshwater discharge rate in BDE is about 252 m³/s (Donnet et al. 2017). The lowest average discharge of about 183 m³/s occurs in August; the largest discharge is found in April with an average rate of 332 m³/s. The BDE power generation plant accounts for about 75% of the total freshwater discharge going into the bay but the natural rivers discharge of the area are large in spring, leading to a discharge peak in April although the power generation discharge peaks in February (Donnet et al. 2017).

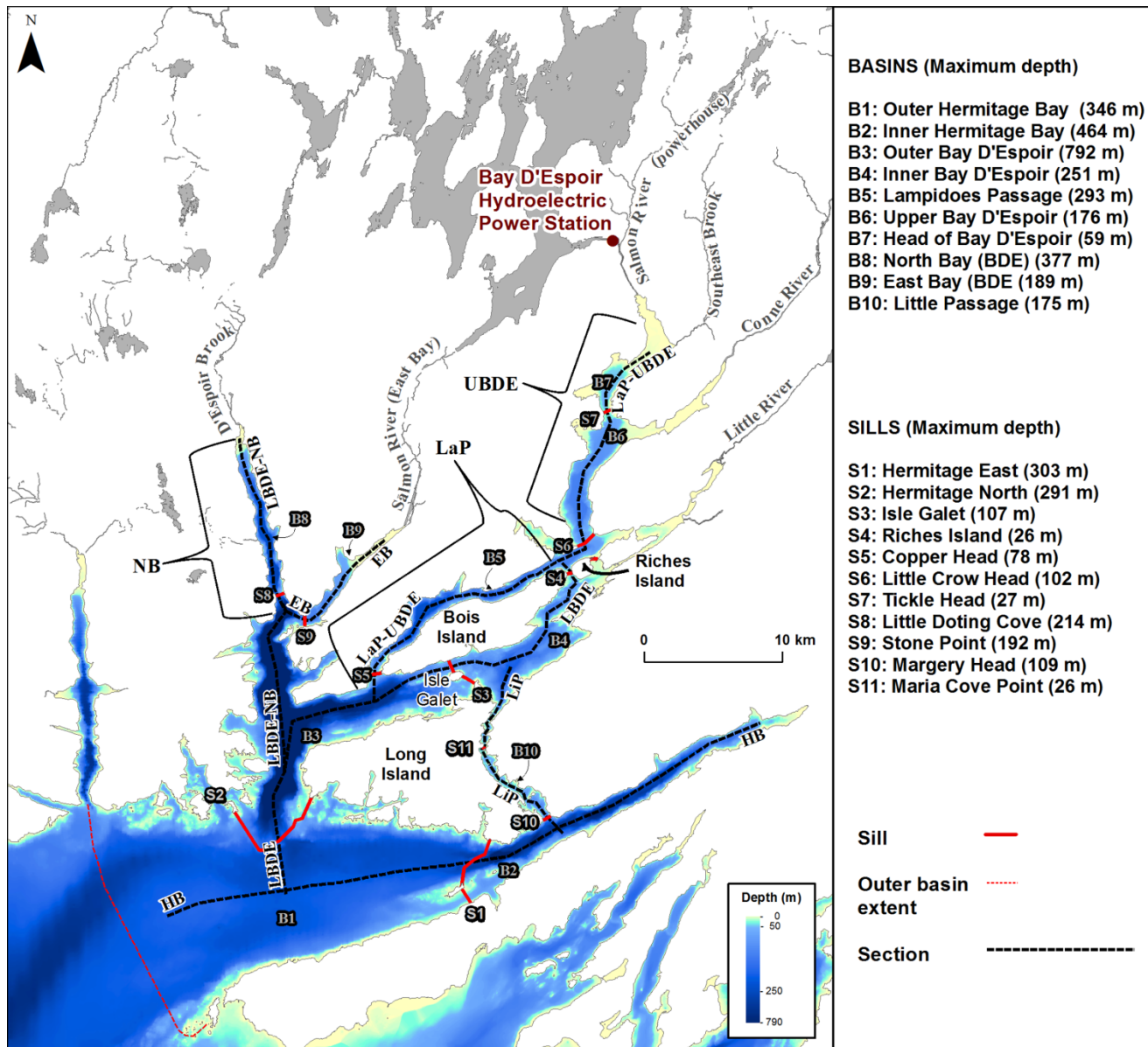


Figure 7: Basins and sills of the Hermitage Bay – Bay d'Espoir (HB-BDE) region.

Near-surface layer (0-20 m)

Freshwater input from the northeast head of BDE (power generation plant) is evident from all of the surveys of the LaP-UBDE section (June 2009, September 2009, April-May 2010 and November 2013) and is a dominant feature of the region (Figure A(i)26, Figure A(i)28, Figure A(i)30, Figure A(i)34 and Figure A(iii)1, Figure A(iii)6, Figure A(iii)10, Figure A(iii)29). The freshwater lens appears uneven, however: patches of low salinity water (less than 15) are separated by smaller areas of higher salinity (22-25). This pattern was best seen in June 2009 (Figure A(iii)1) and April-May 2010 (Figure A(iii)10) but appeared also in September 2009 (Figure A(iii)6). An area of higher salinity was located in the upper part of the bay, at the Conne River inlet mouth (Figure 7, km 30 on LaP-UBDE section), downstream from Tickle Head sill (S7 in Figure 7, km 32 on LaP-UBDE section), in June 2009 (Figure A(iii)1), September 2009 (Figure A(iii)6) and April-May 2010 (Figure A(iii)10); indicating a persistence of the pattern. An area of higher salinity near the head of bay, in B7, was also present in September 2009 (Figure A(iii)6) and in April-May 2010 (Figure A(iii)10) and another to the North of Richies Island, downstream from Little Crow Head sill (S6 in Figure 7, km 20 on LaP-UBDE section) was present in April-May 2010 (Figure A(iii)10). Surface temperatures appear coherent with the salinity and decrease in areas of higher salinity. All these areas seem located near places of flow constriction (presence of a sill and lateral restriction of the channel) and where vertical mixing processes are more likely to take place because of stronger currents. As a result of mixing, the near-surface salinity increase notably from the head of the bay with values near 0-5 downstream to the LaP (B5 in Figure 7, km 3-20 on LaP-UBDE section) where it reaches values around 15-20 in all surveys (Figure A(i)26, Figure A(i)28, Figure A(i)30, Figure A(i)32 and Figure A(i)34). In September 2009 another process yielding to higher salinities in UBDE occurred. This time, the entire UBDE and inner HB featured lower temperatures and higher surface salinities (Figure A(iii)6). Considering the spatial scale of the features and the structures seen in the corresponding vertical section plots (see Figure A(i)3 and Figure A(i)28) which display isotherms and isohalines sloping upward toward the head, it appears that the region was subject to upwelling. However, since the sampling of the stations capturing the upwelling zone were sampled about five days after the other stations of the area, the full spatial extent of this event was not captured and neither was its duration. Relatively strong upwelling favorable winds from the North (about 50 km/h or about 14 m/s) were blowing in the area just before and during UBDE and HB sampling (September 26, Figure E1). It is also worth noting that the isotherms were consistently slanted in all but the November 2013 surface layer (0-20 m) vertical section plots of LaP-UBDE (Figure A(i)26, Figure A(i)28, Figure A(i)30 and Figure A(i)32: colder water is found towards and within UBDE for almost any given depth between 0 and 20 m) which may be the result of estuarine circulation (e.g., see Figure 2.8 in Dyer 1997).

In general, the surface flow originating from the northeastern head of BDE appears to be mainly directed towards and going through the LaP as best illustrated by the surface property maps of June 2009 and April-May 2010 (Figure A(iii)1 and Figure A(iii)10). However, the conditions seen in both September 2009 and November 2013 when a substantial area of low salinity water was measured south of Richies Island (S4 in Figure 7) and down to the inner basin south of Bois Island (B4 in Figure 7), indicate that a surface flow may come through that gate as well from time to time; perhaps more frequently or strongly in the fall (Figure A(iii)6 and Figure A(iii)29; Figure A(i)16 and Figure A(i)24). To the south of Copper Head sill (S5 in Figure 7), towards BDE outer basin, surface salinity increases markedly and generally present an horizontal gradient with increasing values towards the mouth of the bay (Figure A(iii)1, Figure A(iii)6 and Figure A(iii)10). The persistence of this feature suggests that significant mixing of the brackish surface layer occurs at S5 prior being exported towards HB. The flow pattern south of Bois Island is more difficult to deduce. Near-surface and surface gradients of September 2009 (Figure A(i)16 and Figure A(iii)6), April-May 2010 (Figure A(i)18 and Figure A(iii)10) and

November 2013 (Figure A(i)24 and Figure A(iii)29) indicate a downward flow from the Richie's Island towards the outer basin B3. In both September 2009 (Figure A(iii)6) and November 2013 (Figure A(iii)29), similar surface salinities were found in front of and behind Richies Island sill (S4), indicating a lack of vertical mixing at S4 (or weaker than the one occurring at Copper Head sill, S5). A close look at the LBDE 0-20 m vertical section plots of September 2009 and November 2013 (Figure A(i)16 and Figure A(i)24), however, points out that some mixing occurred at the bottom of the halocline (i.e., below about 5 m depth around km 35-40 on LBDE section; best seen in September 2009, Figure A(i)16). Vertical mixing appears also in the April-May 2010 LBDE vertical section plots (Figure A(i)18) and the surface salinity gradient (Figure A(iii)10) from the north of Richies Island to the South is more pronounced. A cross-channel gradient is evident in B4 and the brackish water flow appears restrained along Bois Island (Figure A(iii)10). In June 2009, the surface horizontal field was much more complex in this area and presented strong gradients (Figure A(iii)1). As in April-May 2010 (Figure A(iii)10), the surface cross-channel gradient in B4 of June 2009 (Figure A(iii)1) indicates a downward flow along Bois Island's southern shore but ends with a single low salinity value (about 20 at 2 m depth) east of Isle Galet. Since all the CTD casts west of this later point were taken about two days after (June 23 vs. June 21), it is difficult to differentiate the temporal and spatial aspects of this apparent anomaly. Below this surface level (2 m), the water column was more horizontally homogenous in salinity (around km 25 on LBDE section, Figure A(i)14). Possibly, a local runoff from Bois Island may have been the origin of this low value. On the eastern shore of B4, substantially larger salinity and lower temperature were observed near the coast (about 6°C and 30 in salinity, respectively; Figure A(iii)1), resulting in a surface horizontal gradient of the order of 4°C and 7 in salinity from the main channel; that is within a couple of kilometers. CTD casts were taken the same day in this area, at about 3 hours interval, therefore precluding significant temporal aliasing. Given the coherence in temperature and salinity, this feature may have been due to a local upwelling induced by winds from the east-northeast quadrant. Wind data from Sagona Island (Appendix E) support this hypothesis with blowing wind from east-northeast just before and during sampling of this area (21-23 June, Figure E1).

The other sources of freshwater in BDE and HB, although of much less importance with regard to their discharge rate compared to the power generation plant (Donnet et al. 2017), are also visible from the salinity distribution. Thus, a clear horizontal gradient in salinity could be seen in inner HB, NB and EB and where decreasing salinities were seen towards the head in June 2009 (Figure A(i)2, Figure A(i)36 and Figure A(i)42), September 2009 (NB only, Figure A(i)38), April-May 2010 (NB only, Figure A(i)40) and November 2013 (inner HB only, Figure A(i)12). The extent of the continuous brackish water core coming from the head ($S < 25$ for NB and EB; $S < 30$ for inner HB) was the largest in June 2009 and the smallest in April-May 2010 in all sections. An apparent isolated cell of low salinity water was located around km 5 of the LBDE-NB section in June 2009 (Figure A(i)36). This cell corresponded to an area of low salinity observed along B3 northern cross-channel section (Figure A(iii)1) which was surveyed about two days later than stations located to the north in NB (Figure 7) and to the south toward BDE' entrance. As a result and similarly to the patch to the east of Isle Galet described above (LBDE section of June 2009, Figure A(i)14), it is unclear whether this cell in LBDE-NB was locally generated by river runoff or advected from the eastern arm. In HB, the brackish ($S < 30$) water core extent of November 2013 (Figure A(i)12) was slightly shorter but more vertically mixed than the June 2009 conditions (Figure A(i)2). Of all the spring surveys executed in HB (April-May 2010, May 2012 and May 2013), May 2012 was the freshest and April-May 2010 the most saline with a difference of almost 0.8 between the surface means of the two years (Figure A(i)6, Figure A(i)8, Figure A(i)10 and Table A(ii)1).

In Little Passage, increasing surface salinities were found from the north-end to the south-end during all the surveys done for this section (Figure A(i)46, Figure A(i)48, Figure A(i)50 and

Figure A(i)52), suggesting inflow of the brackish water from B4 towards inner HB (i.e., southward flow). Higher near-surface salinities and weaker stratification were systematically found to the south of Maria Cove Point sill (S11; km 9 on LiP section), suggesting that mixing processes occurs at this location. Given the very restricted width of the channel at this location (down to about 150 m) and the shallow depth (about 28 m maximum depth), both vertical and lateral mixing processes could be expected. A clear evidence of vertical mixing can be seen in the November 2013 0-20 m vertical section plots (Figure A(i)52). Overall, the largest inflow of brackish water appeared in September 2009 (Figure A(i)48) and the smallest inflow in April-May 2010 (Figure A(i)50), consistent with the conditions seen in the LBDE section.

The outer basin of BDE (B3 in Figure 7) appears as a transitory area where surface water from the upper bay branches (LaP-UBDE, LBDE, NB and EB) meet and spill towards HB. The area presents significant surface gradients of temperature and salinity both horizontally and vertically (about 1-2°C/km horizontally at 2 m depth and 0.5-5°C/m in the thermocline; 1-2/km horizontally at 2 m depth and 2-5/m in salinity in the halocline) as seen in June 2009, September 2009, April-May 2010 and November 2013 LBDE 0-20 m vertical section plots (Figure A(i)14, Figure A(i)16, Figure A(i)18 and Figure A(i)24) and in the surface (2 m) property maps (Figure A(iii)1, Figure A(iii)6, Figure A(iii)10 and Figure A(iii)29). In general, near-surface temperatures observed in this area were coherent with the areas of lower salinity. This can be seen in the June 2009, September 2009, April-May 2010 and November 2013 surface (2 m) property maps (Figure A(iii)1, Figure A(iii)6, Figure A(iii)10 and Figure A(iii)29).

Overall (Appendix A(ii)), the lowest near-surface salinities of the region were observed in UBDE, at the head of the northeastern arm, in June 2009 with a value of about 2.2 but the surface layer (0-20 m depth) of the LaP-UBDE section was generally fresher, on average, in September 2012 with a mean salinity of about 26.9 (Table A(ii)3). In all the other sections, except EB, the freshest conditions were seen in either September 2009 or November 2013. In EB, the averaged lowest salinity of the surface layer was seen in June 2009 (Table A(ii)5) but this section was not surveyed in fall which would probably have shown lower salinities in that later season as well, considering the seasonal pattern of the other sections. For the range of temperature and salinity observed (about 0-15°C and about 0-32 in salinity, respectively) the density structure of the near-surface (0-20 m) was governed by the salinity gradients and as evidenced by the equivalent pycnoclines and haloclines depths (i.e., Surface Clines in tables of Appendix A(ii)). Strongest and shallowest stratification was constantly found in BDE, typically presenting a pycnocline within 5 m depth; shallower towards the northeastern head (UBDE, Table A(ii)3) and deeper toward the mouth, particularly in spring (April-May 2010). HB (Table A(ii)1) generally presented weaker vertical salinity gradients than in BDE (of the order of 0.5-2.5/m, maximums, from all surveys, compared to gradients of the order 5-12/m, maximums, observed in LaP-UBDE, Table A(ii)3, from all surveys) and deeper pycnoclines than in BDE (up to about 22 m, on average along HB vs. up to about 7 m, on average along LBDE, Table A(ii)2). It is worth noting that while an halocline (and thus, pycnocline) could be seen in HB during our spring surveys (April-May 2010, May 2012 and May 2013, Figure A(i)5, Figure A(i)7 and Figure A(i)9) much weaker vertical salinity gradients were seen during those periods (<0.1/m, on average, Table A(ii)1) than during the summer periods surveyed (about 0.1/m, on average, in June and September 2009, Table A(ii)1); indicating that the spring freshet does not fully reach HB until later in the year. The surface layer temperatures were similarly strongly stratified. The thermocline depth varied greatly seasonally and spatially, shallow in summer and towards the head of the bay (about 4 m vs. 9 m, on average, in LaP-UBDE and HB in June 2009, Table A(ii)3 and Table A(ii)1, respectively) and deep in fall in the whole region (about 56 m vs. 53 m, on average, in LaP-UBDE and HB in November 2013, Table A(ii)3 and Table A(ii)1, respectively). The highest surface (1-2 m depth) temperature was recorded in the LaP-UBDE section in September 2012 (about 18.2°C, Table A(ii)3) and the lowest was recorded in HB in

April-May 2010 (about 2.5°C, Table A(ii)1). In general, the warmest near-surface temperatures were measured in June 2009 in all the sections but LaP-UBDE with values of the order of 12.7 (HB, Table A(ii)1) - 16.9 (EB, Table A(ii)5)°C and the coldest in April-May 2010 in all the sections with values of the order of 2-6°C. September 2009 near-surface temperatures were comparable to those of June 2009. Near surface temperatures of June 2009 were particularly warm and resulted in a very strong thermocline all across the HB-BDE region (more than 10°C range within the 0-20 m surface layer) while the conditions of September 2009 were more vertically mixed and presented higher temperatures at 20 m depth than in June (by about 1.5-5°C). In general, near-surface temperatures were higher in BDE than in HB and the highest in LaP-UBDE or EB; coherent with the areas of lower salinity. On average over 0-20 m depth, however, LaP temperatures were the smallest in June 2009, September 2009 and April-May 2010, highlighting the strong stratification and low vertical mixing that must occur in this section. Averaged DO concentration and saturation levels within the surface layer (0-20 m) were the highest in April-May 2010 in all sections but LBDE (of the order of 11 mg/L) and lowest in September 2009 (of the order of 8-9 mg/L). Typically, observed DO concentration and saturation decreased from the spring to fall surveys. In spring (e.g., April-May 2010), the surface water column (0-20 m depth) was typically vertically homogenous with regard to DO and highly oxygenated. In summer (e.g., June 2009) and due to substantial surface heating and strong stratification, the surface water column typically presented a vertical gradient; DO increasing in concentration with depth. In fall (e.g., November 2013), the water column was once again more vertically homogenous but presented lower DO concentration and saturation than in both summer and fall. Some spatial variations with regard to DO are worth noting: lower concentration and saturation were consistently found in UBDE (best seen in LaP-UBDE section plots, Figure A(i)25 to Figure A(i)32). In general, DO concentration and saturation in UBDE was about 1-2 mg/L and 10-20% less than in LaP, respectively. NB also presented lower concentrations and saturation in June 2009 (surface and sub-surface, Figure A(i)35-36 and Table A(ii)4) and September 2009 (sub-surface, Figure A(i)37-38 and Table A(ii)4).

Intermediate layer

As observed by Richard and Hay (1984), the CIL water mass was found from the HC up to the northeast end of BDE in our surveys (Figure A(i)13, Figure A(i)15, Figure A(i)17, Figure A(i)23 and Figure A(i)25, Figure A(i)27, Figure A(i)29, Figure A(i)31 and Figure A(i)33); in depths as shallow as 5 m (Figure A(i)30 and Figure A(i)50) and as deep as 185 m (Figure A(i)11). It fills the deep basins of LaP-UBDE (B5) and EB (B9) and is the only water mass found in LiP below the surface layer with the exception of the deepest part of the basin B10, below S11 depth. In the HB, LBDE and NB sections, it is seen as a cold and relatively fresh intermediate layer between the seasonal surface layer and the relatively warm and salty deep water (MSW) in all the surveys.

Colder temperatures are found in spring (April-May 2010) and warmer temperatures in fall (November 2013) with significant inter-annual variations. Colder spring conditions may be attributed as the result of convective overturning of the cooled surface layer during the winter and warmer temperatures in fall as the result of internal mixing with the heated surface layer during the summer. June 2009 was particularly cold (about 1°C on average in HB, Figure A(i)1 and Table A(ii)1) and May 2012 particularly warm (about 1.6°C on average in HB, Table A(ii)1) with respect to our observation period (2009-13). Perhaps due to those cold and warm conditions were September 2009 and May 2013 temperatures similar (i.e., colder late summer 2009 and warmer spring 2013 than 'normal' due to the pre-conditions of a cold spring 2009 and warm spring 2012). Along with colder temperatures, fresher conditions were seen in spring (April-May 2010, May 2012 and May 2013, Table A(ii)1-) and saltier conditions in late summer

to fall (September 2009 and November 2013, Table A(ii)1) with intermediate salinity values seen in our only early-summer survey (late June 2009, Table A(ii)1).

Important seasonal effect of the cold intermediate water layer in the inner parts of BDE (LaP-UBDE and NB) was observed. From Copper Head sill (S5) to the head of UBDE, a horizontal temperature gradient was observed in all surveys but April-May 2010 (Figure A(i)25, Figure A(i)27, Figure A(i)29, Figure A(i)31 and Figure A(i)33). A seasonal pattern is evident: positive gradient in spring to early summer (Figure A(i)25) and negative gradient in late summer to early fall (Figure A(i)27); from cold to warm and from warm to cold towards UBDE, respectively. Such horizontal gradients suggest that a seasonal deep water renewal occur at Copper Head sill (S5 in Figure 7, km 2.5 on LaP-UBDE section): cold intermediate water from the outer basin is being advected in spring (and perhaps also in winter) and warmer intermediate water is being advected in summer/fall.

Striking features occurred in spring 2010 in the outer basin (B3 in Figure 7). In April-May 2010, a large core of super-saturated oxygen along with a large downward displacement of the interface between the intermediate and deep water layers could be seen (Figure A(i)17 and Figure A(i)39). The supersaturated cells extended from the near-surface down to about 100 m depth. The vertical displacements of isotherms and isohalines were of the order of 20-40 m and located about 5 km from the Hermitage Sill for the first cell and between about 10-20 km for the second cell. Temporal aspect complicate the spatial pattern: the only two profiles of the outer basin that did not show any super-saturation cell were taken 1-2 days after all the other ones of the LBDE-NB section (Figure A(i)39). Similar striking features were seen in HB between the 28 and 29 of April on the Hermitage Bank (Figure A(i)5). A large zone of supersaturated DO extended from the near-surface to almost 130 m depth and over about 15 km distance (around km 3-18). A day later, 30 April, further eastward into the bay (just ahead km 20 on HB section), the water column was saturated from the near-surface down to about 50 m depth, but no super-saturation cell was encountered.

Bottom layer

Due to total blockage from Copper Head Sill (S5 in Figure 7), Richies Island sill (S4 in Figure 7) and the Little Passage ridge (culminating at S11 in Figure 7), the deep water mass was not found in the LaP-UBDE, EB and most of the LiP sections (Figure A(i)25, 27, 29, 31 and 33, Figure A(i)41&43 and Figure A(i)45, 47, 49 and 51). Partial blockage from Gallet Island Sill (S3) and Margery Head sill (S10) allowed the mixture of MSW with the CIL, roughly present between 100 m and 150 m depth, to enter into South Bois Island basin (B4 in Figure 7, km 30 on LBDE section) and into the deepest part of Little Passage basin (B10 in Figure 7, km 2.5 on LiP section) (best seen in LBDE and LiP full depth vertical sections of April-May 2010, Figure A(i)17 and Figure A(i)49, respectively).

Consistent with the observations of Richard and Hay (1984), Hermitage North sill (S2 in Figure 7) appears to act as a barrier limiting the influx of MSW into BDE as evidenced by the slanted isolines of the LBDE full depth vertical section plots of June 2009 (Figure A(i)13). The conditions of temperature, salinity and DO measured inside and outside BDE did not indicate significant differences, however. Although generally marginally lower than in B1, the DO concentration did not show evident decay in B3 in any of our survey; supporting the annual (if not more frequent) renewal period suggested by Richard and Hay (1984). Presenting a shallower maximum and mean depth than the Hermitage Sill (S2), Little Doting Cove sill (S8 in Figure 7), which separates the North Bay basin (B8 in Figure 7) from the outer BDE basin (B3 in Figure 7) should act as a stronger barrier. MSW could clearly be seen in B8 during the April-May 2010 measurements (Figure A(i)39), however, and albeit at deeper depth than in B3 (5°C isotherm located below about 230 m vs. 190 m, respectively).

In general (best seen from the summary table of HB section in Appendix A(ii), Table A(ii)1), the bottom layer was found to be warmer and shallower in spring (April-May 2010, May 2012 and May 2013) than in early summer (June 2009) and fall (November 2013) in the HB-BDE region; consistent with the winter upwelling mechanisms described initially by de Young (1983). Some inter-annual variation can also be noted such as between May 2013 and May 2012, showing a difference on the average of up to 0.69°C, though being within its seasonal range of 0.8°C reported by El-Sabh (1977). On a long-term basis, the MSW has been reported to vary the most on timescale of a decade rather than on a yearly timescale (Bugden 1991).

FORTUNE BAY – BELLE BAY (FB – BB)

Geography

The FB-BB region is divided in sections as follow (Figure 6 and Figure 8): Fortune Bay (FB, 11 in Figure 6), Belle Bay West (BBW, 7 in Figure 6), Belle Bay East (BBE, 8 in Figure 6), Belle Bay – Mal Bay (BB-MB, 9 in Figure 6) and Fortune Bay – Long Harbour (FB-LH, 10 in Figure 6) of a total length of about 108 km, 28 km, 28 km, 12 km, 10 km, respectively. The bathymetry of the region, centered on Belle Bay, with its main basins and sills described in Donnet et al. (2017) is reproduced as Figure 8. Interpolated profiles of the full water column and surface layer (0-20 m depth) are presented in Appendix B(i), sorted in the order listed above (FB, BBW, BBE, BB-MB and FB-LH) and chronologically. Corresponding summary tables are presented in Appendix B(ii). Interpolated property maps are presented in Appendix B(iii), sorted in chronological order and from shallow (surface, 2 m depth) to deep (near-bottom).

FB is a large fjord-like embayment, bounded by the Burin Peninsula to the East and by three outer sills (Figure 1): Saint-Pierre sill to the south (about 125 m maximum depth), Miquelon sill to the southwest (about 125 m maximum depth) and Sagona sill to the west (about 112 m maximum depth). FB is both long (about 130 km) and wide (about 20 km) with a large head (BB) oriented towards the northwest (Figure 1). The main basin of FB is made of a relatively shallow bank (less than 200 m depth), Fortune Bank (Figure 1), bordered by two channels of more than 300 m maximum depth (Figure 1 and Figure 6). BB consists of two deep channels (more than 500 m maximum depth) separated by a shallow bank (less than 100 m depth; Figure 8). BB western channel is separated from FB by a sill (S1 in Figure 8) of about 213 m limiting depth. The western channel is very narrow at its entrance behind S1 (about 650 m width using the 200 m contour) and progressively widen towards a relatively large basin forming the head of the bay (B2 in Figure 8). A shallow area, about 170 m at its shallowest point, rise roughly in the middle of the western channel-B2 system, partly as an extension of the shallow bank (S2 in Figure 8) towards the northwest. The eastern channel is a direct prolongation of FB main channel and gets progressively narrower as it extends towards the northeast. This channel is separated from the head of BB (B2 in Figure 8) by a sill (S3 in Figure 8) of about 138 m limiting depth. A number of side bays and inlets are present around BB: Belleoram Barasway (B3 in Figure 8), Corbin Bay (B6 in Figure 8), Cinq Island Bay (B7 in Figure 8), North Bay (B8 in Figure 8), East Bay (B9 in Figure 8), Belle Harbour (B10 in Figure 8), Little Bay (B11 in Figure 8) and Mal Bay (B12 and B13 in Figure 8). All those features are characterized by a sill and a, sometime only slightly, deeper basin.

Freshwater input to BB was assessed by Donnet et al. (2017) which report a yearly averaged discharge rate of about 71 m³/s. The main source of freshwater is from Bay du Nord, which account for about 57% of the total discharge. Altogether, the main rivers flowing to the northwest end of the bay (Salmon River, Bay du Nord, North West Brook, North East Brook, Figure 1 and Figure 8) account for about 76% of the total direct discharge to BB. Discharge is seasonal with two peaks: one in April (largest) and one in December (smallest).

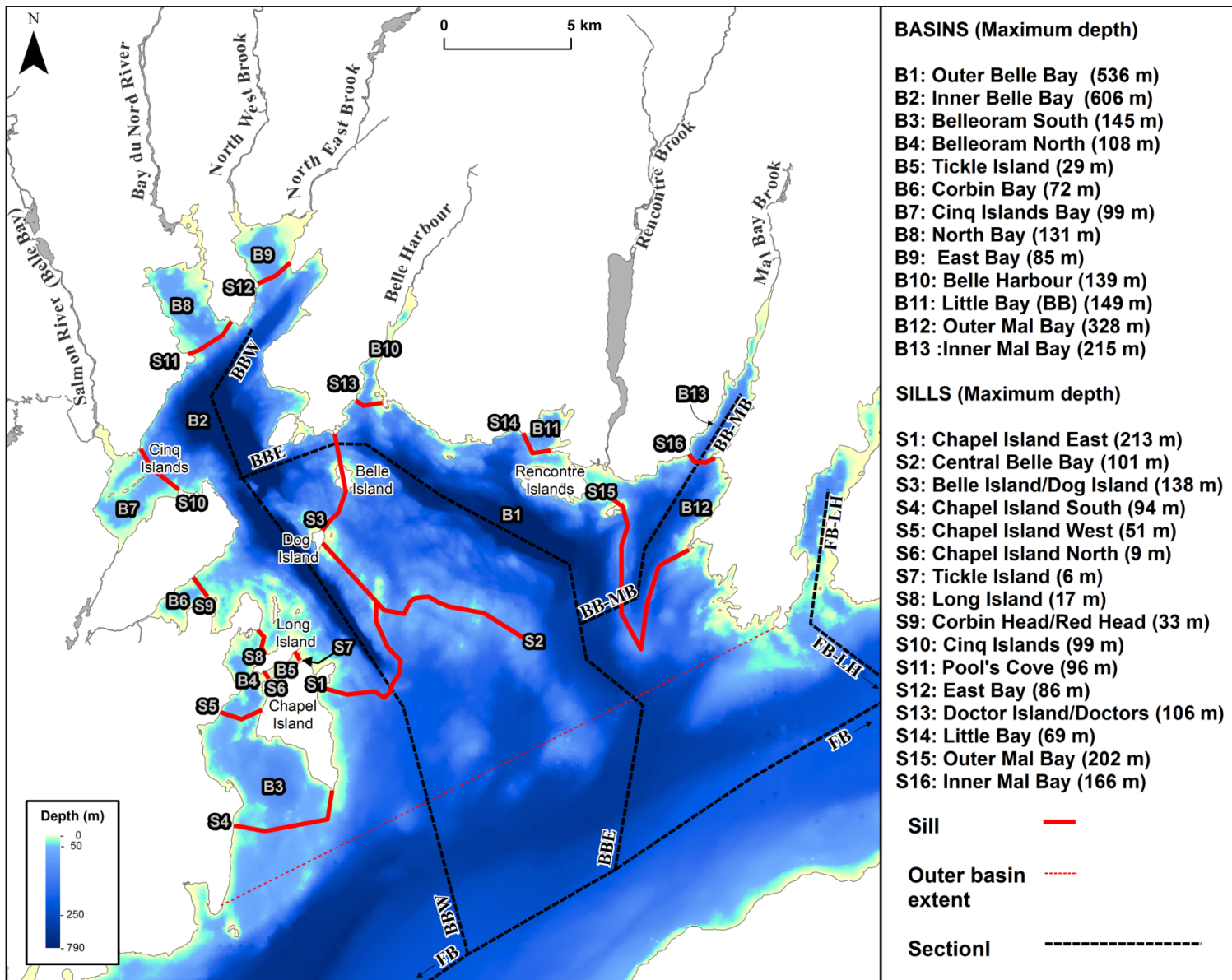


Figure 8: Basins and sills of the Belle Bay (BB) region.

Near-surface layer (0-20 m)

Freshwater input from the rivers of the Northwest of BB and near the mouth of Long Harbour (LH) is evidenced by a clear horizontal gradient of salinity with decreasing values toward the head of the bay and LH inlet, respectively (Figure B(iii)1, Figure B(iii)5 and Figure B(iii)9). In general, near-surface water was warmer and fresher in BB's head and slightly warmer temperatures and lower salinities were observed on the eastern side of BB than on the western side; consistent with the main freshwater discharge occurring in the region.

Surface horizontal temperatures appear coherent with the surface salinities in both May 2011 and July 2011, increasing from the mouth to the head of FB-BB (Figure B(iii)1, Figure B(iii)5 and Figure B(iii)9). A cross-channel gradient in temperature and salinity was clearly observed in May 2011 in FB with colder and saltier water present along the Burin Peninsula coast (Figure B(iii)1). The presence of this colder and saltier water along the southeast side of FB was uneven as shown by the south to north cross-section transects: present in the first transect, almost vanished in the second transect, present in the third transect and not present in the inner, northeastern, part of the bay. FB vertical section plots (Figure B(i)2) show that the water structure was much less stratified in those colder and saltier areas. Since the measurement of the FB stations spanned a period of about three days (May 4 to May 6), the origin of this spatial and/or temporal pattern is difficult to explain. The slanted, near-surface isopleths of FB-LH section (Figure B(i)16) rising towards the head of the inlet could indicate that a local upwelling was occurring at the time of sampling. However, no such feature was observed in the near-by and similarly oriented inlet of MB (Figure B(i)12) which was sampled the same day than LH (May 8) and no wind data are available from the Sagona Island weather station for this period; precluding further inference. In July, the isopleth were, on the other hand, clearly slanted within MB but rising toward the mouth of the bay (Figure B(i)14). In both cases, the stations within MB were sampled the same day (May 8, 2011 and July 4, 2011, respectively), about 0.5 hour apart from each other. In BB, stratification in salinity increased at the head from May to July, as evidenced in the BBW vertical section plots (Figure B(i)4 and Figure B(i)6): while near surface salinities were comparable (about 25-30), saltier water was found further north in the sub-surface in July (e.g., see the isohaline 31 position change).

Surface DO concentration and saturation were high in May 2011 being generally above 10 mg/L and 100%, respectively (Figure B(iii)1 and Figure B(iii)5). Due to warmer conditions observed in July 2011, surface DO concentration decreased in July 2011 in BB to values of the order of 9-9.5 mg/L, but saturation remained high and generally above 100% (Figure B(iii)9). Horizontally, a cross-bay gradient was observed in May with lower surface DO concentration found along the eastern shore of BB (Figure B(iii)5); coherent with the temperature pattern for the most part except in LH where relatively low DO values were measured in colder water temperature. Vertically, the DO concentration generally decreased with depth in May and increased in depth in July (Figure B(i)4, Figure B(i)6 and Figure B(i)8, Figure B(i)10).

Overall (Appendix B(ii)), near-surface layer temperatures ranged from 1.6°C to 5.9°C in May 2011 (FB and BBW, Table B(ii)1 and Table B(ii)2, respectively) and from about 5.8°C to 14.3°C in July 2011 (both in BBW, Table B(ii)2). This represents an increase of about 8°C at the surface and by about 4°C in the sub-surface in just about two months; consistent with the conditions seen in 1982 and reported by de Young (1983) which observed an increase of the order of 7°C at the surface between May and July. Salinity ranged from 25.8 (BBW, Table B(ii)2) to 32.2 (FB-LH, Table B(ii)5) in May and from 25.4 to 31.8 in July (both in BBW, Table B(ii)2). DO concentration ranged from 9.7 (BBE, Table B(ii)3) to 11.6 mg/L (FB, Table B(ii)1) in May and from 9.1 to 10.3 mg/L (about anywhere in BB, Table B(ii)2-4) in July; decreasing by about 1 mg/L at the surface and by about 0.6 mg/L in the sub-surface. Similarly to BDE and though the range of salinity observed is much smaller (about 0-32 in BDE vs. about 25-32 in BB), the

near-surface water column density structure of FB-BB is found to be governed by the salinity gradients. Thermocline depths ranged from about 7 m (FB-LH, Table B(ii)5) to 16 m (BBW, Table B(ii)2) in May; significantly rising in the main basins (B1 and B2) to depths of the order of 3 m (BBW, Table B(ii)2) and slightly deepening in MB (Table B(ii)4) to a mean depth of about 10 m in July. Vertical temperature gradients increased markedly from May to July in the main basins from about 0.1°C/m to 0.4°C/m, on average, while it virtually stayed the same in MB (around 0.2°C/m, on average). Maximum gradients were found in BBW (Table B(ii)2) with a magnitude of the order of 1.6°C/m. Halocline (and thus pycnocline) depths ranged from about 6 m (FB-LH, Table B(ii)5) to about 16 m (FB, Table B(ii)1) in May; significantly rising to a range of about 3 m (BBW, Table B(ii)2) to about 7 m (BB-MB, Table B(ii)4) in July. Vertical salinity gradients were of the order of 0.1/m (BB, Table B(ii)2-4) and 0.06/m (FB, Table B(ii)1) in May; slightly increasing in BBW (Table B(ii)2) to about 0.15/m while decreasing in BBE (Table B(ii)3) and MB (Table B(ii)4) to about 0.08/m and 0.07/m in July, respectively.

Bottom layer

The bottom layer of the whole FB-BB region was found to be generally cold (<2°C) and nearly vertically homogeneous in temperature and salinity; consistent with the observations made in earlier work (e.g., de Young 1983).

In May 2011, FB presented horizontal variations of temperature from mouth to head with intrusion of cold water above 200 m depth at the head, interflow of warmer and colder water between 50 and 200 m depth over the bank and warmer water towards the head (Figure B(i)1). The intrusion of cold water is consistent with previous observations reporting cold LCW flowing over St. Pierre sill in summer (e.g., de Young 1983). The interflow of relatively warm and cold water might be the result of previous inflow of MSW mixture from the HC during late-winter or early spring upwelling events but is more difficult to interpret since spatial and temporal distinction cannot be made. In BBW, a cold to warm temperature gradient was also observed above sill depth (i.e., 200 m depth, Figure B(i)3). Below sill depth, temperatures decreased to values lower than 1°C in B2 (km 12.5 to 20 on BBW section). In contrast, the temperatures slightly increased to values higher than 1.5°C in B1 (Figure B(i)7 and Figure B(iii)8), suggesting some blockage effect of S1 to the intrusion of warmer water from FB during the winter 2010-11. Both FB-LH and MB showed horizontal gradient of temperature with slightly warmer water towards the head of the bays (Figure B(i)15 and Figure B(i)11, respectively); suggesting higher vertical mixing occurring towards the head. Salinity was largely homogeneous horizontally and vertically in all sections and ranged between 32 and 32.5 (see Appendix B(i), any section, Figure B(i)1-15, full depth). DO concentration and saturation were perceptibly lower in the deep basins of inner FB and BB below sill depth with values inferior to 9.5 mg/L and 85%, respectively (Figure B(i)1, Figure B(i)3 and Figure B(i)7). This indicates a lower renewal rate of those basins and/or a progressive decay of the deep water DO while slowly progressing towards the head as suggested by de Young (1983). The effect of the oxygen-poor MSW on those lower DO concentrations is, however, less likely in B2 considering the cold temperatures recorded in this basin (Figure B(i)3). It is also worth to note the horizontal gradient in both DO concentration and saturation in all the sections: lower DO concentration and saturation levels were found towards the head of the bays and indicate a progressive renewal of deep water from the mouth to the heads of FB (Figure B(i)1, Figure B(i)3 and Figure B(i)7).

In July 2011, the CTD casts were limited to the first 200 m of the water column and therefore did not sample the bottom of the deep basins of the region. Surface warming from May was clear and evidenced by the deepening to about 100 m depth of the 2°C isotherm (from about 20 m depth in May, Figure B(i)5 and Figure B(i)9). This warming to deeper level is consistent with and of the same order of magnitude than the results reported by de Young in 1983. Temperature,

salinity and, most notably, DO concentration and oxygen saturation fields were largely horizontally uniform; contrasting with the gradients seen in two month earlier (Figure B(i)5 and Figure B(i)9). This, along with the slightly warmer temperatures and higher DO concentration above 100 m depth, indicates a gradual advection and renewal of the deep water layer associated with mixing; consistent with the summer processes reported by de Young in 1983.

CONNAIGRE PENNISULA (CP)

The CP region is divided in sections as follow (Figure 6 and Figure 9): Outer Connaigre Peninsula (OCP, 16 in Figure 6), Lower Connaigre Bay (LCB, 12 in Figure 6), Upper Connaigre Bay (UCB, 13 in Figure 6), Harbour Breton – Northeast Arm (HB-NA, 14 in Figure 6) and Great Bay De l'Eau (GBDE, 15 in Figure 6) of a total length of about 45 km, 25 km, 11 km, 19 km and 23 km respectively. The bathymetry of the region with its main basins and sills described by Donnet et al. (2017) is reproduced as Figure 9. Interpolated profiles of the full water column and surface layer (0-20 m depth) are presented in Appendix C(i), sorted in the order listed above (OCP, LCB, UCB, HB-NA and GBDE) and chronologically. Corresponding summary tables are presented in Appendix C(ii). Interpolated property maps are presented in Appendix C(iii), sorted in chronological order and from shallow (surface, 2 m depth) to deep (near-bottom).

Geography

The CP consists of two open-bays (CB and GBDE) and 1 narrow inlet (HB-NA). Just offshore those coastal features, the area is characterised by a deep semi-enclosed basin (B1 in Figure 9), bounded by the Sagona sill (S2 in Figure 9) and Miquelon Sill (S1 in Figure 9) to the east and by a long and wide sill to the west (S3 in Figure 9), restricting the connection to the HC. CB and HB-NA entrances present a sill of the order of 100 m limiting depth (S4 and S5 in Figure 9) whereas GBDE entrance sill (S6 in Figure 9) has a much deeper limiting depth (about 200 m) connecting the bay to the deep offshore basin B1. CB consists of 5 main basins (B2, B3, B4, B5 and B6 in Figure 9) separated by sills (S8, S9, S10, S11 and S12 in Figure 9). Two of those basins are more than 200 m maximum depth (B3 and B6); the deepest (B6) being located at the head of the bay and separated from the outer part of the bay by a sill (S12) of about 92 m maximum depth. The others basins are 191 m (B2), 169 m (B4) and 120 m (B5) maximum depth. B3 is separated from the outer basin B2 by a sill of 124 m depth (S8) whereas B4 is bounded by three sills to the west and to the south of limiting depths 131 m (S11), 93 m (S9) and 84 m (S10), respectively.

The shallowest basin B5 is bounded to the west by S9 and S10. HB-NA consists of three main basins separated by sills. The deeper basin (B8 in Figure 9) is located in the middle of the inlet and has a maximum depth of 182 m. The other basins are less than 140 m maximum depth (B7 and B9 in Figure 9). The inner sills separating the basins have 86 m (S13 in Figure 9) and 104 m (S14 in Figure 9) limiting depths, respectively. GBDE consists of one large and deep basin (B10 in Figure 9, 313 m maximum depth), two side-bays (St. John's Bay, B13 and Little Bay, B11 in Figure 9) and one isolated and shallow basin located in the inner part of the bay (B12 in Figure 9, 80 m maximum depth).

Little Bay (B11) is relatively shallow (63 m maximum depth) and separated to the outer basin by a sill of 34 m limiting depth (S15 in Figure 9). St. John's bay (B13) is similarly shallow (74 m maximum depth) and separated from the offshore basin B1 by a wide sill of 42 m limiting depth (S7 in Figure 9).

Freshwater input to the region was assessed by Donnet et al. (2017) which reports small yearly averaged discharge rate of about 2.6 m³/s with 1.4 m³/s and 6 m³/s in CB, HB-NA and GBDE, respectively.

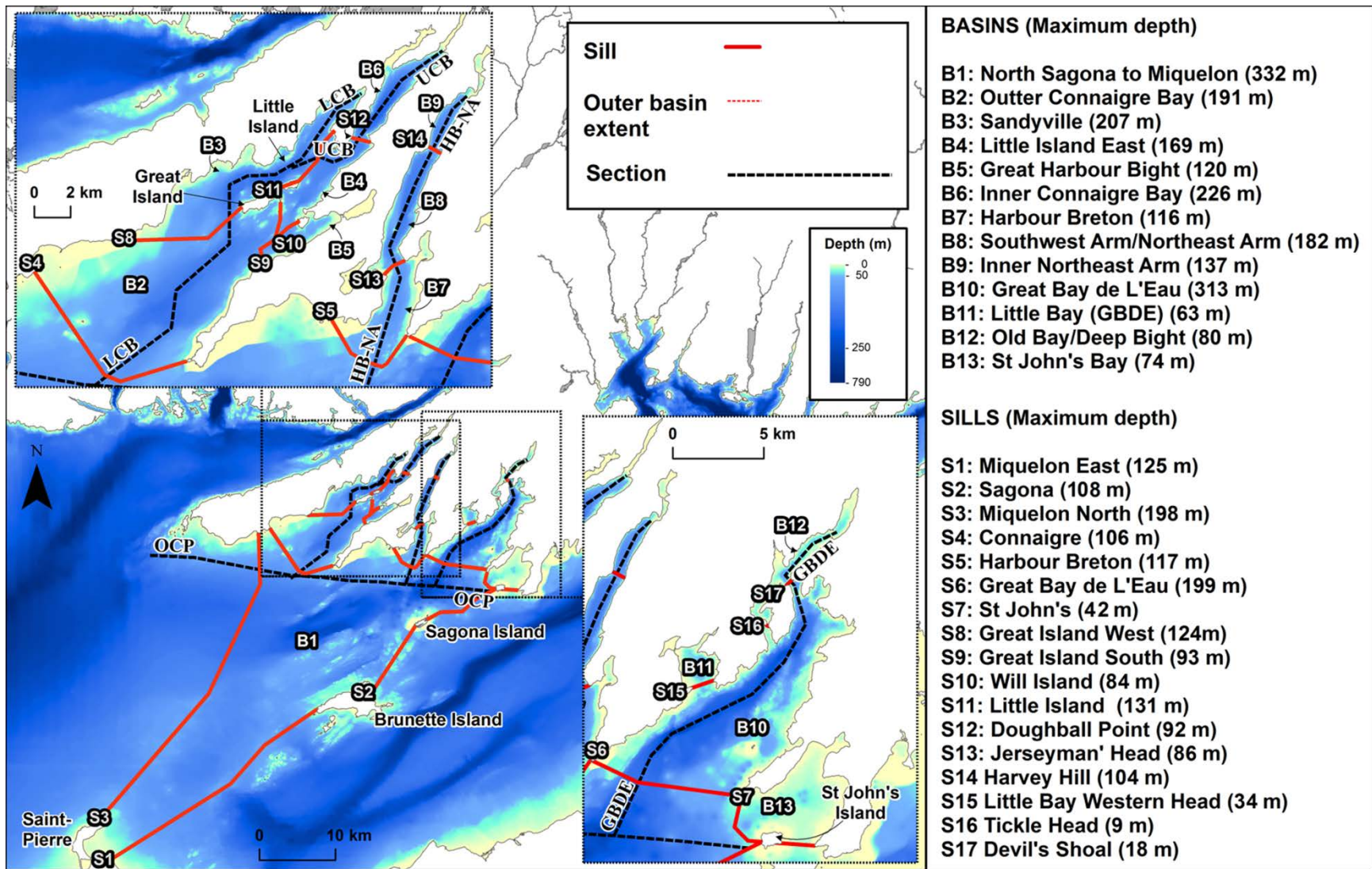


Figure 9: Basins and sills of the CP region.

Near-surface layer (0-20 m)

In comparison to BB and, to a larger extent, BDE, the surface layer of the CP region is much more homogeneous both vertically and horizontally, particularly with regard to the salinity distribution which can be attributed to the region much more limited amount of freshwater discharge.

Despite having the smallest watershed area of the region (Donnet et al. 2017), runoff was the most visible in HB-NA in July 2010; probably due to the inlet small area (Figure C(i)26). Interestingly, runoff appeared larger in the July 2010 HB-NA and GBDE sections than in all spring surveys of May (2011, 2012 and 2013, Figure C(i)28, Figure C(i)30, Figure C(i)32 and Figure C(i)38, Figure C(i)40, Figure C(i)42) despite an annual discharge peak of the Coast of Bays area rivers in April and an annual discharge low in July (Donnet et al. 2017).

In May 2012, it appears that an upwelling was in place when the region was being sampled. Lower temperature and higher salinity were observed at the surface in the inner half of CB (Figure C(iii)9). Similar observations were made in the inner part of GBDE (B12), though to a smaller extent. The feature is also evidenced in the UCB, HB-NA and GBDE vertical sections, all showing rising isopleths towards the head of the respective bay (Figure C(i)17, Figure C(i)29 and Figure C(i)39, respectively). Sampling temporal and spatial resolutions do not allow inferring the full spatial extent of the event. The HB section, however, which was sampled about three days after CB, shows slightly lower temperatures and higher salinities at the surface of the innermost station and a slant in the isopleth within the near-surface layer (Figure A(i)7 and Figure A(i)8). It seems therefore probable that the whole Coast of Bays area was subject to upwelling, most likely due to winds from the northwest or from the northeast. Wind data from Sagona Island (Appendix E) supports this observation: wind from the north-northeast was blowing consistently during the whole duration of the survey (May 4-7, Figure E1).

In spring (as observed in May 2011, 2012 and 2013), the region was generally characterized by surface temperatures of the order of 4-5°C and surface salinities of the order of 31.5 (Figure C(iii)5, Figure C(iii)9 and Figure C(iii)17). With the exception of May 2012 upwelling conditions and of CB to some extent, temperatures generally increased towards the northeast (i.e., towards the head of the bays) along with decreasing salinities. The heads of HB-NA and GBDE were generally the warmest and freshest areas of the region. Offshore, patterns of surface temperature were patchy at times such as in May 2013 (Figure C(iii)17). The surface layer (0-20 m) was the freshest, offshore, in 2012 (about 31.4, OCP section, Table C(ii)1) and the saltiest in 2013 (about 31.7, OCP section, Table C(ii)1), indicating inter-annual variation in discharge rates and/or spring freshet timing or simply the effect of the upwelling acting in 2012 and pushing the brackish surface layer away from the bays. The near-surface (0-20 m) OCP section was also notably warmer, by almost 1°C, in 2012 than in 2013 (Figure C(i)4 vs. Figure C(i)6 and Table C(ii)1).

The limited surveys conducted in summer (July 2010 and July 2012) showed maximum near-surface temperatures of the order of 16°C (HB-NA, July 2010, Table C(ii)4) to 17°C (UCB, July 2012, Table C(ii)3) and minimum surface salinities from about 28.8 (HB-NA, July 2010, Table C(ii)4) to 30.2 (UCB, July 2012, Table C(ii)3). The horizontal structure was generally uniform but the spatial extent of the surveys were too limited for a good representation of the area (Figure C(iii)1, Figure C(iii)2 and Figure C(iii)13, Figure C(iii)14). UCB (July 2012), HB-NA (July 2010) and GBDE (July 2010) vertical sections show continuous temperature and salinity stratifications within 0-20 m and 0-5 m depth, respectively (Figure C(i)20, Figure C(i)26 and Figure C(i)36). DO concentration was relatively uniform horizontally and increasing with depth; coherent with the temperature. Oxygen saturation was high, about 100% or more except in the

GBDE inner basin below 5-10 m depth (B12 in Figure 9; beyond km 17.5 on GBDE section, Figure C(i)36).

In fall, as observed in November 2013, the surface layer was generally uniform horizontally (Figure C(iii)21-22) and vertically (Figure C(i)8, Figure C(i)16, Figure C(i)24 and Figure C(i)34) all across the region with temperatures of the order of 8-8.5°C, salinities of about 31.5 and DO concentrations of the order of 9 mg/L.

Overall (Appendix C(ii)), surface layer (0-20 m) temperatures ranged from about 2°C to 5°C in May; from about 6°C to 17°C in July and from about 7.5°C to 9°C in November across the region. Salinity ranged from 30.5 to 32 in May; from 29 to 32 in July and from 30.5 to 32 in November across the region. DO concentration ranged from 10 to 12 mg/L in May; from 8 to 10.5 mg/L in July and from 8 to 9.5 mg/L in November across the region. In contrast to BDE and FB-BB region, the water column density structure of CP is found to be governed by both salinity and temperature gradients. Thermocline depths ranged from about 10 m to 45 m in May (being, for the most part, significantly shallower in HB-NA, Table C(ii)4, and GBDE, Table C(ii)5, than elsewhere); from about 6 m to 20 m in July and from 29 m (HB-NA, Table C(ii)4) to 77 m (UCB, Table C(ii)3) in November. Vertical temperature gradients ranged from about 0.02°C/m to 0.1°C/m, on average in May; 0.3°C/m to 0.5°C/m in July and ranged from about 0.01°C/m to 0.03°C/m in November. Maximum gradients were found in UCB in July 2012 with a magnitude of the order of 1.7°C/m (Table C(ii)3). Halocline depths ranged from about 14 m (HB-NA, Table C(ii)4) to about 72 m (UCB, Table C(ii)3) in May; from about 3 m (HB-NA, Table C(ii)4) to about 4 m (GBDE, Table C(ii)5) in July and from about 16 m (HB-NA, Table C(ii)4) to about 71 m (UCB, Table C(ii)3) in November. Vertical salinity gradients of the order of 0/m to 0.04/m were measured, on average, in May; 0.1/m in July and 0.01/m to 0.02/m in November. Pycnocline depth was found from about 13 m (HB-NA, Table C(ii)4) to 50 m (UCB, Table C(ii)3) in May; around 3 m (HB-NA, Table C(ii)4) to 6 m (UCB, Table C(ii)3) in July and from about 29 m (HB-NA, Table C(ii)4) to 77 m (UCB, Table C(ii)3) in November (Appendix C(ii)).

Bottom layer

The CIL was observed down to the near-bottom in all the surveys and in the entire region except in the deep offshore basin B1 and in GBDE deep basin B10 where MSW was present (e.g., Figure C(i)3 and Figure C(i)39). The CIL was much less present in May 2012, consistent with HB-BDE observations and, though somewhat less voluminous (except in CB), was colder in May 2013 than in May 2011 (e.g., Figure C(i)27, Figure C(i)29 and Figure C(i)31). In November 2013, the water column was nearly homogeneous from the surface down to about 80 m depth and the CIL drastically decreased in volume in CB (Figure C(i)15) and vanished from the HB-NA (Figure C(i)33) section from May 2013. It also vanished offshore, as illustrated by the OCP transect (Figure C(i)7).

Horizontal gradient of the CIL temperatures from west to east in the OCP section in May 2012 (Figure C(i)3) would suggest a flow of this LCW derived water from the Hermitage Channel rather than from Fortune Bay, in agreement with de Young (1983), but the conditions seen in May 2013 are less clear (Figure C(i)5). In May 2013, a cell of warmer water associated with higher DO concentration and supersaturated oxygen was observed near and eastward of S3 (Figure 9, km 7.5 on OCP section). Most likely, the area of supersaturated oxygen resulted from primary production. Perhaps this area of mixing resulted from internal wave generated on S3 as suggested by Ratsimandresy et al. (2014).

Intrusion of CIL-MSW mixture into the inner basin of CB (B2, B3 and B4 in Figure 9) and HB-NA (B7 and B8 in Figure 9) was observed in most LCB and in all HB-NA transects, as evidenced by the slightly higher temperatures and salinities as well as by lower DO concentrations

(e.g., Figure C(i)11 and). Such intrusions appear more clearly in the May 2011 (Figure C(i)9 and Figure C(i)27) and May 2012 (Figure C(i)11 and Figure C(i)29) transects as well as, to a lesser extent, in the July 2010 (Figure C(i)25) and May 2013 (Figure C(i)31) transects. In November 2013, bottom temperatures were somewhat colder, salinity slightly lower and DO concentration slightly higher in HB-NA; indicating a replacement of the bottom mixture from May 2013 (Figure C(i)33 vs. Figure C(i)31). This seasonal and inter-annual pattern seems consistent with the seasonal upwelling mechanisms described by de Young (1983) and others and with BDE results presented above.

MSW is clearly visible in the near-bottom property maps (Figure C(iii)8, Figure C(iii)12 and Figure C(iii)20) and GBDE vertical transect plots (Figure C(i)35, Figure C(i)37, Figure C(i)39 and Figure C(i)41), with temperatures of the order of 5°C, salinity higher than 33 and DO concentration lower than 6 mg/L within the deep basins B1 and B10 (Figure 9). The water mass was warm and large in July 2010 (Figure C(i)35 and Figure C(iii)4) and in May 2012 (Figure C(i)39, Figure C(iii)12), less warm in May 2011 (Figure C(i)37 and Figure C(iii)8) and even colder or less present in May 2013 (Figure C(i)41 and Figure C(iii)20).

DISCUSSION

HYDROGRAPHIC CHARACTERISTICS

Based on the results of a five year program (2009-13), three distinct regions are described:

- BDE: a fjord of complex geometry and large freshwater discharge resulting in the presence of a sharp and shallow near-surface pycnocline for most of the year. At depth, BDE is subject to the intrusion of both a CIL and a warm and saline deep water layer (MSW); the latter only partially flowing into the fjord due to blockage from inner sills. As a result, the vertical water column structure of BDE is found to be essentially a two layered (in the inner parts) to three layered (in the outer parts) structure from spring to fall; consistent with the description of Richard and Hay (1984). An example of the vertical structure within BDE in spring is shown in Figure 10.
- FB-BB: a large and deep fjord-like bay, subject to noticeable freshwater discharge at its head resulting in a fairly strong seasonal pycnocline from spring to summer (and, perhaps, up to the fall). BB itself is the largest embayment of the Coast of Bays area (in terms of volume and area) and receives a disproportionately large amount of the freshwater discharge flowing into FB; either directly (about 43% of FB total, including BB, input; Donnet et al. 2017, Table B1) or from the near-by LH inlet (representing about 24% of FB total, including BB, input; Donnet et al. 2017, Table B1). Thus, assuming BB would receive the whole input from LH, it could receive up about 67% of FB total input. FB is bounded by a series of sills and islands on its offshore boundaries limiting the influx of the warm MSW from the Hermitage Channel and is characterised by a seasonal deep-water renewal from derived LCW in summer and from the MSW in winter (e.g., Hay and de Young 1989). Thus, from spring to summer (and most likely up the late fall or early winter) when the seasonal surface layer is present FB-BB is, for the most part, characterised by a two layered system. An example of the vertical structure within Belle Bay in spring is shown in Figure 10.
- CP: a region consisting of two open bays (CB and GBDE) and one narrow inlet (HB-NA); all having limited amount of freshwater discharge compared to FB-BB and BDE. As a result of this limited input and a geographically more exposed position, the near-surface water of this region is more oceanic and more vertically mixed. Freshwater input has, nevertheless, a noticeable effect (and at times, dominant) on the stratification in HB-NA and GBDE and brackish water (<32 in salinity) was clearly present all along the peninsula and in all our

surveys (spring to fall). At depth, the CIL is found everywhere and down to the near-bottom. MSW is, however, well present in the deep offshore basin located just outside GBDE (B1 in Figure 9) and in GBDE itself (B10 in Figure 9). Some MSW mixture was also found in the outer and inner basins of CB (B2 and B3 in Figure 9) and inner basins of HB-NA (B7 and B8 in Figure 9) in spring (2012 and 2013 in particular); disappearing in fall. The CP region is, therefore, essentially a two layered system from spring to fall, with some three layered structure areas (GBDE and offshore basin B3, notably). An example of the vertical structure within the CP region in spring is shown in Figure 10.

Near-surface layer (0-20 m)

The salinity has a dominant influence on the density structure of the Coast of Bays water column; both at the surface due to the rivers freshwater discharge and at depth due to the cold and relatively small range of temperatures. In all three regions studied (HB-BDE, FB-BB and CP), near-surface temperature gradients appear generally coherent with near-surface salinity gradient, indicating a potential effect of stabilisation of the freshwater input on the vertical structure, reducing vertical mixing and thermal diffusion to deeper depth. As a result, near-surface stratification was stronger in BDE and weaker in CP, as inferred from the vertical mixing rate estimated in Donnet et al. (2017) from archived temperature data. As a whole, and based on the dominant effect of the salinity on the near-surface water structure, the Coast of Bays area may be considered as a Region of Freshwater Influence (ROFI, Simpson 1997; see more details in Donnet et al. 2017).

Surprisingly, the BDE April-May 2010 survey (Figure A(iii)10) revealed less runoff than both June 2009 (Figure A(iii)1) and September 2009 (Figure A(iii)6) even though the rivers' discharge peak in the region typically occurs in April (Donnet et al. 2017). In BB, although the effect of the spring freshet appears evident on the eastern side (i.e., along BBE section), similar low salinity values (25-30) were observed at the head of the bay from May to July (Figure B(iii)5 and Figure B(iii)9) suggesting some sort of 'containment' of the brackish water plume towards the head and, in CP, both HB-NA and GBDE surface salinities were lower in July 2010 (Figure C(iii)1) than in any of the spring surveys (May 2011, 2012 and 2013; Figure C(iii)5, Figure C(iii)9 and Figure C(iii)17). Prevailing winds from the southwest containing the freshwater discharge towards the head of the bays may, in part, explain these observations. This hypothesis was first proposed by Richard and Hay (1984) to explain the difference of near-surface salinity seen between their spring and fall surveys in BDE. In their case, however, some of the low salinity value observed in BDE in November may have also been the result of the fall freshet experienced by the local rivers (shown in Donnet et al. 2017; Figure 5). Nevertheless, there is little doubt that the wind is a major force in the area, as indicated by the simple scale analysis discussed in Donnet et al. (2017) for BDE and the drifter observations executed in BDE and HB-NA of Ratsimandresy et al. (2012). In addition, while the observed salinity distributions within HB clearly show the influence of the BDE and inner HB runoff (e.g., Figure A(iii)1) they do not seem to indicate an offshore influence from the Gulf of St Lawrence as was suggested by Richard and Hay (1984). The present dataset is, however, insufficient to rule-out this hypothesis. Based on this dataset, there does not seem to be any visible connection (i.e., water exchange) across the three regions studied (i.e., between BDE, FB-BB and CP). With the exception of the probable upwelling conditions of May 2012, surface salinity within CP was generally decreasing toward the head of the bays, indicating an effect of local land runoff; thus precluding an offshore influence of lower salinity waters (i.e., $S < 31$) from either BDE or FB. The surface (2 m) maps of May 2011 and May 2013 do show, nevertheless, relatively low surface salinity offshore the bays, particularly to the south of HB-NA and GBDE. Nonetheless, our data appear insufficient to infer the origin of this pattern, here also (i.e., temporal and spatial resolution is too limited).

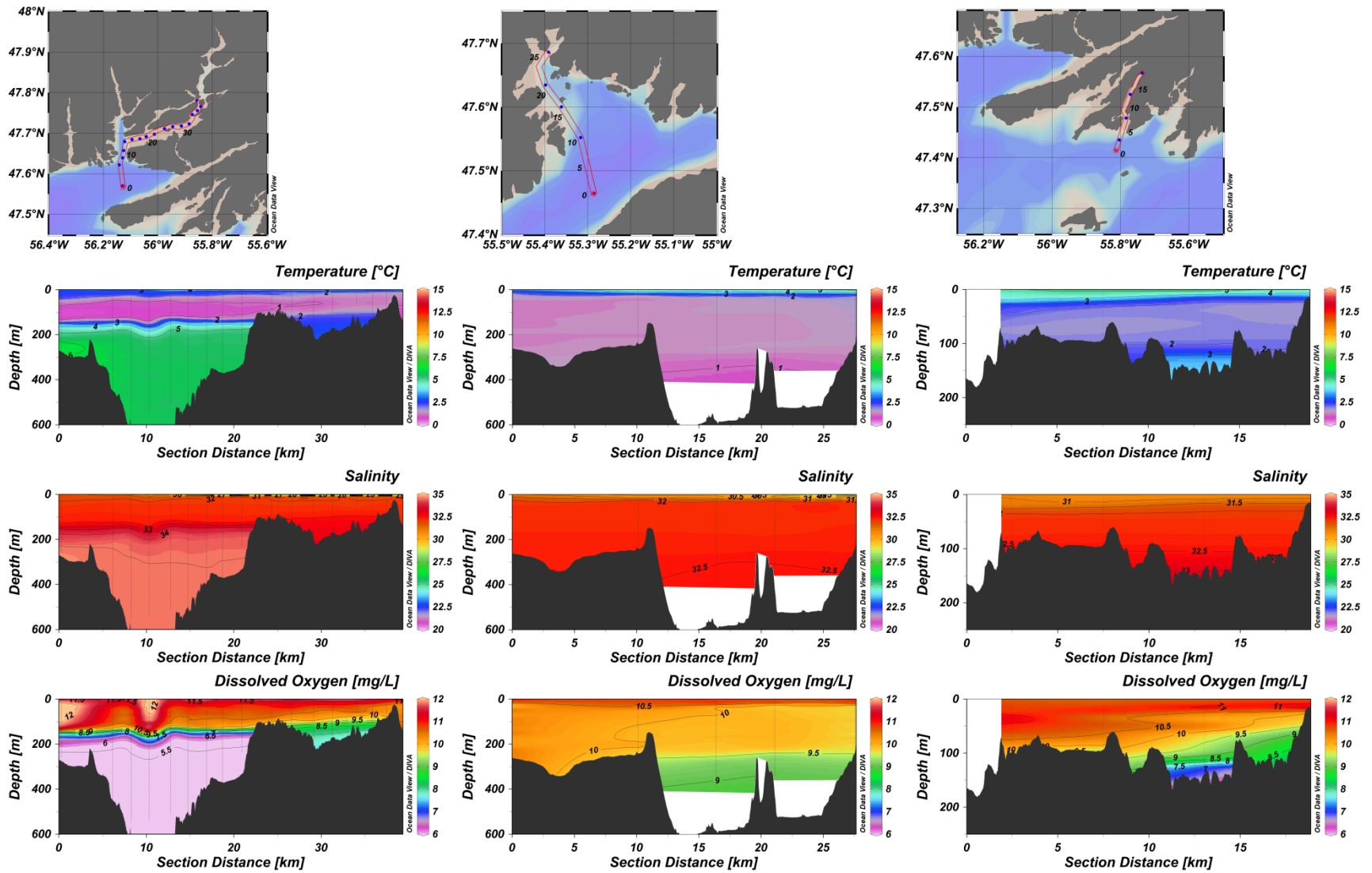


Figure 10: BDE (April-May 2010), BB (May 2011) and CP (May 2011) hydrographic sections.

The halocline (and thus, pycnocline) depth in UBDE was found to be consistently around 3-3.5 m, in agreement with the previous studies of MSRL (1980), Tlusty et al. (1999) and Pepper et al. (2003 and 2004). In HB, the pycnocline deepened to depths as shallow as 6 m (May 2013) and as deep as 22 m (November 2013). In FB-BB, the pycnocline ranged from 6 m to 16 m in May and from 3 m to 7 m in July; similar to HB. In CP, the pycnocline depths were generally much deeper (order of 20-40 m) but was also observed as shallow as 3 m in HB-NA (July 2010) and as 6 m in UCB (July 2012).

With regard to DO, lower concentration and saturation were consistently found in UBDE and NB also presented lower concentrations and saturation in June 2009 (surface and sub-surface) and September 2009 (sub-surface). As suggested by Richard and Hay (1984), isolation by winter ice may have caused some of the lower values observed (e.g. June 2009 and April-May 2010), but the conditions seen late in the summer (September 2009 and September 2012) are more difficult to explain. These observations also contrast with the results presented in BDE-DA (1984) which reported oxygen saturation at all depths during summer and winter. It also contrasts somewhat with the winter observation of Tlusty et al. (1999) which reported concentration above 8 mg/L on average at all measured depths (i.e., 1 m, 3 m, 5 m and 1 m above bottom). The effect of finfish farming on these local lower DO levels cannot be ruled out either but would necessitate more investigations. Hypoxic conditions (i.e., $DO < 6$ mg/L) as reported in Burt et al. (2011) within fish cages were not observed in the sections and areas surveyed in BB. This result indicates that weak flow conditions (leading to a low flushing rate) rather than low regional DO concentration would be responsible for the hypoxic events observed. Horizontal gradient found in May at depth and disappearing in July, however, indicates progressive (and perhaps slow) renewal of water from the mouth to the head of FB from spring to summer (e.g., Figure B(i)3 vs. Figure B(i)5); consistent with de Young (1983) description. Near-surface oxygen saturation found in July in BB of about 100% contrast, however, with the maximum values of about 70% measured in June 1982 and reported by de Young (1983).

Intermediate and bottom layer (20 m - bottom)

In agreement with Richard and Hay (1984), we find that the CIL water mass varies seasonally and inter-annually in volume, temperature and salinity. Fresher conditions were seen in spring (April-May 2010, May 2012 and May 2013), saltier conditions in late summer to fall (September 2009 and November 2013) and intermediate salinity values seen in our only early-summer survey (late June 2009). As pointed out by Richard and Hay (1984), this seasonal salinity pattern may be the result of internal mixing with the deep MSW. In fact, two processes of internal mixing possibly occur with the cold intermediate water mass from spring to fall: one with the surface layer bringing warmer (and fresher) water down and one with the deep water layer (MSW) bringing saltier (and warmer) water up. Taking 2°C as water mass boundary, the mixing with the deep MSW appears to dominate the effect on salinity during spring to fall by bringing up saltier and warmer water and winter convection appears to dominate effect on salinity during winter by bringing down cooled and relatively fresh surface water to intermediate depth.

The coldest CIL conditions were observed during the summer 2009 survey (June 18-23); even colder than the conditions seen in subsequent spring of 2010 (28 April - 03 May), 2012 (May 4-7) and 2013 (May 3-9). The warmest CIL conditions were observed during the fall 2013 survey (November 3-9; about 1.7°C in HB); however closely followed by the conditions seen in the spring 2012 survey (about 1.6°C in HB). The cold conditions of 2009 appear consistent with the offshore conditions annually reported by Colbourne et al. (e.g., Colbourne et al. 2015) which show positive anomalies (i.e., colder conditions than normal) all across the Labrador shelf to the Flemish Cap region (Figures 33 and 34 in Colbourne et al. 2015). The notably warm 2012

conditions seen in our study area, however, are more surprising. Offshore conditions showed weakly positive CIL anomalies only that year (Figures 33 and 34 in Colbourne et al. 2015), implying near-normal conditions, but conditions at station 27 (historical hydrographic station located off St. John's, 47°32.8' N, 52°35.2' W), do show 2012 as a warm year, although less so than 2010 and 2011 (Figure 20 in Colbourne et al. 2015). Since station 27 represents the conditions of the inner Labrador shelf current (see Loder et al. 1998 for an overall description of the Labrador Current branches and transport) its conditions are more likely to be coherent with those seen within the Coast of Bays albeit with some time lag. Nevertheless, 2012 contrasted with the years 2010, 2011 that showed strong positive anomalies and thus, much warmer than normal conditions. This discrepancy may indicate important local effects such as, perhaps, the strength of local winter convective overturning process, strength and frequency MSW upwelling/downwelling events and/or strength of internal mixing due to internal waves. In addition, the effect of the LCW type ($T=-0.5$ to -1 ; $S=33$) expected to happen from late spring to early fall (de Young, 1983) and clearly seen in the June 1982 and November 1983 surveys reported by Richard and Hay (1984) appears to be minimal from our surveys: no temperatures below 0°C were recorded and intrusion of cold (less than 1°C) and slightly more saline water were not seen in any of the vertical sections (see HB section in particular). Time lag (i.e., time for the cold water to be transported along with the inner branch might also play a significant role. Our results presented, however, are not sufficient to assess the possible seasonality and/or inter-annual variability of the LCW transport and its effect on the CIL.

Spring conditions in LaP-UBDE are consistent with the observations made by Richard and Hay (1984) but late-summer to fall conditions, showing an horizontal gradient with colder water towards the head of the bay (Figure A(i)27, Figure A(i)31 and Figure A(i)33) appears to differ from their horizontally uniform observations. Pointing down the exact mechanism responsible for the deep water renewal at this location is difficult and our dataset does not provide with much more clue than the previous observations. The upwelling event seen in September 2009 and described above appears to be an important mechanism judging on the clearly visible intrusion of warmer water into LaP basin in the vertical section plots (Figure A(i)27). The interpretation of this intrusion is problematic, however, since the casts located near S5 were obtained about five days prior to the ones obtained in UBDE. Estuarine circulation may play a role also in migrating the cold water up towards the head of the bay from spring to fall and in bringing water from the outer basin below the pycnocline. Internal tides could be another important mechanism, as previously suggested by Richard and Hay (1984), and as commonly seen at steep sills of stratified fjords (e.g., Farmer and Freeland 1983). In FB, the seasonal gradient of temperature (mouth to head) from cold to warm and warm to cold, first described by de Young (1983), was also observed in our data. Apparent blockage by the S1 sill of the relatively warm deep water inflow to B1 (Figure 8) is noted; contrasting with de Young (1983) May 1982 observations.

The inflow of the CIL-MSW mixture into the basin south of Bois Island (B4 in Figure 7) and the deep Little Passage basin (B10 in Figure 7) appears to be seasonal and to occur in spring or winter; consistent with previous observations indicating that this water mass is upwelled during winter-spring north-westerly to north-easterly prevailing wind (de Young 1983, Richard and Hay 1984, Hay and de Young 1989). Recent observations indicated that the response of the embayment to such forcing can be fast, showing vertical displacement of the water mass of the order of 60 m over a period of about five days (Ratsimandresy et al. 2014). The presence of CIL-MSW mixture, most notable in spring, with temperatures of the order of 3°C in BDE basins B4 (bounded by the sill S3 of 107 m limiting depth) and B10 (S10, 109 m) and in CB basins B2 (S4, 106 m), B3 (S8, 124 m), B4 (S11, 131 m) and HB-NA basins B7 (S5, 117 m), B8 (S13, 86 m), support this seasonal inflow and a vertical displacement of the pycnocline of the order of 50 m or more (the 3°C isotherm being located at about 150-200 m depth in HB). In fact, Hay and

de Young (1989) reported a vertical displacement as large as 100 m from their observations around Miquelon Sill.

Hydrographic zones

Based on the above analysis, hydrographic zones (i.e., zone of common or similar hydrographic characteristics) are proposed (Figure 11 to Figure 13). Each zone is defined by a somewhat unique set of characteristics based on: surface (2 m) temperature, salinity and DO, near-surface (0-20 m) vertical gradient of temperature and salinity, pycnocline depth (0-100 m) and deep (>100 m) water characteristics.

In BDE, the following zones are proposed:

- UBDE: very low surface salinity (<5-15), very shallow pycnocline (<5 m) and large near-surface vertical gradients salinity (5-12/m, maximums, respectively) outside areas of mixing (e.g., Tickle Head, S7 in Figure 7) associated with large horizontal gradient of temperature and salinity (up to ~3°C/km and ~5/km, respectively), relatively low sub-surface DO concentration and saturation in fall (<9 mg/L and <90%, respectively) and zone potentially subject to upwelling
- LaP: low surface salinity with significant horizontal gradient (10-20) with values increasing downstream, high surface temperature (>5°C in spring to >18°C in summer) and shallow pycnocline (<5 m), warmer sub-surface temperature than UBDE in fall (colder in spring to early summer), no presence of MSW at depth and high sub-surface DO levels from spring to fall, separated from UBDE, BIS and LBDE by sills (S6, S4 and S5 in Figure 7, respectively) which either impede deep water exchange (S4 and S5) and/or induce vertical mixing (S4, S5 and S6)
- BIS (Bois Island South): low surface salinity particularly in fall (~15-20 in summer-fall; ~24-28 in spring), strong horizontal cross channel gradients of salinity and temperature (~1.5/km and up to 2°C/km, respectively), zone potentially subject to upwelling on its eastern side, presence of MSW mixture at depth (i.e., slightly colder and fresher water than MSW), shallow pycnocline (~5 m), separated from LBDE and LiP zones by sills restricting deep flow and inducing vertical mixing (S3 and S11, respectively)
- LBDE: transition zone receiving input from the upper branch of the fjord resulting in significant surface horizontal gradients of temperature and salinity (~1-2°C/km and 1-2/km, respectively), shallow pycnocline (~5-10 m), high surface temperature (12-16°C in summer, ~9°C in fall and ~4-5°C in spring), brackish surface salinity (~20-30 in summer-fall, ~25-30 in spring), presence of MSW at depth (deepest parts), zone potentially subject to large burst of sub-surface primary production in spring
- NB: brackish surface salinity with clear influence of runoff from the head (~22-26 in summer and ~25-30 in spring), high temperature (~12-16°C in summer, ~4-6°C in spring), relatively low surface and sub-surface DO (<8 mg/L) in early to late summer; pycnocline depth from ~5 m (early summer) to ~10 m (late summer and spring) stronger towards the head, presence of MSW at depth, separated from LBDE by the sill S8 (Figure 7) limiting the inflow of MSW and potentially inducing sub-surface mixing
- EB: brackish surface salinity with clear influence of runoff from the head (S~20-23 in summer, S<30 in spring), high temperatures (>15°C in summer and increasing onshore, >3°C in spring and increasing onshore), low surface DO levels in early summer (<8 mg/L); slight MSW mixture (T>2°C, S>32 and DO<8 mg/L in summer, DO<11 mg/L in spring) within the deepest basin located just behind S9 (Figure 7)

-
- LiP: brackish surface salinity gradient (~25-30 in summer-fall to 30-31 in spring) indicating a southward flow restricted at S11 (Figure 7) which induces vertical mixing, slightly cooler surface temperature than in LBDE (~13°C in summer, ~8°C in fall and ~3°C in spring), shallow pycnocline (~5-10 m), presence of MSW mixture limited to the deepest basin located just behind S10 (Figure 7)
 - IHB: brackish surface salinity with clear influence of runoff from the head (~28-30 in summer-fall and 30-31 in spring), slightly lower surface temperature than in most of BDE (~12 in summer, 8 in fall and 3-5°C in spring), pycnocline depth varying from ~5 m (in spring) to ~20 m (in fall), presence of MSW at depth, and zone potentially subject to upwelling
 - OHB (Outer HB): surface salinity almost oceanic (~30-31 in summer-fall and ~31 in spring), lower surface temperature than in BDE (~10-12°C in summer, ~7°C in fall and ~3-5°C in spring), near-surface vertical temperature and salinity gradient of about 0.1-5°C/m and 0.5-2.5 m, respectively (weaker than in BDE), pycnocline depth varying from ~5 m (in spring) to ~20 m (in fall), presence of MSW at depth, zone potentially subject to large burst of sub-surface primary production in spring.

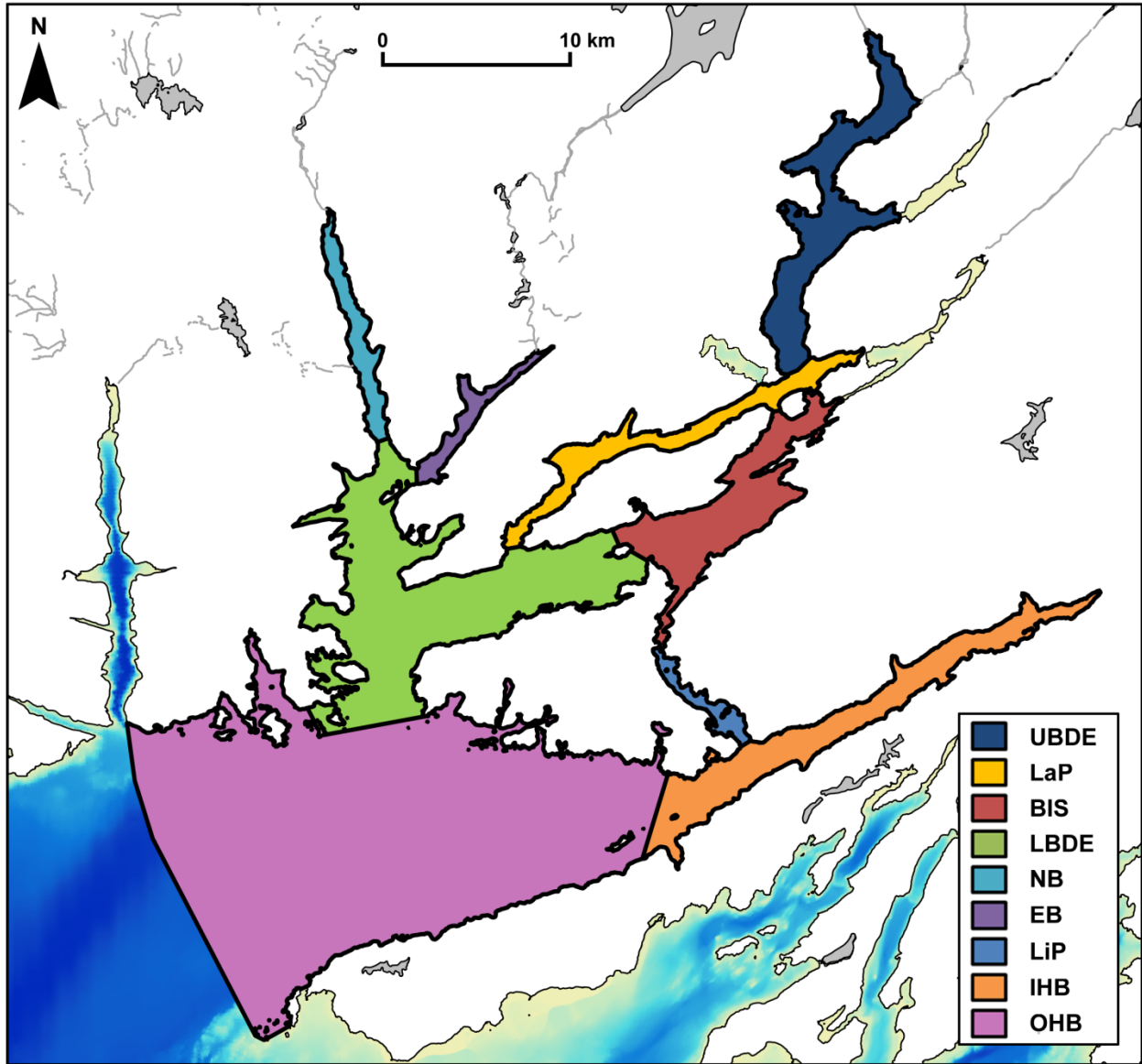


Figure 11: BDE hydrographic zones.

In BB, the following zones are proposed:

- BBN (BB North): large horizontal gradient of surface salinity ($\sim 1\text{-}2.5/\text{km}$), high surface temperature ($\sim 5\text{-}7^\circ\text{C}$ in spring and $\sim 12\text{-}15^\circ\text{C}$ in summer) and low surface salinity ($\sim 25\text{-}29$ in both spring and summer), very shallow pycnocline (< 5 m in both spring and summer).
- BBW: surface salinity $\sim 29\text{-}30.5$ in both spring and summer, surface temperature $\sim 4\text{-}5^\circ\text{C}$ in spring and $\sim 11\text{-}12^\circ\text{C}$ in early summer, more strongly stratified in early summer than spring (near-surface vertical density gradient of $\sim 3 \text{ kg/m}^3/\text{m}$ vs $\sim 2 \text{ kg/m}^3/\text{m}$, maximums, respectively), no apparent influence of MSW mixture at depth.
- BBE: slightly lower surface salinity ($\sim 29\text{-}30$) and higher surface temperature ($> 5^\circ\text{C}$ for the most part) than BBW in spring, much less stratified than BBW ($\sim 0.5 \text{ kg/m}^3/\text{m}$ in spring and $\sim 0.8 \text{ kg/m}^3/\text{m}$, maximums, respectively), small MSW mixture at depth (deepest parts).

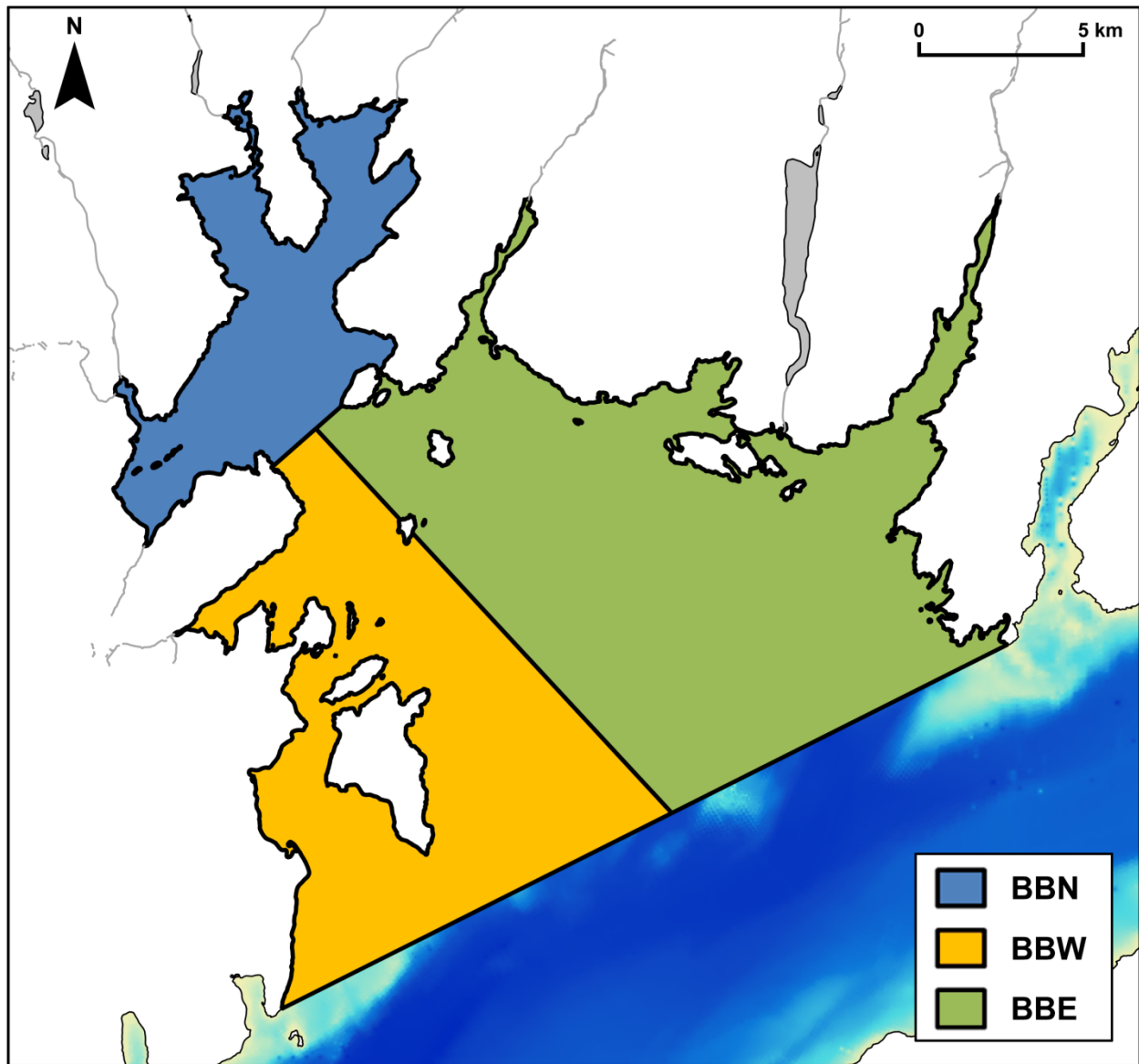


Figure 12: BB hydrographic zones.

In CP, the following zones are proposed:

- UCB: zone potentially subject to upwelling, no presence of MSW as depth, no evidence of freshwater runoff effect, surface salinity ~32 in spring and ~31.5 in fall but could be as low as about 30 in summer, surface temperature ~4°C in spring and ~8°C in fall, surface DO ~11 mg/L in spring and ~9 mg/L in fall, pycnocline ~20 m in spring and ~80 m in fall, separated from CCB by S12 impeding inflow of MSW origin water.
- CCB (Central CB): zone subject to limited inflow of MSW mixture at depth in spring or winter (and maybe not every year) and appears subject to local runoff at the surface, surface salinity ~31-32 in spring and ~31 in fall with potential local runoff effects, surface temperature ~4°C in spring and ~8°C in fall, surface DO ~11 mg/L in spring and ~8-9 mg/L in fall, pycnocline depth ~25-45 m in spring to ~70 m in fall, separated from OCB and GHB by S8 and S9&S10, respectively (Figure 9).

- GHB (Great Harbour Bight): basin isolated from inflow of MSW mixture at depth (deduced from maximum sill depths and conditions seen in nearby CCB and OCB basins), zone does not seem to be subject to local runoff, surface temperature, surface salinity and surface DO conditions equivalent to conditions in OCB.
- OCB (Outer CB): seasonal presence of MSW mixture at depth, surface salinity ~31.5 in spring and fall, surface temperature ~4-5°C in spring and 8-9°C in fall, surface DO ~11 mg/L in spring and ~9 mg/L in fall, pycnocline depth ~25-45 m in spring to ~70 m in fall.
- UHB-NA (Upper HB-NA): zone potentially subject to upwelling, no presence of MSW at depth, surface salinity ~31-31.5 in spring, ~29 in early summer and ~30.5-31 in fall, surface temperature ~5°C in spring, >16°C in summer and ~8°C in fall, surface DO ~10-11 mg/L in spring, ~8-9 mg/L in summer, and ~9 mg/L in fall, pycnocline depth ~15-30 m in spring, <5 m in summer and ~30 m in fall, separated from LHB-NA by S14.
- LHB-NA (Lower HB-NA): seasonal presence of MSW mixture at depth, surface salinity ~31.5 in spring, ~29 in early summer and ~31 in fall, surface temperature ~4-5 in spring, >16 in summer and 8-9°C in fall, surface DO ~10-11 mg/L in spring, ~8-9 mg/L in summer, and ~9 mg/L in fall, pycnocline depth ~15-30 m in spring, <5 m in summer and ~30 m in fall.
- UGBDE (Upper GBDE): zone potentially subject to upwelling, no presence of MSW mixture at depth, surface salinity <30 (or less) to ~31.5 in spring and 29-30 in summer, surface temperature ~5-6°C in spring and >14°C in summer, surface DO ~10-11 mg/L in spring and ~9 mg/L in summer, pycnocline depth ~20-25 m in spring and <5 m in summer.
- LGBDE (Lower GBDE): presence of MSW at depth (maybe year-round), surface salinity ~30-31.5 in spring and ~29-30.5 in summer, surface temperature ~4-5°C in spring and >14°C in summer, surface DO ~10-11 mg/L in spring, ~8-9 mg/L in summer, and ~9 mg/L in fall, pycnocline depth ~15-30 m in spring, <5 m in summer and ~30 m in fall.

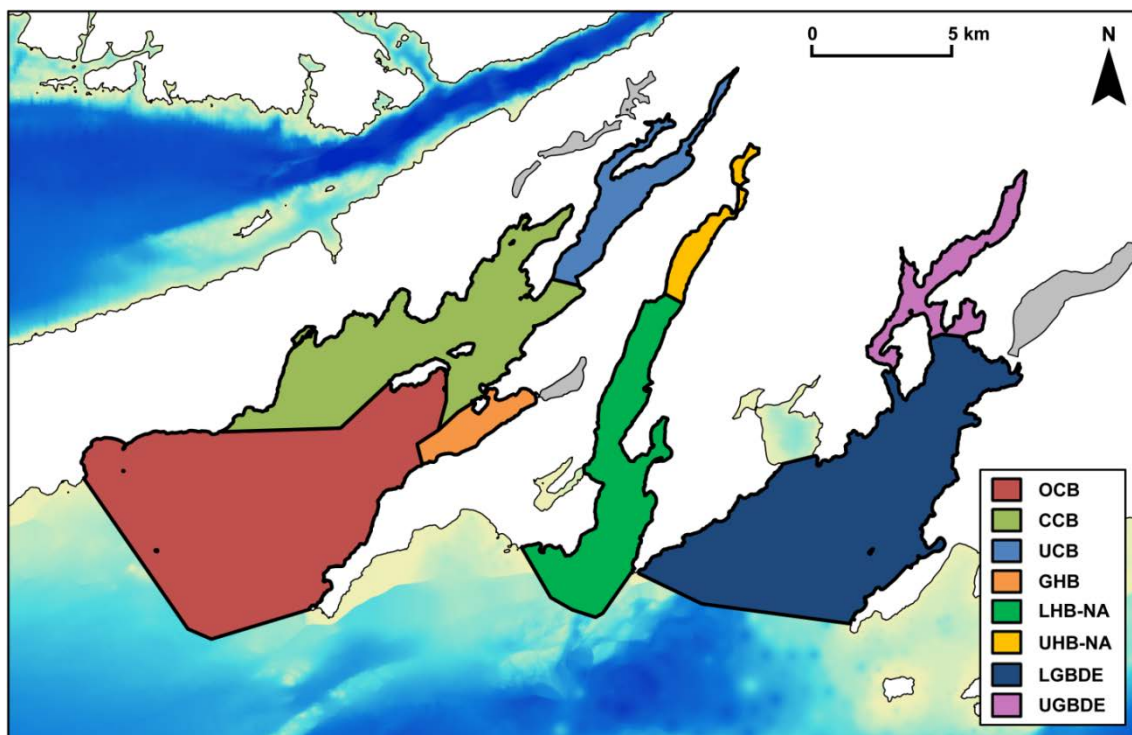


Figure 13: CP hydrographic zones.

SHORT TERM VARIATIONS

Upwelling features were seen in all three regions during our 2009-13 surveys: in September 2009 in the HB-BDE region, in May 2011 in LH (FB region) and in May 2012 in the CP and HB regions. To the exception of the event of May 2011 in LH, all upwelling events were supported by Sagona Island weather station data (Appendix E), located to the south of Connaigre Peninsula (Figure 1) and indicating winds blowing from the northern quadrant during each of those events (Figure E1). These findings are consistent with the mechanism described in Hay and de Young (1989) for a two layers system, in winter (i.e., deep water renewal) and our data suggest that a similar mechanism can also occur in spring-summer, in a two to three layers system (i.e., surface and intermediate water advection). These findings, however, contrast with the description proposed by Yurick and Vanstone (1983) which indicated a lack of upwelling events in the region.

Large supersaturated DO cells were found in both HB and in the deep outer basin of BDE (B3 in Figure 7) coinciding with vertical displacement of the deep pycnocline depth. While the vertical displacement of the isopleths are thought to be due to internal oscillations (potentially internal tide generated at Hermitage Sill, S2, Figure 7, and at the Hermitage Bank, Figure 1) and that the super-saturation are thought to be due phytoplankton bloom, the origin of the supposedly short-lived “burst” in primary production is unclear since no large vertical mixing associated with the isopleths displacement is apparent. In addition, since the stations of those transects were taken one to two days apart, the distinction between the temporal and spatial aspects of these large features cannot really be made.

Notable temperatures and salinity variation were seen along FB in May 2011. Here again, the distinction between the temporal and spatial aspects cannot be made due to the sampling limitation. Possible mechanisms that could be at the origin of this feature, however, could be upwelling and/or coastal trapped waves such as those reported in Conception Bay by de Young and co-workers in the 1990's (e.g., de Young et al. 1993).

STUDY LIMITATIONS

While a comprehensive spatial coverage of the region has been obtained through the 2009-13 PARR program, the temporal resolution is still scarce and does not allow a good understanding of the large short-term (order of hours to days), seasonal and inter-annual variations. In particular, and due to logistical constraints (weather and access to a suitable boat), no data were collected neither during the warmest nor during the coldest months of the year (July-August, and February-March, respectively and as reported in Donnet et al. 2017).

The interpretation of important short-term changes/events (upwelling events, DO super-saturation and deep pycnocline vertical displacement, freshwater runoff) are presently impeded by the lack of data (time series in particular); requiring further data collection to better understand the related forcing.

Data needs to be collected in the winter to better understand why the UBDE region offers relatively more favourable temperature conditions for over-wintering than other areas in NL as originally reported by Taylor in 1975 and the MSRL report in 1980. If there is little doubt that ice cover is responsible for an effective thermal isolation from the cold atmosphere and, at the same time, a reduced vertical mixing, in some areas such as Roti Bay in BDE, it is not known why other ice-covered sites such as the inlets along Hermitage Bay reported in MSRL (1980) and BDE-DA (1984) presented less favourable sub-surface water temperature conditions. In particular, the horizontal homogeneity of relatively warm water in the sub-surface layer reported by Richard and Hay (1984) in the LaP-UBDE section in fall contrasts with the horizontal gradient from relatively warm to cold water towards UBDE seen in our observations which undermine the

idea of a pre-conditioning. It is possible, however, that the slightly warmer sub-surface water that we observed in the first part of the LaP-UBDE in September 2009 and November 2013 migrated its way towards the head of bay during the fall-early winter, driven by larger freshwater discharge and favourable winds from the northern quadrant occurring during that time of the year (Donnet et al. 2017). Clearly, a better understanding of the processes responsible for these regional differences would be useful for the management of the expected aquaculture expansion to other regions along the South Coast of NL.

CONCLUSION AND RECOMMENDATIONS

This study significantly updates previous hydrographic knowledge of the BDE and FB-BB region and presents, for the first time, the conditions within the bays of the CP region. The results of this study show the presence of two main water masses topped by a seasonal surface layer within the Coast of Bays area (Figure 1). The distribution of these main water masses varies from a bay to another (or a region to another) due, mainly, to topographic features (i.e., sills) which impede or limit water exchanges. The surface layer is strongly affected by freshwater runoff which varies greatly from a bay to another but is also not distributed evenly within a given bay. As a result of these geographical differences, three main hydrographic regions as well as a number of hydrographic zones within those regions are defined (Figure 11 to Figure 13). While those zones can help with the delineation of BMAs, they should be considered neither alone nor definitive. i.e., they would likely change upon further research and a better understanding of the area. In particular, a better spatial and temporal resolution in the assessment of short-term (i.e., order of hours to days), seasonal and inter-annual variations is needed. Within the aquaculture activities context, the creation of water structure climatology for each of the bays, or regions, of the Coast of Bays area and an assessment of short-term variability are necessary. To this aim, further analyses of existing data are required and additional CTD data collection is recommended. This climatology and additional analyses are needed for further development of the numerical model currently being implemented by Fisheries and Oceans Canada and for the understanding of the following:

- Water structure seasonality and inter-annual variability; which would provide input data to the numerical model (baroclinic mode) as well as providing key information on sea-lice proliferation potential (e.g., understanding the seasons more at risk).
- Water structure short-term variations due, for instance, to wind events and/or internal waves; of interest to fish health (e.g., physical environment conditions inducing stress and/or affecting wellbeing).
- Winter conditions and potential processes leading to more sheltered/favourable over-wintering conditions.
- Water stratification build-up and destruction timescales and vertical extent; of interest to fish-health and the understanding of superchill events.
- Effect of climate change on the area and how it relates to the offshore and regional/larger scale conditions presently being regularly monitored by the Atlantic Zone Monitoring Program (AZMP). This aspect having important and various implications to the sustainability of the aquaculture development.

ACKNOWLEDGEMENTS

This work was funded by DFO's Program for Aquaculture Regulatory Research (PARR). The authors thank the technical staff from the aquaculture and biotechnology section of DFO (Northwest Atlantic Fisheries Centre), for their help and effort in collecting the data. The authors also thank Mike Foreman, Eugene Colbourne, Brian Petrie and Dounia Hamoutene for their helpful review and comments which significantly improved this work.

REFERENCES

- Bay d'Espoir Development Association (BDE-DA). 1984. Salmonid Aquaculture in Bay d'Espoir – a Development Plan. Volume III. Bay d'Espoir Development Association, St. Alban's.
- Bugden, G. L. 1991. Changes in temperature-salinity characteristics of the deeper waters of the Gulf of St. Lawrence over the past several decades. *In* The Gulf of St. Lawrence: small ocean or big estuary? Edited by J.-C. Therriault. Can. Spec. Publ. Fish. Aquat. Sci. 113. p. 139-147.
- Chang, B.D., Coombs, K.A. and Page, F.H. 2014b. The development of the salmon aquaculture industry in southwestern New Brunswick, Bay of Fundy, including steps toward integrated coastal zone management. *Aquaculture Economics and Management*. 18(1): 1-27.
- Chang, B.D., Page, F.H., Losier, R.J., Lawton, P., Singh, R., and Greenberg, D.A. 2007. [Evaluation of Bay Management Area Scenarios for the Southwestern New Brunswick Salmon Aquaculture Industry: Aquaculture Collaborative Research and Development Program Final Project Report](#). Can. Tech. Rep. Fish. Aquat. Sci. 2722: v + 69 p.
- Colbourne, E. B. and Murphy, E. F. 2008. [Physical oceanographic conditions in NAFO Division 3P during 2007 - potential influences on the distribution and abundance of Atlantic cod \(*Gadus morhua*\)](#). DFO Can. Sci. Advis. Sec. Res. Doc. 2008/027. iv + 22 p.
- Colbourne, E., Holden, J., Senciall, D., Bailey, W., Craig, J. and S. Snook. 2015. [Physical Oceanographic Conditions on the Newfoundland and Labrador Shelf during 2014](#). DFO Can. Sci. Advis. Sec. Res. Doc. 2015/053. v+ 37 p.
- de Young, B., and Hay, A.E., 1987. Density current flow into Fortune Bay, Newfoundland. *Physical Oceanography*. 17(7): 1066-1070.
- de Young, B., Otterson, T. and Greatbatch, R. J. 1993. The Local and Nonlocal Response of Conception Bay to Wind Forcing. *Physical Oceanography*. 23(12): 2636-2649.
- de Young, B.S. 1983. Deep water exchange in Fortune Bay. Theses (M.Sc.) Memorial University of Newfoundland, St. John's, NL.
- Department of Fisheries and Aquaculture. 2014a. Economic Impacts of the Newfoundland and Labrador Aquaculture Industry. Government of Newfoundland and Labrador.
- Department of Fisheries and Aquaculture. 2014b. Newfoundland and Labrador Sustainable Aquaculture Strategy 2014. Government of Newfoundland and Labrador.
- Department of Fisheries and Aquaculture. 2015. [Locations of aquaculture licences](#). Accessed November 2015.
- Donnet, S., Ratsimandresy, A.W., Goulet, P., Doody, C., Burke, S., and Cross, S. 2017. Coast of Bays Metrics: Geography, Hydrology and Physical Oceanography of an Aquaculture Area of the South Coast of Newfoundland. DFO Can. Sci. Advis. Sec. Res. Doc. 2017/076. x+ 108 p

-
- Dyer, K.R. 1997. *Estuaries: A Physical Introduction*. Second edition. John Wiley and Sons Ltd., West Sussex.
- El-Sabh, M. I. 1977. Oceanographic Features, Currents, and Transport in Cabot Strait. Fisheries Research Board of Canada. 34(4): 516-528.
- Farmer, D. M. and Freeland, H. J. 1983. The Physical Oceanography of Fjords. *Progress in Oceanography*. 12(2): 147-194.
- Fofonoff, N. P. and Millard, R. C. 1983. Algorithms for computation of fundamental properties of seawater. Unesco (44). Paris, France. 55 p.
- Garcia, H. E. and Gordon, L. I., 1992. Oxygen solubility in seawater: Better fitting equations. *Limnology and Oceanography*. 37(6): 1307–1312.
- Hay, A. E. and de Young, B. 1989. An Oceanographic Flip-Flop: Deep Water Exchange in Fortune Bay, Newfoundland. *Geophysical Research*. 94(C1): 843-853.
- Intergovernmental Oceanographic Commission (IOC). 2010. [The international thermodynamic equation of seawater – 2010: Calculation and use of thermodynamic properties](#). IOC Manuals and Guides No. 56. Paris, France.
- Marine Sciences Research Laboratory (MSRL), 1980. Bay d'Espoir Aquaculture Feasibility Study. Marine Sciences Research Laboratory. St John's, NL:
- McLellan, H. J. 1957. On the Distinctness and Origin of the Slope Water off the Scotian Shelf and its Easterly Flow South of the Grand Banks. Fisheries Research Board of Canada. 14(2): 213-239.
- Owens, W. B. and Millard, R. C. 1985. A New Algorithm for CTD Oxygen Calibration. *Physical Oceanography*. 15(5): 621–631.
- Pepper, V.A., Nicolls, T., Collier, C., Watkins, V., Barlow, E., and Tlusty, M.F. 2003. [Quantitative performance measurement of alternative North American salmonid strains for Newfoundland aquaculture](#). Can. Tech. Rep. Fish. Aquat. Sci. 2502: vi + 53 p.
- Pepper, V.A., Withler, R., Nicholls, T. and Collier, C., 2004. [Quantitative marine performance evaluation of a Newfoundland Atlantic salmon strain for Bay d'Espoir aquaculture](#). Can. Tech. Rep. Fish. Aquatic. Sci. 2540: vi +44 p.
- Petrie, B., Akenhead, S., Lazier, J. & Loder, J., 1988. The Cold Intermediate Layer on the Labrador and Northeast Newfoundland Shelves, 1978-86, Dartmouth, NS: NAFO.
- Petrie, B., K. Drinkwater, D. Gregory, R. Pettipas and A. Sandstrom. 1996a. [Temperature and salinity atlas for the Scotian Shelf and the Gulf of Maine](#). Can. Tech. Rep. Hydrogr. Ocean Sci. 171: v + 398 pp.
- Petrie, B., K. Drinkwater, A. Sandstrom, R. Pettipas, D. Gregory, D. Gilbert and P. Sekhon. 1996b. [Temperature, salinity and sigma-t atlas for the Gulf of St. Lawrence](#). Can. Tech. Rep. Hydrogr. Ocean Sci. 178: v + 256 pp.
- Ratsimandresy, A.W., Page, F., Mabrouk, G., Losier, R., Drover, D., Ings, D., and McCurdy, P. 2012. [Aquaculture Drifter Programme: Progress Update 2010](#). DFO Can. Sci. Advis. Sec. Res. Doc. 2011/127. vi + 41 p.
- Ratsimandresy, A.W., Donnet, S., Goulet, P., Bachmayer, R., and Claus, B 2014. [Variation in the structure of the water column as captured by Slocum glider CTD and by CTD from a research vessel and assessment of internal waves](#). IEEE. St. John's, NL.
-

-
- Richard, J.M., and Hay, A.E., 1984. The physical oceanography of Bay d'Espoir, Newfoundland. Memorial University of Newfoundland. Newfoundland Institute for Cold Ocean Science, St. John's, Newfoundland.
- Schlitzer, R. 2015. [Ocean Data View](#). Accessed August 2017.
- Simpson, J.H. 1997. Physical processes in the ROFI regime. *Marine Systems*. 12(1-4): 3-15.
- Taylor, V.R. 1975. A Preliminary Assessment of Newfoundland Near-Shore Areas as Potential Sites for Salmonid Mariculture. Environment Canada, Fisheries and Marine Service, St. John's:
- Thomson, R.E., and Emery, W. J. 2014. *Data Analysis Methods in Physical Oceanography*. Third Edition. Elsevier, Waltham, MA. 728 p.
- Thrusty, M.F., Pepper, V.A. and Anderson, M.R. 1999. [Environmental monitoring of finfish aquaculture sites in Bay d'Espoir Newfoundland during the winter of 1997](#). Can. Tech. Rep. Fish. Aquat. Sci. No. 2273: vi + 34 p.
- Troupin, C., Barth, A., Sirjacobs, D., Ouberdous, M., Brankart, J M., Brasseur, P, Rixen, M., Alvera-Azcárate, A., Belounis. M., Capet, A., Lenartz. F., Toussaint, M.-E., and Beckers. J.-M. 2012. Generation of analysis and consistent error fields using the Data Interpolating Variational Analysis (Diva). *Ocean Modelling*. 52-53: 90-101.
- White, M., and Hay, A.E. 1994. Dense overflow into a large silled embayment: Tidal modulation, fronts and basin modes. *Marine Research*. 52(3): 459-487.
- Yurick, D.B., and Vanstone, M.C.1983. A Biological and Oceanographic Study of the Baie D'Espoir Region, Newfoundland, Volume 1. Final Report To: Parks Canada, Department of the Environment, Ottawa.

**APPENDIX A(I): HERMITAGE BAY – BAY D'ESPOIR (HB-BDE) VERTICAL
SECTIONS**

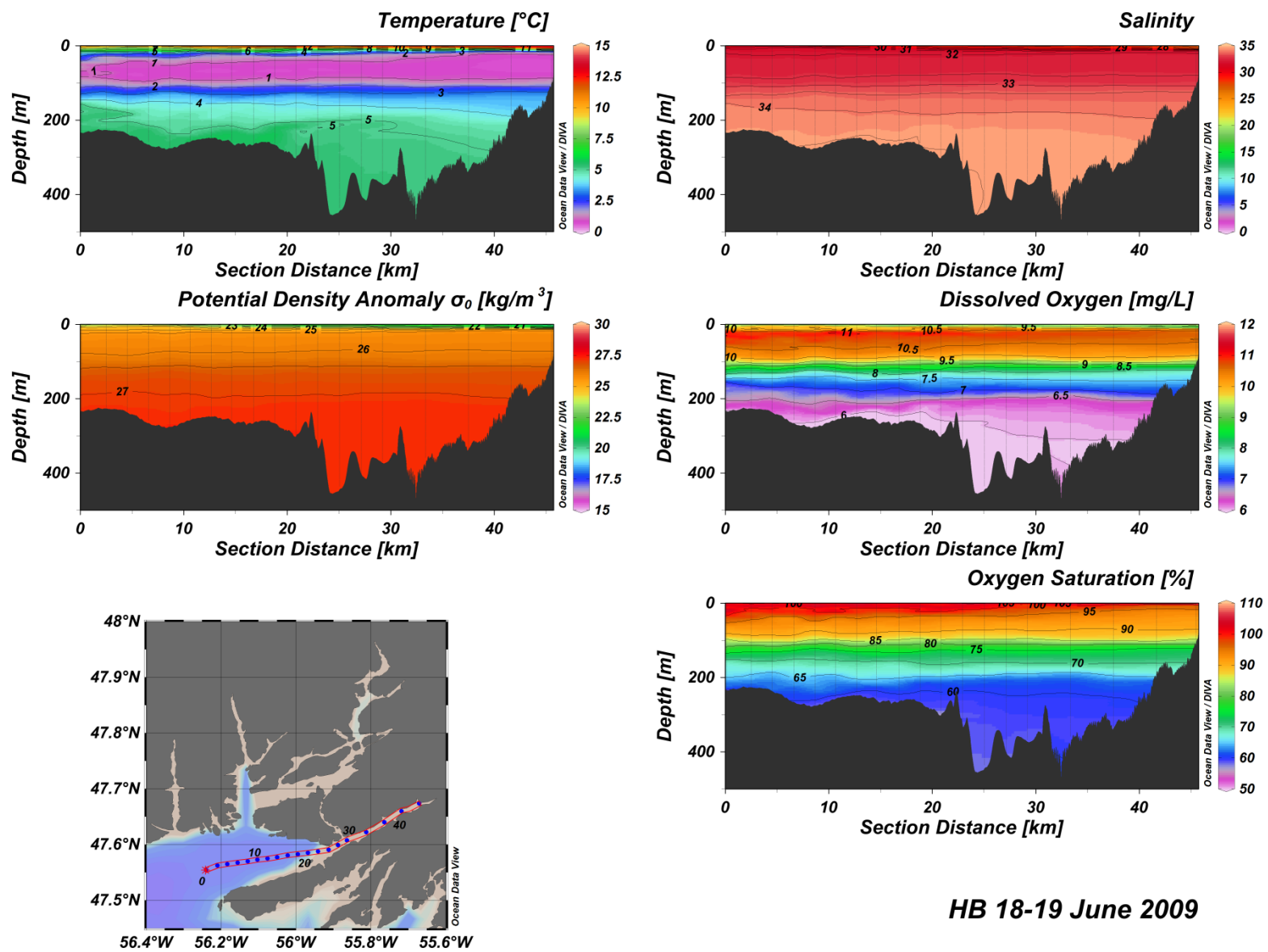


Figure A(i)1: Hermitage Bay water column vertical structure.

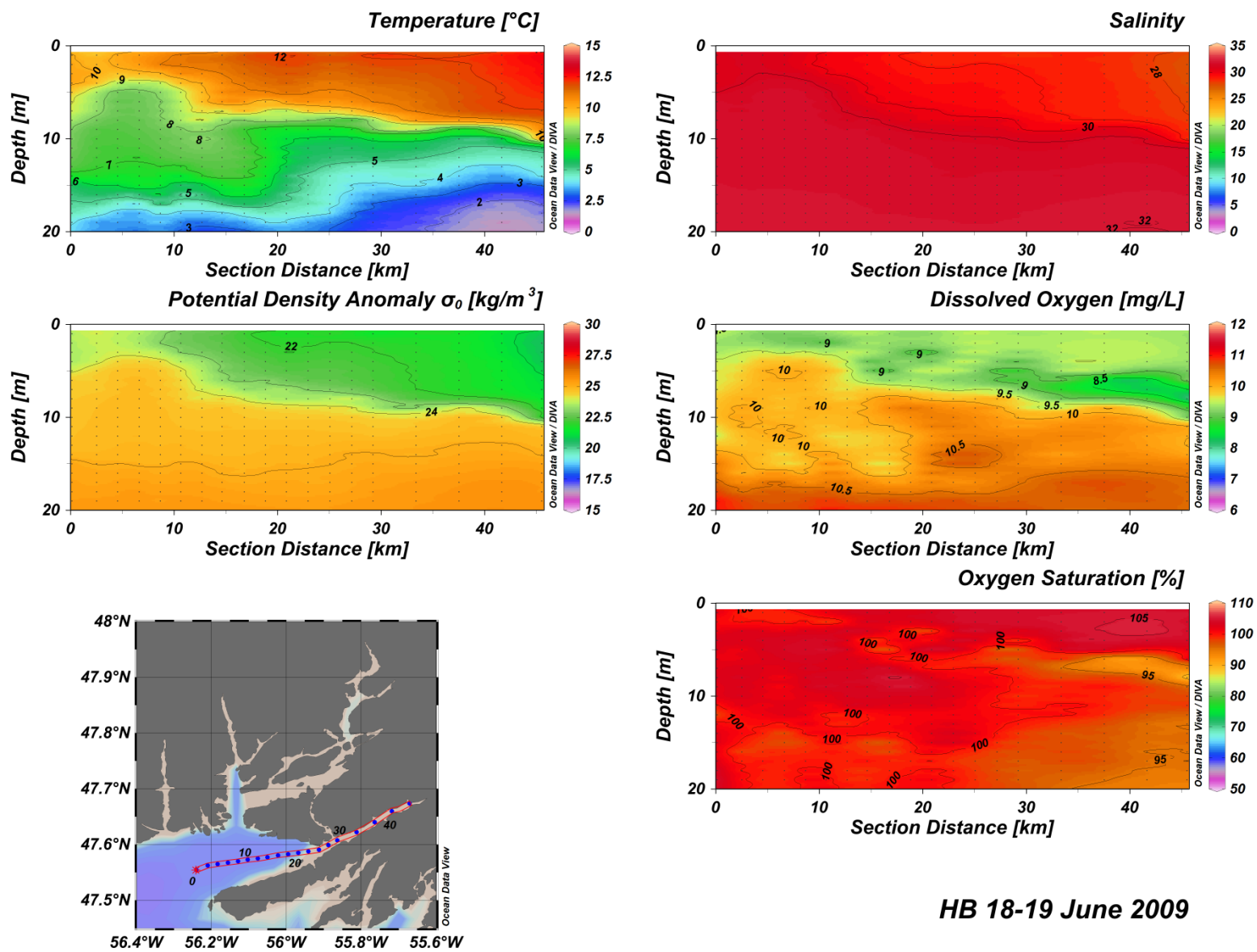
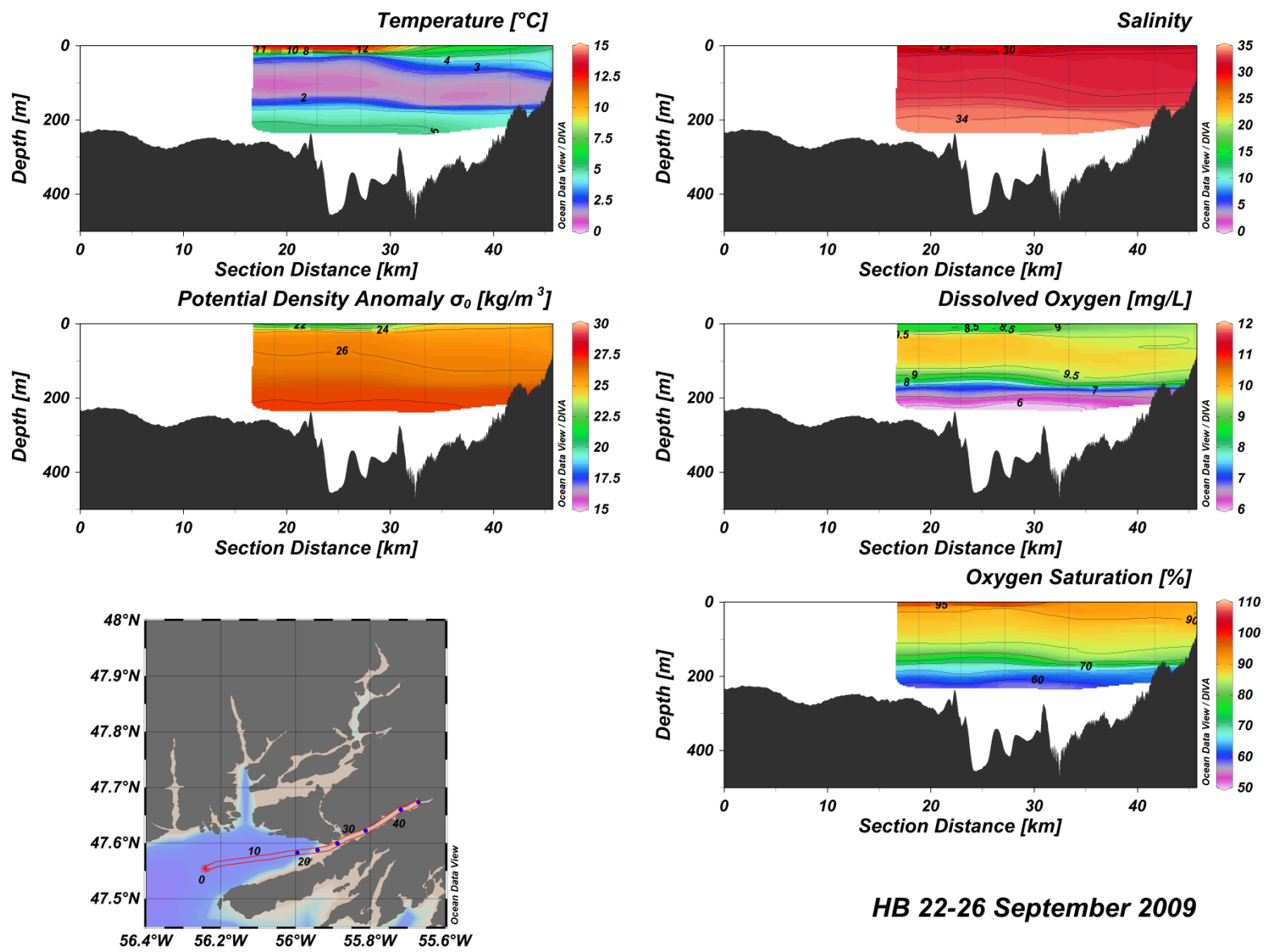


Figure A(i)2: Hermitage Bay water column vertical structure.



HB 22-26 September 2009

Figure A(i)3: Hermitage Bay water column vertical structure.

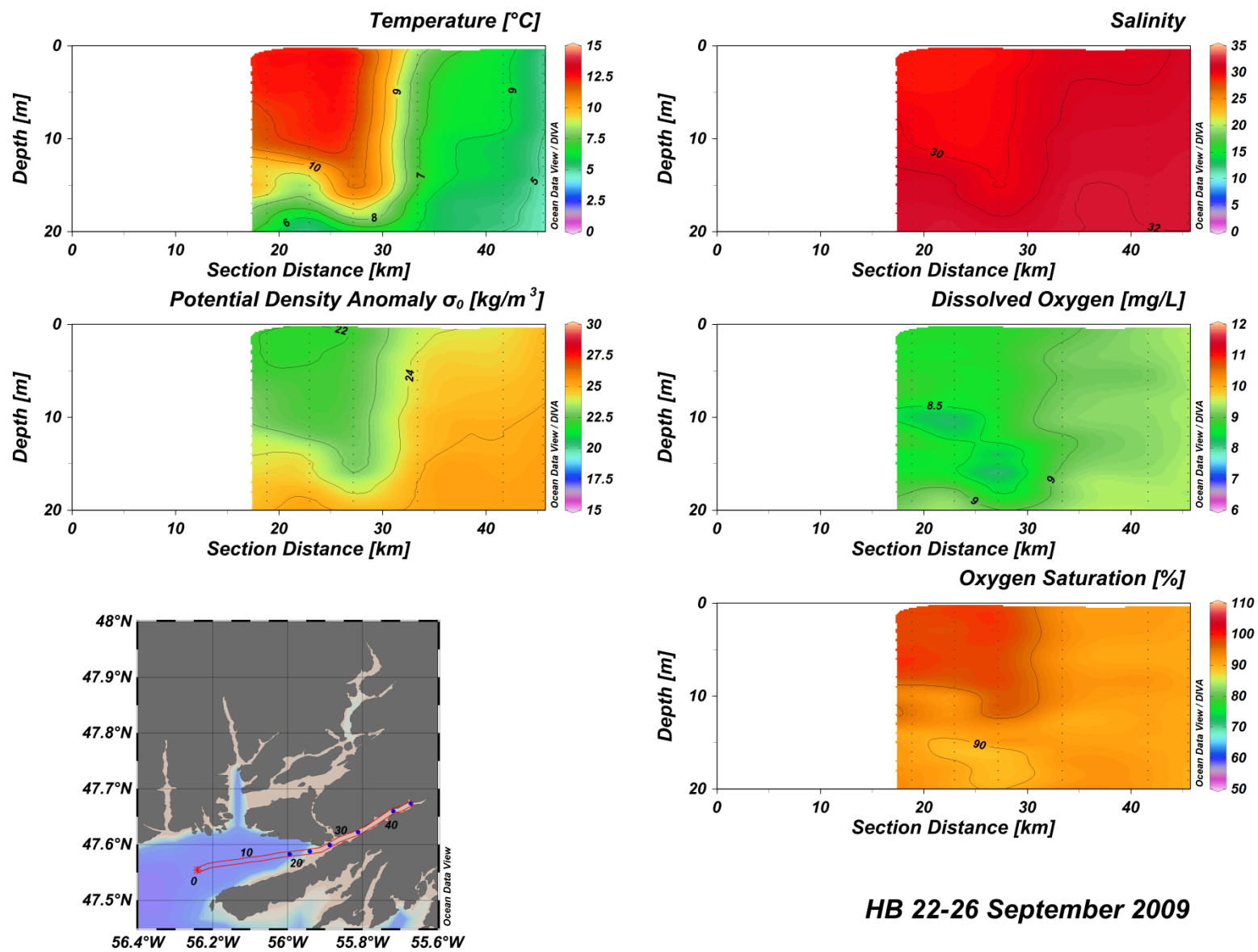


Figure A(i)4: Hermitage Bay water column vertical structure.

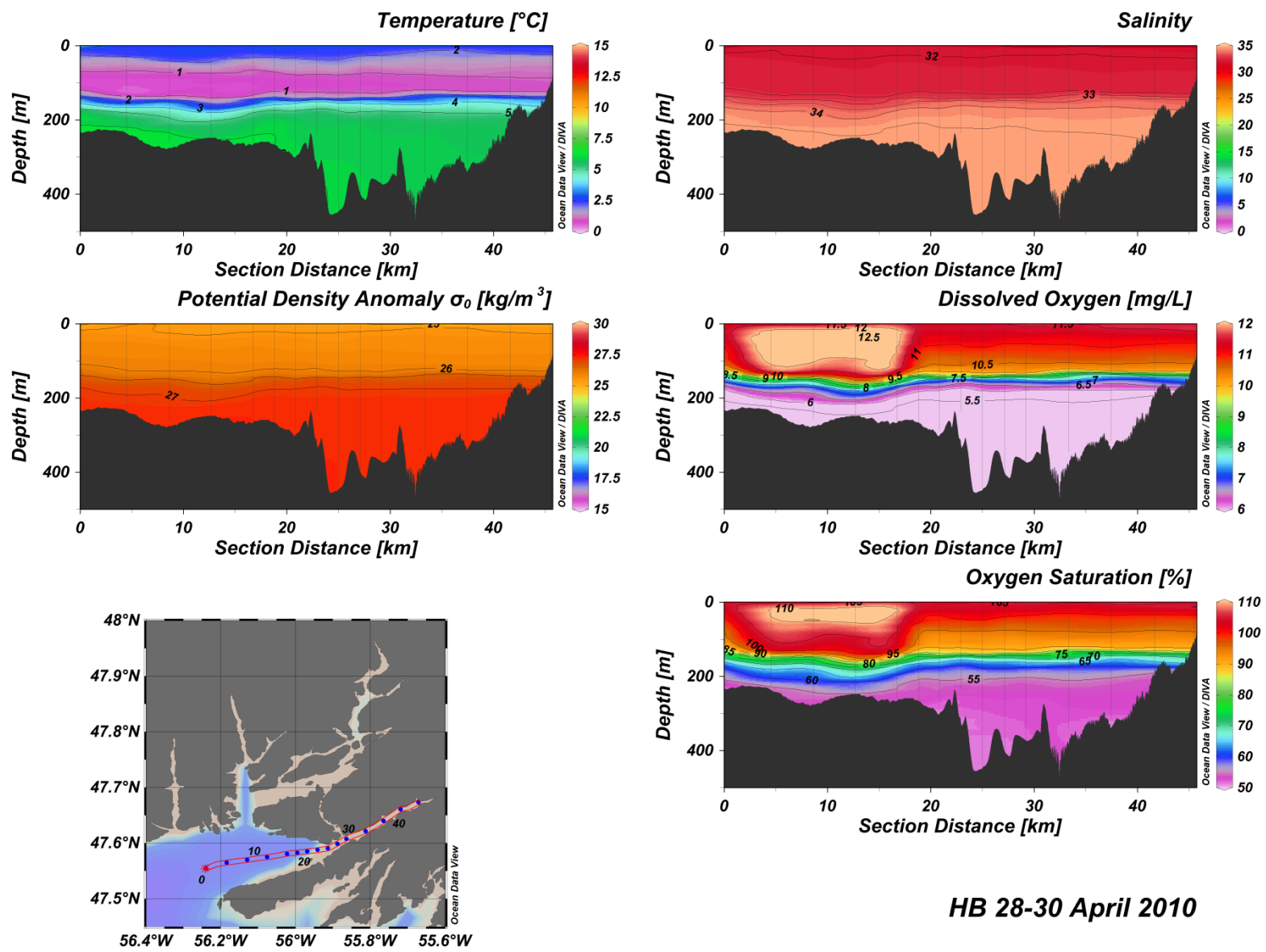
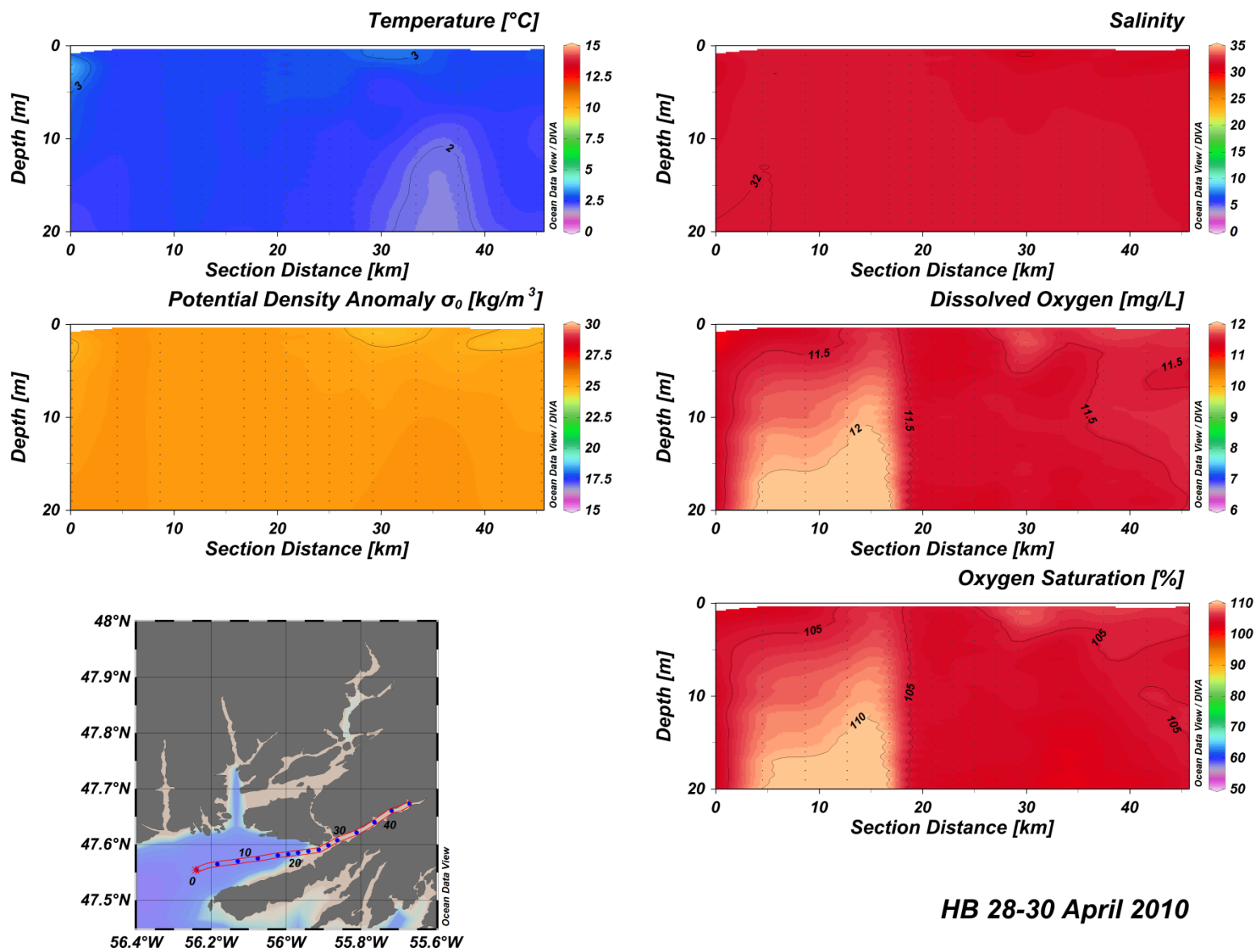
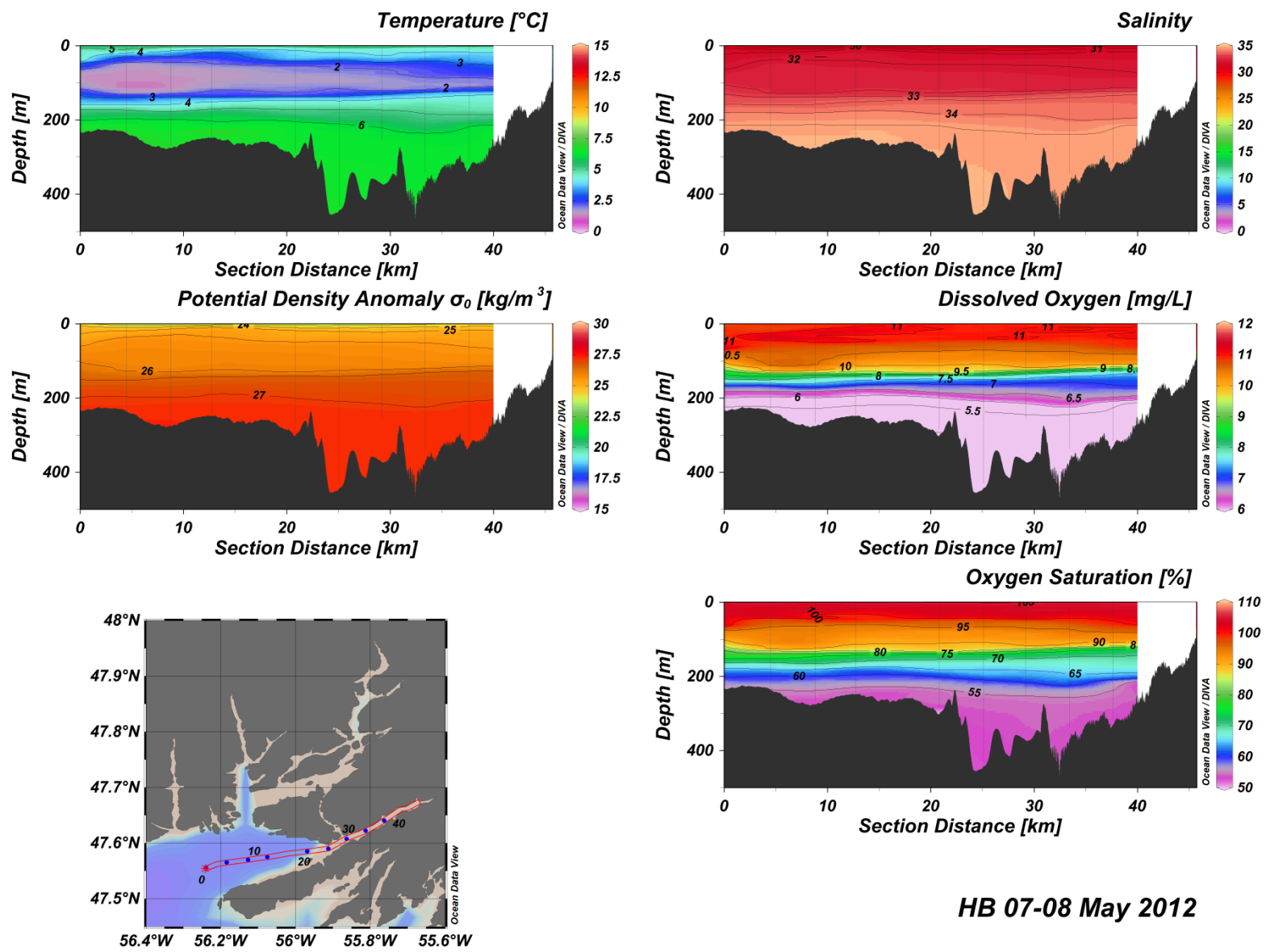


Figure A(i)5: Hermitage Bay water column vertical structure.



HB 28-30 April 2010

Figure A(i)6: Hermitage Bay water column vertical structure.



HB 07-08 May 2012

Figure A(i)7: Hermitage Bay water column vertical structure.

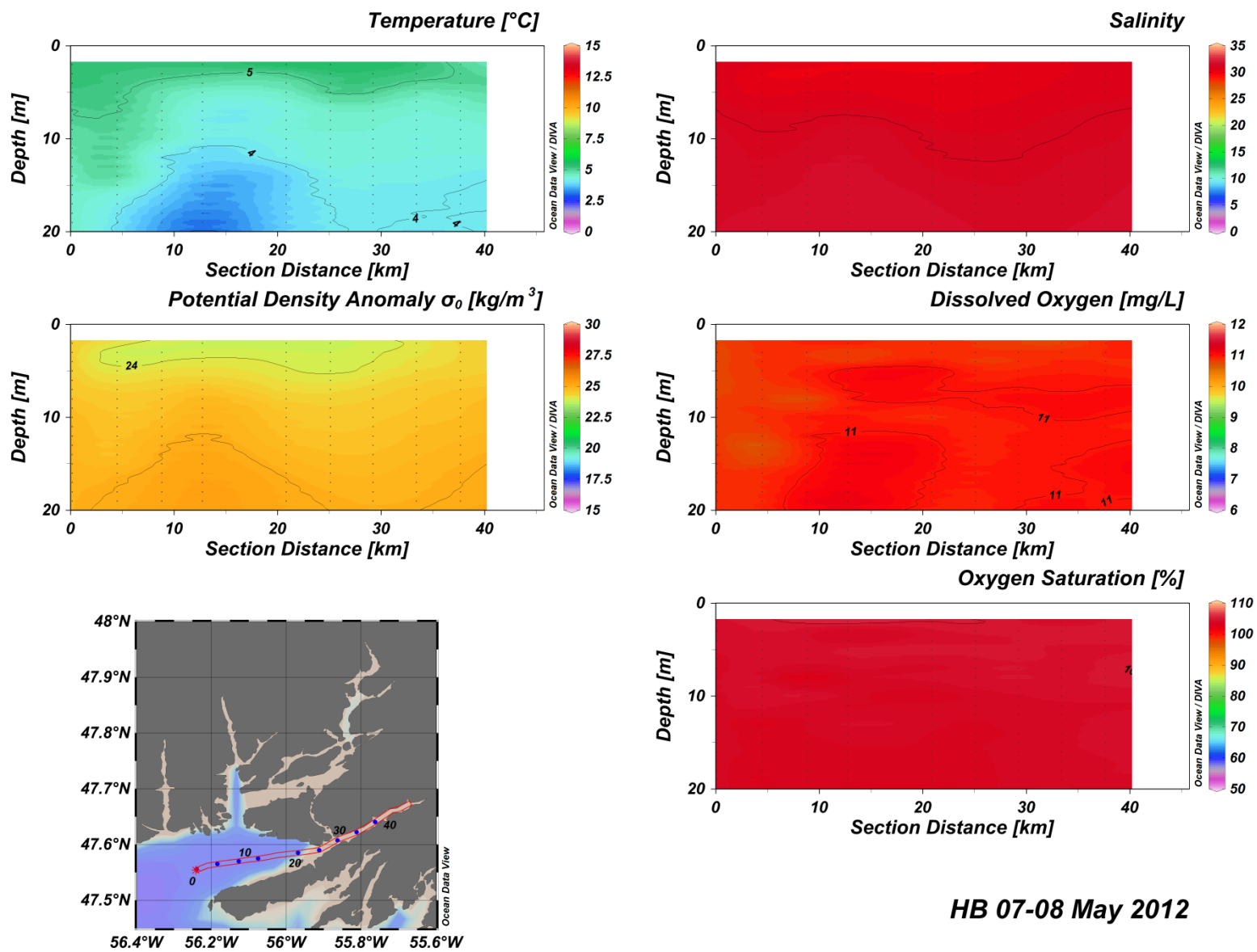


Figure A(i)8: Hermitage Bay water column vertical structure.

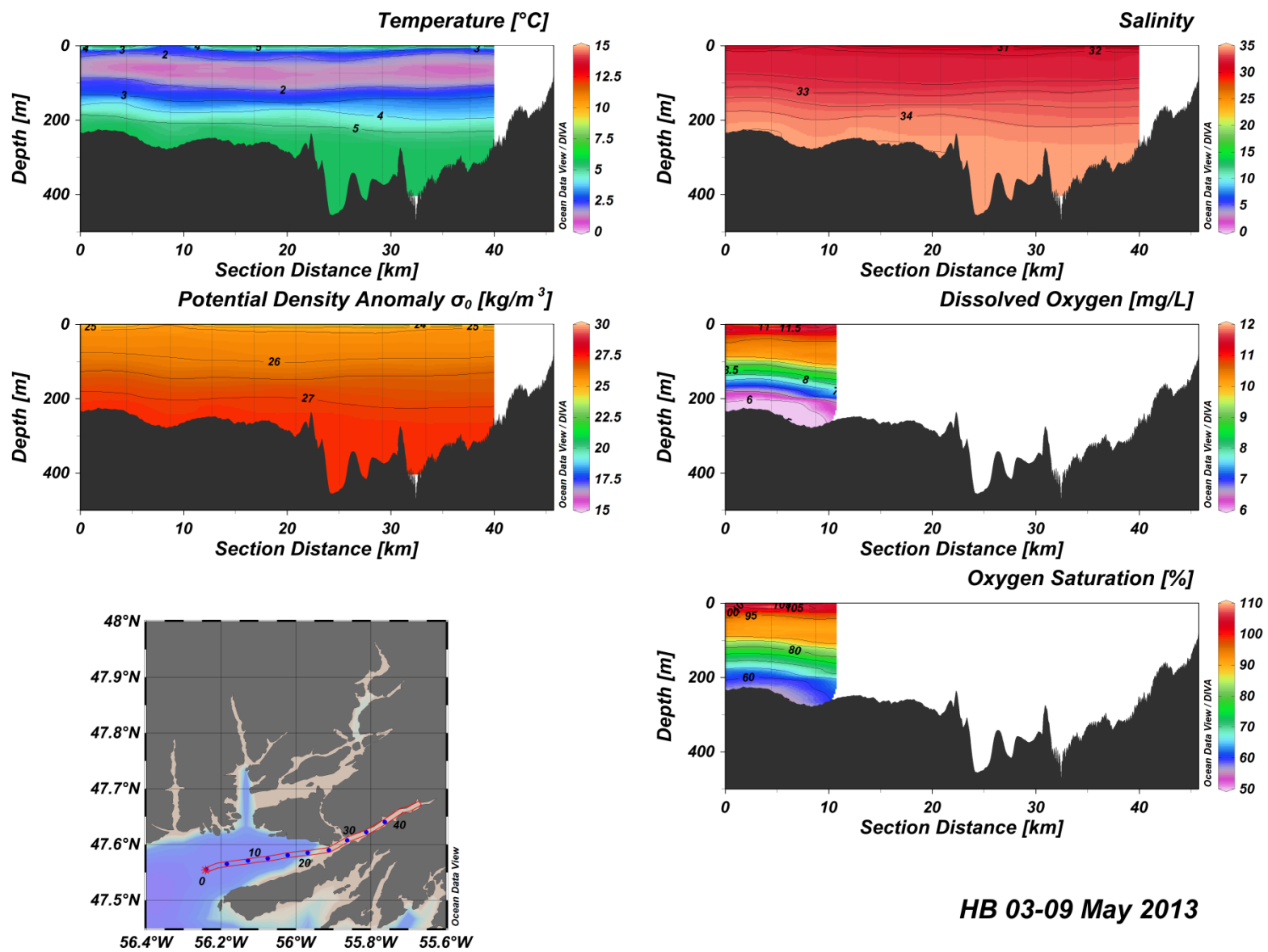


Figure A(i)9: Hermitage Bay water column vertical structure.

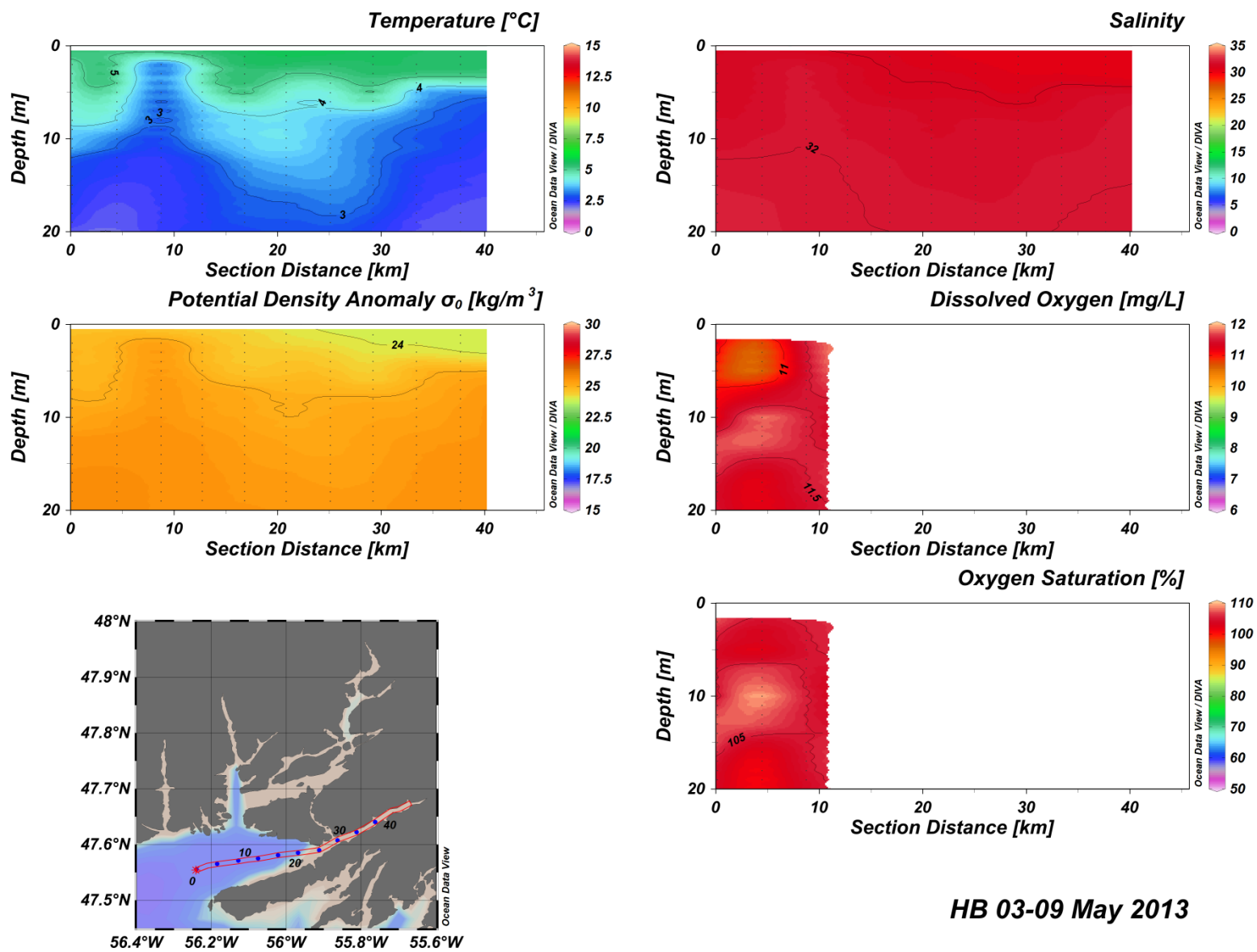


Figure A(i)10: Hermitage Bay water column vertical structure.

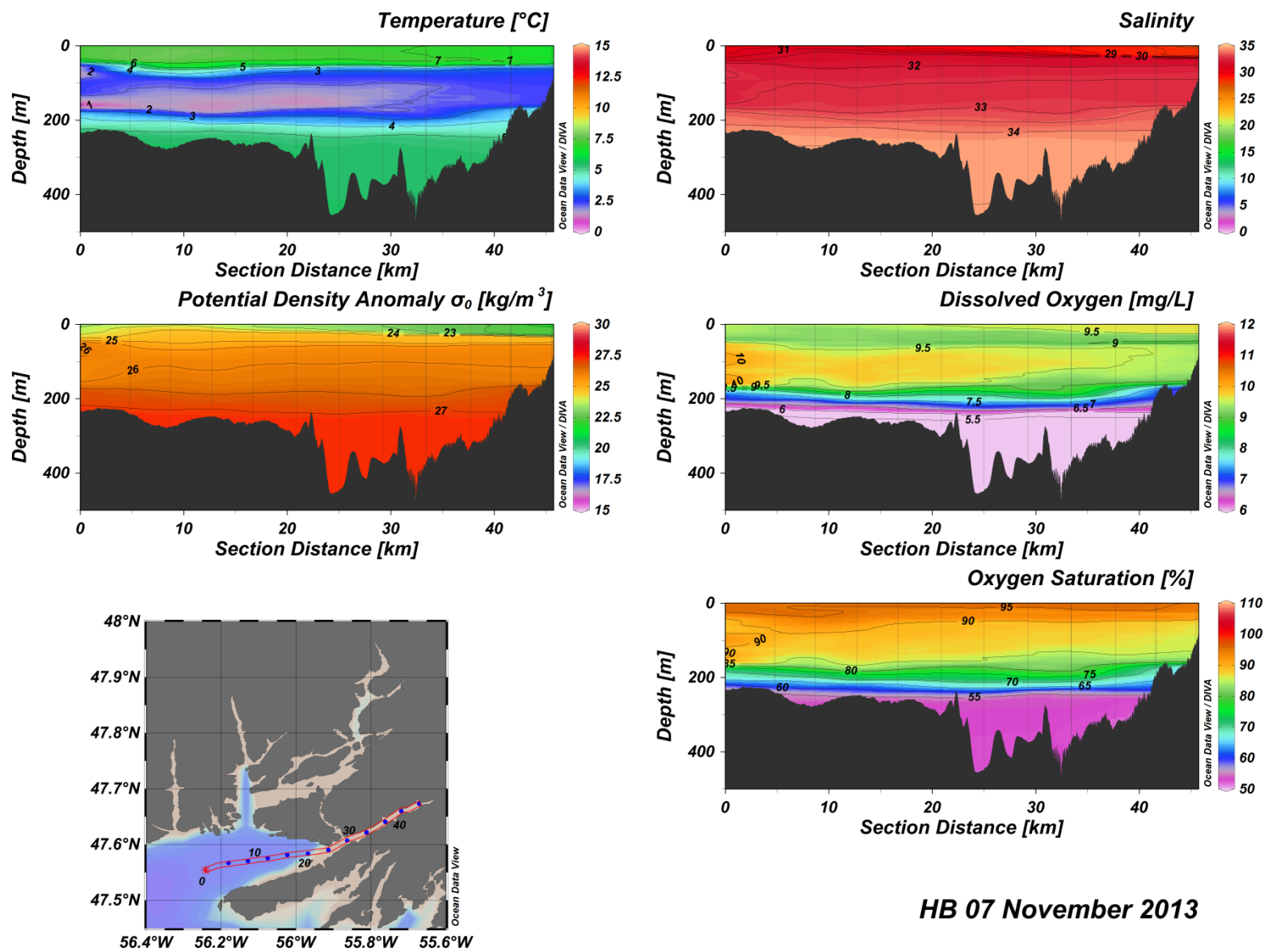


Figure A(i)11: Hermitage Bay water column vertical structure.

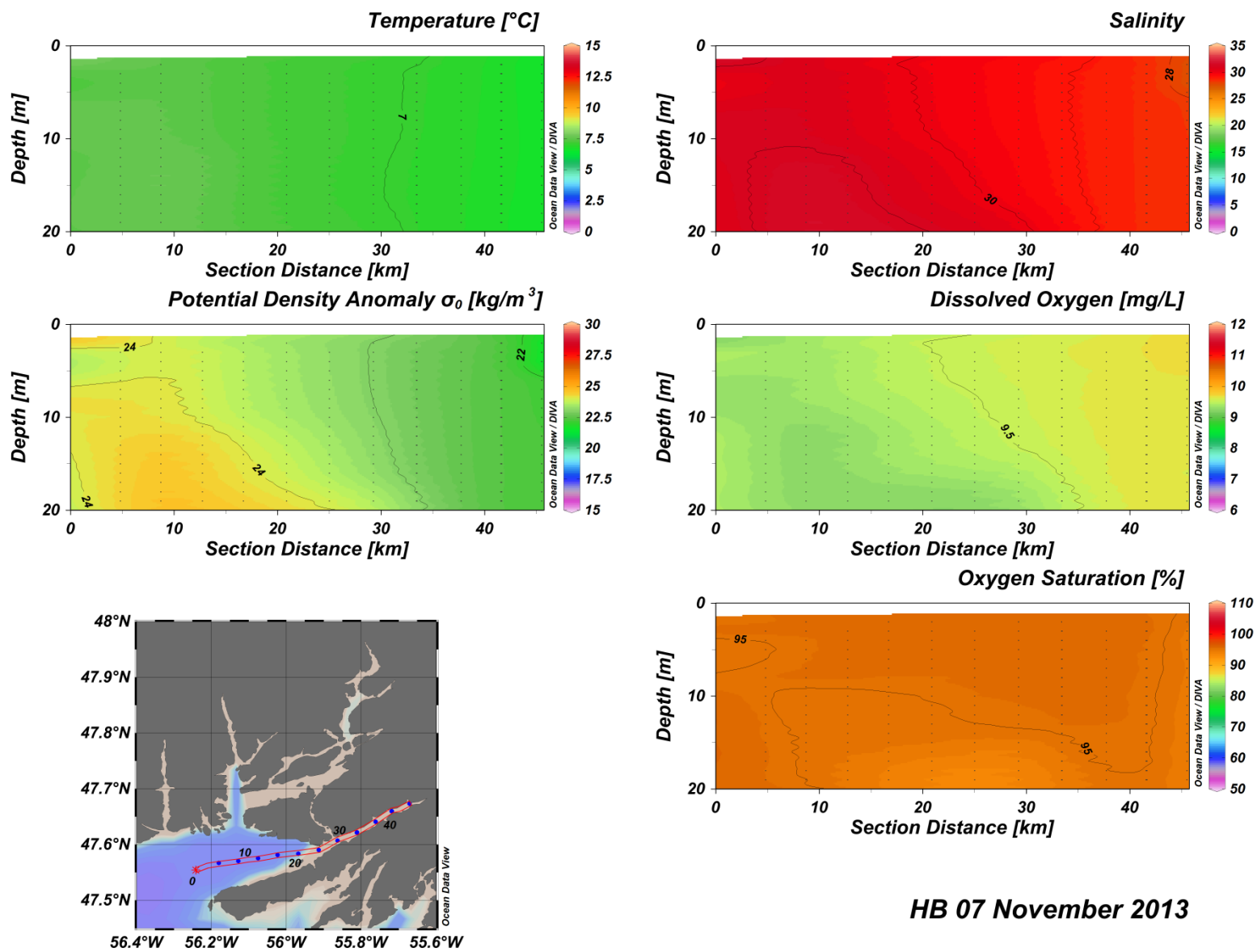


Figure A(i)12: Hermitage Bay water column vertical structure.

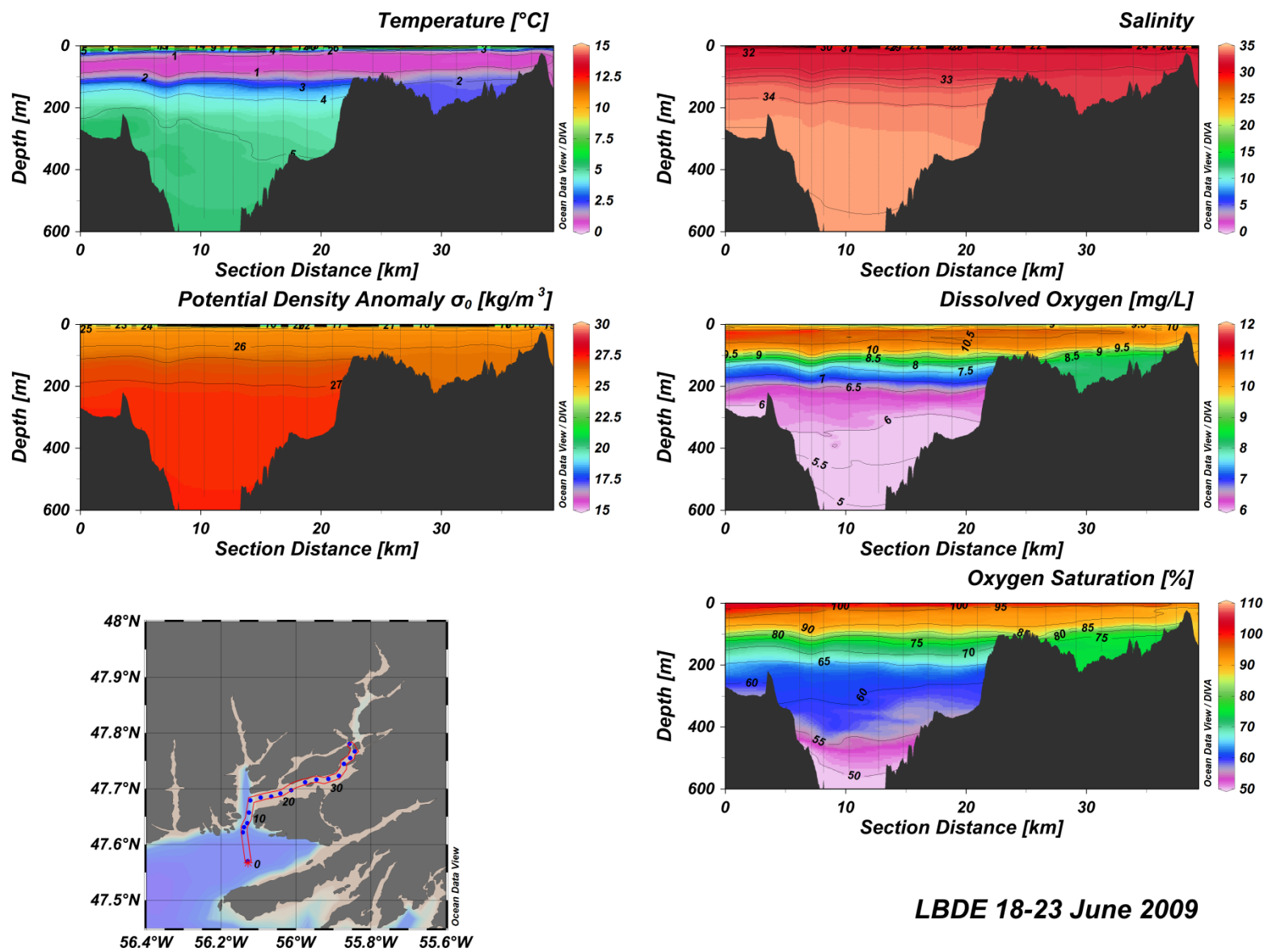


Figure A(i)13: Lower Bay d'Espoir water column vertical structure.

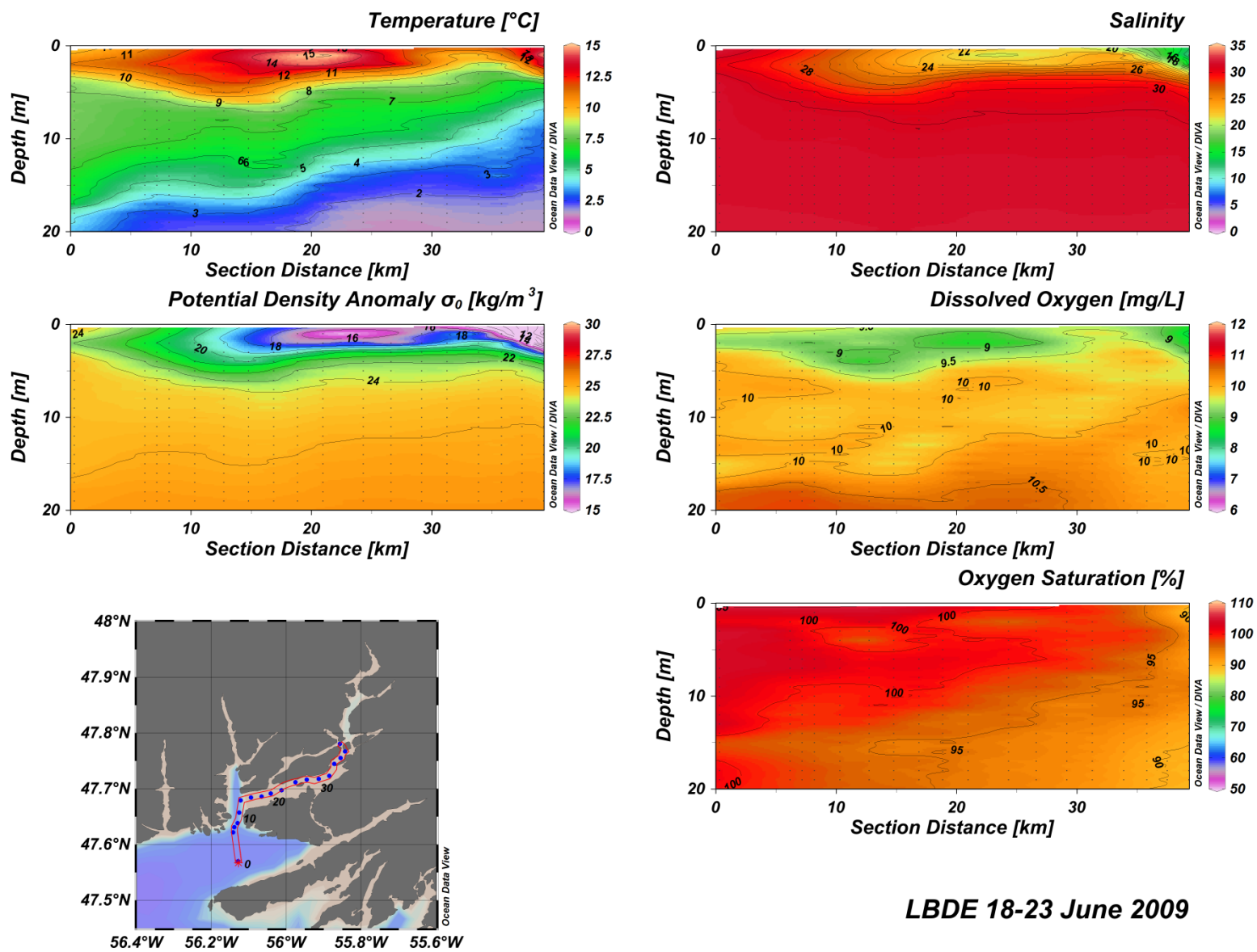


Figure A(i)14: Lower Bay d'Espoir water column vertical structure.

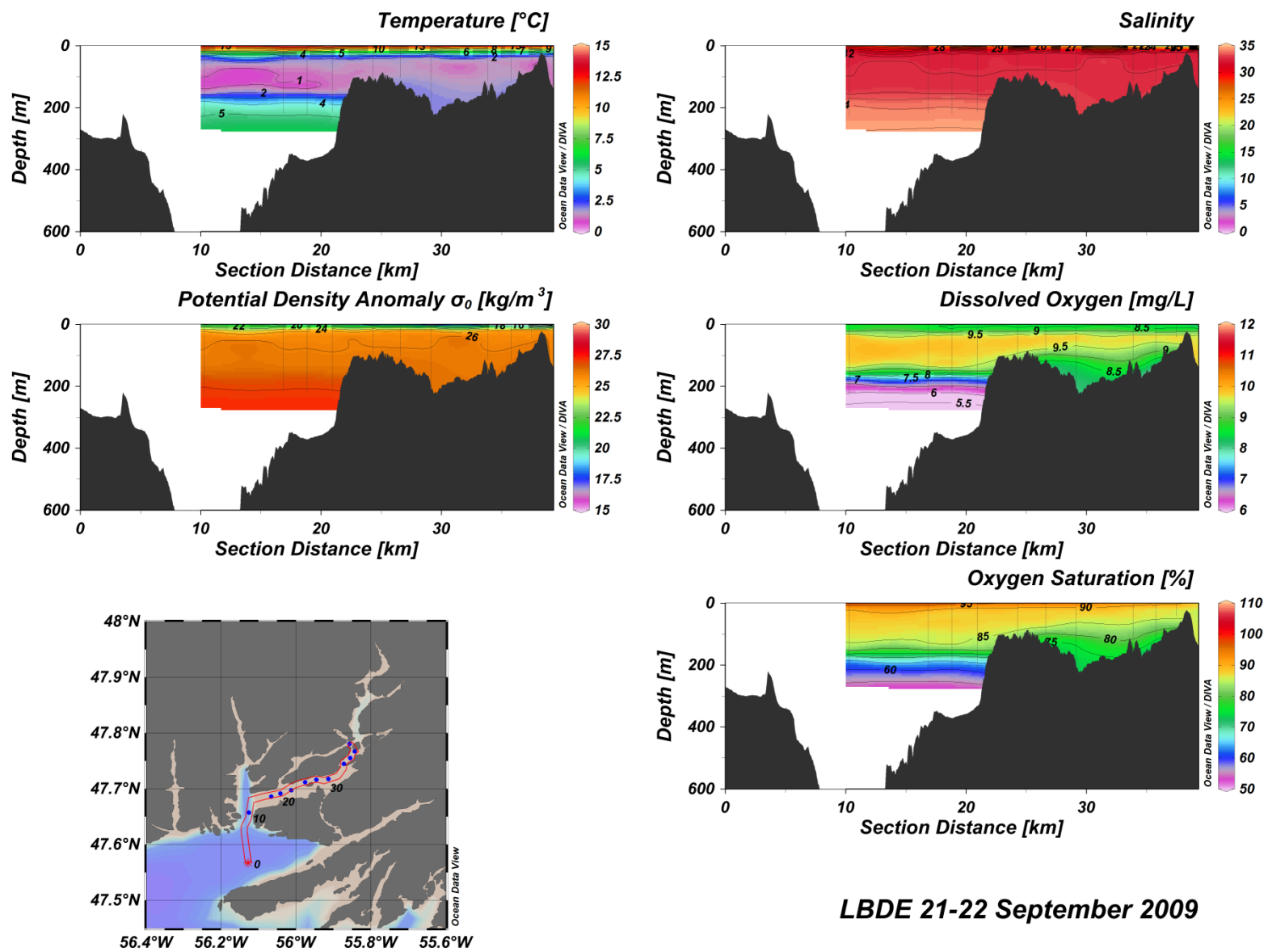


Figure A(i)15: Lower Bay d'Espoir water column vertical structure.

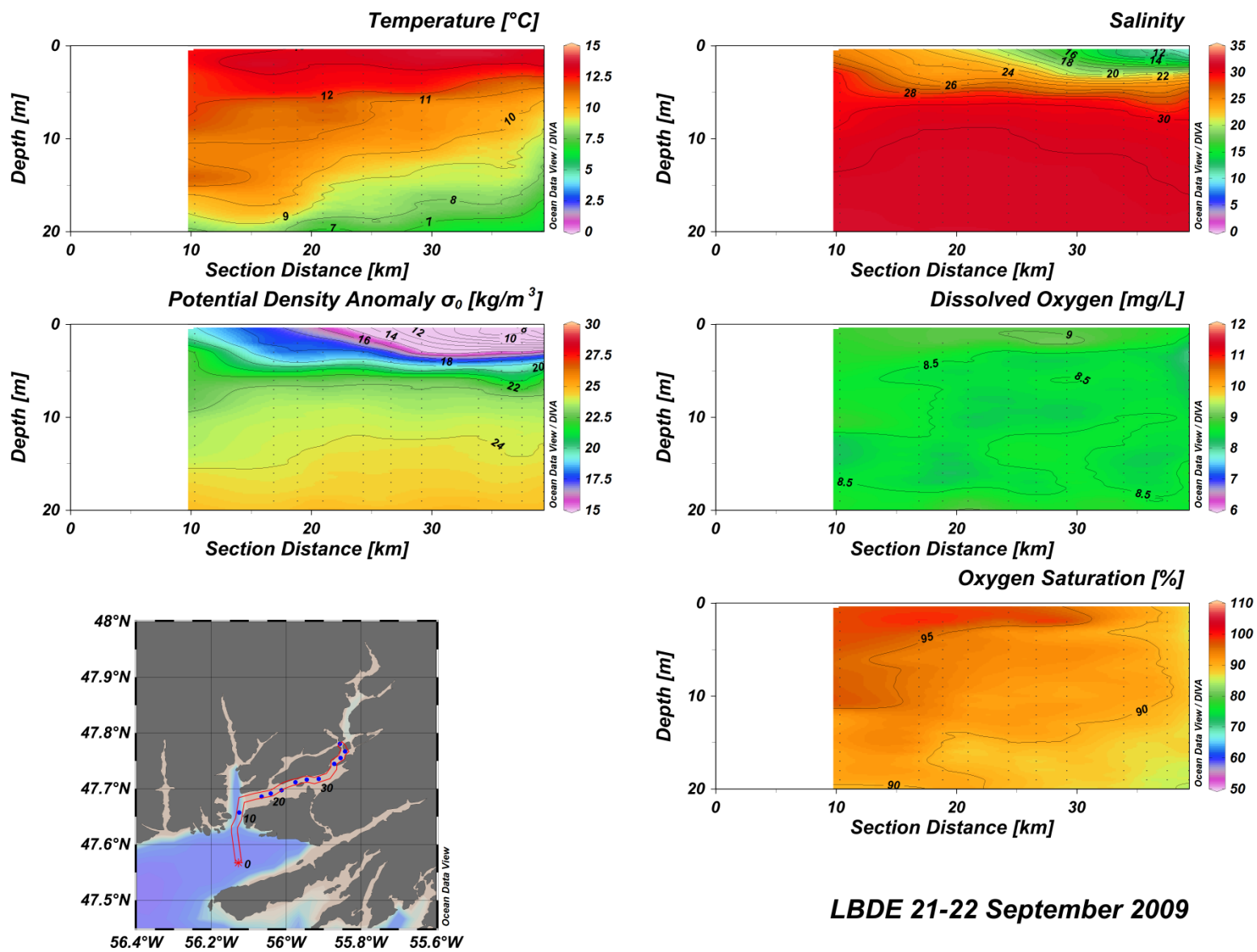


Figure A(i)16: Lower Bay d'Espoir water column vertical structure.

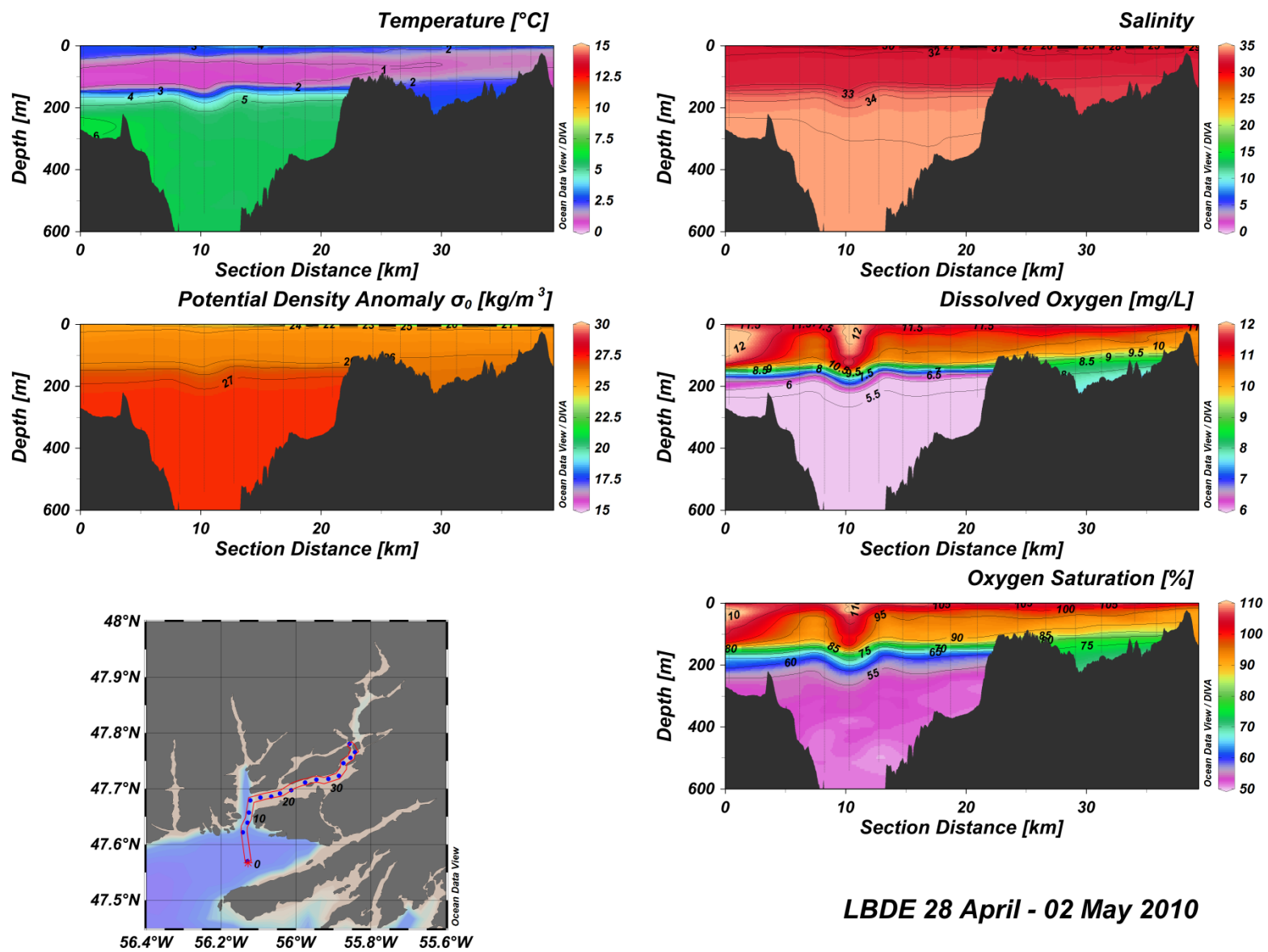


Figure A(i)17: Lower Bay d'Espoir water column vertical structure.

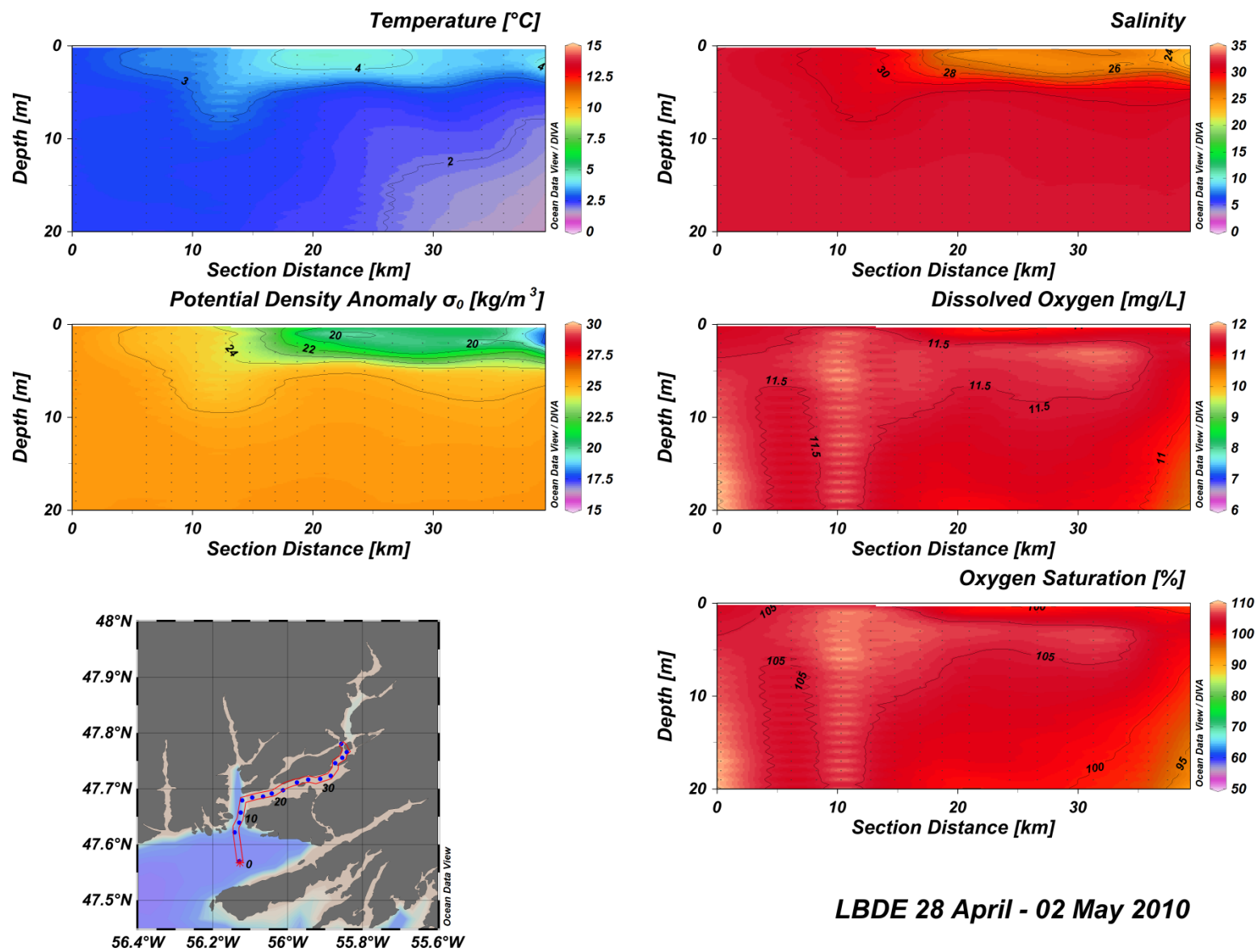
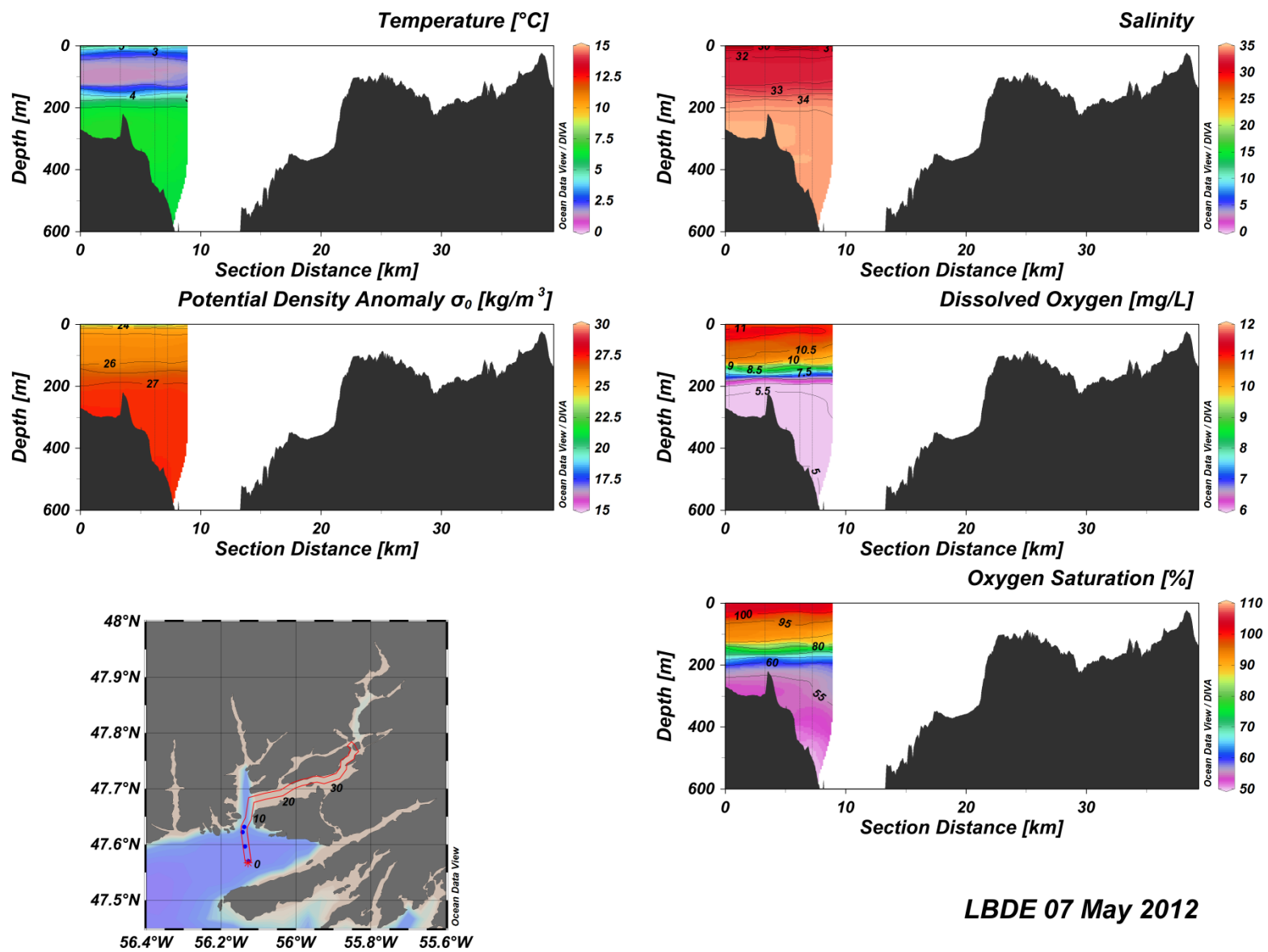


Figure A(i)18: Lower Bay d'Espoir water column vertical structure.



LBDE 07 May 2012

Figure A(i)19: Lower Bay d'Espoir water column vertical structure.

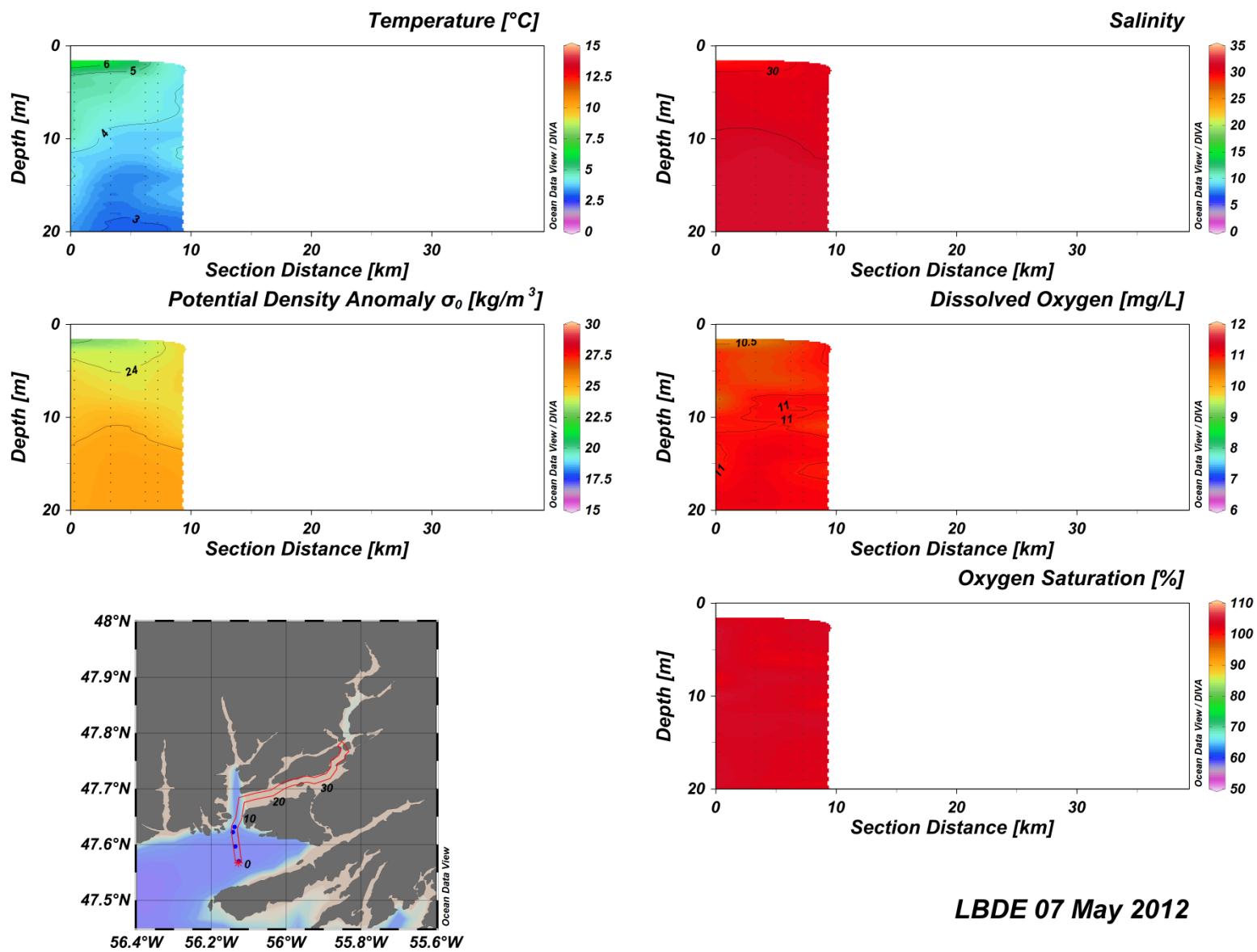


Figure A(i)20: Lower Bay d'Espoir water column vertical structure.

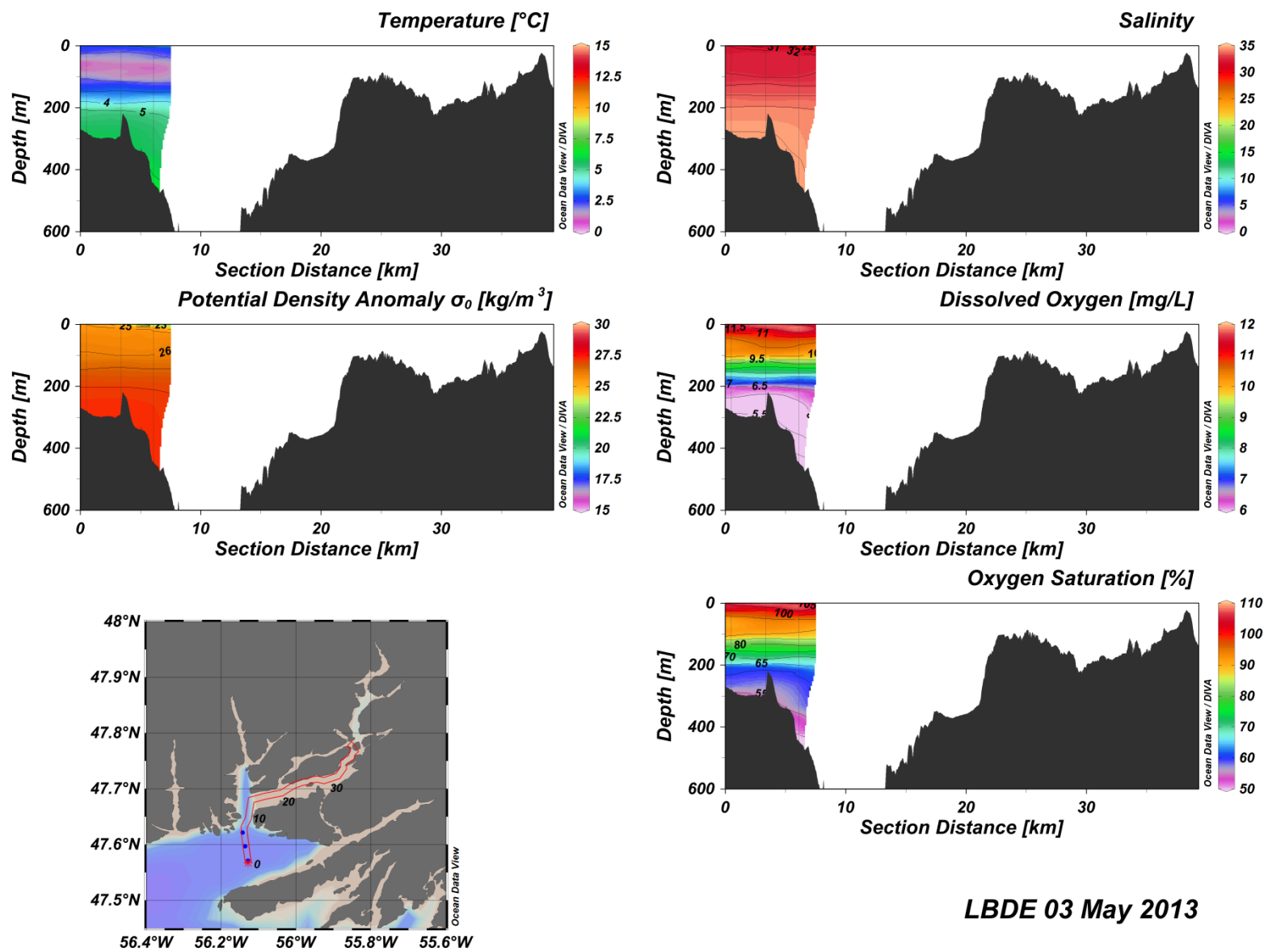


Figure A(i)21: Lower Bay d'Espoir water column vertical structure.

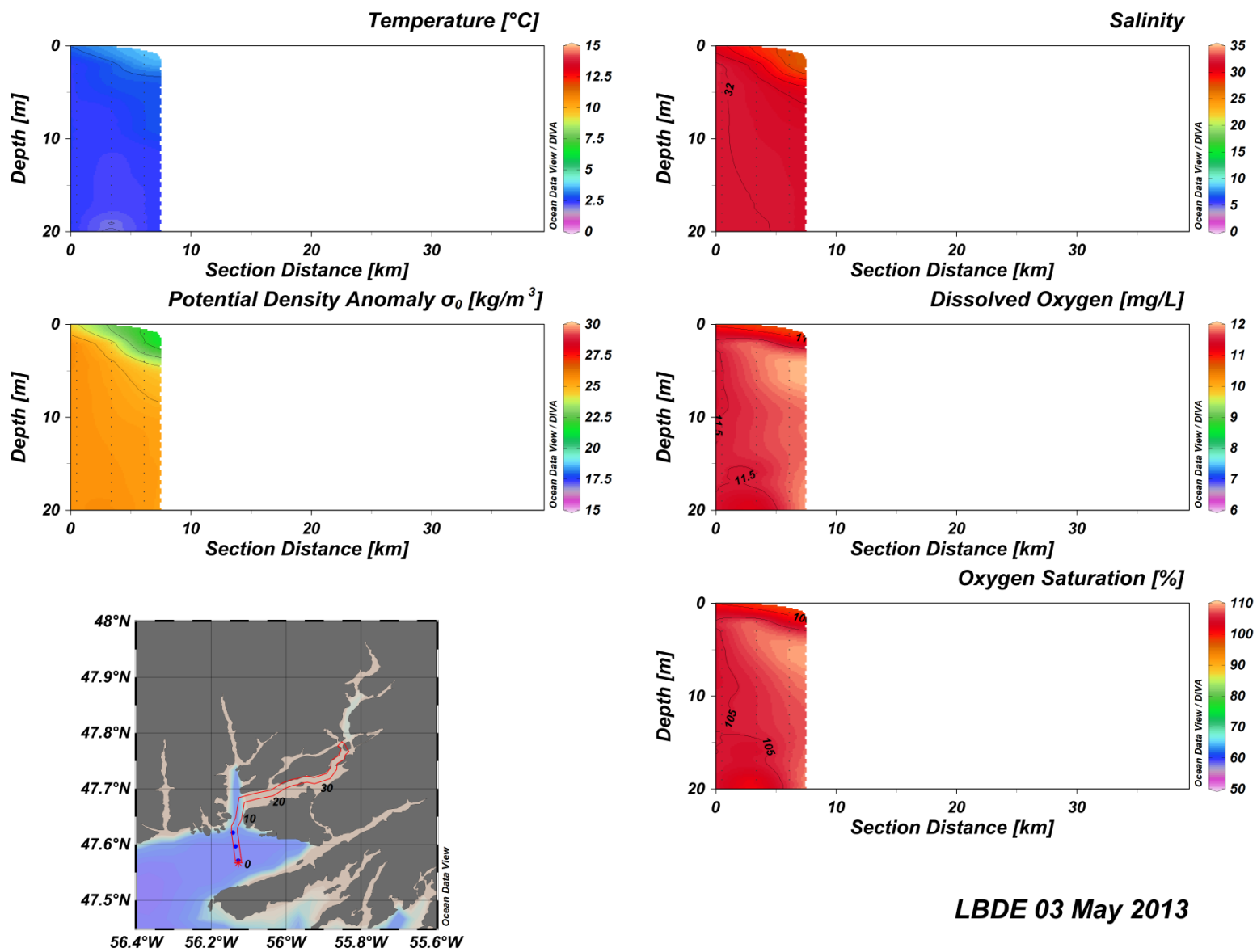


Figure A(i)22: Lower Bay d'Espoir water column vertical structure.

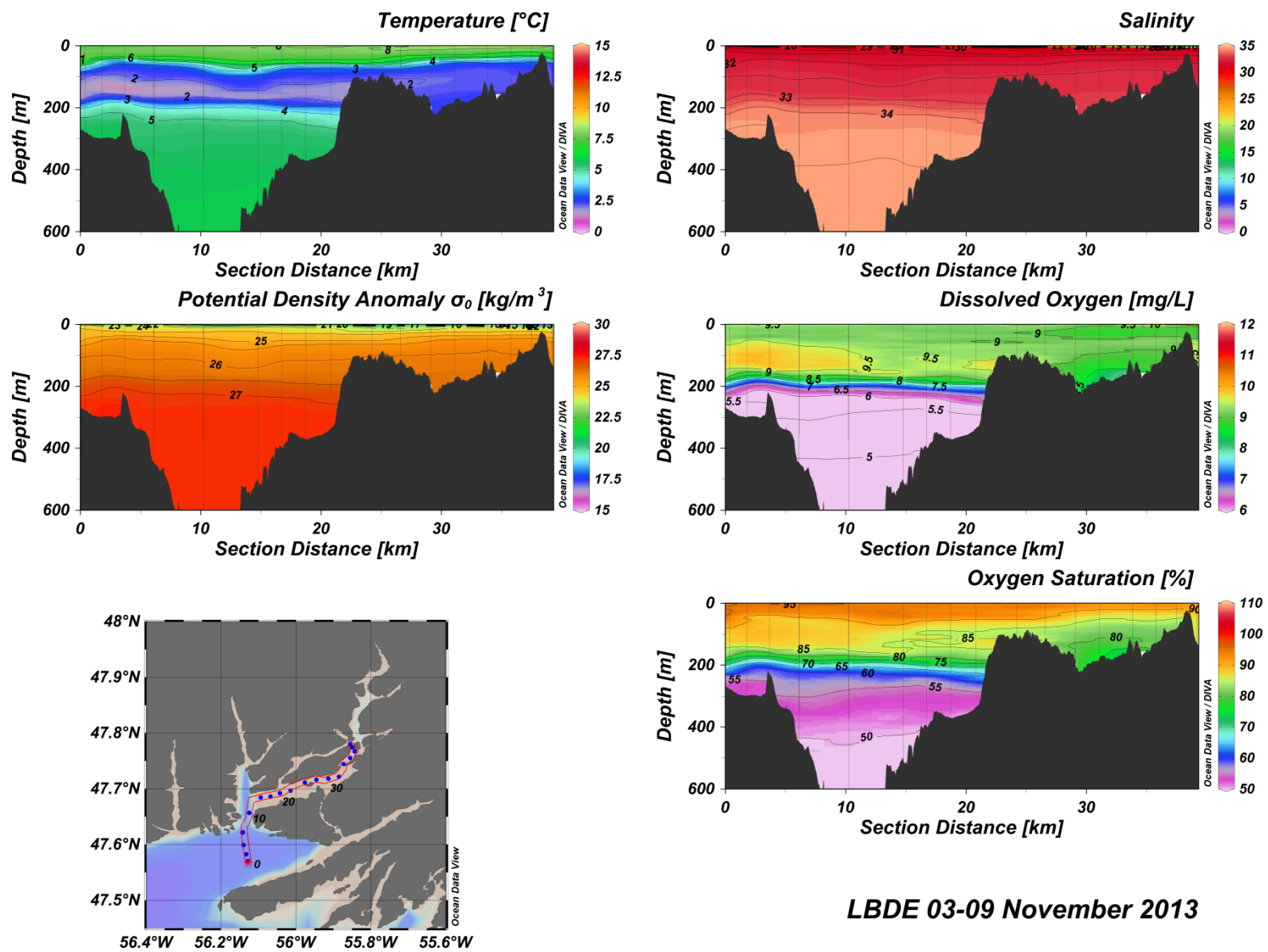


Figure A(i)23: Lower Bay d'Espoir water column vertical structure.

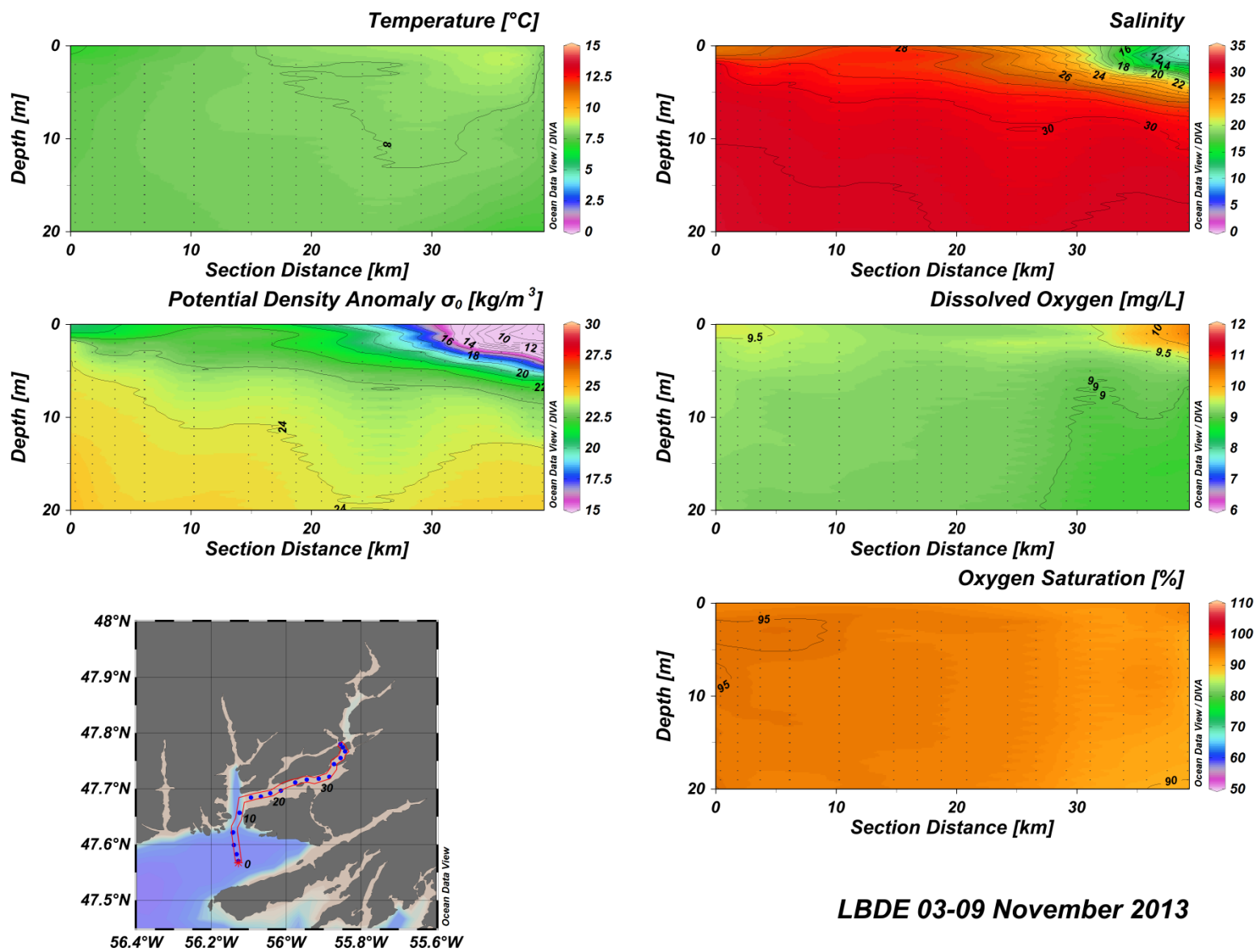


Figure A(i)24: Lower Bay d'Espoir water column vertical structure.

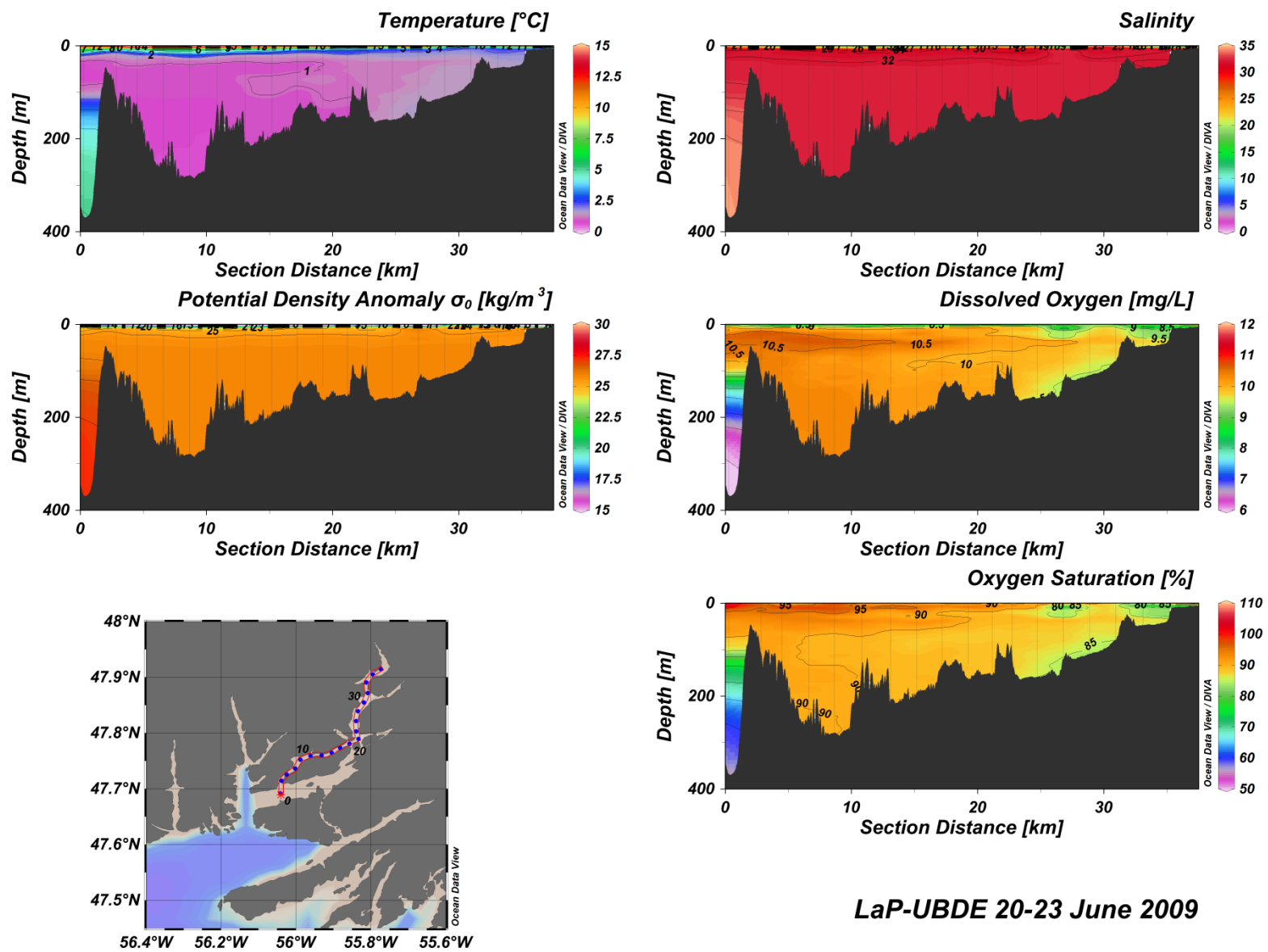


Figure A(i)25: Lampidoes Passage – Upper Bay d'Espoir water column vertical structure.

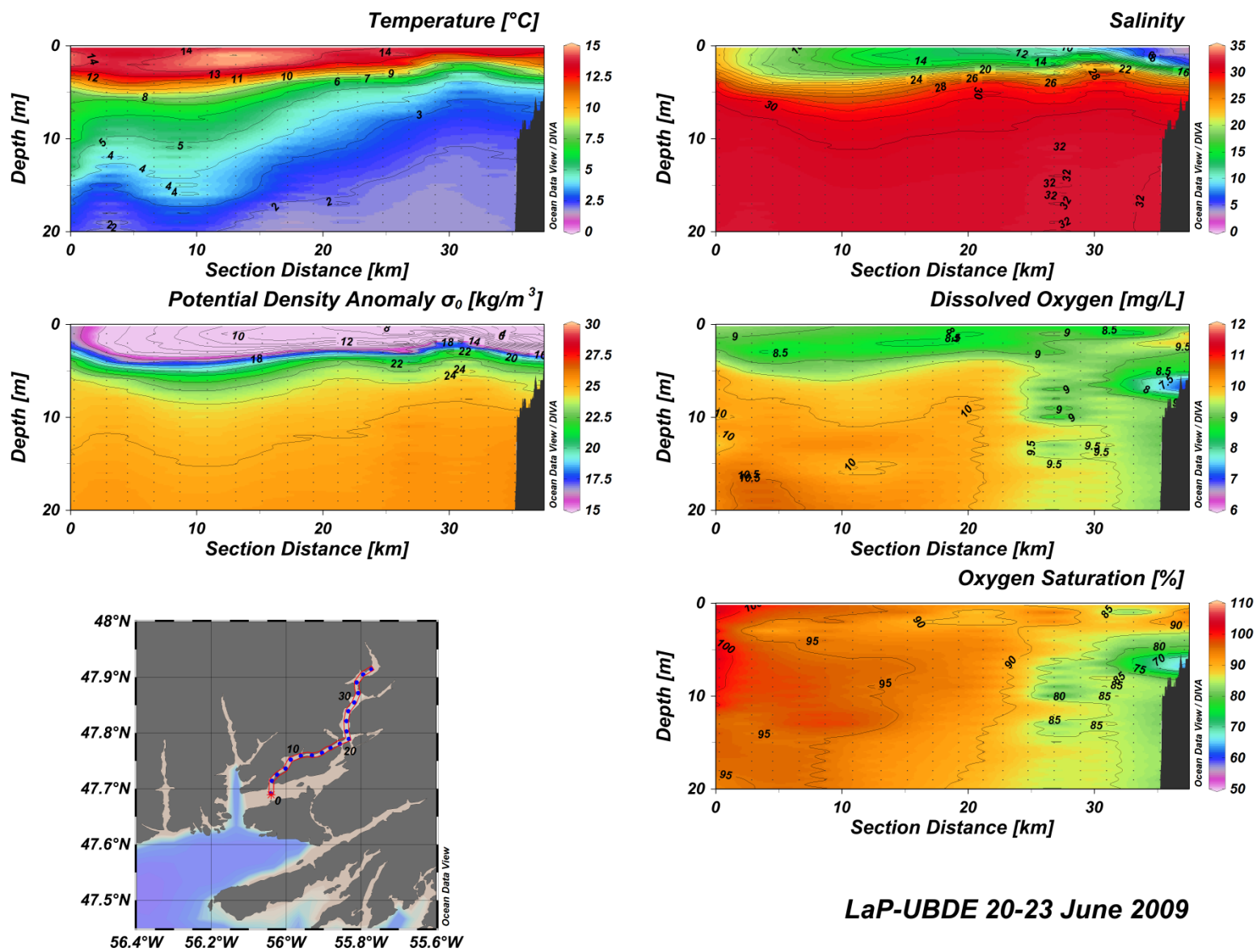
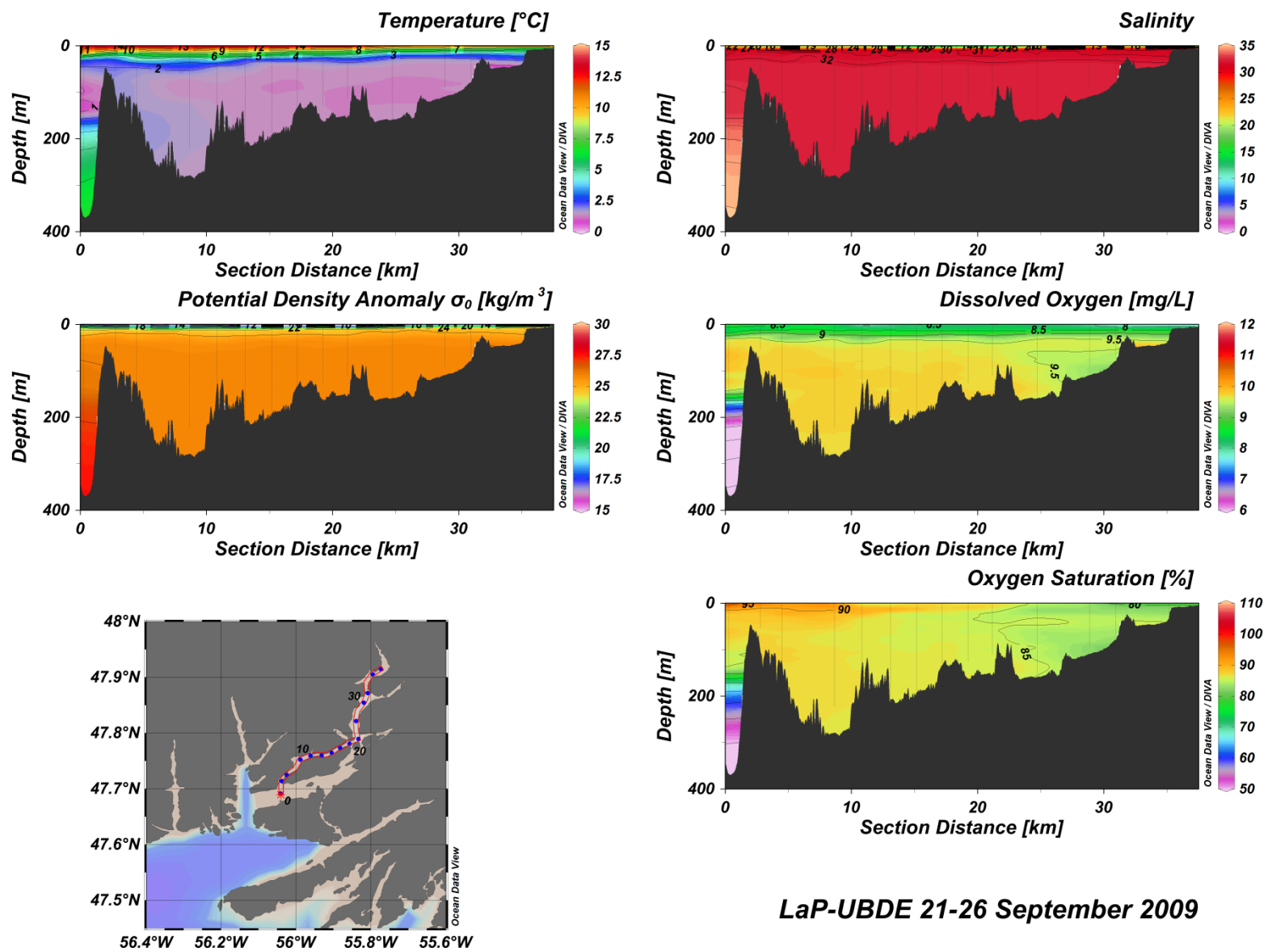


Figure A(i)26: Lampidoes Passage – Upper Bay d’Espoir water column vertical structure.



LaP-UBDE 21-26 September 2009

Figure A(i)27: Lampidoes Passage – Upper Bay d’Espoir water column vertical structure.

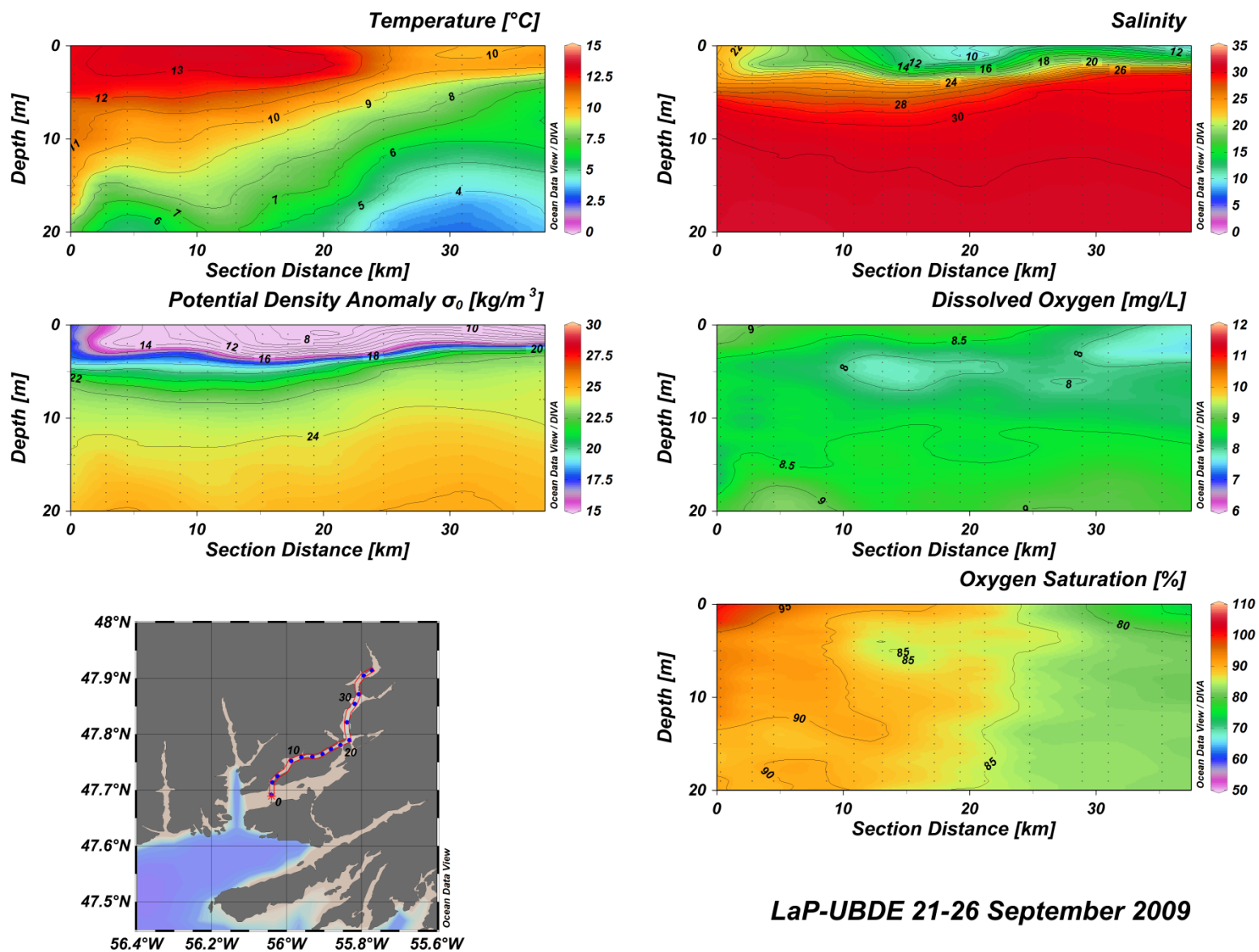


Figure A(i)28: Lampidoes Passage – Upper Bay d’Espoir water column vertical structure.

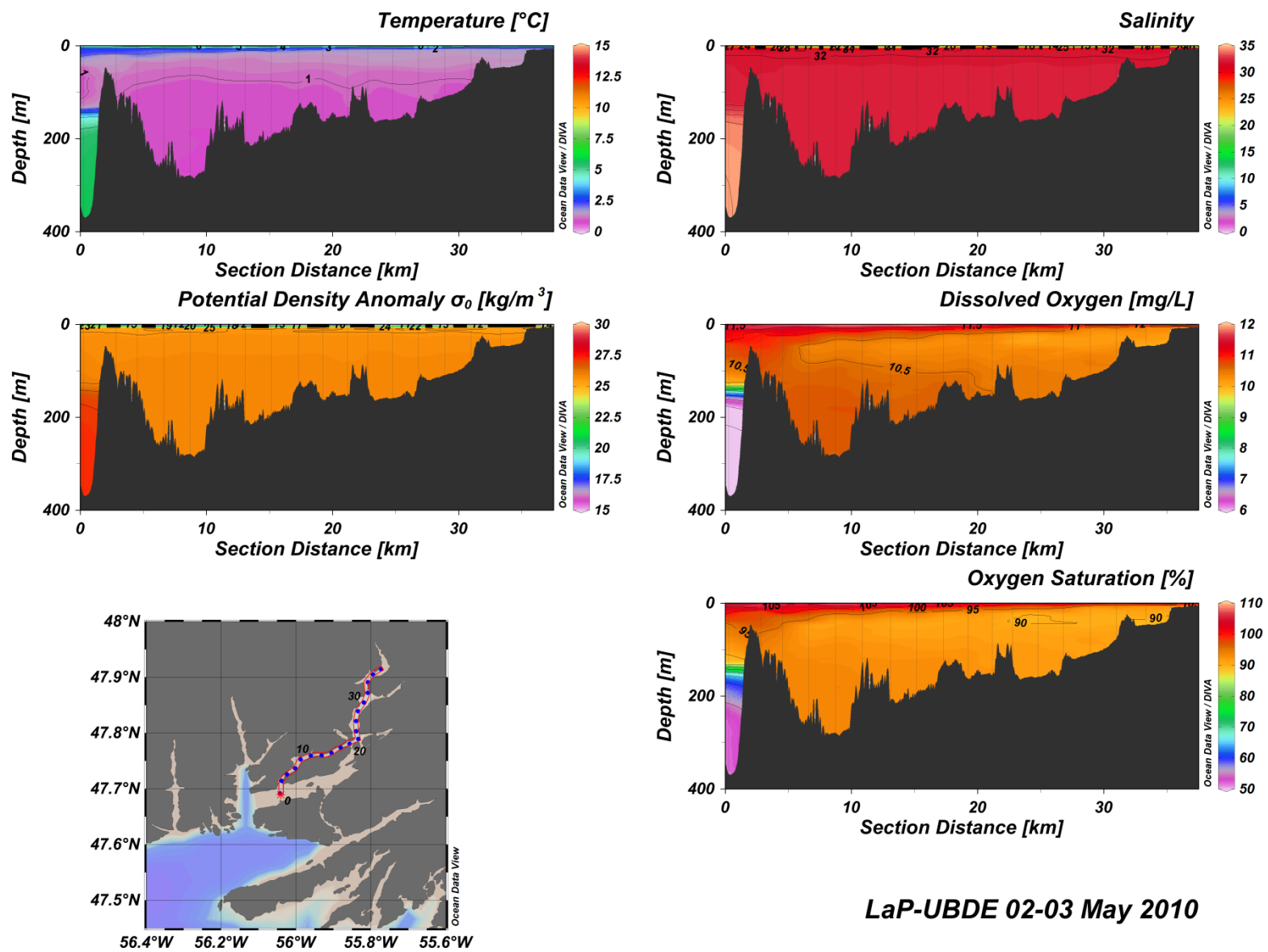


Figure A(i)29: Lampidoes Passage – Upper Bay d’Espoir water column vertical structure.

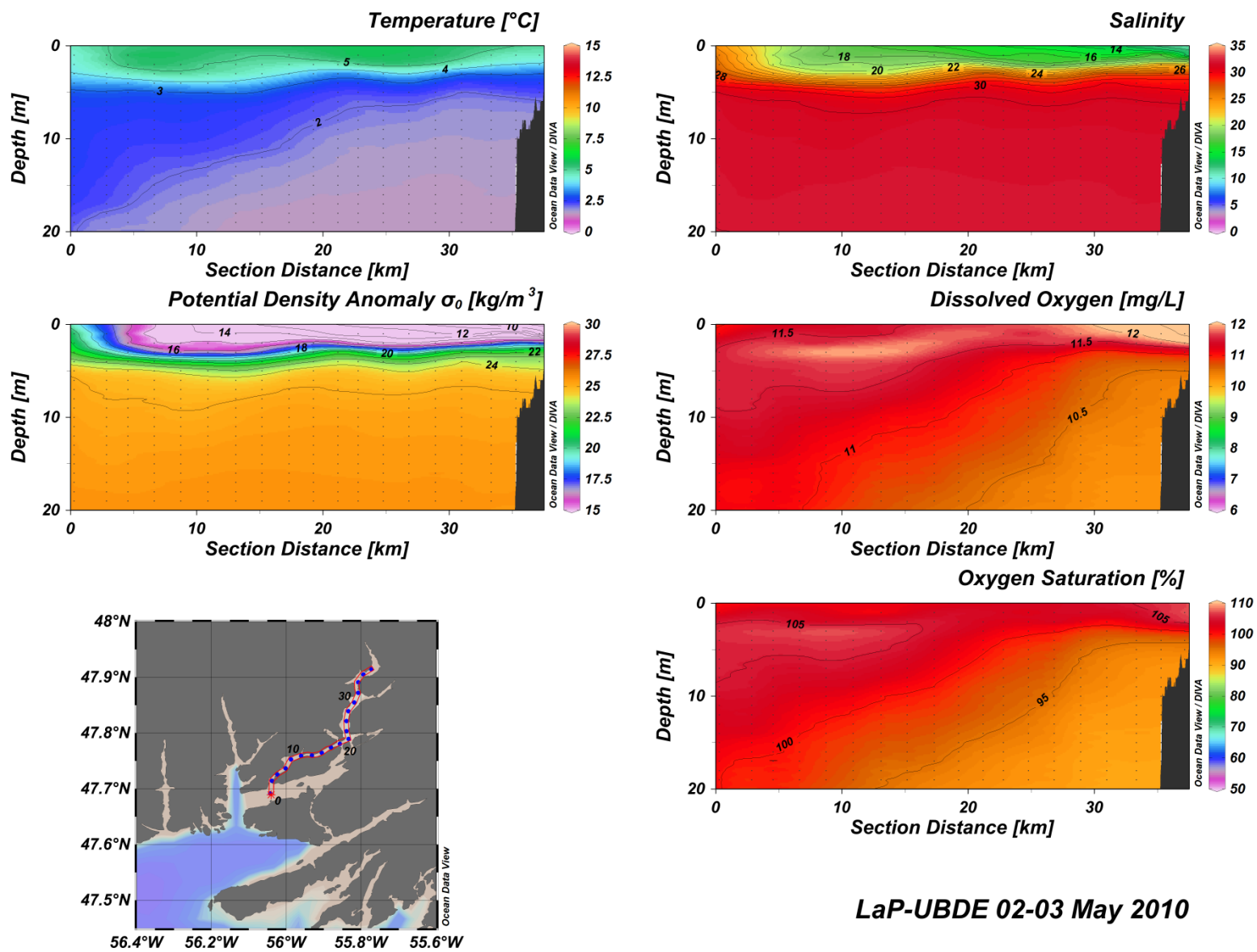


Figure A(i)30: Lampidoes Passage – Upper Bay d’Espoir water column vertical structure.

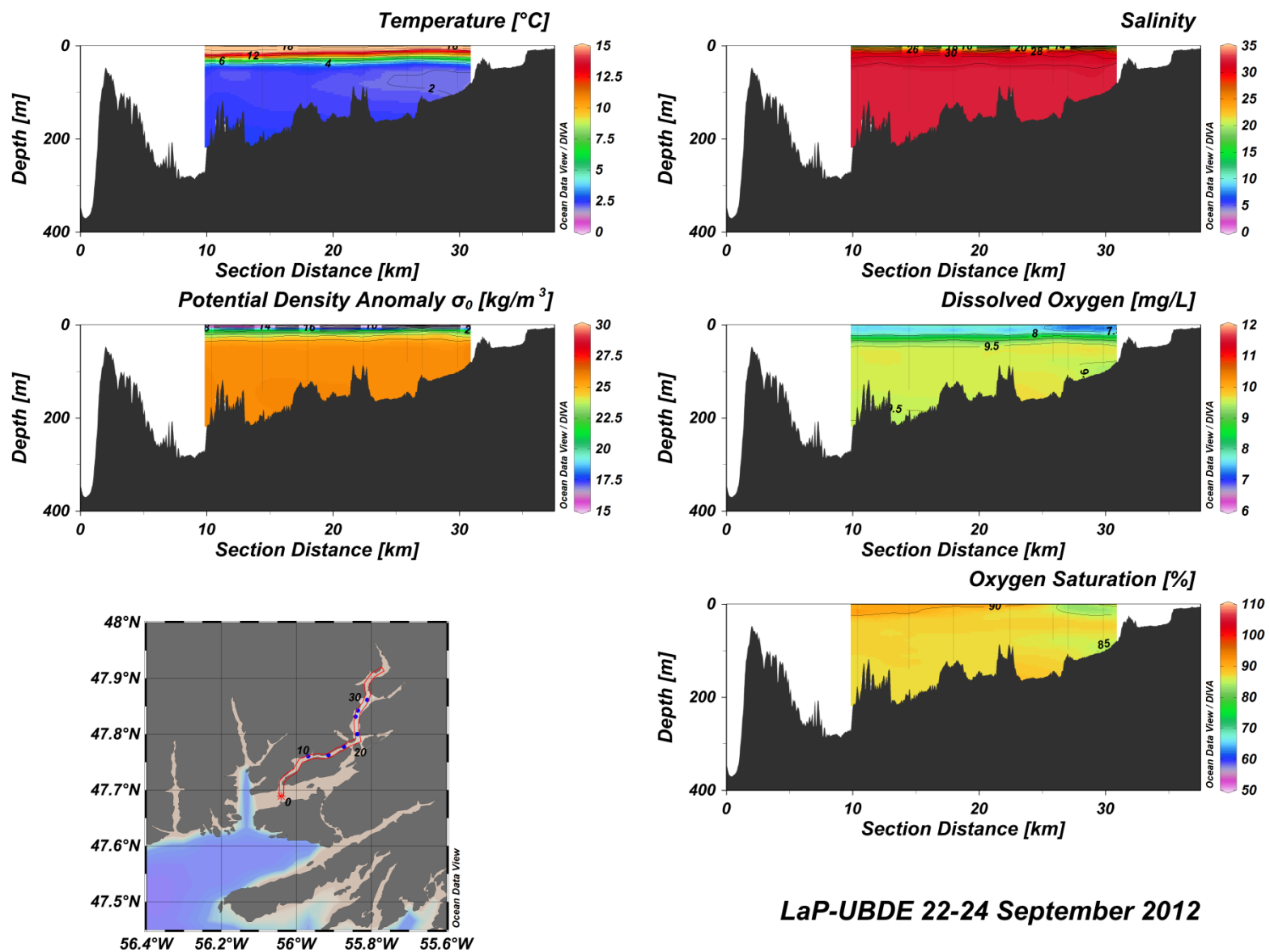
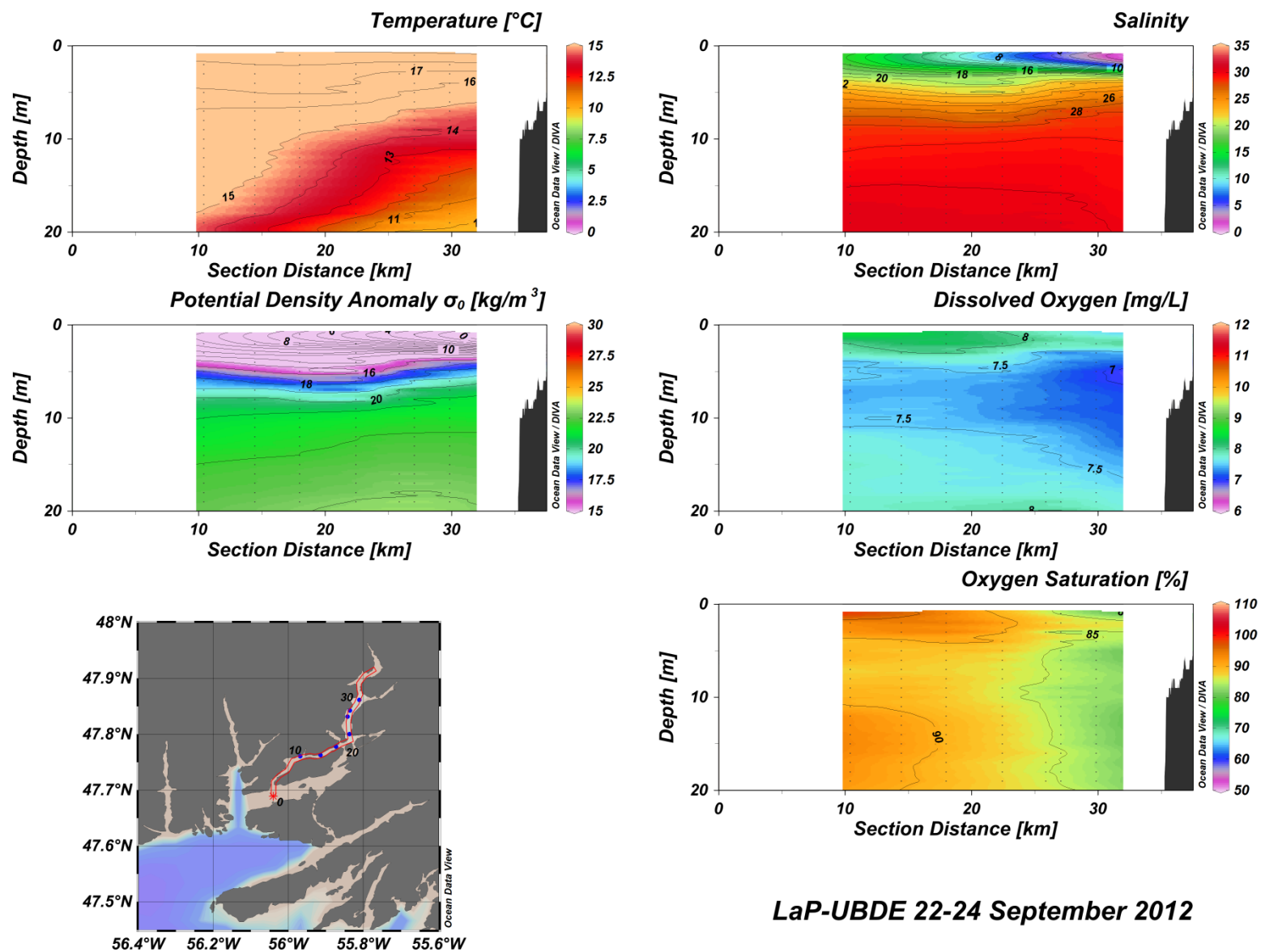


Figure A(i)31: Lampidoes Passage – Upper Bay d'Espoir water column vertical structure.



LaP-UBDE 22-24 September 2012

Figure A(i)32: Lampidoes Passage – Upper Bay d'Espoir water column vertical structure.

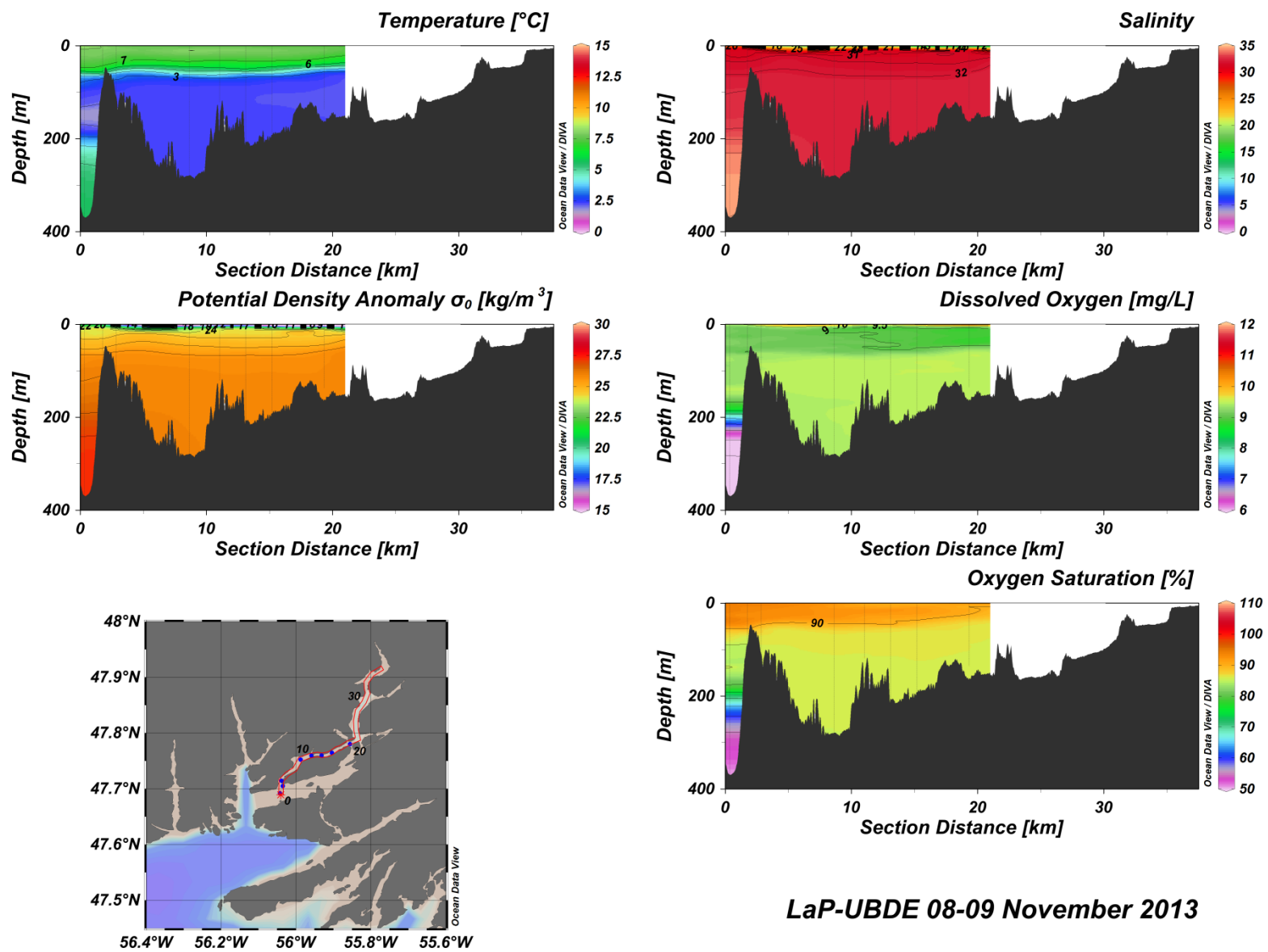


Figure A(i)33: Lampidoes Passage – Upper Bay d’Espoir water column vertical structure.

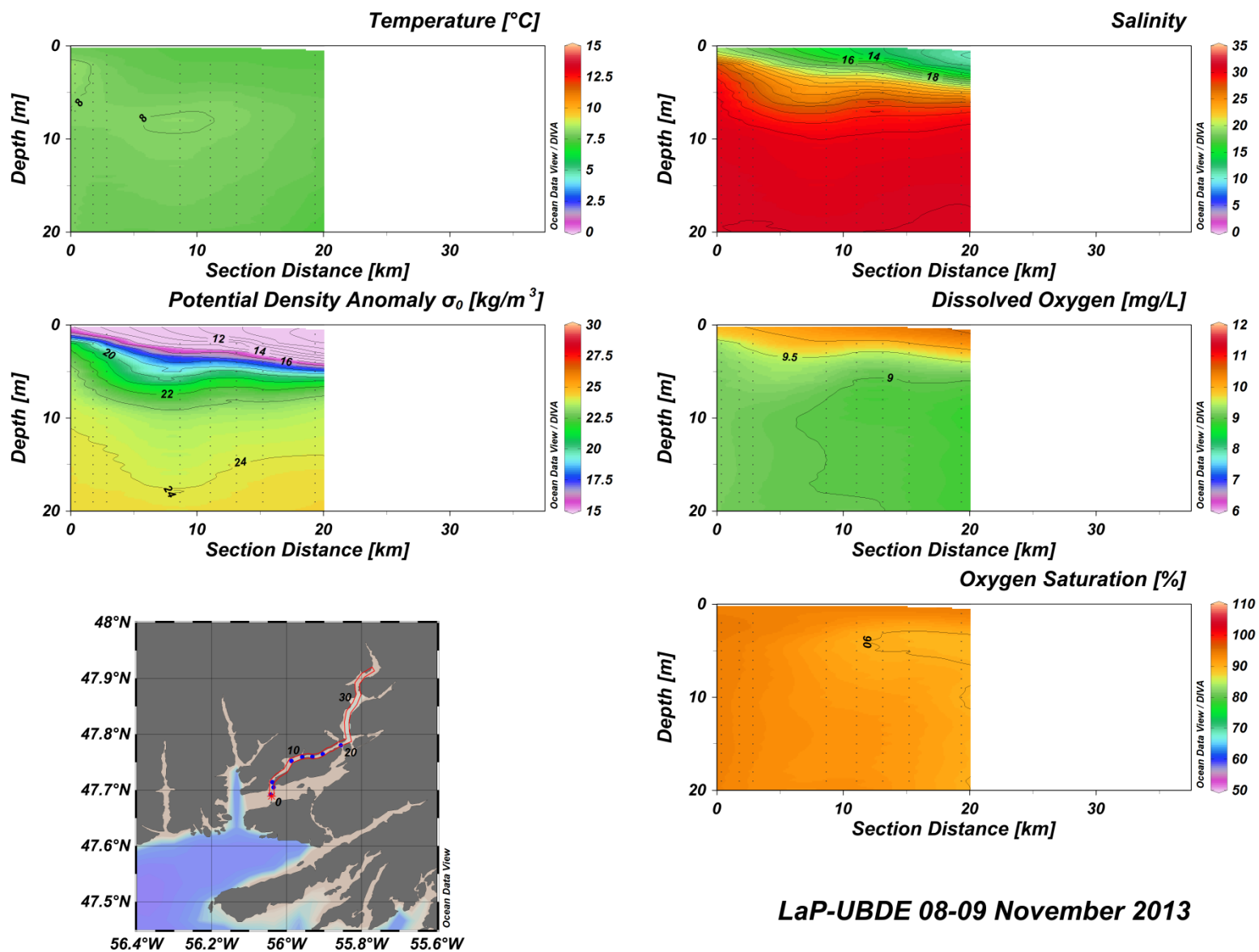


Figure A(i)34: Lampidoes Passage – Upper Bay d'Espoir water column vertical structure.

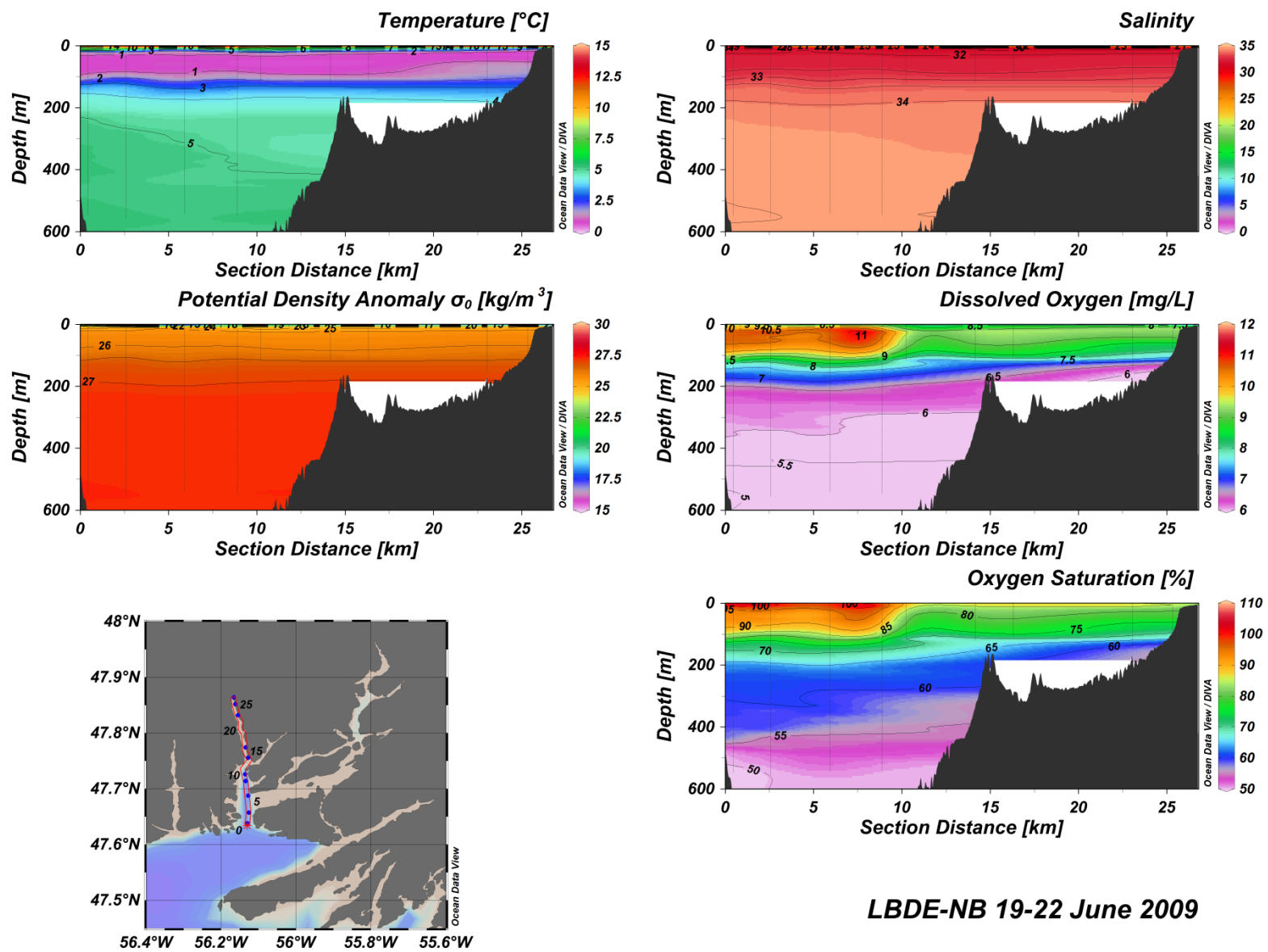


Figure A(i)35: Lower Bay d'Espoir– North Bay water column vertical structure.

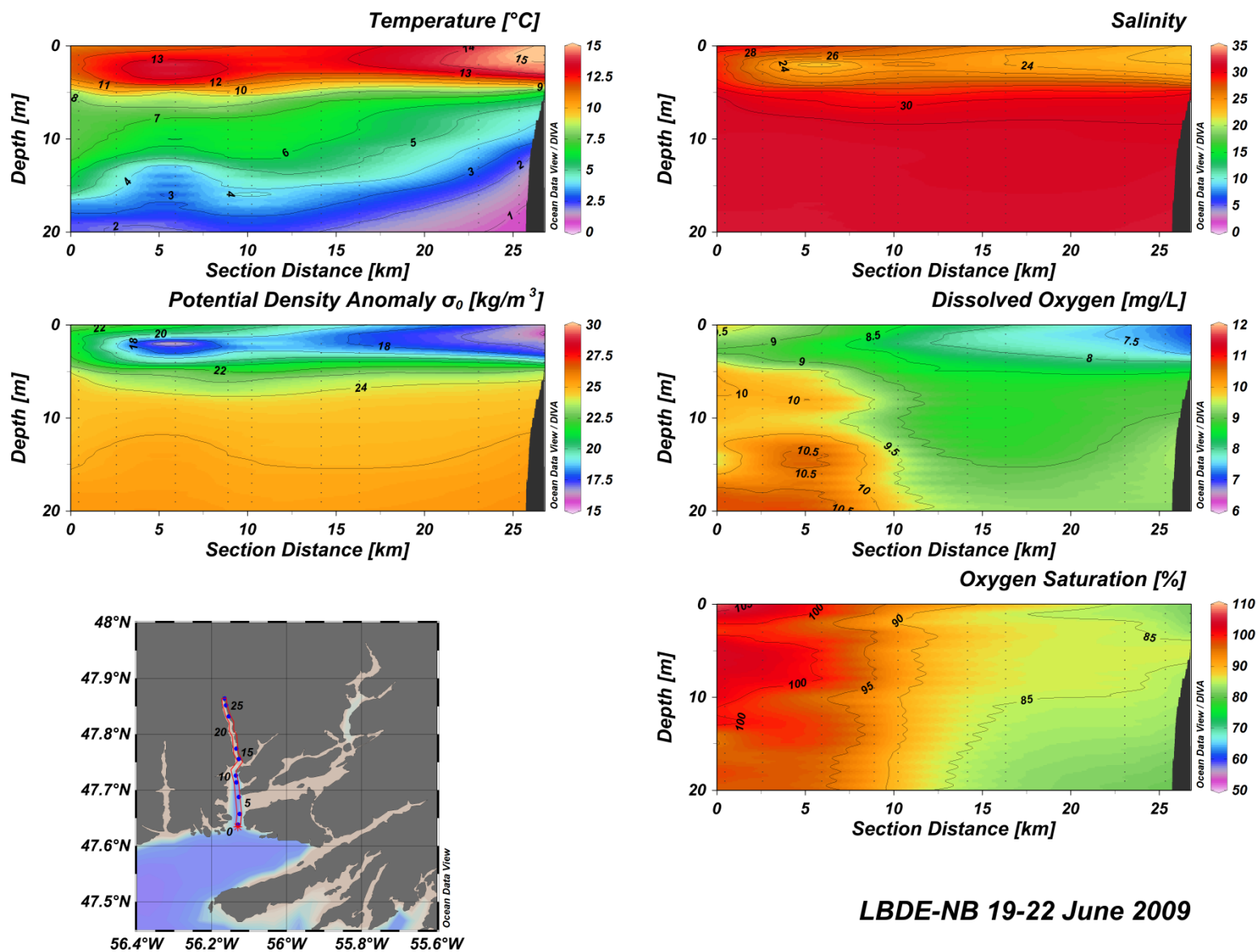
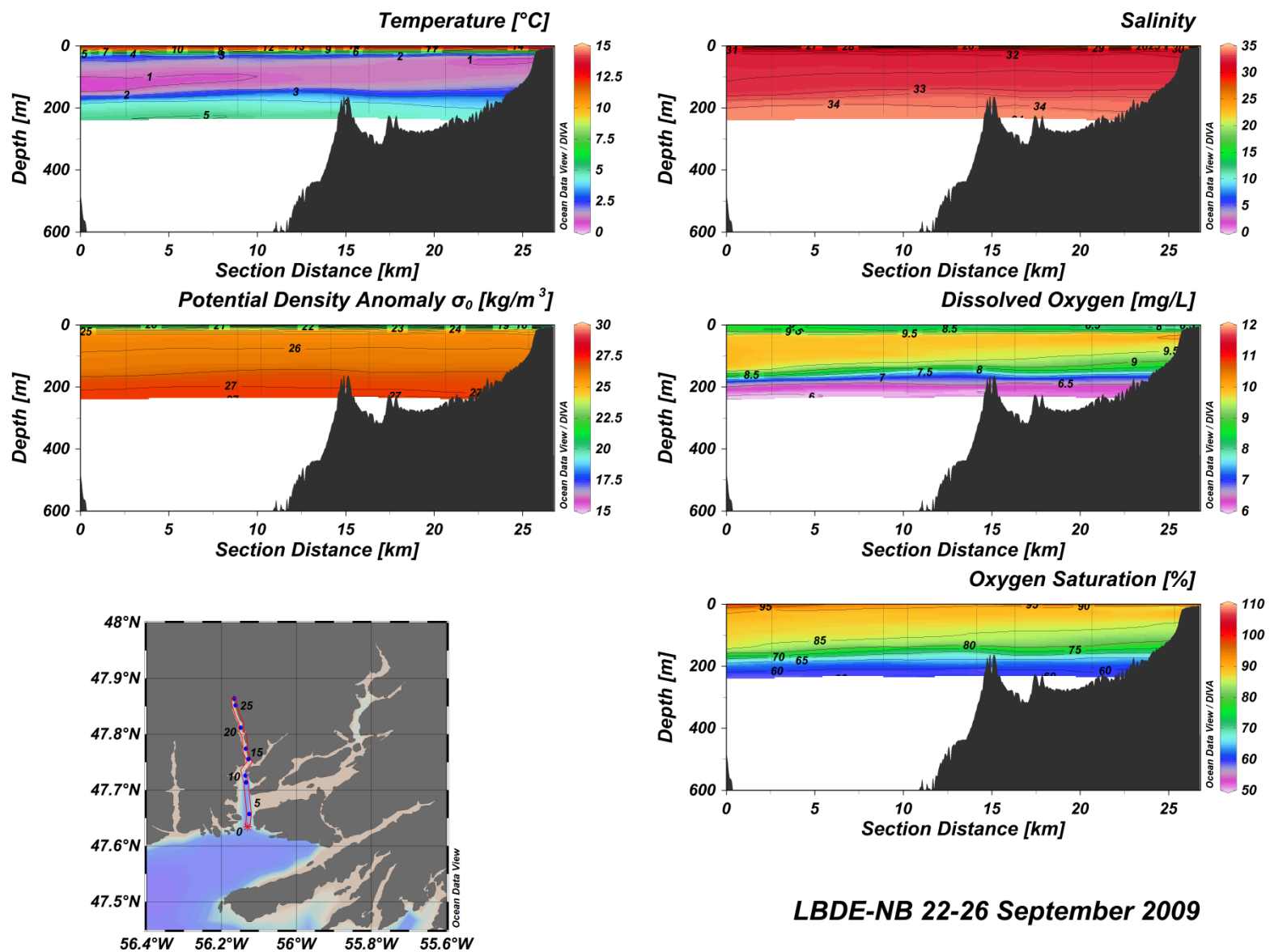


Figure A(i)36: Lower Bay d'Espoir– North Bay water column vertical structure.



LBDE-NB 22-26 September 2009

Figure A(i)37: Lower Bay d'Espoir– North Bay water column vertical structure.

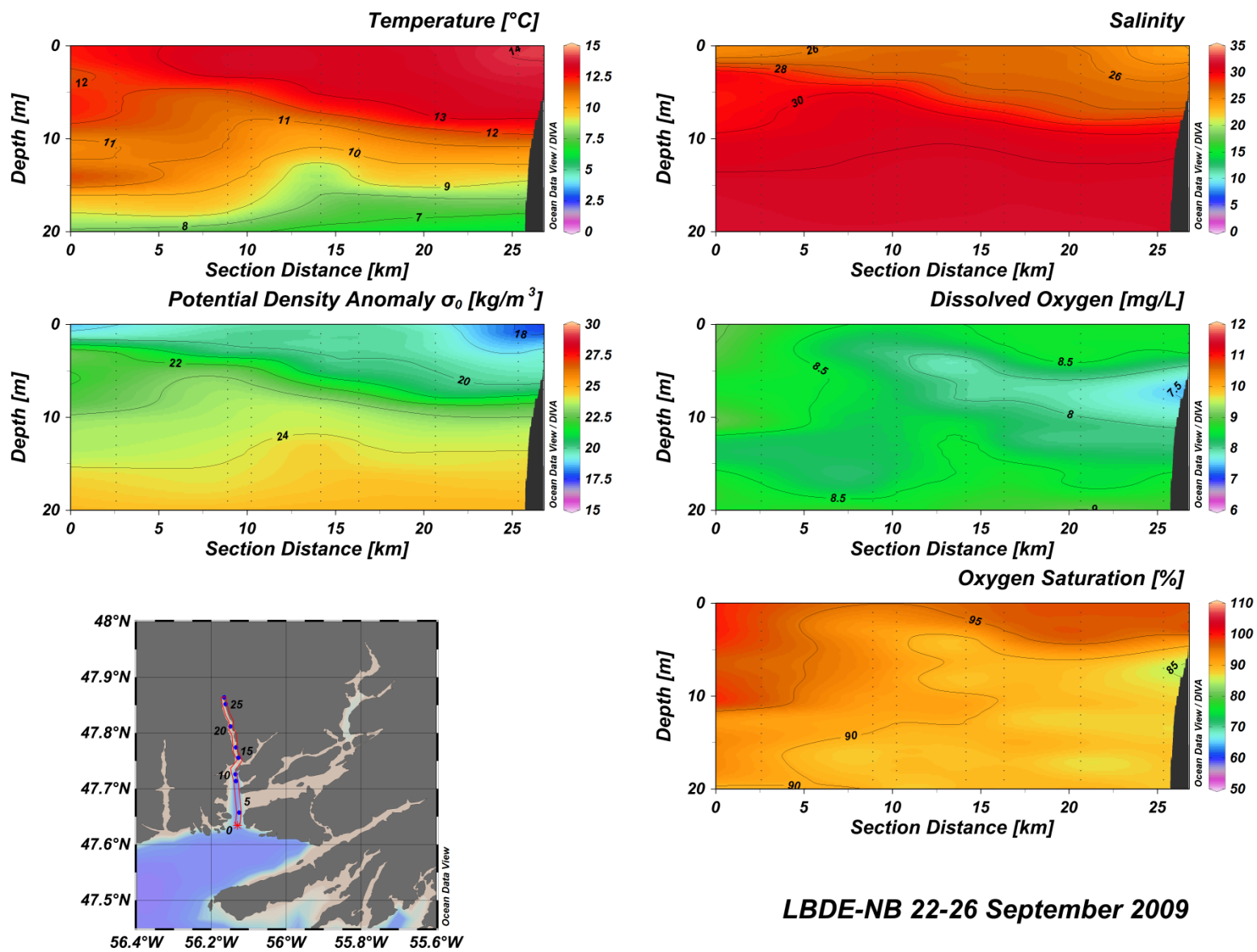


Figure A(i)38: Lower Bay d'Espoir– North Bay water column vertical structure.

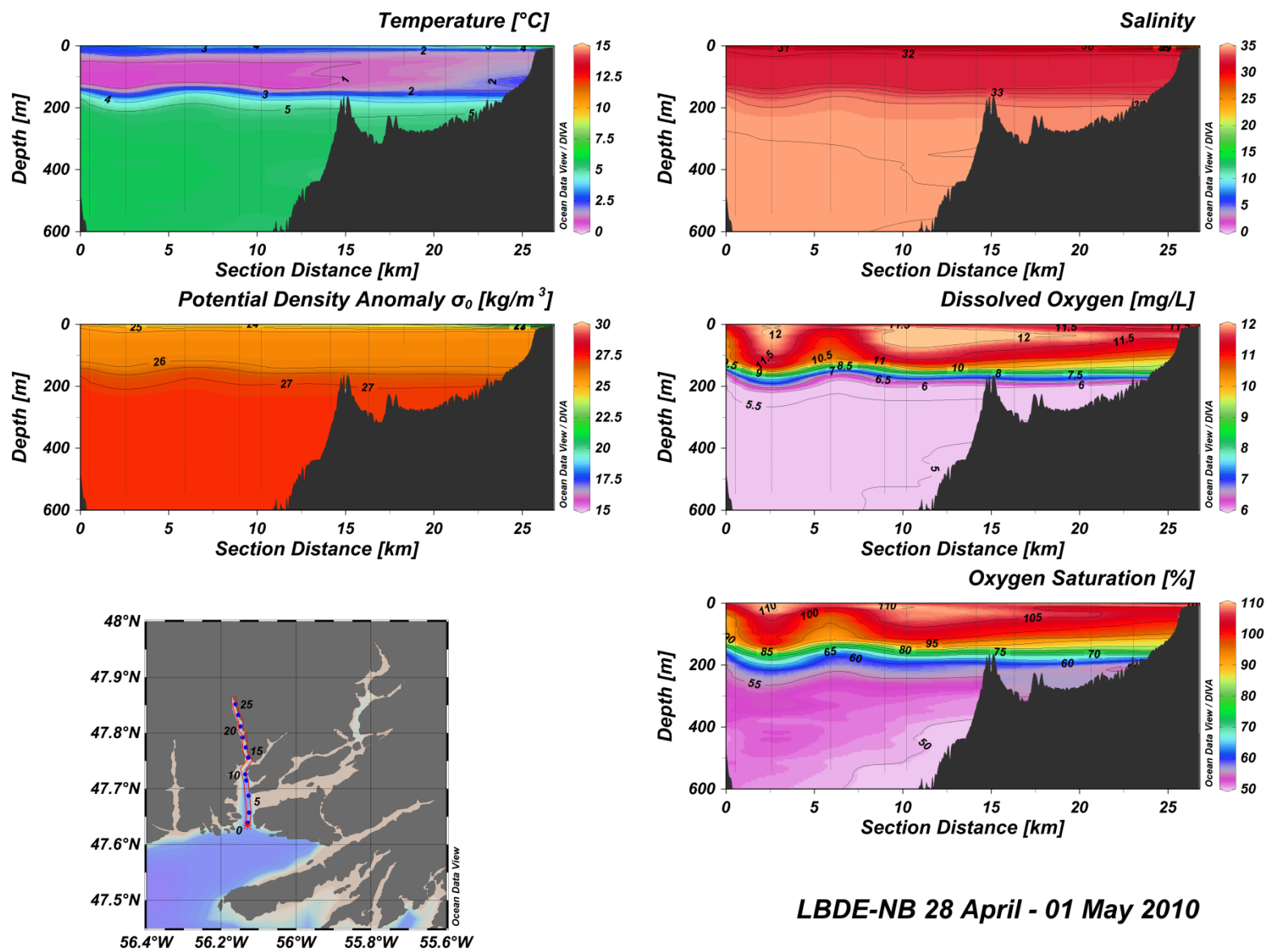


Figure A(i)39: Lower Bay d'Espoir– North Bay water column vertical structure.

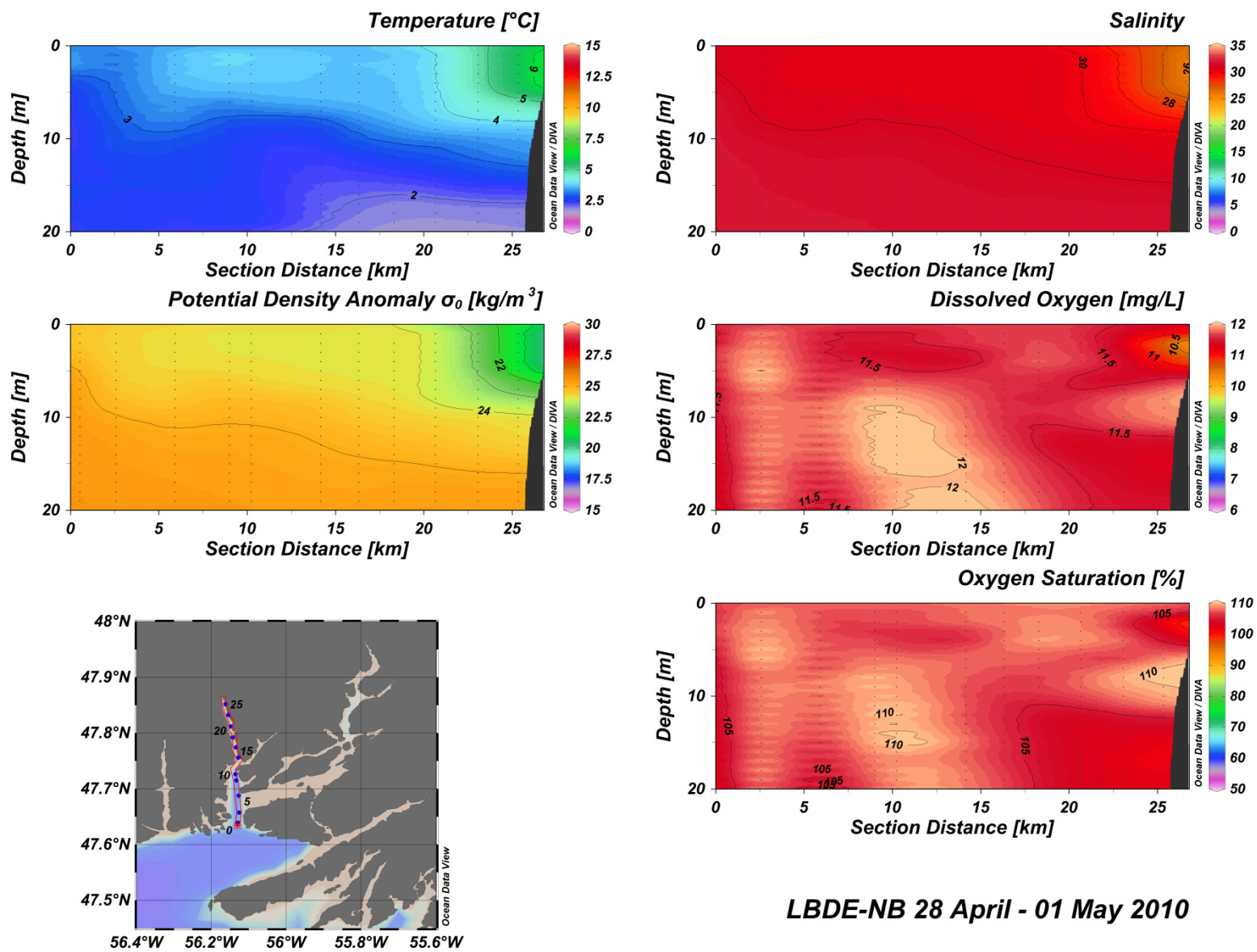
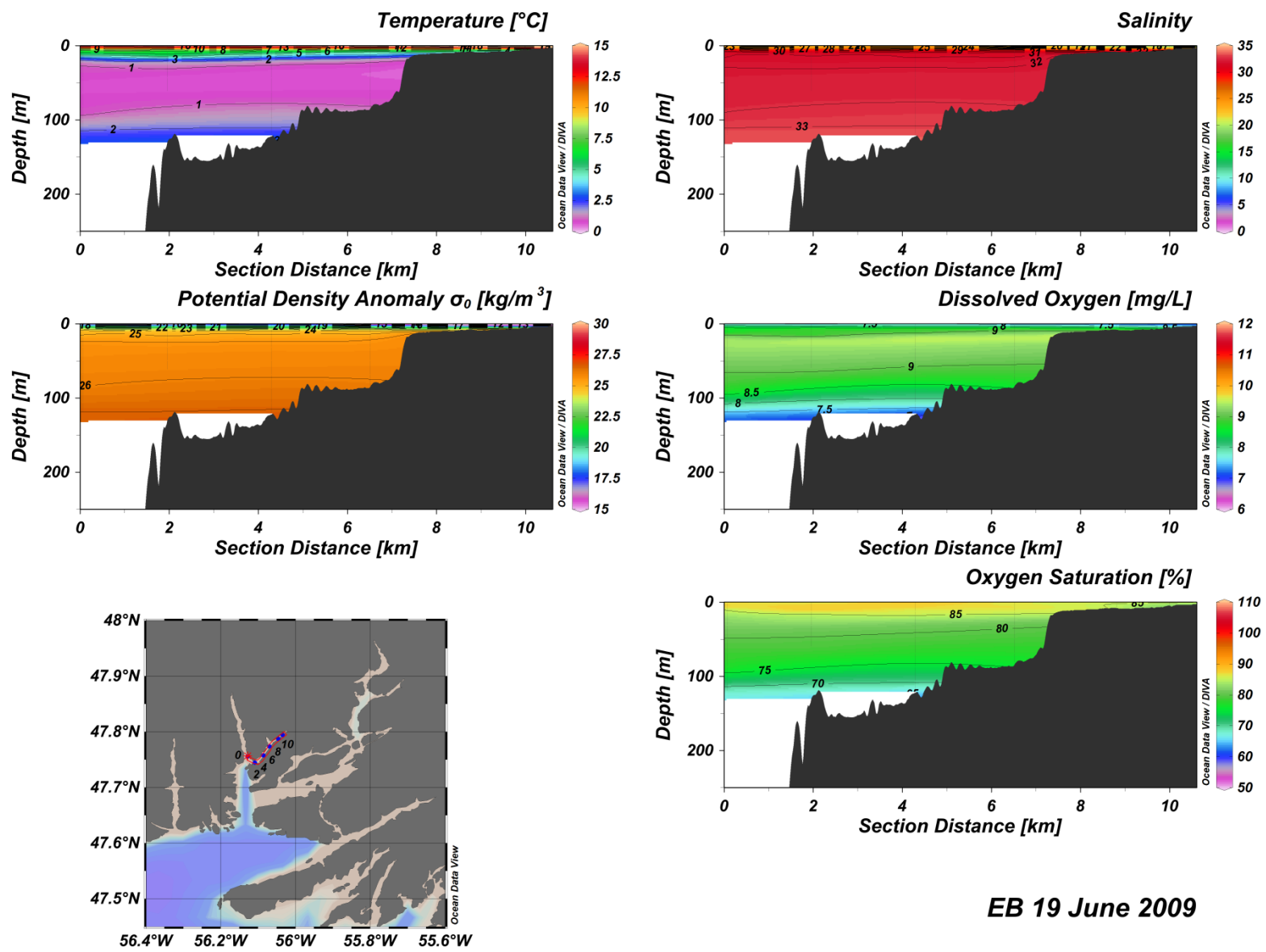


Figure A(i)40: Lower Bay d'Espoir– North Bay water column vertical structure.



EB 19 June 2009

Figure A(i)41: East Bay water column vertical structure.

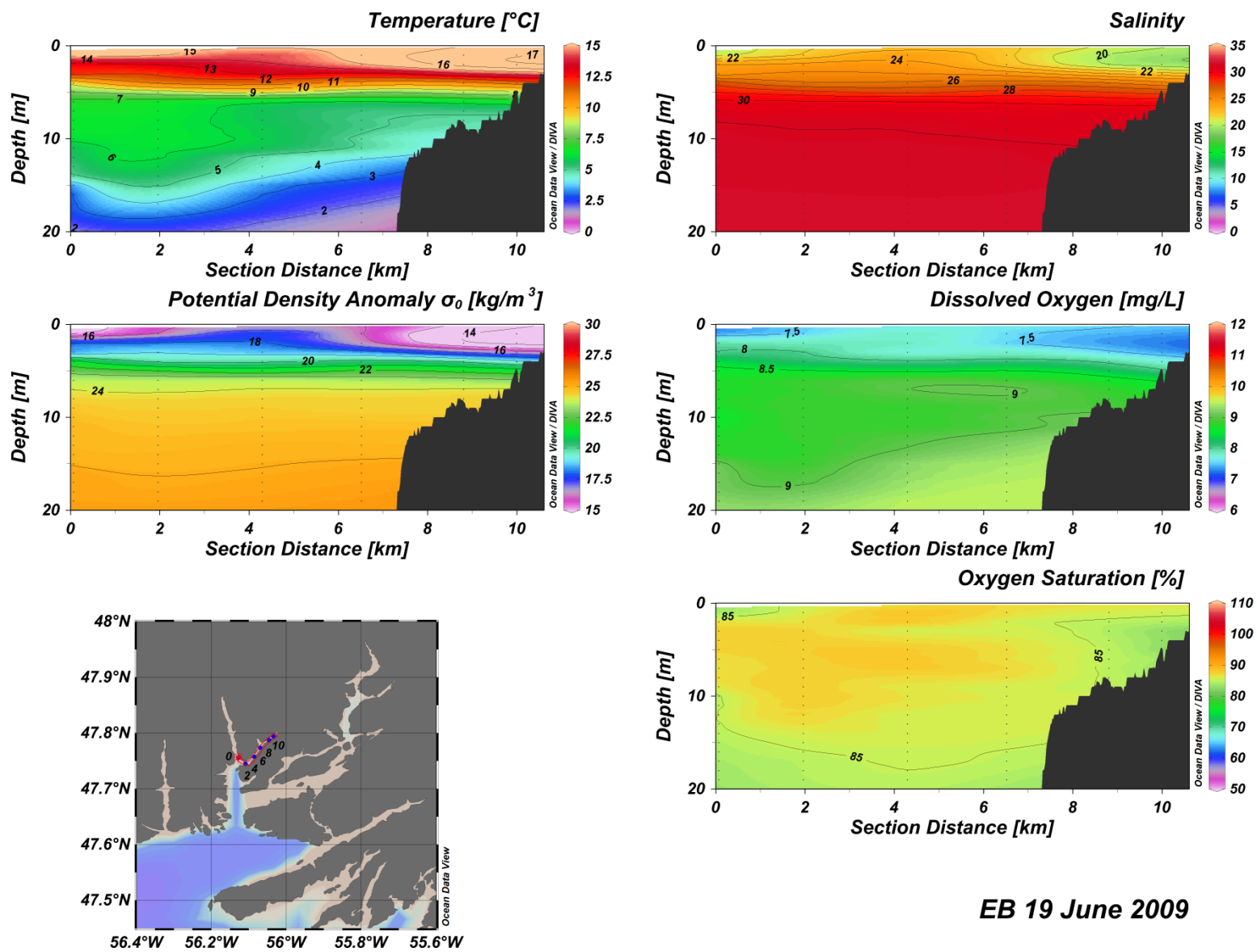
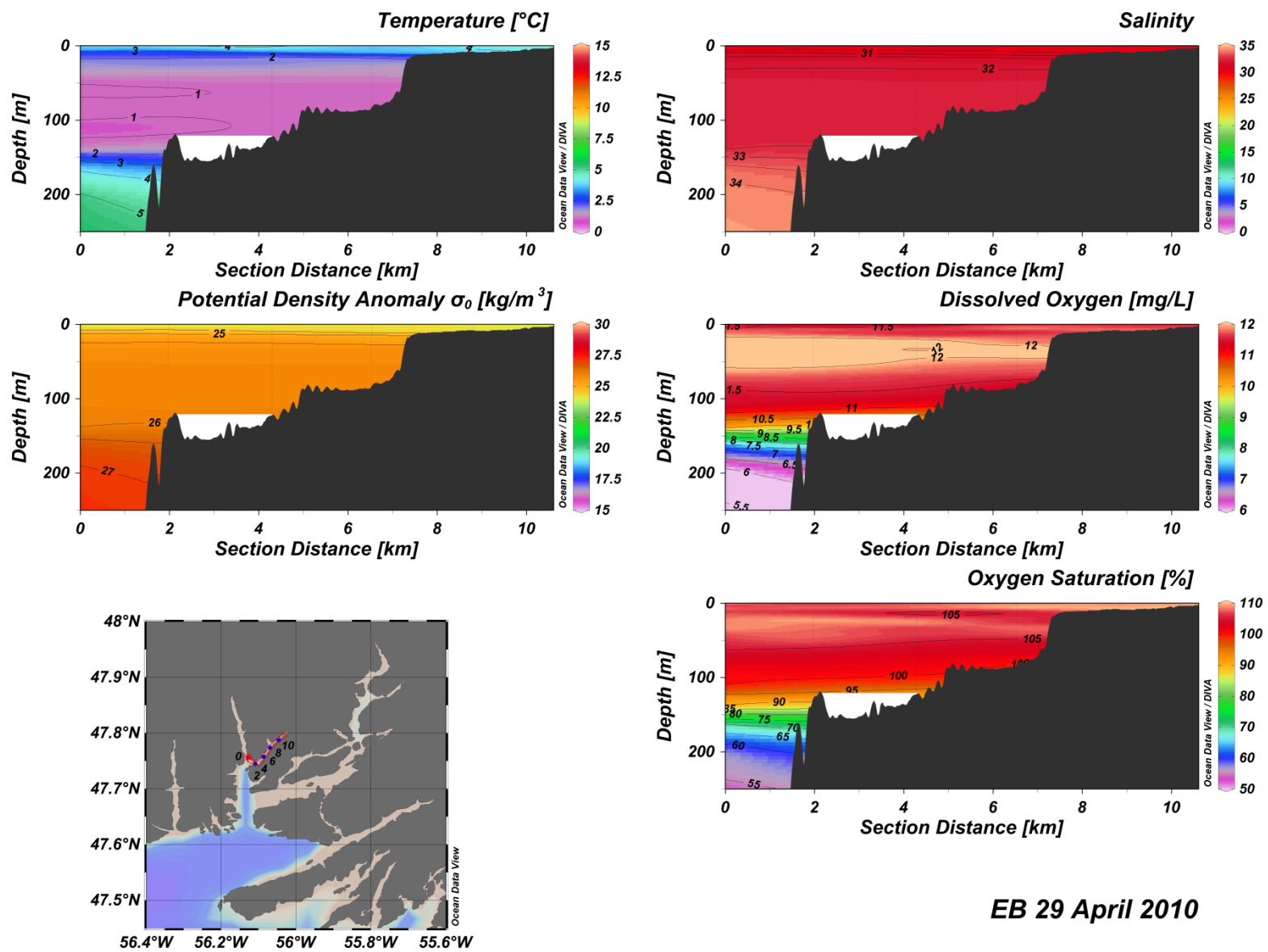


Figure A(i)42: East Bay water column vertical structure.



EB 29 April 2010

Figure A(i)43: East Bay water column vertical structure.

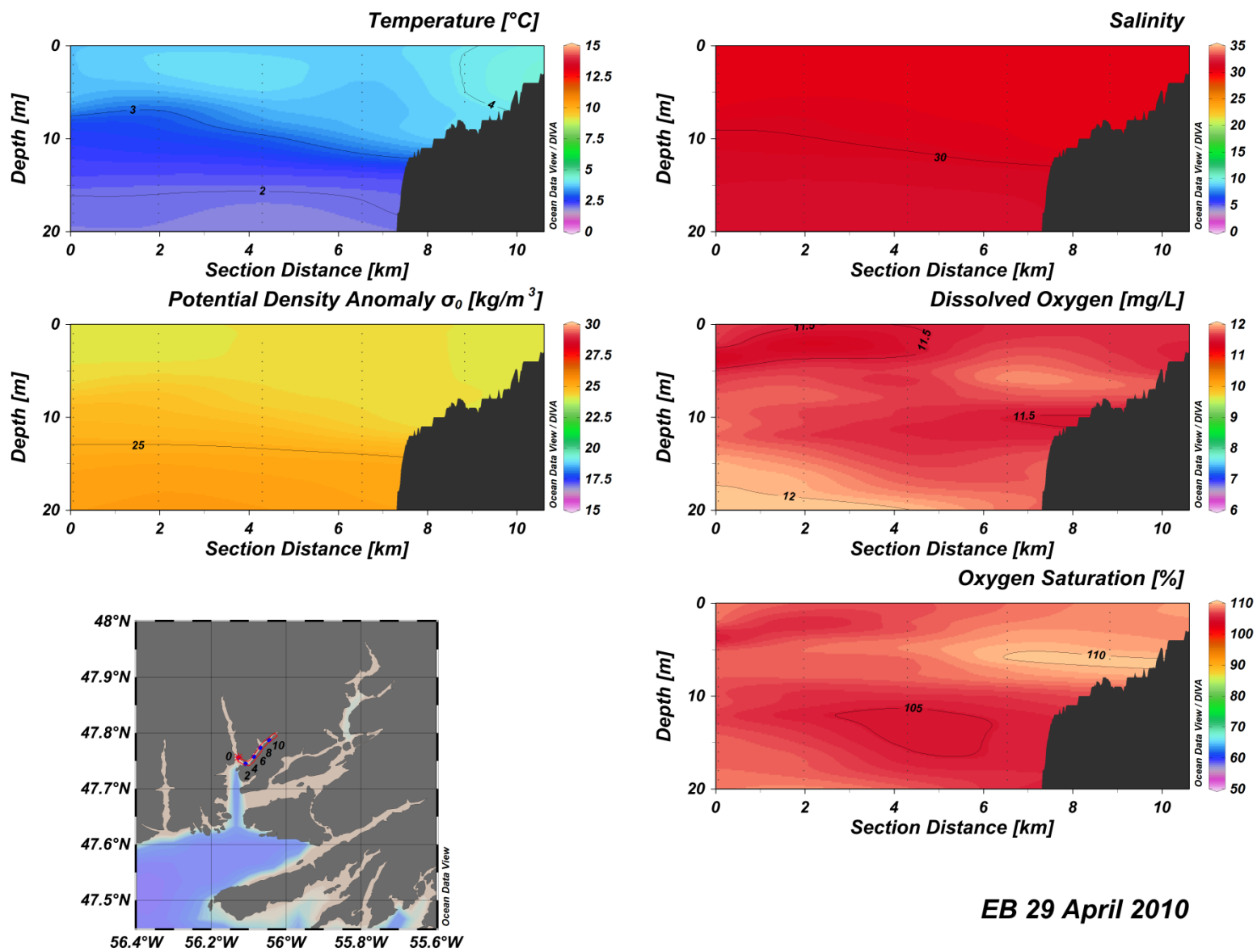
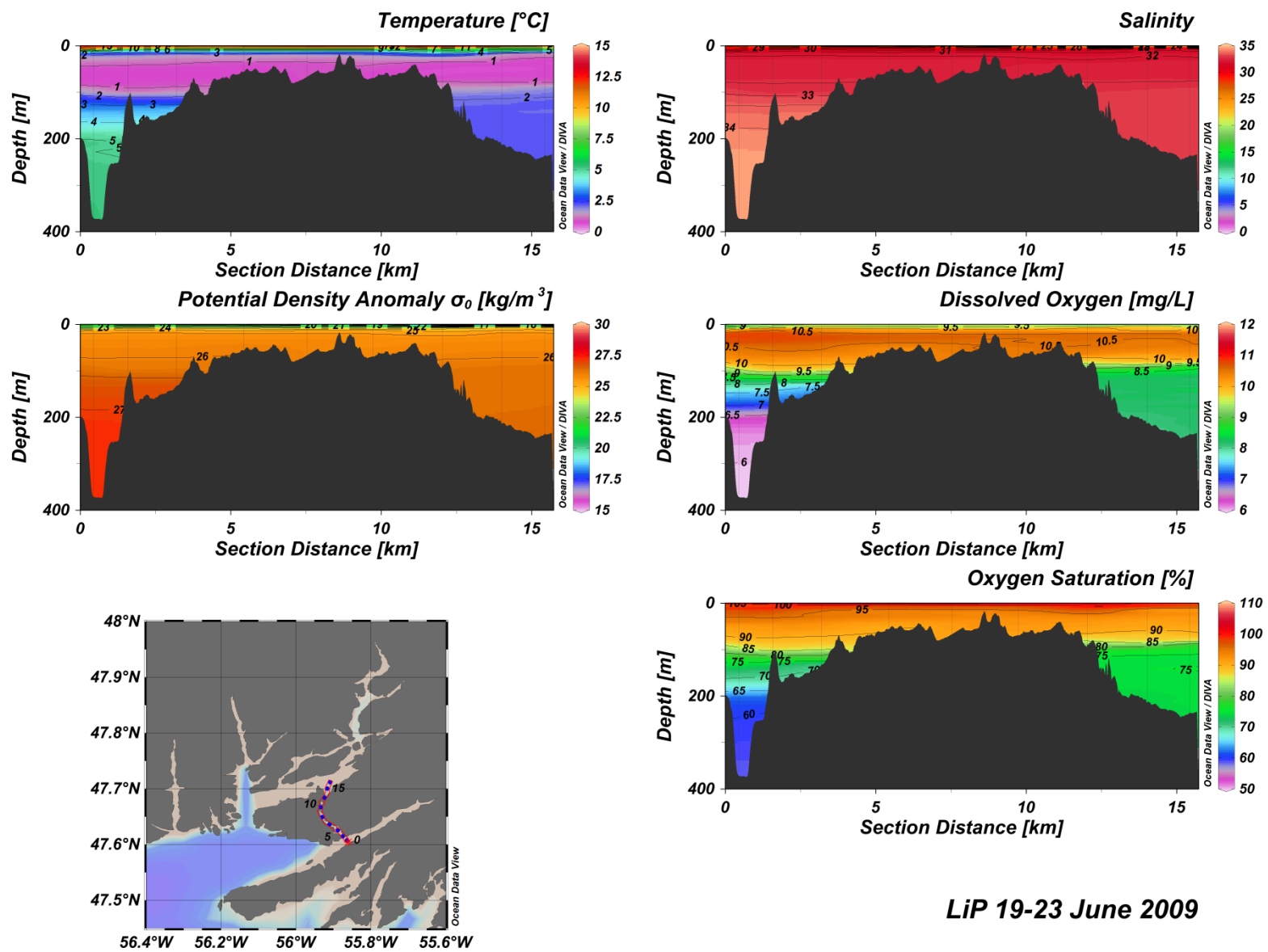
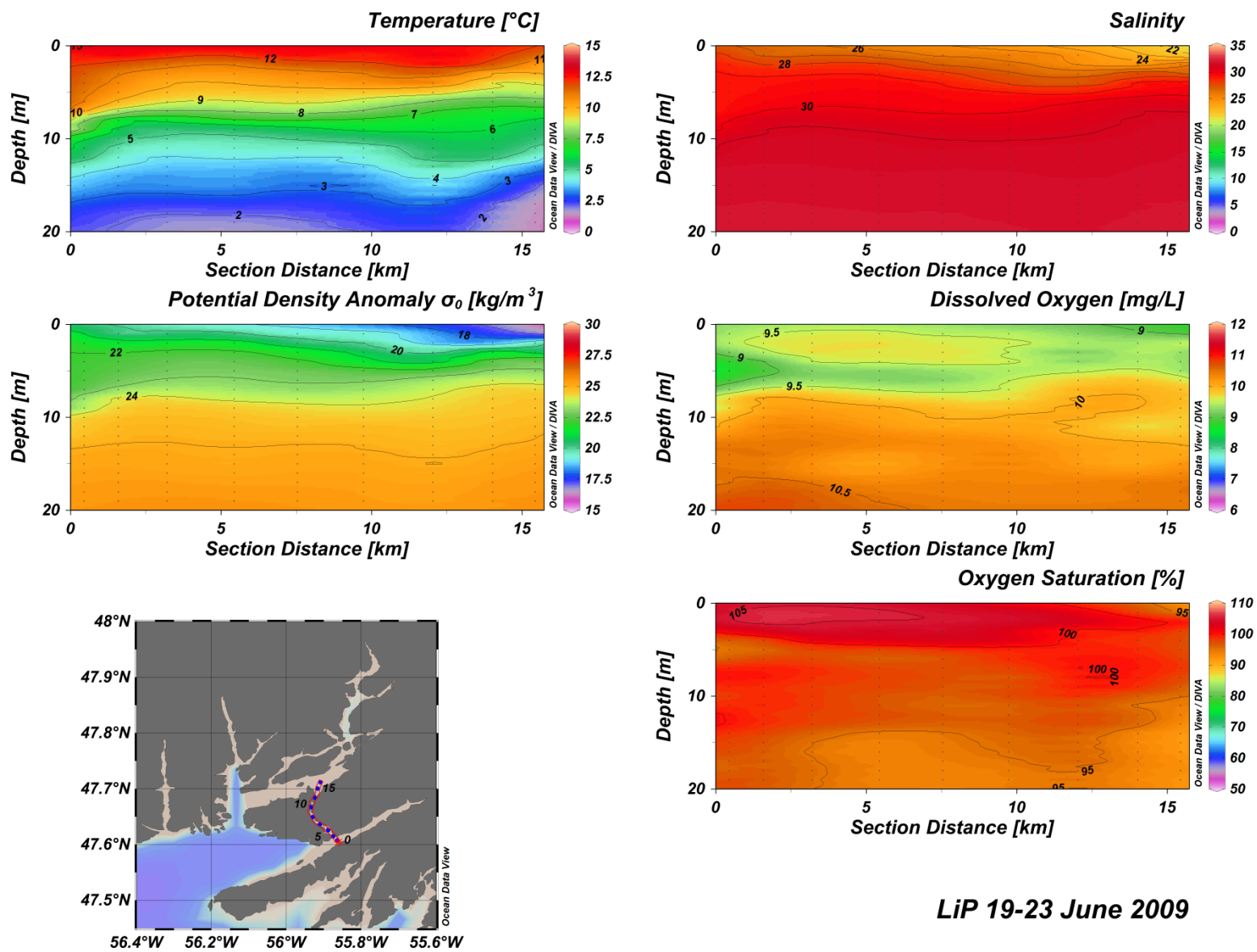


Figure A(i)44: East Bay water column vertical structure.



LIP 19-23 June 2009

Figure A(i)45: Little Passage water column vertical structure.



LiP 19-23 June 2009

Figure A(i)46: Little Passage water column vertical structure.

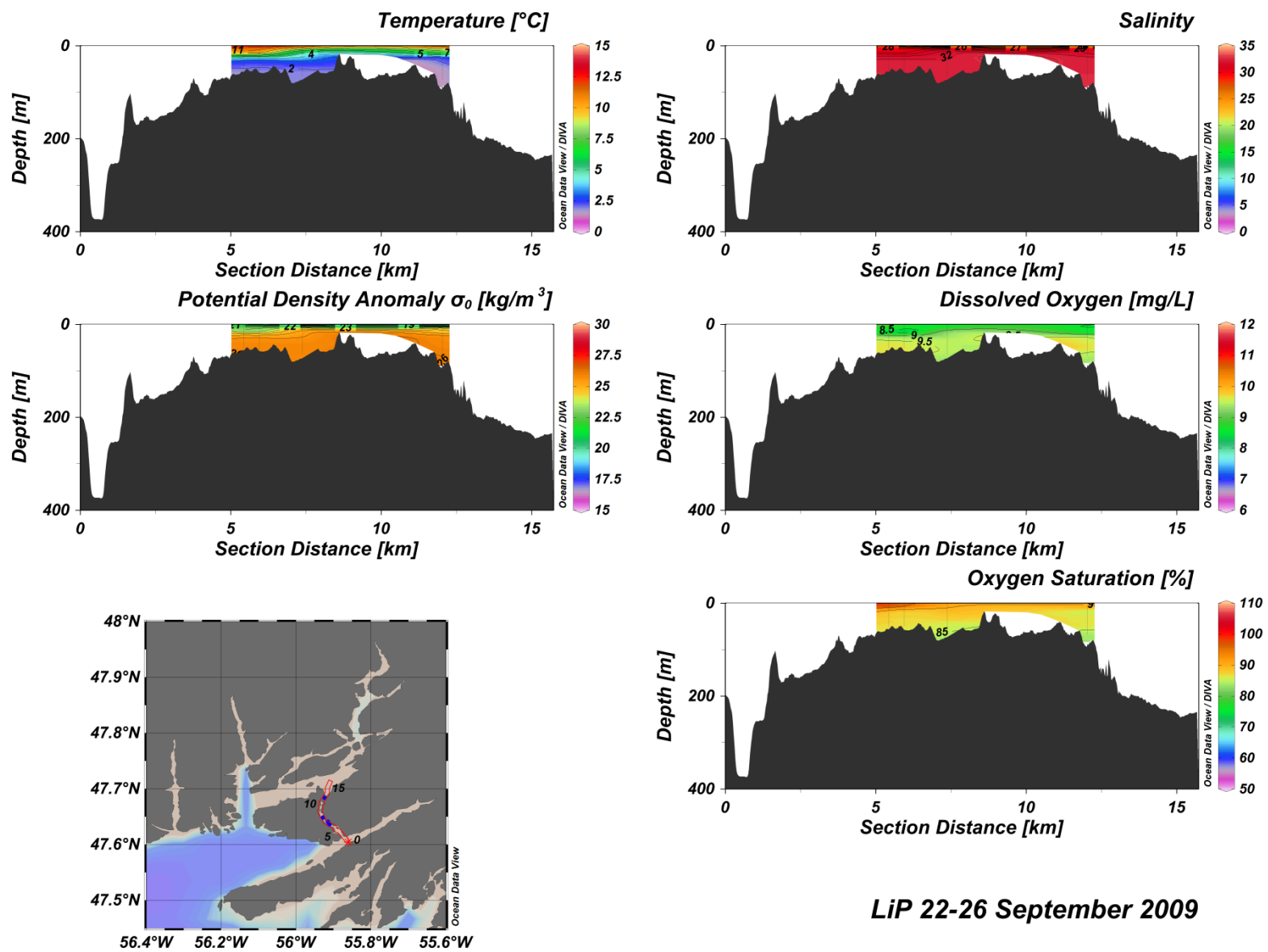


Figure A(i)47: Little Passage water column vertical structure.

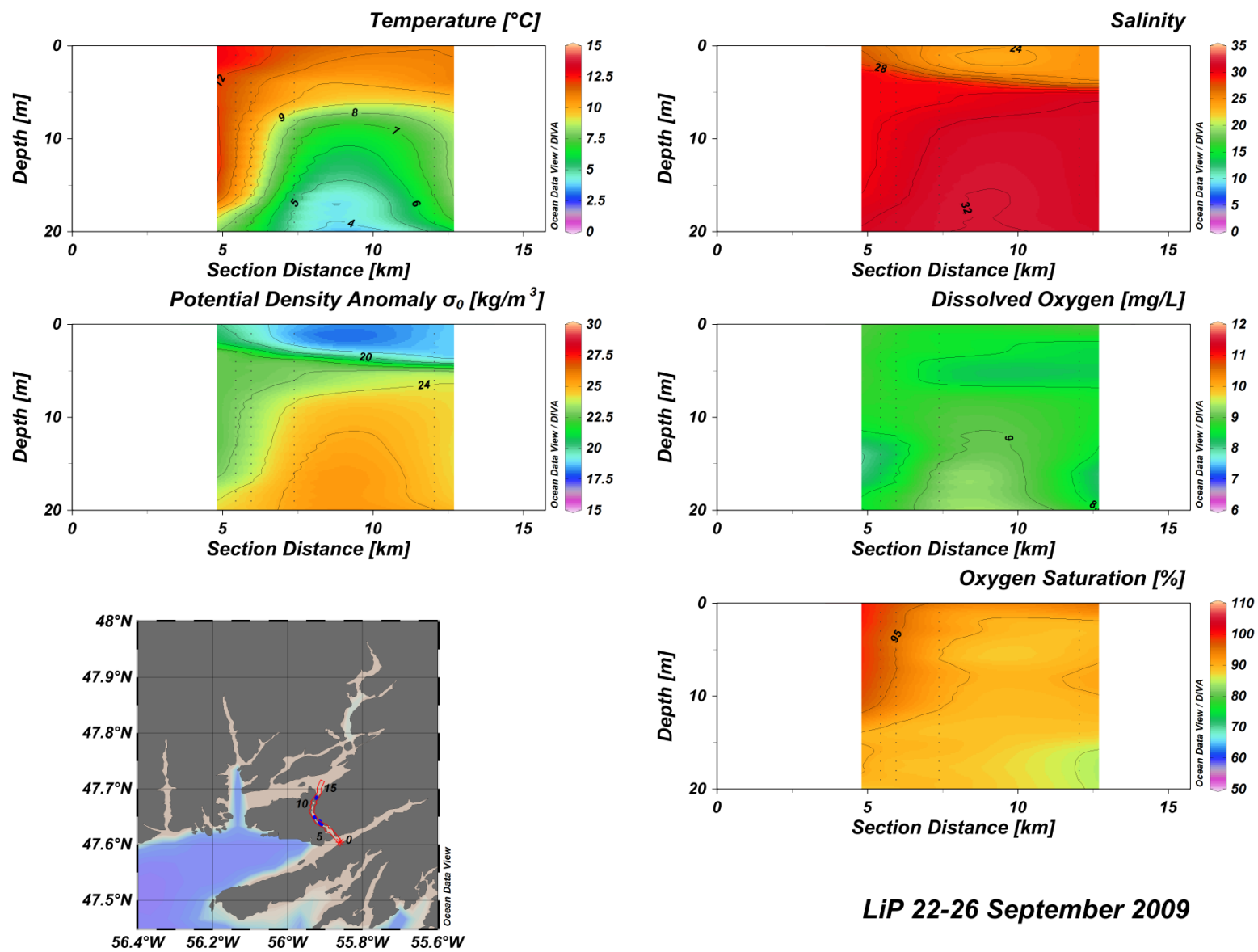
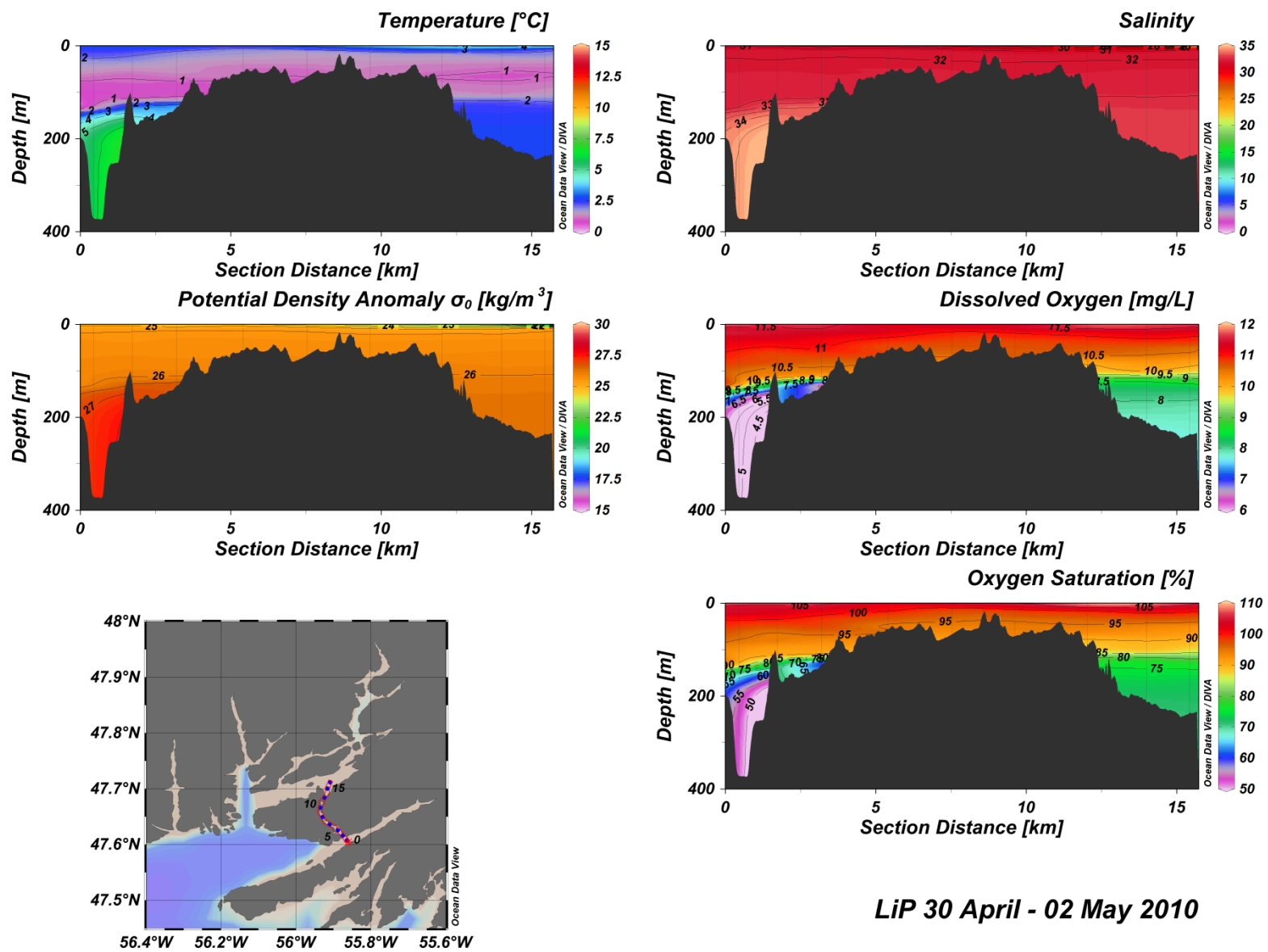


Figure A(i)48: Little Passage water column vertical structure.



LiP 30 April - 02 May 2010

Figure A(i)49: Little Passage water column vertical structure.

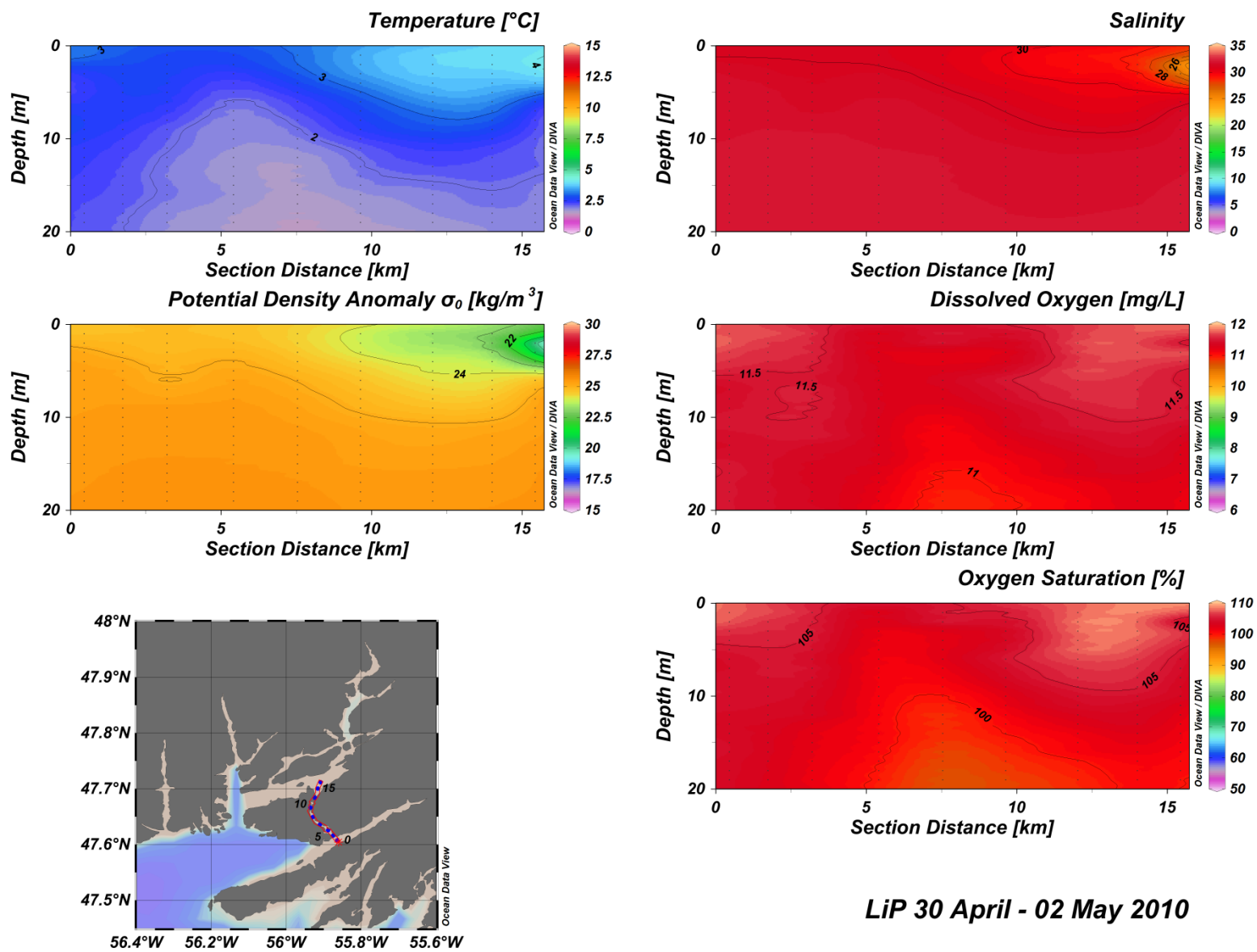


Figure A(i)50: Little Passage water column vertical structure.

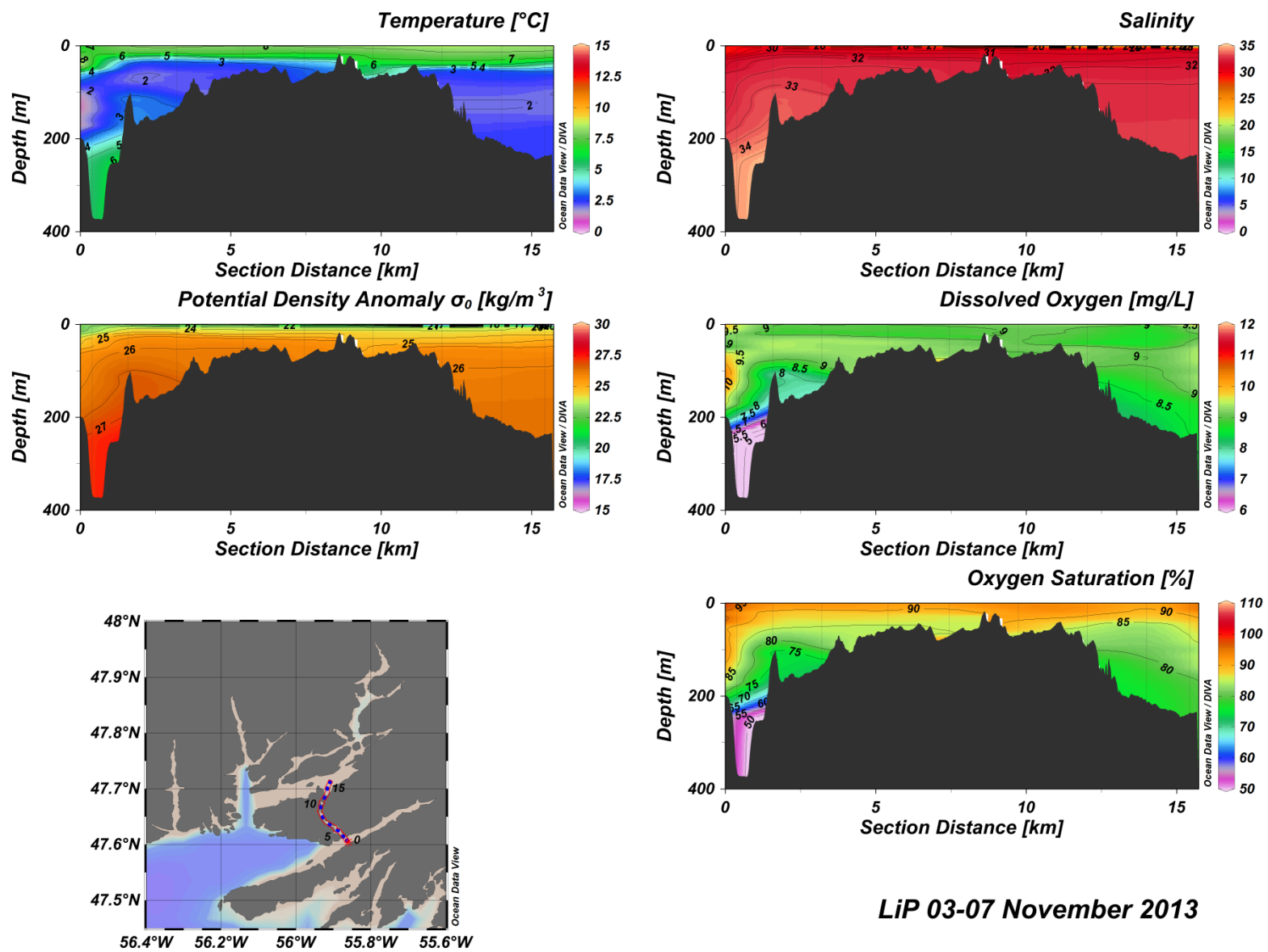


Figure A(i)51: Little Passage water column vertical structure.

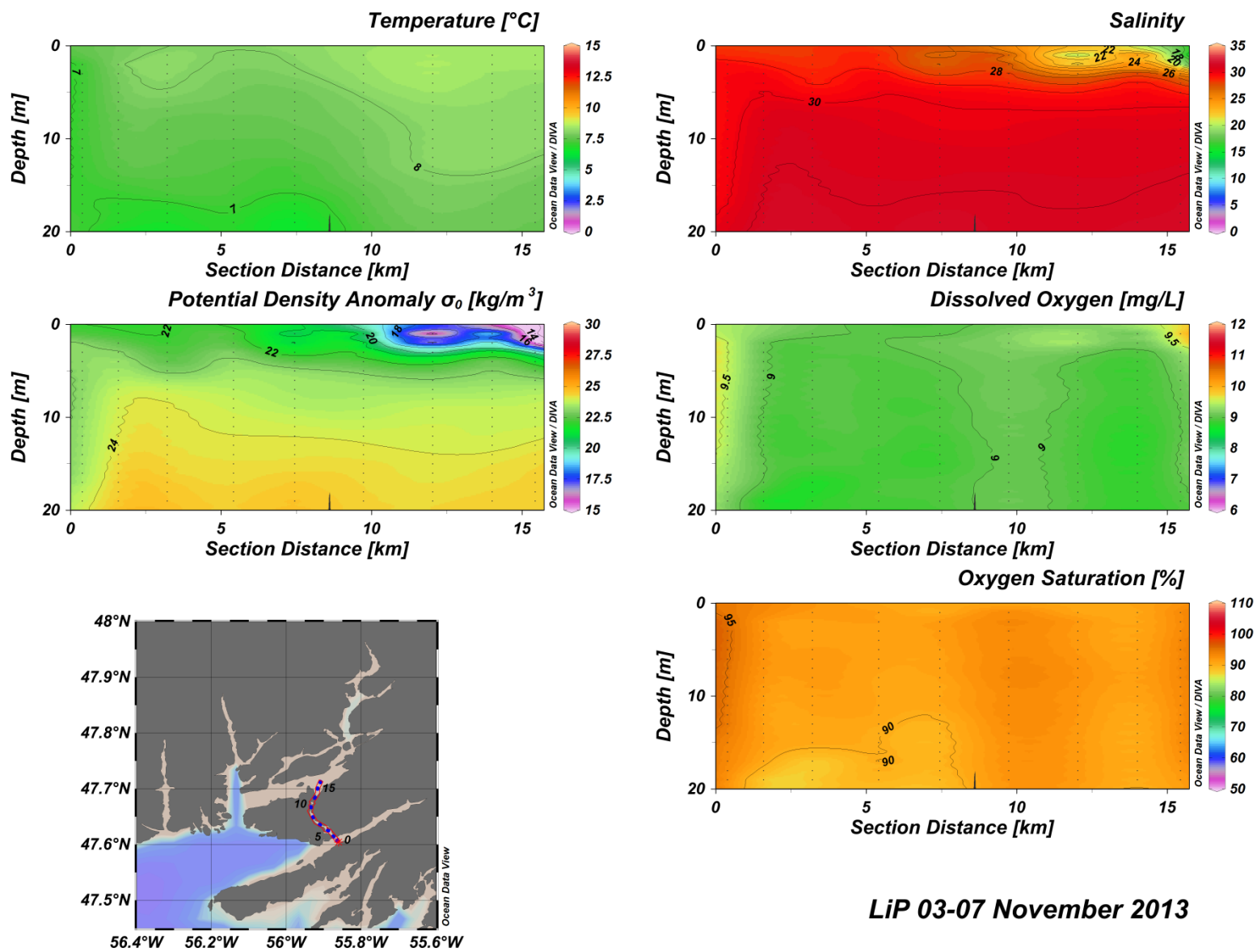


Figure A(i)52: Little Passage water column vertical structure.

**APPENDIX A(II): HERMITAGE BAY – BAY D’ESPOIR(HB-BDE) VERTICAL
SECTIONS SUMMARY TABLES**

Table A(ii)1: Hermitage Bay (HB) vertical sections summary statistics.

18-19 June 2009	T_min	T_max	T_mean	S_min	S_max	S_mean	DO_min	DO_max	DO_mean	ST_min	ST_max	ST_mean
Surface	1.22	12.65	7.17	27.36	32.03	30.9	8.12	11.13	9.93	20.55	25.65	24.13
Surface Gradients	0	4.69	0.47	0	2.51	0.14	0	1	0.17	0	2.61	0.17
Surface Clines	3	16	8.89	3	11	7.26	3	19	9	3	11	7.47
Intermediate 2°C_D = 30-110 m Dz = 80 m	0.56	2	1.06	31.93	33.08	32.44	8.83	11.1	10.25	-	-	-
Deep 5°C_D = 212.5 m Dz = N/A	5	5.65	5.21	34.05	34.54	34.42	5.74	6.96	6.08	-	-	-
22-26 September 2009	T_min	T_max	T_mean	S_min	S_max	S_mean	DO_min	DO_max	DO_mean	ST_min	ST_max	ST_mean
Surface	4.6	12.56	8.3	29.08	32.01	30.83	8.13	9.45	8.95	21.9	25.34	23.92
Surface Gradients	0	1.54	0.22	0	0.6	0.1	0	0.32	0.07	0	0.72	0.11
Surface Clines	12	67	23.5	6	17	12	9	67	25.33	6	17	12
Intermediate 2°C_D = 55-152.5 m Dz = 97.5 m	1	1.99	1.42	32.29	33.05	32.54	8.63	9.91	9.59	-	-	-
Deep 5°C_D = 212.5 m Dz = N/A	5	5.18	5.09	34.14	34.32	34.22	5.85	6.27	6.07	-	-	-
28-30 April 2010	T_min	T_max	T_mean	S_min	S_max	S_mean	DO_min	DO_max	DO_mean	ST_min	ST_max	ST_mean
Surface	1.9	3.51	2.49	30.96	32.03	31.83	11.09	12.21	11.54	24.66	25.58	25.39
Surface Gradients	0	0.3	0.03	0	0.43	0.02	0	0.12	0.03	0	0.35	0.02
Surface Clines	3	56	21.87	2	41	14.67	2	74	19.2	2	41	14.67
Intermediate 2°C_D = 28.5-143.5 m Dz = 115 m	0.45	1.99	1.13	31.85	33	32.26	8.9	12.44	11.02	-	-	-
Deep 5°C_D = 185 m Dz = N/A	5.01	6.25	5.73	34.07	34.65	34.49	5.06	6.66	5.42	-	-	-
07-08 May 2012	T_min	T_max	T_mean	S_min	S_max	S_mean	DO_min	DO_max	DO_mean	ST_min	ST_max	ST_mean
Surface	2.82	5.45	4.41	30.15	31.82	31.06	10.6	11.19	10.93	23.79	25.36	24.62
Surface Gradients	0	0.47	0.09	0	0.32	0.07	0	0.24	0.04	0	0.27	0.06
Surface Clines	3	48	17.9	5	9	7	3	45	20.5	5	9	7
Intermediate 2°C_D = 64-120 m Dz = 56 m	1.15	2	1.59	32.03	32.69	32.26	9.41	11.11	10.42	-	-	-
Deep 5°C_D = 177.5 m Dz = N/A	5	6.91	6.12	33.9	34.78	34.45	5.12	6.82	5.69	-	-	-

Table A(ii)1: Continued.

03-09 May 2013	T_min	T_max	T_mean	S_min	S_max	S_mean	DO_min	DO_max	DO_mean	ST_min	ST_max	ST_mean
Surface	1.98	5.63	3.45	29.25	32.17	31.62	10.56	11.82	11.34	23.13	25.71	25.14
Surface Gradients	0	1.15	0.15	0	0.65	0.06	0	0.37	0.07	0	0.62	0.06
Surface Clines	3	47	11.1	3	12	6	7	23	14	3	12	5.9
Intermediate 2°C_D = 30-101.5 m Dz = 71.5 m	0.99	2	1.45	32.06	32.83	32.36	9.4	11.16	10.42	-	-	-
Deep 5°C_D = 207.5 m Dz = N/A	5	5.76	5.43	34.2	34.55	34.39	5.59	6.31	5.94	-	-	-
07 November 2013	T_min	T_max	T_mean	S_min	S_max	S_mean	DO_min	DO_max	DO_mean	ST_min	ST_max	ST_mean
Surface	6.54	7.71	7.08	27.42	31.62	29.64	9.19	9.71	9.48	21.51	24.67	23.19
Surface Gradients	0	0.11	0.01	0	0.42	0.04	0	0.07	0.01	0	0.33	0.03
Surface Clines	46	61	53.38	6	34	22.23	26	58	48.92	6	34	21.62
Intermediate 2°C_D = 112.5-170 m Dz = 57.5 m	1.06	2	1.68	32.49	33.04	32.69	8.77	9.88	9.54	-	-	-
Deep 5°C_D = 234 m Dz = N/A	5	5.55	5.35	34.14	34.53	34.43	5.21	6.18	5.38	-	-	-

Table A(ii)2: Lower Bay d'Espoir (LBDE) vertical sections summary statistics.

18-23 June 2009	T_min	T_max	T_mean	S_min	S_max	S_mean	DO_min	DO_max	DO_mean	ST_min	ST_max	ST_mean
Surface	1.08	15.62	5.76	12.1	32.07	30.48	8.31	10.99	9.94	8.42	25.69	23.96
Surface Gradients	0	4.31	0.57	0	7.97	0.44	0	0.64	0.15	0	6.67	0.41
Surface Clines	2	13	5.06	2	7	4.06	3	17	6.78	2	7	4.11
Intermediate 2°C_D = 20-115 m Dz = 95 m	0.6	2	1.07	31.64	33.08	32.39	8.25	11.04	10.06	-	-	-
Deep 5°C_D = 297.5 m Dz = N/A	5	5.41	5.15	34.31	34.54	34.45	4.97	6.33	5.7	-	-	-
21-22 September 2009	T_min	T_max	T_mean	S_min	S_max	S_mean	DO_min	DO_max	DO_mean	ST_min	ST_max	ST_mean
Surface	5.94	13.7	10.1	10.42	31.67	29.1	7.95	9.17	8.49	7.41	24.92	22.33
Surface Gradients	0	1.44	0.35	0	6.84	0.67	0	0.58	0.09	0.01	5.4	0.57
Surface Clines	4	25	15.73	3	6	4	3	23	7.27	3	6	4.18
Intermediate 2°C_D = 47.5-157.5 m Dz = 115 m	0.8	1.99	1.4	32.02	33.03	32.5	8.07	9.91	9.44	-	-	-
Deep 5°C_D = N/A Dz = N/A	5.01	5.01	5.01	34.28	34.28	34.28	N/A	N/A	N/A	-	-	-
28 April – 02 May 2010	T_min	T_max	T_mean	S_min	S_max	S_mean	DO_min	DO_max	DO_mean	ST_min	ST_max	ST_mean
Surface	1.35	4.44	2.52	21.85	32	31.08	10.55	12.23	11.4	17.31	25.58	24.8
Surface Gradients	0	0.8	0.1	0	3.44	0.25	0	0.33	0.04	0	2.8	0.21
Surface Clines	3	46	8.53	3	41	7	2	98	14.24	3	41	7
Intermediate 2°C_D = 25-131.5 m Dz = 106.5 m	0.61	2	1.13	31.46	32.96	32.23	8.76	12.44	10.63	-	-	-
Deep 5°C_D = 194 m Dz = N/A	5	6.15	5.6	34.16	34.59	34.48	5.04	6.33	5.34	-	-	-
03-09 November 2013	T_min	T_max	T_mean	S_min	S_max	S_mean	DO_min	DO_max	DO_mean	ST_min	ST_max	ST_mean
Surface	6.74	8.7	7.86	10.07	31.62	29.33	8.46	10.48	9.11	7.69	24.67	22.84
Surface Gradients	0	0.37	0.04	0	8.52	0.48	0	0.5	0.04	0	6.67	0.38
Surface Clines	6	80	45.88	2	13	4.27	2	71	22.31	2	13	4.27
Intermediate 2°C_D = 122.5-167.5 m Dz = 45 m	1.19	2	1.7	32.5	33	32.68	8.77	9.98	9.5	-	-	-
Deep 5°C_D = 235 m Dz = N/A	5	5.85	5.52	34.16	34.59	34.46	4.75	6.03	5.26	-	-	-

Table A(ii)3: Lampidoes Passage – Upper Bay d'Espoir (LaP-UBDE) vertical sections summary statistics.

20-23 June 2009	T_min	T_max	T_mean	S_min	S_max	S_mean	DO_min	DO_max	DO_mean	ST_min	ST_max	ST_mean
Surface	1.48	16.22	4.87	2.24	32.72	28.83	7.62	10.73	9.63	1.02	26.11	22.77
Surface Gradients	0	6.45	0.65	0	11.7	0.99	0	1.66	0.17	0	9.43	0.85
Surface Clines	2	6	3.84	1	6	3.53	2	11	3.95	1	6	3.53
Intermediate 2°C_D = 17.5-116 m Dz = 98.5 m	0.66	2	1.05	31.53	33.07	32.21	8.45	10.73	10.13	-	-	-
Deep 5°C_D = 360 m Dz = N/A	5	5.04	5.03	34.41	34.43	34.42	5.57	5.71	5.65	-	-	-
21-26 September 2009	T_min	T_max	T_mean	S_min	S_max	S_mean	DO_min	DO_max	DO_mean	ST_min	ST_max	ST_mean
Surface	2.91	13.39	8.59	7.86	31.73	28.55	7.56	9.22	8.43	5.46	25.14	22.11
Surface Gradients	0.01	1.87	0.4	0	10.04	0.91	0	0.57	0.1	0.01	7.92	0.76
Surface Clines	3	26	11.73	2	5	3.4	2	26	6.13	2	6	3.53
Intermediate 2°C_D = 40-157 m Dz = 117 m	0.84	1.99	1.37	31.88	33.03	32.28	8.68	9.91	9.67	-	-	-
Deep 5°C_D = N/A Dz = N/A	N/A	N/A	N/A	N/A	N/A	N/A	N/A	N/A	N/A	-	-	-
02-03 May 2010	T_min	T_max	T_mean	S_min	S_max	S_mean	DO_min	DO_max	DO_mean	ST_min	ST_max	ST_mean
Surface	1.31	5.74	2.33	9.79	32.02	29.94	10.18	12.86	10.98	7.75	25.64	23.9
Surface Gradients	0	1.79	0.19	0	10.78	0.74	0	0.94	0.08	0	8.58	0.6
Surface Clines	3	5	3.68	2	4	3.42	2	15	3.63	2	4	3.42
Intermediate 2°C_D = 13.5-137 m Dz = 123.5 m	0.82	2	1.06	30.93	32.86	32.14	9.03	11.24	10.5	-	-	-
Deep 5°C_D = 180 m Dz = N/A	5.05	5.63	5.5	34.21	34.52	34.45	5.13	5.95	5.33	-	-	-
22-24 September 2012	T_min	T_max	T_mean	S_min	S_max	S_mean	DO_min	DO_max	DO_mean	ST_min	ST_max	ST_mean
Surface	9.02	18.25	14.36	4.4	30.78	26.88	7.04	8.29	7.58	1.93	23.82	19.85
Surface Gradients	0	1.26	0.36	0.02	11.5	1	0	0.67	0.09	0.03	8.98	0.83
Surface Clines	3	28	16.25	3	4	3.13	3	28	11.75	3	4	3.13
Intermediate 2°C_D = 61-92 m Dz = 31 m	1.92	2	1.97	32.14	32.19	32.17	9.39	9.65	9.54	-	-	-
Deep 5°C_D = N/A Dz = N/A	N/A	N/A	N/A	N/A	N/A	N/A	N/A	N/A	N/A	-	-	-

Table A(ii)3: Lampidoes Passage – Upper Bay d'Espoir (LaP-UBDE) vertical sections summary statistics.

08-09 November 2013	T_min	T_max	T_mean	S_min	S_max	S_mean	DO_min	DO_max	DO_mean	ST_min	ST_max	ST_mean
Surface	7.25	8.26	7.77	10.95	31.19	28.58	8.8	10.48	9.12	8.49	24.35	22.27
Surface Gradients	0	0.2	0.04	0	5.43	0.67	0	0.5	0.05	0	4.25	0.52
Surface Clines	44	62	55.75	3	5	3.63	3	62	10.88	3	5	3.63
Intermediate 2°C_D = N/A Dz = N/A	1.69	2	1.84	32.61	32.91	32.7	8.95	9.46	9.3	-	-	-
Deep 5°C_D = N/A Dz = N/A	5	5.63	5.42	34.22	34.51	34.42	5.02	5.84	5.33	-	-	-

Table A(ii)4: Lower Bay d'Espoir– North Bay (LBDE-NB) vertical sections summary statistics.

19-22 June 2009	T_min	T_max	T_mean	S_min	S_max	S_mean	DO_min	DO_max	DO_mean	ST_min	ST_max	ST_mean
Surface	0.83	15.69	6.33	19.54	31.92	30.08	7.04	10.79	9.22	14.16	25.56	23.57
Surface Gradients	0.01	5.46	0.68	0	5.09	0.44	0	0.97	0.14	0	4.82	0.43
Surface Clines	4	8	5.2	4	6	4.8	3	7	4.8	4	6	4.8
Intermediate 2°C_D = 17.5-111 m Dz = 93.5 m	0.63	2	1.05	31.51	33.09	32.39	7.57	10.89	9.4	-	-	-
Deep 5°C_D = 319 m Dz = N/A	5	5.23	5.13	34.35	34.51	34.45	4.98	6.21	5.64	-	-	-
22-26 September 2009	T_min	T_max	T_mean	S_min	S_max	S_mean	DO_min	DO_max	DO_mean	ST_min	ST_max	ST_mean
Surface	6.07	14.08	10.83	24.23	31.66	29.63	7.55	9.03	8.35	17.87	24.85	22.61
Surface Gradients	0	1.13	0.35	0	2.07	0.29	0	0.39	0.1	0	1.67	0.28
Surface Clines	3	24	15.5	2	9	5.63	3	22	9.38	2	9	5.63
Intermediate 2°C_D = 40.5-149 m Dz = 108.5 m	0.8	1.99	1.26	31.85	33.02	32.51	8.44	10.07	9.61	-	-	-
Deep 5°C_D = N/A Dz = N/A	5.01	5.01	5.01	34.28	34.28	34.28	N/A	N/A	N/A	-	-	-
28 April – 01 May 2010	T_min	T_max	T_mean	S_min	S_max	S_mean	DO_min	DO_max	DO_mean	ST_min	ST_max	ST_mean
Surface	1.66	5.73	2.98	26.77	31.99	30.88	10.58	12.28	11.65	21.08	25.53	24.6
Surface Gradients	0	0.67	0.11	0	0.89	0.1	0	0.54	0.06	0	0.77	0.09
Surface Clines	3	31	10.55	5	15	8.91	2	16	8.09	5	15	8.91
Intermediate 2°C_D = 25.5-143.5 m Dz = 118 m	0.7	2	1.2	31.47	32.92	32.25	8.96	12.27	11.22	-	-	-
Deep 5°C_D = 107.5 m Dz = N/A	5	5.78	5.52	34.17	34.56	34.47	4.96	6.22	5.28	-	-	-

Table A(ii)5: East Bay (EB) vertical sections summary statistics.

19 June 2009	T_min	T_max	T_mean	S_min	S_max	S_mean	DO_min	DO_max	DO_mean	ST_min	ST_max	ST_mean
Surface	1.27	16.87	6.68	19.51	31.78	29.29	7.27	9.47	8.66	13.7	25.44	22.91
Surface Gradients	0.01	3.27	0.78	0	3.11	0.6	0	0.51	0.12	0	2.97	0.57
Surface Clines	4	6	5	3	6	4.33	4	6	4.67	3	6	4.33
Intermediate 2°C_D = 18.5-112.5 m Dz = 94 m	0.54	1.98	0.92	31.65	33.08	32.3	7.69	9.47	8.94	-	-	-
Deep 5°C_D = N/A Dz = N/A	N/A	N/A	N/A	N/A	N/A	N/A	N/A	N/A	N/A	-	-	-
29 April 2010	T_min	T_max	T_mean	S_min	S_max	S_mean	DO_min	DO_max	DO_mean	ST_min	ST_max	ST_mean
Surface	1.79	4.02	2.88	30.31	31.8	30.95	11.32	12.11	11.71	24.07	25.41	24.66
Surface Gradients	0	0.42	0.1	0	0.31	0.07	0	0.22	0.06	0	0.28	0.06
Surface Clines	6	13	8.8	6	13	9.2	4	9	5.6	6	13	9.2
Intermediate 2°C_D = 16-145 m Dz = 129 m	0.92	2	1.22	31.51	32.75	32.16	9.2	12.24	11.63	-	-	-
Deep 5°C_D = 202 m Dz = N/A	5.01	5.46	5.34	34.22	34.47	34.38	5.22	5.84	5.49	-	-	-

Table A(ii)6: Little Passage (LiP) vertical sections summary statistics.

19-23 June 2009	T_min	T_max	T_mean	S_min	S_max	S_mean	DO_min	DO_max	DO_mean	ST_min	ST_max	ST_mean
Surface	1.3	13.16	6.01	23.07	31.97	30.41	8.71	10.8	9.95	17.34	25.59	23.87
Surface Gradients	0.04	2.47	0.55	0	4.5	0.31	0	0.62	0.13	0.01	3.87	0.32
Surface Clines	3	10	7.67	2	10	4	4	85	16.44	2	10	4
Intermediate 2°C_D = 19-111 m Dz = 92 m	0.62	2	1.07	31.75	33.05	32.35	8.26	10.86	10.15	-	-	-
Deep 5°C_D = 200 m Dz = N/A	5	5.2	5.12	34.29	34.47	34.43	5.9	6.34	6.04	-	-	-
22-26 September 2009	T_min	T_max	T_mean	S_min	S_max	S_mean	DO_min	DO_max	DO_mean	ST_min	ST_max	ST_mean
Surface	4.31	12.58	9.18	24.12	31.95	29.98	8.16	9.32	8.64	18.25	25.34	23.15
Surface Gradients	0.01	1.27	0.31	0	4.7	0.33	0	0.3	0.08	0	3.78	0.3
Surface Clines	8	20	16	3	5	3.75	2	18	9.75	3	5	3.75
Intermediate 2°C_D = 43.5 m Dz = N/A	1.44	2	1.74	32.26	32.49	32.38	9.42	9.71	9.55	-	-	-
Deep 5°C_D = N/A; Dz = N/A	N/A	N/A	N/A	N/A	N/A	N/A	N/A	N/A	N/A	-	-	-
30 April – 02 May 2010	T_min	T_max	T_mean	S_min	S_max	S_mean	DO_min	DO_max	DO_mean	ST_min	ST_max	ST_mean
Surface	1.43	4.01	2.33	25.27	31.96	31.34	10.88	11.74	11.37	20.06	25.56	25.02
Surface Gradients	0	0.5	0.08	0	2.02	0.11	0	0.27	0.04	0	1.65	0.1
Surface Clines	3	10	6.33	2	9	4.56	3	20	9.67	2	9	4.56
Intermediate 2°C_D = 16.5-130 m Dz = 113.5 m	0.8	2	1.26	31.61	32.91	32.16	8.53	11.51	10.62	-	-	-
Deep 5°C_D = 175 m Dz = N/A	5.02	5.85	5.73	34.16	34.58	34.52	5.14	6.1	5.31	-	-	-
03-07 November 2013	T_min	T_max	T_mean	S_min	S_max	S_mean	DO_min	DO_max	DO_mean	ST_min	ST_max	ST_mean
Surface	6.3	8.49	7.66	16.26	31.49	29.99	8.45	9.84	8.97	12.56	24.71	23.39
Surface Gradients	0	0.33	0.06	0	6.6	0.32	0	0.4	0.03	0	5.16	0.26
Surface Clines	21	68	36.63	2	18	4.56	2	48	18.75	2	18	4.63
Intermediate 2°C_D = N/A Dz = N/A	1.62	2	1.88	32.53	32.98	32.69	8.68	9.7	9.23	-	-	-
Deep 5°C_D = N/A Dz = N/A	5.02	5.45	5.38	34.26	34.49	34.45	5.27	5.71	5.35	-	-	-

APPENDIX A(III): HERMITAGE BAY – BAY D’ESPOIR(HB-BDE) SURFACE MAPS

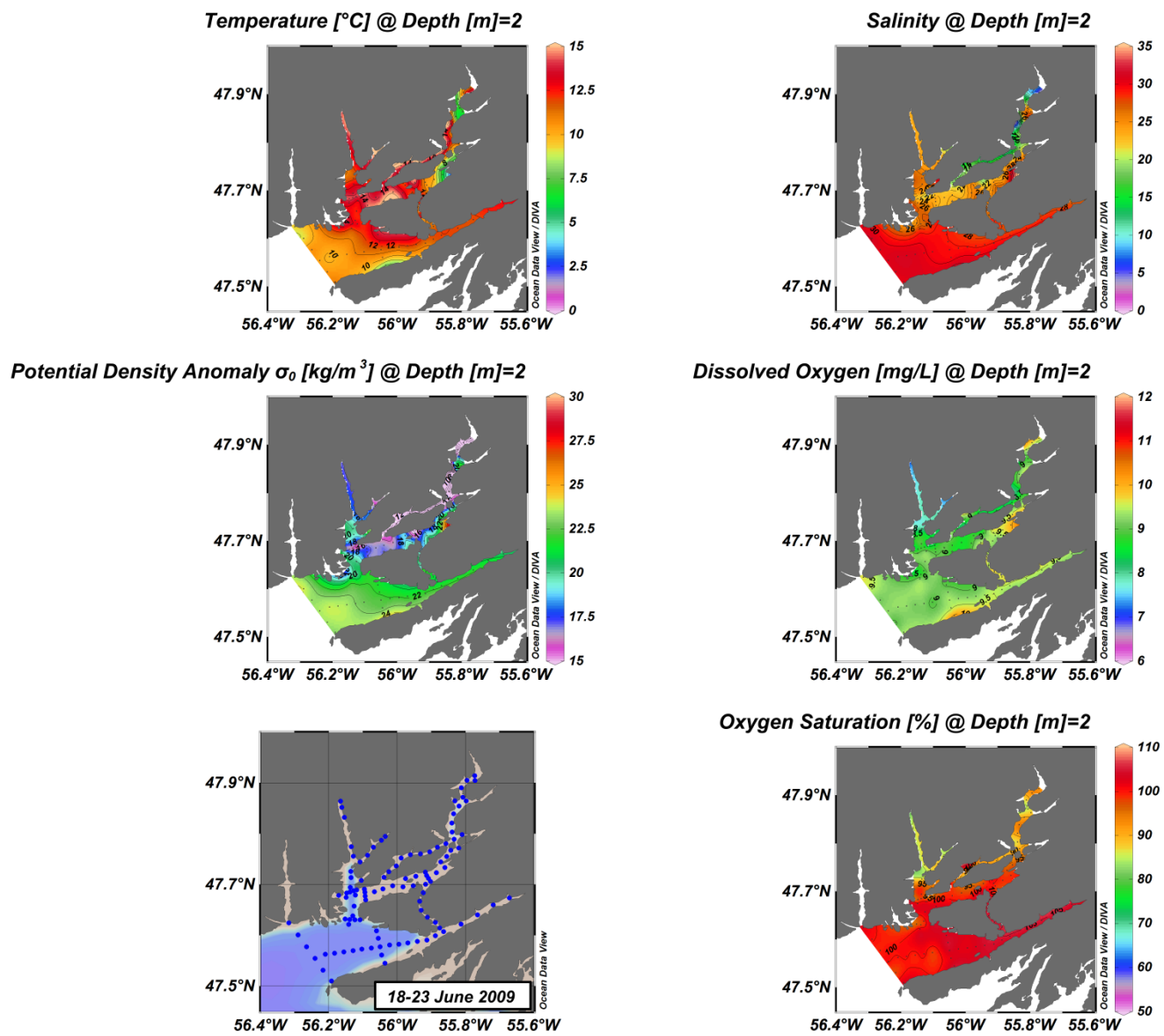


Figure A(iii)1: Hermitage Bay – Bay d'Espoirs surface structure.

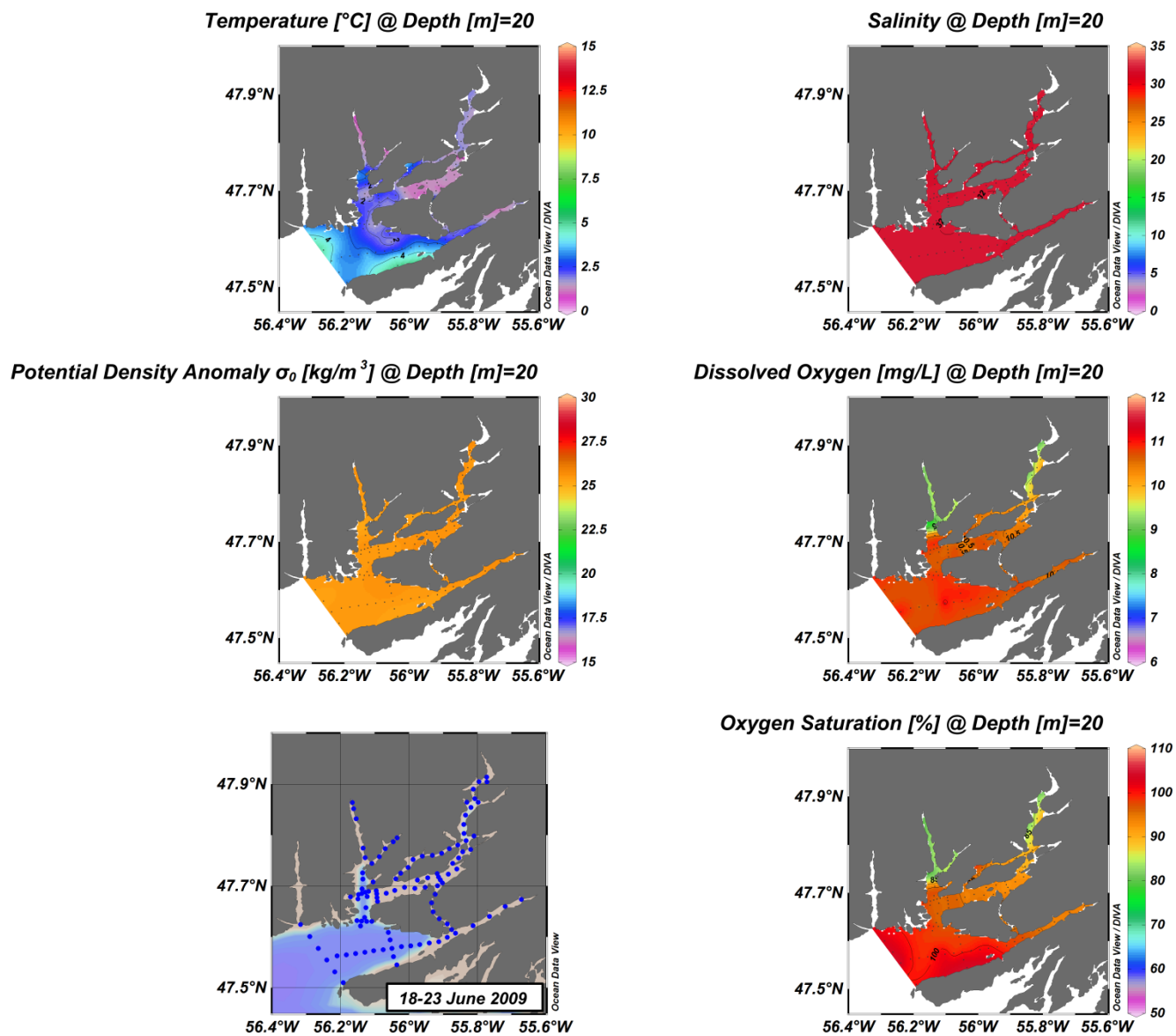


Figure A(iii)2: Hermitage Bay – Bay d'Espoirs surface structure.

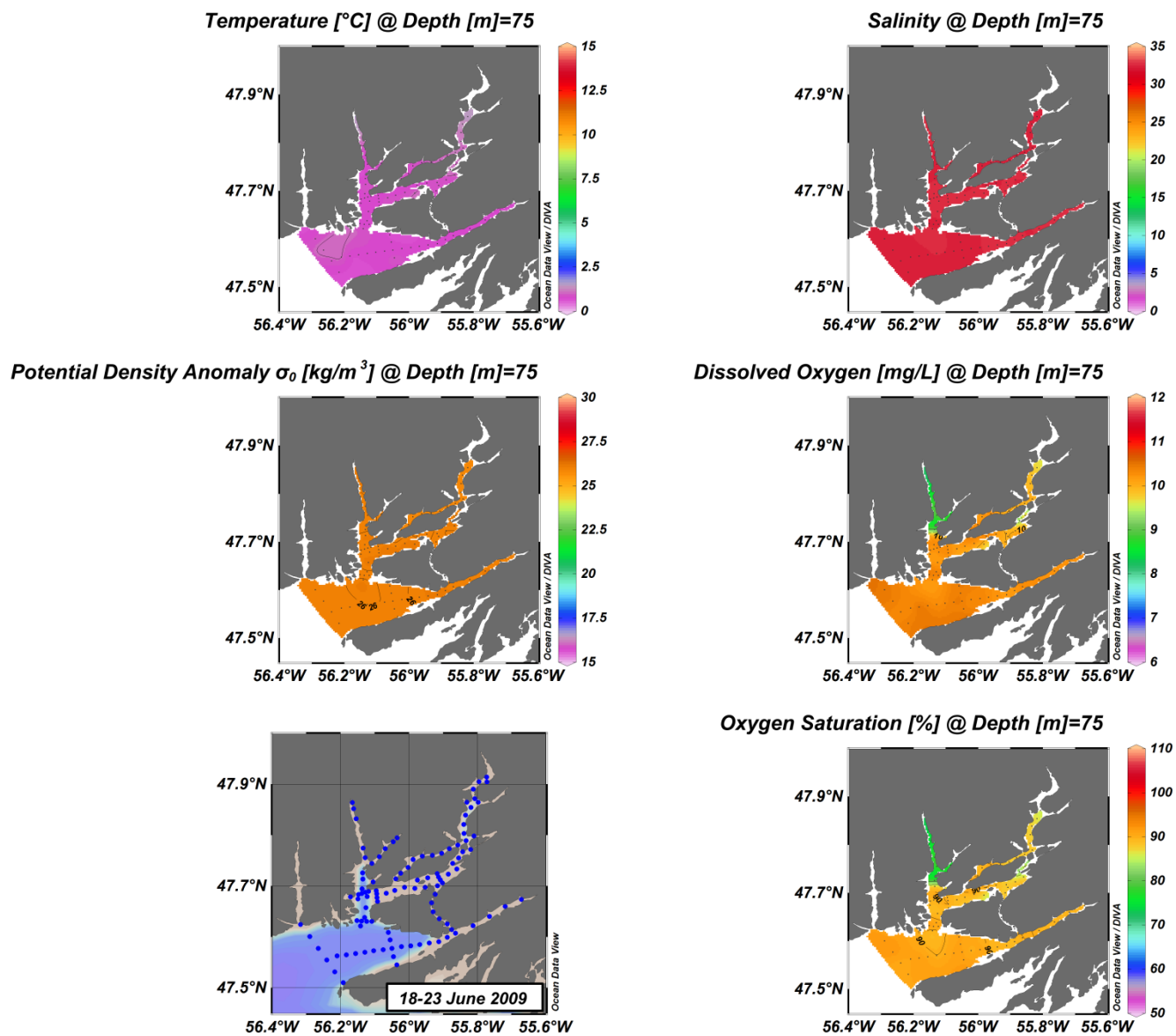


Figure A(iii)3: Hermitage Bay – Bay d'Espoirs surface structure.

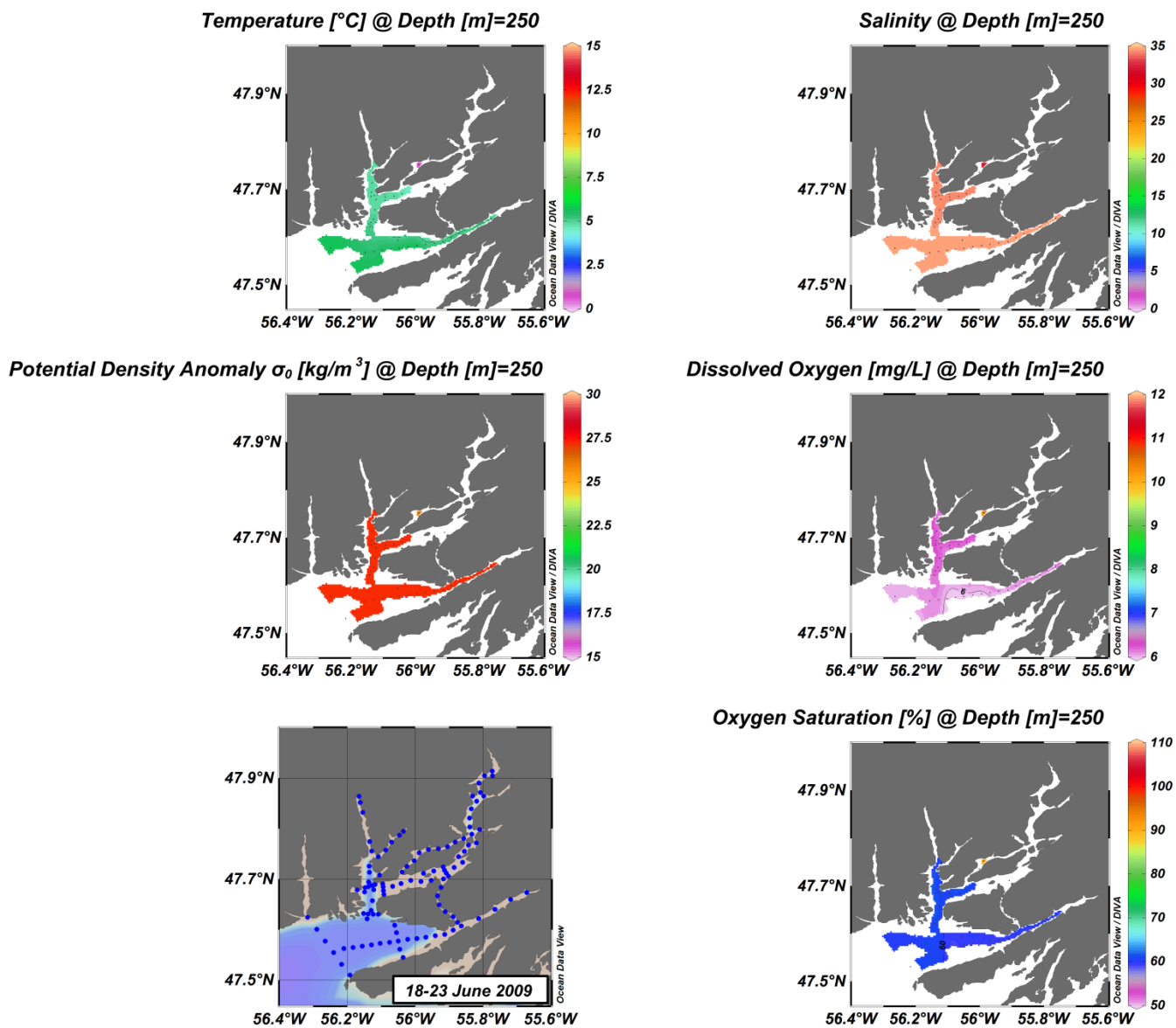


Figure A(iii)4: Hermitage Bay – Bay d'Espoirs surface structure.

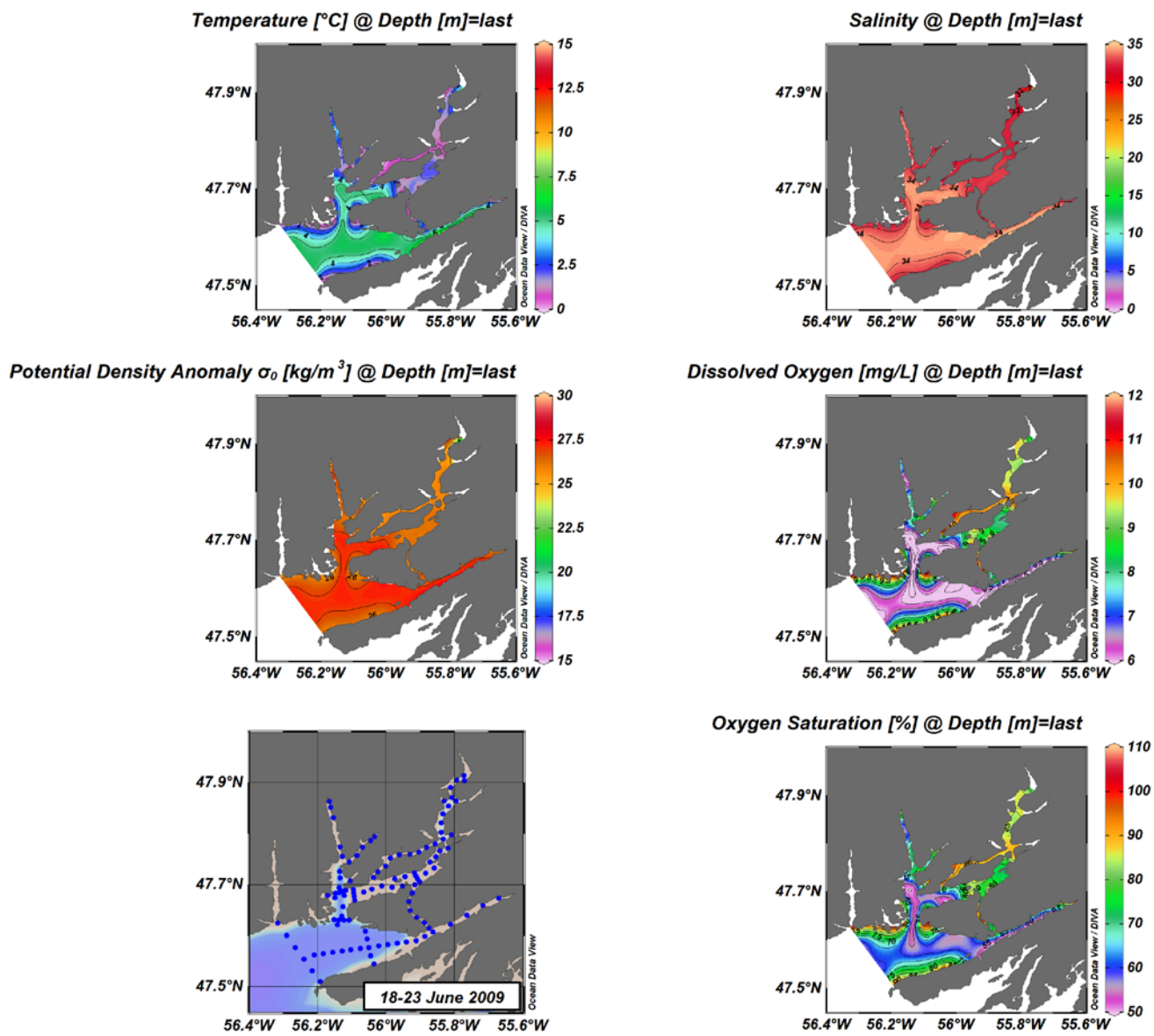


Figure A(iii)5: Hermitage Bay – Bay d'Espoirs surface structure.

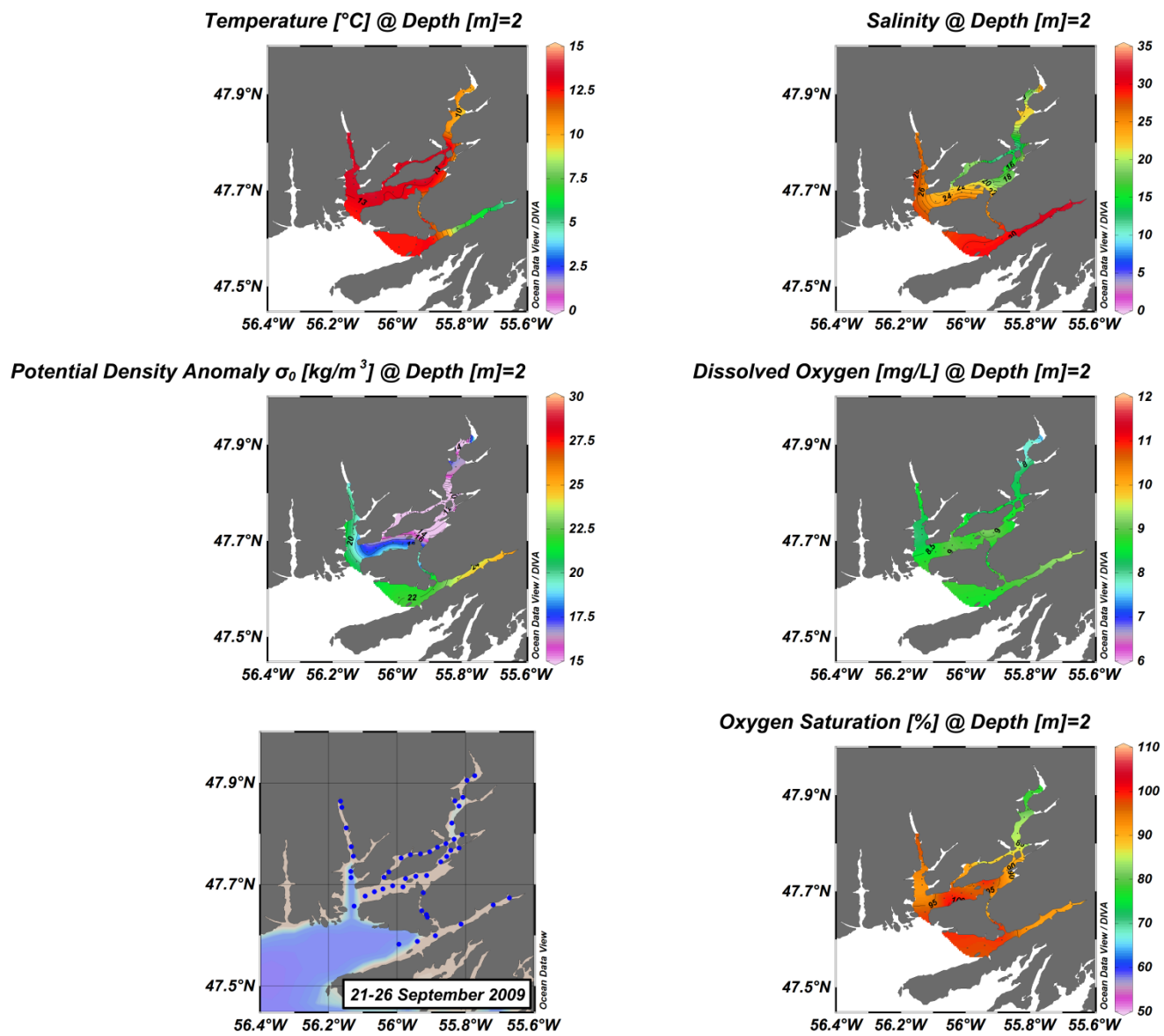


Figure A(iii)6: Hermitage Bay – Bay d'Espoirs surface structure.

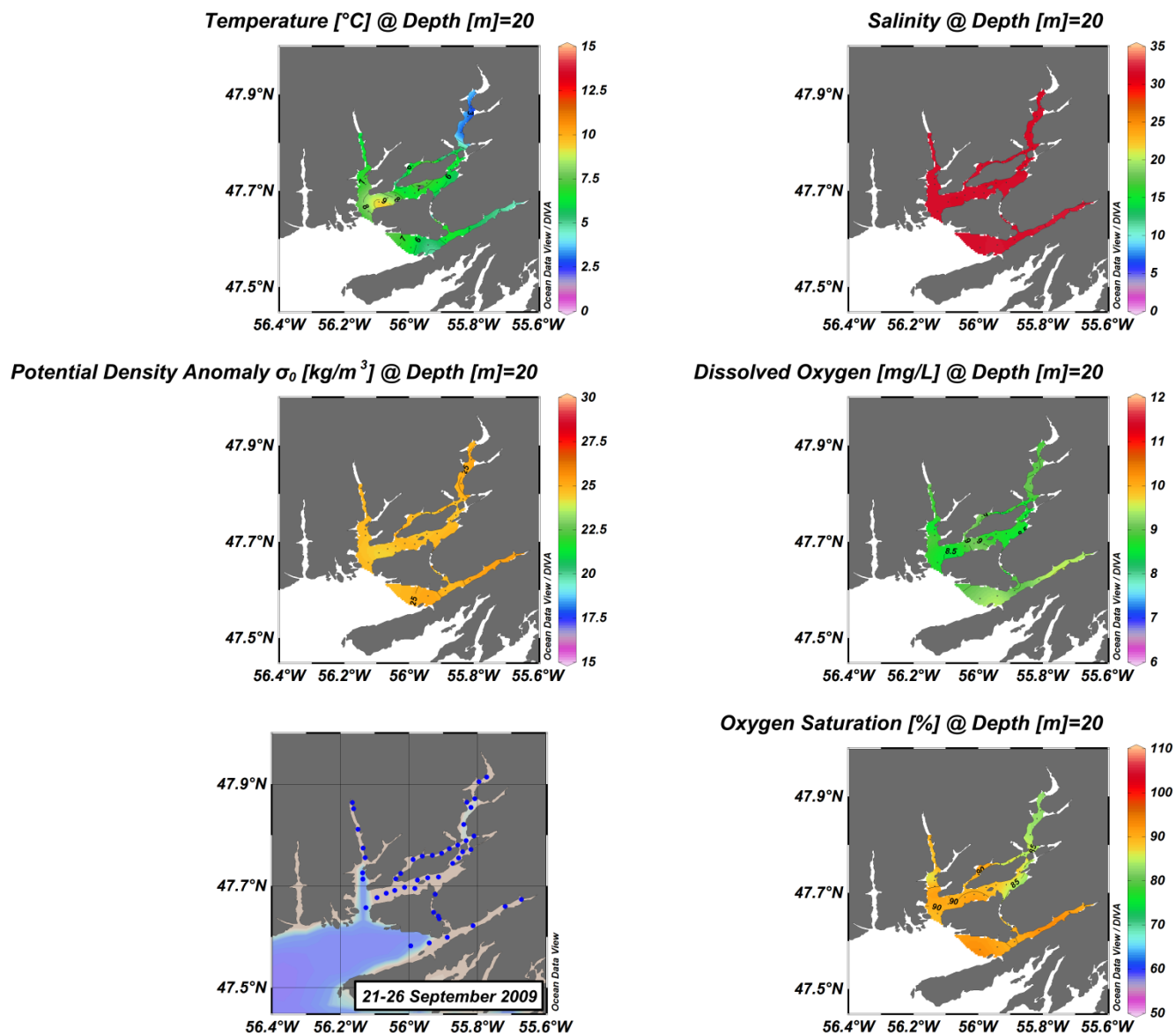


Figure A(iii)7: Hermitage Bay – Bay d'Espoirs surface structure.

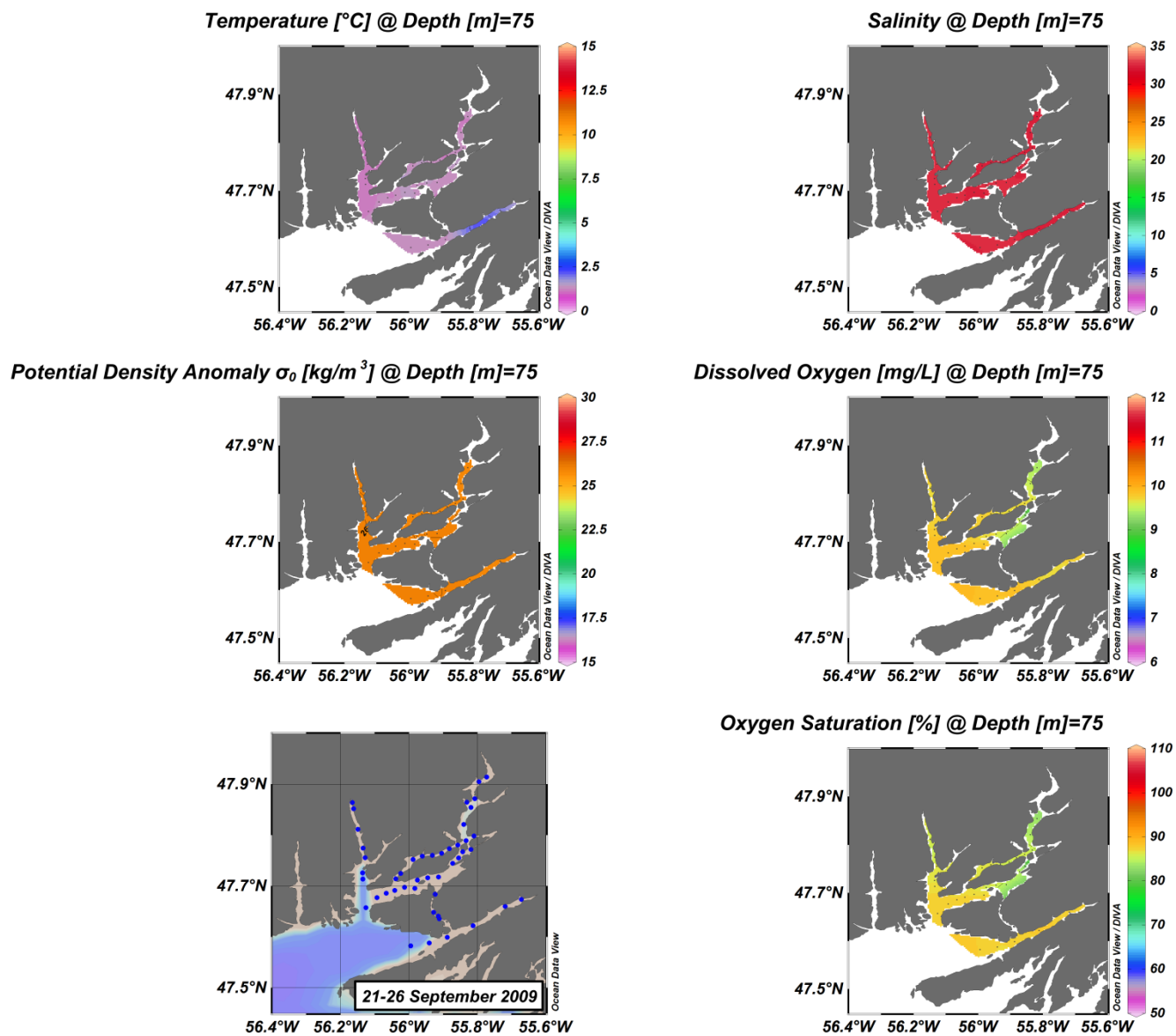


Figure A(iii)8: Hermitage Bay – Bay d'Espoirs surface structure.

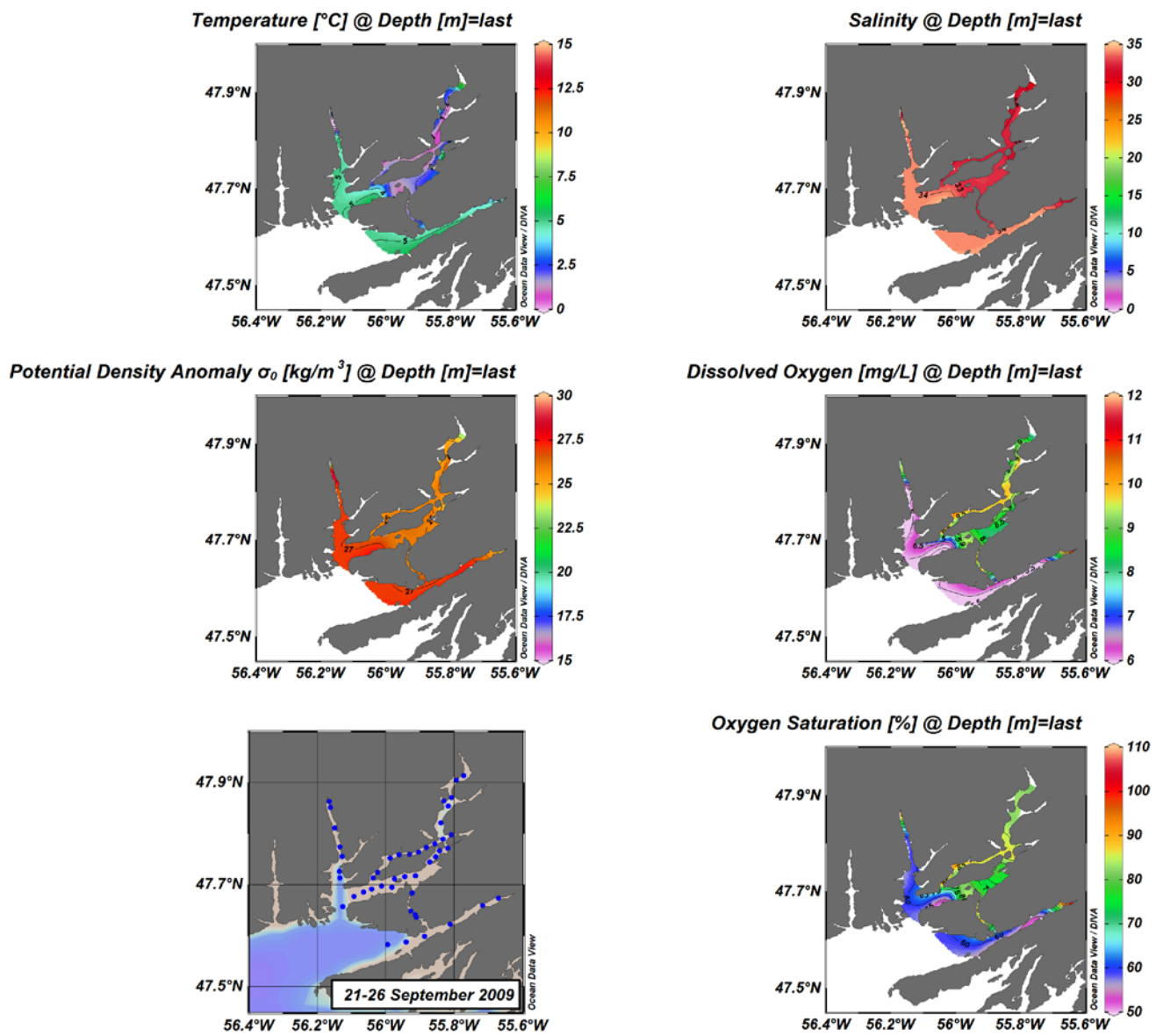


Figure A(iii)9: Hermitage Bay – Bay d'Espoirs surface structure.

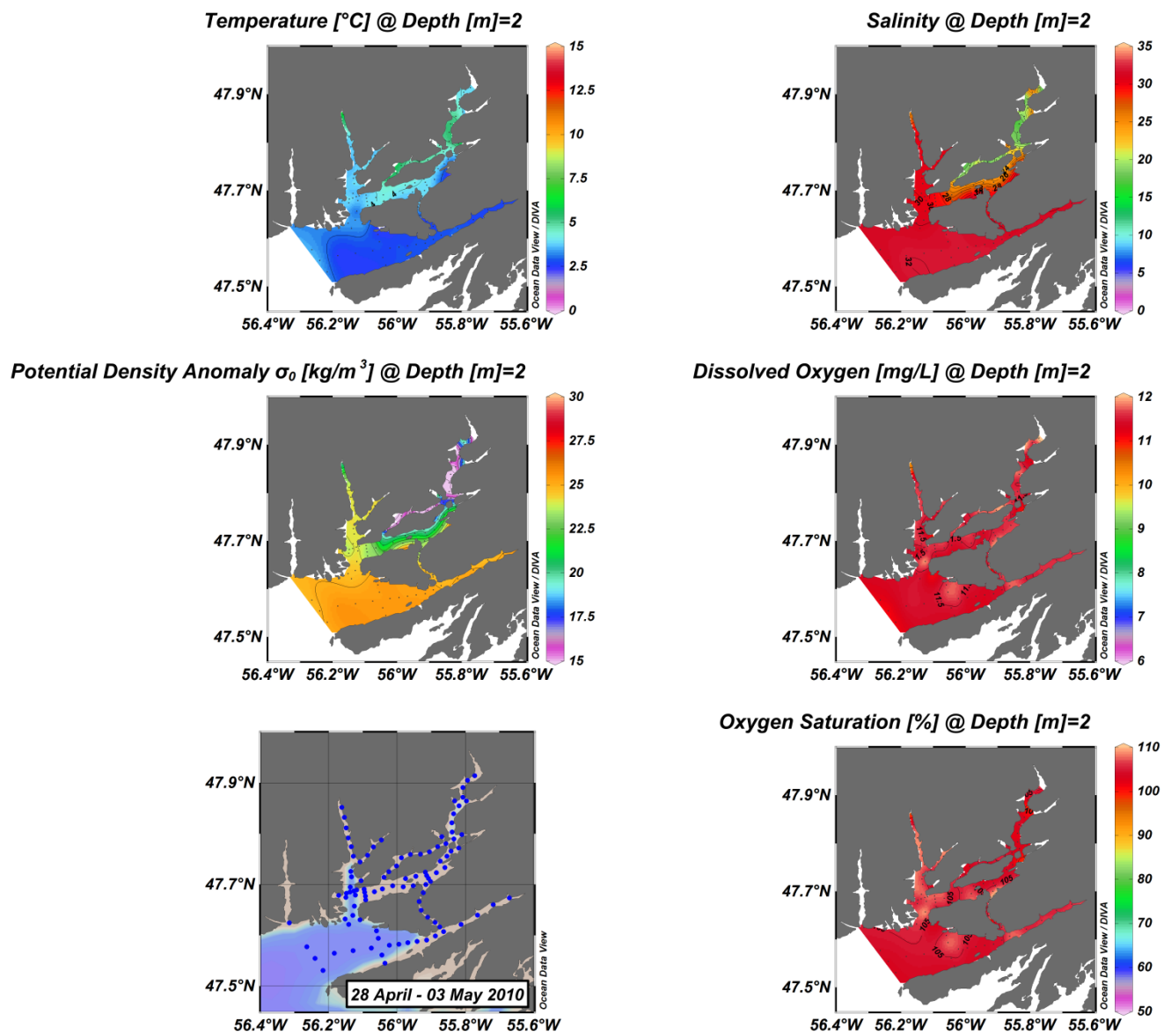


Figure A(iii)10: Hermitage Bay – Bay d'Espoir surface structure.

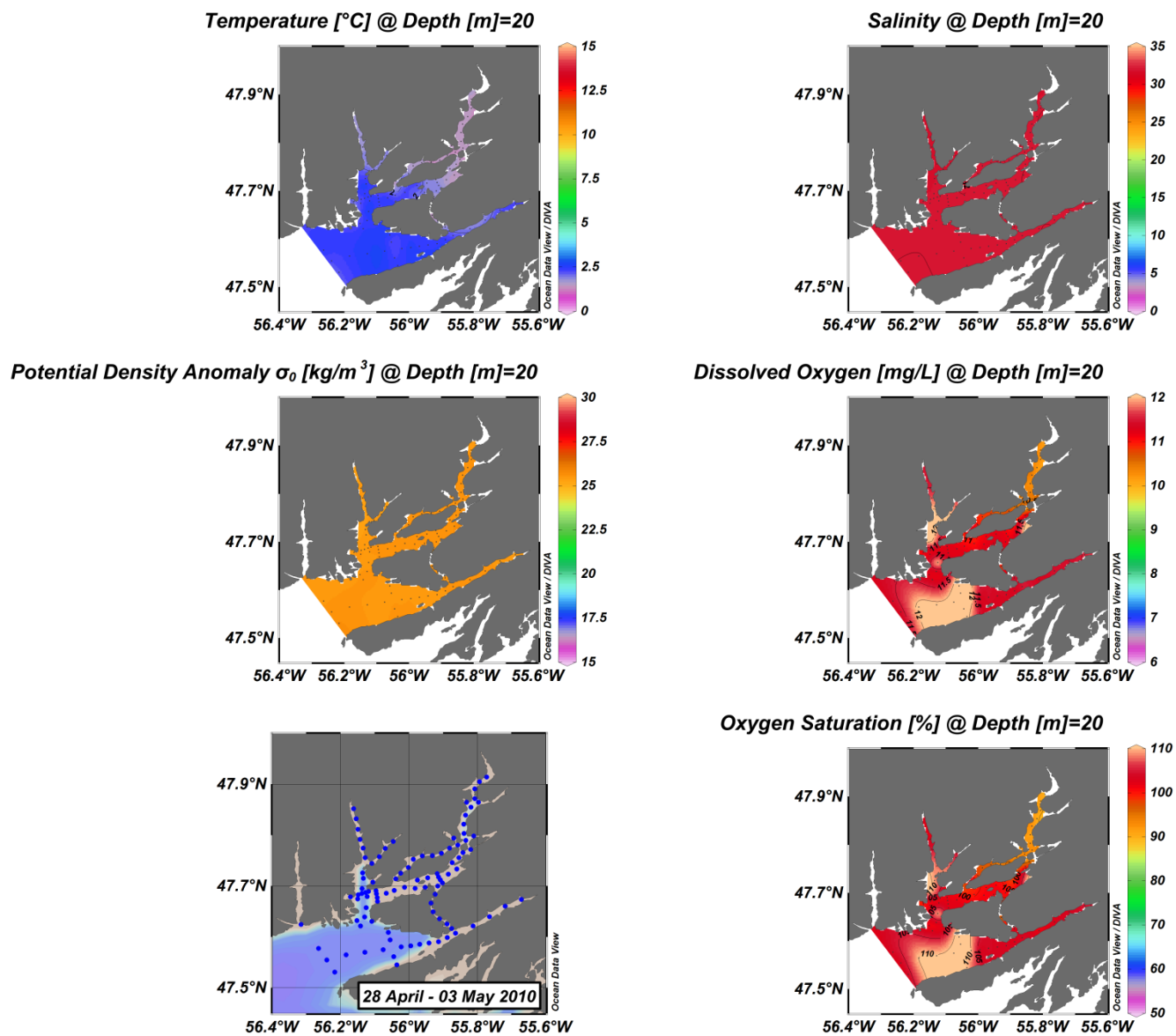


Figure A(iii)11: Hermitage Bay – Bay d'Espoir surface structure.

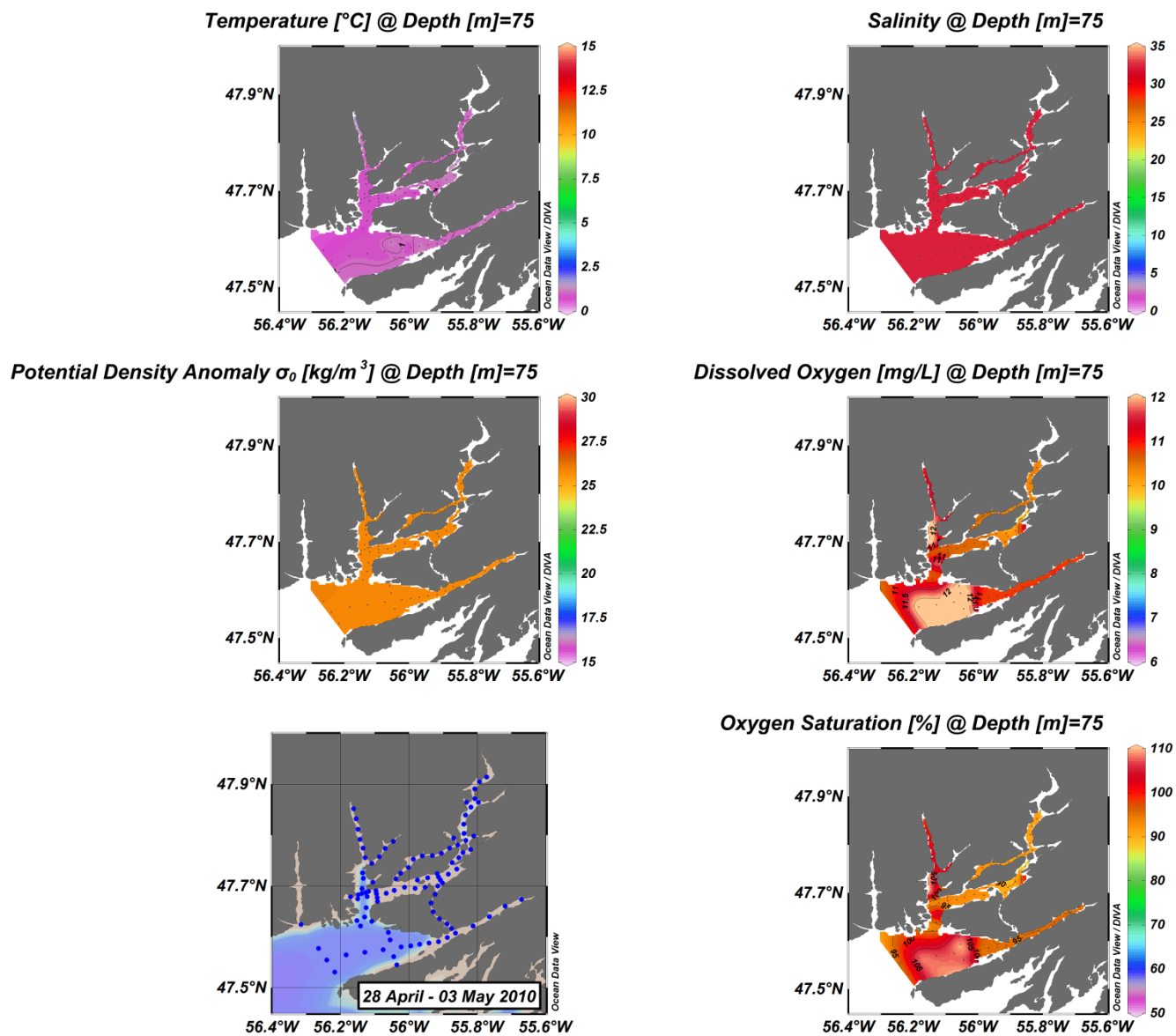


Figure A(iii)12: Hermitage Bay – Bay d'Espoir surface structure.

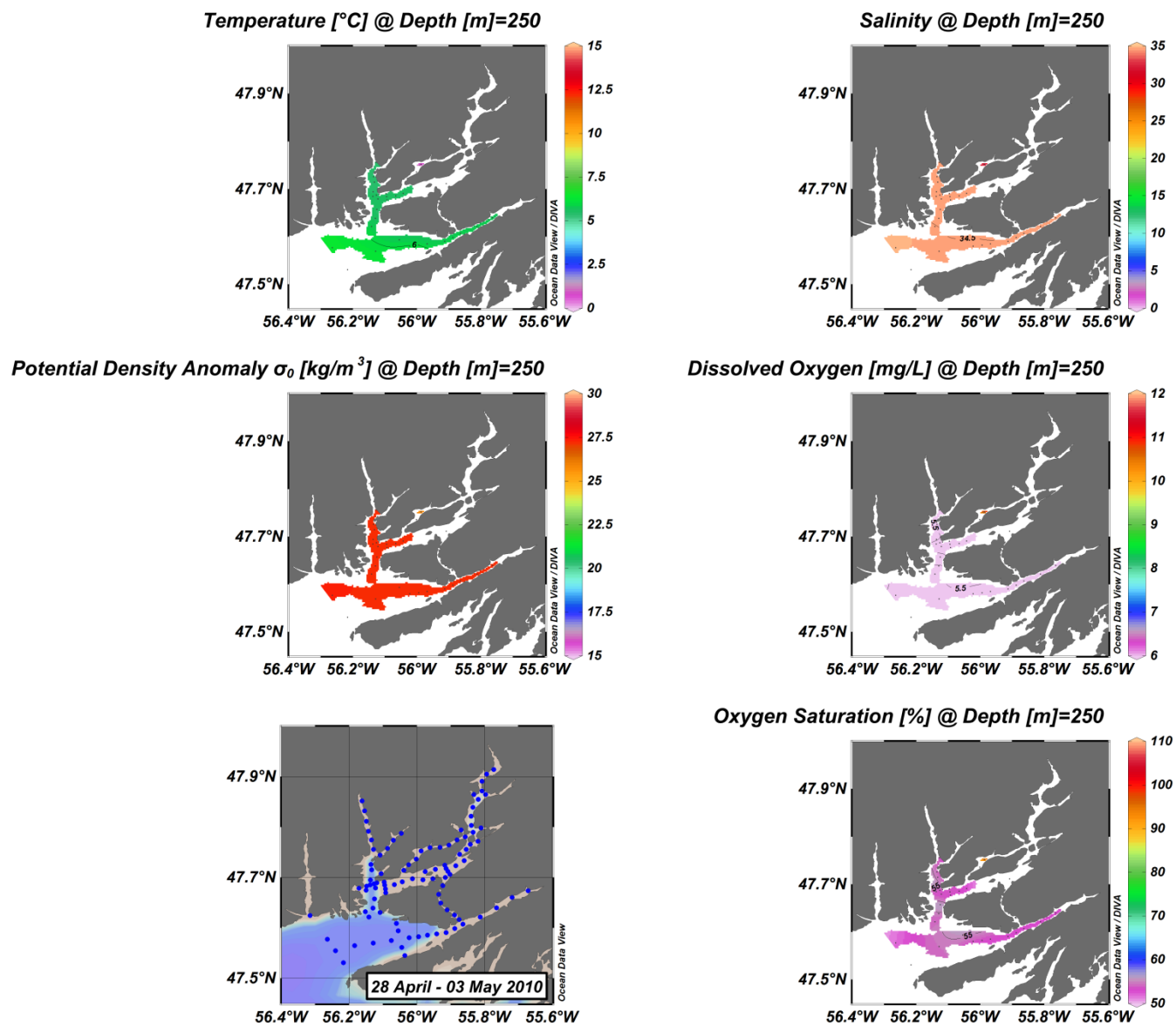


Figure A(iii)13: Hermitage Bay – Bay d'Espoir surface structure.

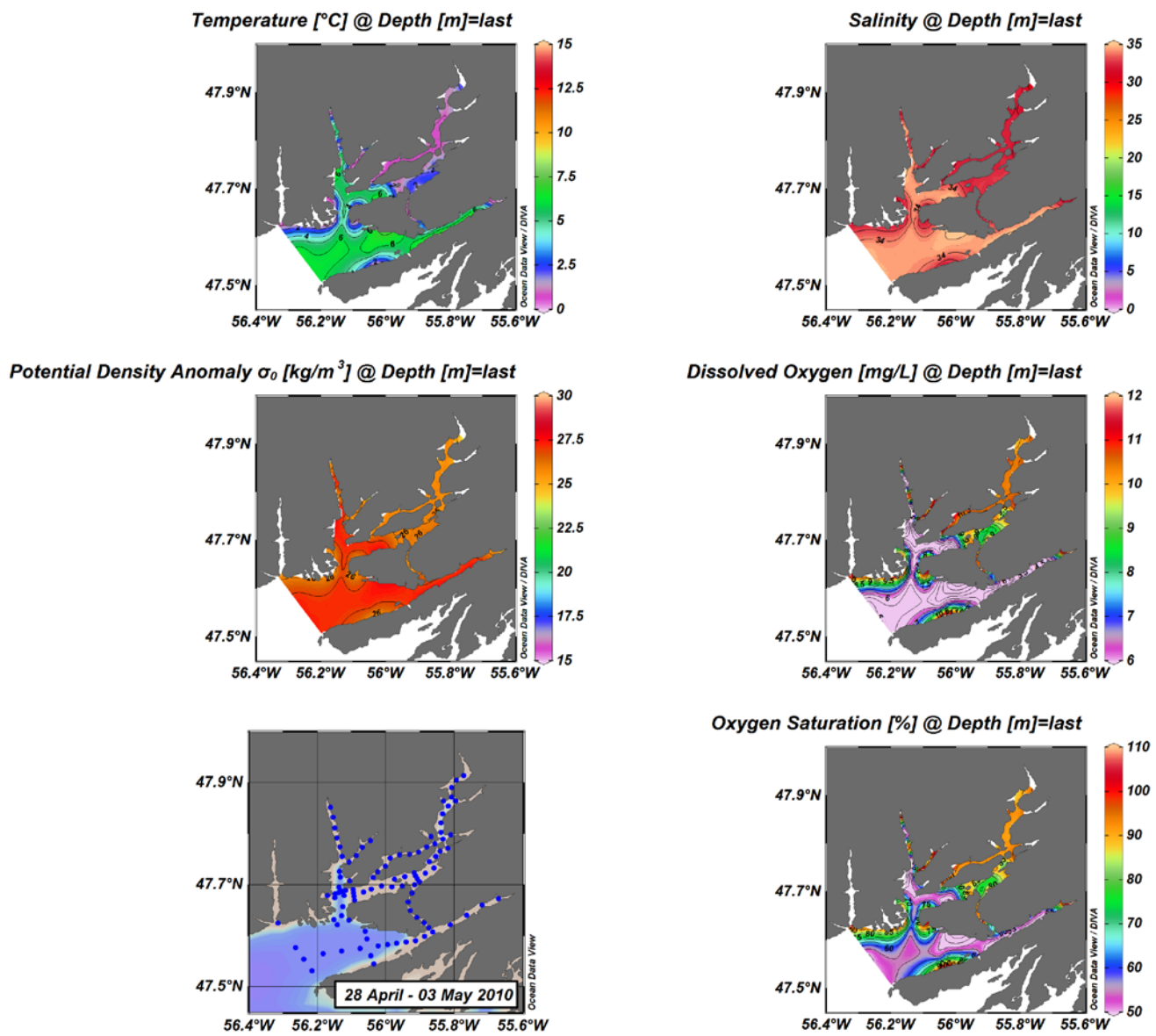


Figure A(iii)14: Hermitage Bay – Bay d'Espoirs surface structure.

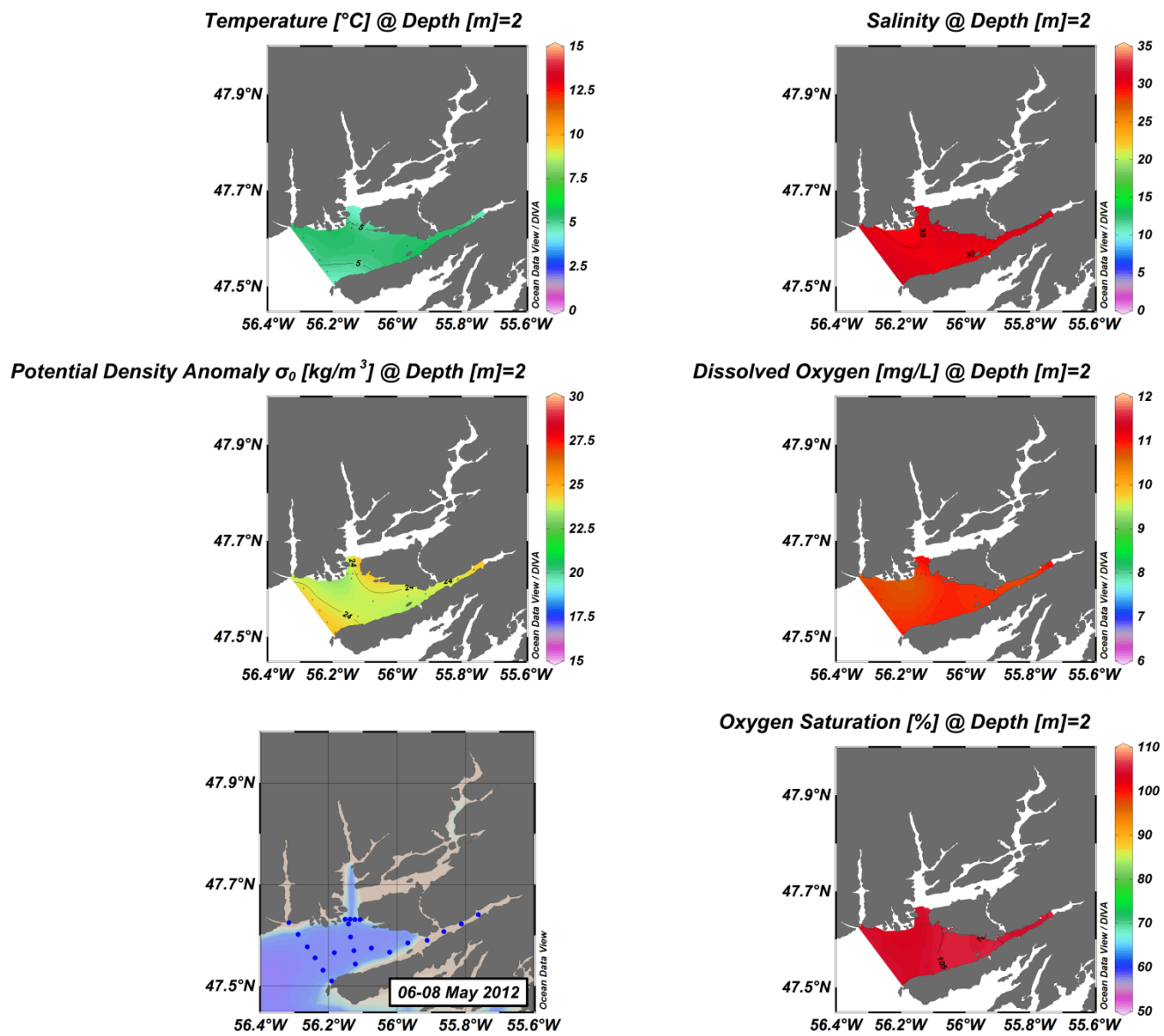


Figure A(iii)15: Hermitage Bay – Bay d'Espoir surface structure.

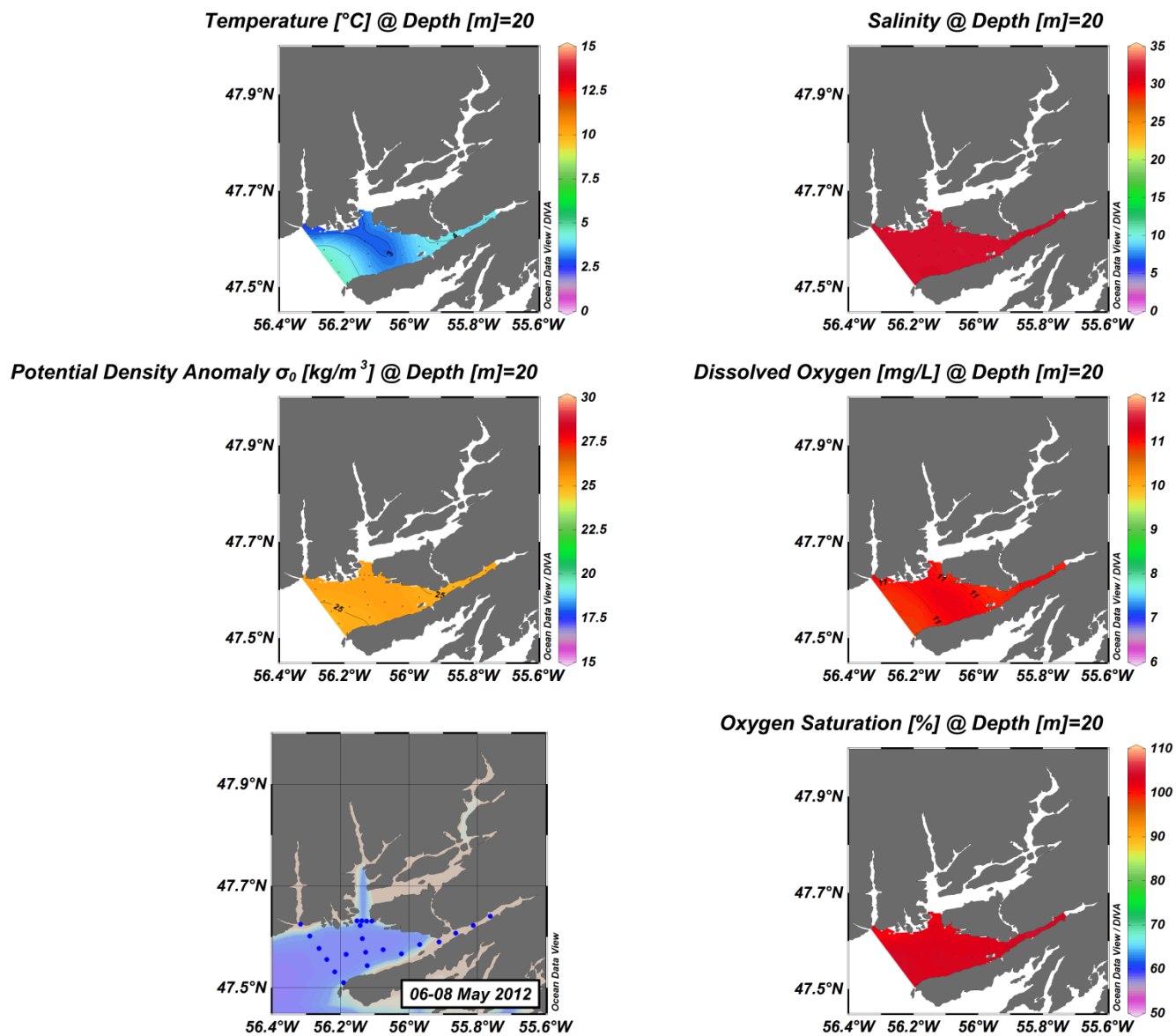


Figure A(iii)16: Hermitage Bay – Bay d'Espoir surface structure.

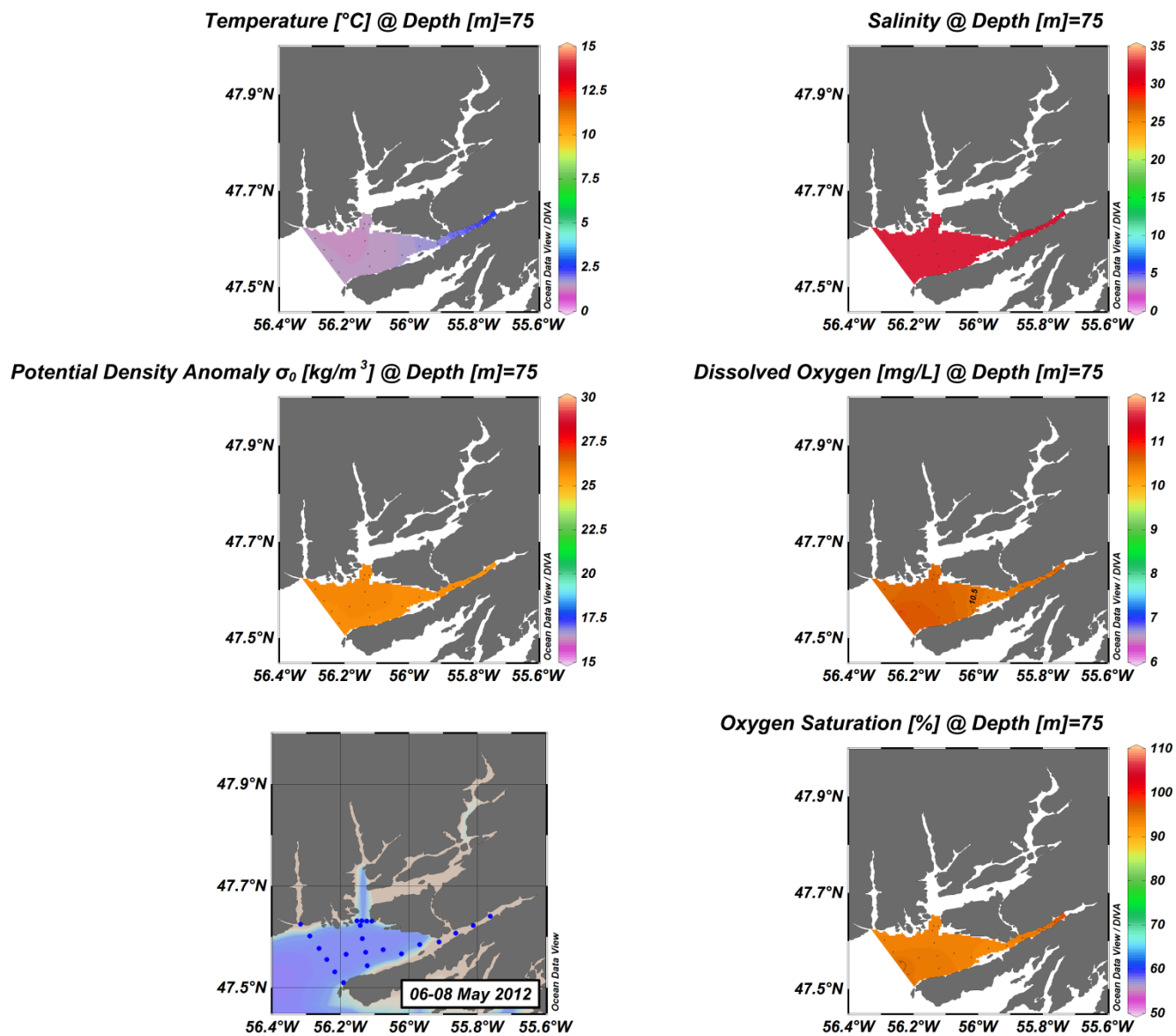


Figure A(iii)17: Hermitage Bay – Bay d'Espoir surface structure.

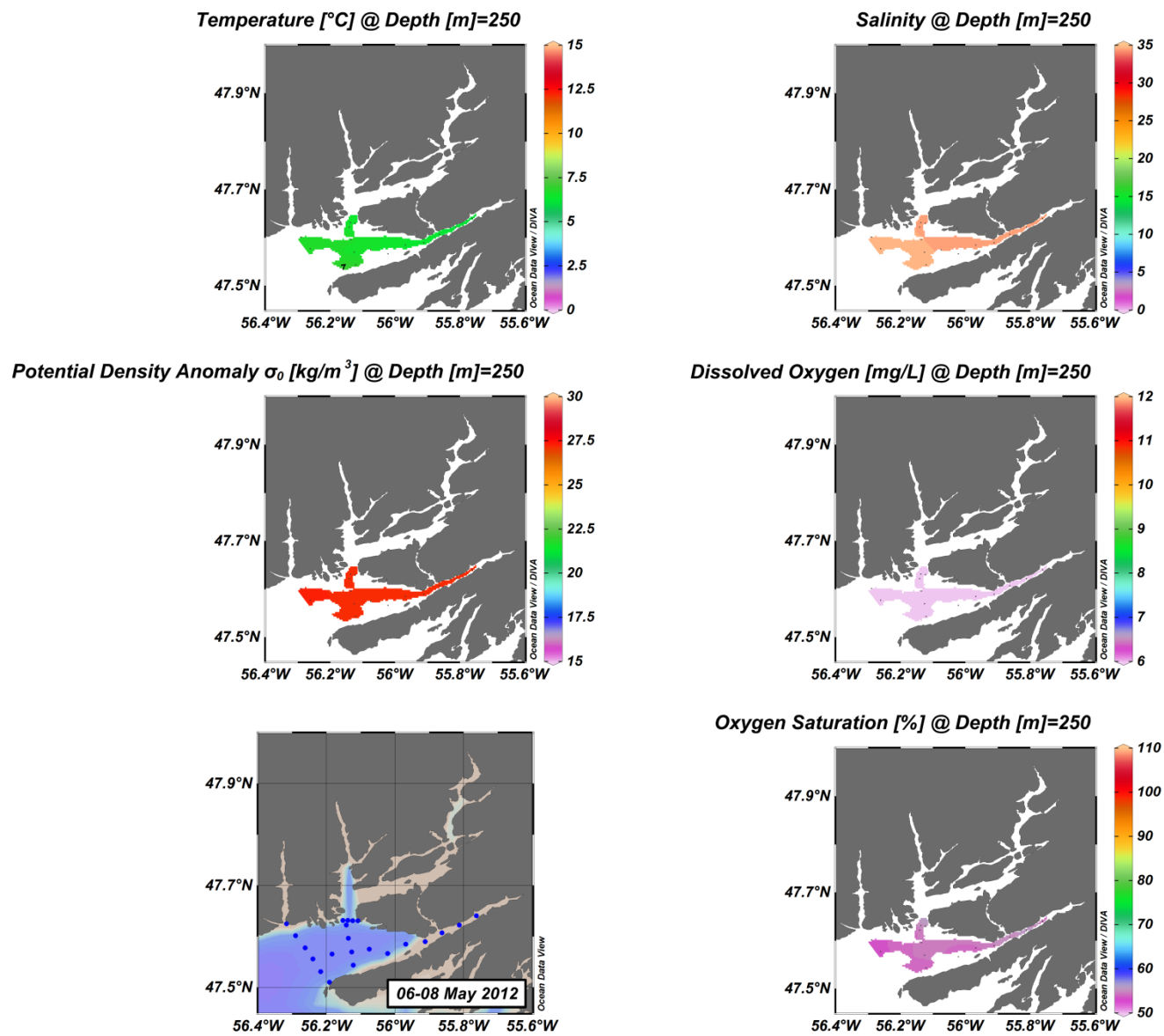


Figure A(iii)18: Hermitage Bay – Bay d'Espoir surface structure.

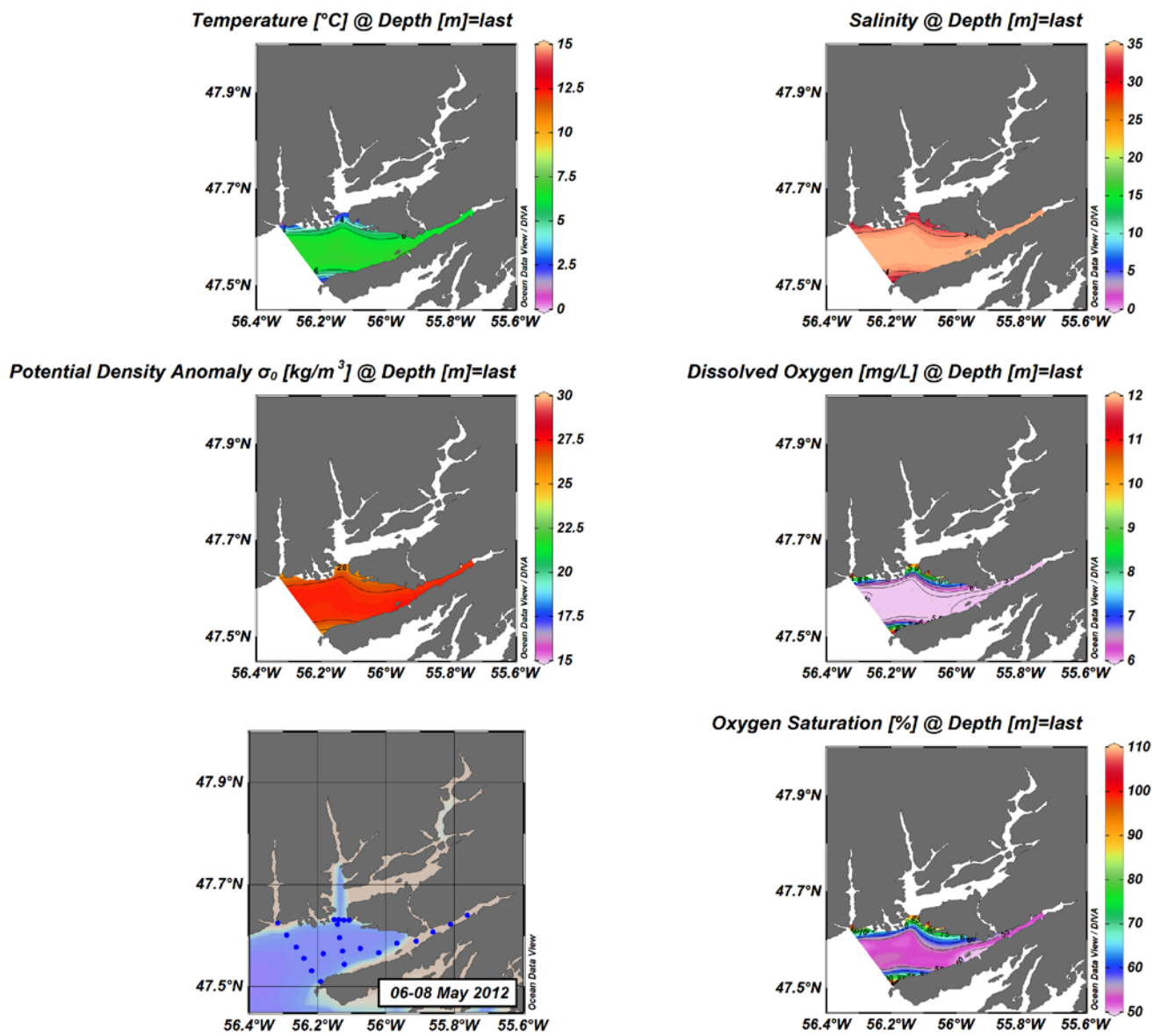


Figure A(iii)19: Hermitage Bay – Bay d'Espoirs surface structure.

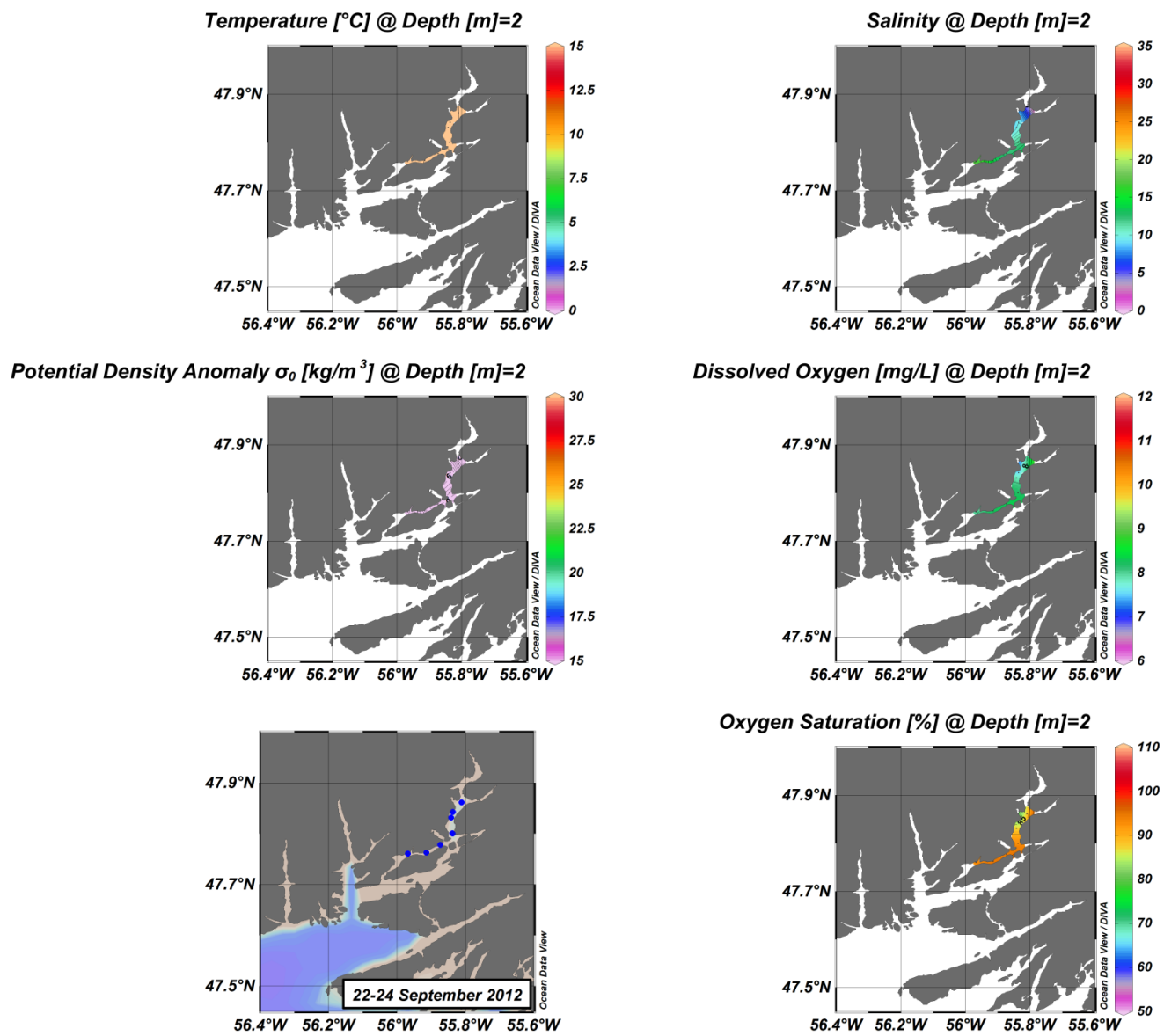


Figure A(iii)20: Hermitage Bay – Bay d'Espoirs surface structure.

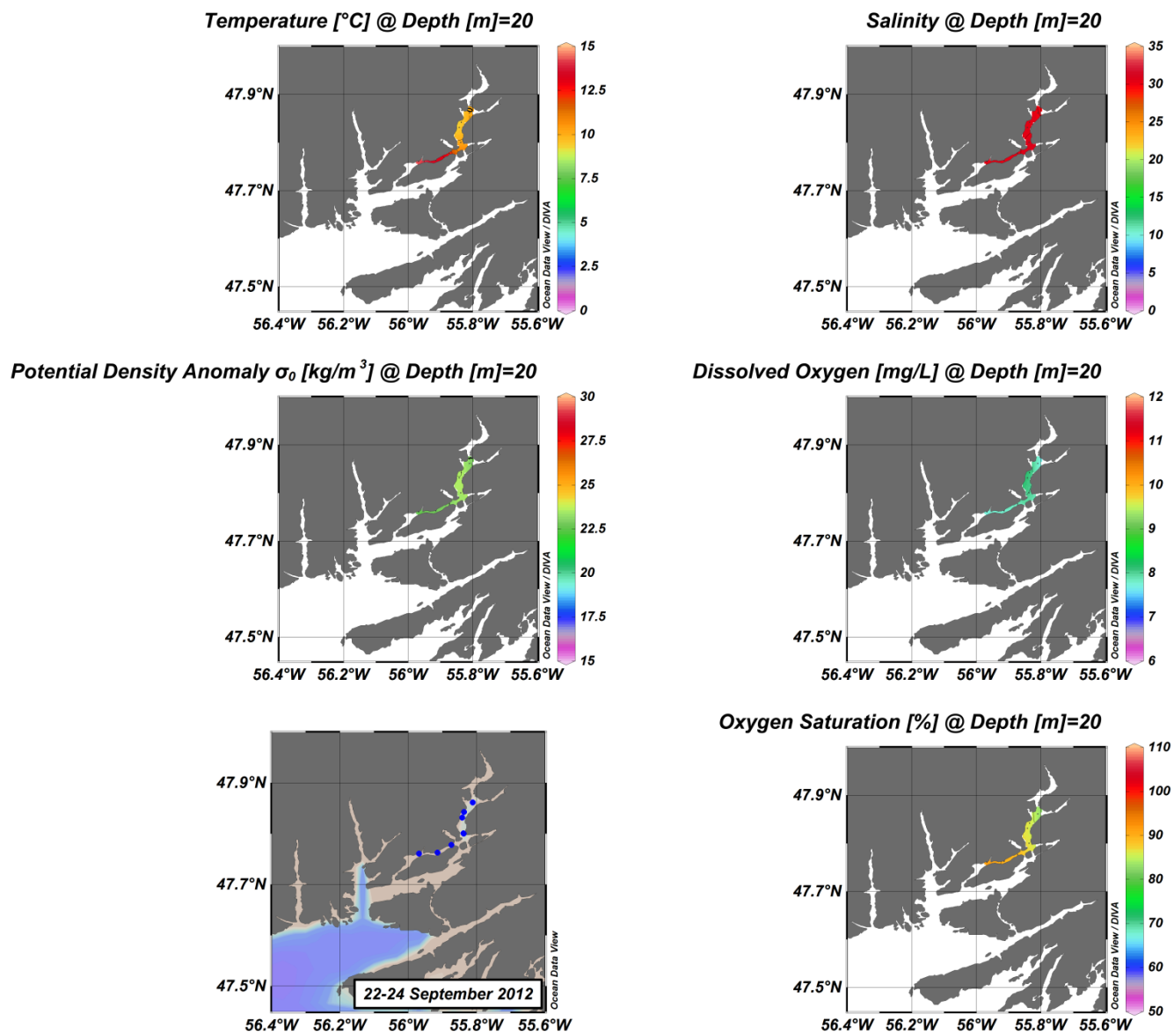


Figure A(iii)21: Hermitage Bay – Bay d'Espoir surface structure.

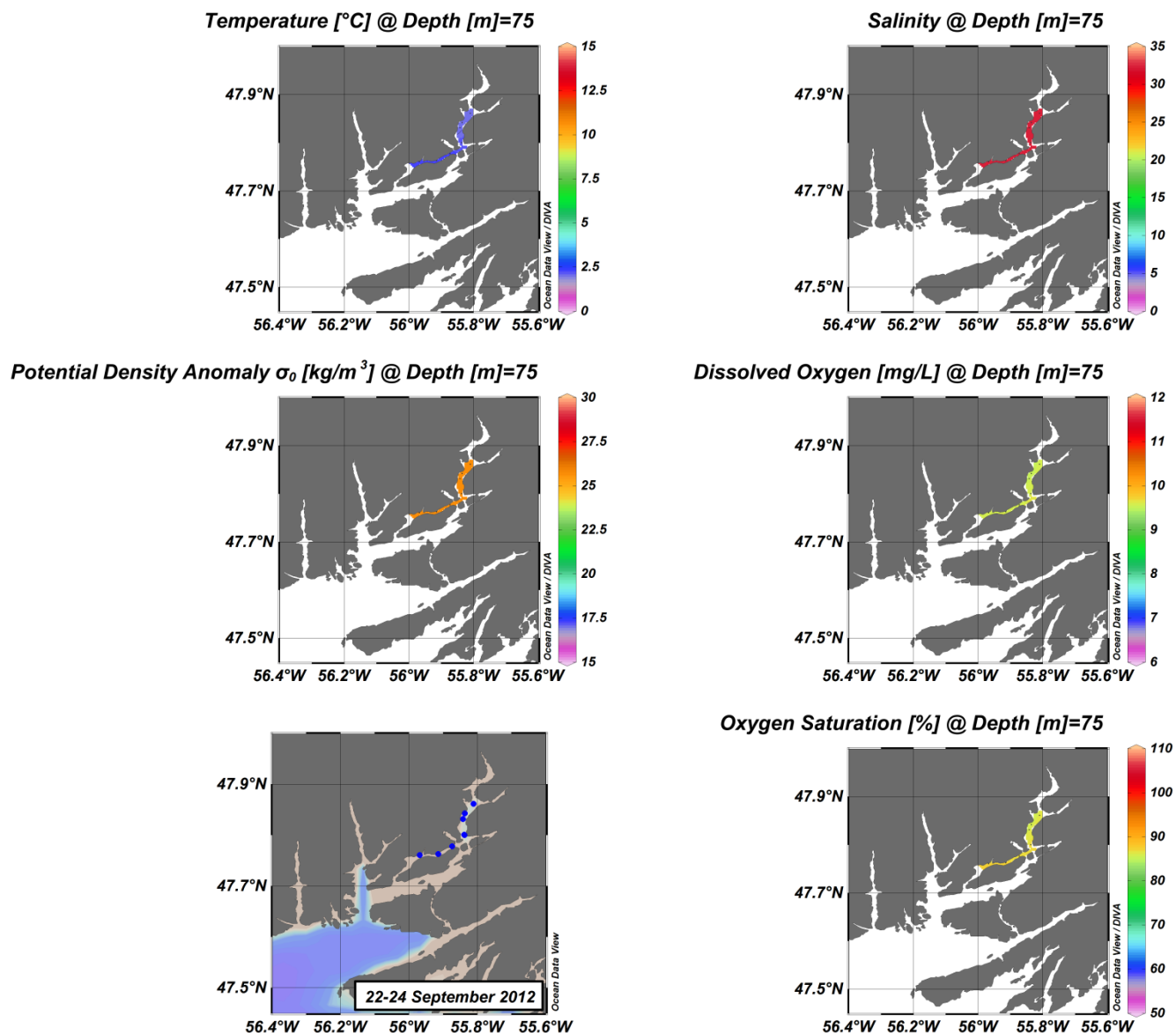


Figure A(iii)22: Hermitage Bay – Bay d'Espoirs surface structure.

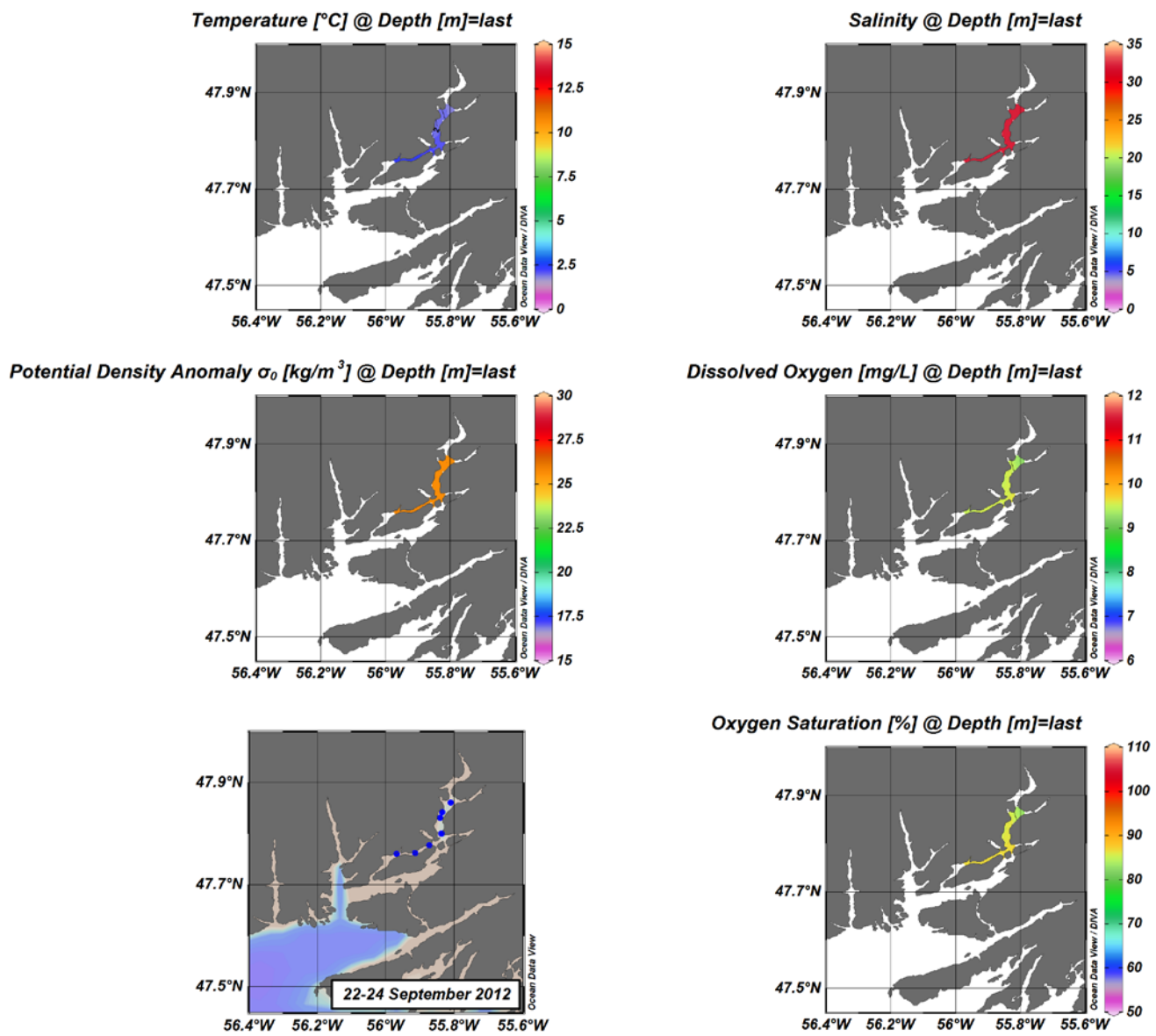


Figure A(iii)23: Hermitage Bay – Bay d'Espoir surface structure.

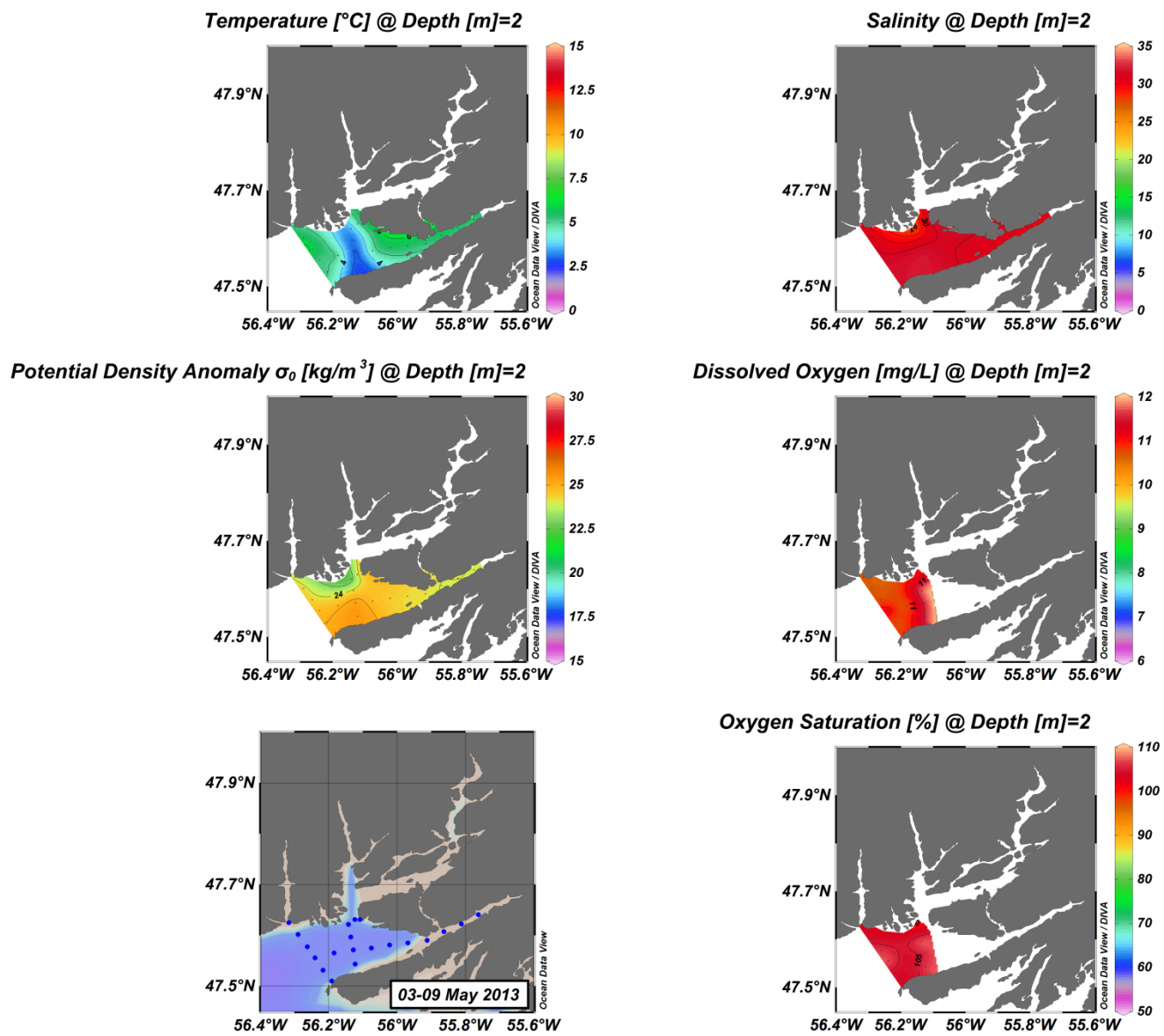


Figure A(iii)24: Hermitage Bay – Bay d'Espoir surface structure.

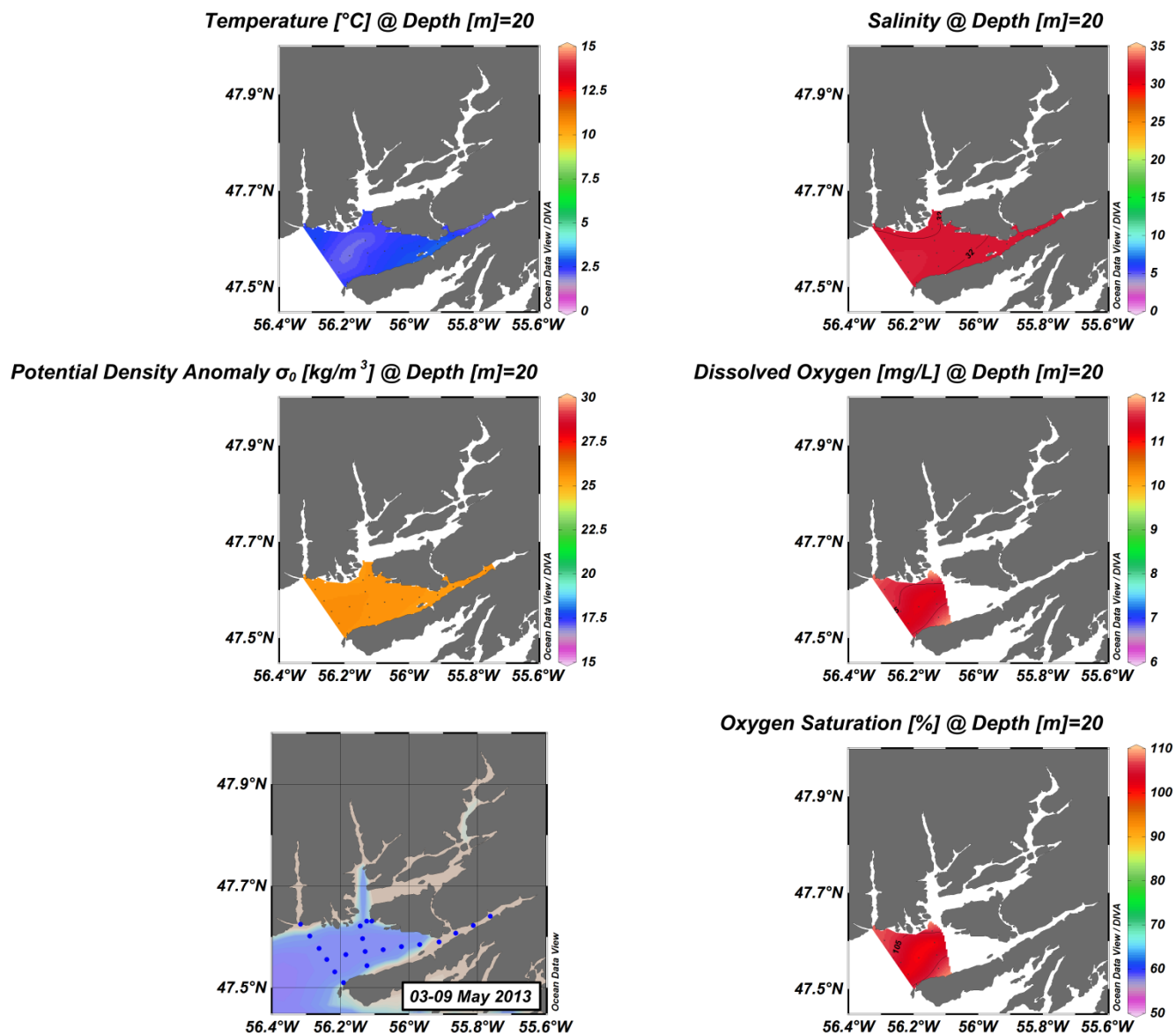


Figure A(iii)25: Hermitage Bay – Bay d'Espoir surface structure.

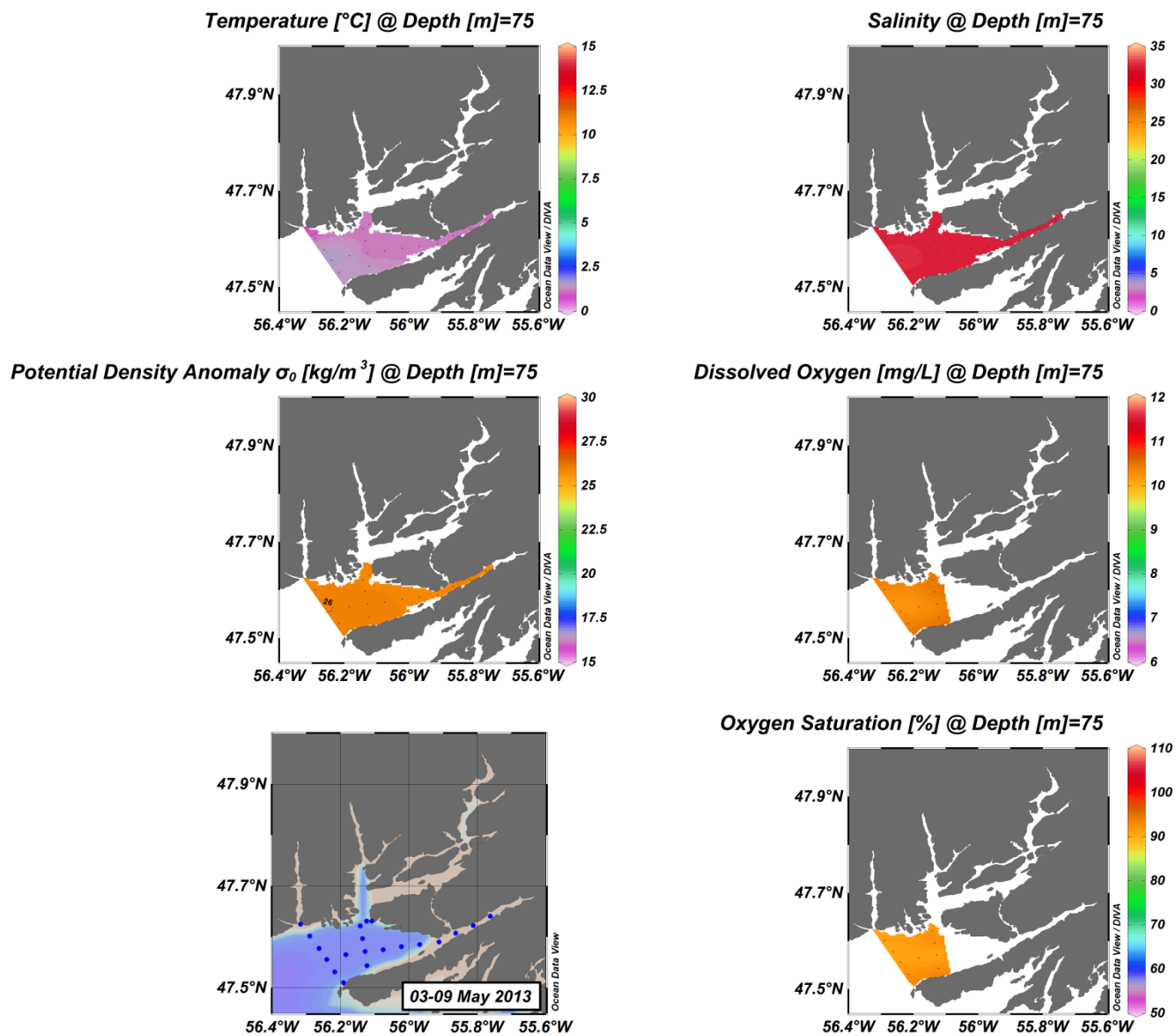


Figure A(iii)26: Hermitage Bay – Bay d'Espoir surface structure.

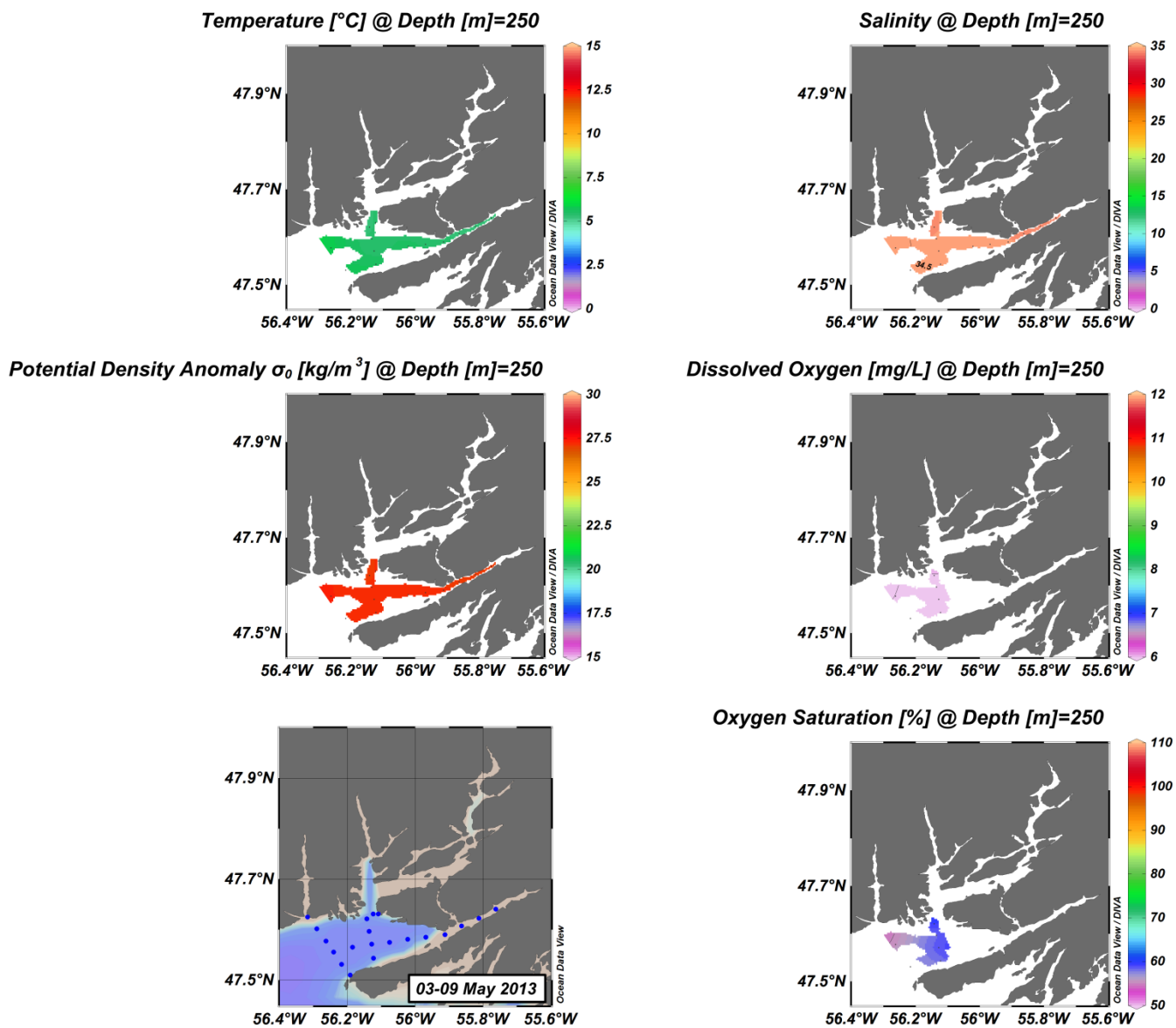


Figure A(iii)27: Hermitage Bay – Bay d'Espoir surface structure.

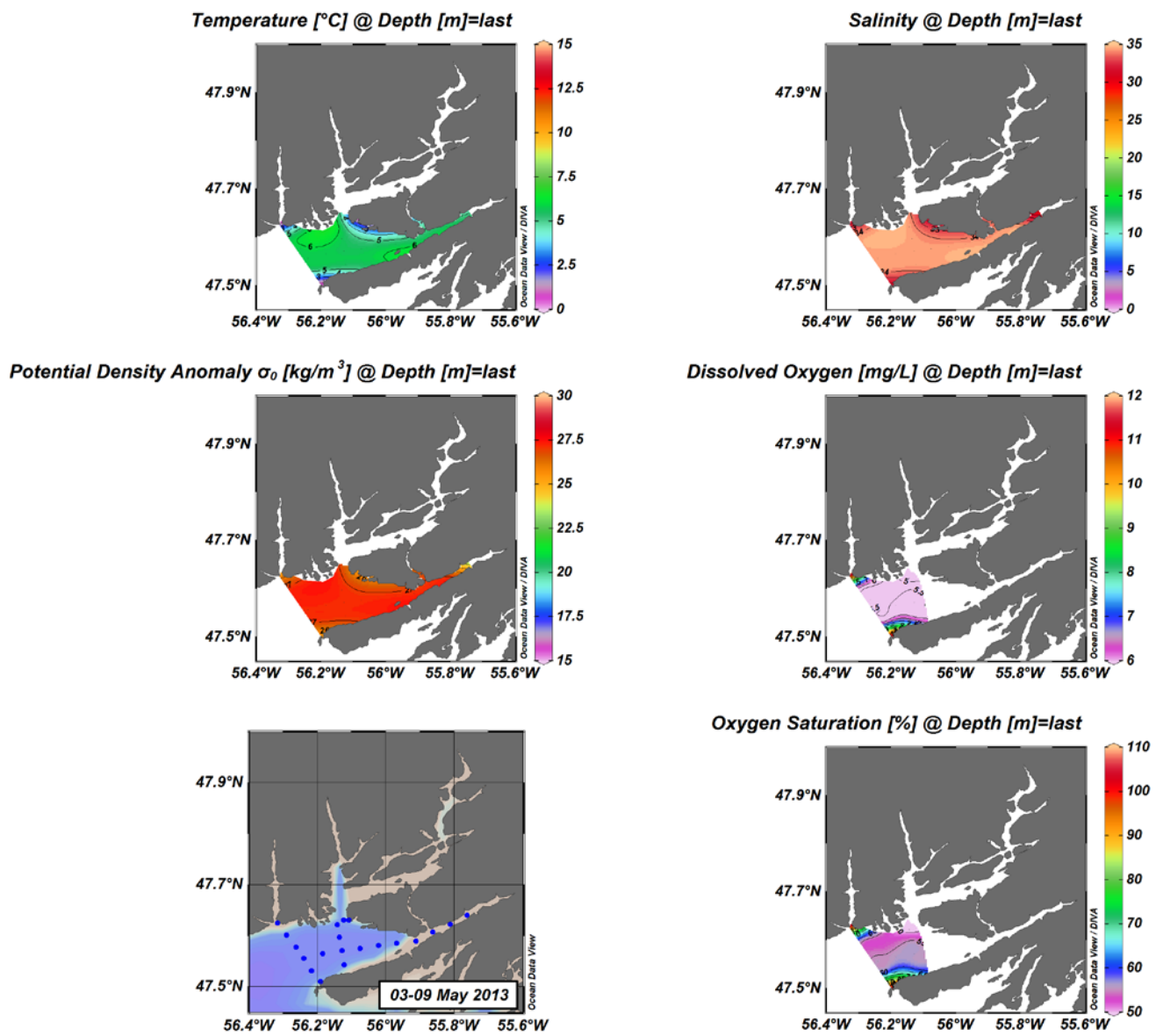


Figure A(iii)28: Hermitage Bay – Bay d'Espoir surface structure.

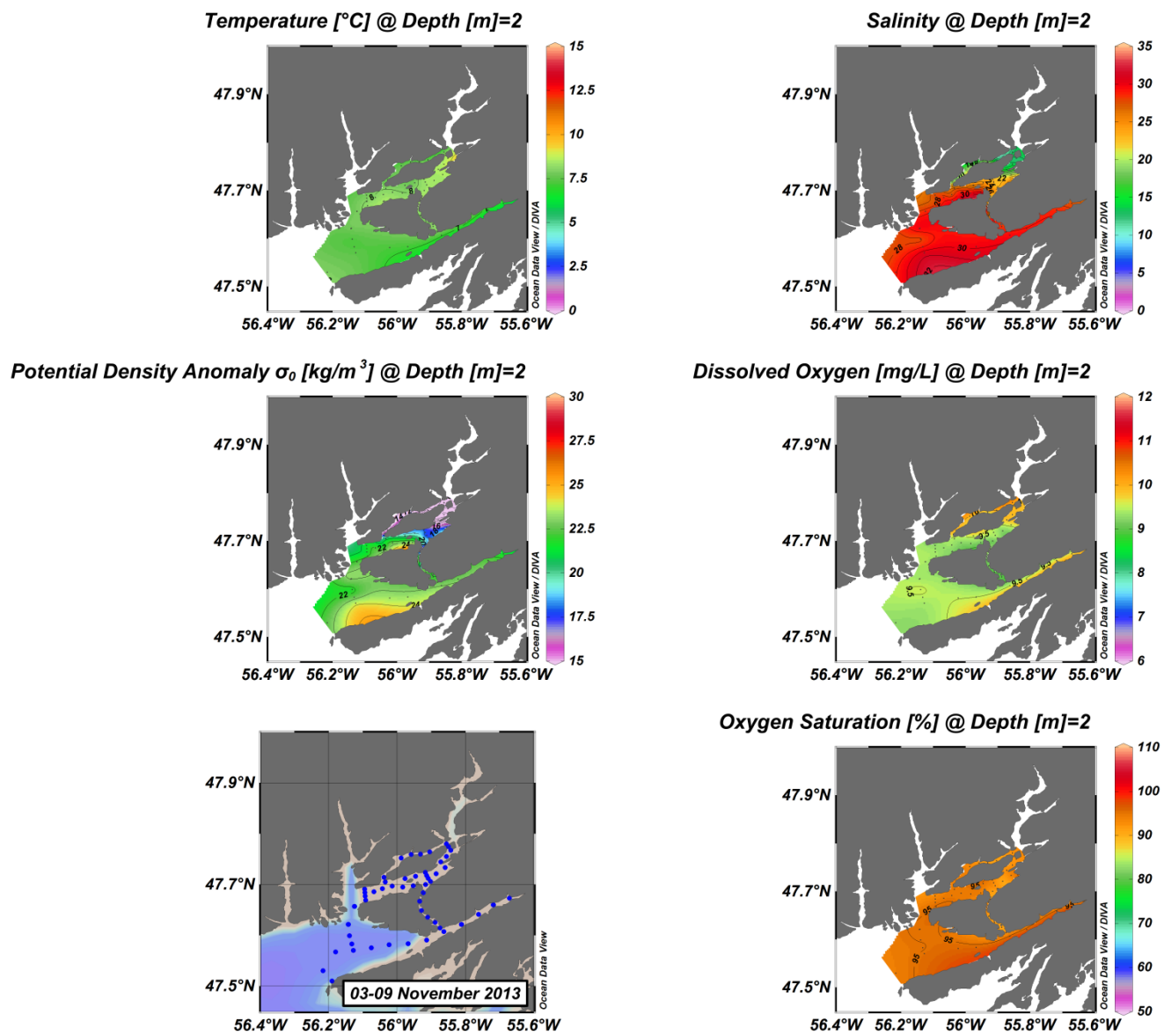


Figure A(iii)29: Hermitage Bay – Bay d'Espoirs surface structure.

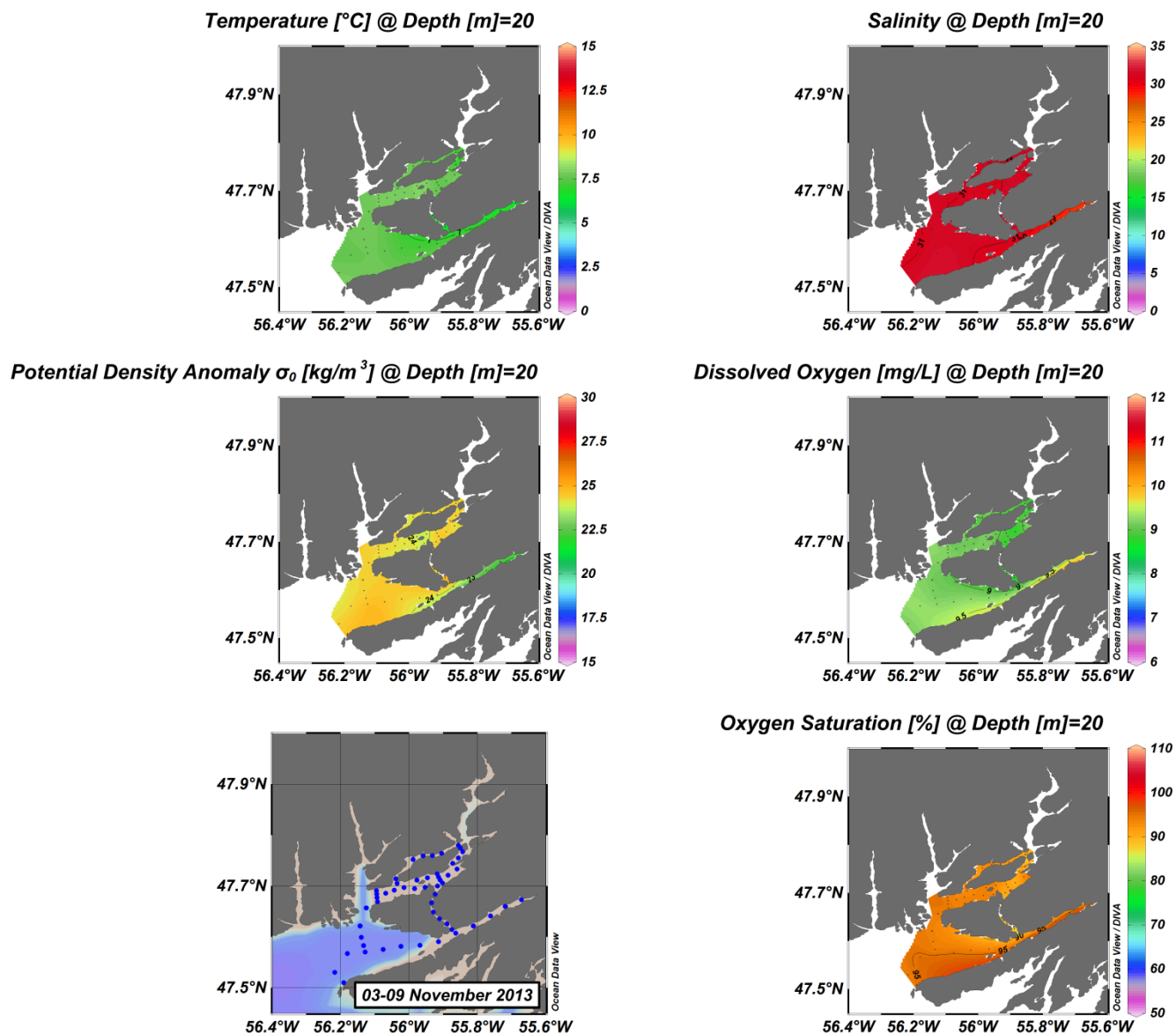


Figure A(iii)30: Hermitage Bay – Bay d'Espoir surface structure.

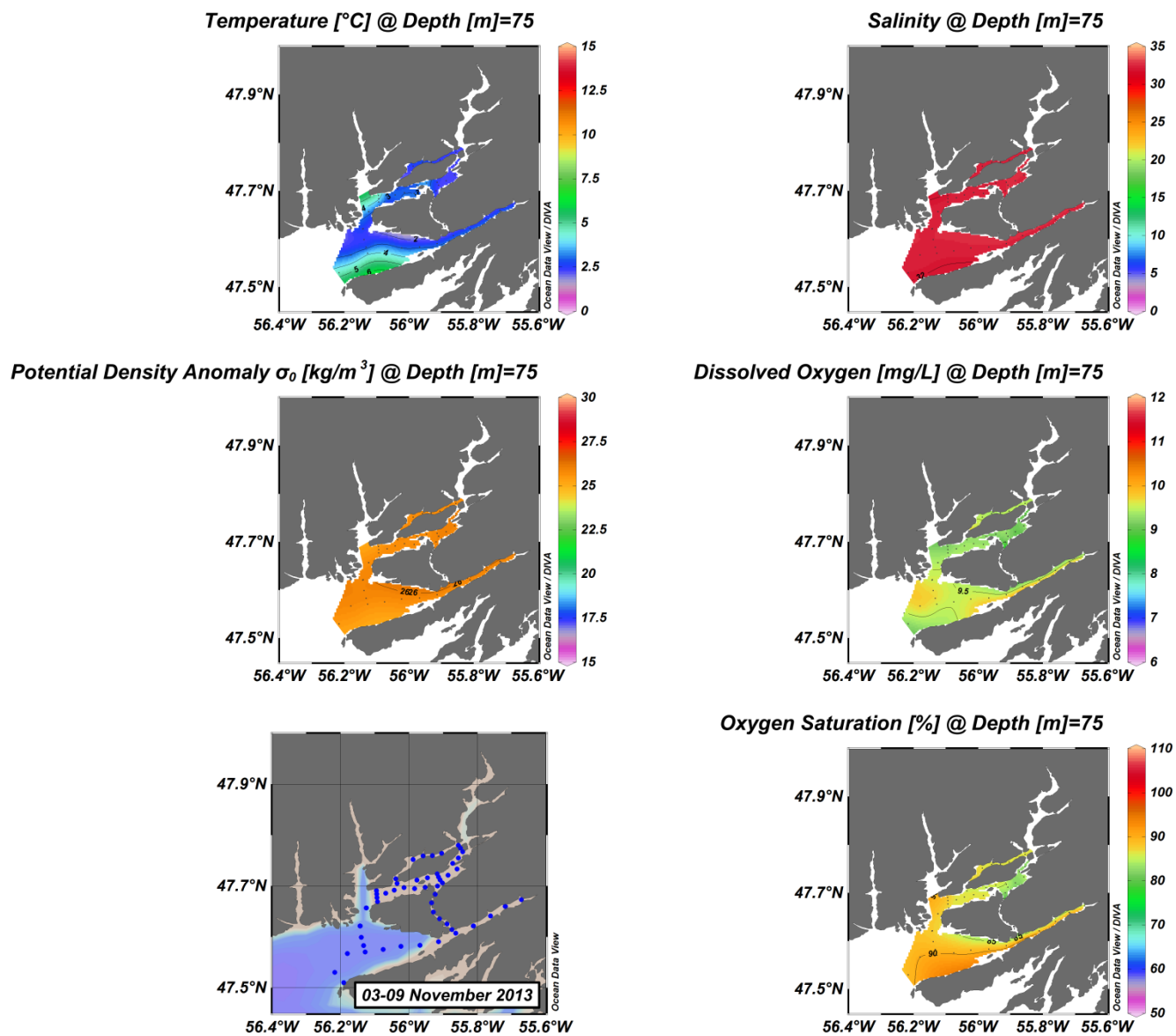


Figure A(iii)31: Hermitage Bay – Bay d'Espoir surface structure.

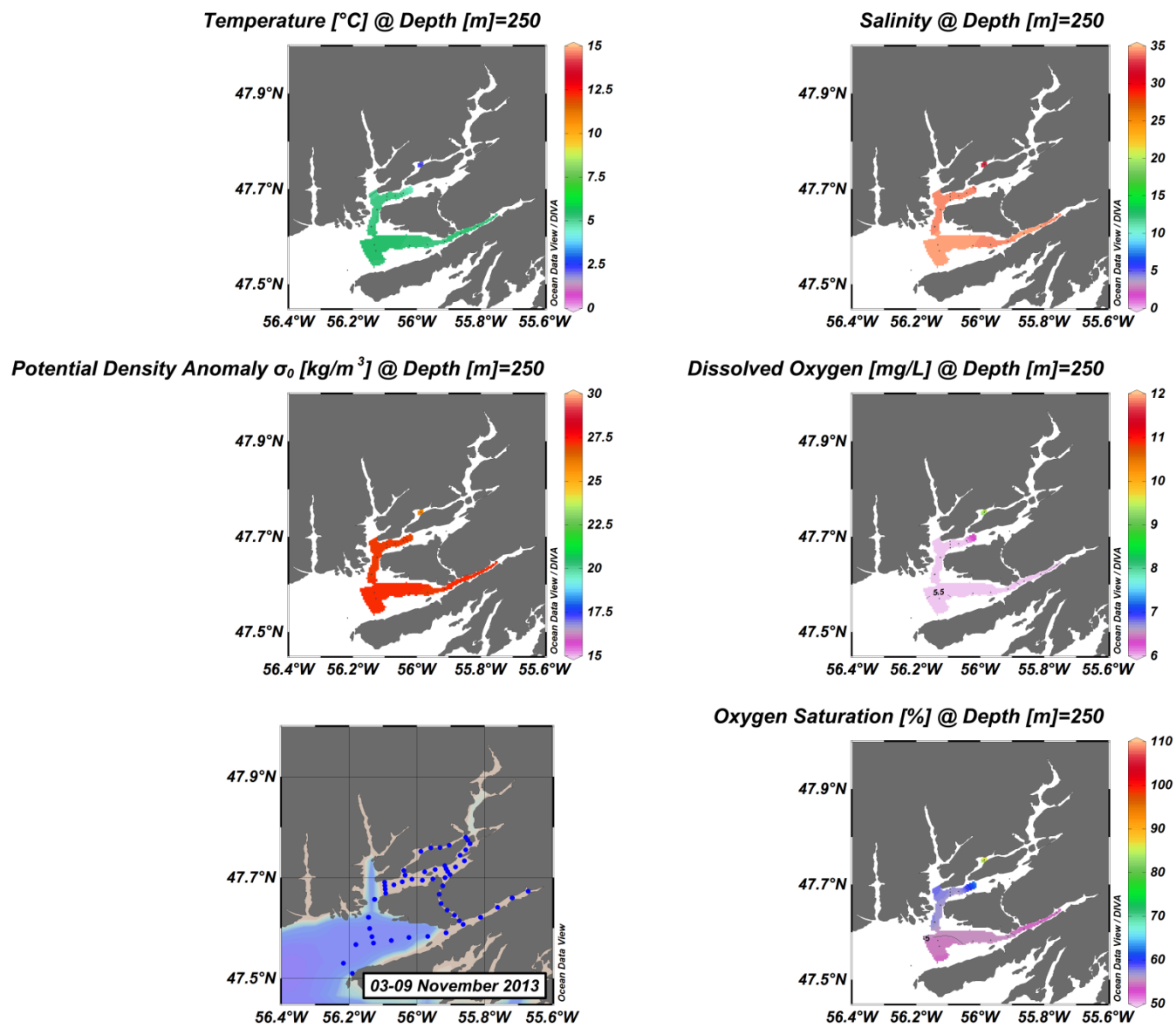


Figure A(iii)32: Hermitage Bay – Bay d'Espoir surface structure.

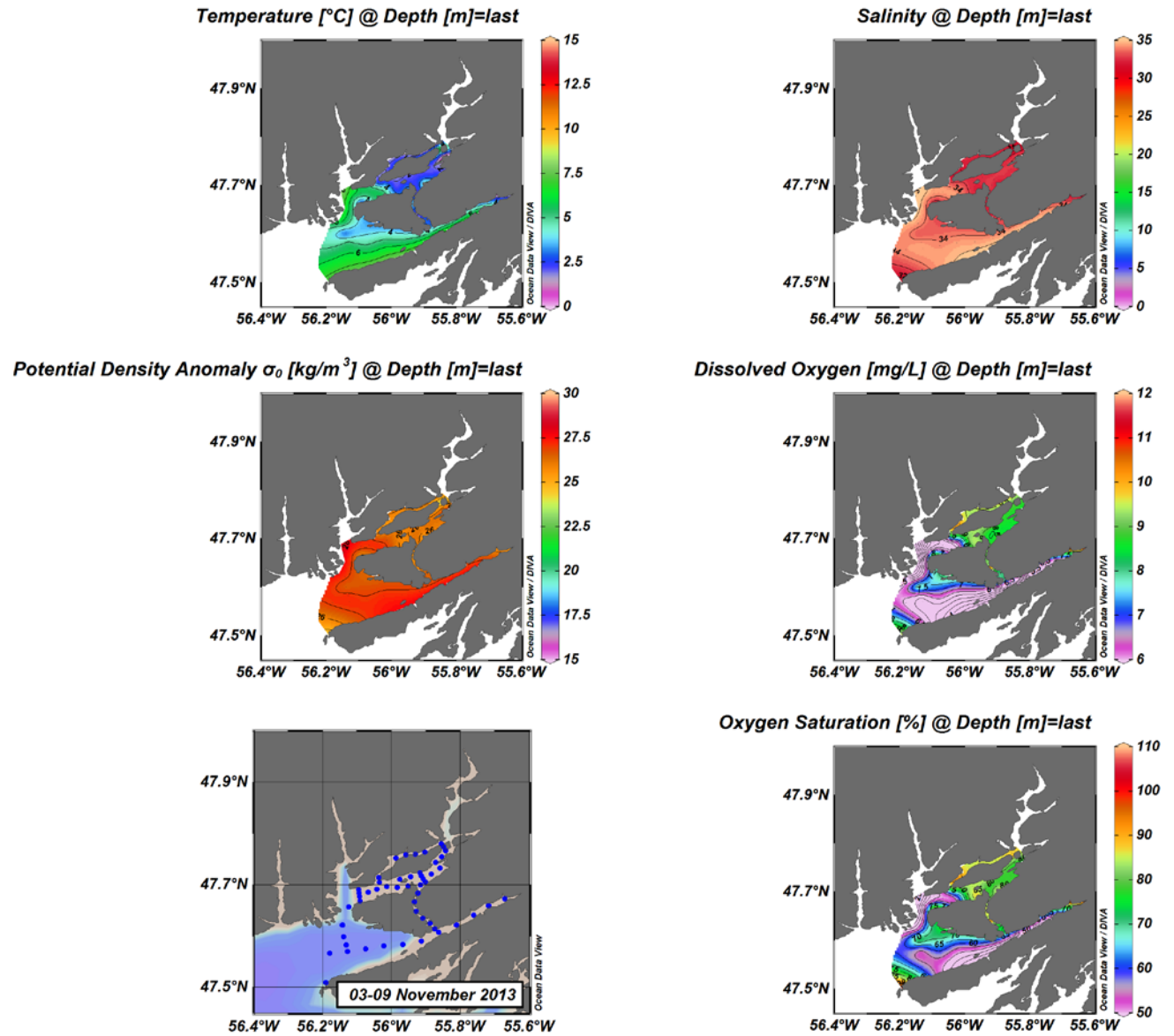
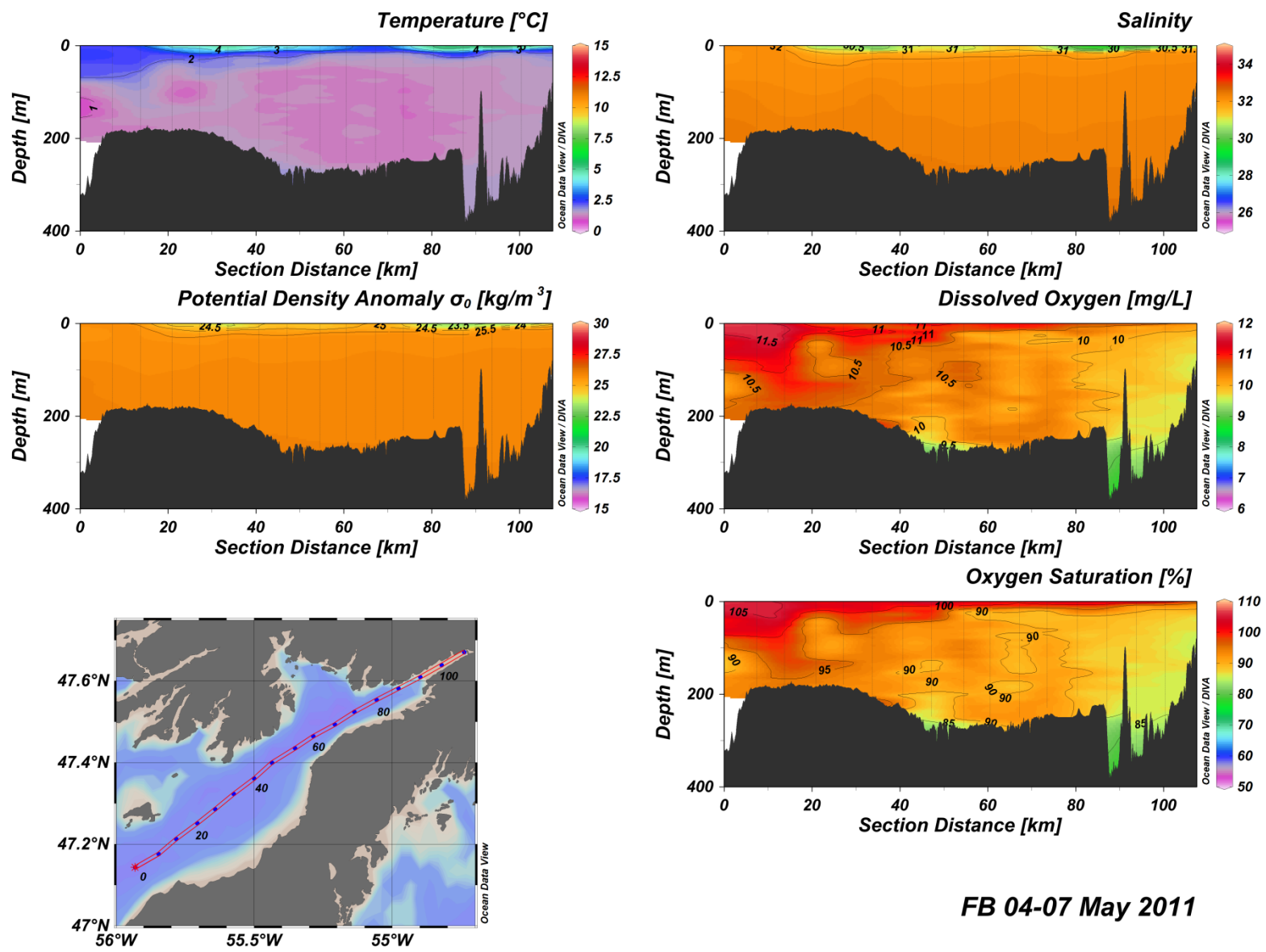


Figure A(iii)33: Hermitage Bay – Bay d'Espoirs surface structure.

APPENDIX B(I): FORTUNE BAY – BELLE BAY (FB-BB) VERTICAL SECTIONS



FB 04-07 May 2011

Figure B(i)1: Fortune Bay water column vertical structure.

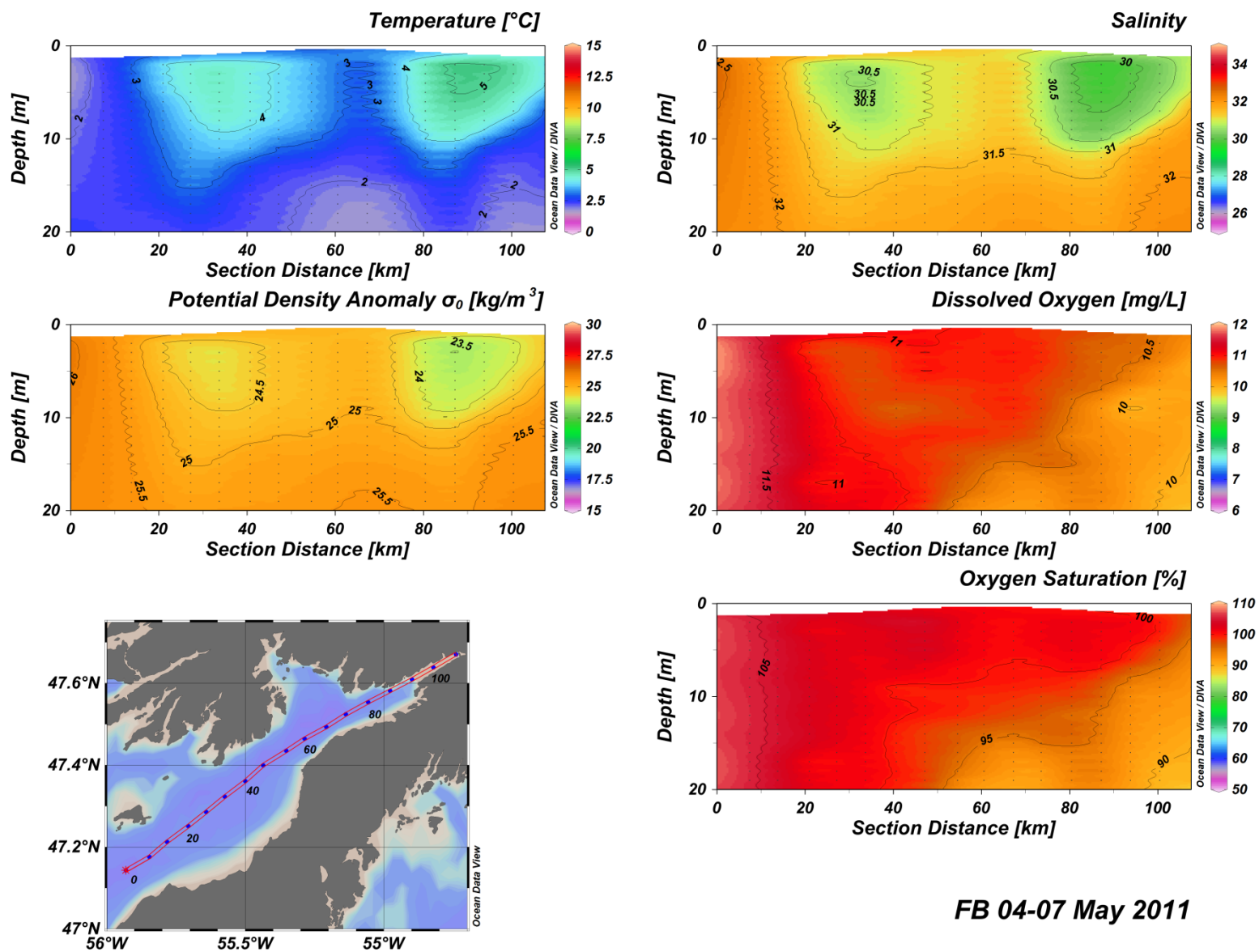


Figure B(i)2: Fortune Bay water column vertical structure.

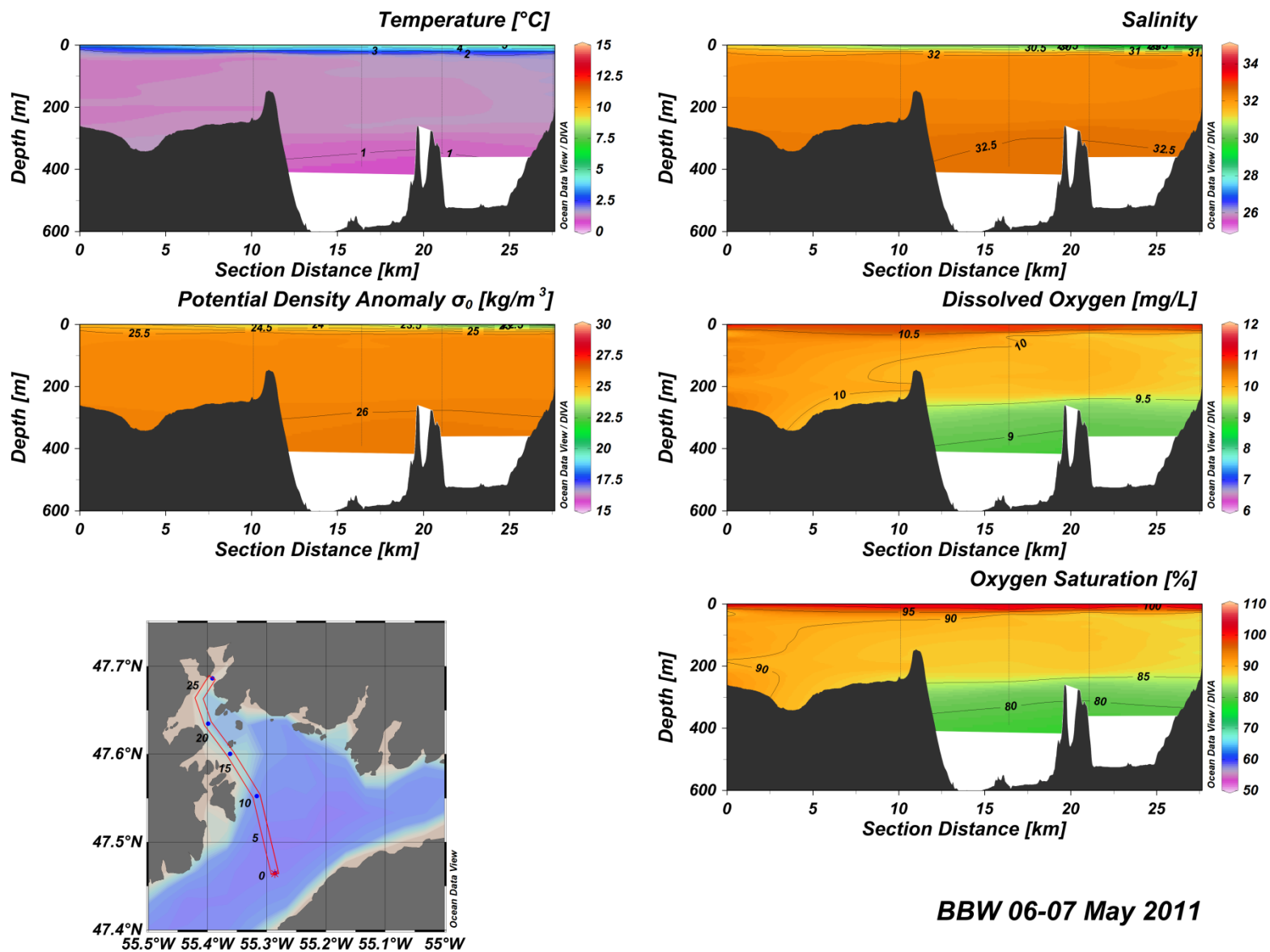


Figure B(i)3: Belle Bay West water column vertical structure.

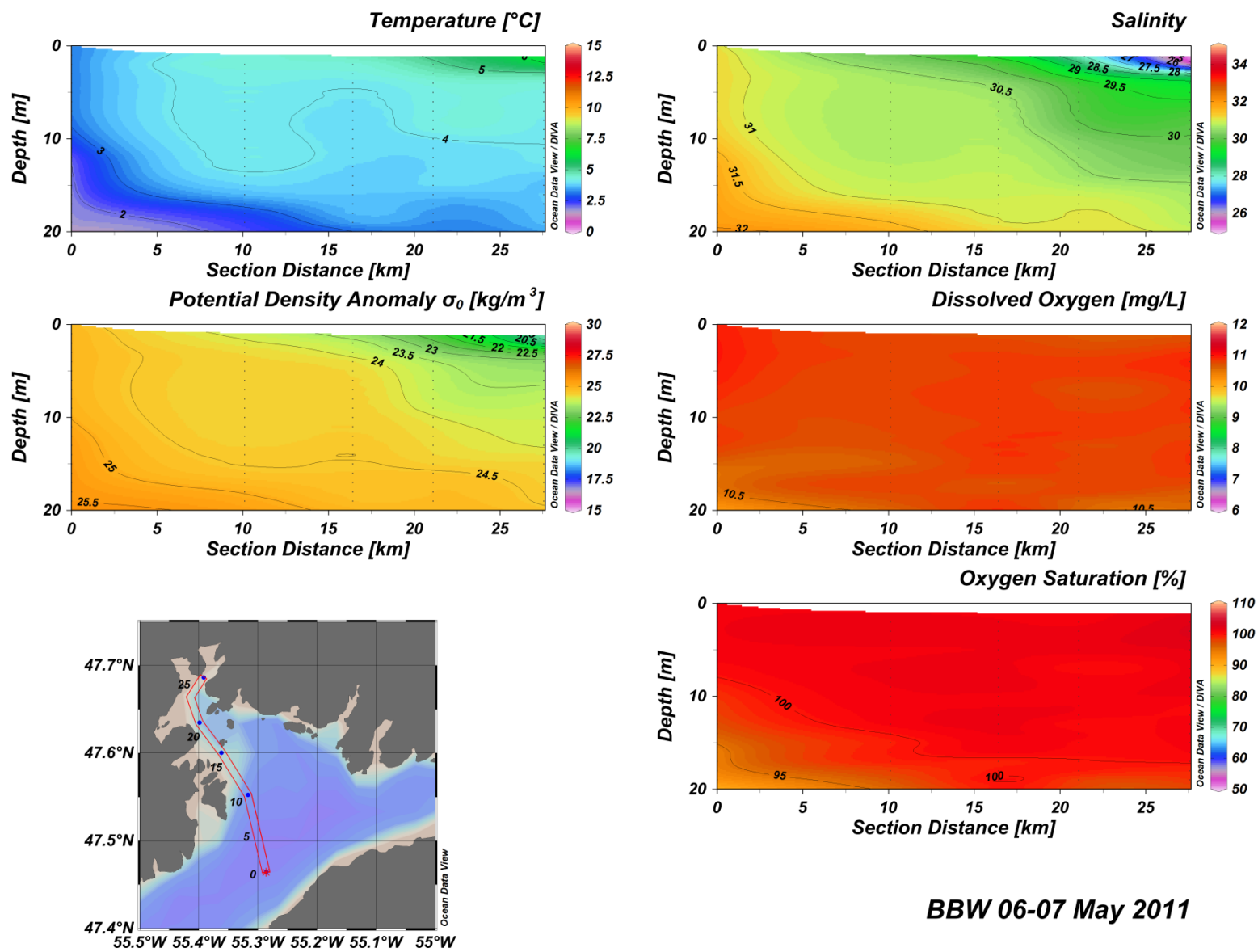


Figure B(i)4: Belle Bay West water column vertical structure.

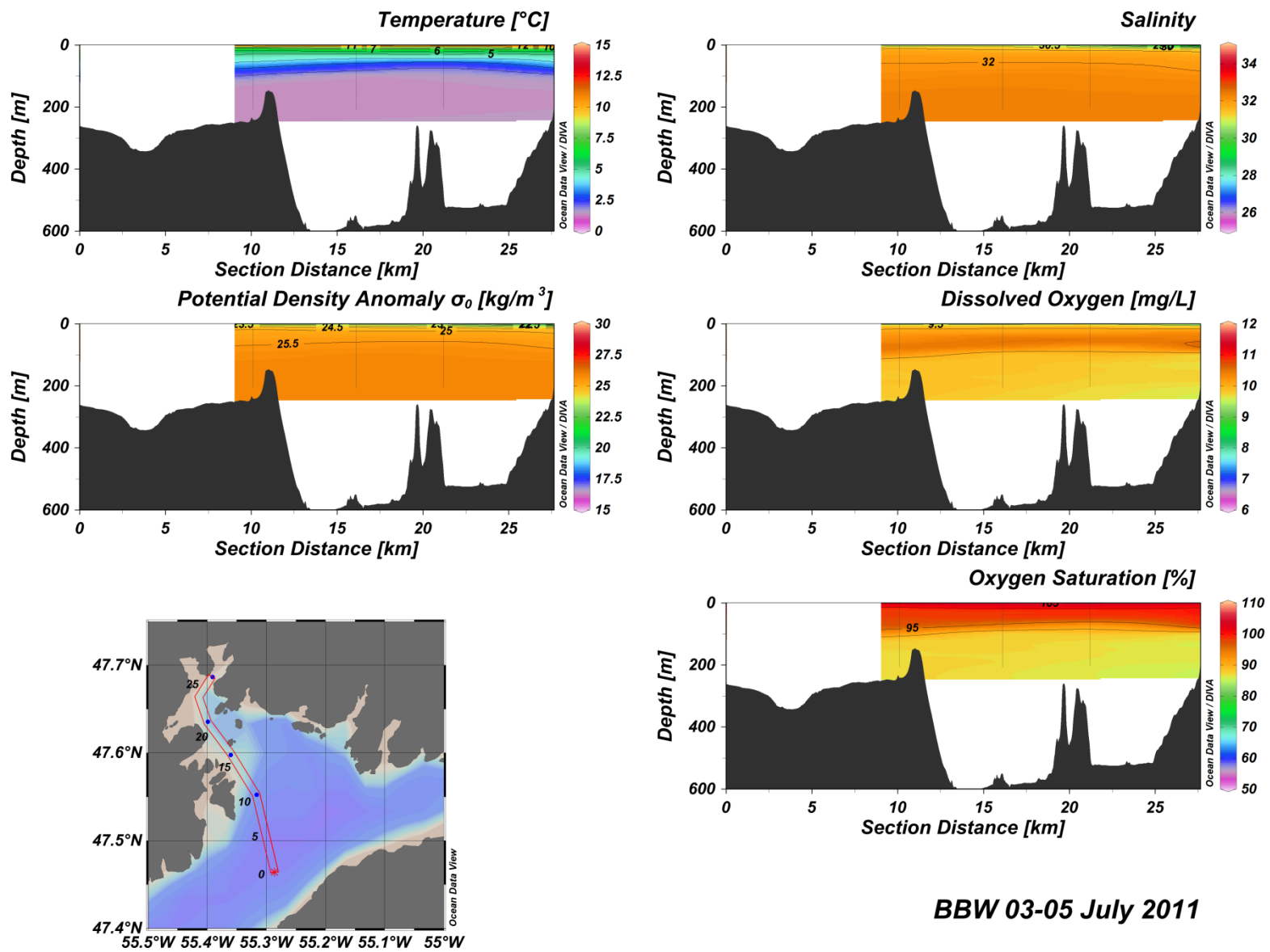


Figure B(i)5: Belle Bay West water column vertical structure.

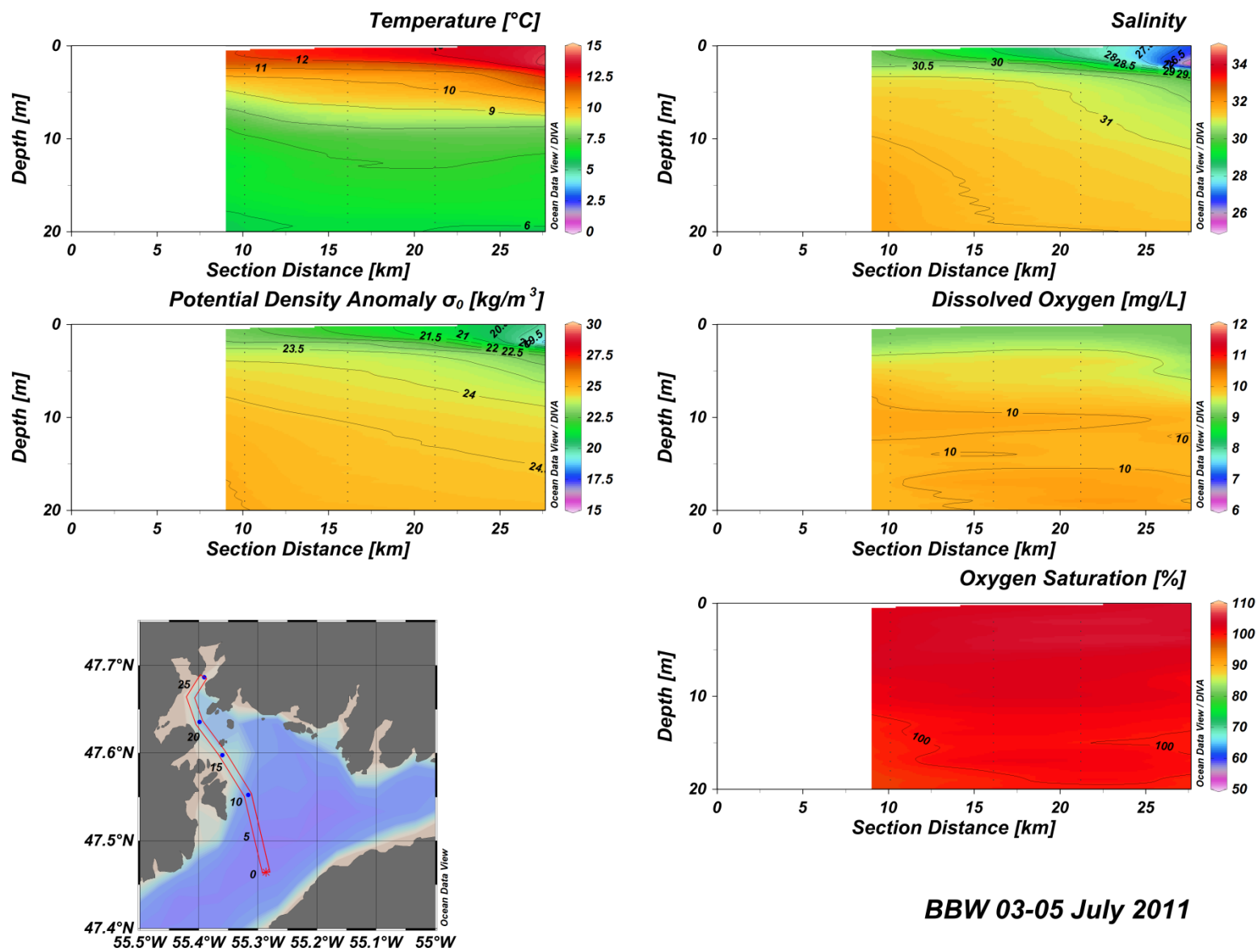
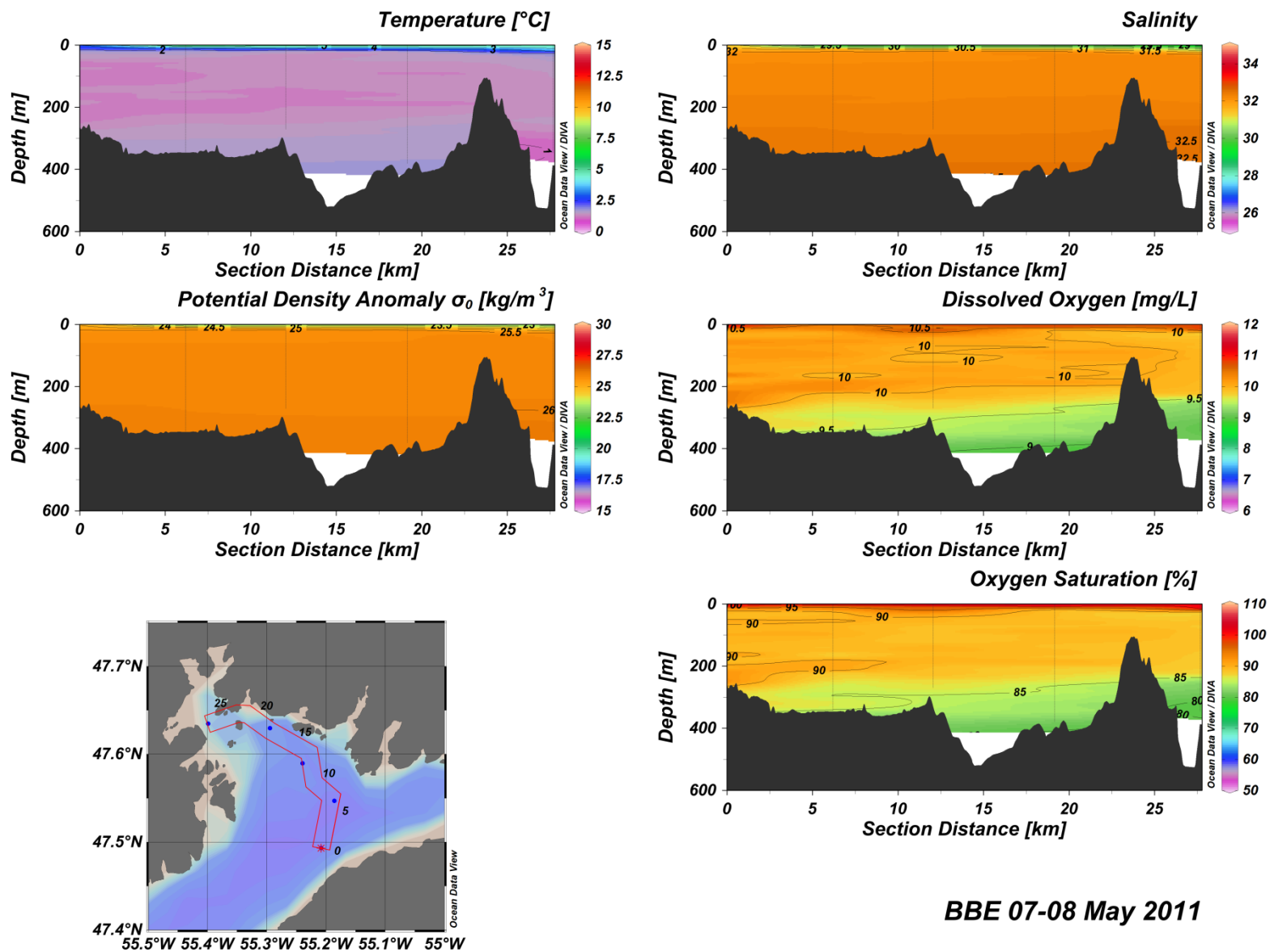


Figure B(i)6: Belle Bay West water column vertical structure.



BBE 07-08 May 2011

Figure B(i)7: Belle Bay East water column vertical structure.

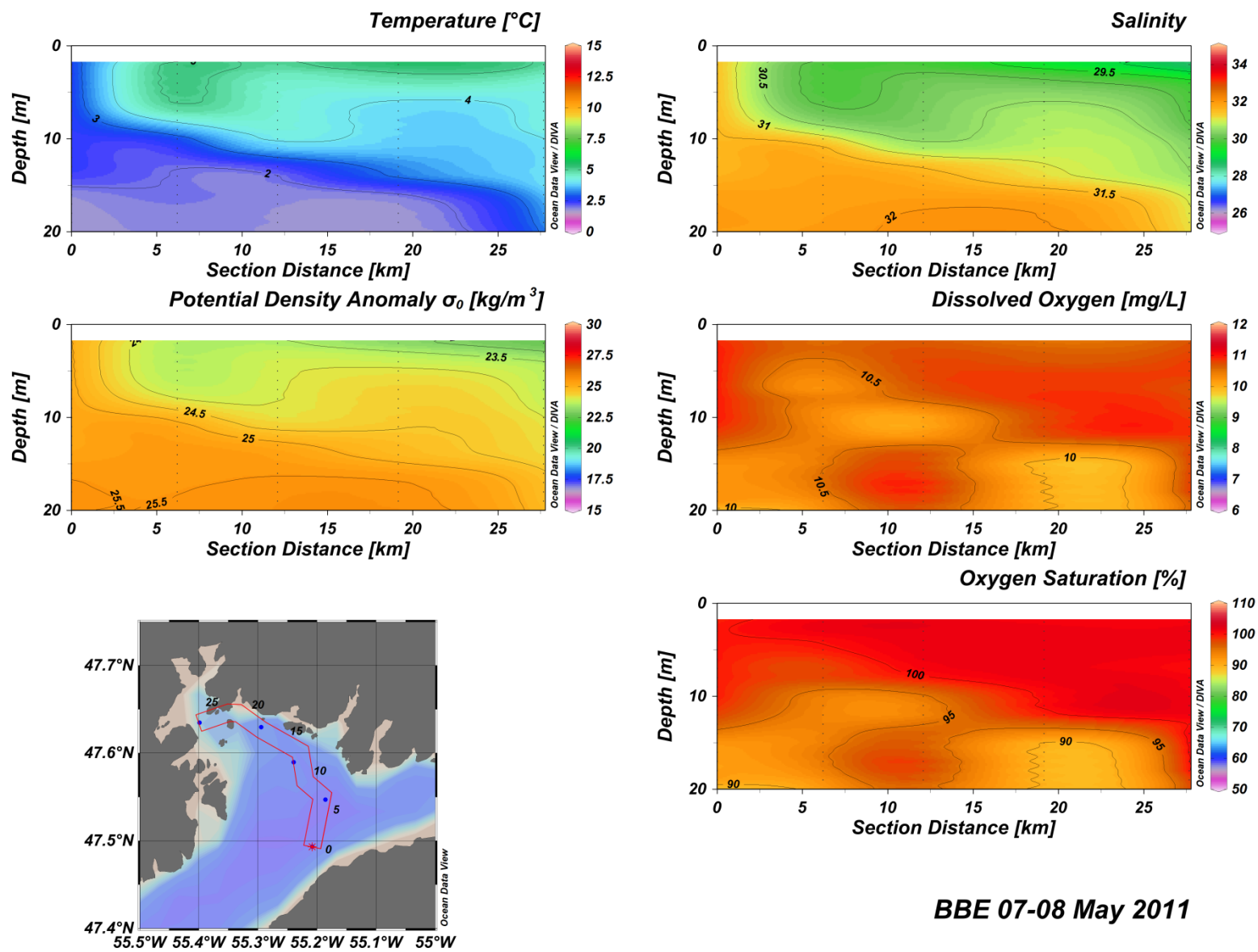


Figure B(i)8: Belle Bay East water column vertical structure.

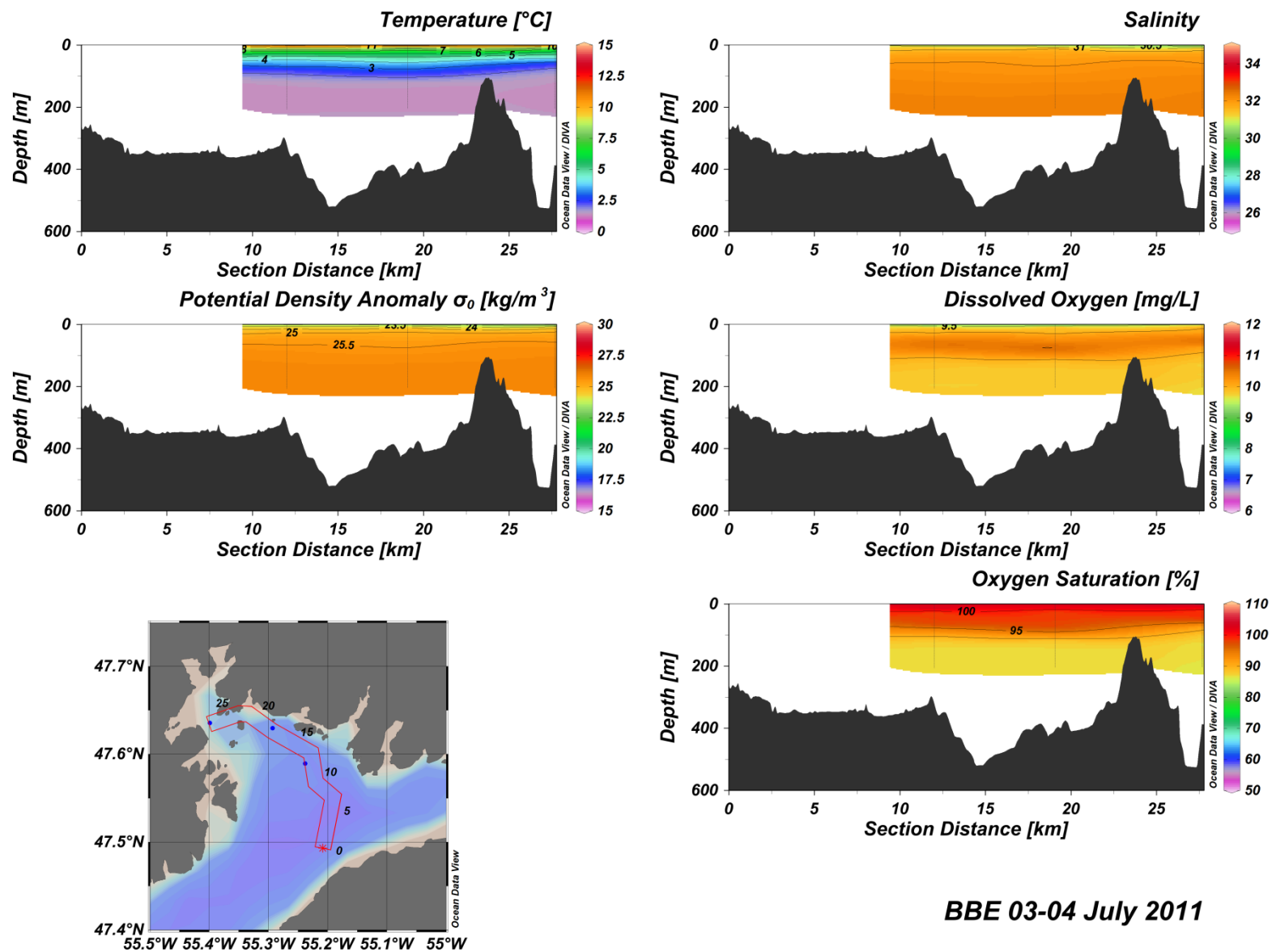


Figure B(i)9: Belle Bay East water column vertical structure.

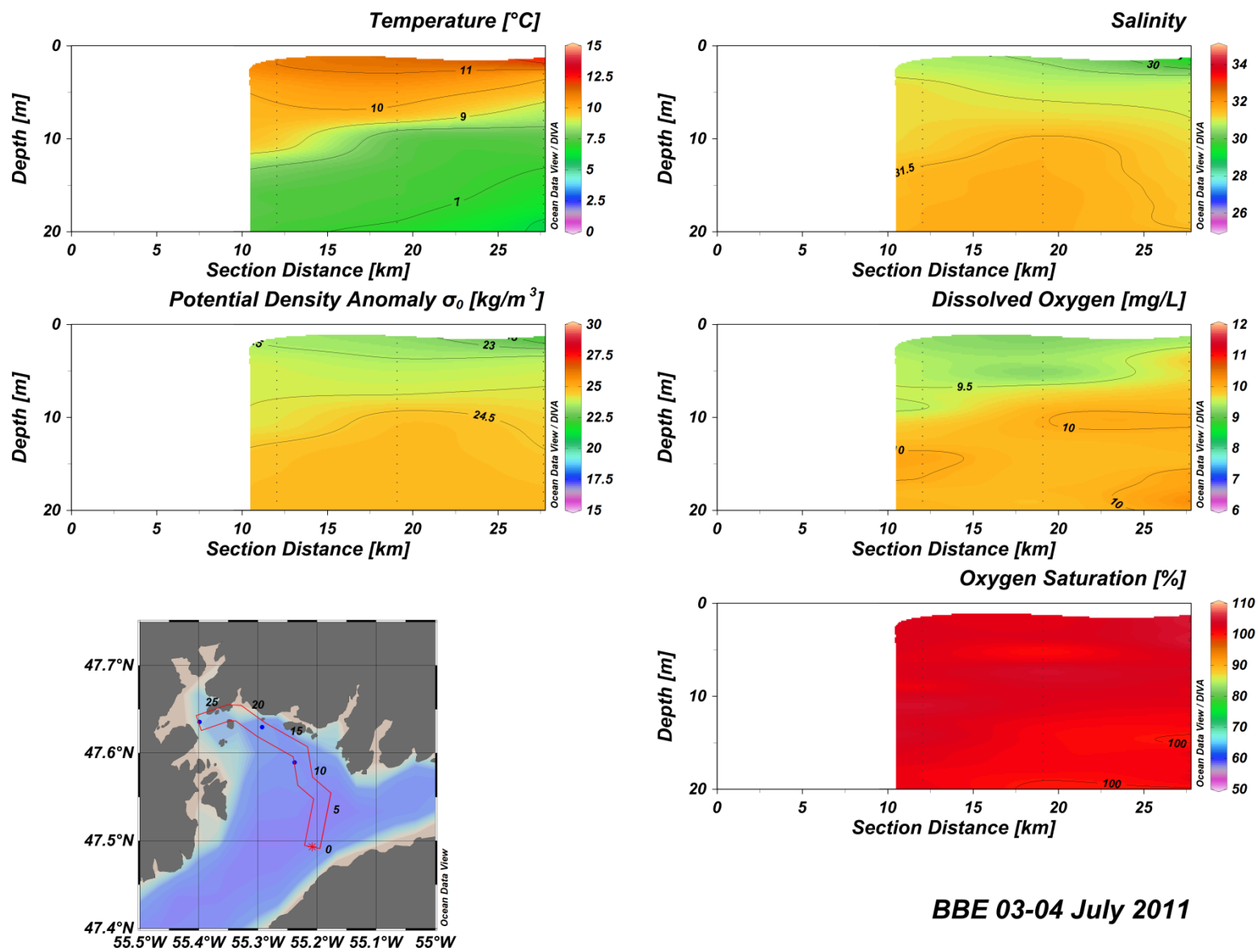


Figure B(i)10: Belle Bay East water column vertical structure.

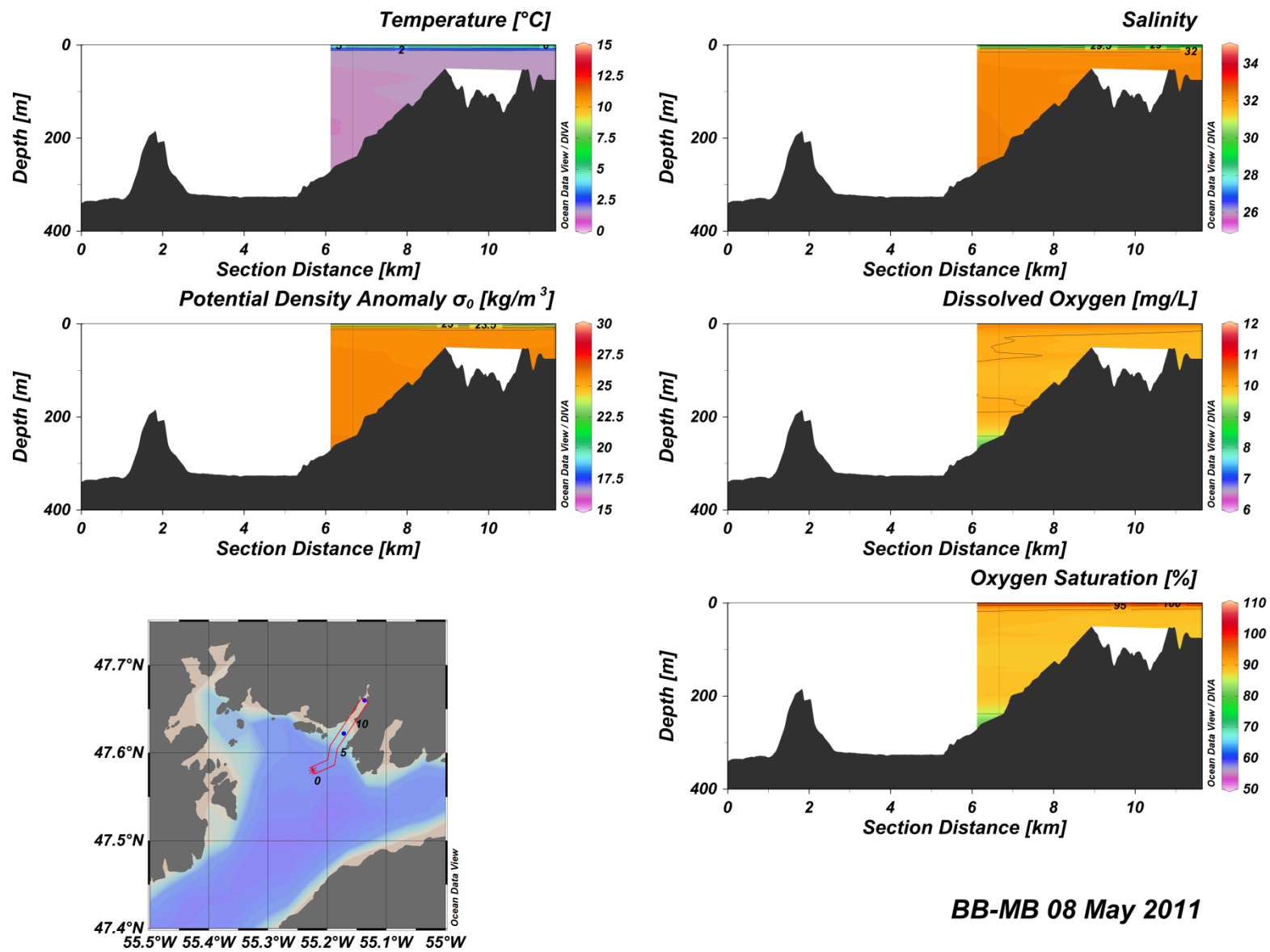


Figure B(i)11: Belle Bay East water column vertical structure.

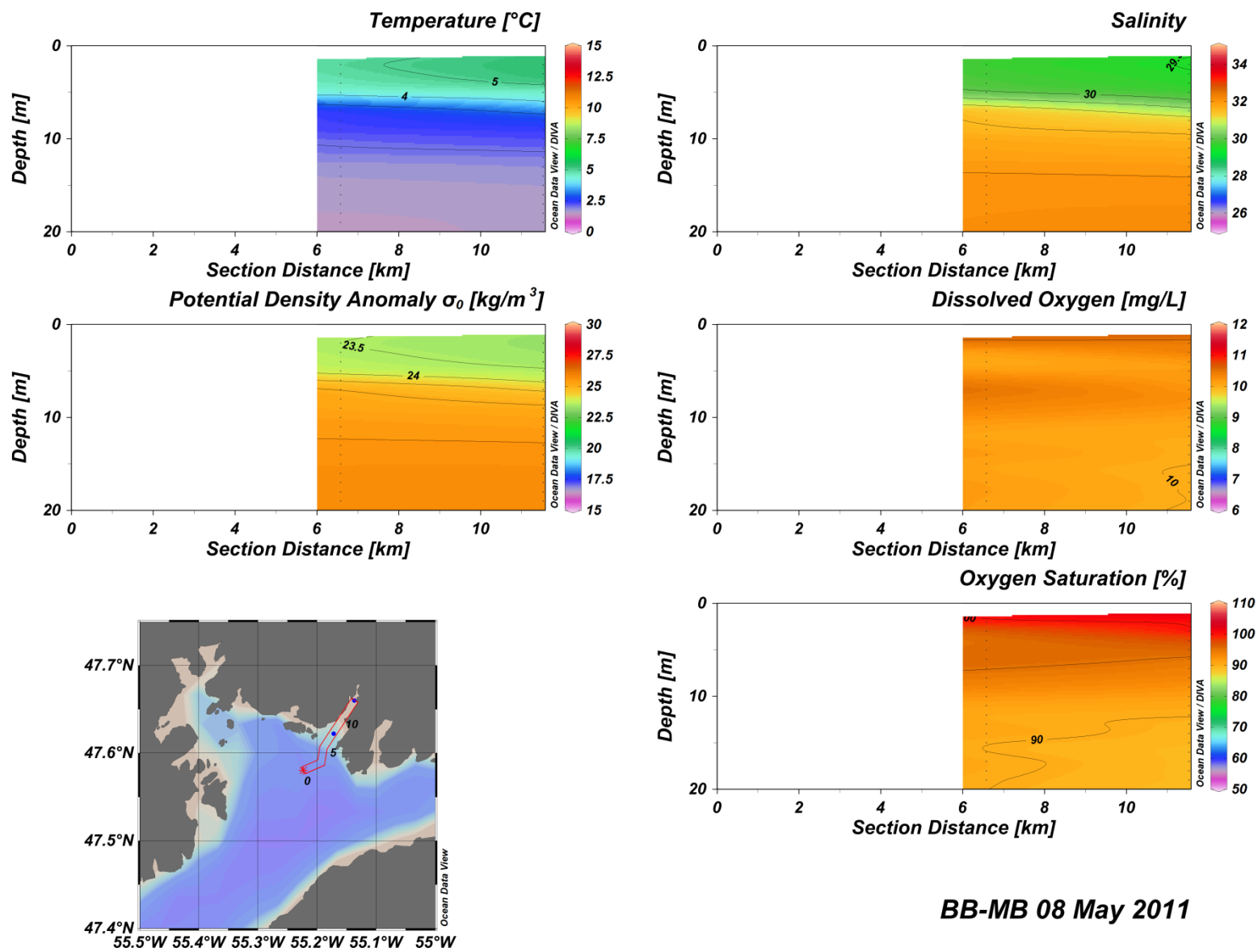


Figure B(i)12: Belle Bay – Mal Bay water column vertical structure.

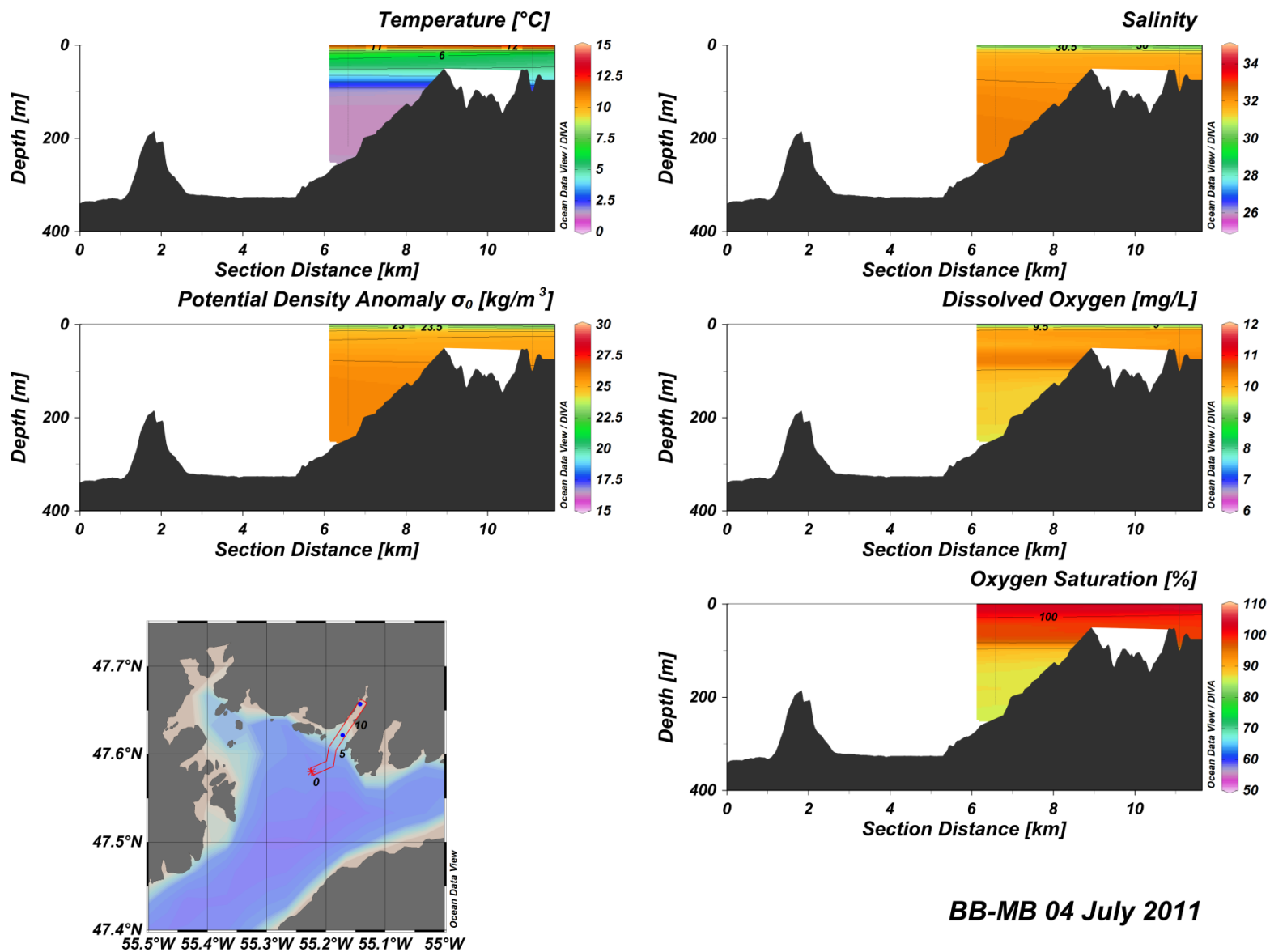


Figure B(i)13: Belle Bay – Mal Bay water column vertical structure.

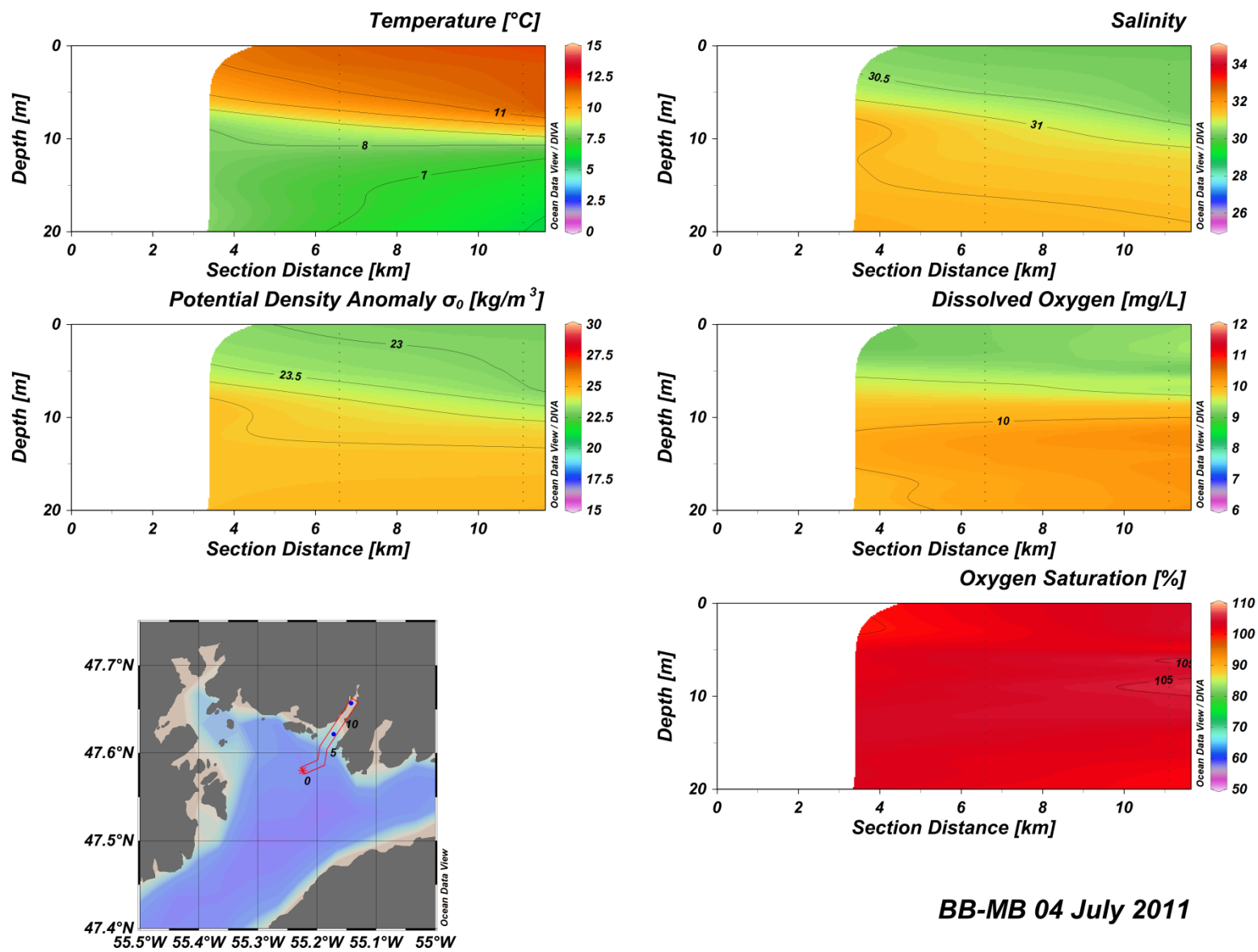


Figure B(i)14: Belle Bay – Mal Bay water column vertical structure.

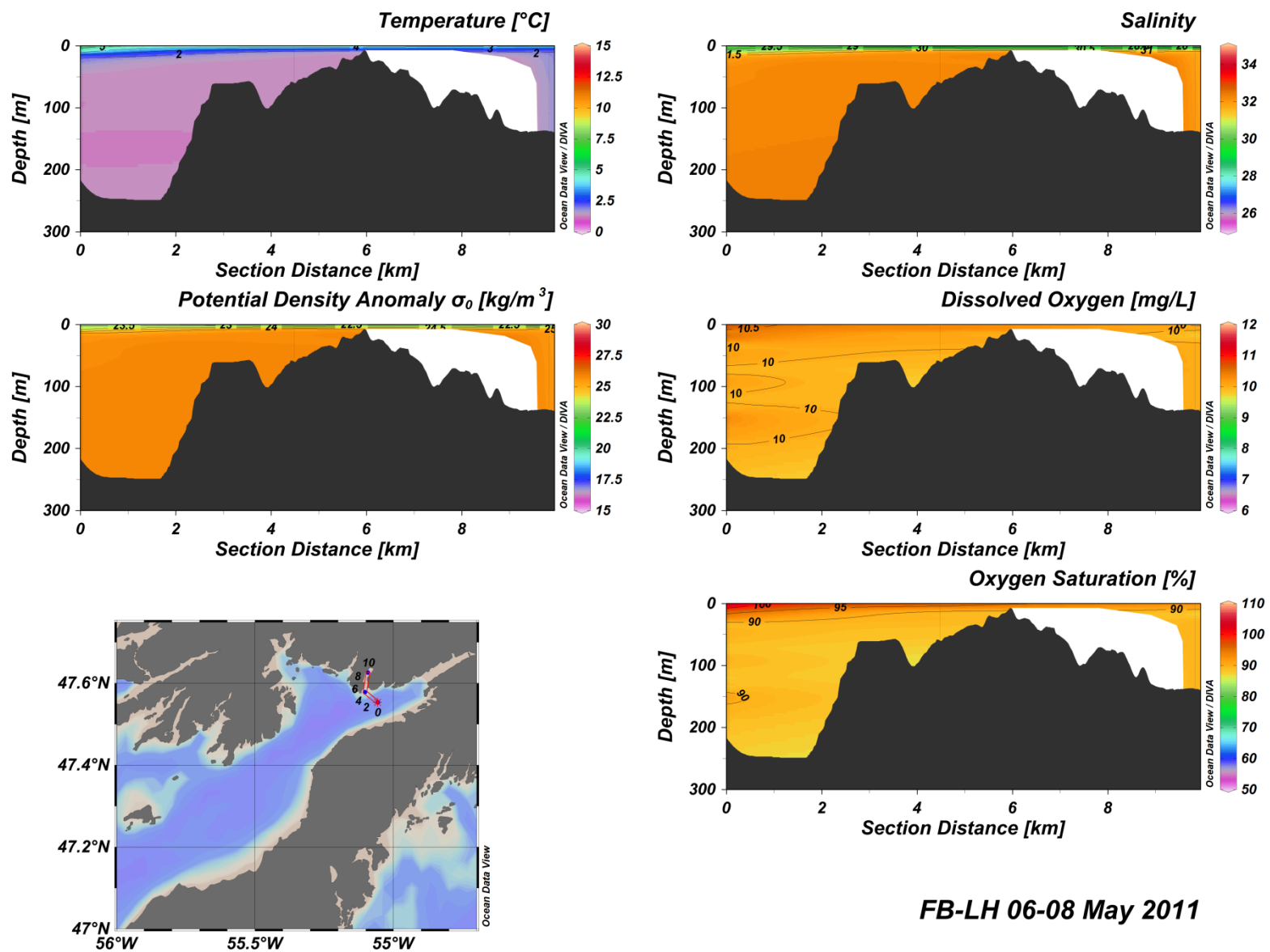


Figure B(i)15: Fortune Bay – Long Harbour water column vertical structure.

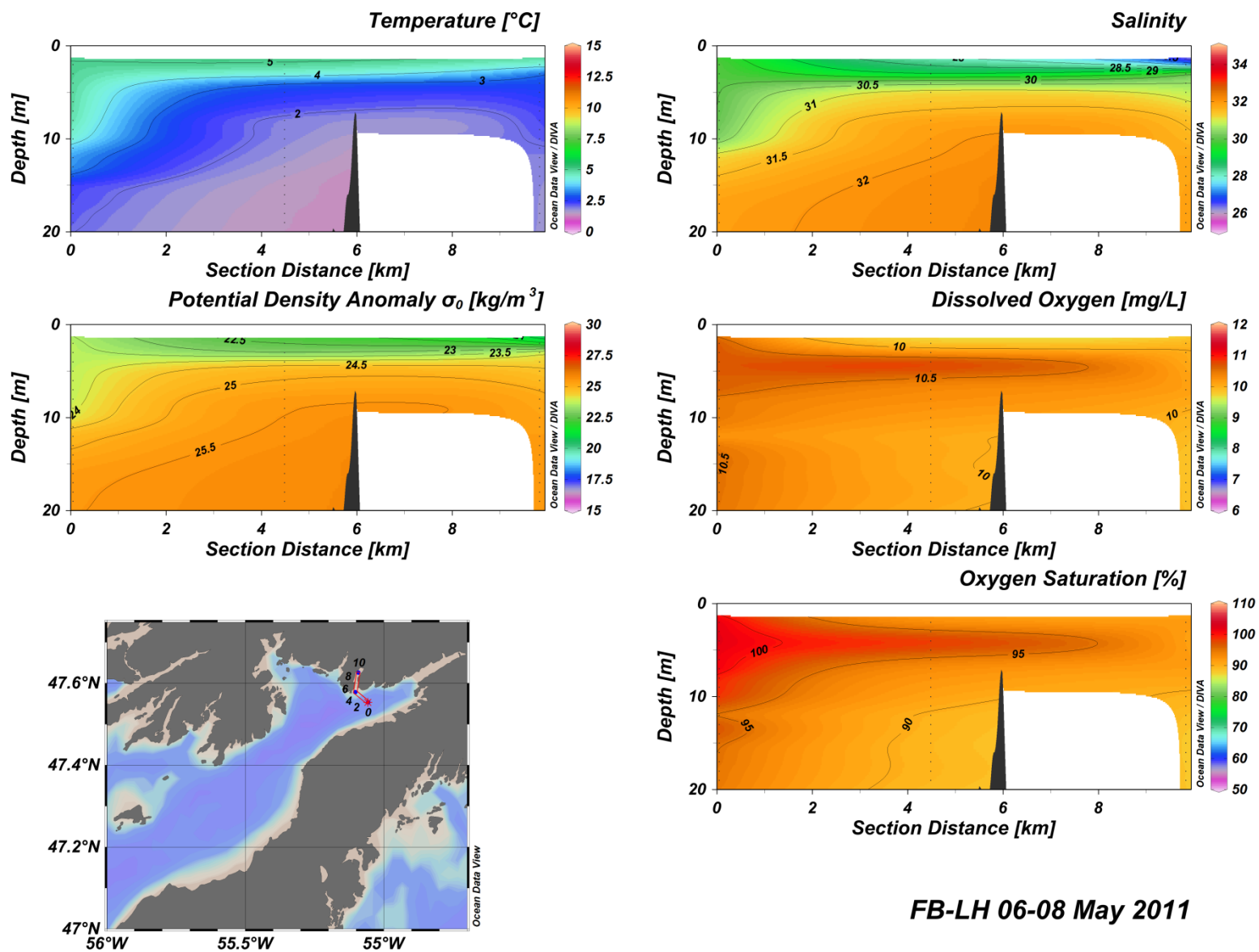


Figure B(i)16: Fortune Bay – Long Harbour water column vertical structure.

**APPENDIX B(II): FORTUNE BAY – BELLE BAY (FB-BB) VERTICAL SECTIONS
SUMMARY TABLES**

Table B(ii)1: Fortune Bay (FB) vertical sections summary statistics.

04-07 May 2011	T_min	T_max	T_mean	S_min	S_max	S_mean	DO_min	DO_max	DO_mean	ST_min	ST_max	ST_mean
Surface	1.65	5.04	2.9	29.65	32.11	31.44	9.76	11.62	10.72	23.43	25.67	25.05
Surface Gradients	0	1.04	0.1	0	0.76	0.06	0	0.37	0.05	0	0.7	0.06
Surface Clines	4	40	13.05	4	74	16.35	4	80	23.25	4	74	16.4
Intermediate 2°C_D = 38.5 m Dz = N/A	1.08	2	1.37	31.66	32.44	32.24	8.83	11.28	10.14	-	-	-
Deep 5°C_D = N/A Dz = N/A	N/A	N/A	N/A	N/A	N/A	N/A	N/A	N/A	N/A	-	-	-

Table B(ii)2: Belle Bay West (BBW) vertical sections summary statistics.

07 May 2011	T_min	T_max	T_mean	S_min	S_max	S_mean	DO_min	DO_max	DO_mean	ST_min	ST_max	ST_mean
Surface	1.72	5.91	3.66	25.79	31.89	30.56	10.24	10.98	10.74	20.29	25.5	24.29
Surface Gradients	0	1.01	0.11	0	2.42	0.12	0	0.19	0.05	0	2.01	0.11
Surface Clines	3	22	16.17	3	18	7.5	19	46	27.33	3	18	7.5
Intermediate 2°C_D = 21.5 m Dz = N/A	0.95	1.99	1.32	31.6	32.52	32.28	8.84	10.82	9.76	-	-	-
Deep 5°C_D = N/A Dz = N/A	N/A	N/A	N/A	N/A	N/A	N/A	N/A	N/A	N/A	-	-	-
03-05 July 2011	T_min	T_max	T_mean	S_min	S_max	S_mean	DO_min	DO_max	DO_mean	ST_min	ST_max	ST_mean
Surface	5.77	14.3	7.97	25.42	31.76	31.07	9.09	10.27	9.84	18.74	25.02	24.18
Surface Gradients	0.01	1.62	0.36	0	3.72	0.15	0	0.23	0.07	0.01	3.18	0.17
Surface Clines	3	3	3	3	3	3	3	18	8.25	3	3	3
Intermediate 2°C_D = 84 m Dz = N/A	1.3	2	1.41	32.06	32.31	32.24	9.61	10.26	9.82	-	-	-
Deep 5°C_D = N/A Dz = N/A	N/A	N/A	N/A	N/A	N/A	N/A	N/A	N/A	N/A	-	-	-

Table B(ii)3: Belle Bay East (BBE) vertical sections summary statistics

07-08 May 2011	T_min	T_max	T_mean	S_min	S_max	S_mean	DO_min	DO_max	DO_mean	ST_min	ST_max	ST_mean
Surface	1.64	5.46	3.31	28.62	32.06	30.86	9.71	10.97	10.51	22.63	25.65	24.55
Surface Gradients	0	0.84	0.15	0	0.52	0.12	0	0.35	0.07	0	0.48	0.11
Surface Clines	9	22	15.25	3	15	7.88	8	23	14.88	3	15	7.88
Intermediate 2°C_D = 18.5 m Dz = N/A	1	1.99	1.34	31.68	32.51	32.28	8.84	10.96	9.79	-	-	-
Deep 5°C_D = N/A Dz = N/A	N/A	N/A	N/A	N/A	N/A	N/A	N/A	N/A	N/A	-	-	-
03-04 July 2011	T_min	T_max	T_mean	S_min	S_max	S_mean	DO_min	DO_max	DO_mean	ST_min	ST_max	ST_mean
Surface	5.86	11.89	8.38	29.66	31.68	31.25	9.22	10.27	9.78	22.47	24.84	24.26
Surface Gradients	0	1.54	0.27	0	0.74	0.08	0	0.3	0.07	0.01	0.84	0.1
Surface Clines	3	12	8	3	9	5.33	3	10	6.67	3	9	5.33
Intermediate 2°C_D = 88 m Dz = N/A	1.3	2	1.42	32.09	32.31	32.24	9.69	10.24	9.84	-	-	-
Deep 5°C_D = N/A Dz = N/A	N/A	N/A	N/A	N/A	N/A	N/A	N/A	N/A	N/A	-	-	-

Table B(ii)4: Belle Bay – Mal Bay (BB-MB) vertical sections summary statistics

08 May 2011	T_min	T_max	T_mean	S_min	S_max	S_mean	DO_min	DO_max	DO_mean	ST_min	ST_max	ST_mean
Surface	1.46	5.32	2.74	29.48	32.12	31.24	9.88	10.71	10.19	23.27	25.69	24.9
Surface Gradients	0	0.99	0.19	0	0.71	0.13	0	0.32	0.07	0	0.65	0.12
Surface Clines	6	12	7.75	6	12	7.75	3	9	4.75	6	12	7.75
Intermediate 2°C_D = 12 m Dz = N/A	1.21	1.99	1.33	31.68	32.5	32.26	8.62	10.71	9.72	-	-	-
Deep 5°C_D = N/A Dz = N/A	N/A	N/A	N/A	N/A	N/A	N/A	N/A	N/A	N/A	-	-	-
04 July 2011	T_min	T_max	T_mean	S_min	S_max	S_mean	DO_min	DO_max	DO_mean	ST_min	ST_max	ST_mean
Surface	6	11.67	8.76	30.22	31.65	31.09	9.12	10.28	9.79	22.94	24.82	24.08
Surface Gradients	0	1.06	0.26	0	0.22	0.07	0	0.35	0.07	0.01	0.34	0.09
Surface Clines	8	12	9.67	4	9	6.67	6	10	8.33	4	9	7
Intermediate 2°C_D = 96 m Dz = N/A	1.3	1.99	1.43	32.09	32.32	32.23	9.64	10.19	9.81	-	-	-
Deep 5°C_D = N/A Dz = N/A	N/A	N/A	N/A	N/A	N/A	N/A	N/A	N/A	N/A	-	-	-

Table B(ii)5: Fortune Bay – Long Harbour (FB-LH) vertical sections summary statistics

06-08 May 2011	T_min	T_max	T_mean	S_min	S_max	S_mean	DO_min	DO_max	DO_mean	ST_min	ST_max	ST_mean
Surface	1.37	4.96	2.65	27.28	32.15	31.18	9.8	10.72	10.21	21.62	25.74	24.86
Surface Gradients	0	1.29	0.17	0	2.56	0.19	0	0.52	0.06	0	2.13	0.17
Surface Clines	3	15	7.33	3	11	6	3	13	6.67	3	11	6
Intermediate 2°C_D = 13.5 m Dz = N/A	1.13	1.97	1.43	31.66	32.28	32.1	9.83	10.46	10.04	-	-	-
Deep 5°C_D = N/A Dz = N/A	N/A	N/A	N/A	N/A	N/A	N/A	N/A	N/A	N/A	-	-	-

APPENDIX B(III): FORTUNE BAY – BELLE BAY (FB-BB) SURFACE MAPS

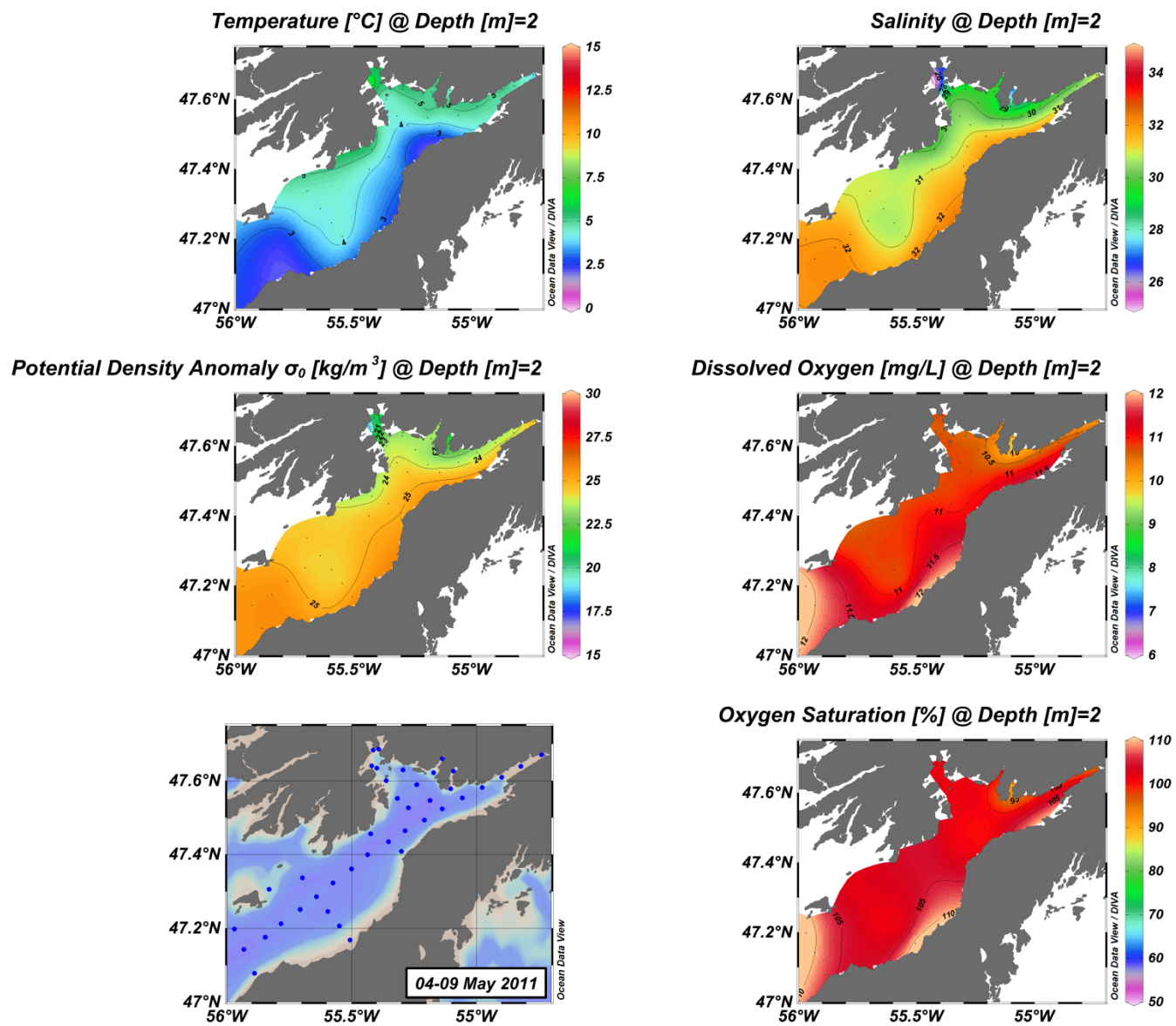


Figure B(iii)1: Fortune Bay – Belle Bay surface structure.

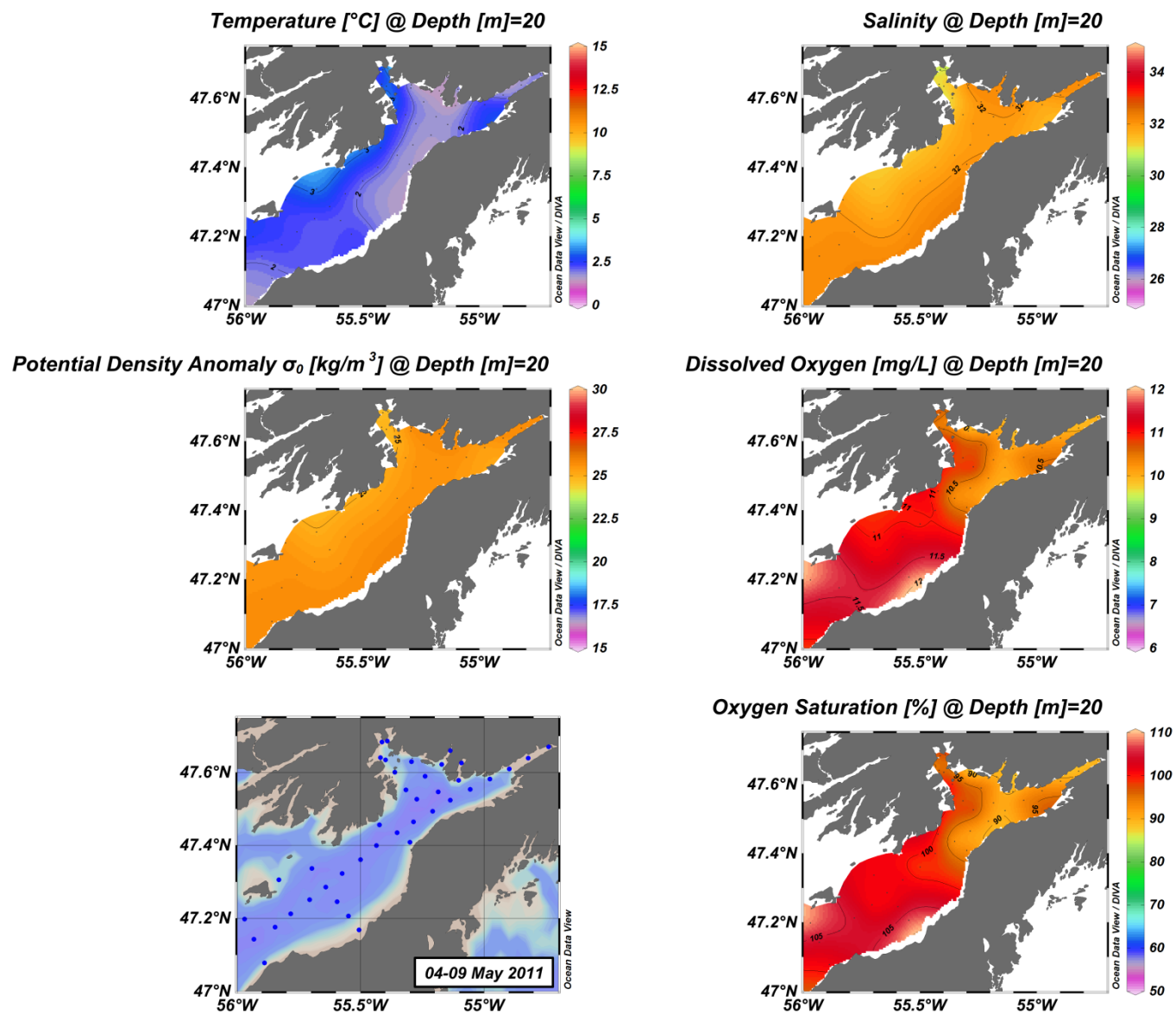


Figure B(iii)2: Fortune Bay – Belle Bay surface structure.

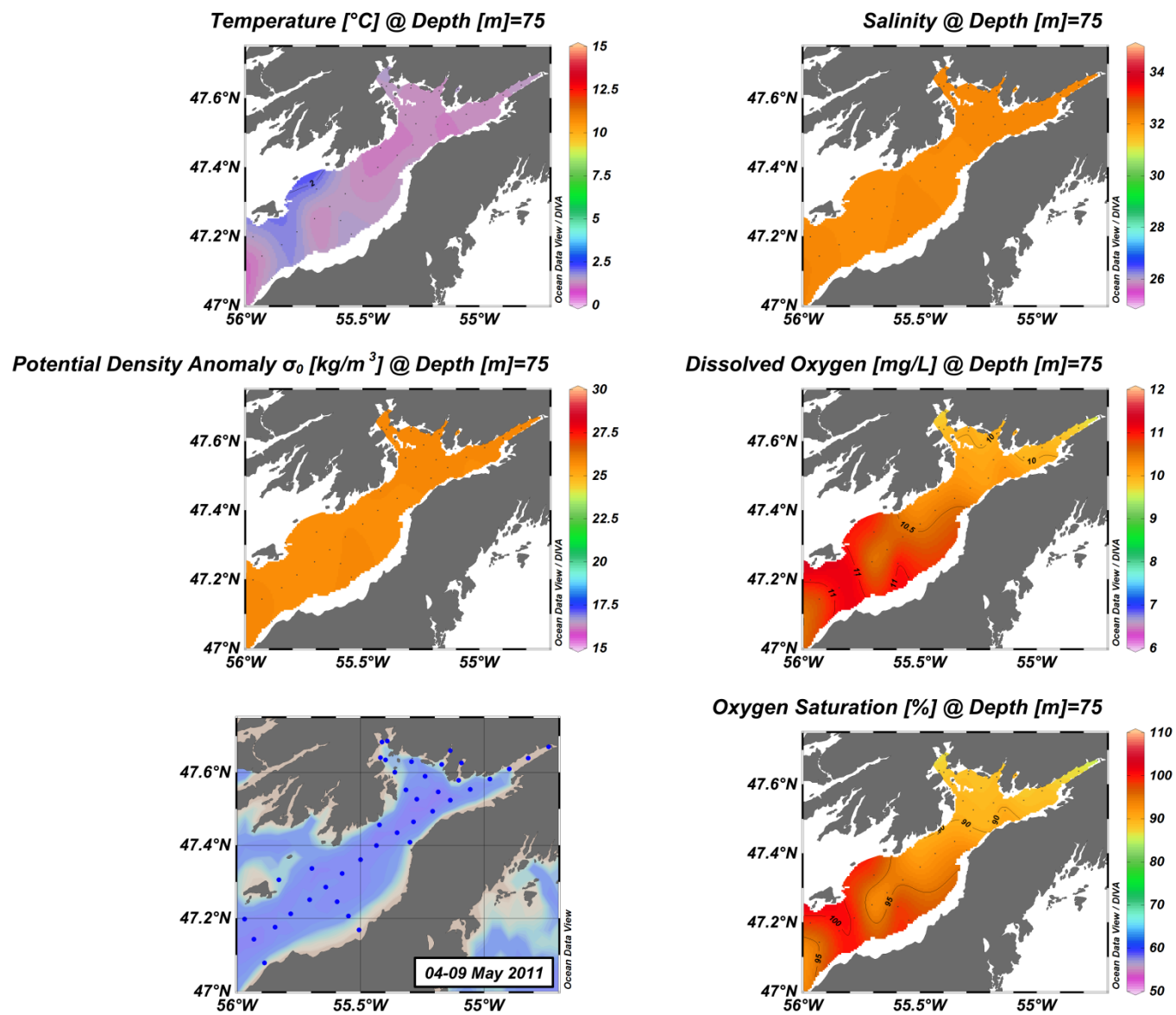


Figure B(iii)3: Fortune Bay – Belle Bay surface structure.

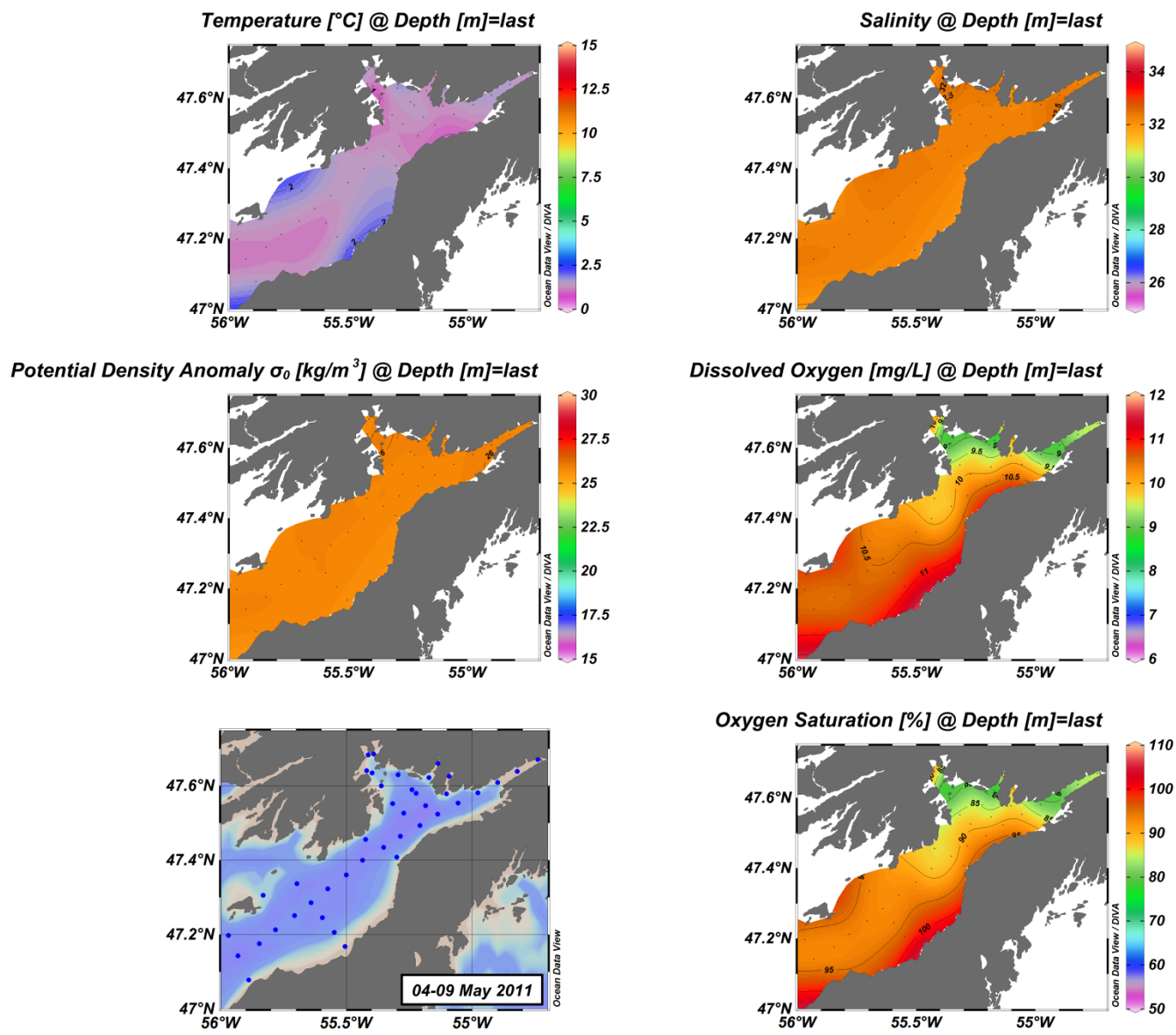


Figure B(iii)4: Fortune Bay – Belle Bay surface structure.

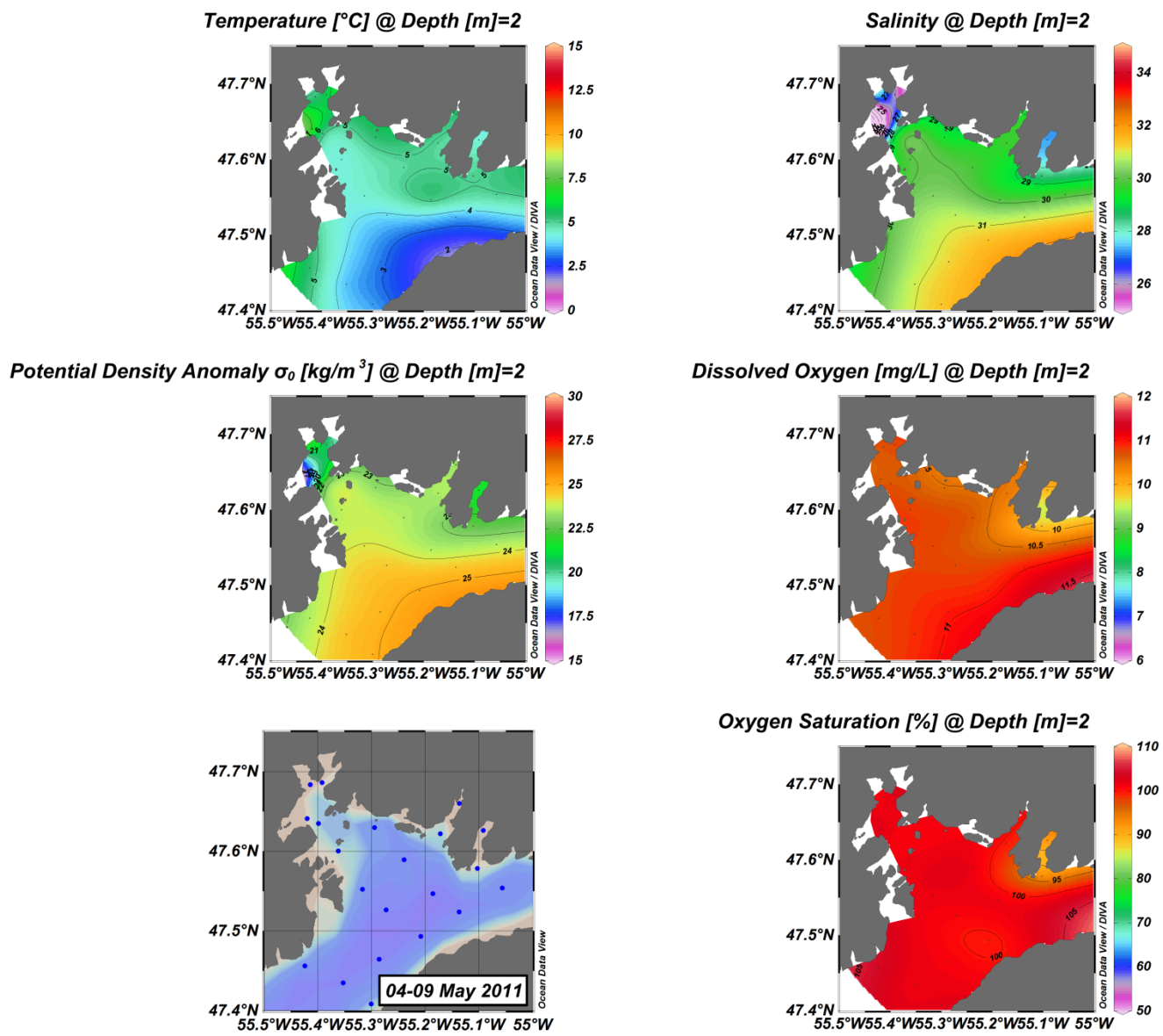


Figure B(iii)5: Belle Bay surface structure.

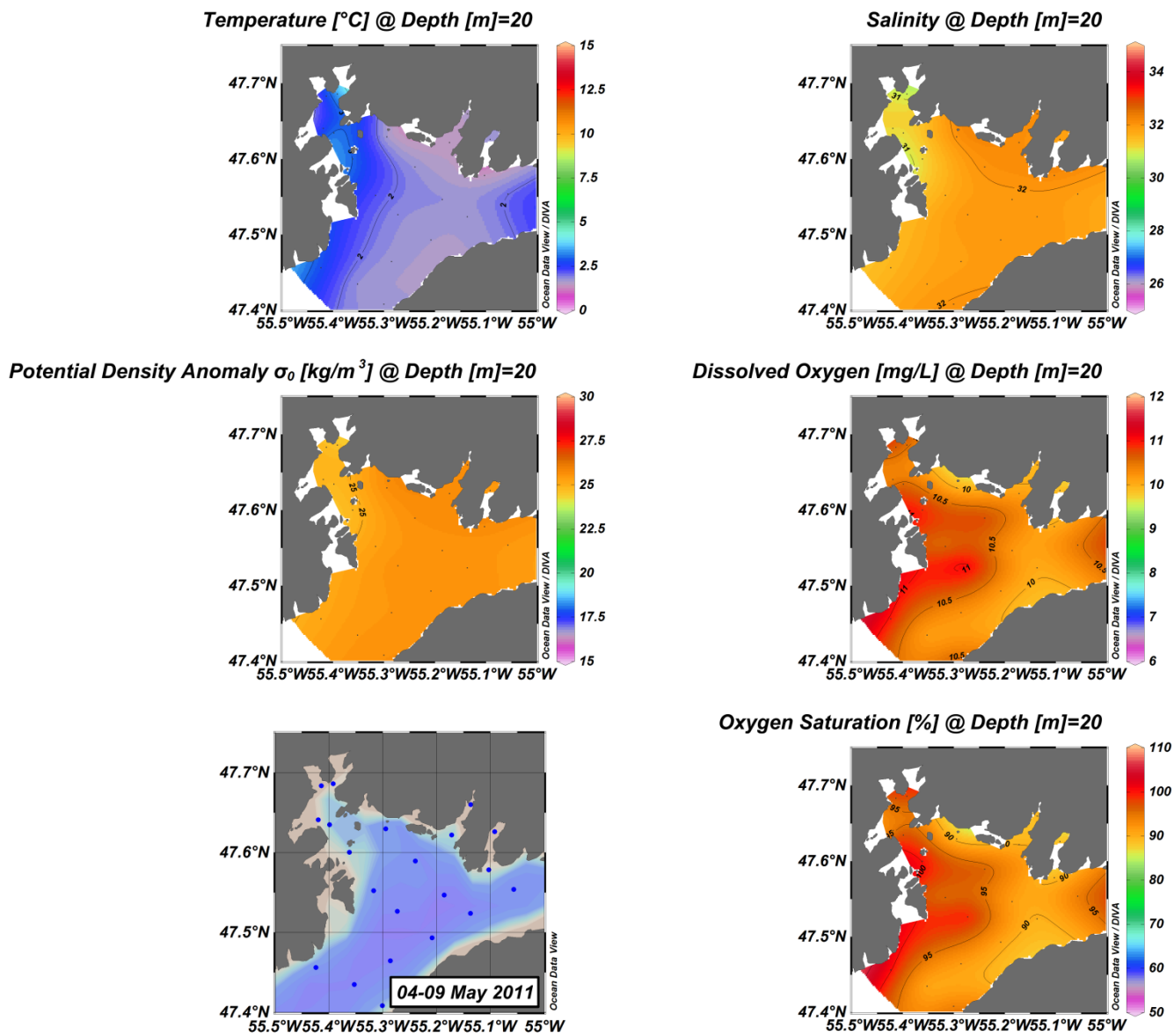


Figure B(iii)6: Belle Bay surface structure.

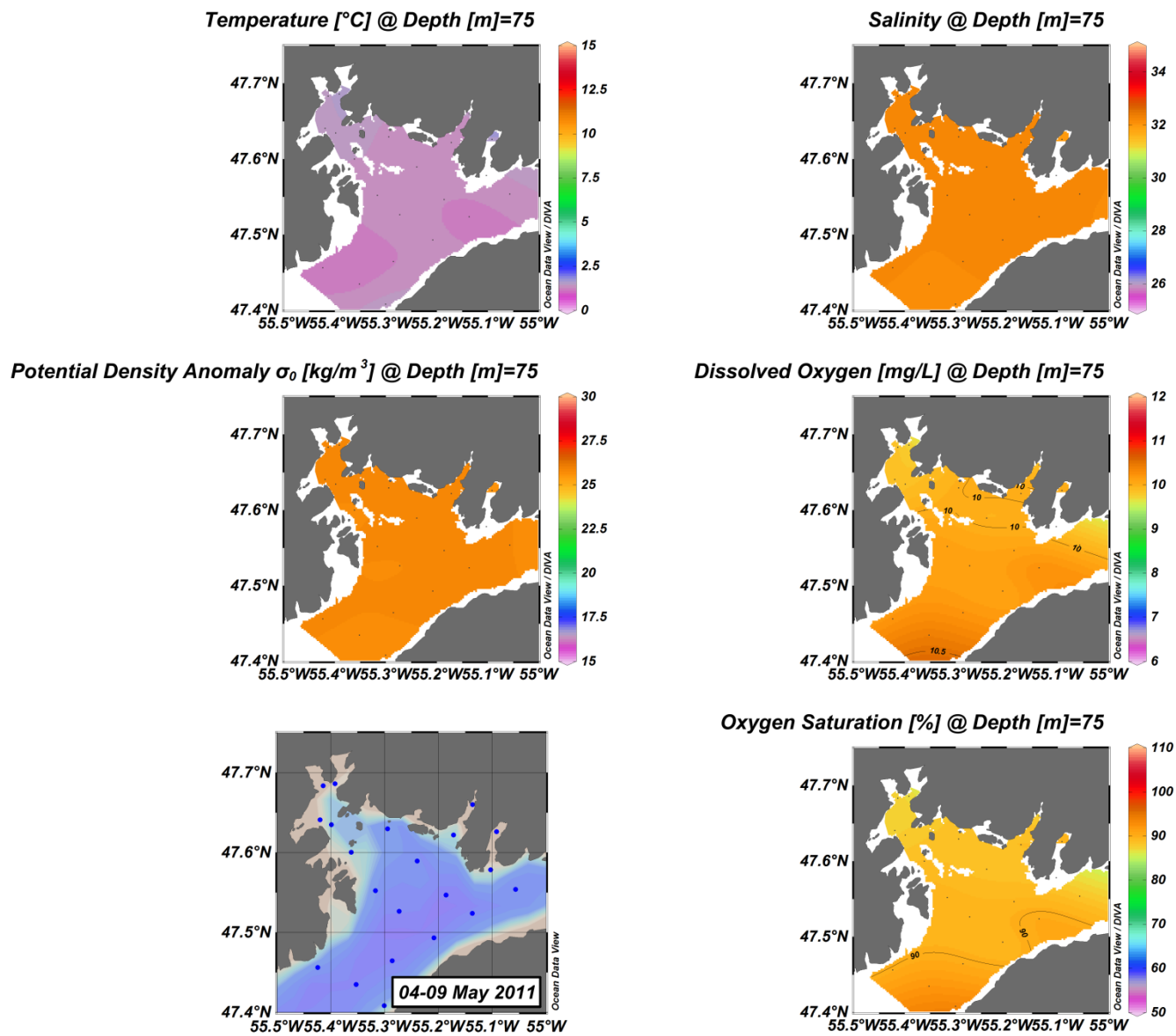


Figure B(iii)7: Belle Bay surface structure.

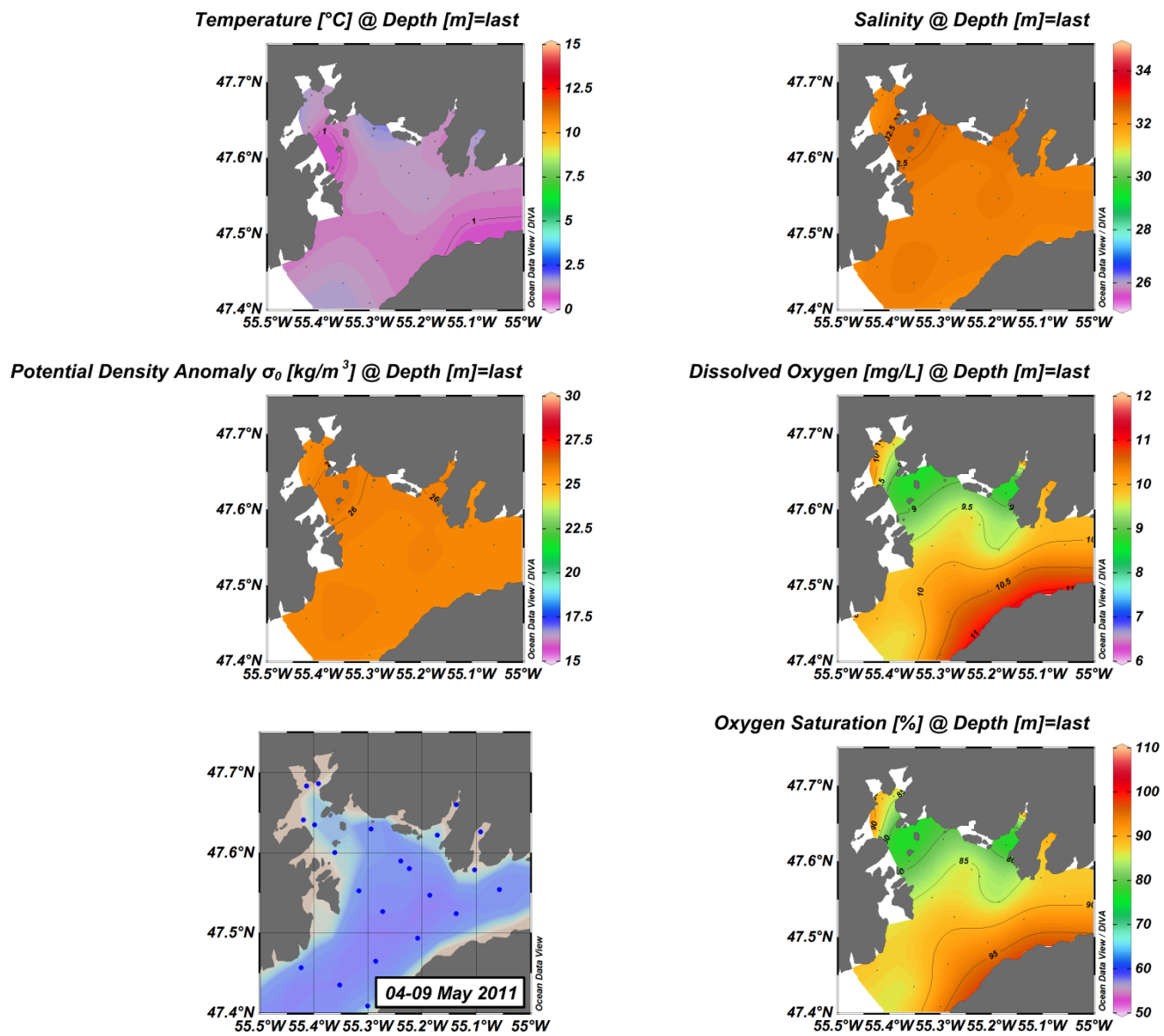


Figure B(iii)8: Belle Bay surface structure.

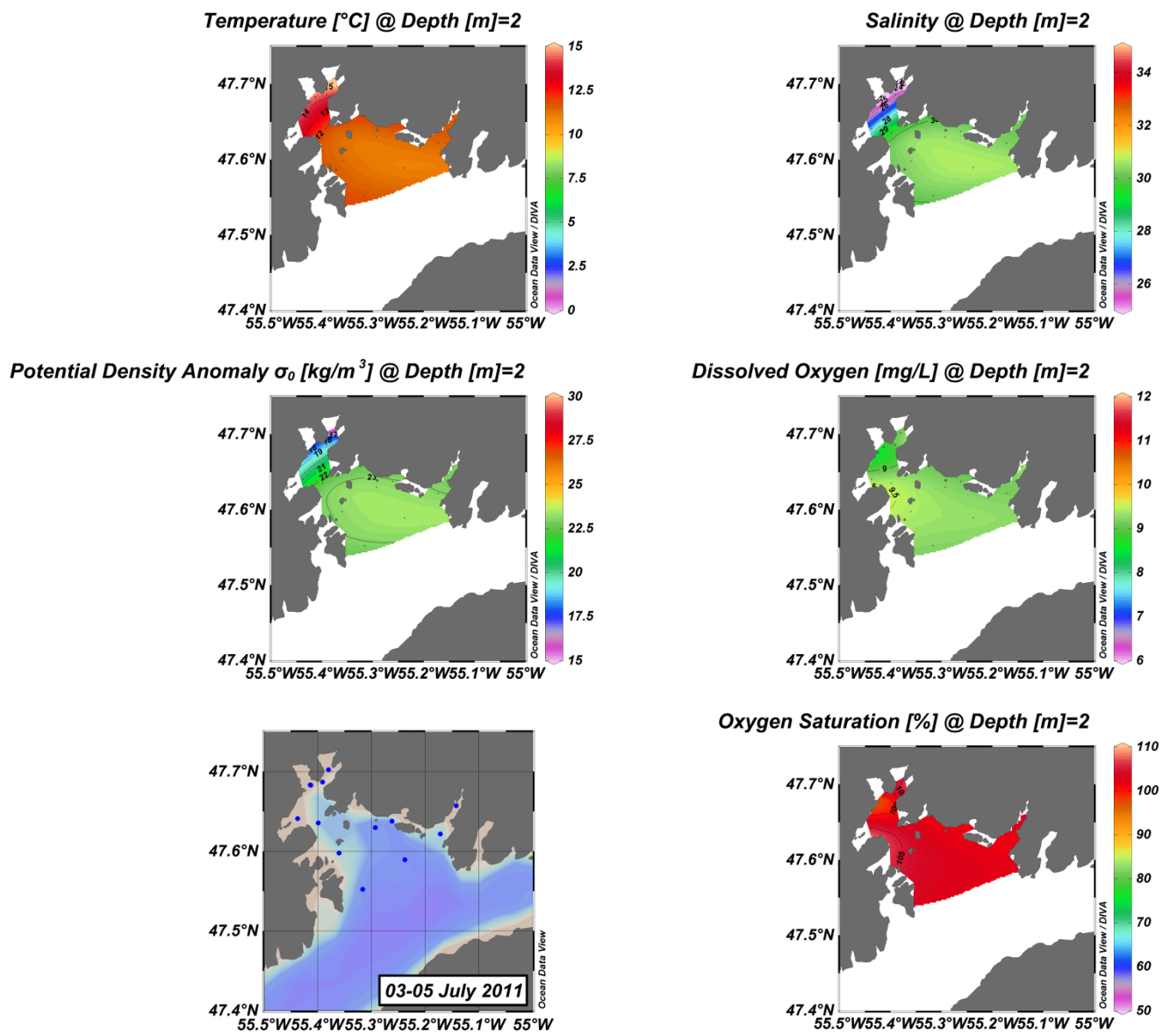


Figure B(iii)9: Belle Bay surface structure.

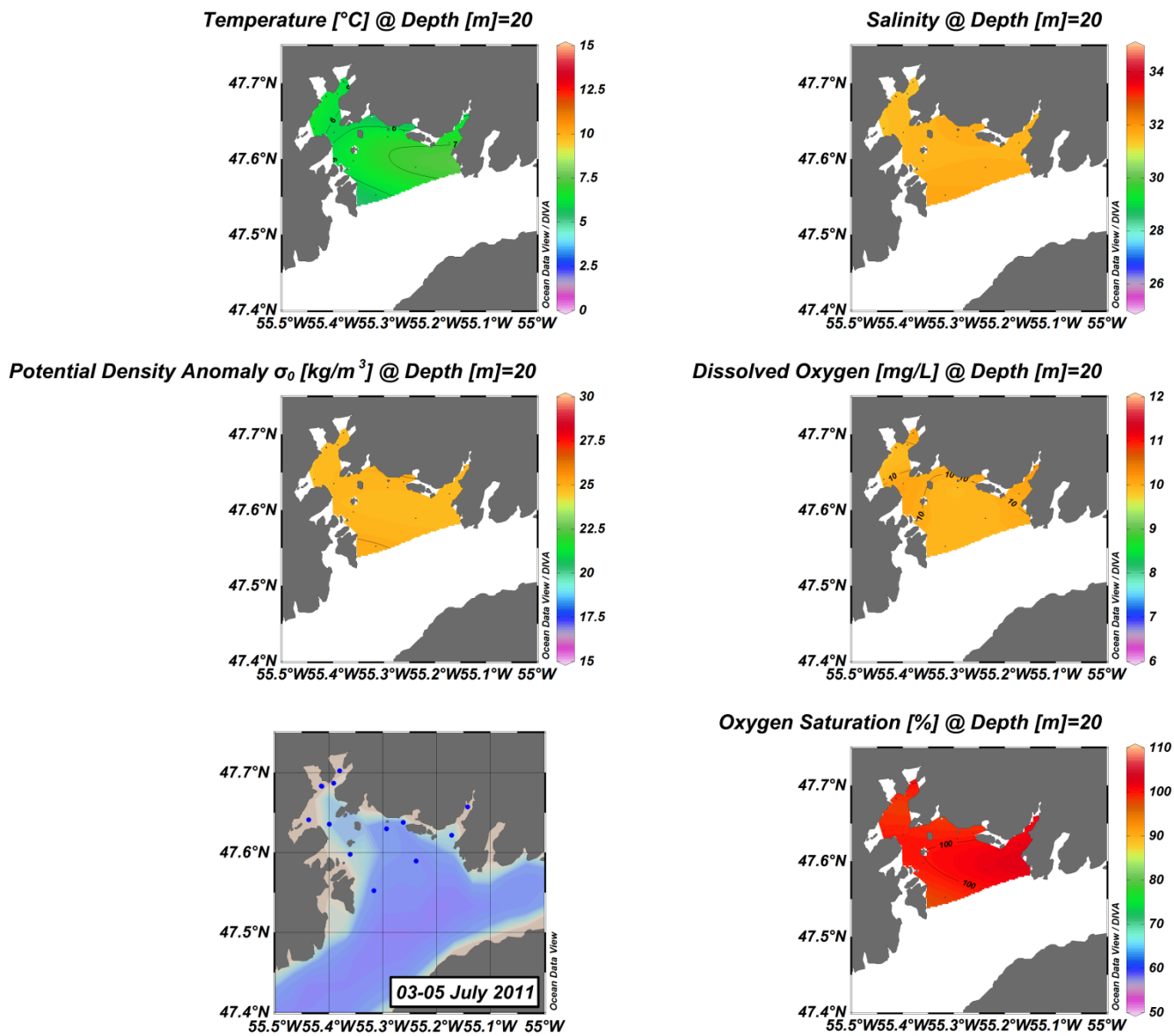


Figure B(iii)10: Belle Bay surface structure.

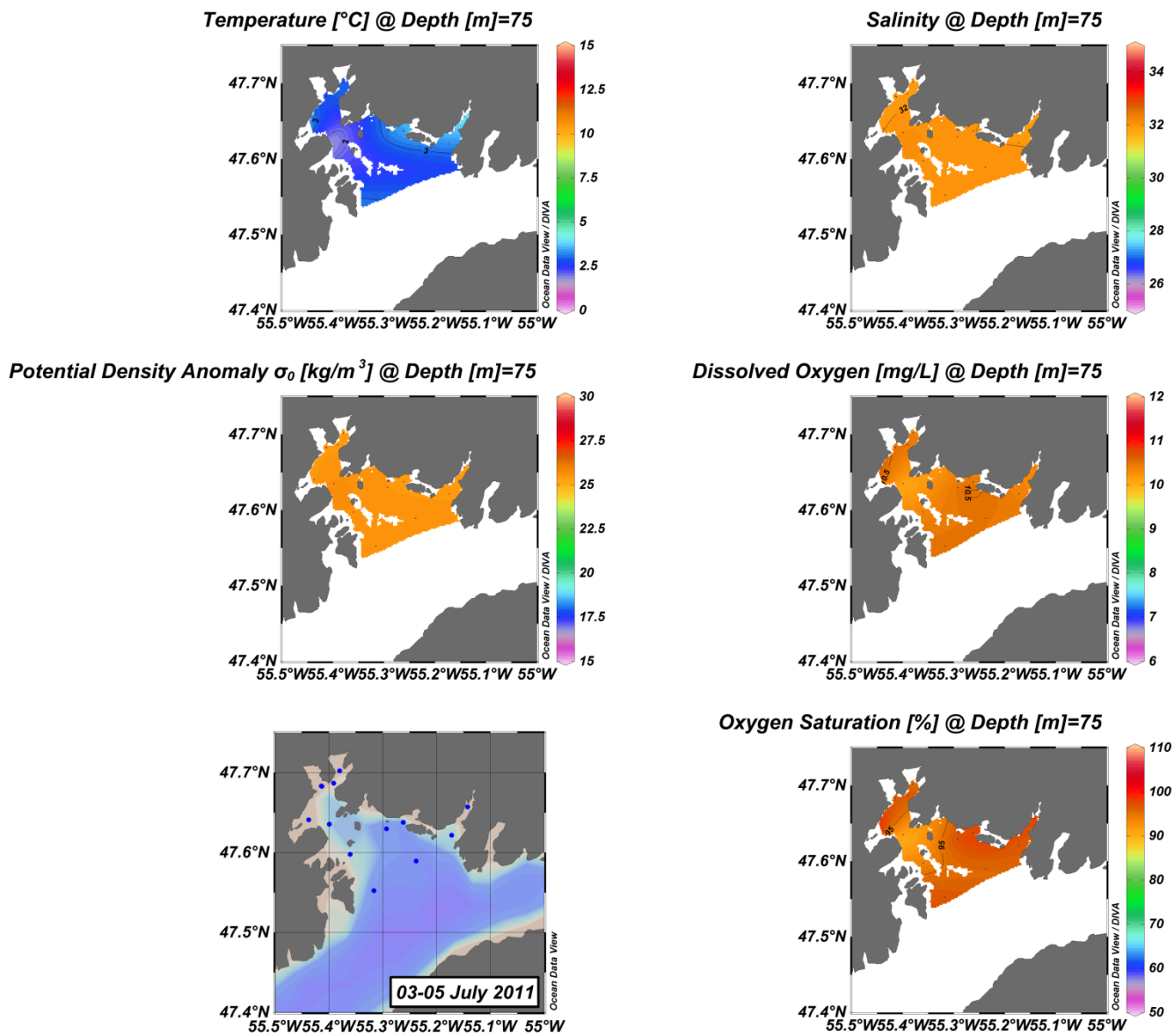


Figure B(iii)11: Belle Bay surface structure.

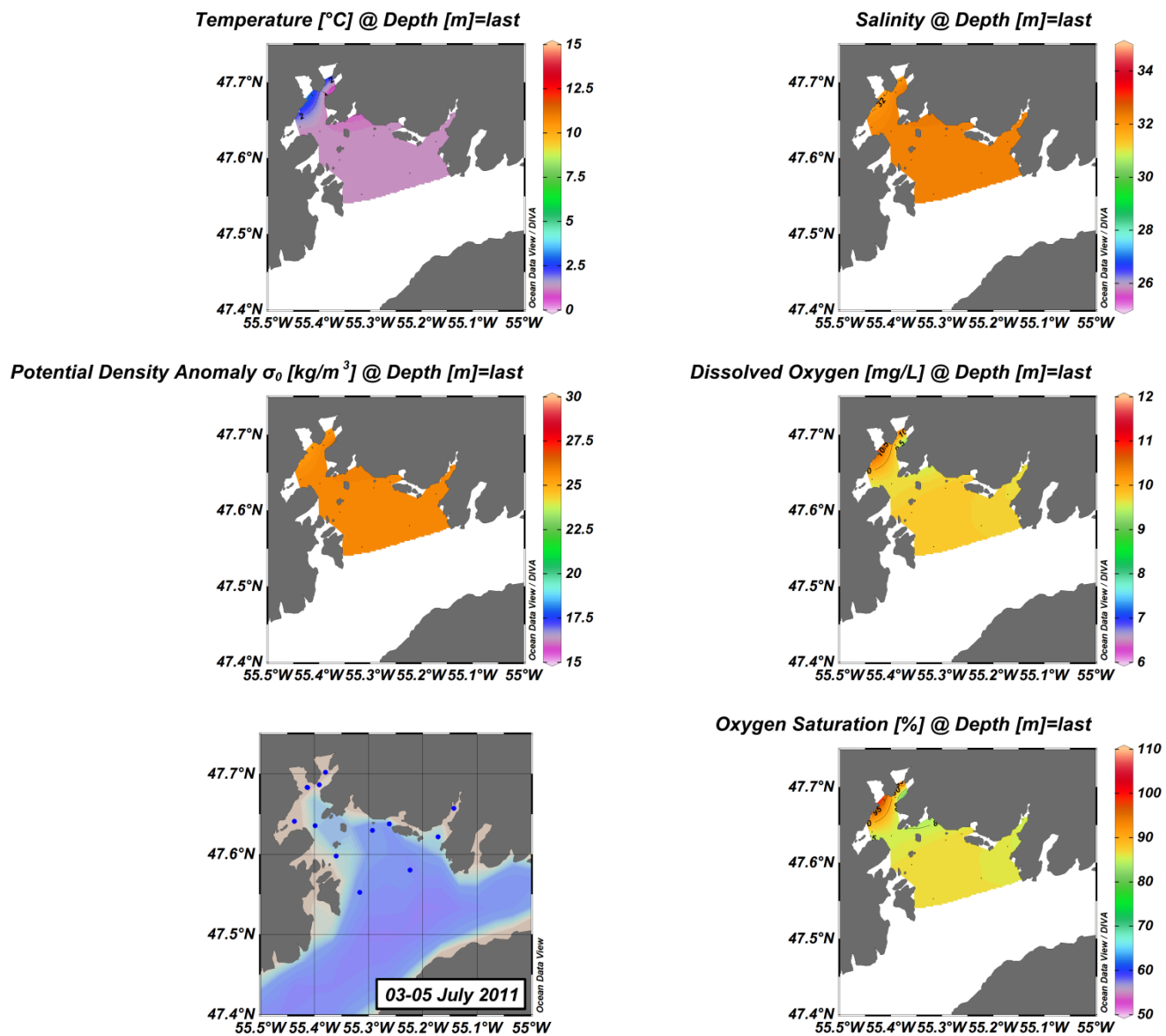


Figure B(iii)12: Belle Bay surface structure (maximum depth of the casts ~200m for this survey).

APPENDIX C(I): CONNAIGRE PENINSULA (CP) VERTICAL SECTIONS

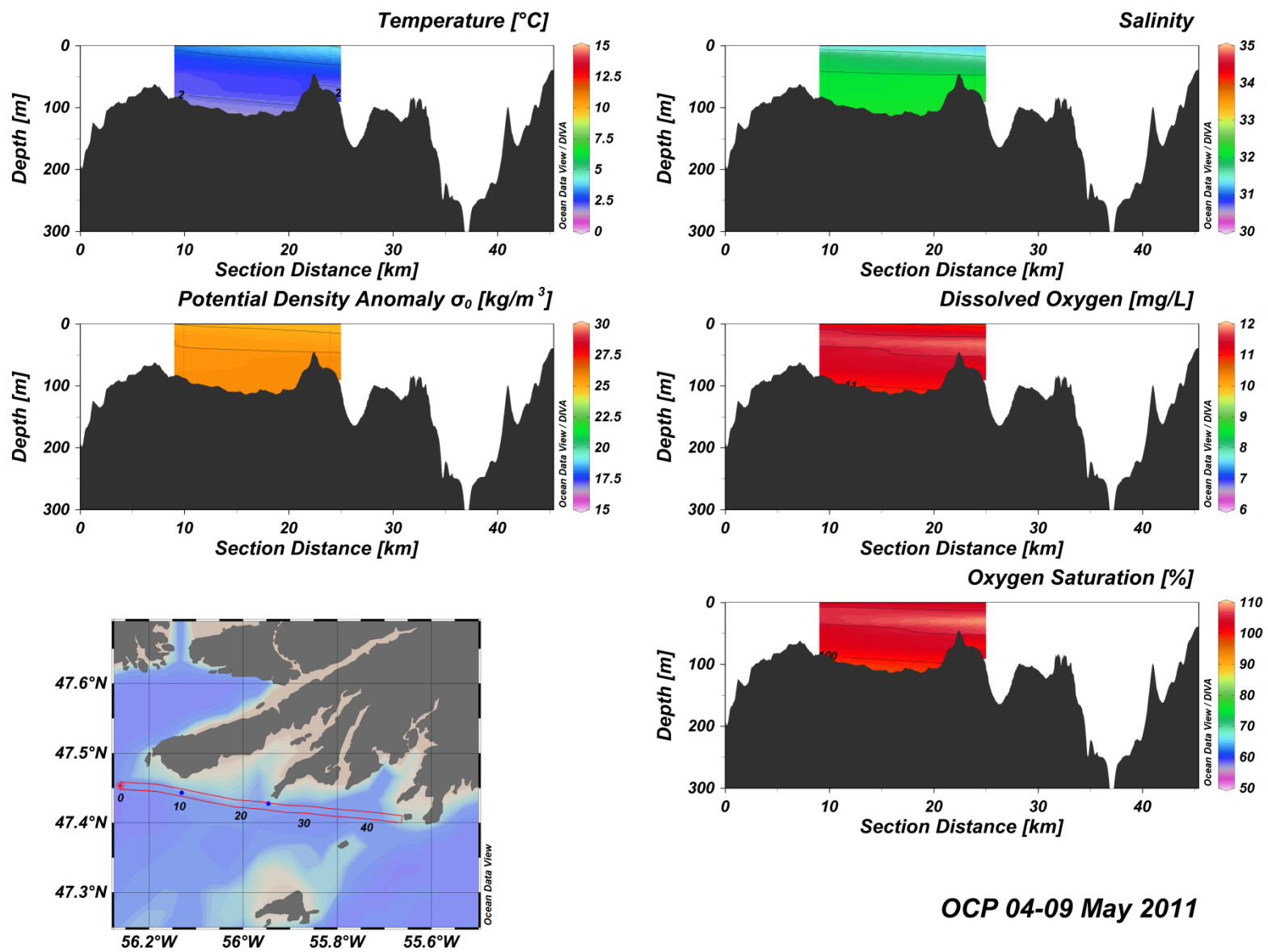


Figure C(i)1: Outer Connaigre Peninsula water column vertical structure.

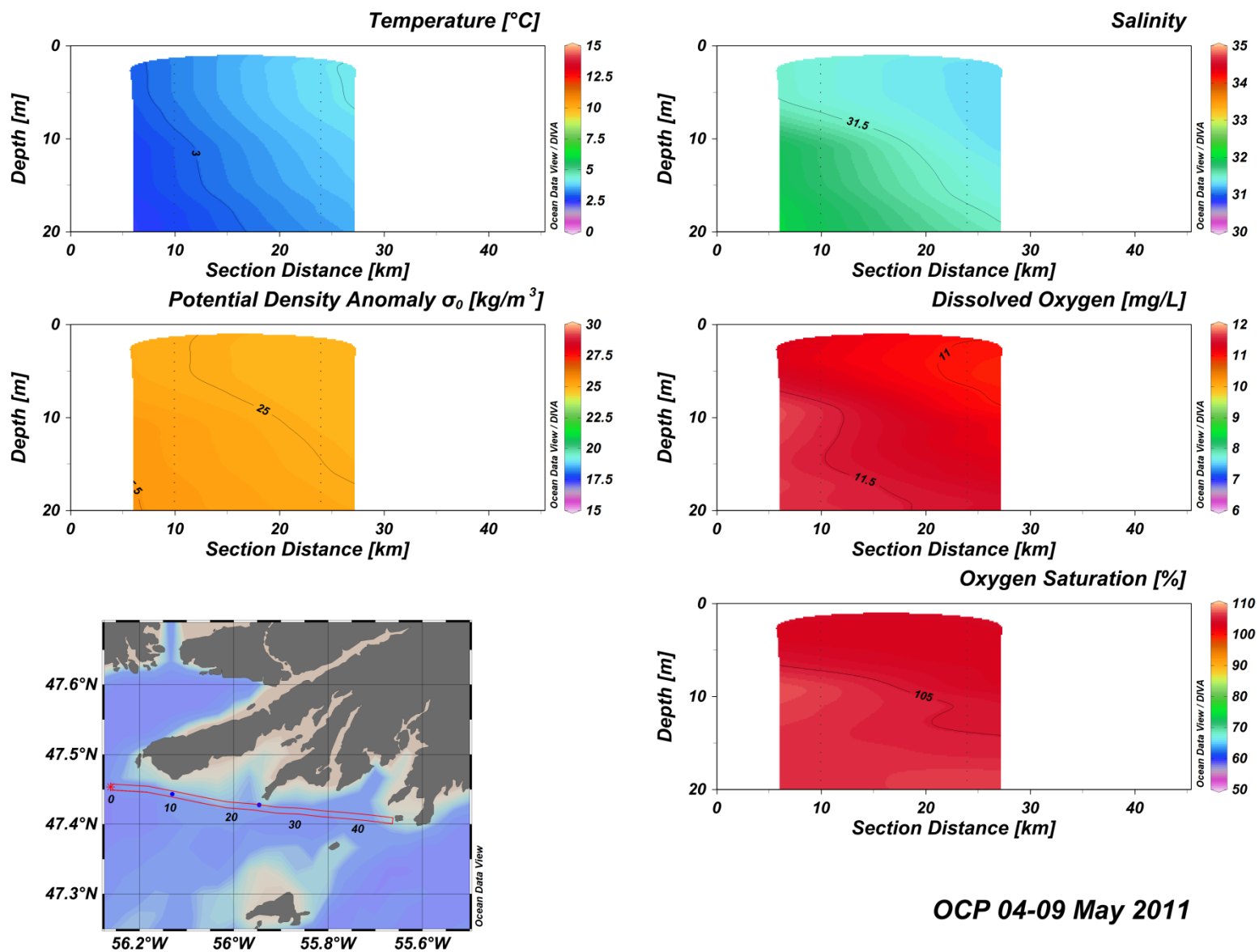


Figure C(i)2: Outer Connaigre Peninsula water column vertical structure.

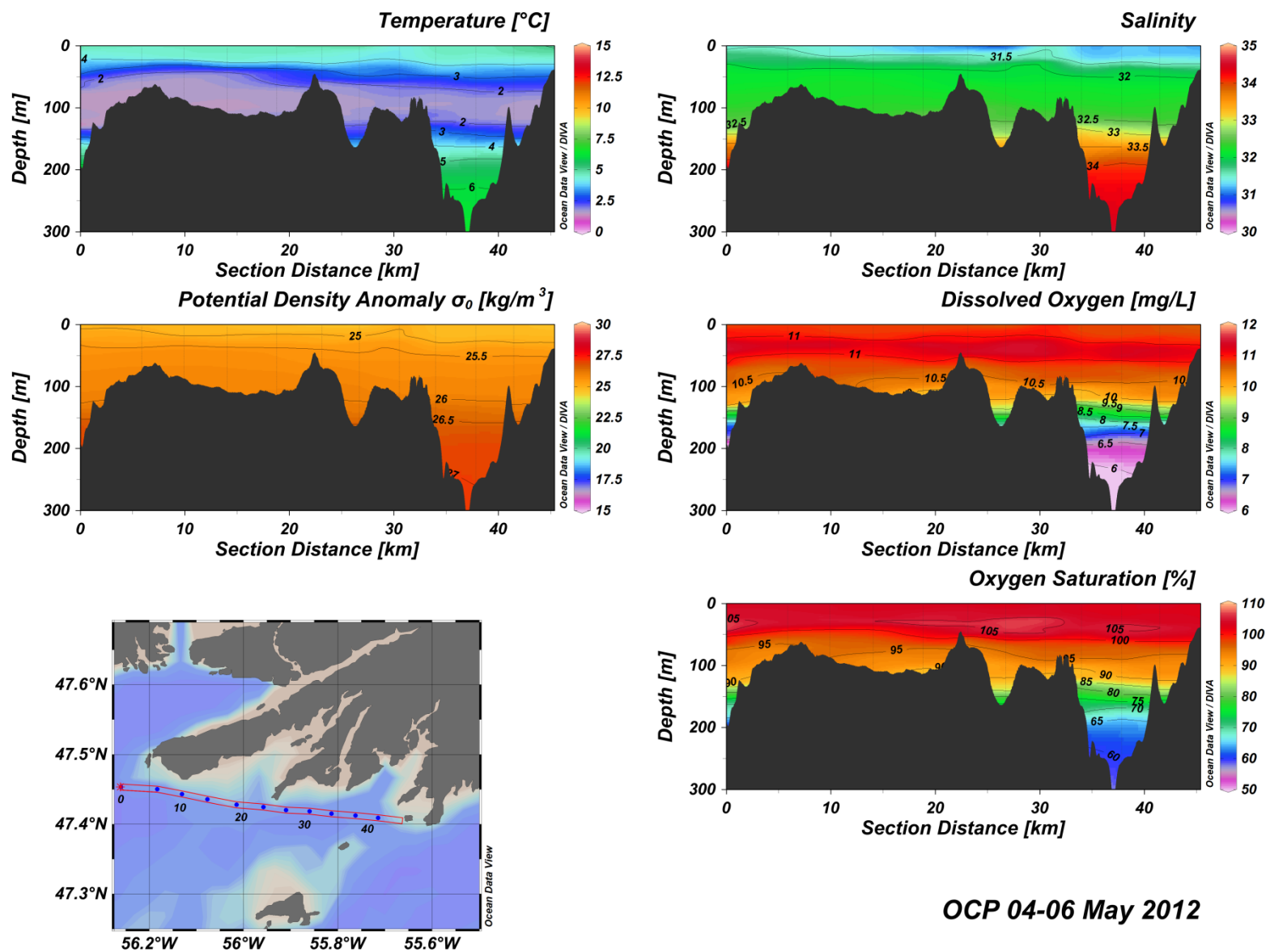


Figure C(i)3: Outer Connaigre Peninsula water column vertical structure.

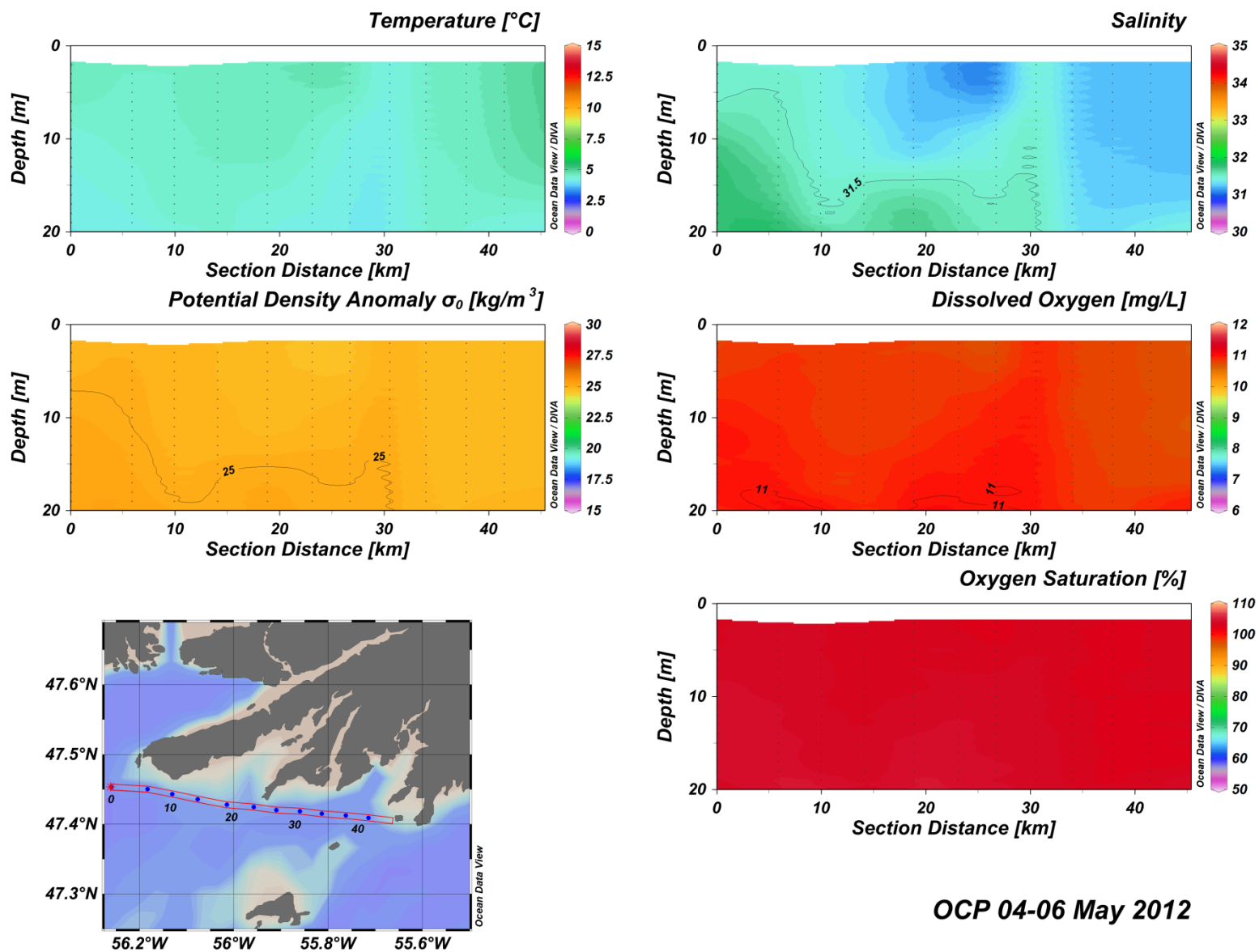
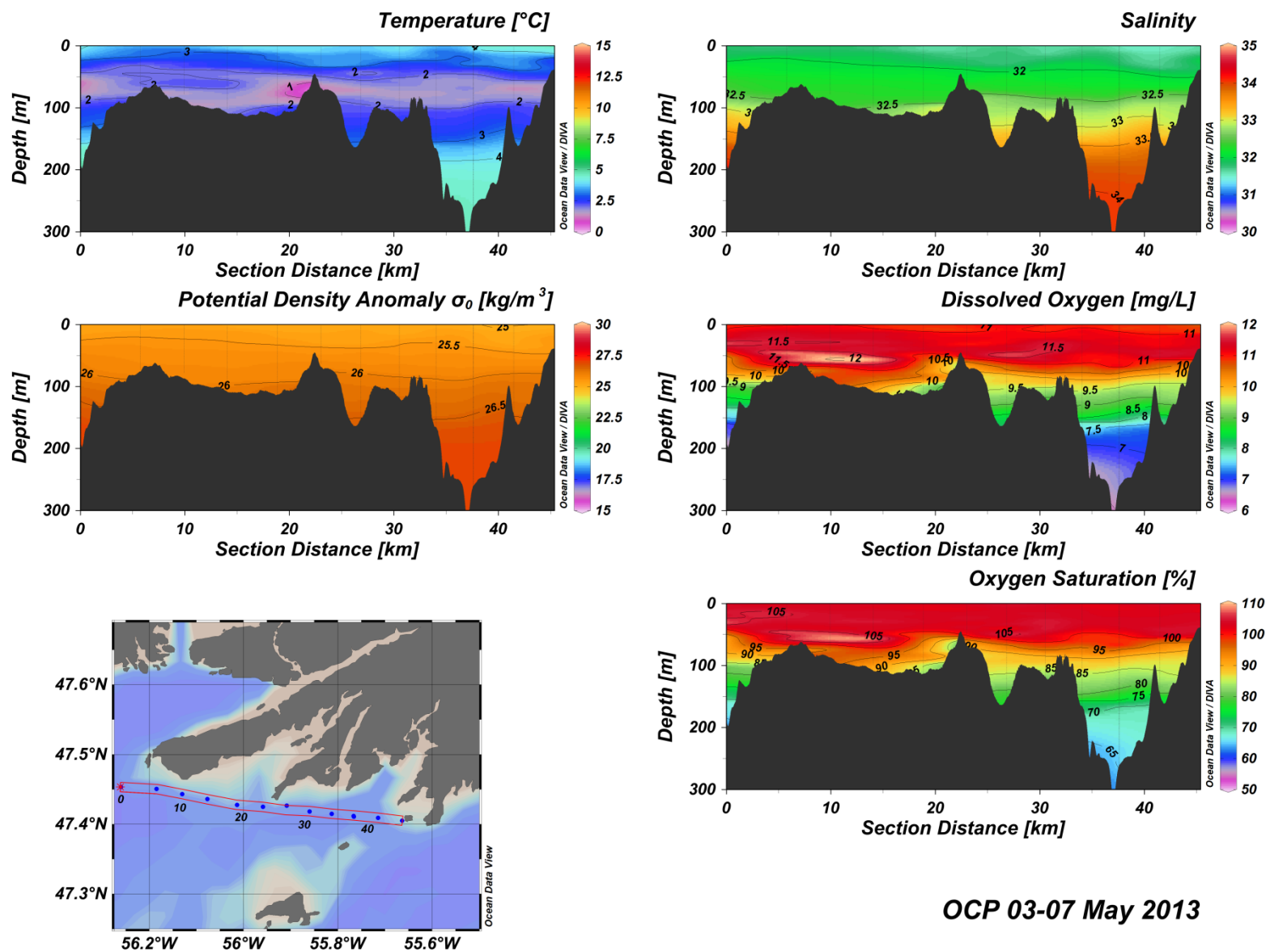


Figure C(i)4: Outer Connaigre Peninsula water column vertical structure.



OCP 03-07 May 2013

Figure C(i)5: Outer Connaigre Peninsula water column vertical structure.

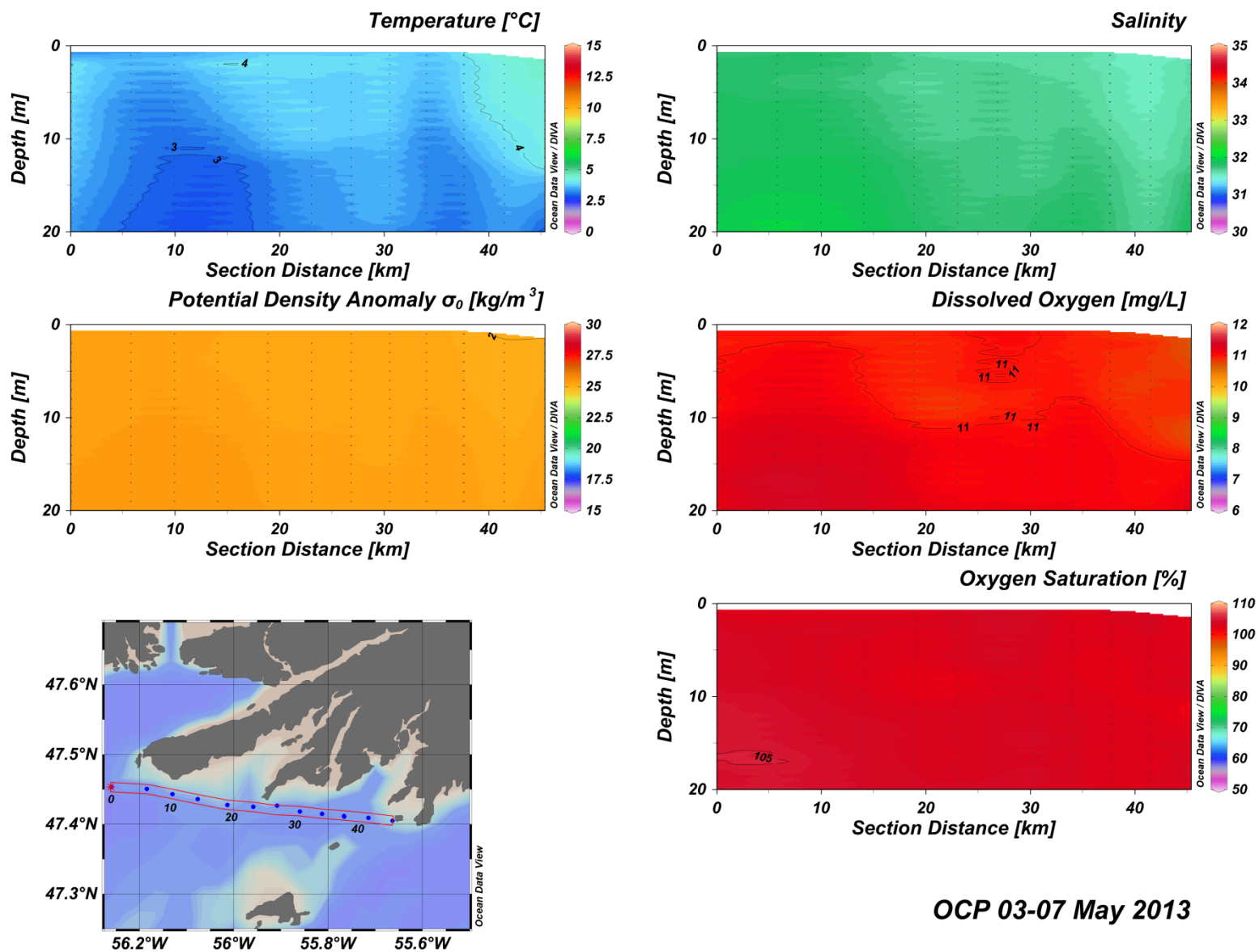


Figure C(i)6: Outer Connaigre Peninsula water column vertical structure.

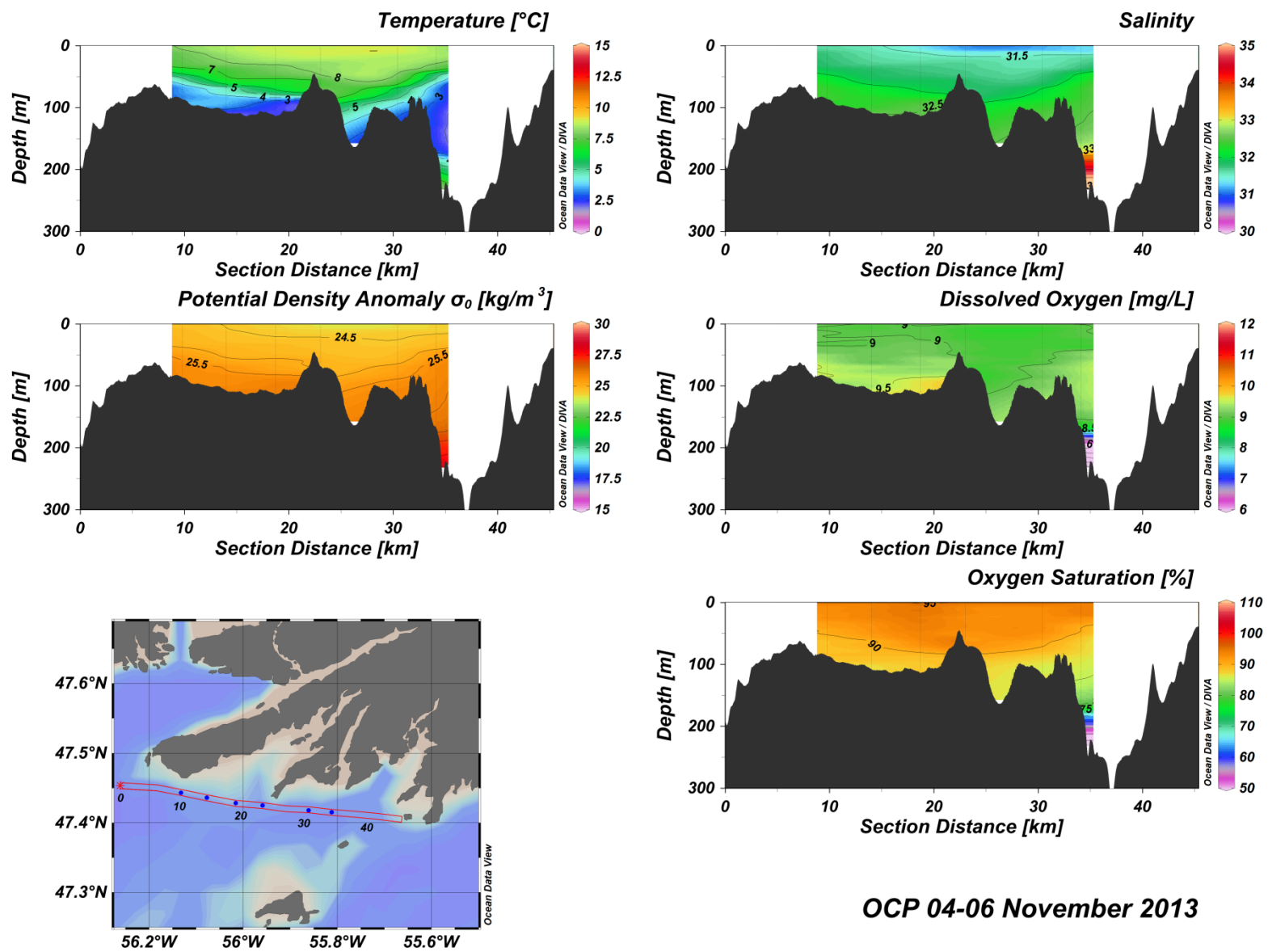


Figure C(i)7: Outer Connaigre Peninsula water column vertical structure.

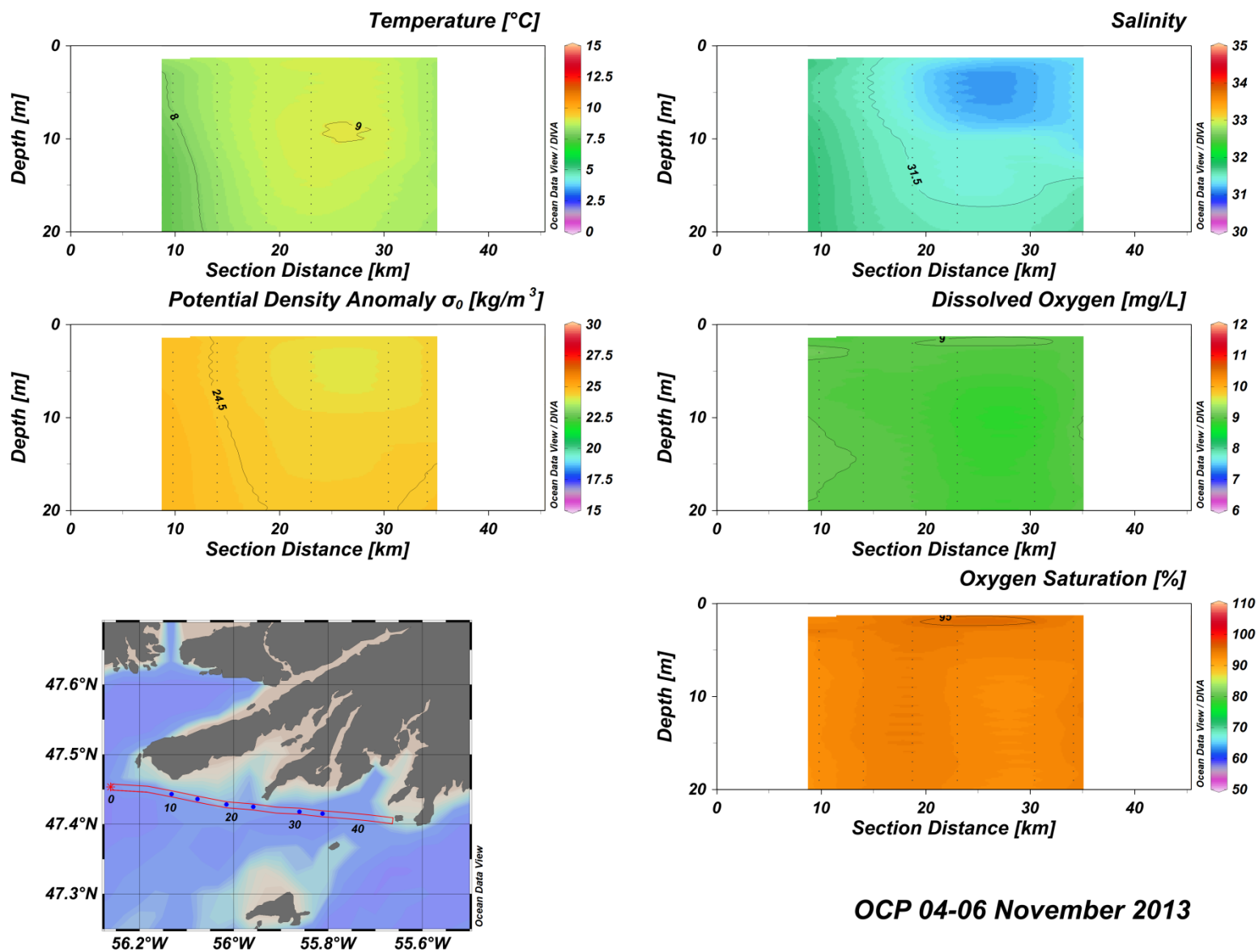


Figure C(i)8: Outer Connaigre Peninsula water column vertical structure.

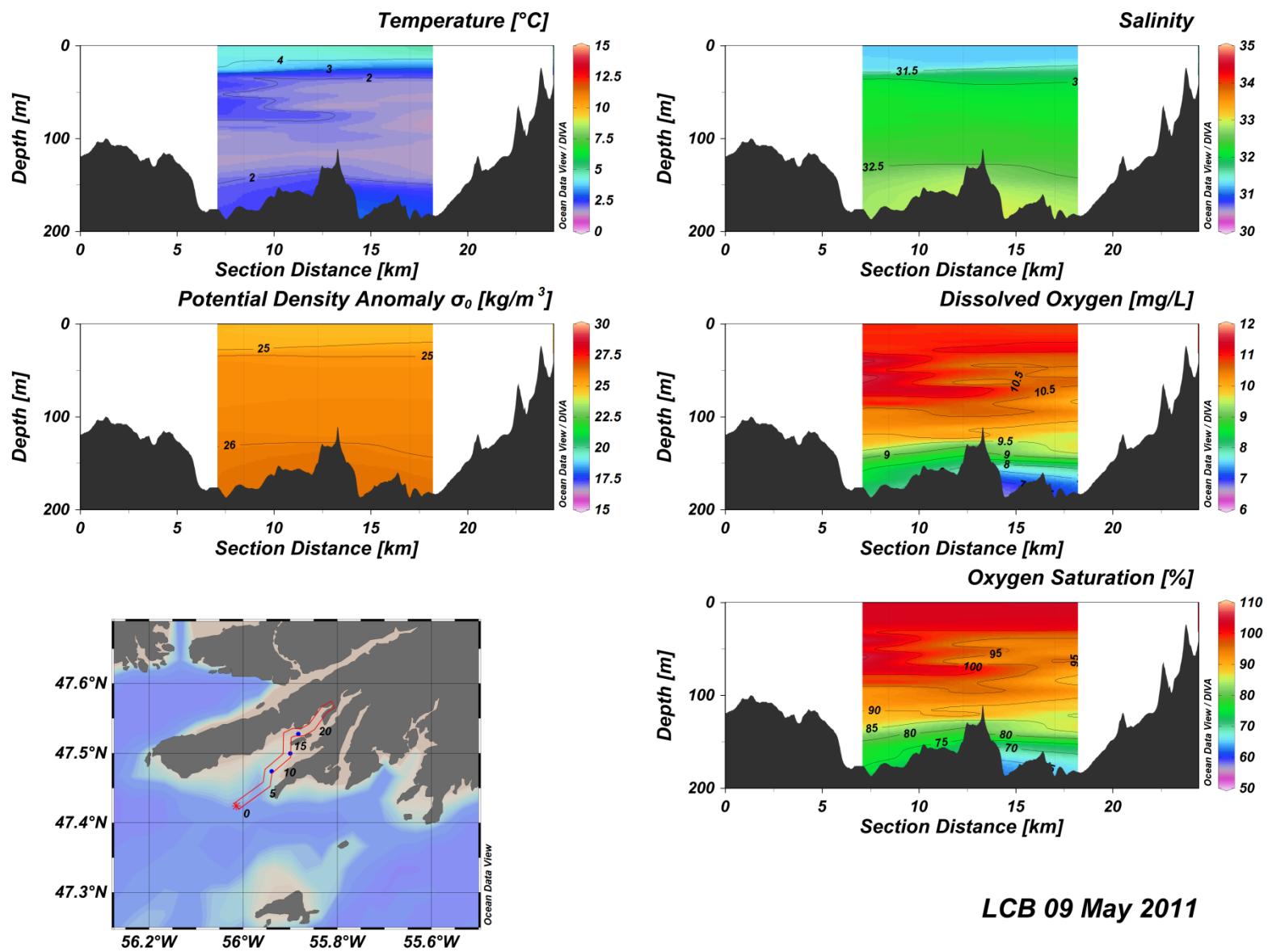


Figure C(i)9: Lower Connaigre Bay water column vertical structure.

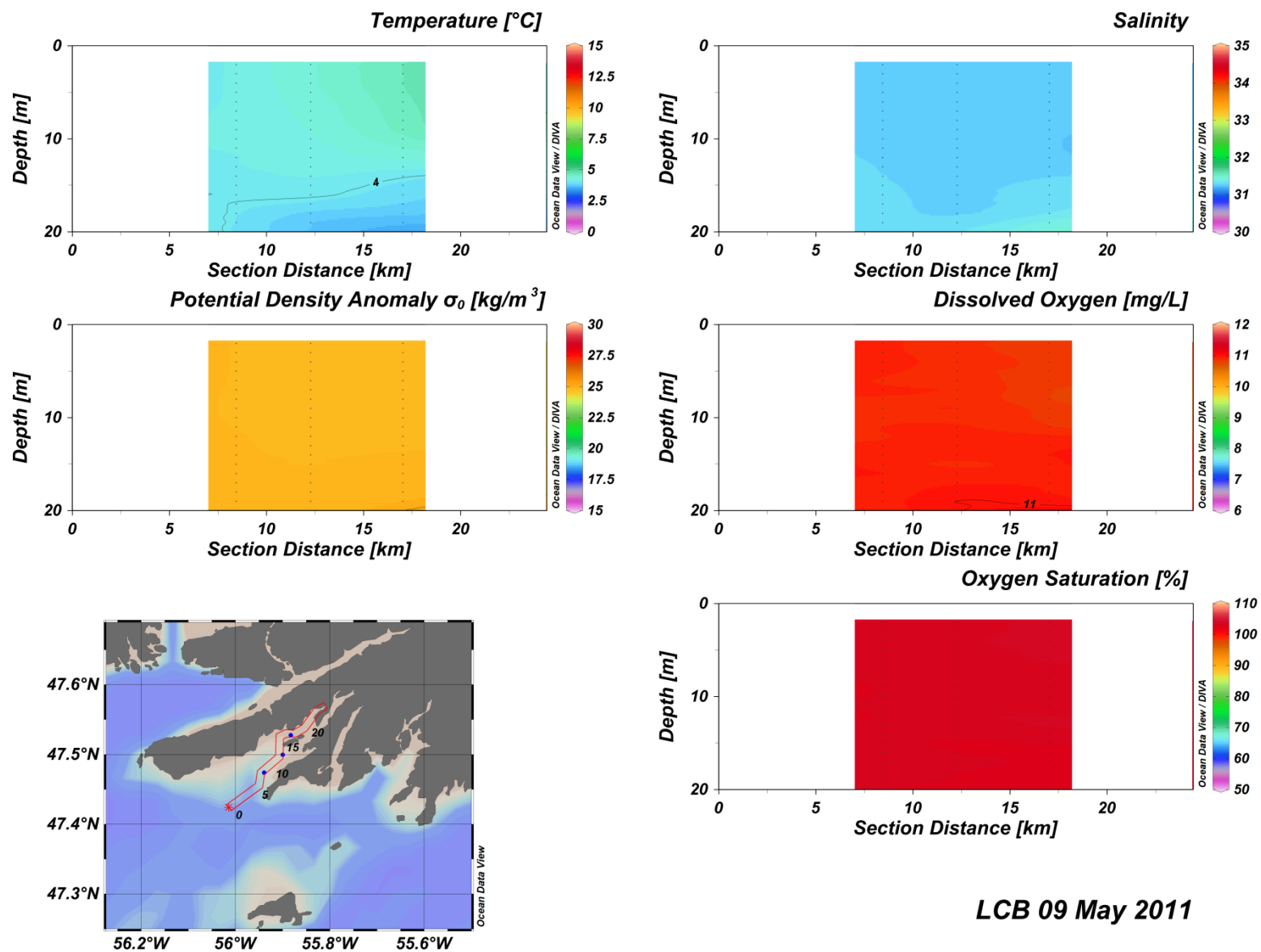


Figure C(i)10: Lower Connaigre Bay water column vertical structure.

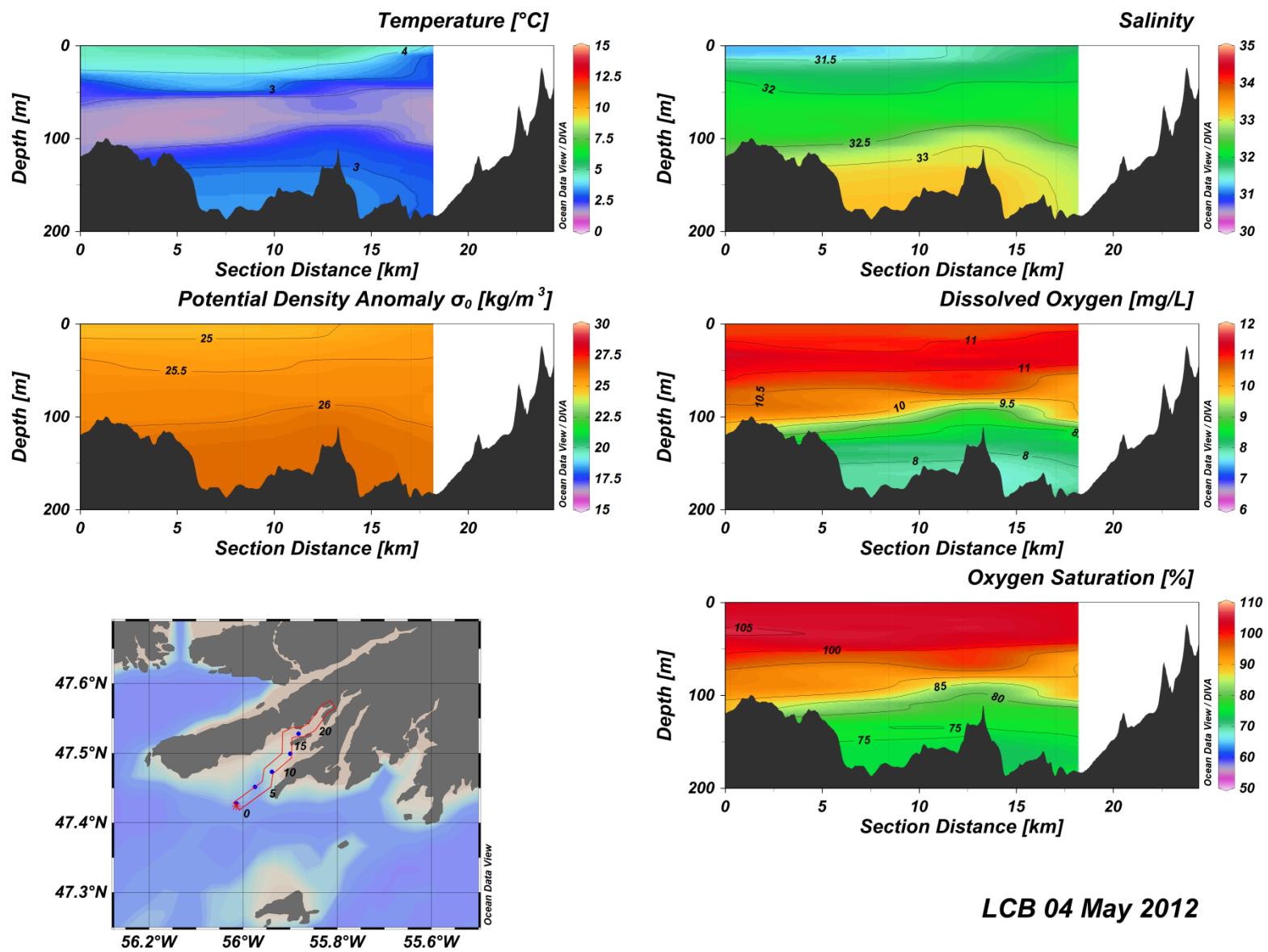


Figure C(i)11: Lower Connaigre Bay water column vertical structure.

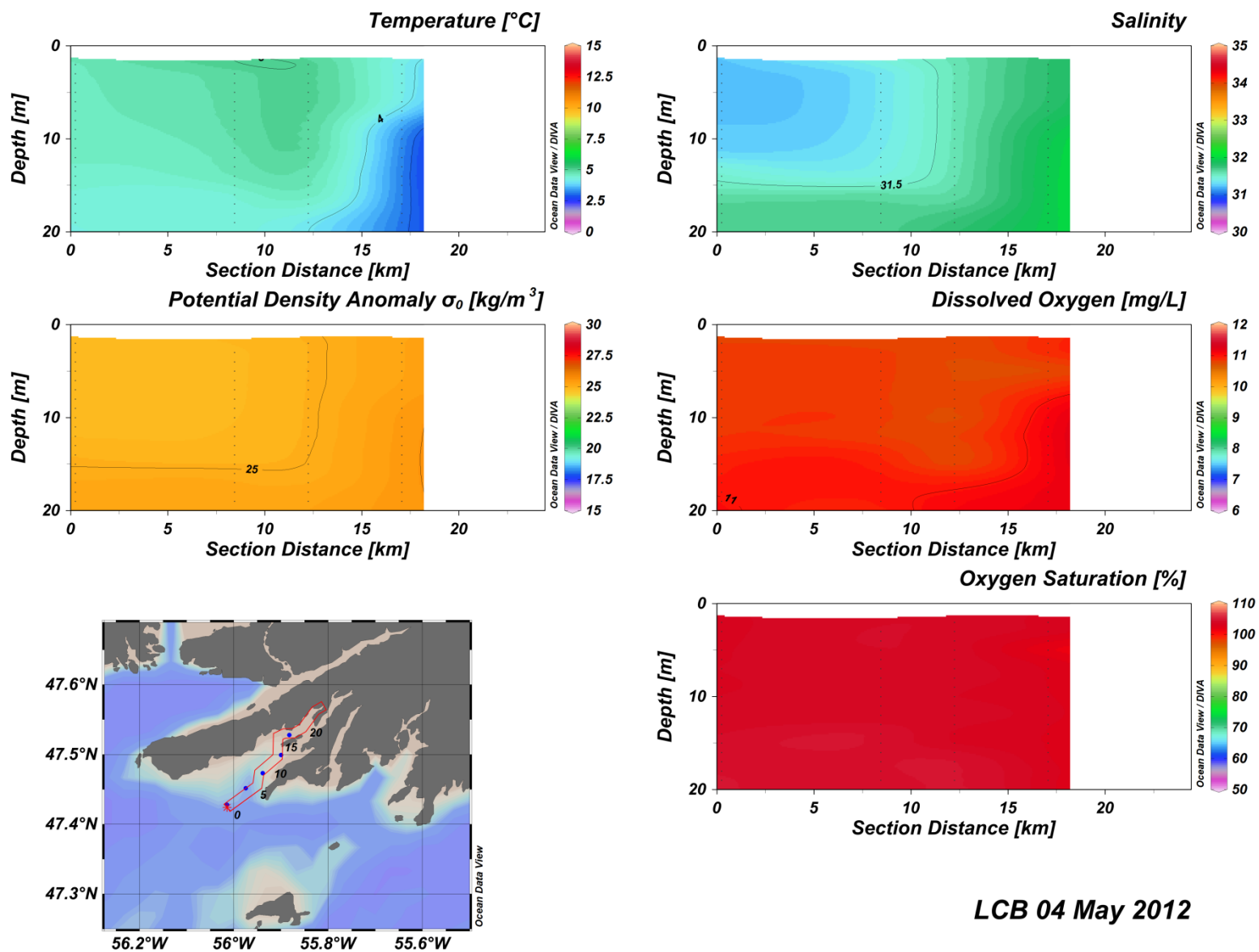


Figure C(i)12: Lower Connaigre Bay water column vertical structure.

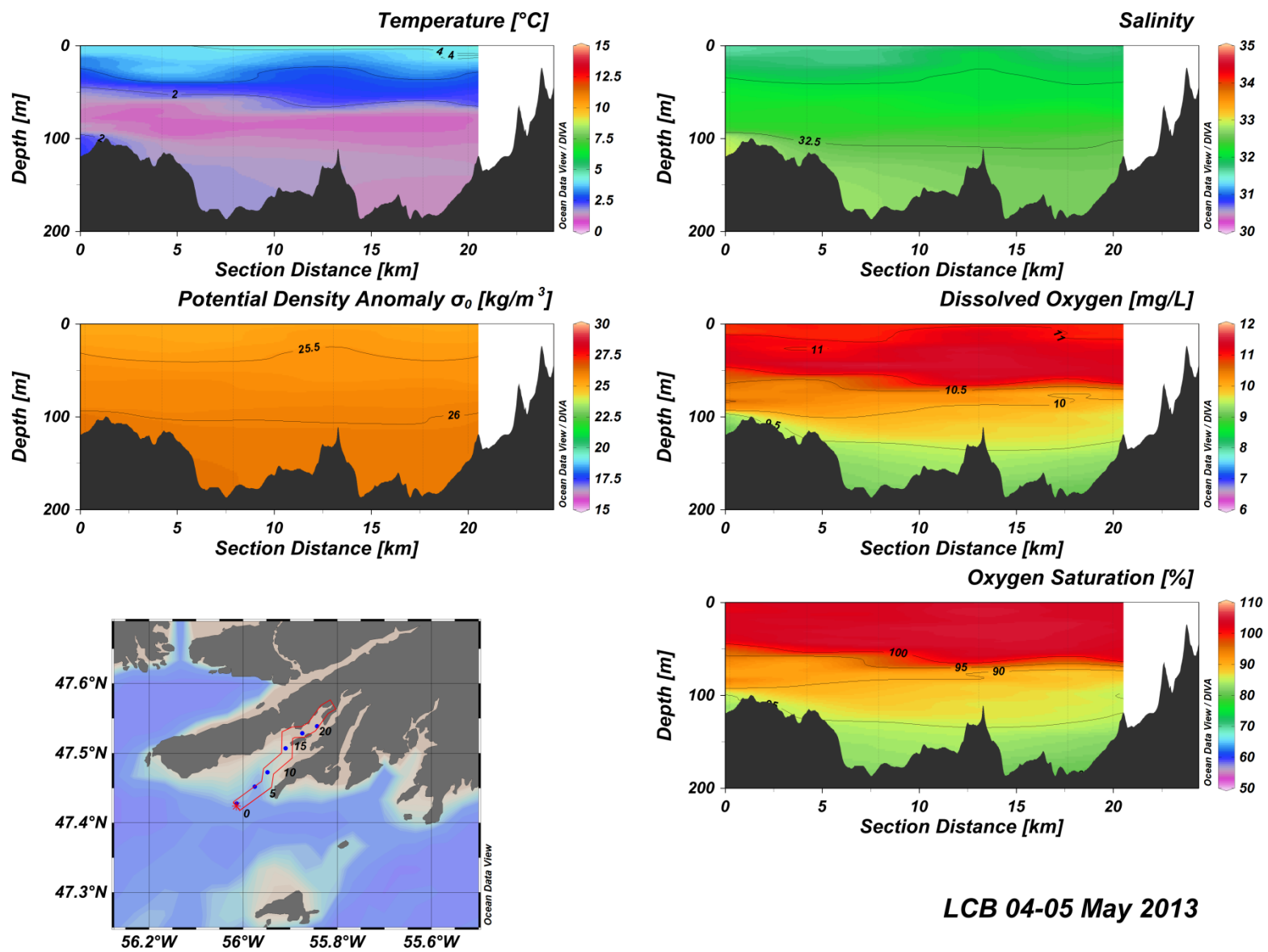


Figure C(i)13: Lower Connaigre Bay water column vertical structure.

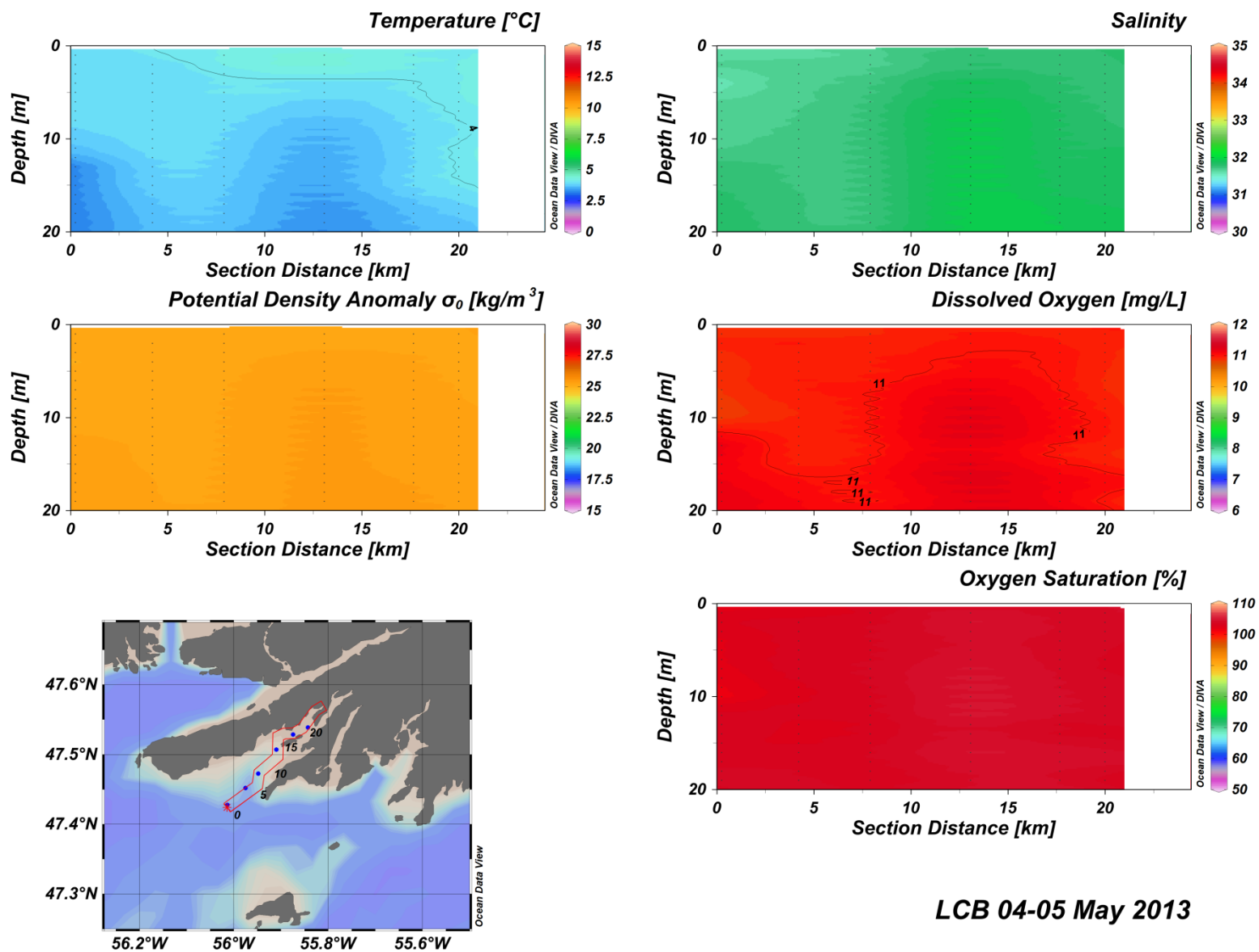


Figure C(i)14: Lower Connaigre Bay water column vertical structure.

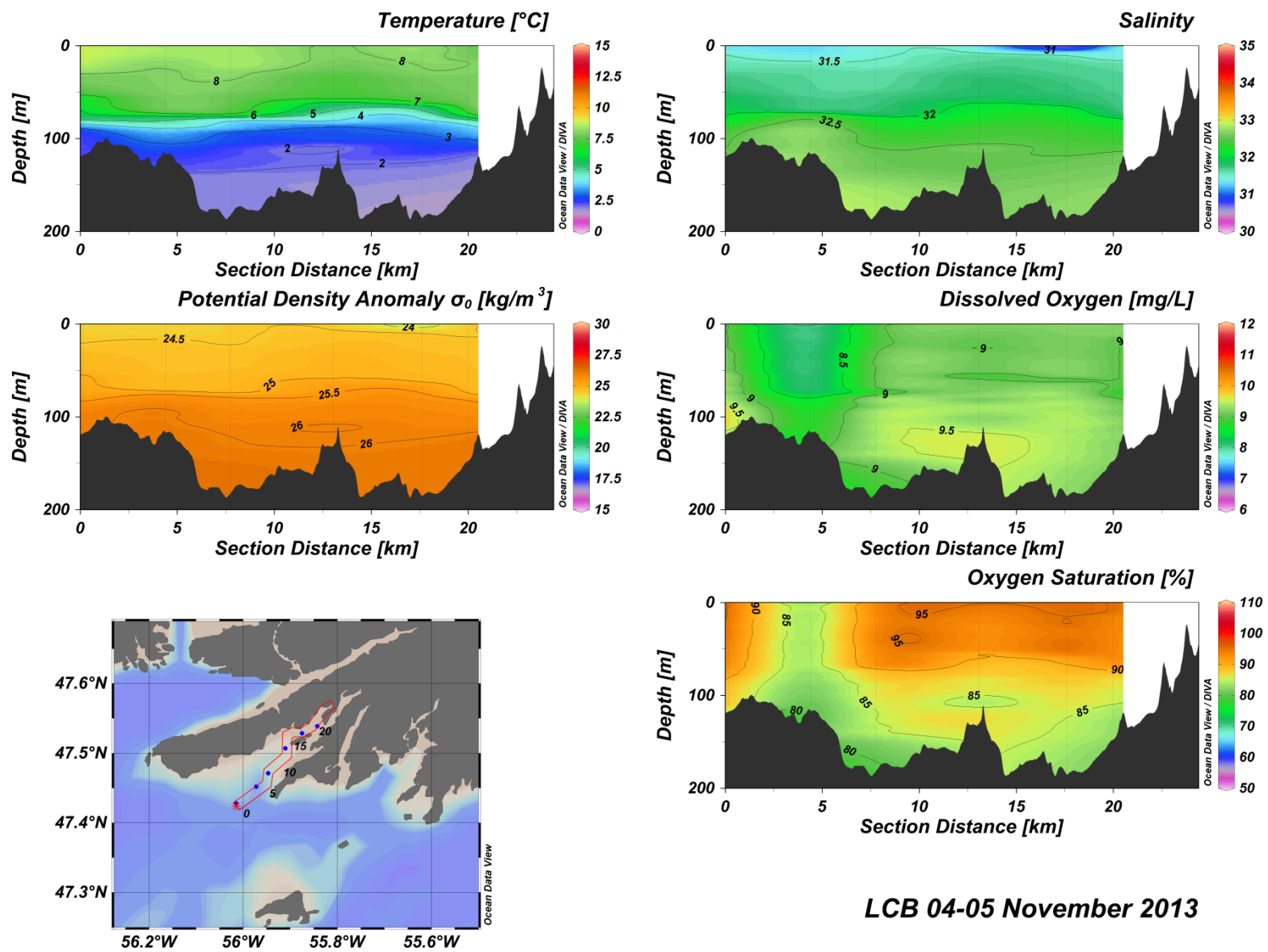


Figure C(i)15: Lower Connaigre Bay water column vertical structure.

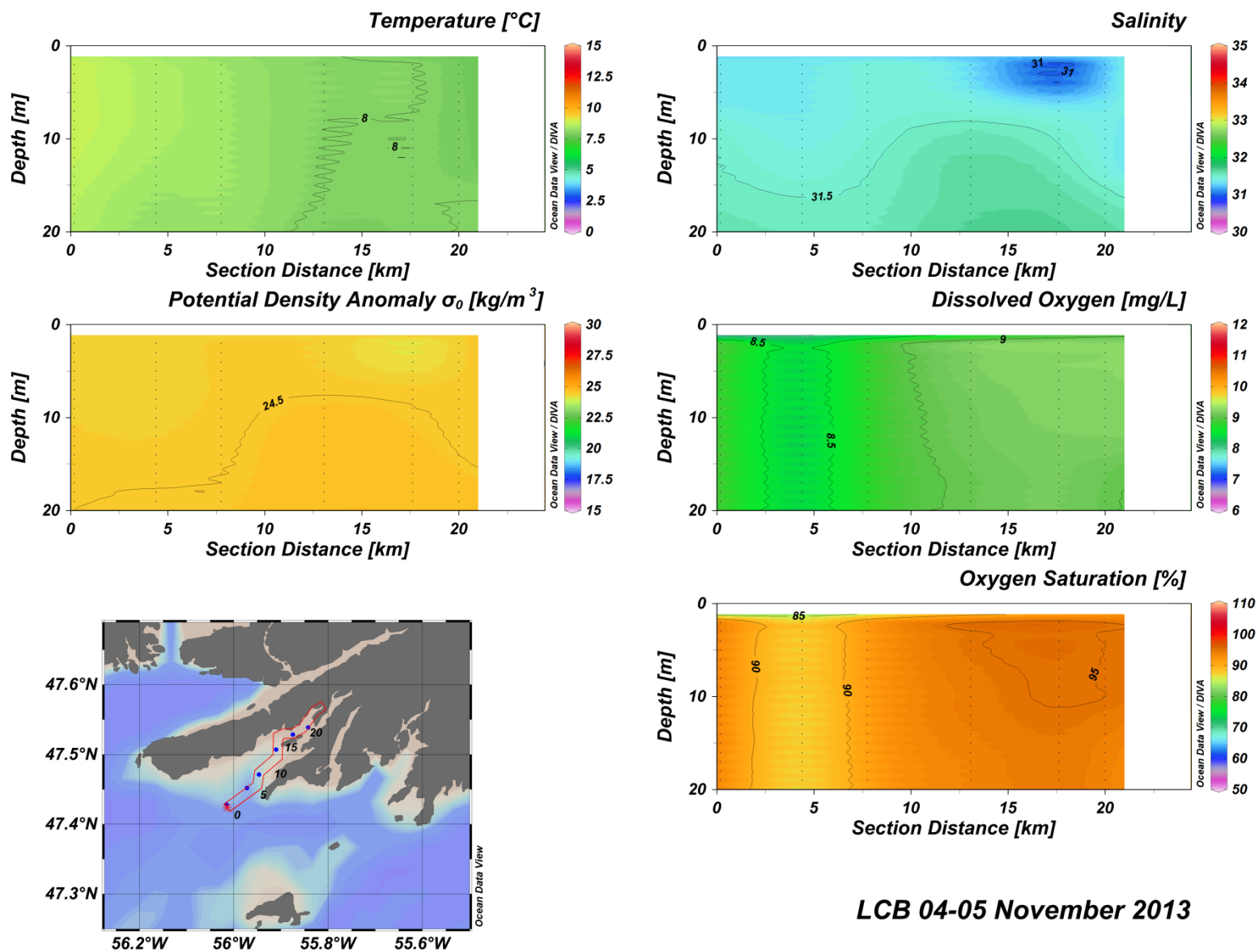


Figure C(i)16: Lower Connaigre Bay water column vertical structure.

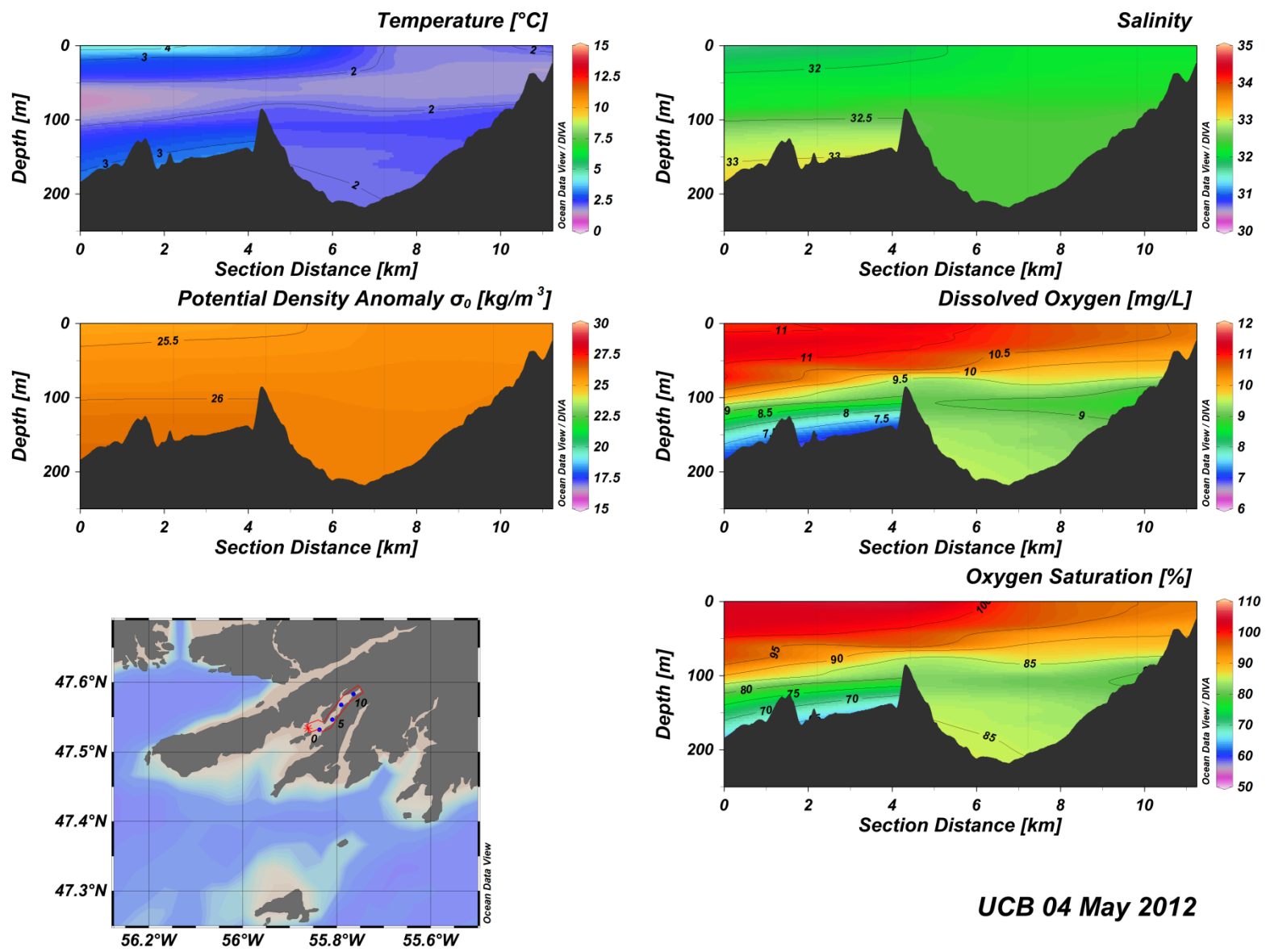


Figure C(i)17: Upper Connaigre Bay water column vertical structure.

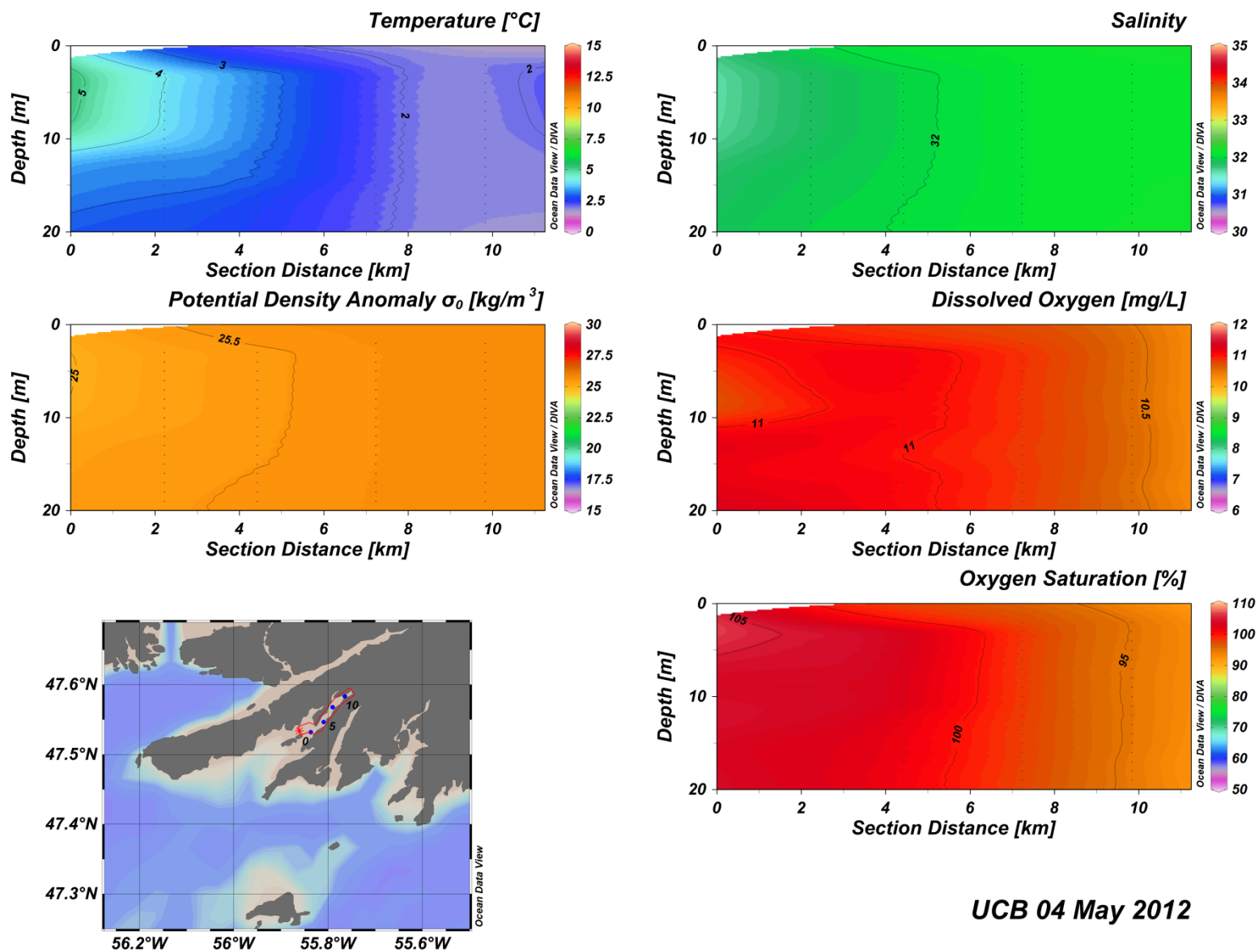
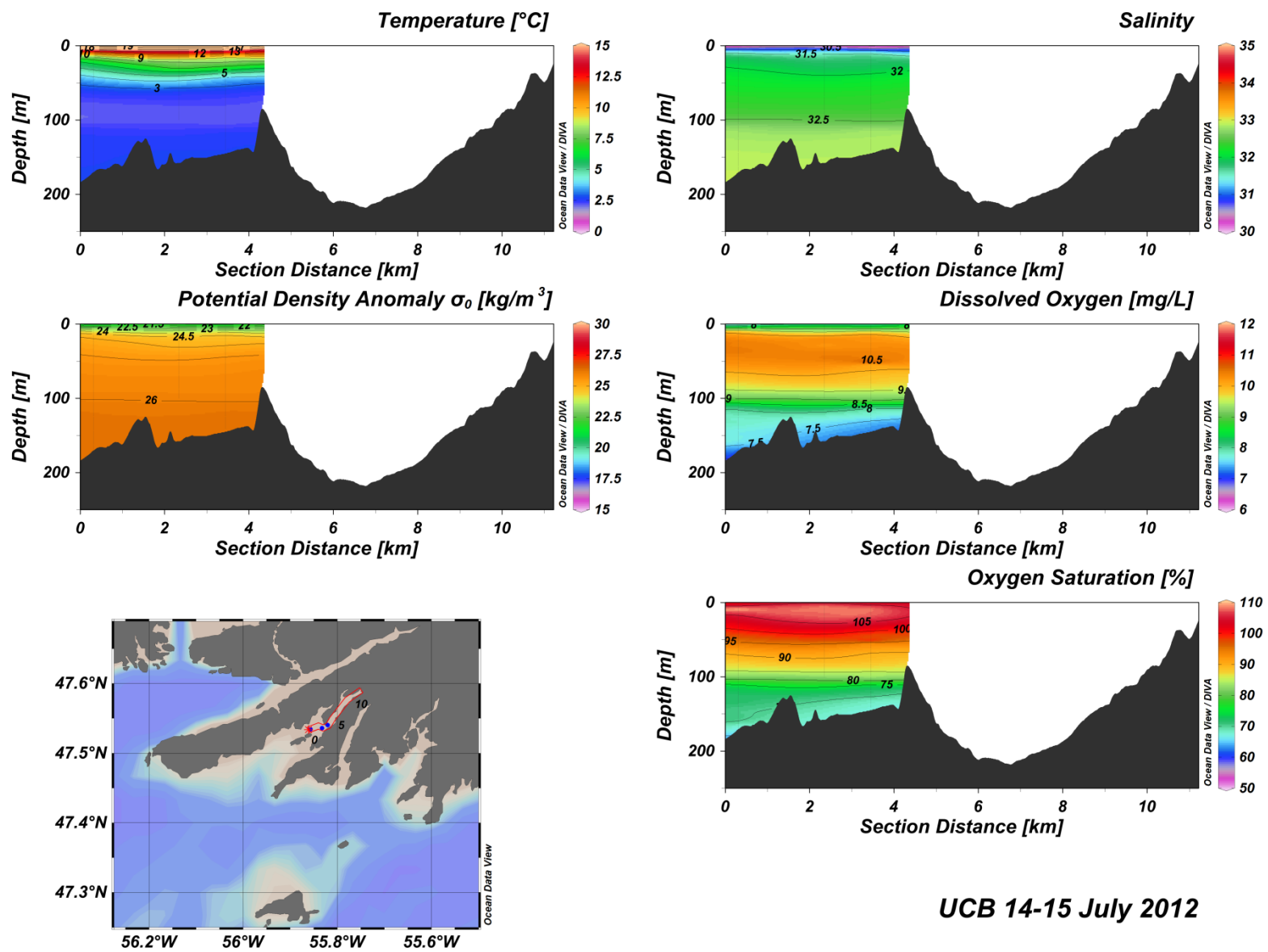


Figure C(i)18: Upper Connaigre Bay water column vertical structure.



UCB 14-15 July 2012

Figure C(i)19: Upper Connaigre Bay water column vertical structure.

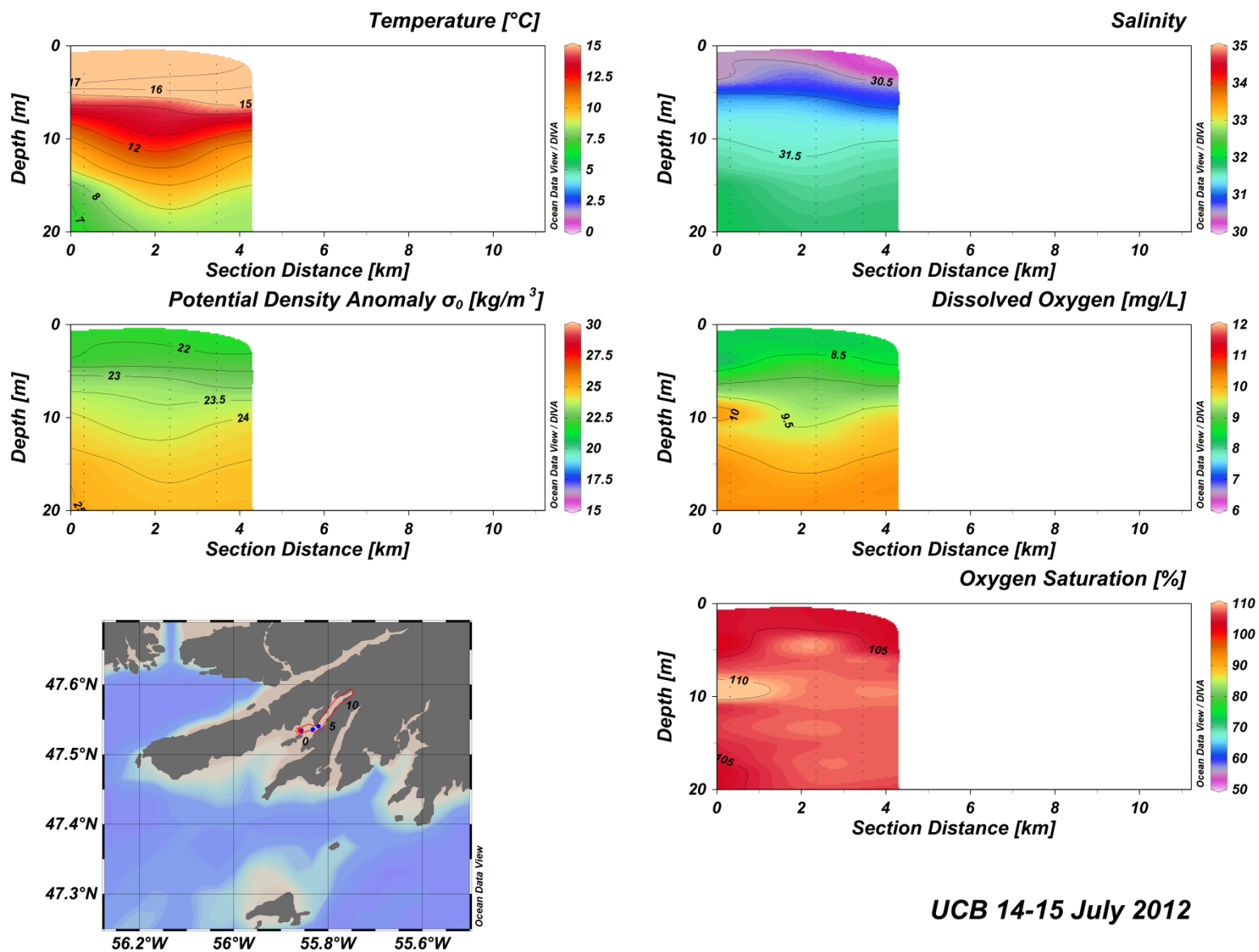


Figure C(i)20: Upper Connaigre Bay water column vertical structure.

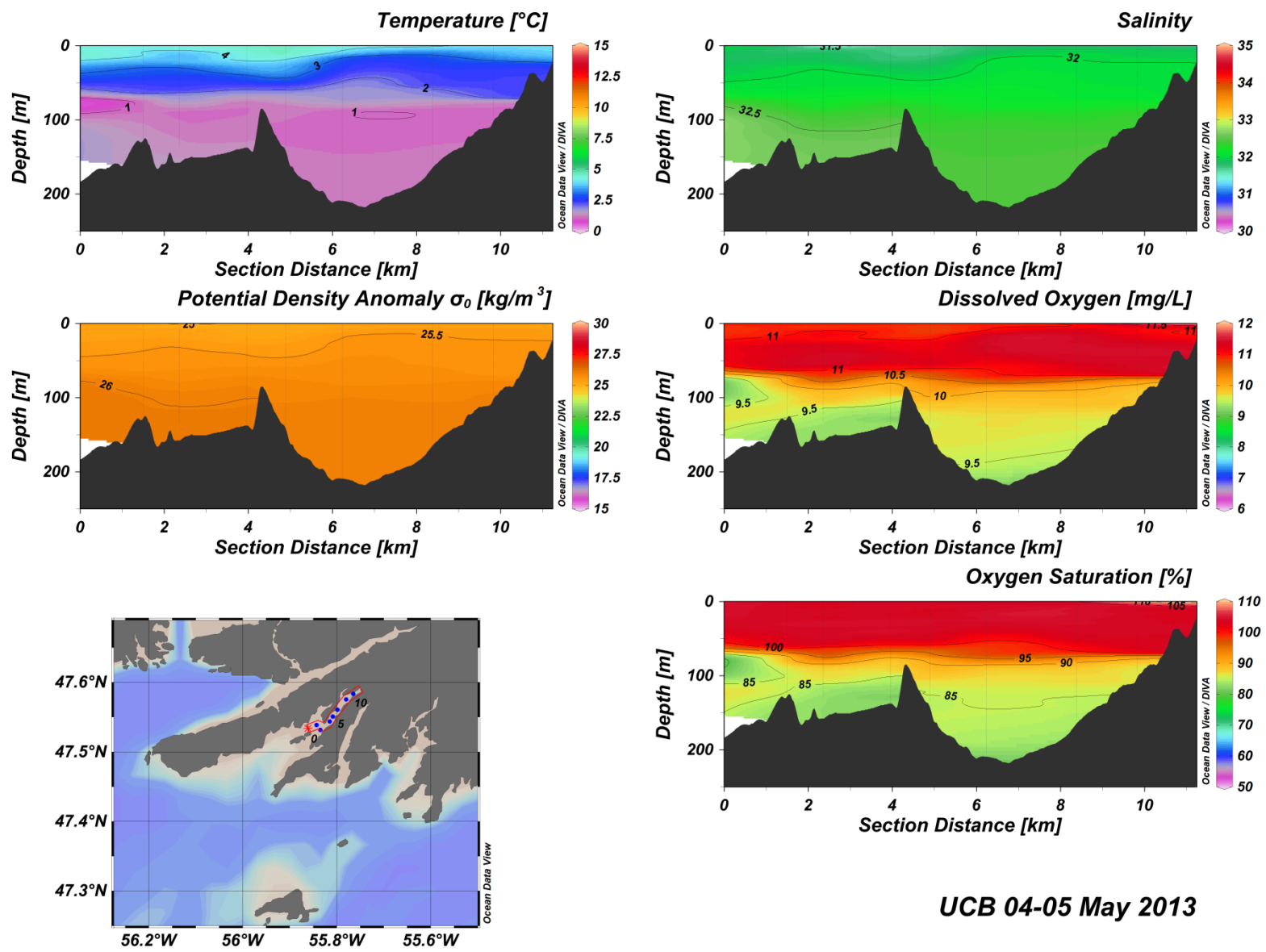


Figure C(i)21: Upper Connaigre Bay water column vertical structure.

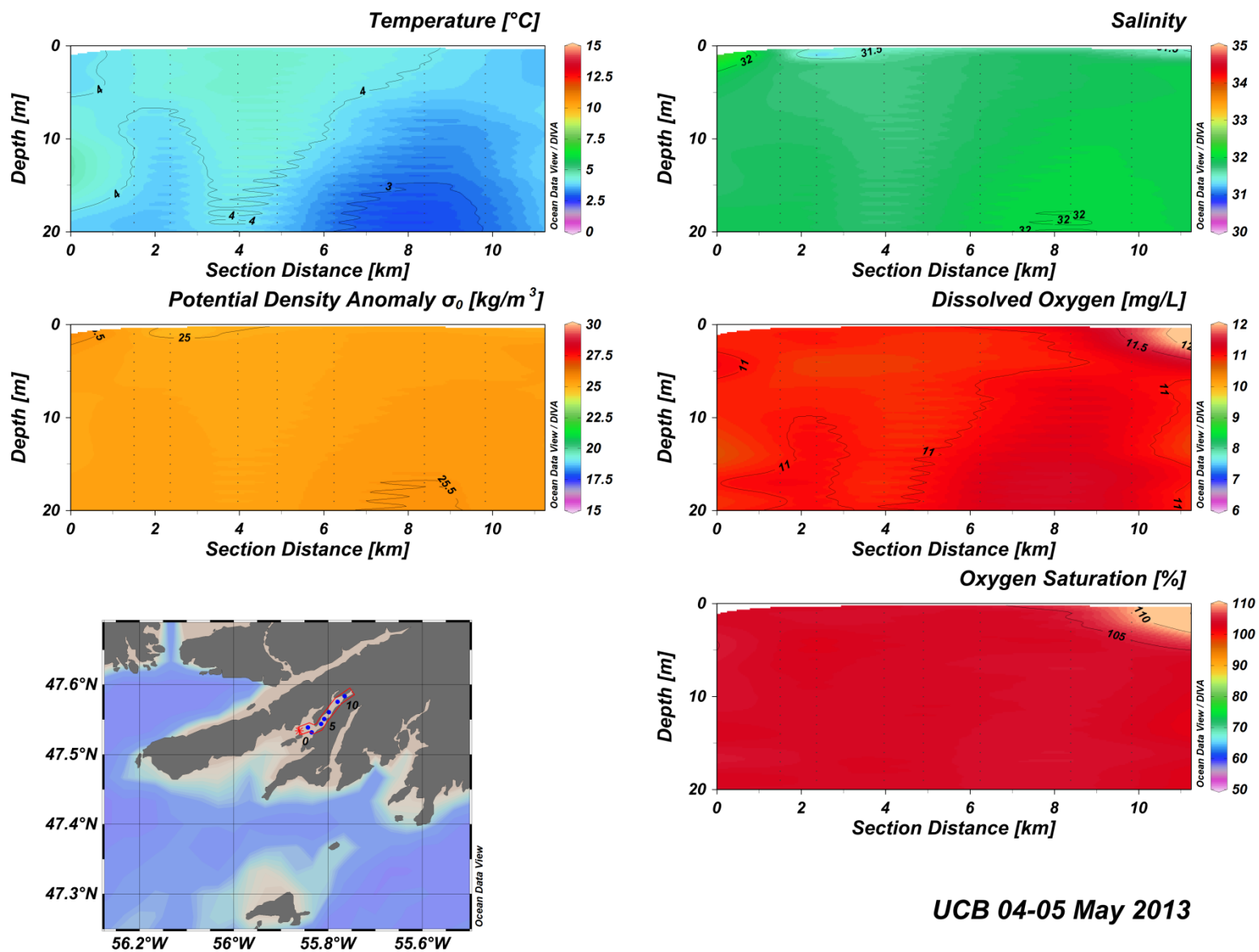


Figure C(i)22: Upper Connaigre Bay water column vertical structure.

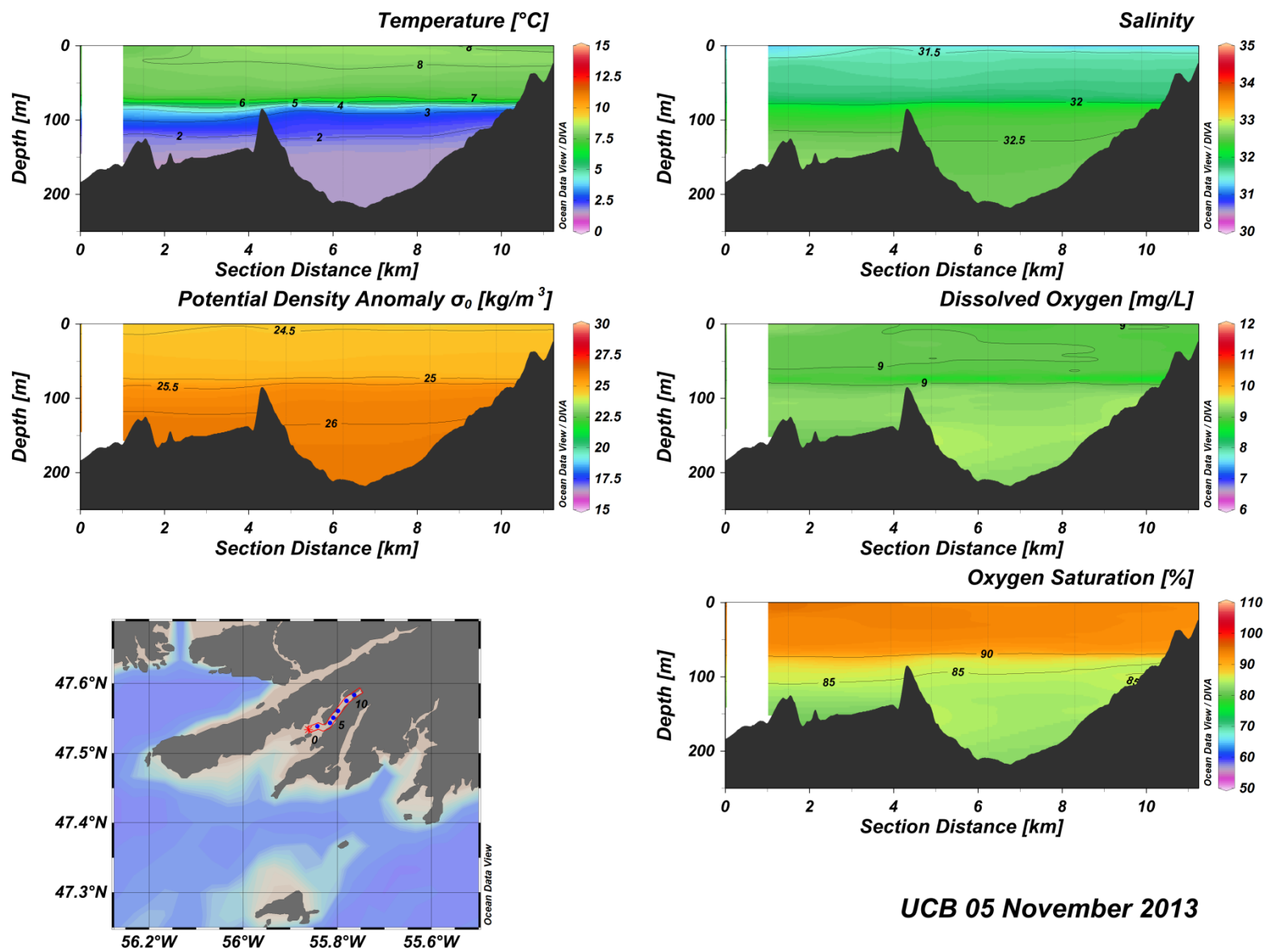
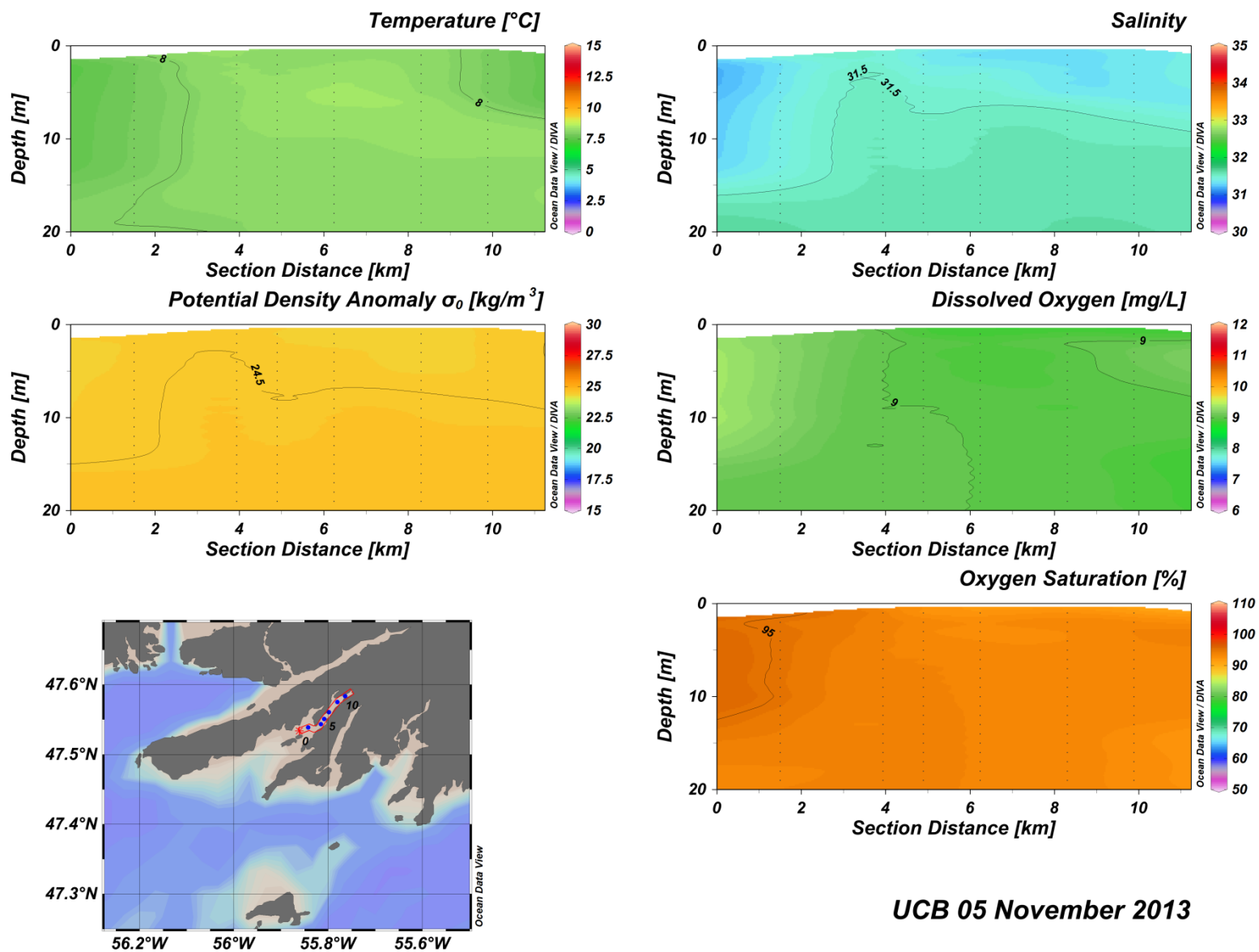
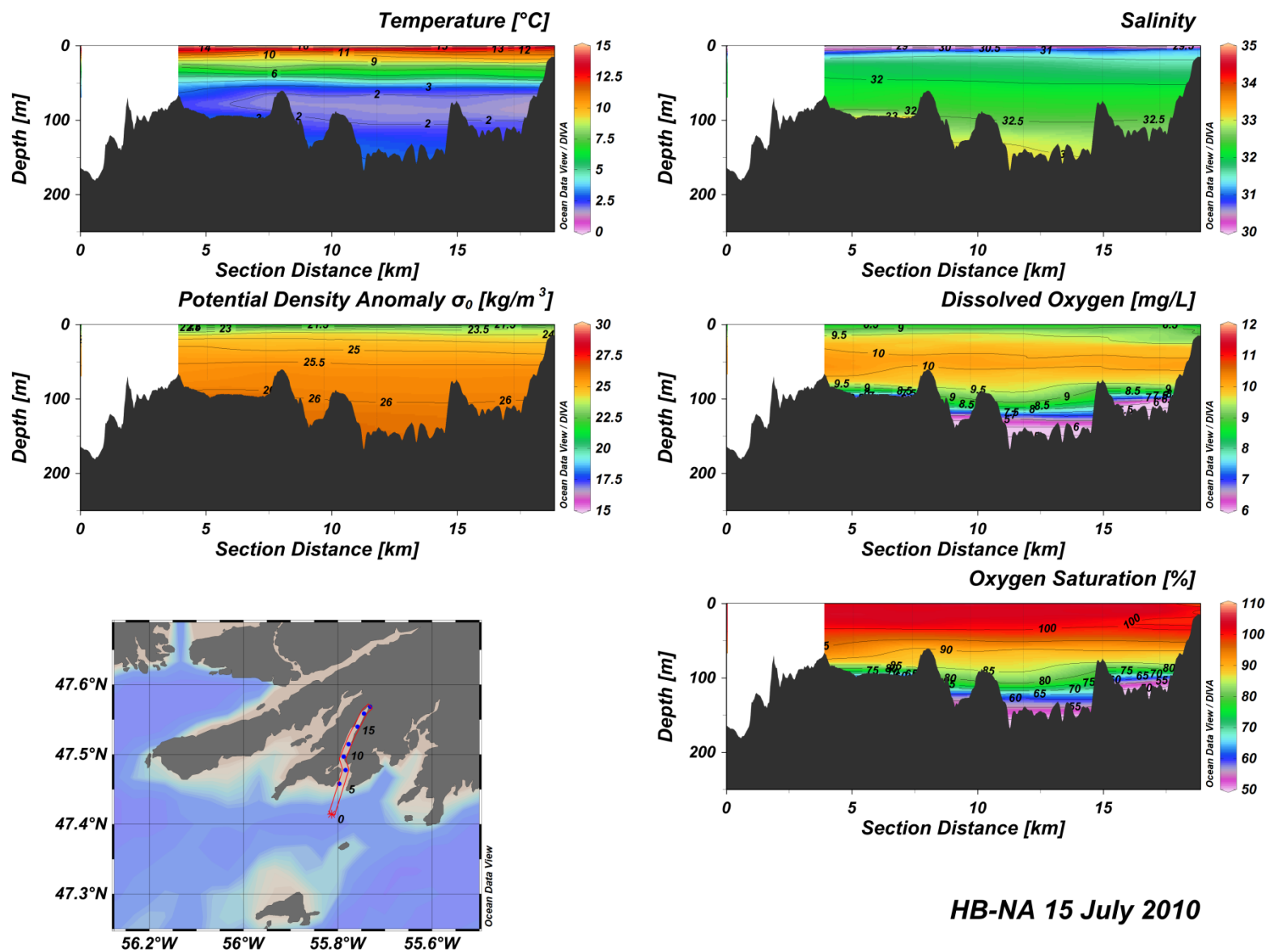


Figure C(i)23: Upper Connaigre Bay water column vertical structure.



UCB 05 November 2013

Figure C(i)24: Upper Connaigre Bay water column vertical structure.



HB-NA 15 July 2010

Figure C(i)25: Harbour Breton – Northeast Arm water column vertical structure.

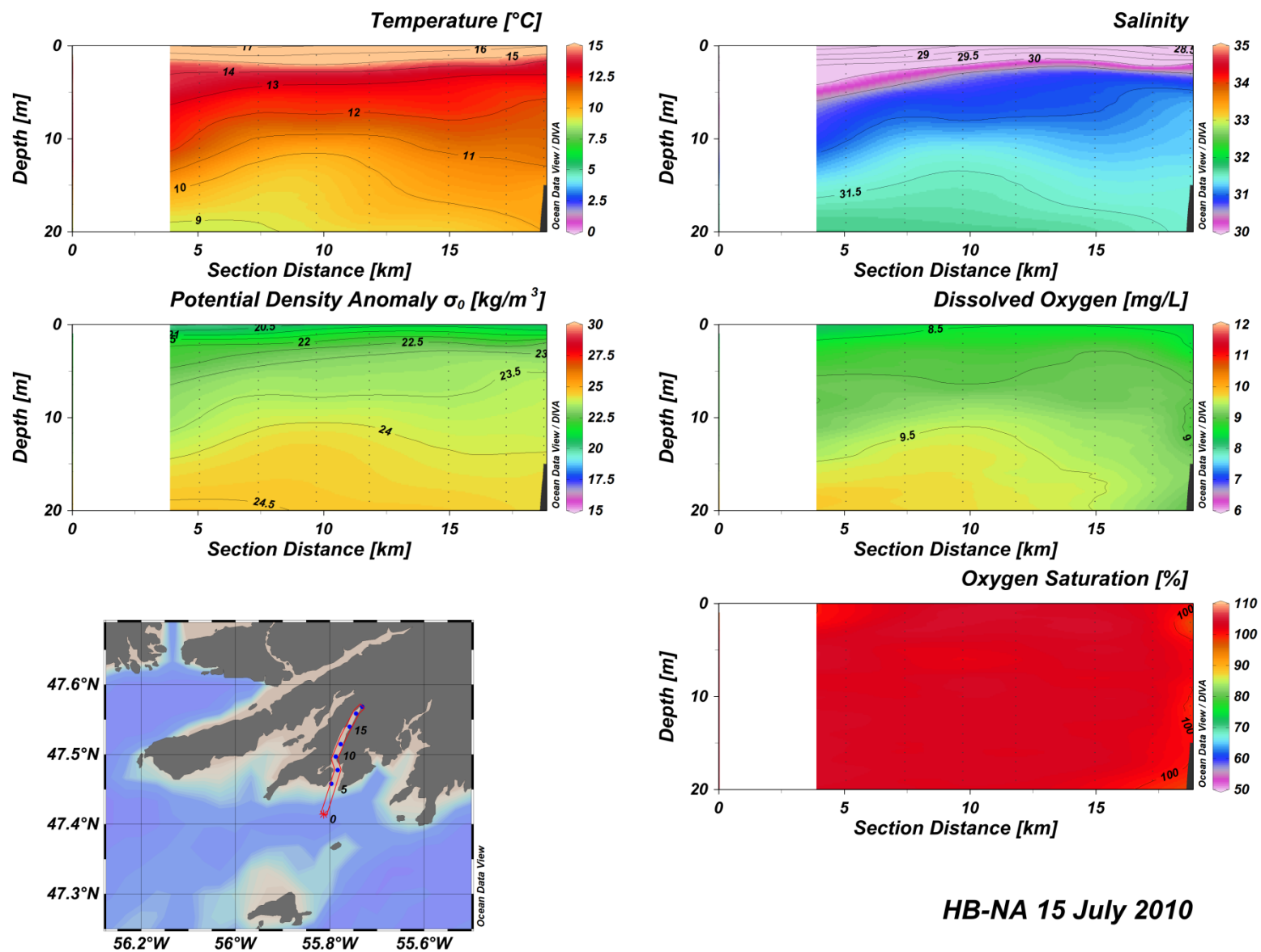
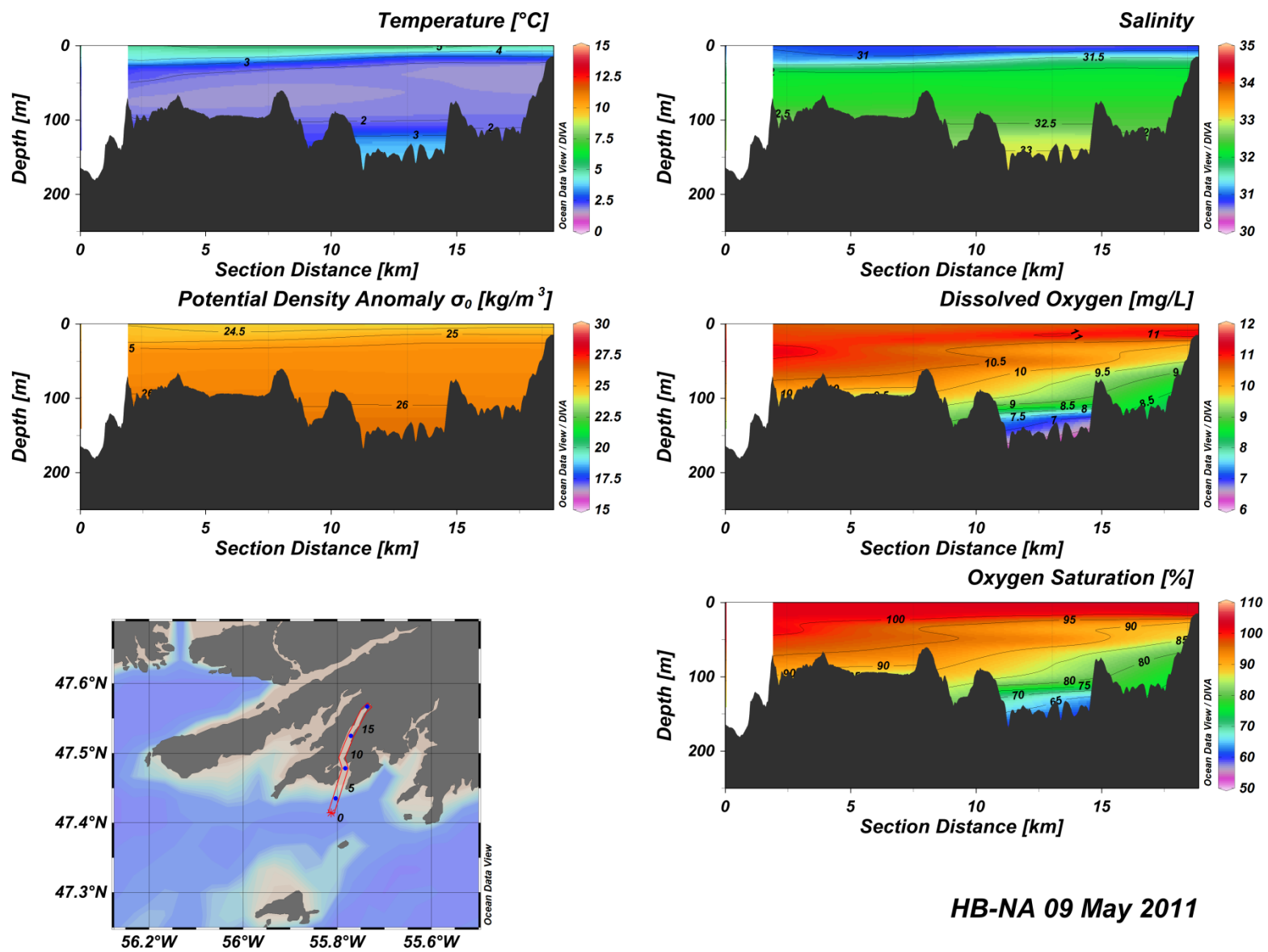


Figure C(i)26: Harbour Breton – Northeast Arm water column vertical structure.



HB-NA 09 May 2011

Figure C(i)27: Harbour Breton – Northeast Arm water column vertical structure.

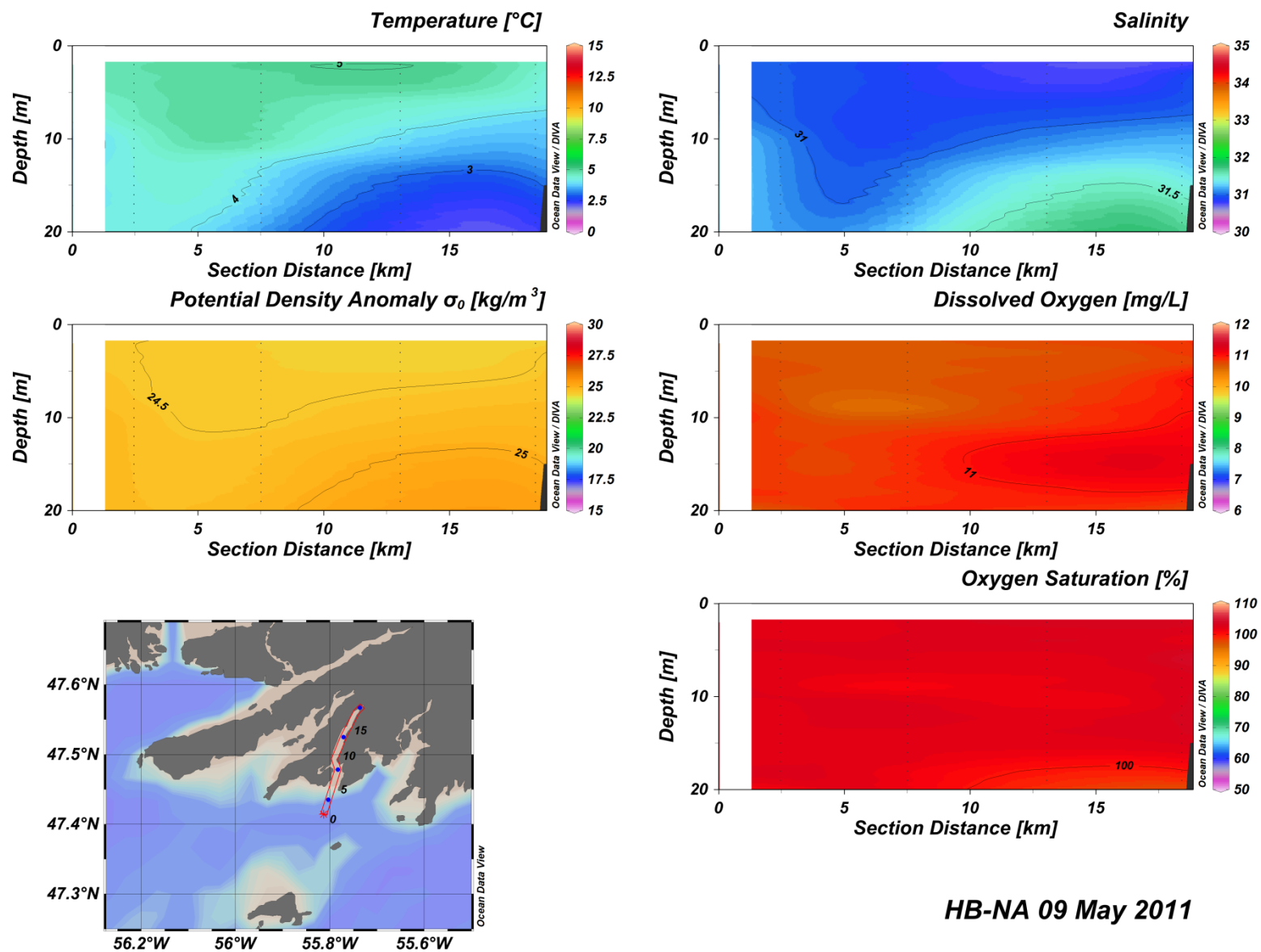
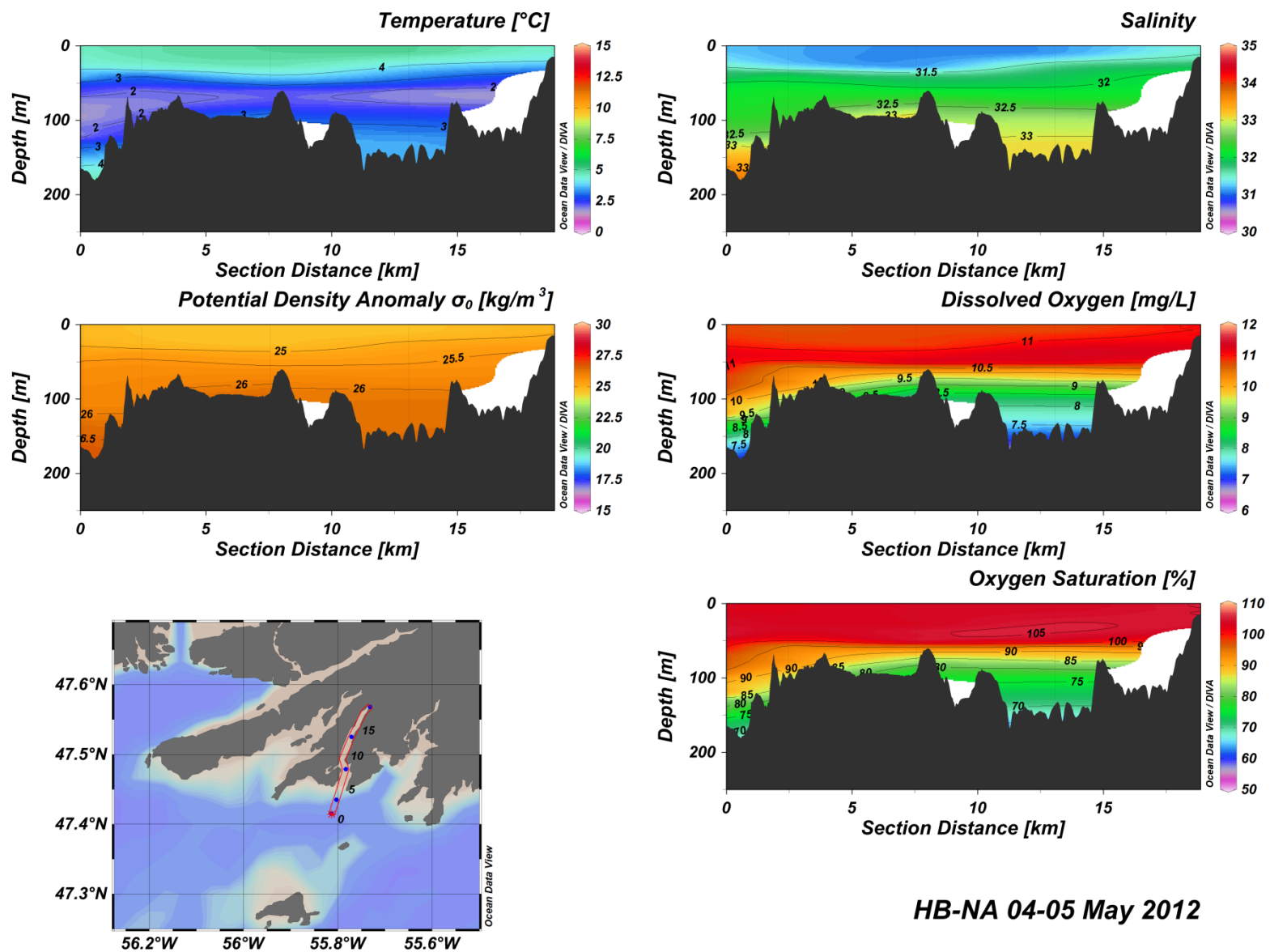


Figure C(i)28: Harbour Breton – Northeast Arm water column vertical structure.



HB-NA 04-05 May 2012

Figure C(i)29: Harbour Breton – Northeast Arm water column vertical structure.

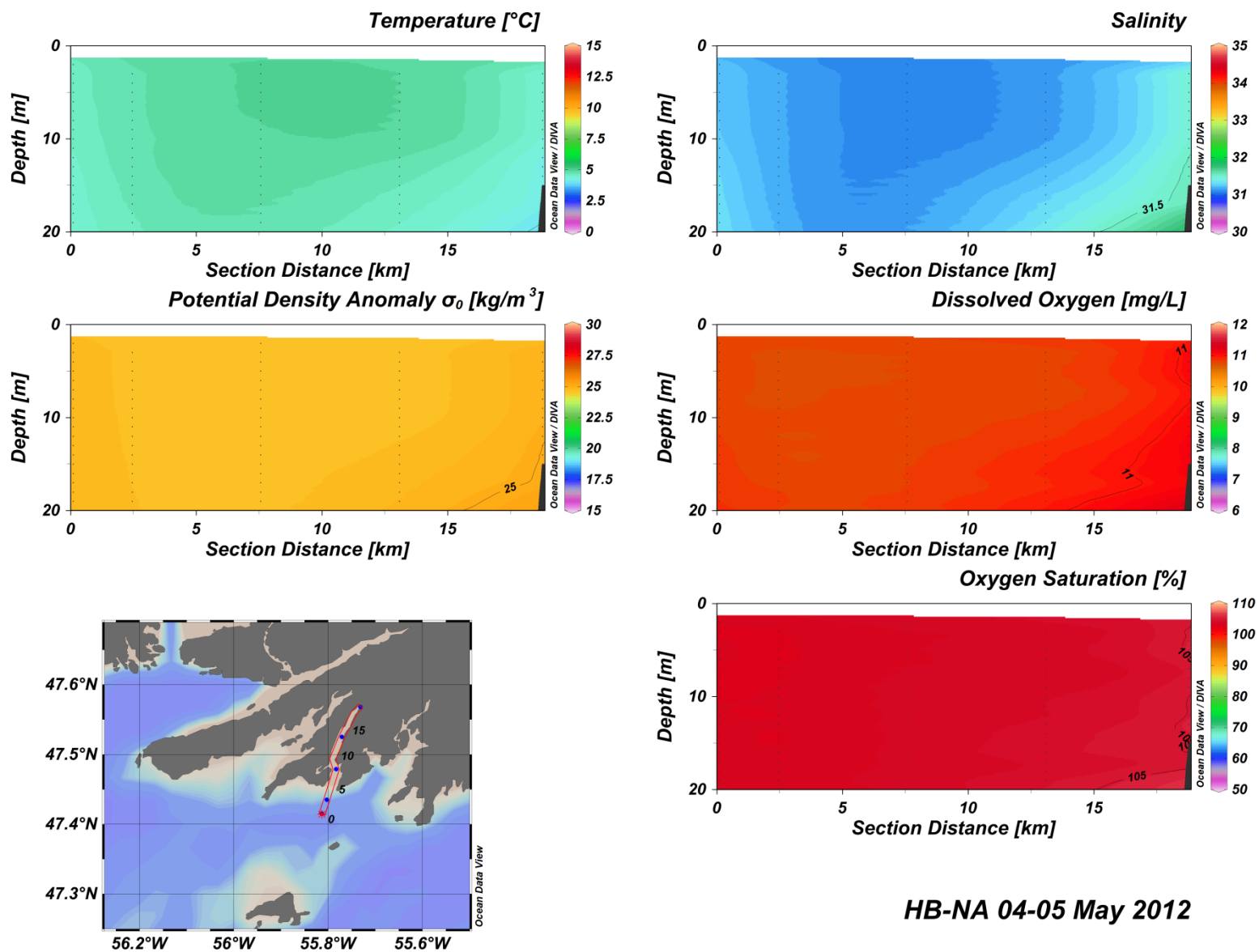
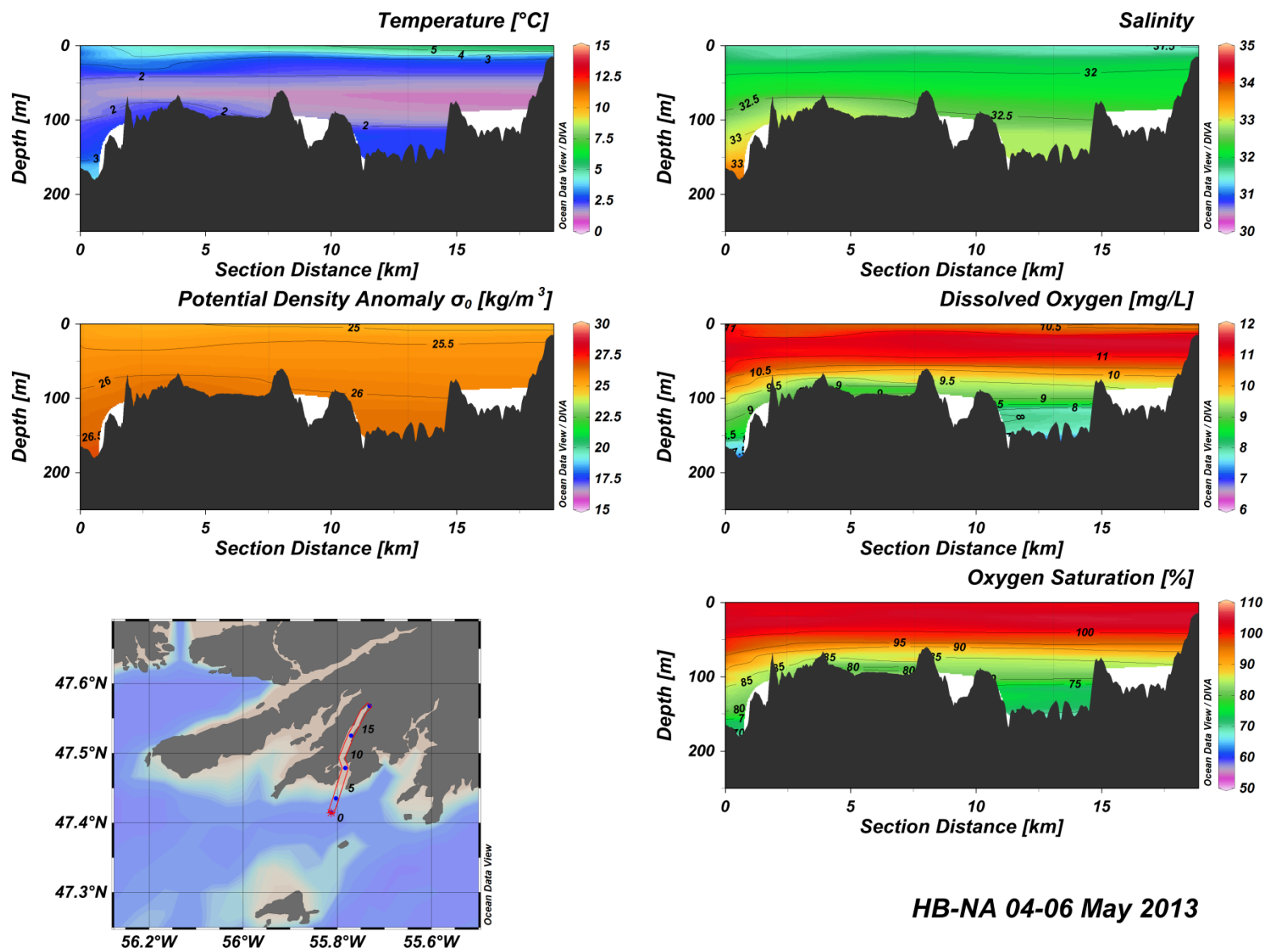


Figure C(i)30: Harbour Breton – Northeast Arm water column vertical structure.



HB-NA 04-06 May 2013

Figure C(i)31: Harbour Breton – Northeast Arm water column vertical structure.

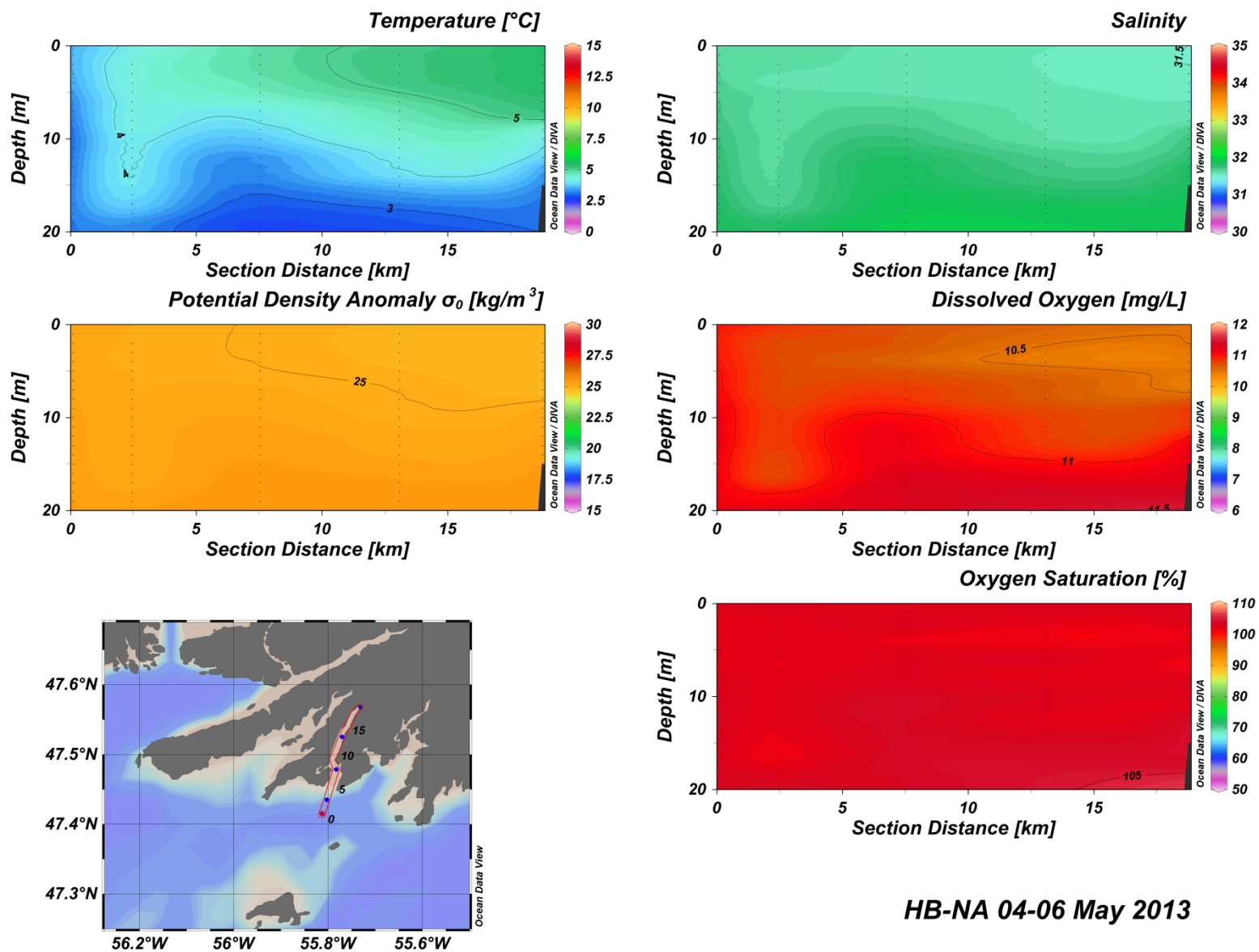
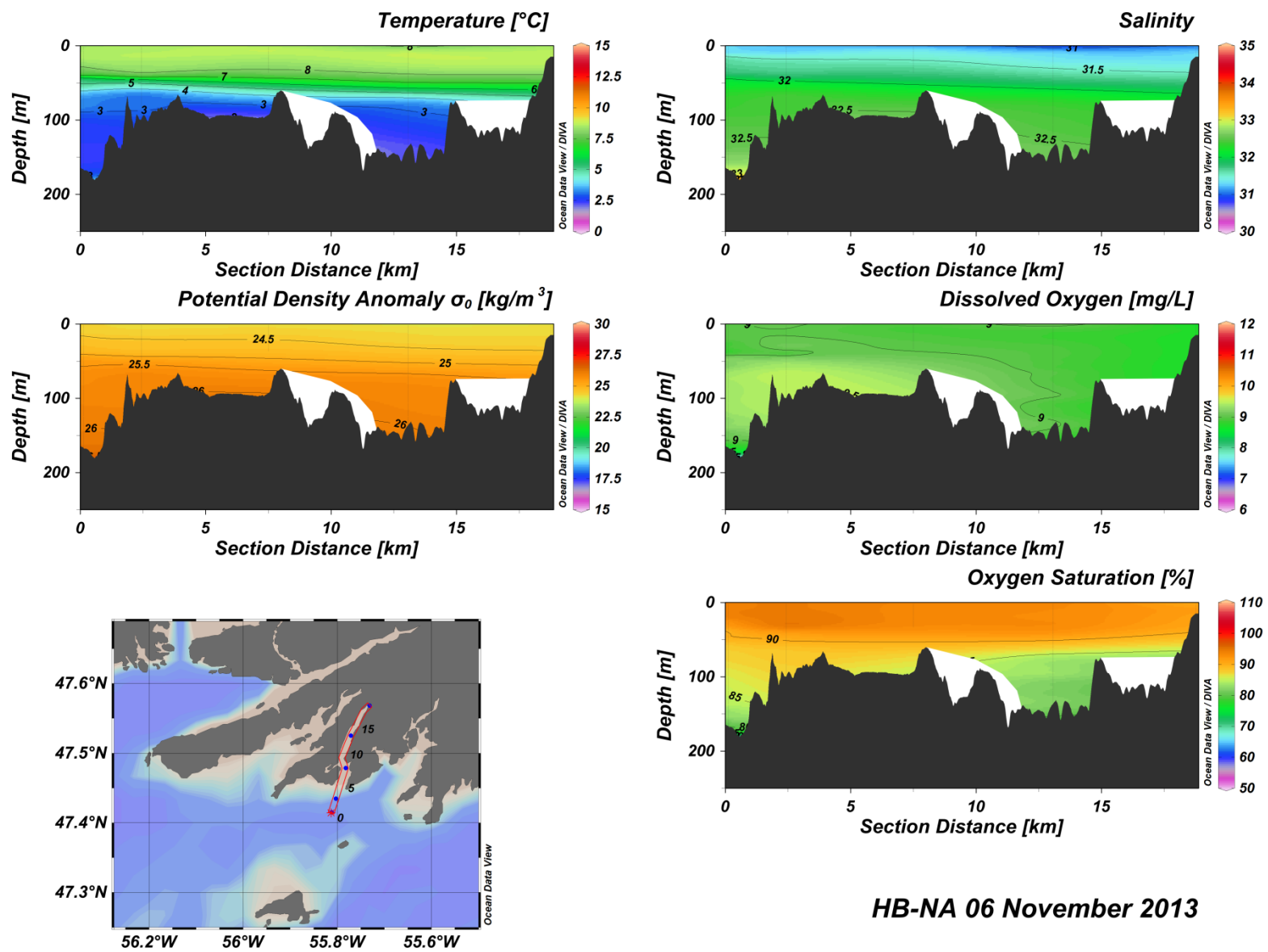


Figure C(i)32: Harbour Breton – Northeast Arm water column vertical structure.



HB-NA 06 November 2013

Figure C(i)33: Harbour Breton – Northeast Arm water column vertical structure.

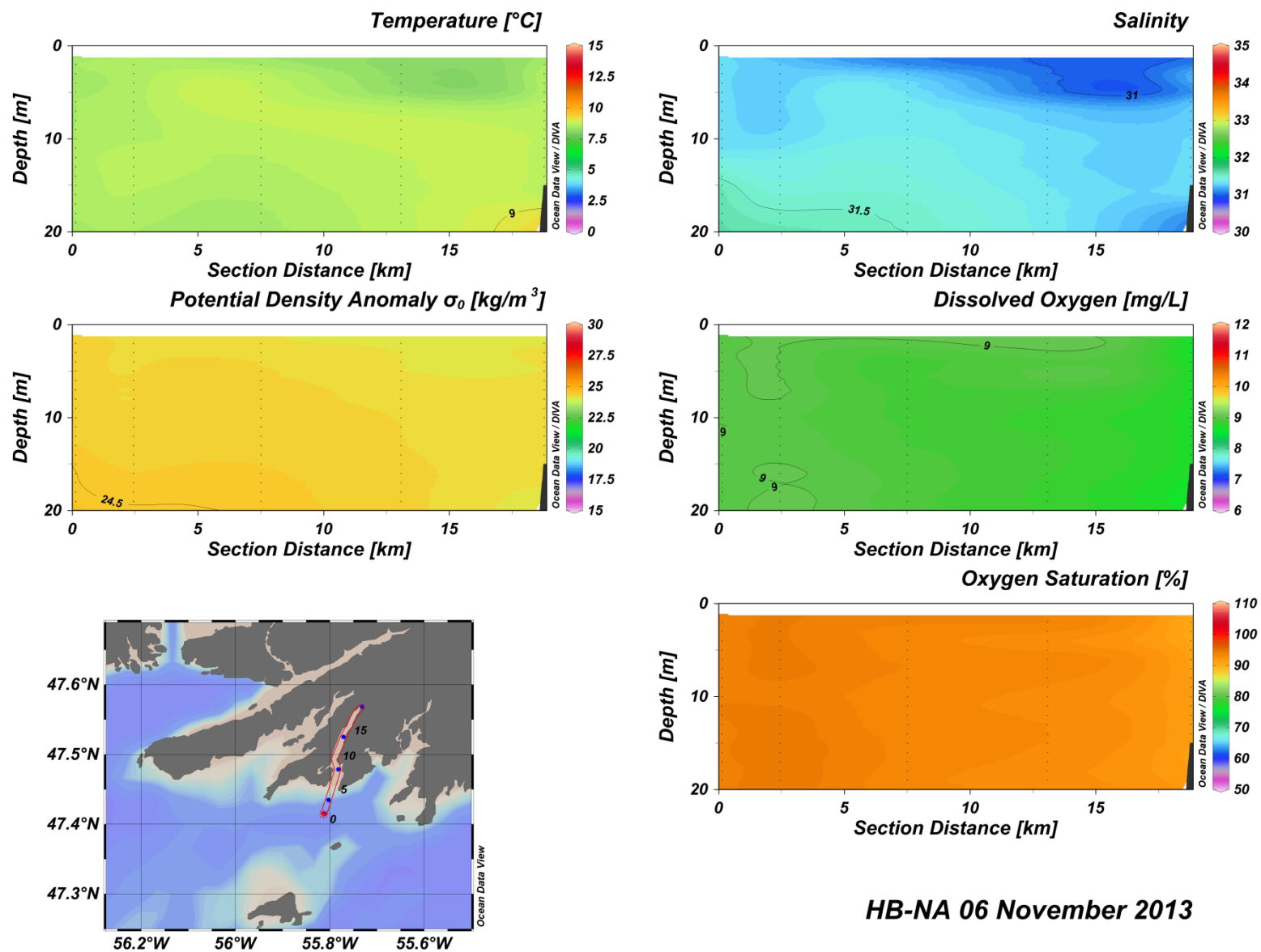


Figure C(i)34: Harbour Breton – Northeast Arm water column vertical structure.

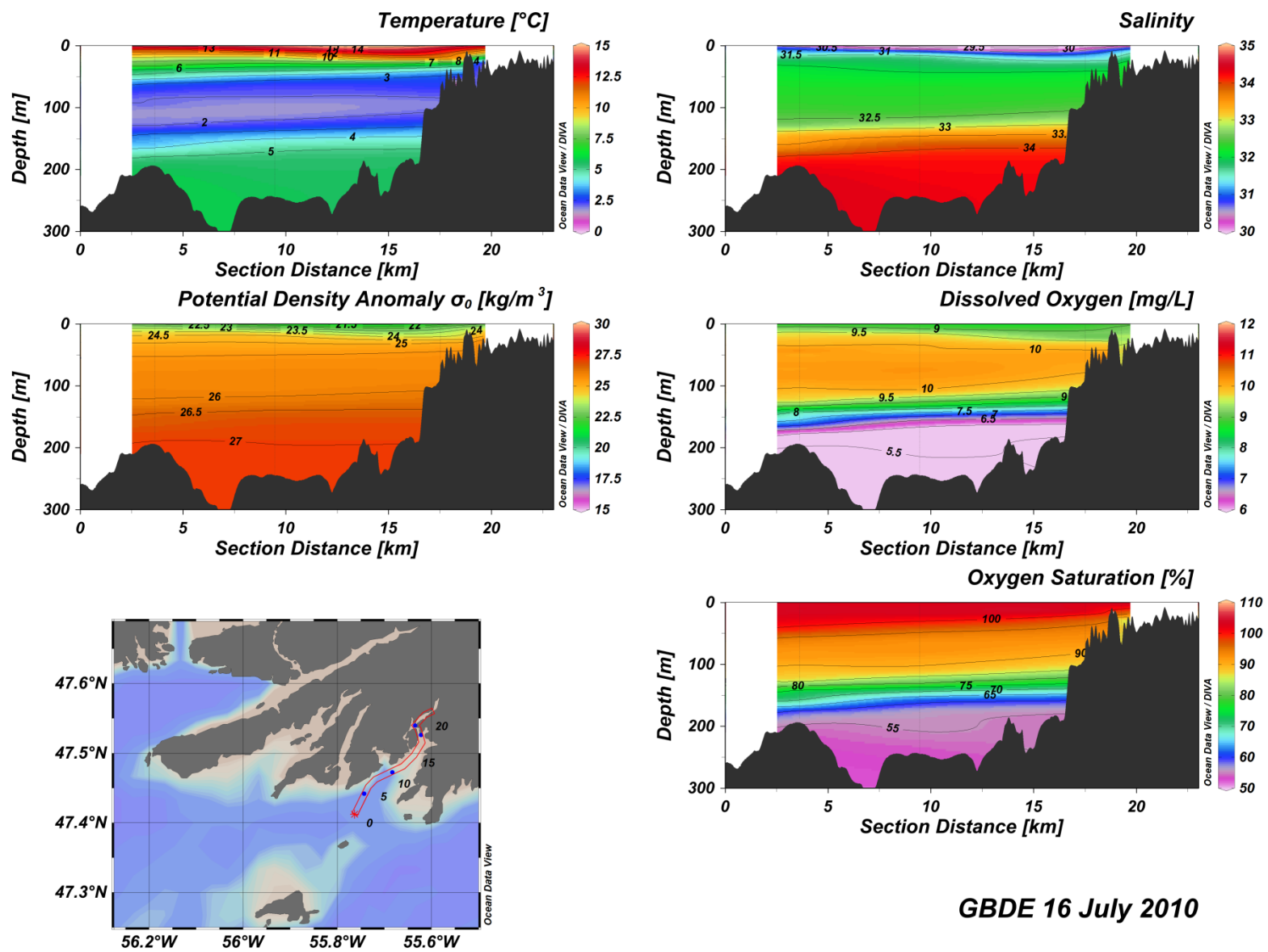


Figure C(i)35: Great Bay De L'Eau water column vertical structure.

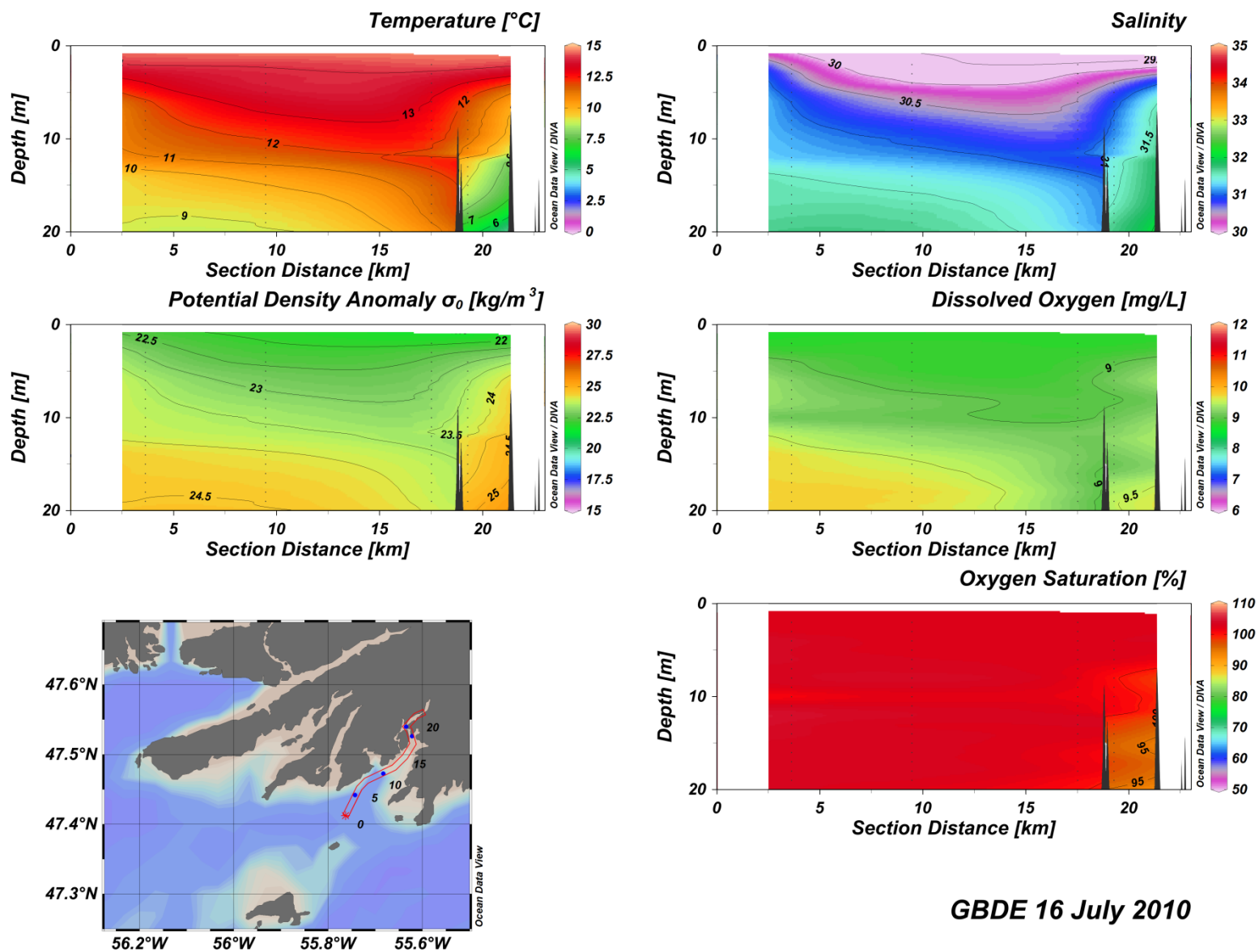
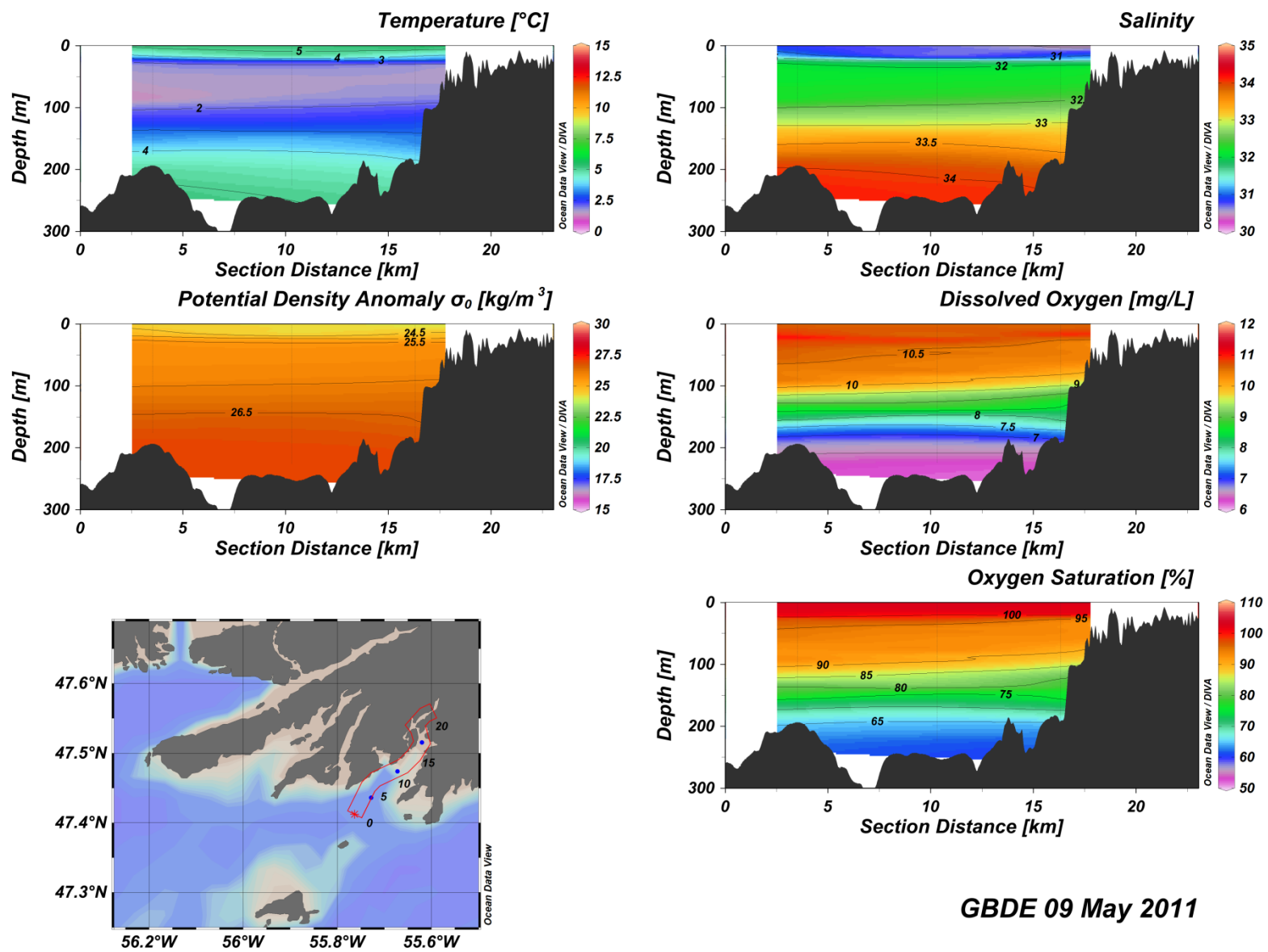


Figure C(i)36: Great Bay De L'Eau water column vertical structure.



GBDE 09 May 2011

Figure C(i)37: Great Bay De L'Eau water column vertical structure.

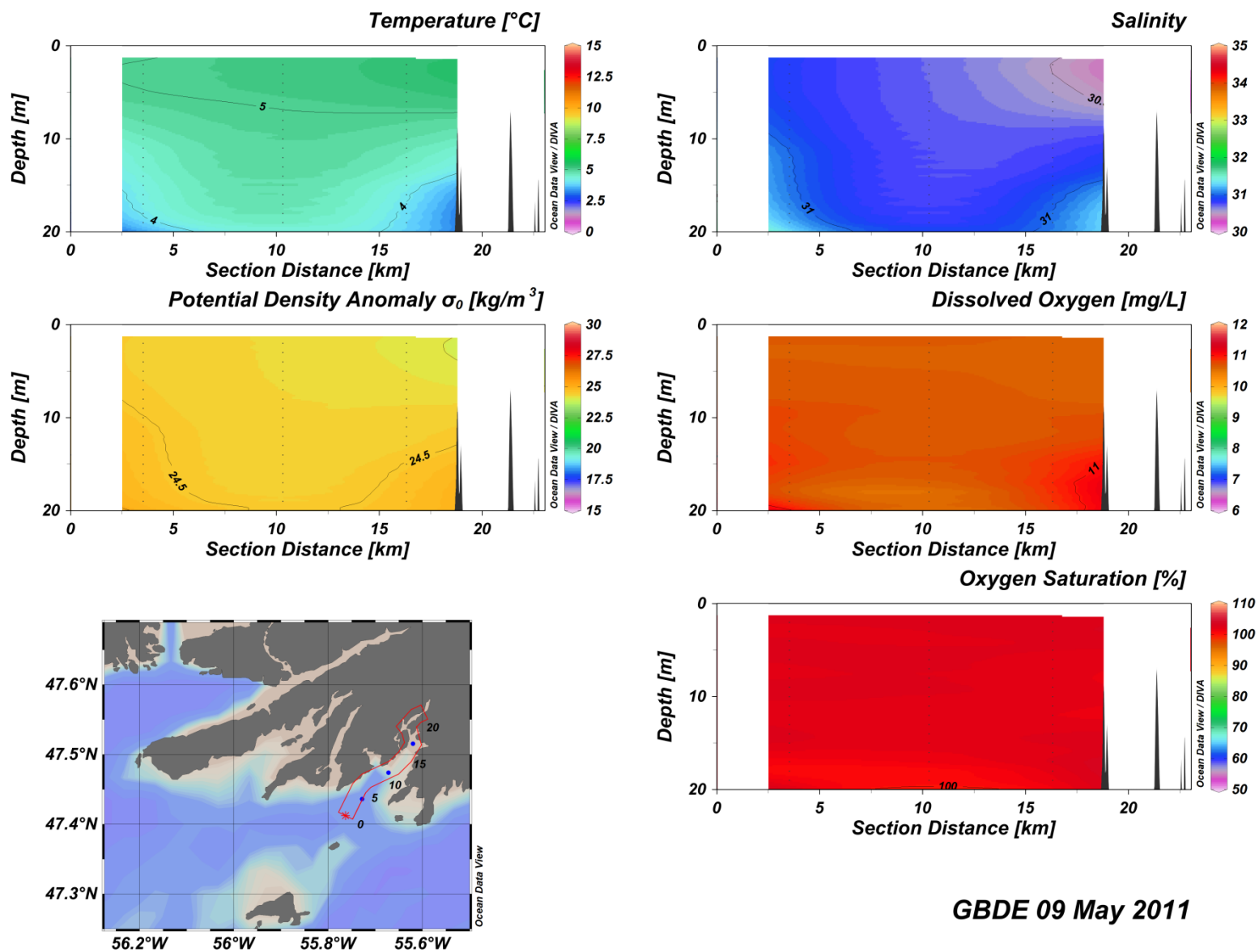
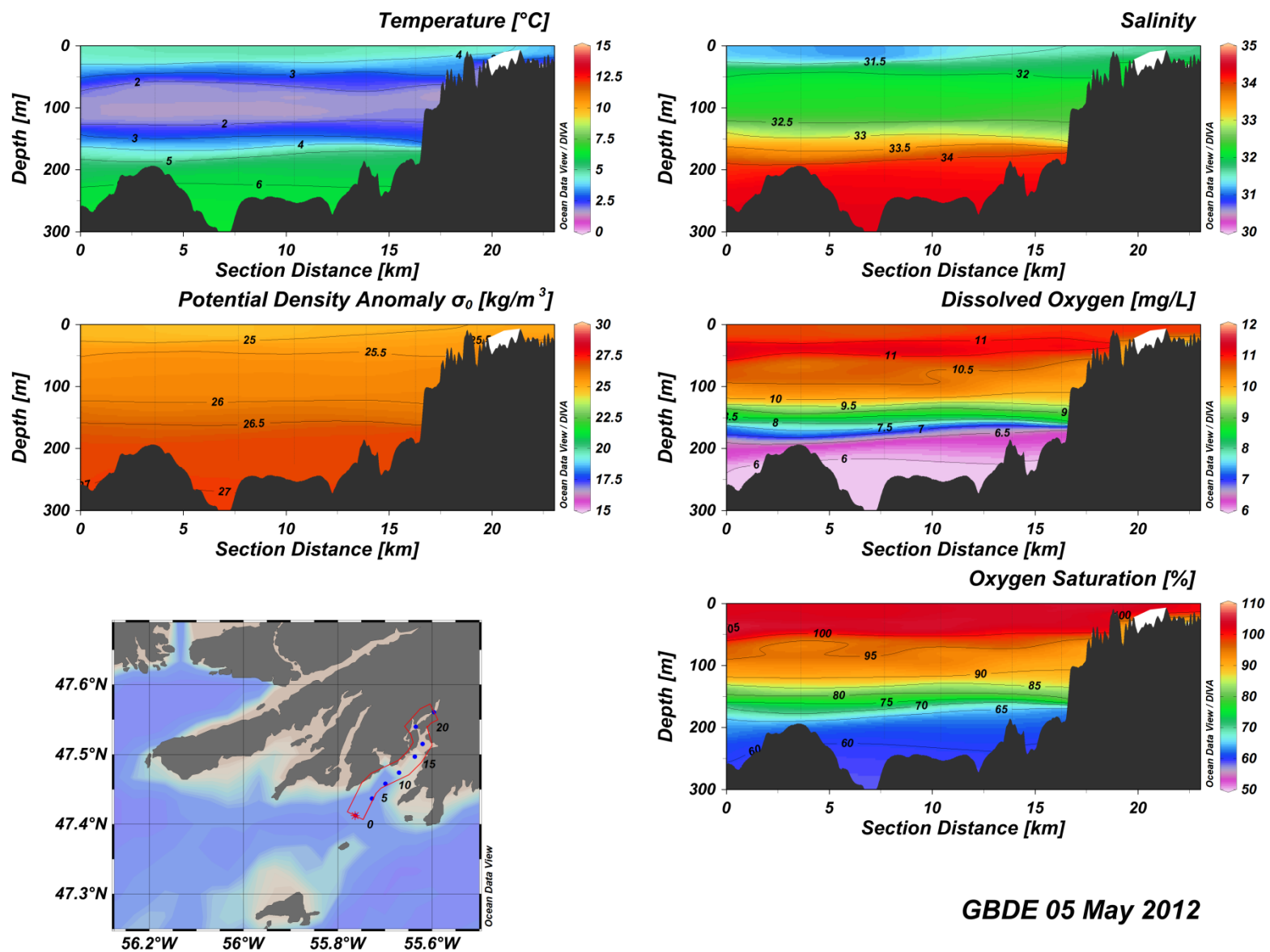


Figure C(i)38: Great Bay De L'Eau water column vertical structure.



GBDE 05 May 2012

Figure C(i)39: Great Bay De L'Eau water column vertical structure.

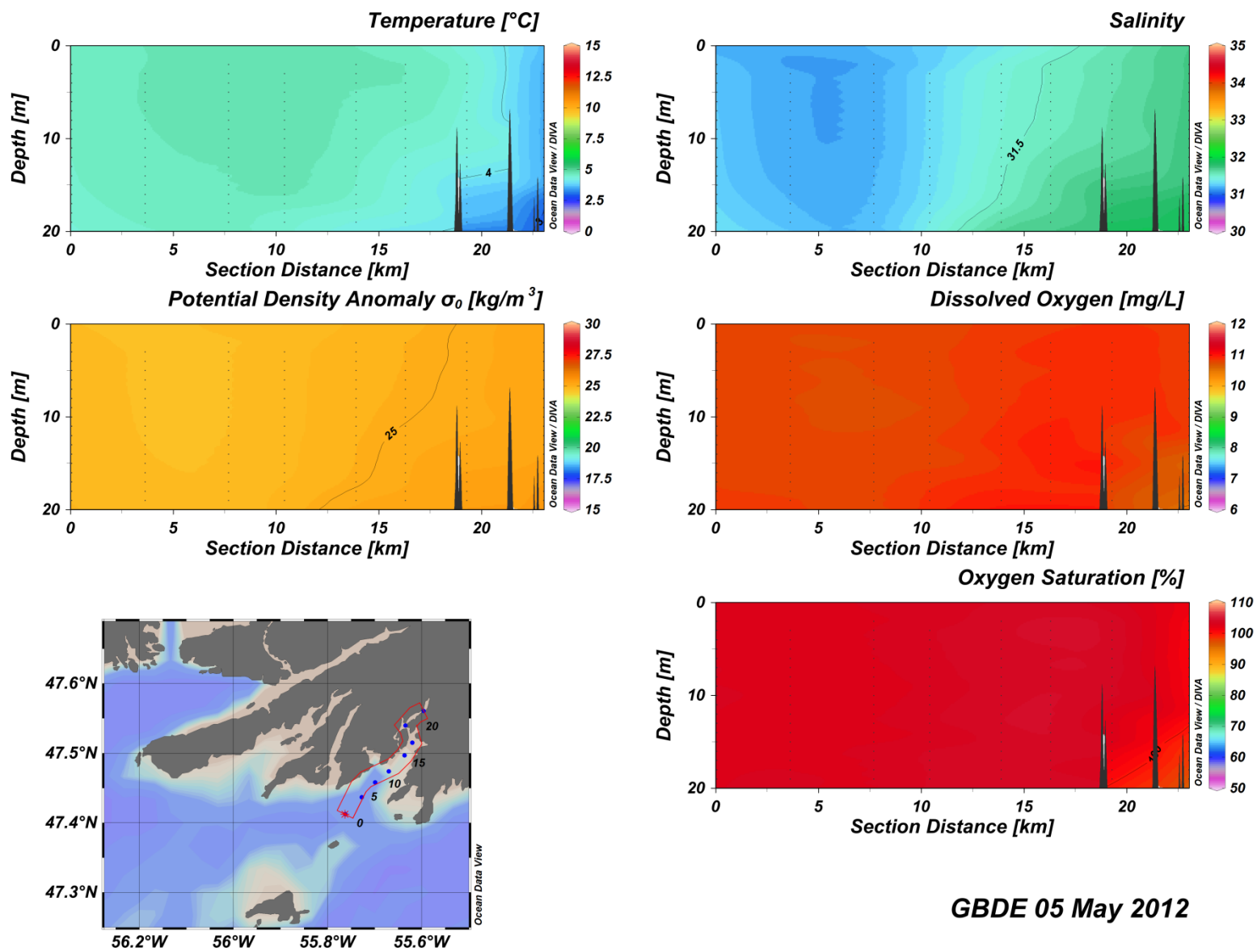


Figure C(i)40: Great Bay De L'Eau water column vertical structure.

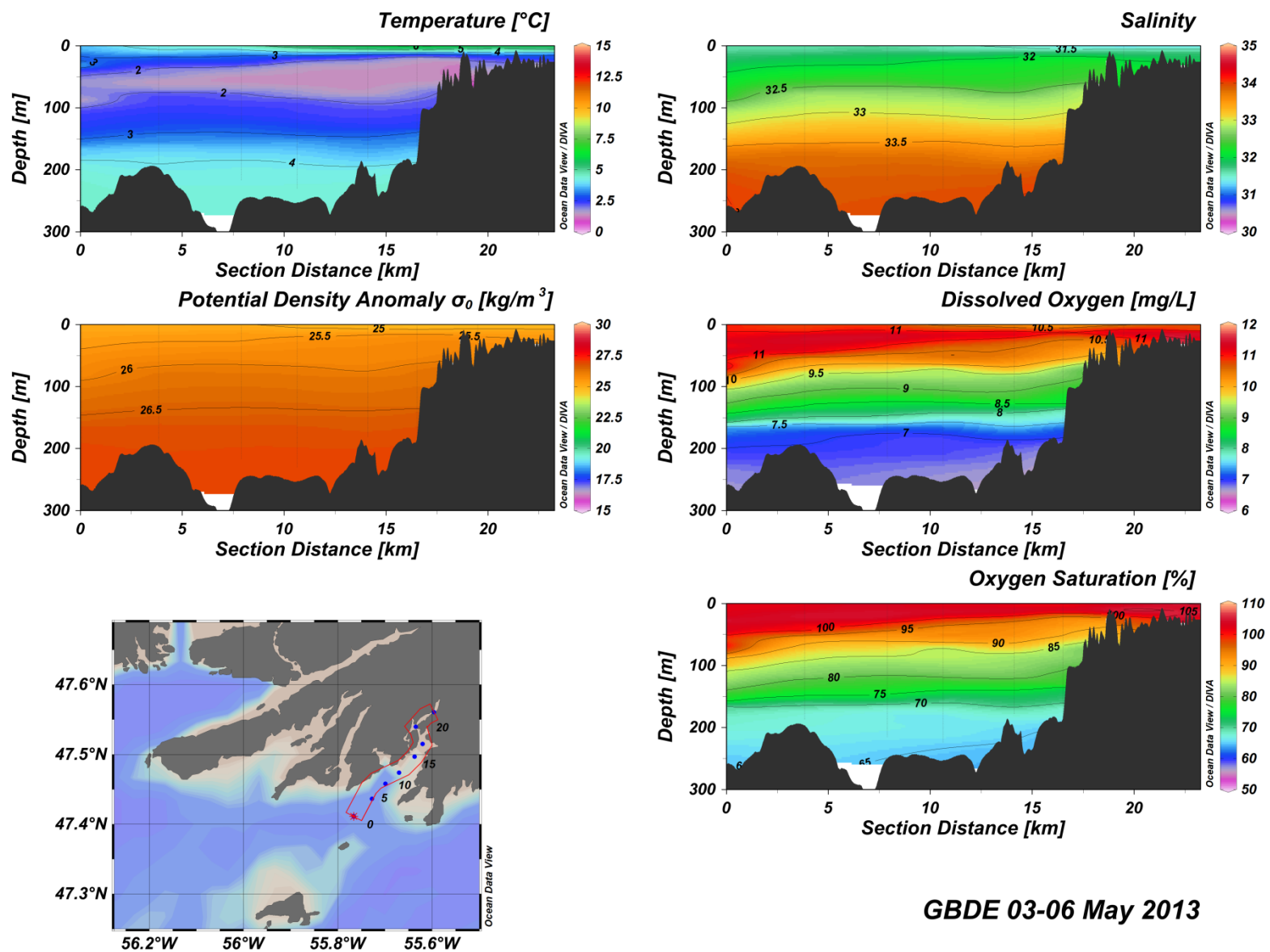


Figure C(i)41: Great Bay De L'Eau water column vertical structure.

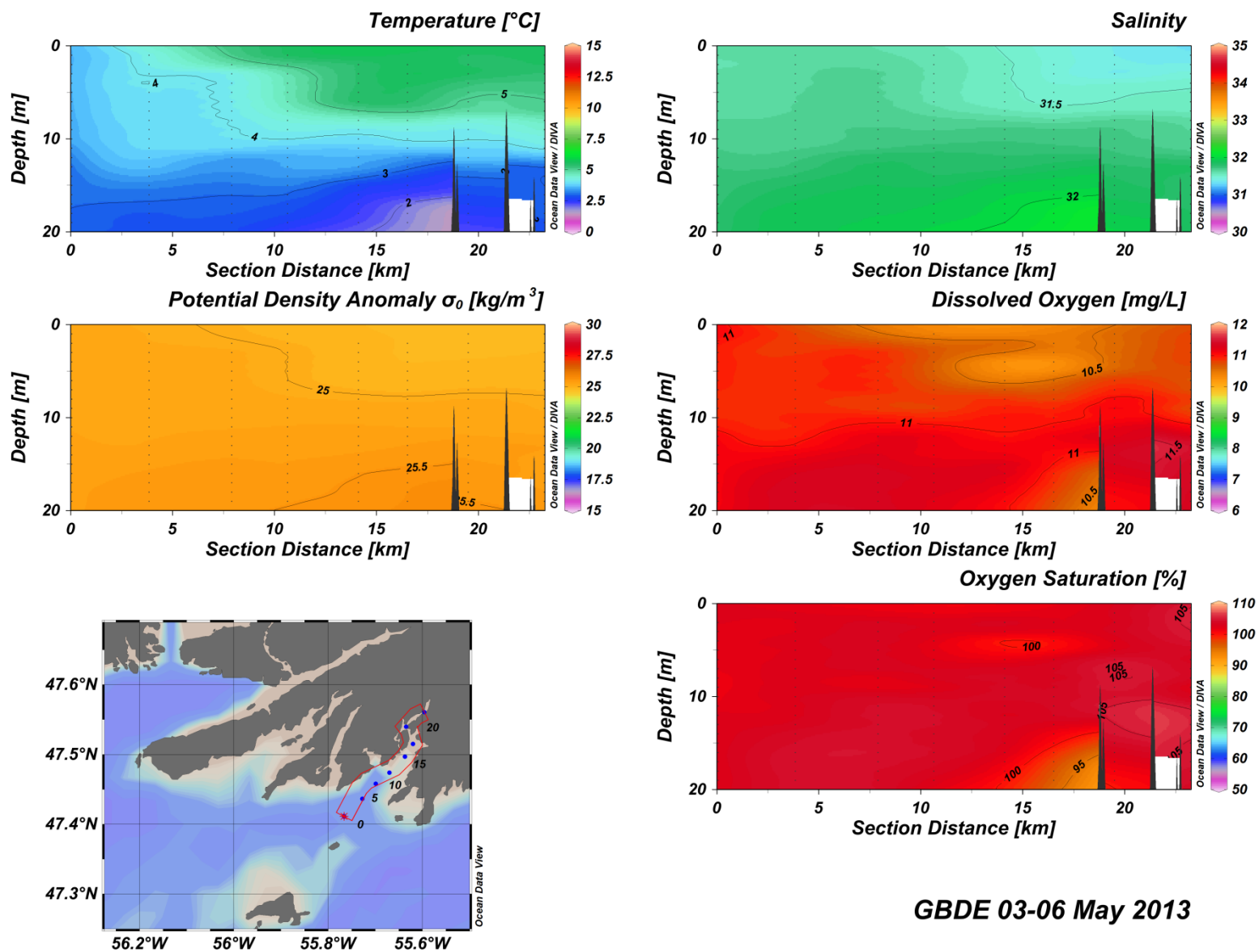


Figure C(i)42: Great Bay De L'Eau water column vertical structure.

**APPENDIX C(II): CONNAIGRE PENINSULA (CP) VERTICAL SECTIONS SUMMARY
TABLES**

Table C(ii)1: Outer Connaigre Peninsula (OCP) vertical sections summary statistics.

04-09 May 2011	T_min	T_max	T_mean	S_min	S_max	S_mean	DO_min	DO_max	DO_mean	ST_min	ST_max	ST_mean
Surface	2.63	3.95	3.31	31.31	31.89	31.53	10.97	11.73	11.38	24.86	25.43	25.09
Surface Gradients	0	0.07	0.03	0	0.08	0.02	0	0.1	0.03	0	0.07	0.02
Surface Clines	17	78	47.5	10	96	53	8	94	51	10	96	53
Intermediate 2°C_D = 79 m Dz = N/A	1.81	1.99	1.92	32.09	32.6	32.28	10.09	11.36	10.9	-	-	-
Deep 5°C_D = N/A Dz = N/A	N/A	N/A	N/A	N/A	N/A	N/A	N/A	N/A	N/A	-	-	-
04-06 May 2012	T_min	T_max	T_mean	S_min	S_max	S_mean	DO_min	DO_max	DO_mean	ST_min	ST_max	ST_mean
Surface	3.43	4.78	4.39	31.05	31.8	31.41	10.56	11.13	10.86	24.58	25.26	24.9
Surface Gradients	0	0.38	0.02	0	0.15	0.02	0	0.57	0.02	0	0.16	0.02
Surface Clines	12	57	36.71	8	34	22.94	6	97	32.82	8	34	22.71
Intermediate 2°C_D = 59-130 m Dz = 71 m	1.21	2	1.69	32.09	32.66	32.28	9.46	11.06	10.46	-	-	-
Deep 5°C_D = 182 m Dz = N/A	5.02	6.18	5.74	33.89	34.33	34.16	5.9	6.82	6.23	-	-	-
03-07 May 2013	T_min	T_max	T_mean	S_min	S_max	S_mean	DO_min	DO_max	DO_mean	ST_min	ST_max	ST_mean
Surface	2.71	4.52	3.5	31.5	32.01	31.72	10.65	11.43	11.05	24.98	25.51	25.23
Surface Gradients	0	0.37	0.05	0	0.08	0.01	0	0.17	0.03	0	0.09	0.01
Surface Clines	3	94	38.53	3	99	45.8	14	94	61.38	3	94	31.13
Intermediate 2°C_D = 42.5-95 m Dz = 52.5 m	1.1	2	1.71	31.98	32.72	32.3	9.57	11.98	10.63	-	-	-
Deep 5°C_D = N/A Dz = N/A	N/A	N/A	N/A	N/A	N/A	N/A	N/A	N/A	N/A	-	-	-
04-06 November 2013	T_min	T_max	T_mean	S_min	S_max	S_mean	DO_min	DO_max	DO_mean	ST_min	ST_max	ST_mean
Surface	7.61	9	8.38	31.1	31.75	31.5	6.62	9.17	8.78	24.1	24.77	24.47
Surface Gradients	0	0.16	0.02	0	0.16	0.01	0	0.24	0.01	0	0.12	0.01
Surface Clines	39	83	56.46	9	68	33.38	4	76	47.62	10	84	45.54
Intermediate 2°C_D = N/A Dz = N/A	N/A	N/A	N/A	N/A	N/A	N/A	N/A	N/A	N/A	-	-	-
Deep 5°C_D = N/A Dz = N/A	5	5.18	5.14	34.07	34.17	34.15	6.03	6.23	6.13	-	-	-

Table C(ii)2: Lower Connaigre Bay (LCB) vertical sections summary statistics.

09 May 2011	T_min	T_max	T_mean	S_min	S_max	S_mean	DO_min	DO_max	DO_mean	ST_min	ST_max	ST_mean
Surface	3.47	4.64	4.15	31.23	31.43	31.27	10.79	11.04	10.91	24.73	25	24.81
Surface Gradients	0	0.16	0.04	0	0.06	0.01	0	0.07	0.02	0	0.06	0.01
Surface Clines	26	29	27.33	19	32	25.67	30	88	62	19	29	24.67
Intermediate 2°C_D = 35-148 m Dz = 113 m	1.51	2	1.72	31.92	32.71	32.29	8.52	11.46	10.23	-	-	-
Deep 5°C_D = N/A Dz = N/A	N/A	N/A	N/A	N/A	N/A	N/A	N/A	N/A	N/A	-	-	-
04 May 2012	T_min	T_max	T_mean	S_min	S_max	S_mean	DO_min	DO_max	DO_mean	ST_min	ST_max	ST_mean
Surface	3.08	4.98	4.37	31.22	31.94	31.53	10.72	11.14	10.88	24.72	25.43	24.99
Surface Gradients	0	0.32	0.04	0	0.12	0.02	0	0.1	0.02	0	0.11	0.02
Surface Clines	8	53	31.6	8	92	28.4	30	79	49.2	8	92	28.4
Intermediate 2°C_D = 47.5-100 m Dz = 52.5 m	1.52	1.99	1.69	32.06	32.53	32.25	9.31	10.98	10.32	-	-	-
Deep 5°C_D = N/A Dz = N/A	N/A	N/A	N/A	N/A	N/A	N/A	N/A	N/A	N/A	-	-	-
03-05 May 2013	T_min	T_max	T_mean	S_min	S_max	S_mean	DO_min	DO_max	DO_mean	ST_min	ST_max	ST_mean
Surface	3.16	4.33	3.82	31.57	31.99	31.77	10.82	11.27	11.01	25.07	25.47	25.24
Surface Gradients	0	0.24	0.03	0	0.08	0.01	0	0.12	0.02	0	0.08	0.01
Surface Clines	4	94	46.38	4	100	65.63	53	94	66.67	4	94	43.75
Intermediate 2°C_D = 52.5 m Dz = N/A	1.06	2	1.38	32.08	32.73	32.44	8.96	11.21	9.88	-	-	-
Deep 5°C_D = N/A Dz = N/A	N/A	N/A	N/A	N/A	N/A	N/A	N/A	N/A	N/A	-	-	-
04-05 November 2013	T_min	T_max	T_mean	S_min	S_max	S_mean	DO_min	DO_max	DO_mean	ST_min	ST_max	ST_mean
Surface	7.75	8.85	8.13	30.64	31.67	31.49	7.83	9.34	8.95	23.82	24.69	24.5
Surface Gradients	0	0.1	0.01	0	0.26	0.01	0	0.16	0.01	0	0.21	0.01
Surface Clines	59	83	71.45	6	80	55.09	2	78	61.45	6	84	66.27
Intermediate 2°C_D = 121.5 m Dz = N/A	1.54	2	1.8	32.55	32.85	32.69	8.73	9.55	9.21	-	-	-
Deep 5°C_D = N/A Dz = N/A	N/A	N/A	N/A	N/A	N/A	N/A	N/A	N/A	N/A	-	-	-

Table C(ii)3: Upper Connaigre Bay (UCB) vertical sections summary statistics.

04 May 2012	T_min	T_max	T_mean	S_min	S_max	S_mean	DO_min	DO_max	DO_mean	ST_min	ST_max	ST_mean
Surface	1.78	3.94	2.58	31.84	32.14	32.03	10.54	11.16	10.87	25.28	25.7	25.54
Surface Gradients	0	0.31	0.03	0	0.02	0	0	0.08	0.01	0	0.04	0
Surface Clines	12	86	35	43	94	72	65	84	78.5	12	77	49.75
Intermediate 2°C_D = 36.5-91 m Dz = 54.5 m	1.58	2	1.8	32.08	32.46	32.19	9.19	10.95	10.23	-	-	-
Deep 5°C_D = N/A Dz = N/A	N/A	N/A	N/A	N/A	N/A	N/A	N/A	N/A	N/A	-	-	-
14-15 July 2012	T_min	T_max	T_mean	S_min	S_max	S_mean	DO_min	DO_max	DO_mean	ST_min	ST_max	ST_mean
Surface	6.89	17.4	11.83	30.19	31.89	31.37	8.25	10.3	9.53	21.77	24.99	23.75
Surface Gradients	0.05	1.74	0.53	0	0.38	0.08	0	0.43	0.13	0.02	0.68	0.16
Surface Clines	5	8	6.33	4	6	5	4	53	22	5	8	6.33
Intermediate 2°C_D = N/A Dz = N/A	N/A	N/A	N/A	N/A	N/A	N/A	N/A	N/A	N/A	-	-	-
Deep 5°C_D = N/A Dz = N/A	N/A	N/A	N/A	N/A	N/A	N/A	N/A	N/A	N/A	-	-	-
04-05 May 2013	T_min	T_max	T_mean	S_min	S_max	S_mean	DO_min	DO_max	DO_mean	ST_min	ST_max	ST_mean
Surface	2.67	4.56	3.84	31.2	32	31.83	10.75	11.66	11.03	24.74	25.52	25.28
Surface Gradients	0	0.26	0.05	0	0.54	0.01	0	0.22	0.03	0	0.43	0.01
Surface Clines	6	74	37	2	94	29.75	3	83	54	2	67	17.5
Intermediate 2°C_D = 57.5 m Dz = N/A	1.01	1.98	1.24	32.07	32.6	32.35	9.19	11.24	9.94	-	-	-
Deep 5°C_D = N/A Dz = N/A	N/A	N/A	N/A	N/A	N/A	N/A	N/A	N/A	N/A	-	-	-
05 November 2013	T_min	T_max	T_mean	S_min	S_max	S_mean	DO_min	DO_max	DO_mean	ST_min	ST_max	ST_mean
Surface	7.75	8.37	8.1	31.31	31.61	31.5	8.76	9.34	9.01	24.36	24.62	24.51
Surface Gradients	0	0.16	0.02	0	0.12	0.01	0	0.07	0.01	0	0.08	0.01
Surface Clines	76	80	77.42	3	80	71.17	72	79	76.33	76	78	77.25
Intermediate 2°C_D = 125 m Dz = N/A	1.52	2	1.69	32.49	32.62	32.54	9.07	9.52	9.32	-	-	-
Deep 5°C_D = N/A Dz = N/A	N/A	N/A	N/A	N/A	N/A	N/A	N/A	N/A	N/A	-	-	-

Table C(ii)4: Harbour Breton – Northeast Arm (HB-NA) vertical sections summary statistics.

15 July 2010	T_min	T_max	T_mean	S_min	S_max	S_mean	DO_min	DO_max	DO_mean	ST_min	ST_max	ST_mean
Surface	8.87	16.18	11.34	28.78	31.69	31.08	8.42	9.76	9.22	20.93	24.55	23.65
Surface Gradients	0.02	1.46	0.32	0.01	0.94	0.12	0	0.28	0.06	0.01	0.99	0.15
Surface Clines	2	29	6.86	2	5	2.86	2	99	29.86	2	5	3
Intermediate 2°C_D = 67.5-96 m Dz = 28.5 m	1.55	2	1.82	32.16	32.55	32.33	6.61	9.89	9.41	-	-	-
Deep 5°C_D = N/A Dz = N/A	N/A	N/A	N/A	N/A	N/A	N/A	N/A	N/A	N/A	-	-	-
09 May 2011	T_min	T_max	T_mean	S_min	S_max	S_mean	DO_min	DO_max	DO_mean	ST_min	ST_max	ST_mean
Surface	2.25	5.02	3.82	30.72	31.72	31.14	10.36	11.15	10.8	24.28	25.32	24.73
Surface Gradients	0	0.36	0.11	0	0.12	0.04	0	0.2	0.05	0	0.11	0.04
Surface Clines	6	23	10.5	3	29	14.17	6	91	55.83	3	24	13.33
Intermediate 2°C_D = 34-103 m Dz = 69 m	1.65	1.99	1.8	31.83	32.51	32.19	8.98	10.94	9.9	-	-	-
Deep 5°C_D = N/A Dz = N/A	N/A	N/A	N/A	N/A	N/A	N/A	N/A	N/A	N/A	-	-	-
04-05 May 2012	T_min	T_max	T_mean	S_min	S_max	S_mean	DO_min	DO_max	DO_mean	ST_min	ST_max	ST_mean
Surface	4.02	4.93	4.62	31.07	31.59	31.24	10.72	11.09	10.84	24.57	25.08	24.73
Surface Gradients	0	0.09	0.02	0	0.04	0.01	0	0.04	0.01	0	0.03	0.01
Surface Clines	22	57	43.8	21	85	39.8	20	97	55.6	20	35	28
Intermediate 2°C_D = 65-101 m Dz = 36 m	1.6	2	1.85	32.04	32.57	32.26	9.44	10.76	10.22	-	-	-
Deep 5°C_D = N/A Dz = N/A	5.06	6.03	5.7	33.91	34.26	34.15	6.08	6.7	6.25	-	-	-
04-06 May 2013	T_min	T_max	T_mean	S_min	S_max	S_mean	DO_min	DO_max	DO_mean	ST_min	ST_max	ST_mean
Surface	2.67	5.4	3.85	31.5	31.93	31.71	10.43	11.43	10.92	24.86	25.46	25.18
Surface Gradients	0	0.67	0.1	0	0.09	0.02	0	0.2	0.04	0	0.13	0.02
Surface Clines	7	26	15.2	9	85	28.2	9	83	45.4	7	26	15.4
Intermediate 2°C_D = 42.5-93.5 m Dz = 51 m	1.17	2	1.62	32.03	32.72	32.32	8.5	11.17	10.13	-	-	-
Deep 5°C_D = N/A Dz = N/A	N/A	N/A	N/A	N/A	N/A	N/A	N/A	N/A	N/A	-	-	-

Table C(ii)4: Continued.

06 November 2013	T_min	T_max	T_mean	S_min	S_max	S_mean	DO_min	DO_max	DO_mean	ST_min	ST_max	ST_mean
Surface	8.08	8.79	8.56	30.99	31.61	31.32	8.53	9.11	8.88	24.11	24.55	24.31
Surface Gradients	0	0.26	0.03	0	0.14	0.02	0	0.08	0.01	0	0.08	0.01
Surface Clines	3	63	28.57	3	44	16.43	3	43	19.86	3	63	28.57
Intermediate 2°C_D = N/A Dz = N/A	N/A	N/A	N/A	N/A	N/A	N/A	N/A	N/A	N/A	-	-	-
Deep 5°C_D = N/A Dz = N/A	5	5.18	5.14	34.07	34.17	34.15	6.03	6.23	6.13	-	-	-

Table C(ii)5: Great Bay De L'Eau (GBDE) vertical sections summary statistics.

16 July 2010	T_min	T_max	T_mean	S_min	S_max	S_mean	DO_min	DO_max	DO_mean	ST_min	ST_max	ST_mean
Surface	6.35	14.35	11.21	29.54	31.7	31.03	8.74	9.73	9.19	21.93	24.9	23.64
Surface Gradients	0	0.78	0.29	0.01	0.51	0.09	0	0.25	0.06	0.02	0.49	0.12
Surface Clines	13	28	20	3	5	4	11	24	16.5	3	5	4
Intermediate 2°C_D = 76-120 m Dz = 44 m	1.66	2	1.82	32.28	32.65	32.4	9.31	10.19	9.93	-	-	-
Deep 5°C_D = 170 m Dz = N/A	5.02	5.67	5.47	34.06	34.31	34.23	5.32	5.91	5.52	-	-	-
09 May 2011	T_min	T_max	T_mean	S_min	S_max	S_mean	DO_min	DO_max	DO_mean	ST_min	ST_max	ST_mean
Surface	3.39	5.29	4.66	30.49	31.34	30.82	10.44	11.06	10.69	24.07	24.93	24.4
Surface Gradients	0	0.37	0.07	0	0.13	0.02	0	0.23	0.03	0	0.13	0.03
Surface Clines	21	24	22.67	21	25	23	20	22	21	21	25	23
Intermediate 2°C_D = 30-97.5 m Dz = 67.5 m	1.33	2	1.67	31.93	32.56	32.22	9.65	10.76	10.36	-	-	-
Deep 5°C_D = N/A Dz = N/A	N/A	N/A	N/A	N/A	N/A	N/A	N/A	N/A	N/A	-	-	-
05 May 2012	T_min	T_max	T_mean	S_min	S_max	S_mean	DO_min	DO_max	DO_mean	ST_min	ST_max	ST_mean
Surface	2.91	4.78	4.35	31.13	31.88	31.42	10.47	10.98	10.81	24.65	25.4	24.91
Surface Gradients	0	0.26	0.03	0	0.05	0.01	0	0.1	0.01	0	0.06	0.01
Surface Clines	16	54	29.25	16	33	24	21	73	42.25	16	33	24
Intermediate 2°C_D = 66.5-124 m Dz = 57.5 m	1.49	2	1.75	32.06	32.6	32.27	9.51	10.72	10.27	-	-	-
Deep 5°C_D = 177.5 m Dz = N/A	5.02	6.18	5.68	33.89	34.33	34.14	5.9	6.69	6.21	-	-	-
03-06 May 2013	T_min	T_max	T_mean	S_min	S_max	S_mean	DO_min	DO_max	DO_mean	ST_min	ST_max	ST_mean
Surface	1.76	5.69	3.71	31.33	32.09	31.72	10.23	11.44	10.96	24.71	25.66	25.2
Surface Gradients	0	0.76	0.13	0	0.11	0.02	0	0.31	0.06	0	0.14	0.03
Surface Clines	2	38	14.6	3	99	19.1	3	82	22	3	86	17.6
Intermediate 2°C_D = 26.5-85 m Dz = 58.5 m	1.12	2	1.58	32	32.83	32.32	9.12	11.33	10.25	-	-	-
Deep 5°C_D = N/A Dz = N/A	N/A	N/A	N/A	N/A	N/A	N/A	N/A	N/A	N/A	-	-	-

APPENDIX C(III): CONNAIGRE PENINSULA (CP) SURFACE MAPS

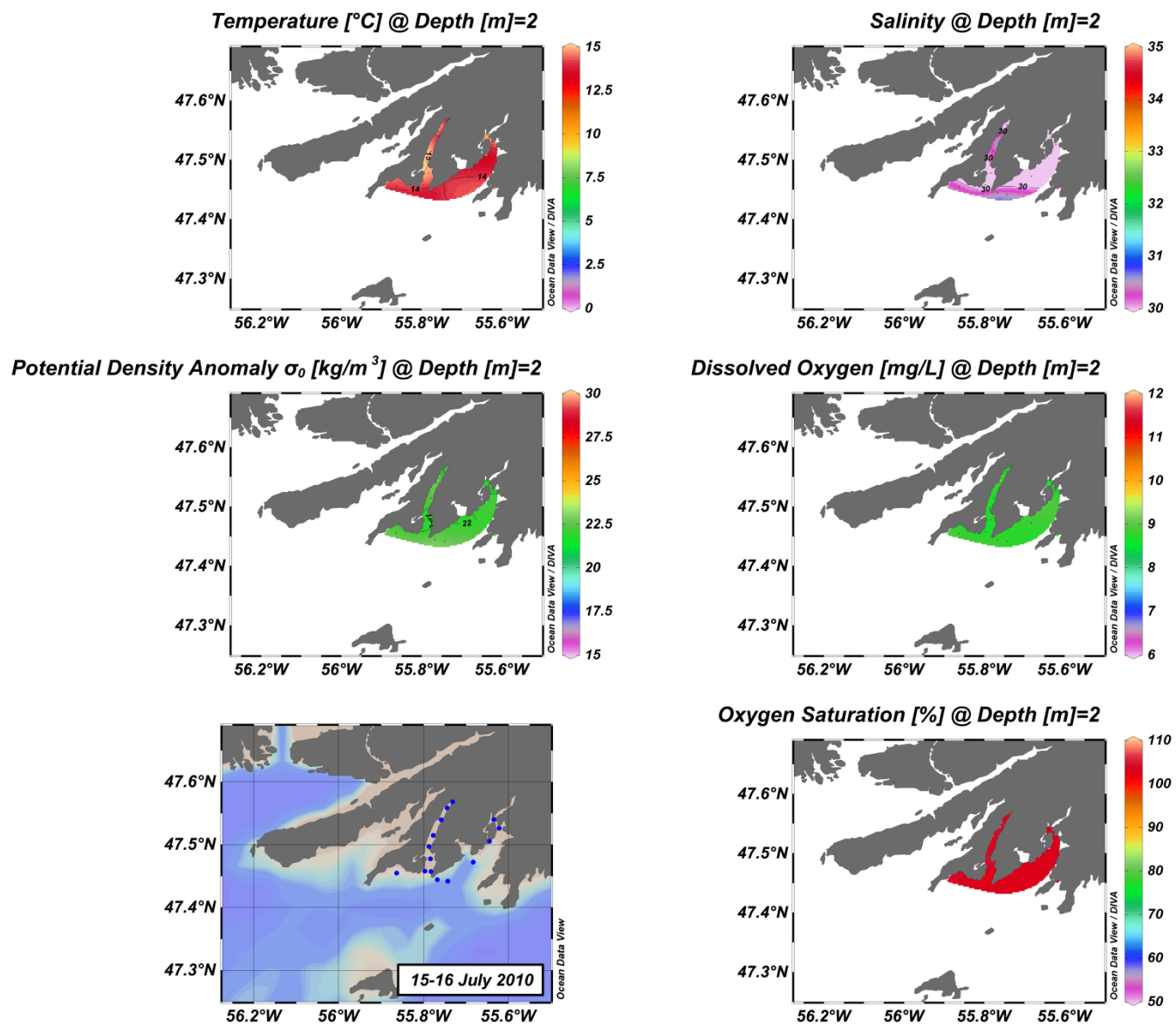


Figure C(iii)1: Connaigre Peninsula surface structure.

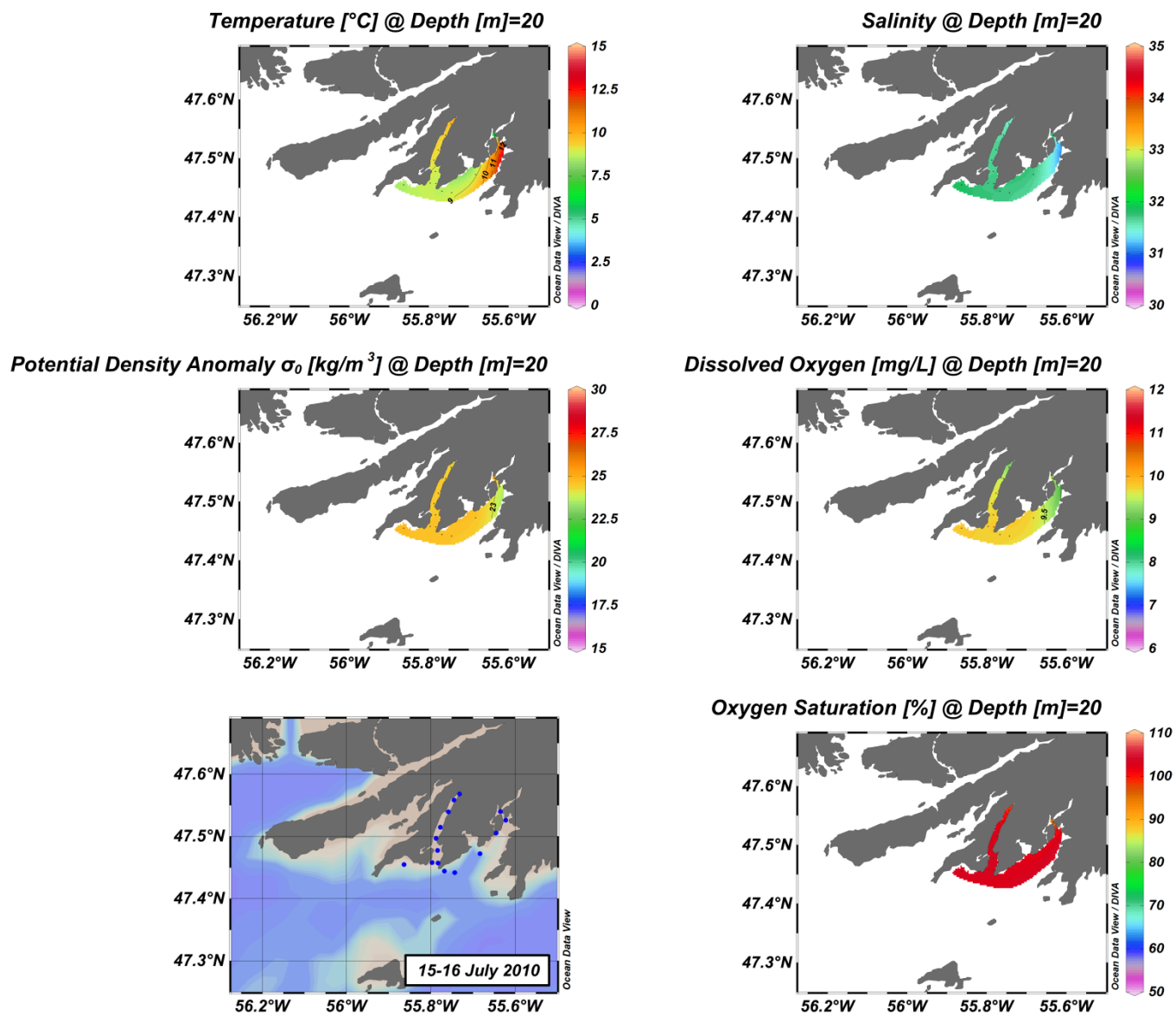


Figure C(iii)2: Connaigre Peninsula surface structure.

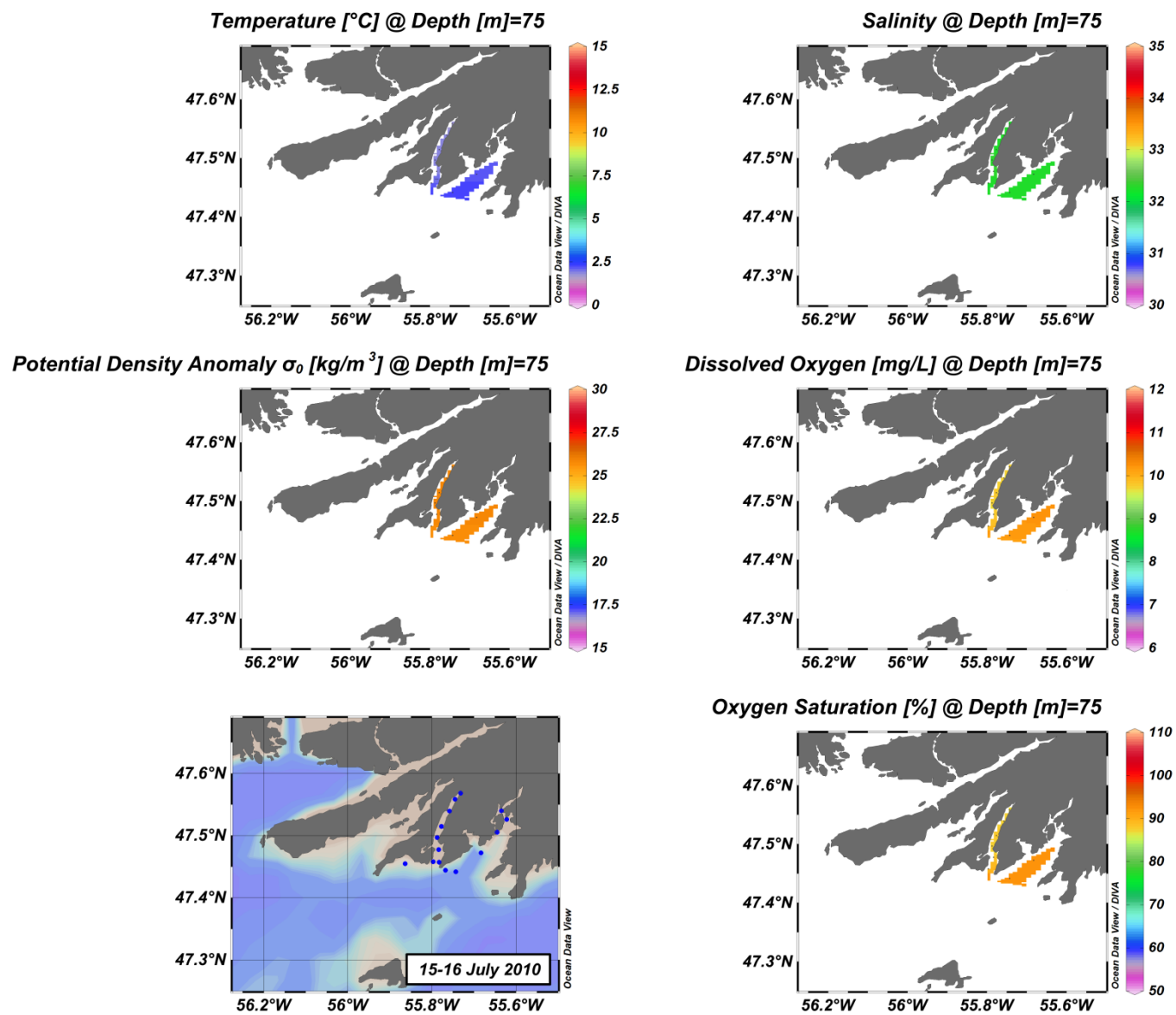


Figure C(iii)3: Connaigre Peninsula surface structure.

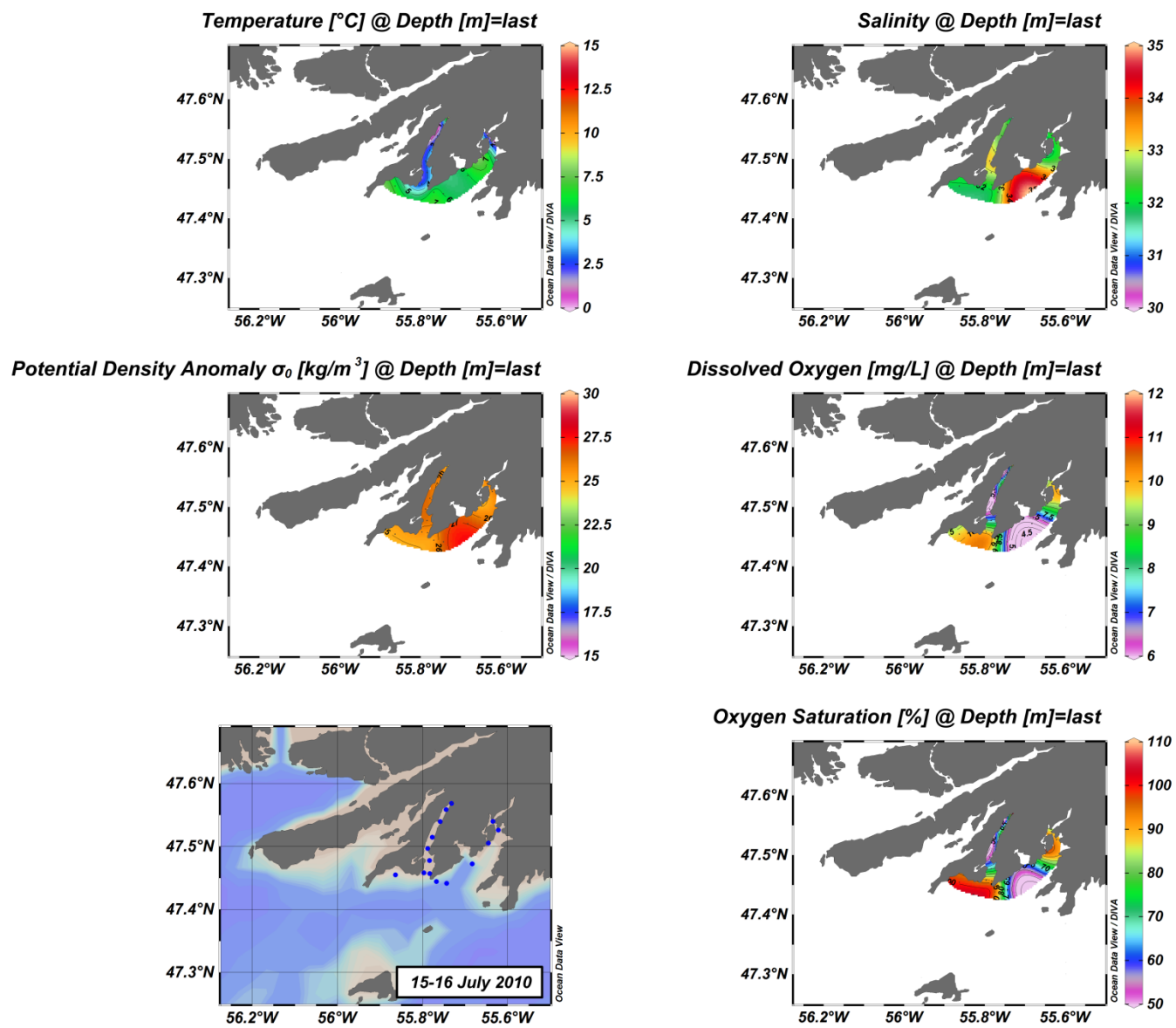


Figure C(iii)4: Connaigre Peninsula surface structure.

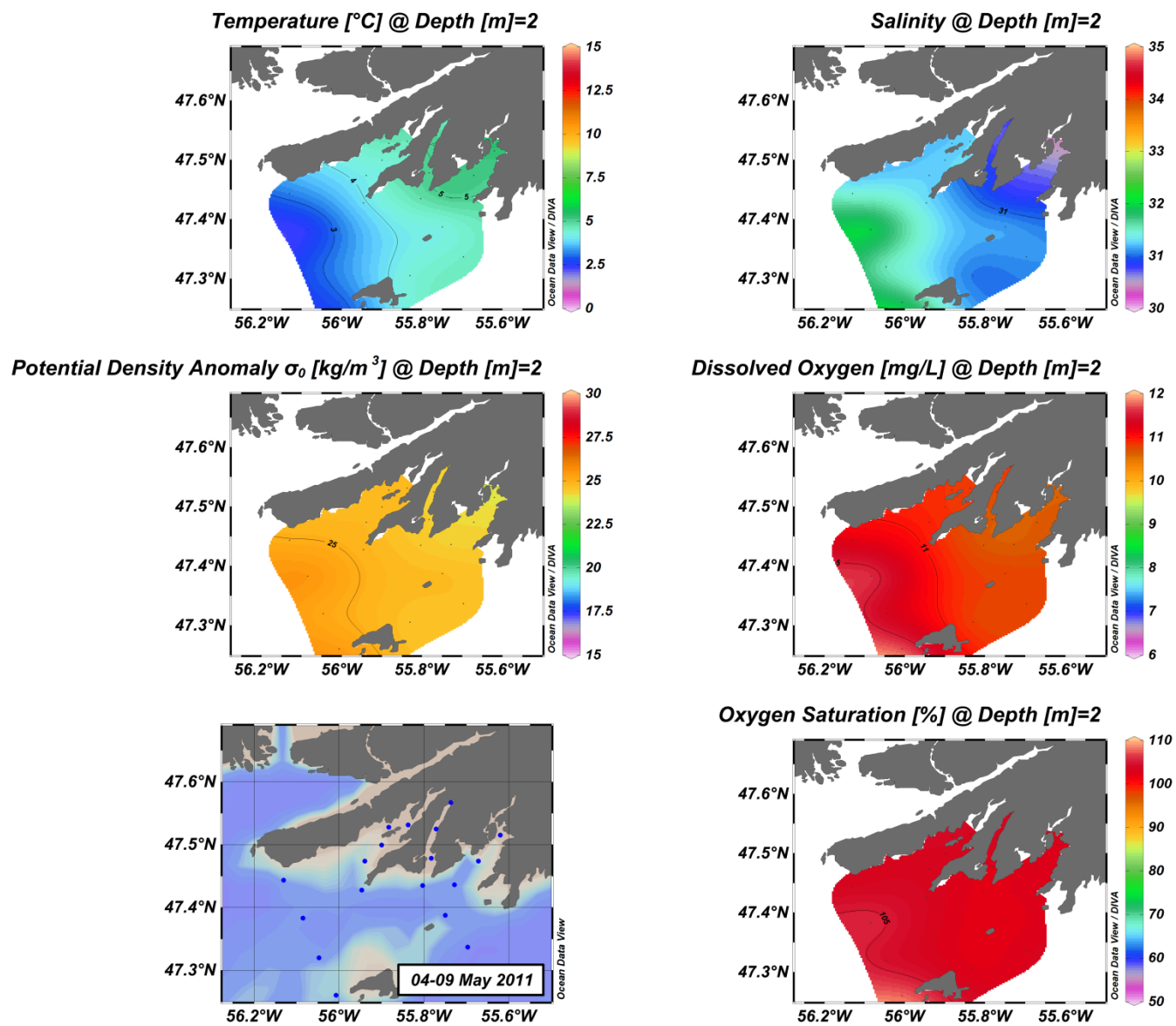


Figure C(iii)5: Connaigre Peninsula surface structure.

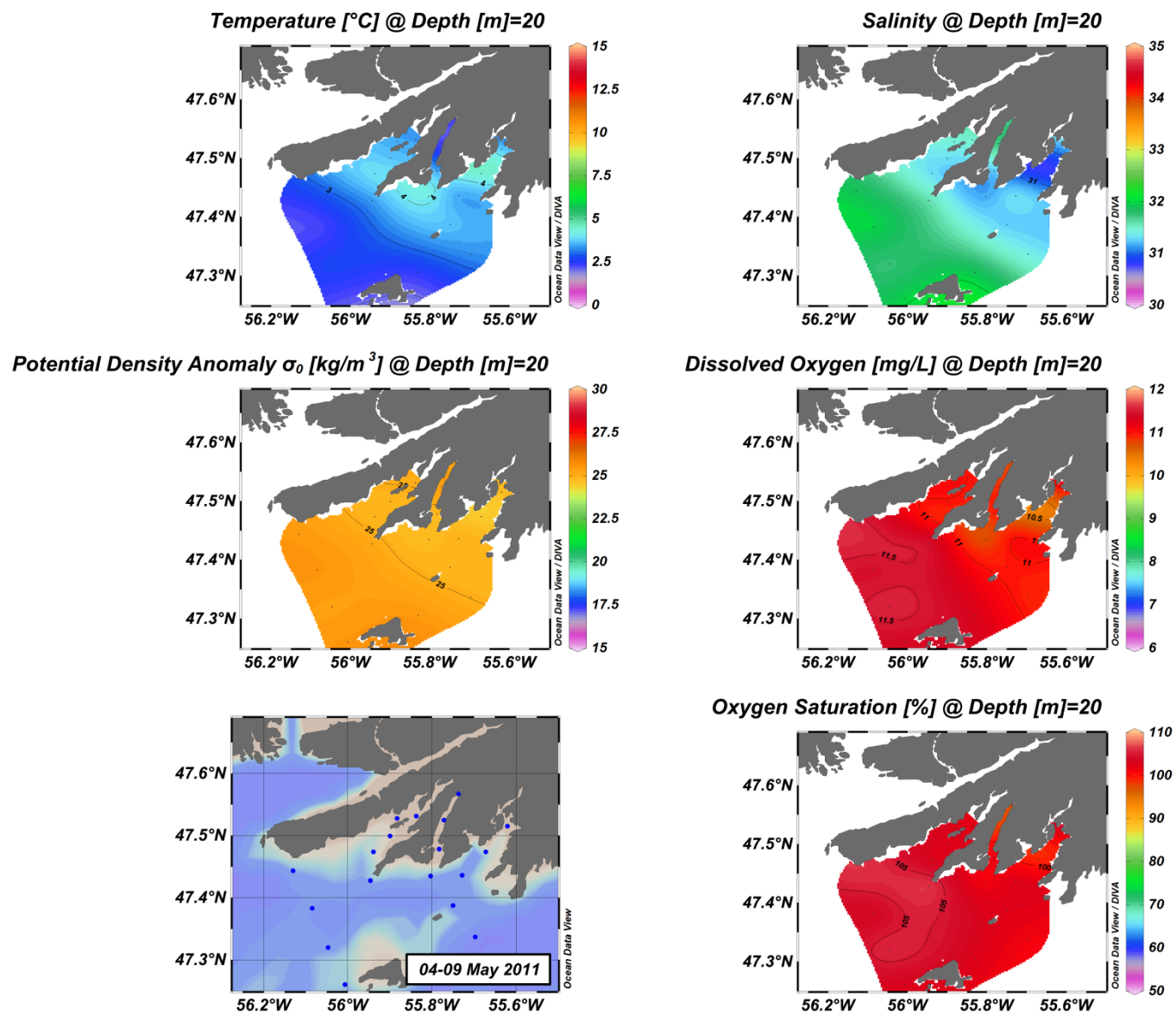


Figure C(iii)6: Connaigre Peninsula surface structure.

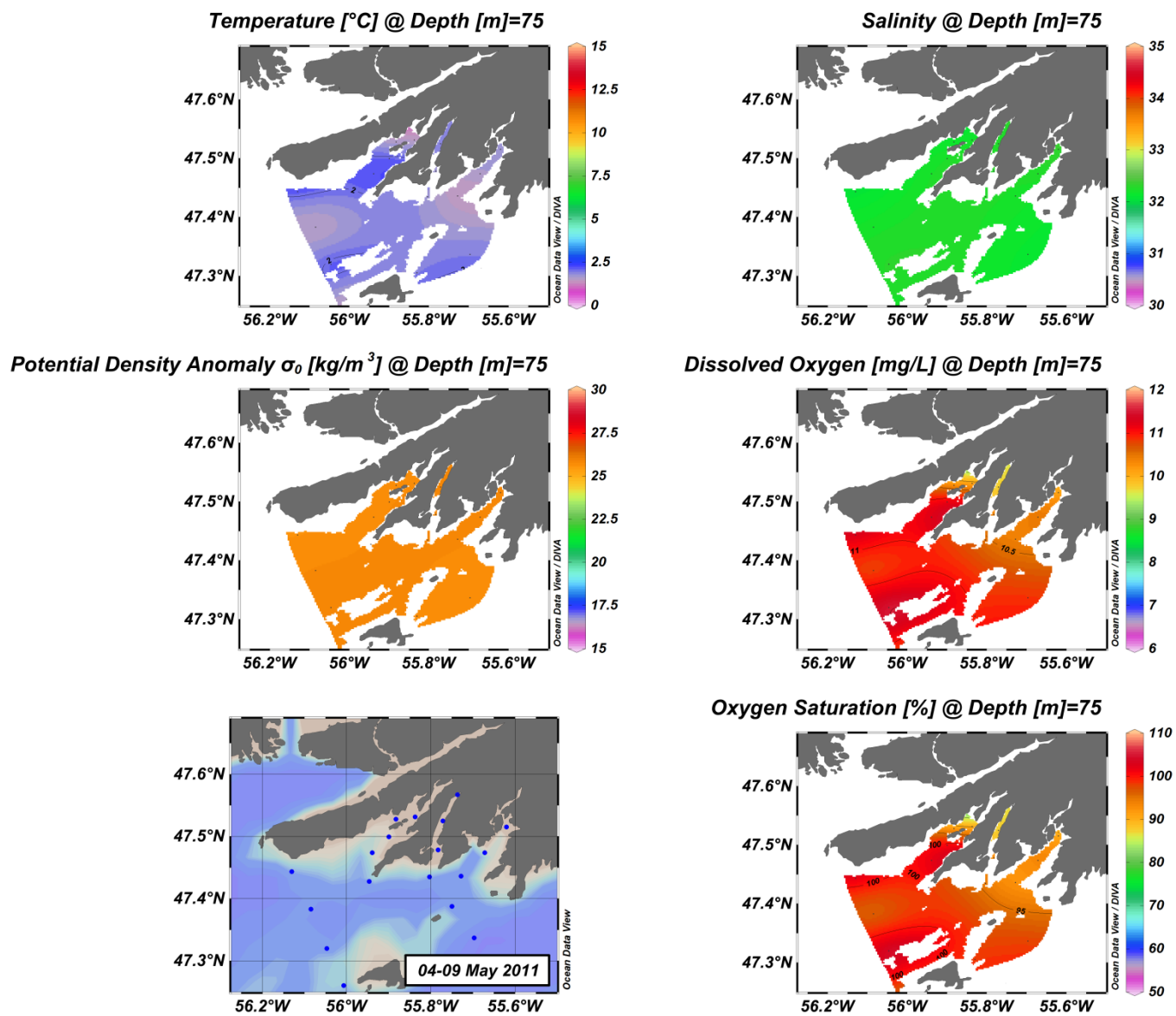


Figure C(iii)7: Connaigre Peninsula surface structure.

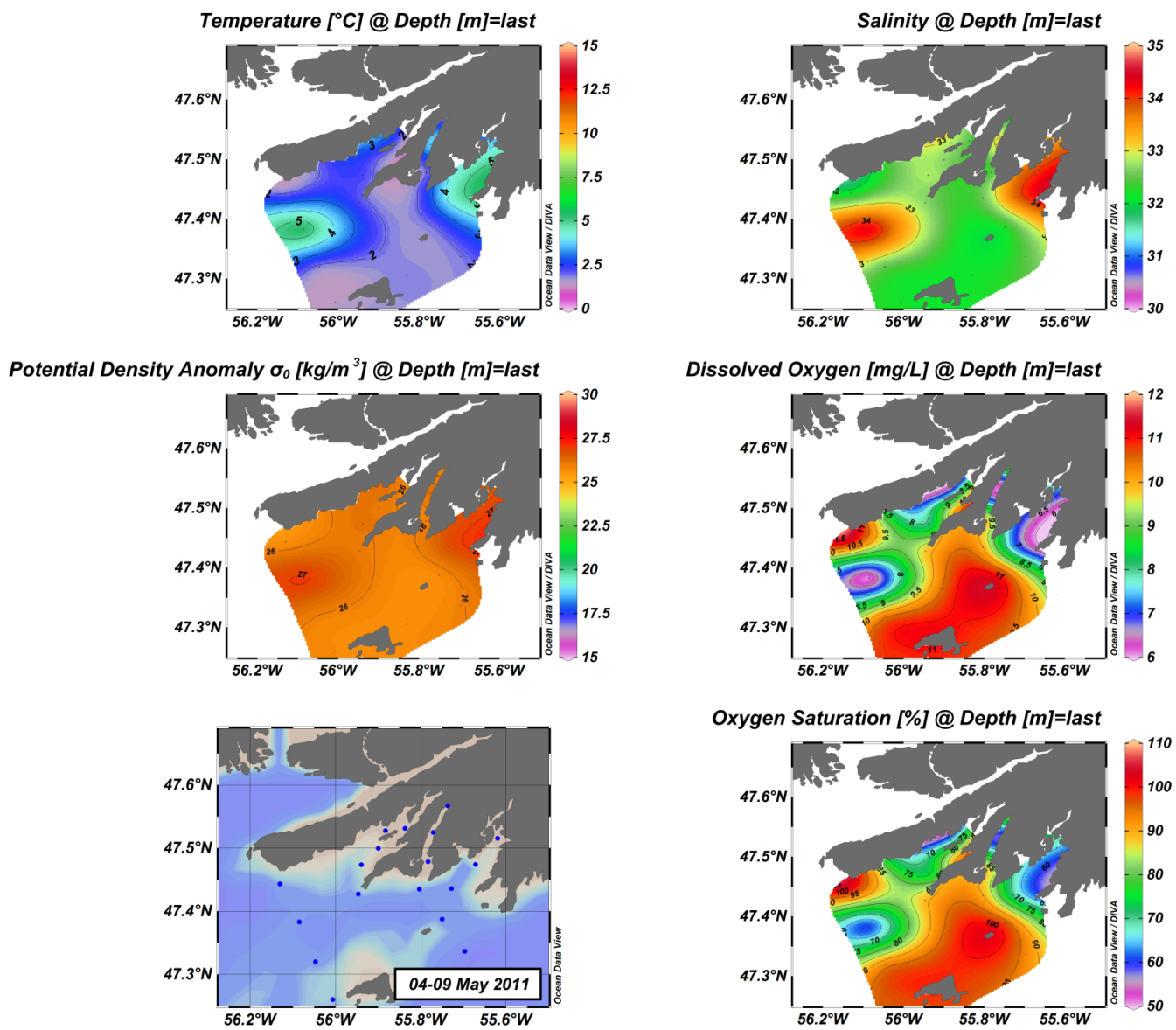


Figure C(iii)8: Connaigre Peninsula surface structure.

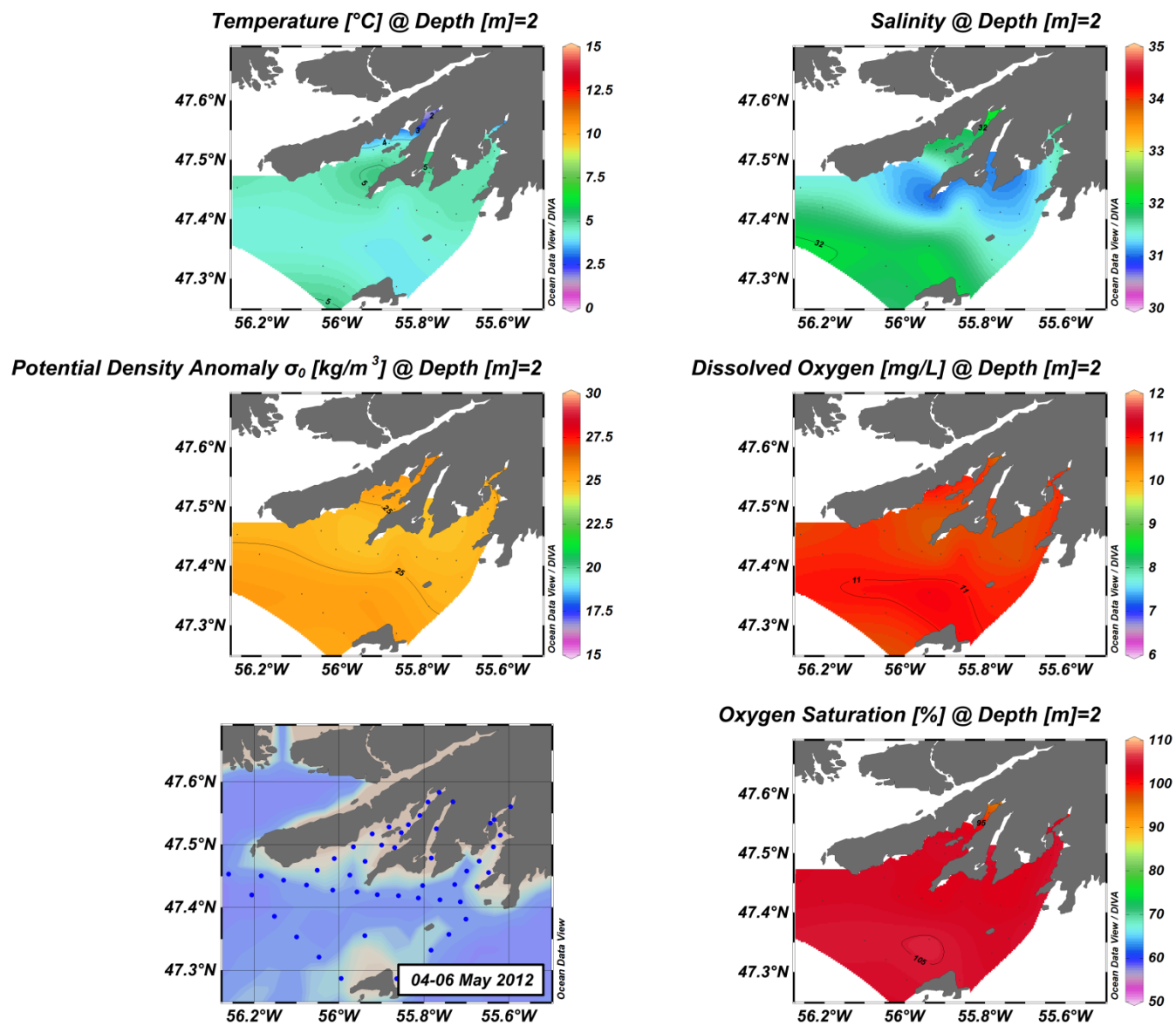


Figure C(iii)9: Connaigre Peninsula surface structure.

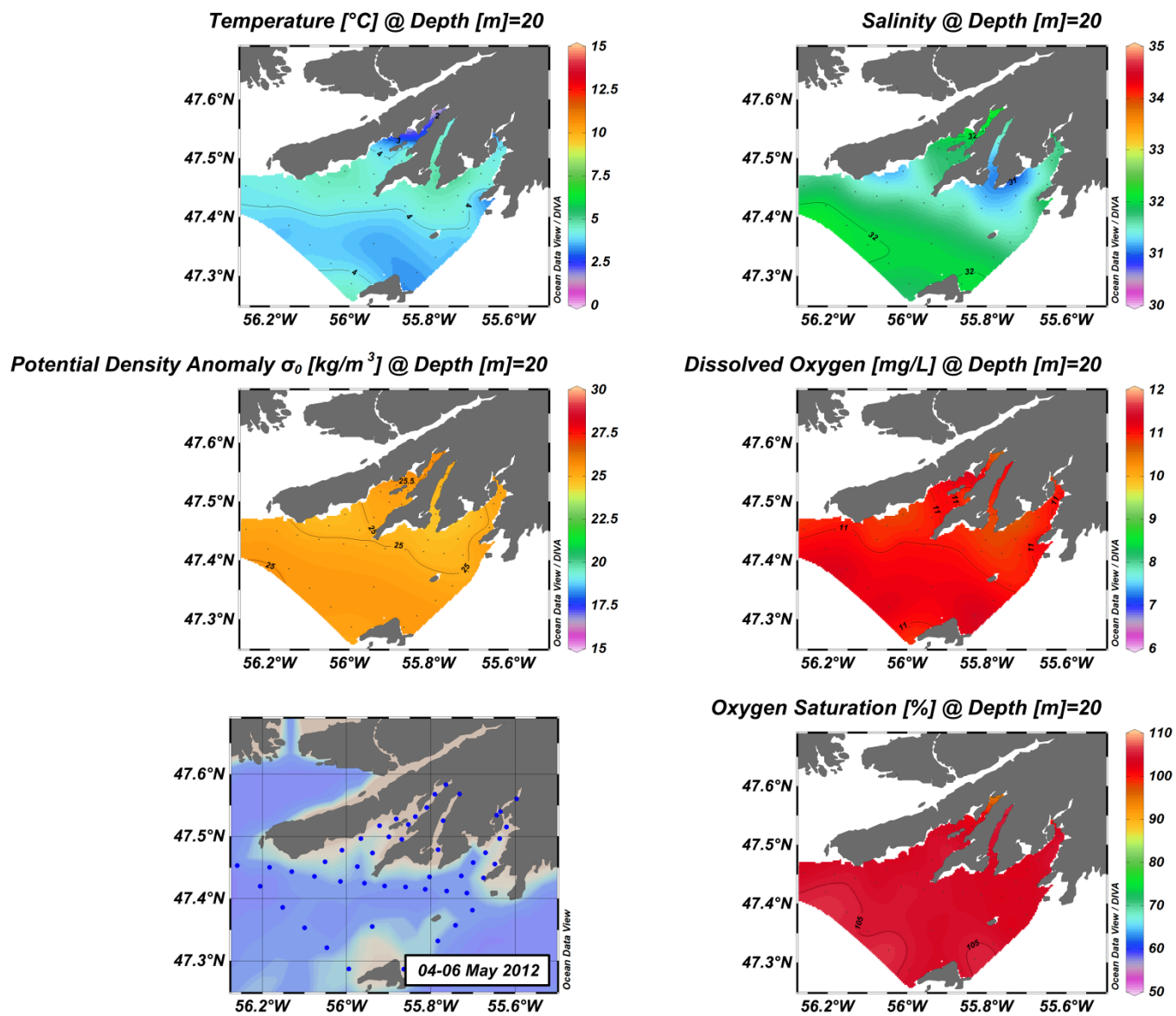


Figure C(iii)10: Connaigre Peninsula surface structure.

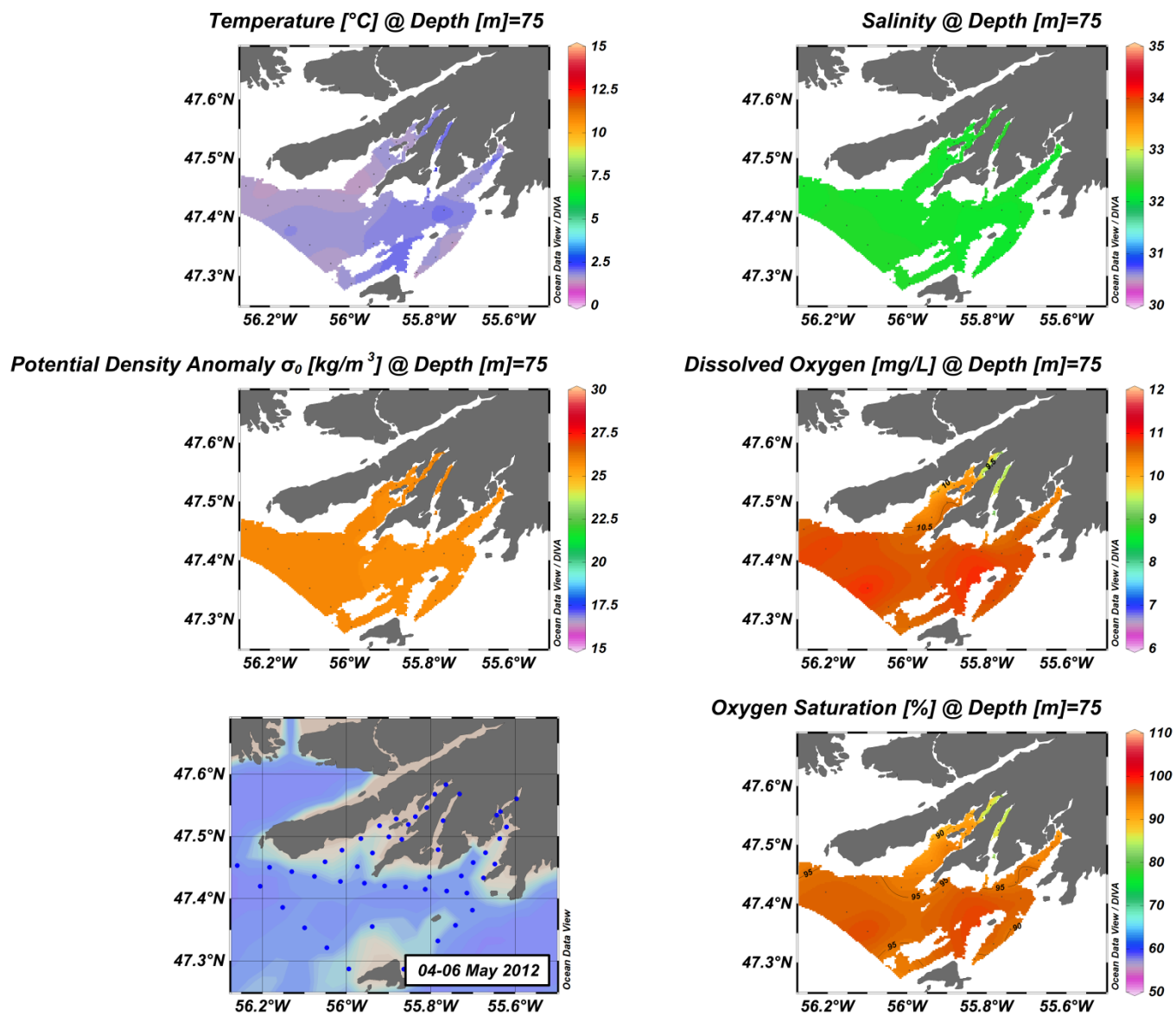


Figure C(iii)11: Connaigre Peninsula surface structure.

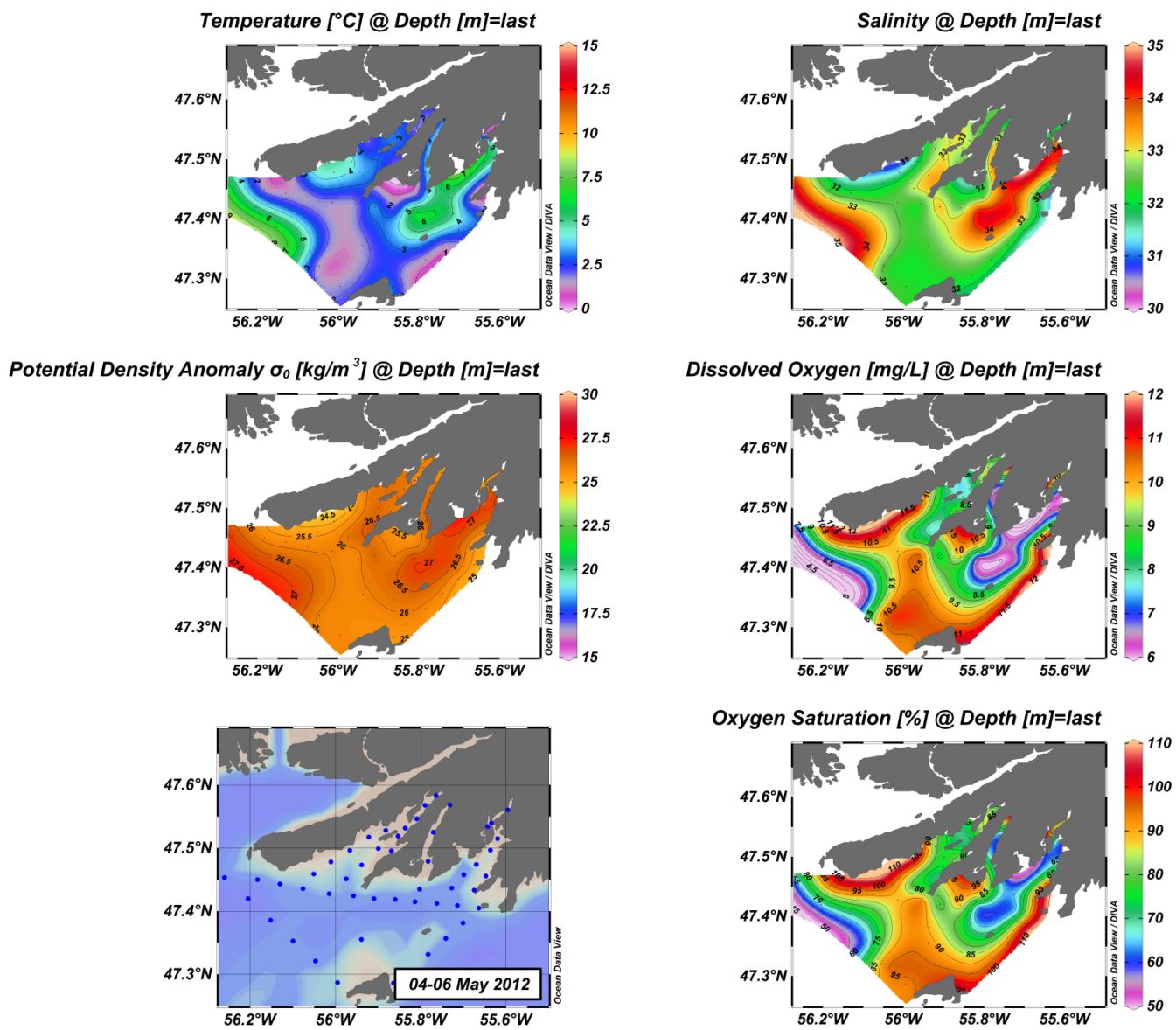


Figure C(iii)12: Connaigre Peninsula surface structure.

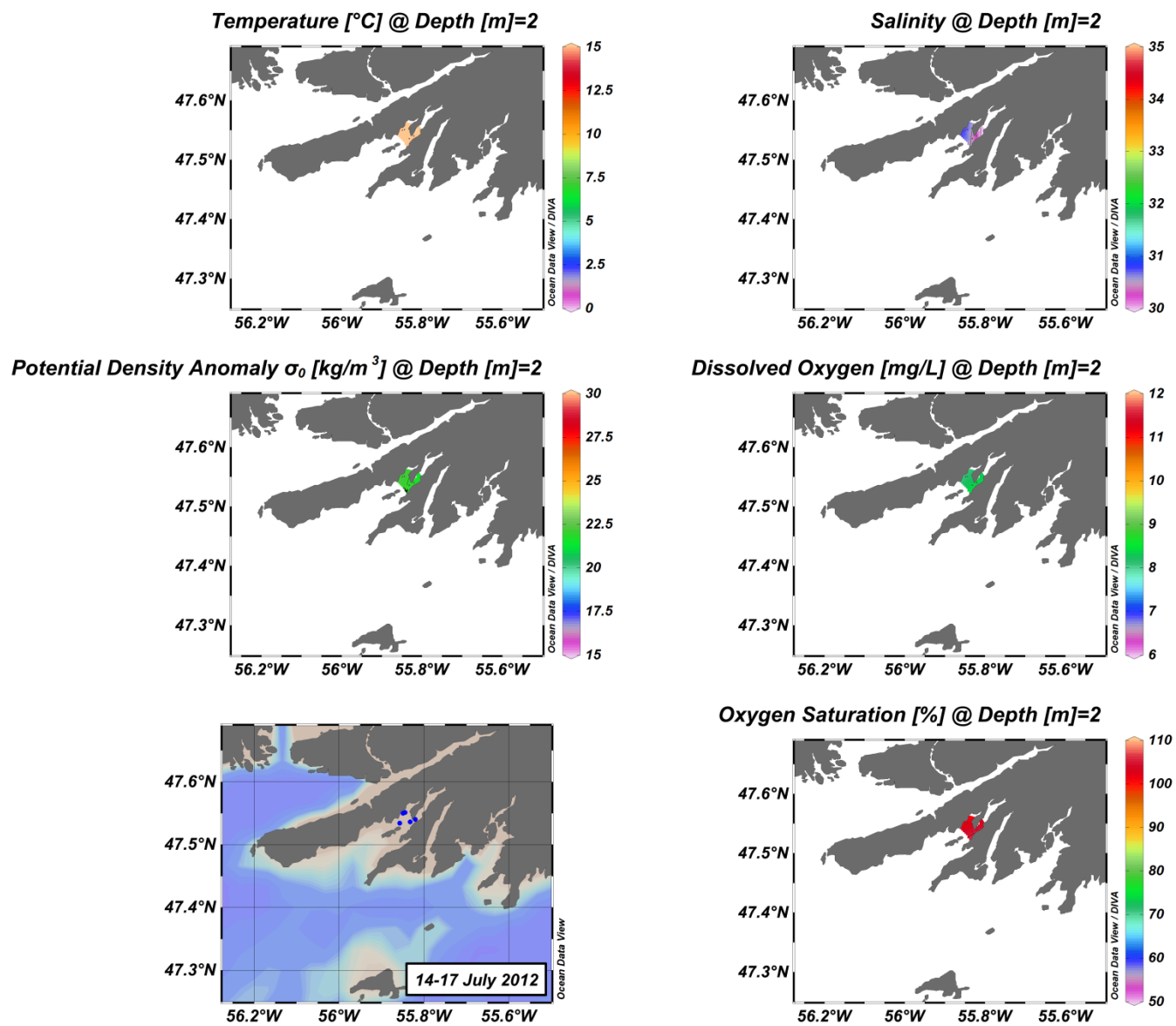


Figure C(iii)13: Connaigre Peninsula surface structure.

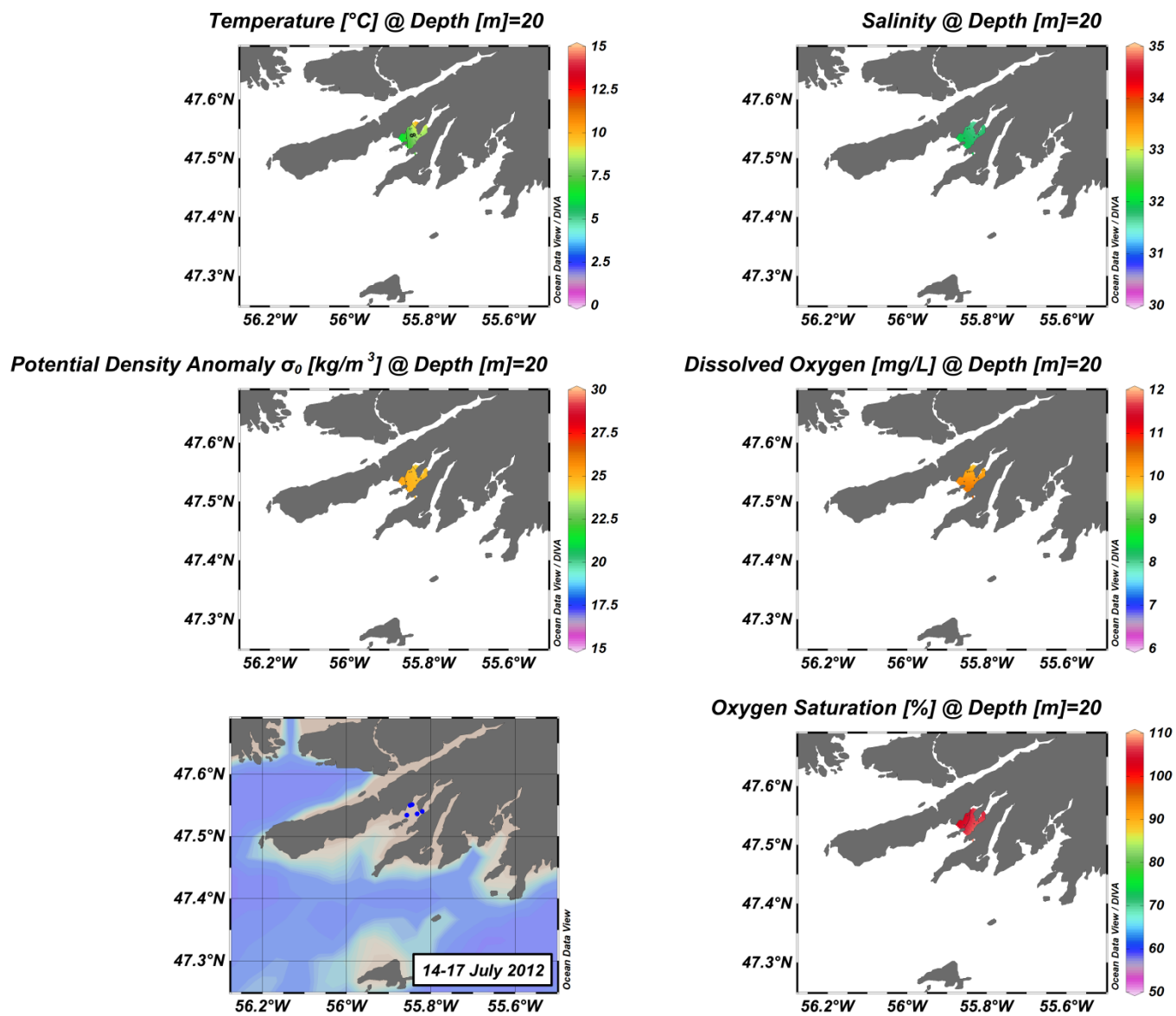


Figure C(iii)14: Connaigre Peninsula surface structure.

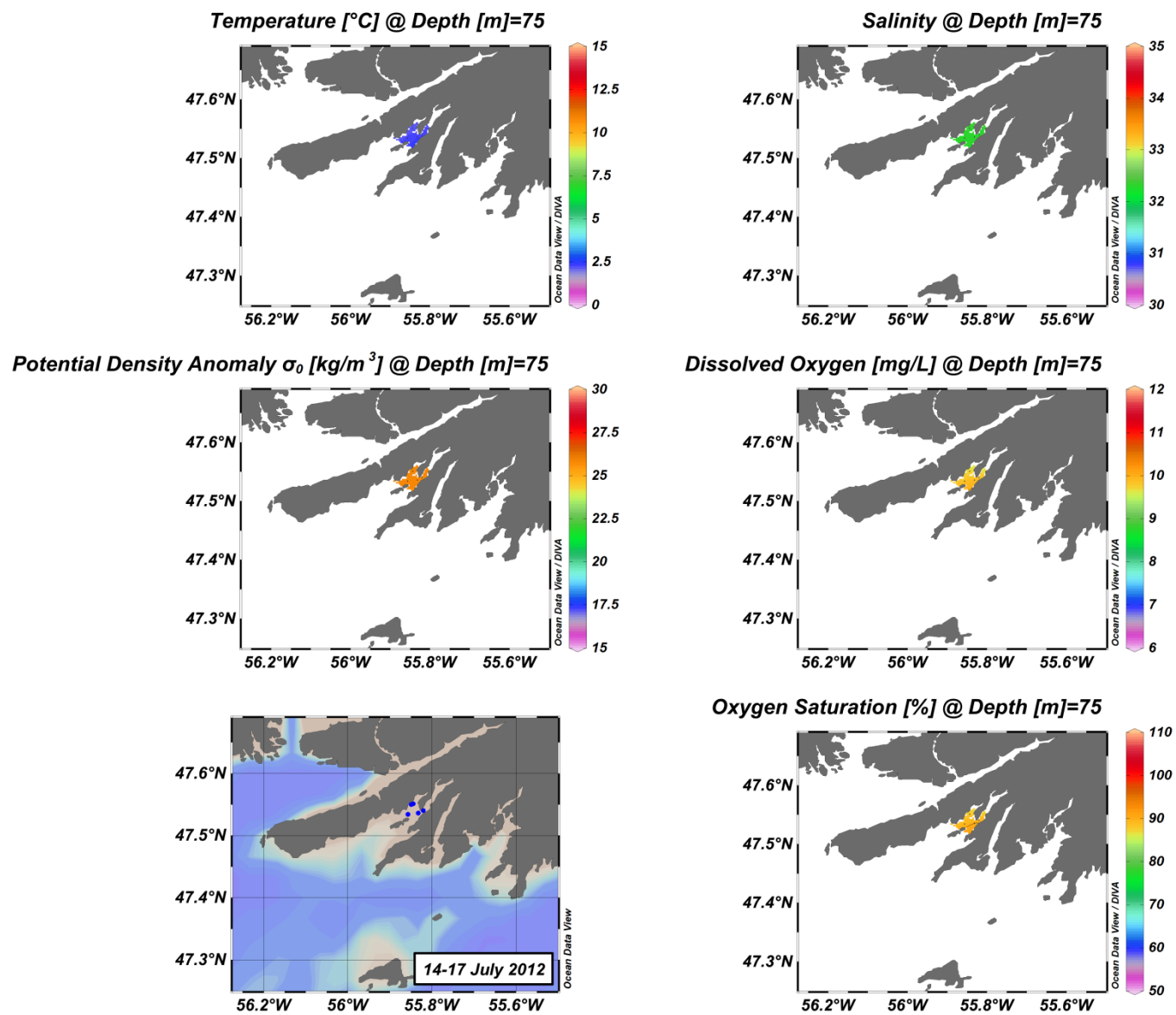


Figure C(iii)15: Connaigre Peninsula surface structure.

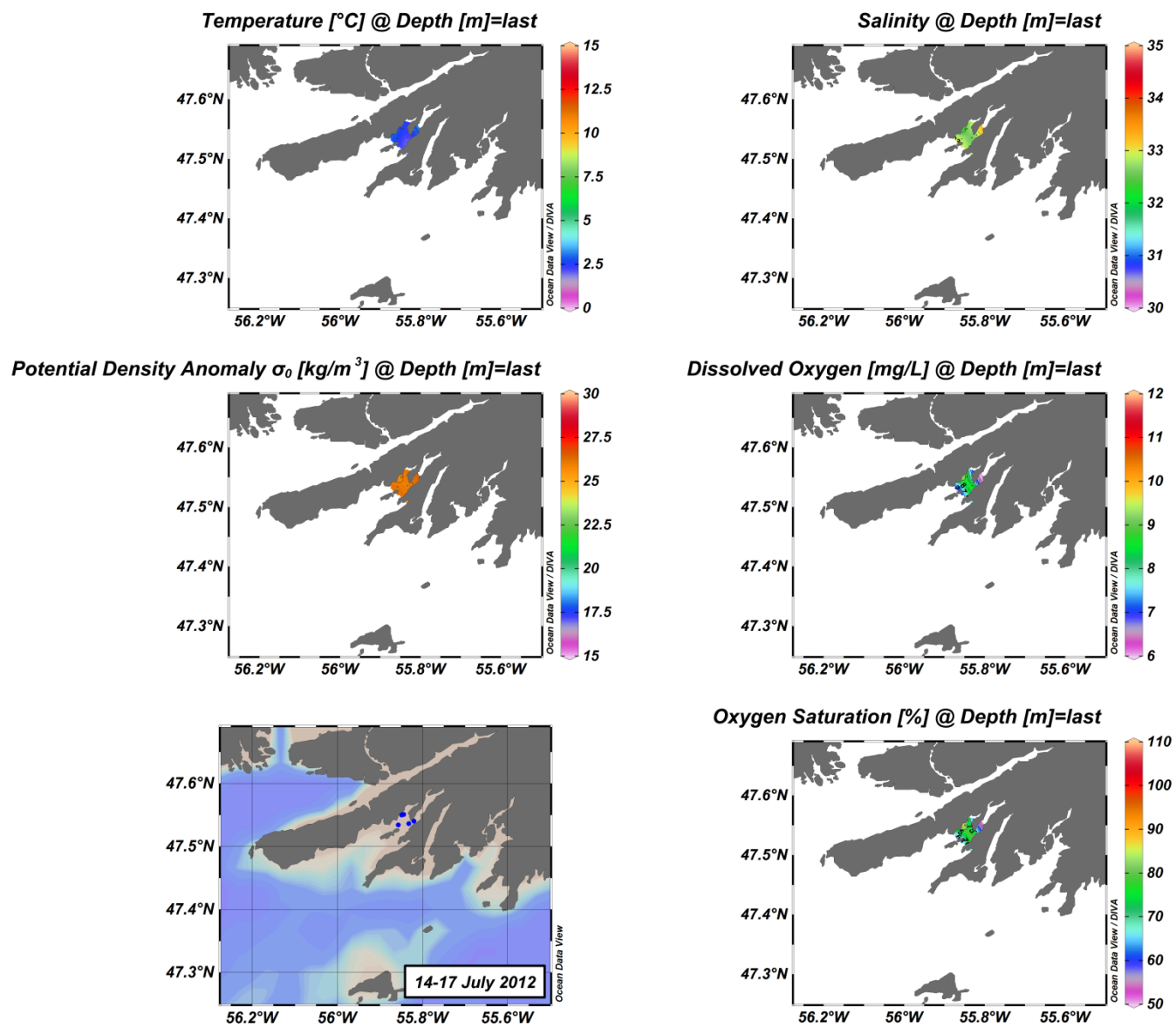


Figure C(iii)16: Connaigre Peninsula surface structure.

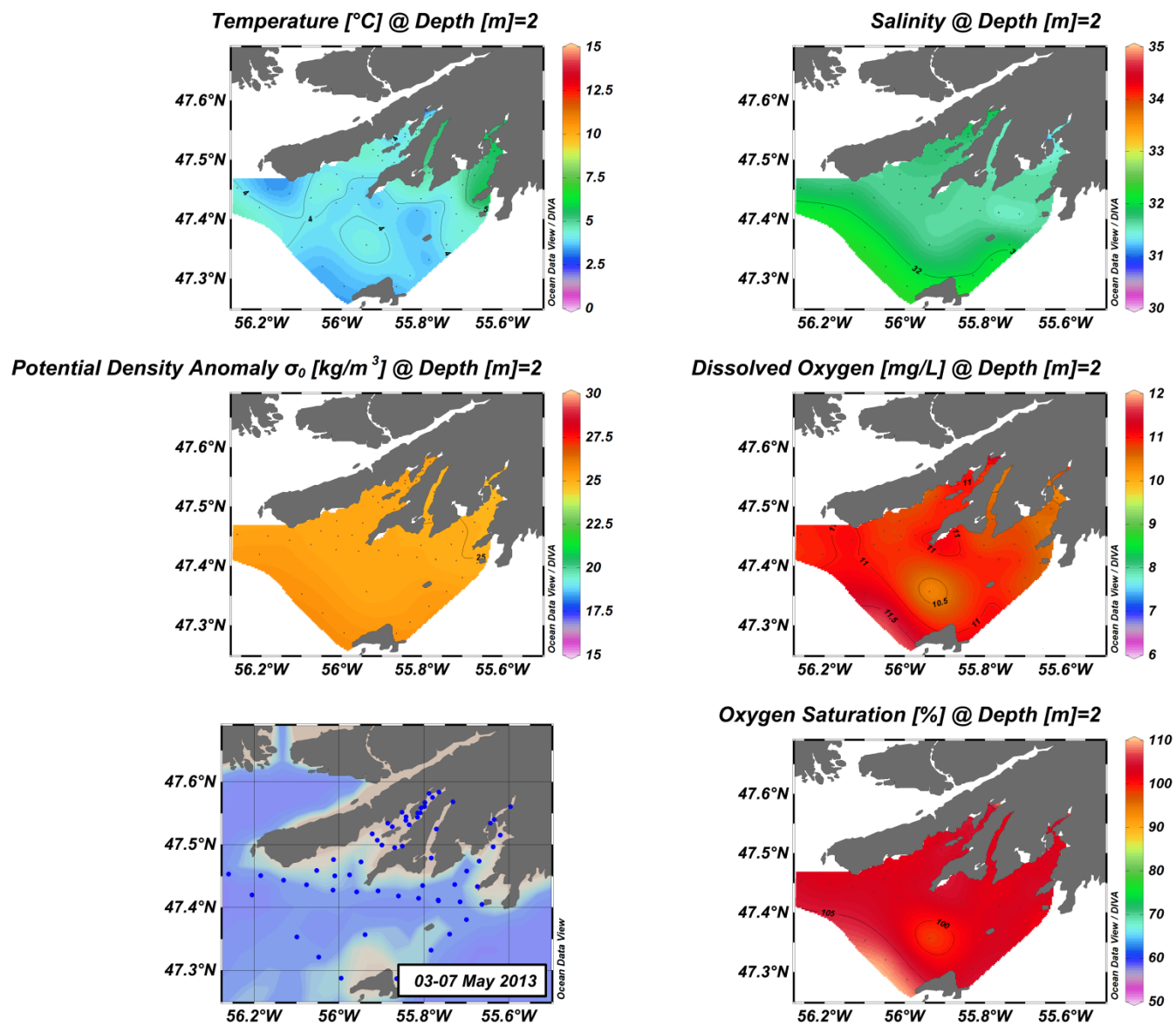


Figure C(iii)17: Connaigre Peninsula surface structure.

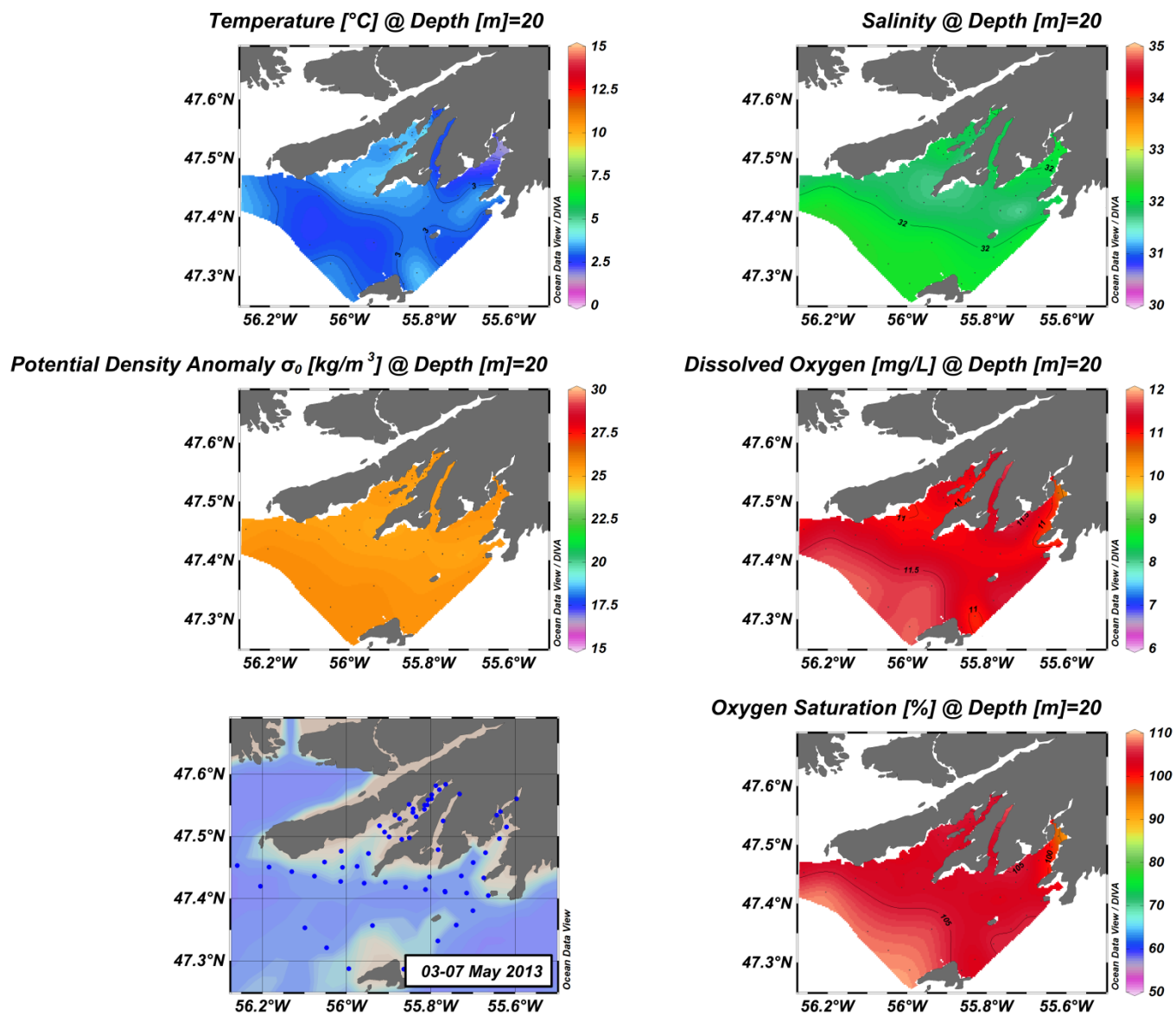


Figure C(iii)18: Connaigre Peninsula surface structure.

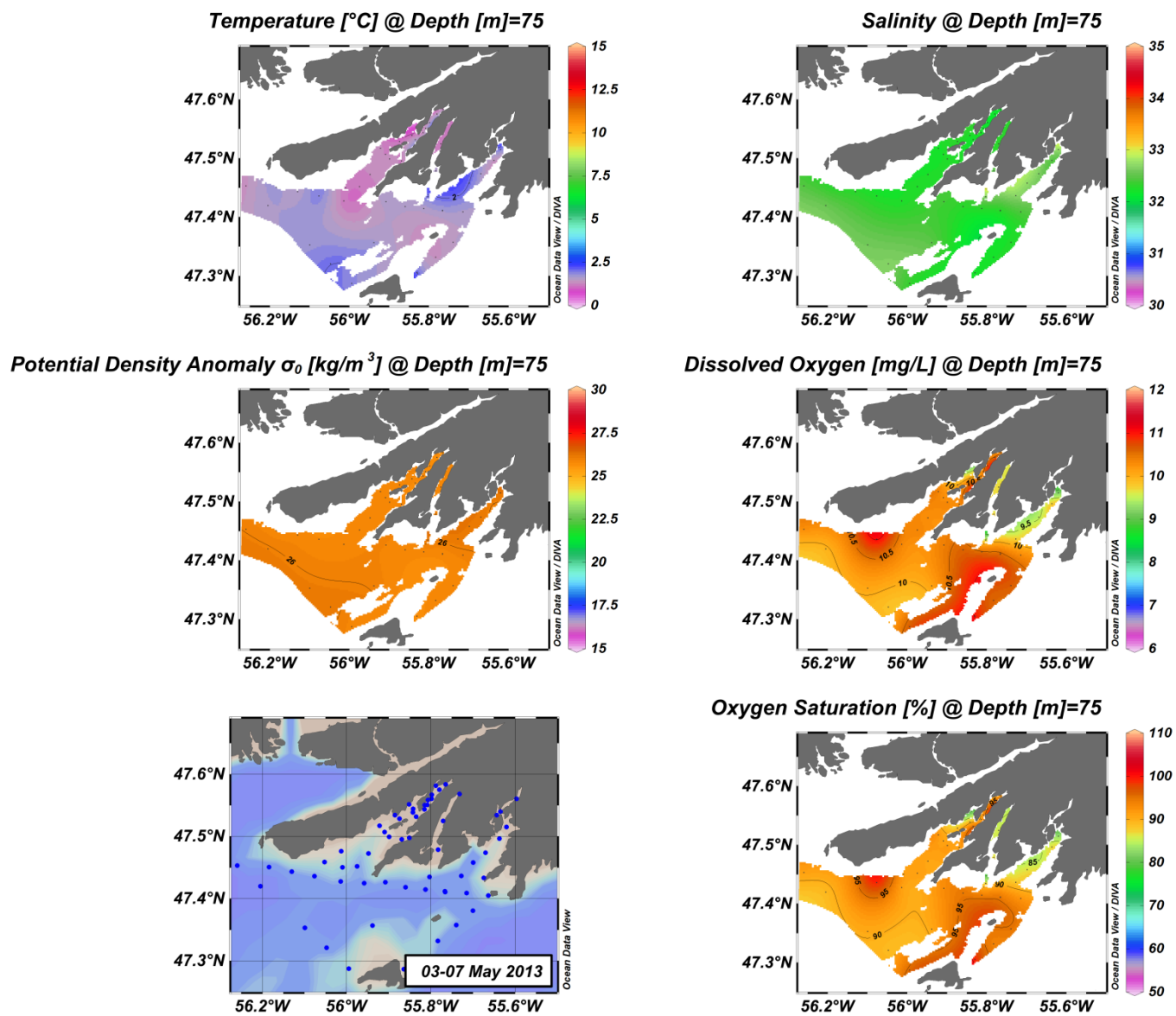


Figure C(iii)19: Connaigre Peninsula surface structure.

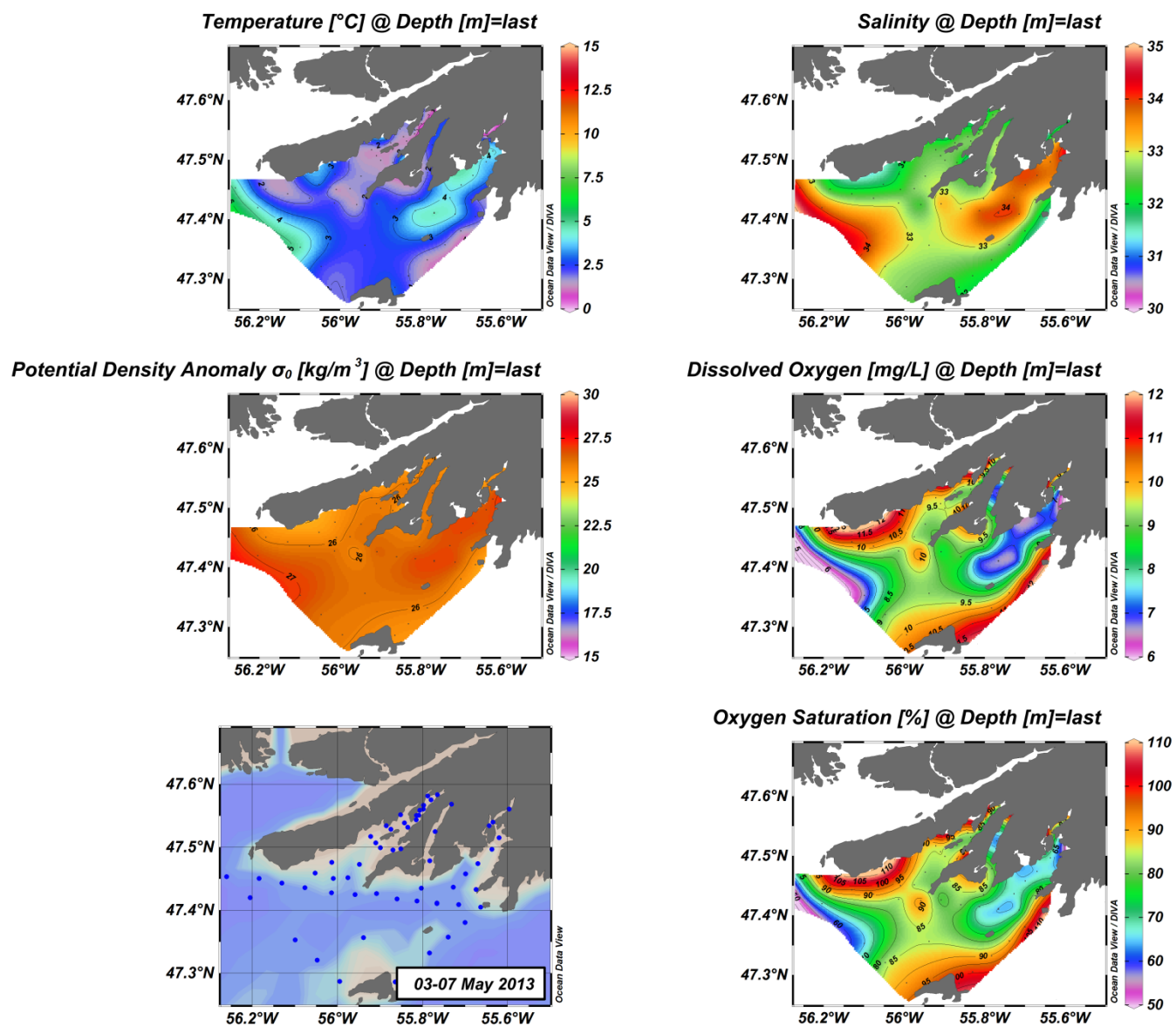


Figure C(iii)20: Connaigre Peninsula surface structure.

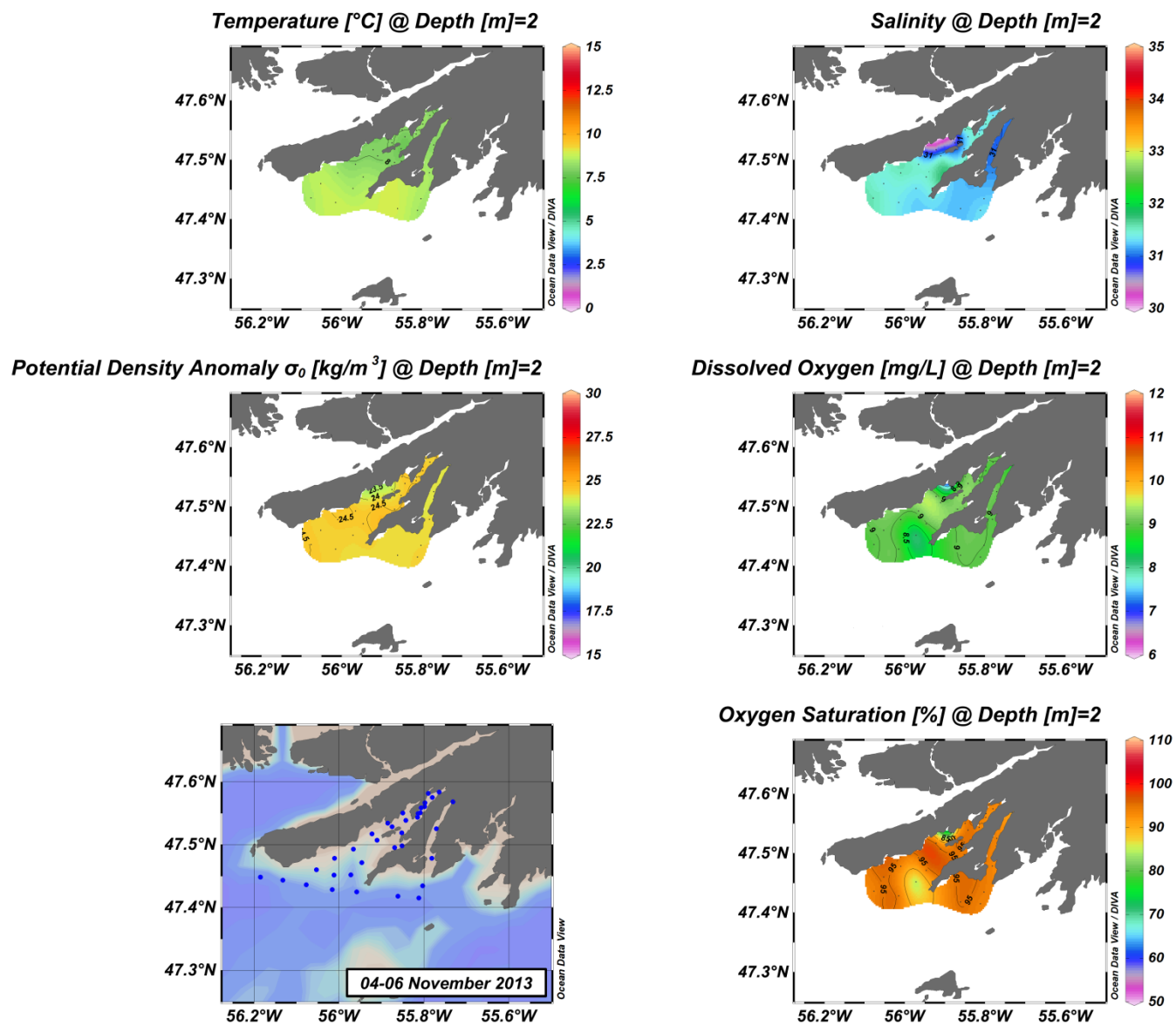


Figure C(iii)21: Connaigre Peninsula surface structure.

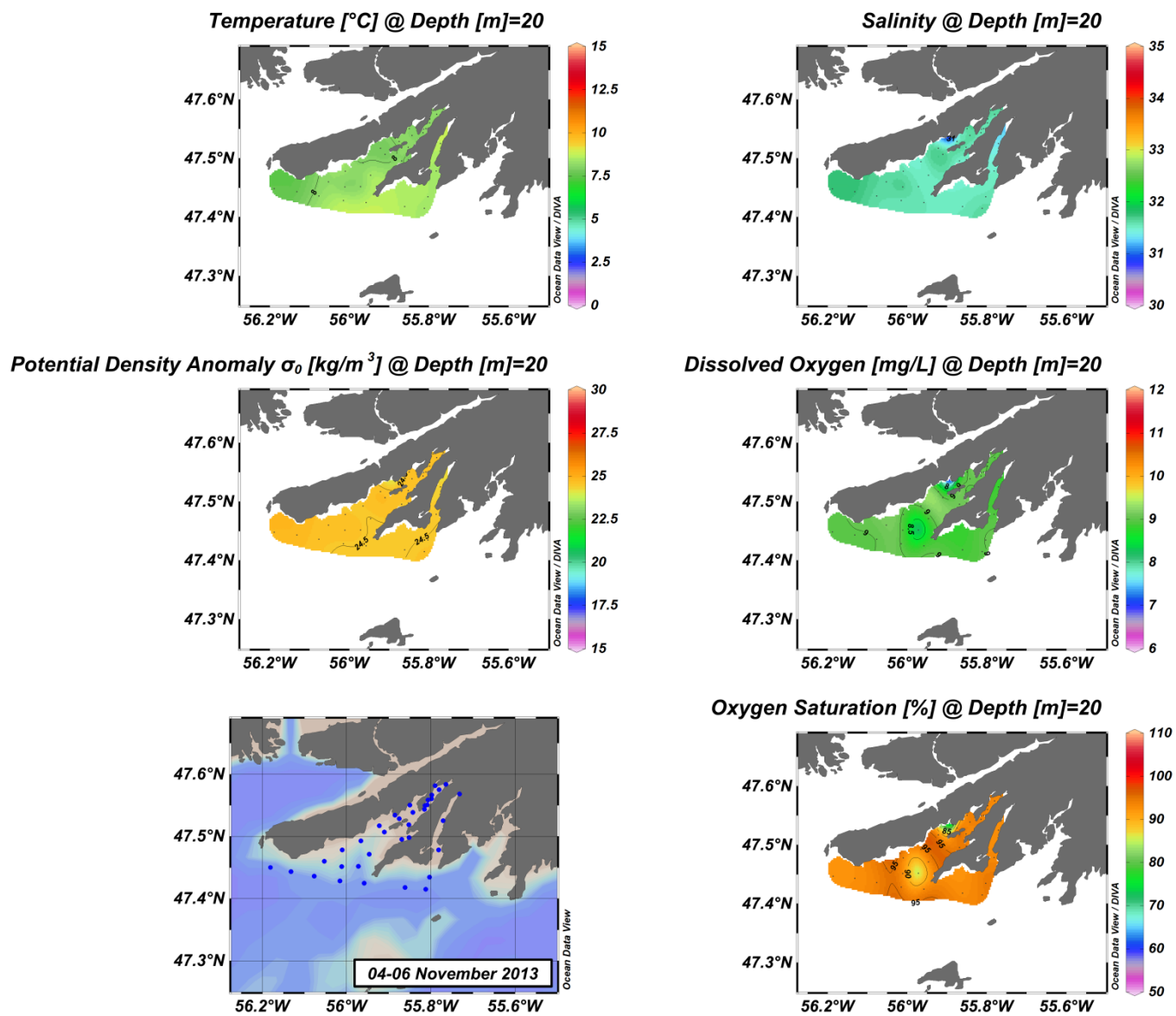


Figure C(iii)22: Connaigre Peninsula surface structure.

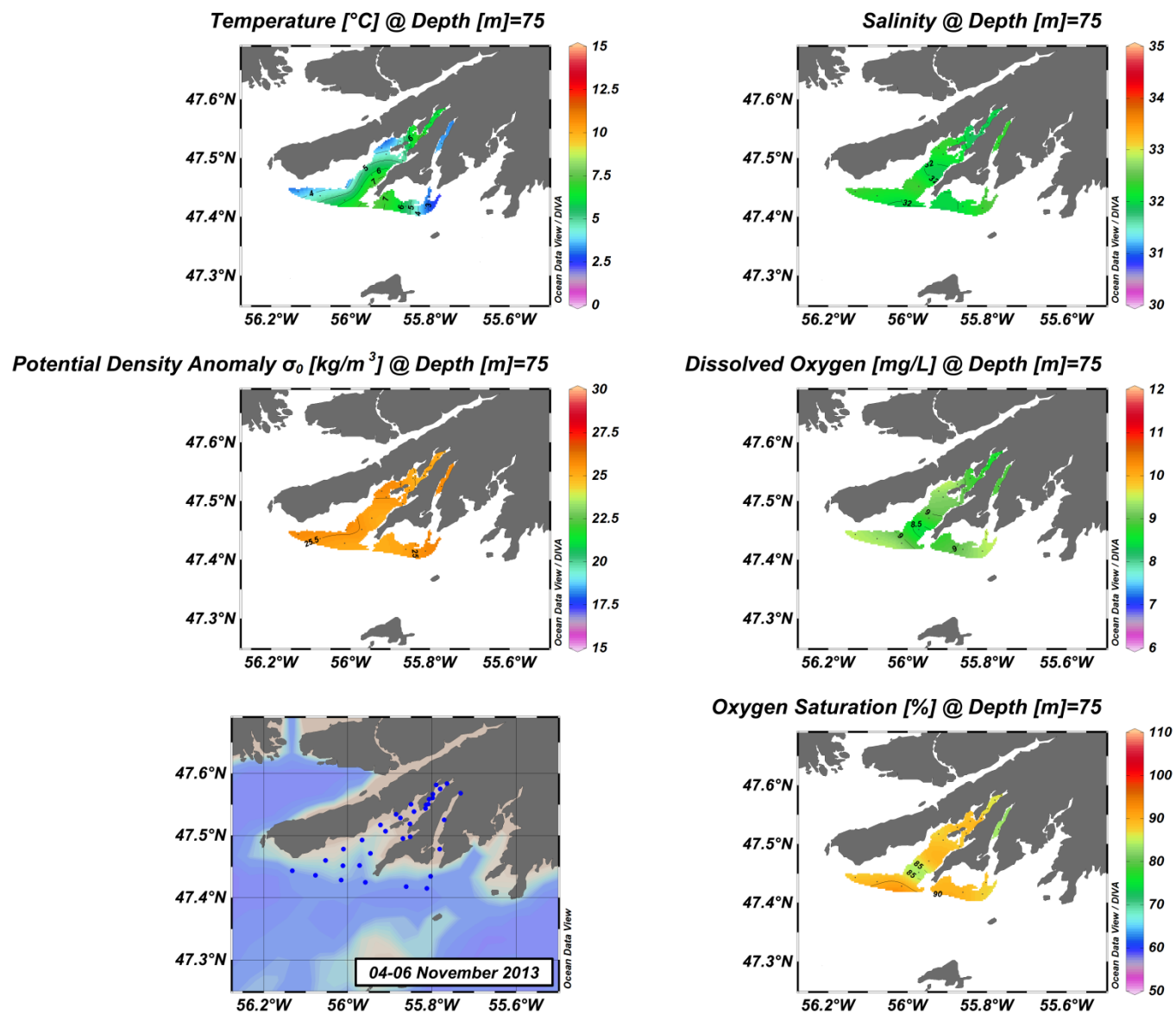


Figure C(iii)23: Connaigre Peninsula surface structure.

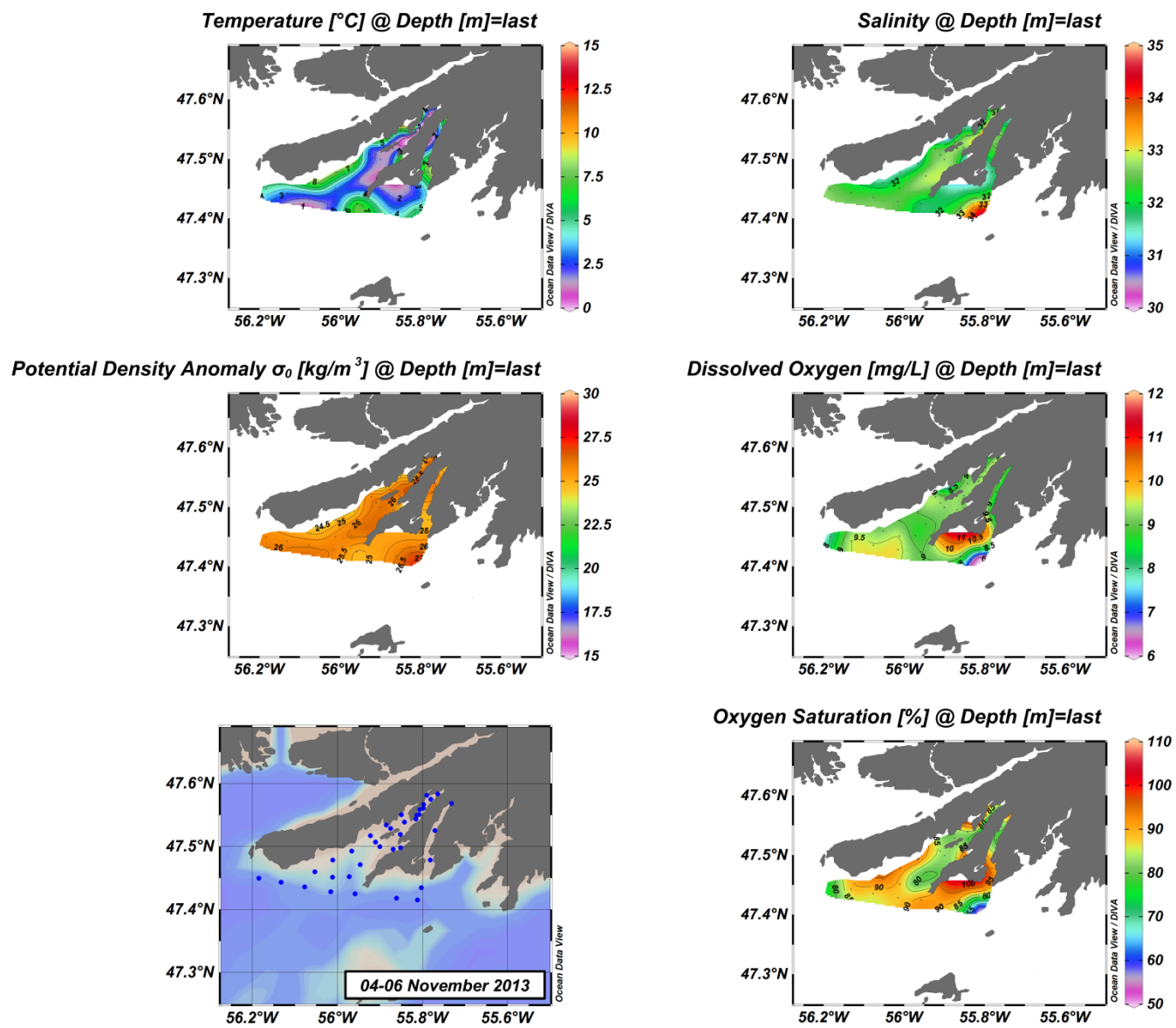


Figure C(iii)24: Connaigre Peninsula surface structure.

APPENDIX D: CTD DATA PROCESSING STEPS

The bullet points below summarise the step by step procedure followed to process the raw data using SBE data processing software ([version 7.22.5a](#)):

1.) Data conversion

Convert the binaries raw data to ASCII data as engineering units (e.g., pressure in dbar).

2. Filter

Uses a low-pass filter the temperature and conductivity data to make their time constant match (i.e., smooth high frequency signals).

3. Align CTD

Compensate for inherent sensors' response time, physical misalignment of the sensors in depth and the water transit time delays in pumped plumbing. This step essentially ensures that the data from the same parcel of water is being provided.

4. Cell Thermal Mass

Compensate for the inherent thermal lag in the conductivity cell. Thermal lag causes an over-estimation of conductivity measurement (and hence, of derived salinity) when sampling from warm to cold waters and vice-versa.

5. Loop Edit

Test the data for pressure reversal (loop in the instrument's trajectory; e.g., due to ship' heave) and for velocities that fall below a user-defined minimum. A threshold of 0.25 m/s was selected for all our dataset. Additionally to this test, the loop-edit tool was used to remove the 'surface soak' based on the assumption that the instrument soaking depth generally fell between 0.5 to 2 m depth.

6. Derive

Uses pressure, temperature, conductivity and auxiliary sensors (e.g., DO) data to calculate derived parameters such as the salinity and density of sea-water. For our datasets, the following parameters were derived: depth (m), specific conductance (uS/cm), salinity, density (kg/m³), sound velocity (m/s), descent rate (m/s) and oxygen, when available (ml/l, mg/l and % saturation). SBE data processing software uses standard UNESCO algorithms to derive those parameters (Fofonoff and Millard, 1983), temperature reported here is based on the International Temperature Scale 1990 (ITS- 90, SeaBird, 2010), sound velocity is based on Chen and Millero (1977) algorithm (Fofonoff and Millard, 1983), oxygen concentration is based on Owens and Millard (1985) and oxygen saturation on Garcia and Gordon (1992) (SeaBird, 2013).

7. Bin Average

Average data values at user-defined intervals based on pressure range, depth range, scan number range or time range. A bin size of one meter was chosen for all the data presented in this report. Since the results of the loop-edit technique was not entirely satisfactory, an 'in-house' filter was developed (see results in Figure D1) and applied along with the bin average as a step 7. To bin average, data located half a bin-size away from the wanted depths were averaged (e.g., data within 0.5 to 1.5 m for a bin centered at 1 m depth); similarly to the SBE data processing software.

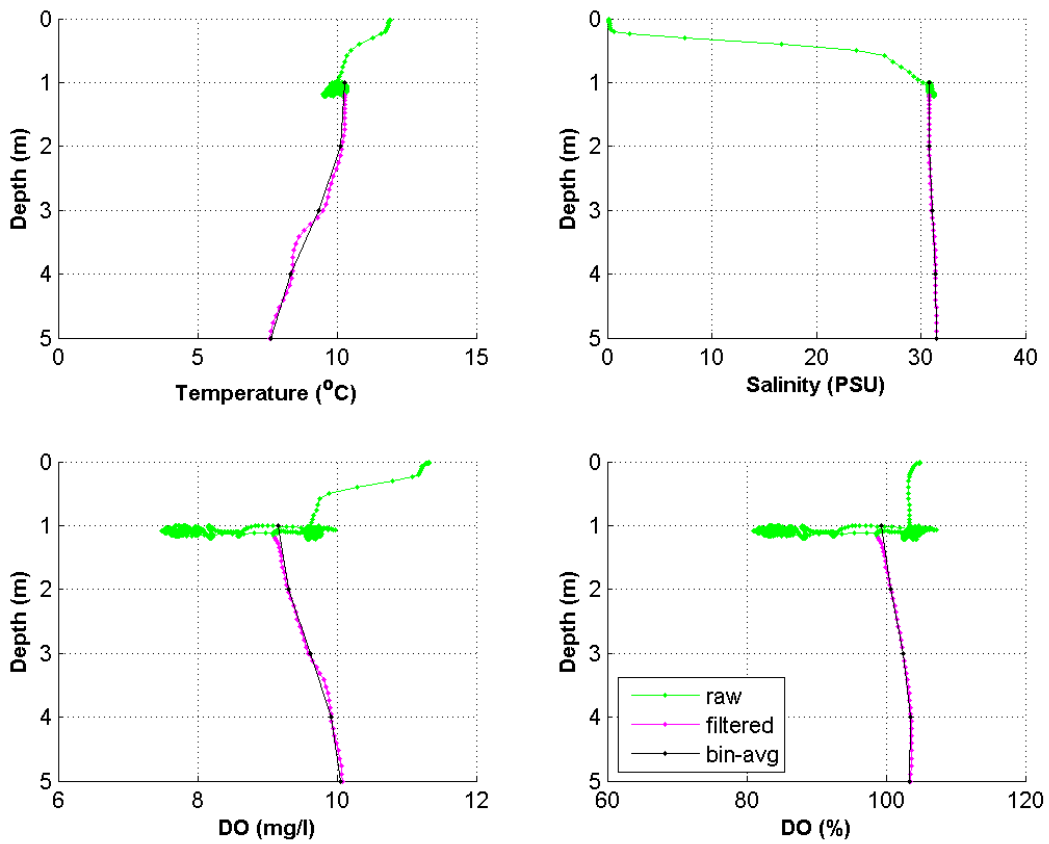


Figure D1: Illustration of the in-house surface removal filter: in green is the raw data as available from the SBE data processing software after step 6 and without removing the data flagged by the loop-edit tool (step 5), in pink is the data as coming out from the in-house surface removal filter and in black is the result from 1 m bin-averaging of the filtered data.

APPENDIX E: SAGONA ISLAND WIND RECORDS

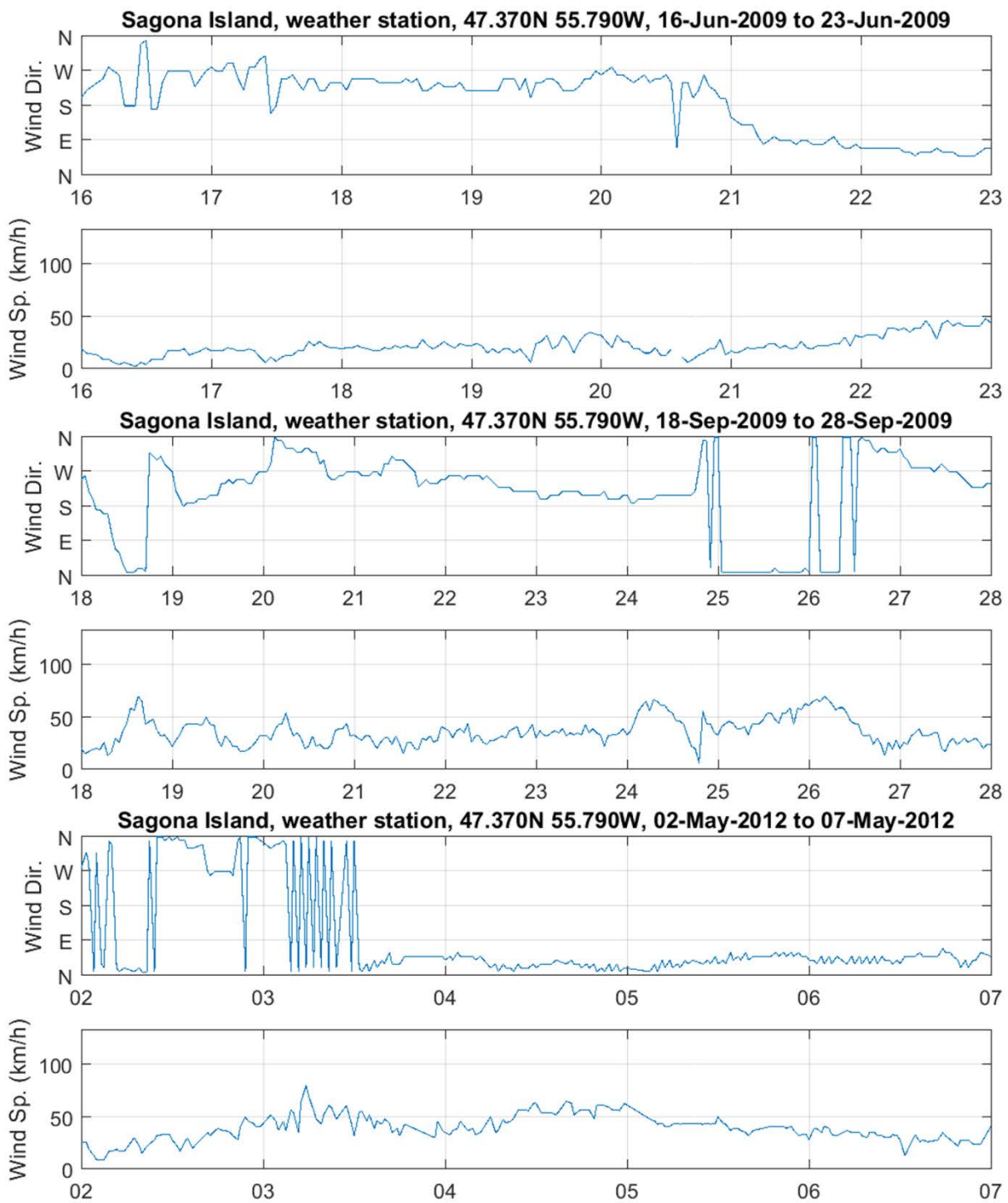


Figure E1: Sagona Island weather station wind records from June 16 to June 23, 2009, September 18 to September 28, 2009 and May 2 to May 7, 2012.